The Osmoadaptive Response of the Wine Yeast *Saccharomyces cerevisiae* K1-V1116 during Icewine Fermentation

Stephanie J. Martin, B.Sc. Hon.

Submitted to the Centre for Biotechnology in partial fulfillment of the requirements for the degree of Doctor of Philosophy

August 2008

Brock University

St. Catharines, Ontario

ABSTRACT

The adapted metabolic response of commercial wine yeast under prolonged exposure to concentrated solutes present in Icewine juice is not fully understood. Presently, there is no information regarding the transcriptomic changes in gene expression associated with the adaptive stress response of wine yeast during Icewine fermentation compared to table wine fermentation. To understand how and why wine yeast respond differently at the genomic level and ultimately at the metabolic level during Icewine fermentation, the focus of this project was to identify and compare these differences in the wine yeast *Saccharomyces cerevisiae* K1-V1116 using cDNA microarray technology during the first five days of fermentation. Significant differences in yeast gene expression patterns between fermentation conditions were correlated to differences in nutrient utilization and metabolite production. Sugar consumption, nitrogen usage and metabolite levels were measured using enzyme assays and HPLC. Also, a small subset of differentially expressed genes was verified using Northern analysis. The high osmotic stress experienced by wine yeast throughout Icewine fermentation elicited changes in cell growth and metabolism correlating to several fermentation difficulties, including reduced biomass accumulation and fermentation rate. Genes associated with carbohydrate and nitrogen transport and metabolism were expressed at lower levels in Icewine juice fermenting cells compared to dilute juice fermenting cells. Osmotic stress, not nutrient availability during Icewine fermentation appears to impede sugar and nitrogen utilization. Previous studies have established that glycerol and acetic acid production are increased in yeast during Icewine fermentation. A gene encoding for a glycerol/H^+ symporter (*STL1*) was found to be highly expressed up to 25-fold in the

Icewine juice condition using microarray and Northern analysis. Active glycerol transport by yeast under hyperosmotic conditions to increase cytosolic glycerol concentration may contribute to reduced cell growth observed in the Icewine juice condition. Additionally, genes encoding for two acetyl CoA synthetase isoforms (*ACS1* and *ACS2*) were found to be highly expressed, 19- and 11-fold respectively, in dilute juice fermenting cells relative to the Icewine juice condition. Therefore, decreased conversion of acetate to acetyl-CoA may contribute to increased acetic acid production during Icewine fermentation. These results further help to explain the response of wine yeast as they adapt to Icewine juice fermentation.

ACKNOWLEDGEMENTS

I would like to personally thank my supervisor Dr. Debra Inglis for providing me the opportunity to be a part of a wonderful lab group. Your guidance and encouragement allowed me to develop and more importantly, have confidence in, my research skills. I truly appreciate all of your help over the years and I am thrilled that I have been one of your students.

I also want to thank Dr. Gary Pigeau, a very talented researcher whose enviable technical skills and academic expertise always set me in the right direction.

To everyone in the IH210 lab group- past and present members (Ai Lin, Shiri, Qing, Fei, Heidi, Lisa, Eric, Wendy and Matilda)- you are a fantastic collection of exceptionally talented people and all of whom are extremely funny, sweet and best of all, supportive. Each of you have influenced my life in so many amazing ways and for that, I thank you all.

I also want to extend my deepest appreciation and thanks for all the faculty and staff of CCOVI, Department of Biology and Department of Chemistry I had the privilege of working with throughout my graduate studies.

Last, but definitely not least, I would like to thank my mother and father for their continuing love, support, guidance and patience. Thank you both for always giving me the drive to pursue my dreams.

TABLE OF CONTENTS

LIST OF TABLES

LIST OF FIGURES

1. INTRODUCTION

1.1. INTRODUCTION TO THE PROBLEM

Icewine is an intensely sweet specialty dessert wine fermented from the juice of grapes frozen naturally on the vine. Canada is now globally the leading producer by volume of Icewine as production of Canadian Icewines has increased considerably over recent years from 364,635 L in 2000 to 1,177,484 L in 2006 (Vintners Quality Alliance Ontario, 2001 and 2007). However, Icewine production offers many challenges to winemakers such as sluggish fermentation rates, difficulties in reaching 10-11% (v/v) ethanol in the wine before the yeast stop fermenting and controlling volatile acidity in the form of acetic acid (Kontkanen *et al.*, 2004). These fermentation difficulties result from the high concentrations of naturally concentrated soluble solids in the juice, like sugar, that place commercial wine yeast under extreme hyperosmotic stress as they ferment the juice into wine. Although the response of laboratory yeast strains to hyperosmotic stress in an aerobic environment is well understood (reviewed in Hohmann, 2002), there is still limited information on how wine yeast strains respond to stress especially within an oenological environment (reviewed in Pretorius, 2000). Wine yeast strains display physiological properties that are distinct from laboratory strains and these differences can impact the organoleptic properties of wine (reviewed in Remize *et al.*, 1999; Hauser *et al.*, 2001; Rossignol *et al.*, 2003). Although wine yeast have been selected for their oenological properties, there is still much we do not understand about how they differ from laboratory strains, such as their responses to hyperosmotic stress during Icewine fermentation. Also, since Icewine fermentations typically take weeks to months to complete, the initial response by wine yeast to hyperosmotic stress may differ

considerably from their adapted response throughout the fermentation of Icewine juice in addition to differing from the well-characterized initial responses of laboratory strains (reviewed in Hohmann, 2002). Wine yeast responses during stressful fermentations are not well characterized at the molecular level. This lack of understanding is a problem because this stress response leads to production of metabolites that ultimately affects wine quality (Kontkanen *et al.*, 2004; Pigeau and Inglis, 2005; Pigeau *et al.*, 2007) and our limited understanding of the response limits our ability to select and/or design strains better suited to these fermentations.

1.2. OBJECTIVES

The fundamental goal of this project was to gain a more complete understanding of how wine yeast metabolism adapts in response to prolonged exposure to hyperosmotic stress, especially to high concentrations of fermentable sugars found in Icewine juice and how these responses affect metabolite production such that this information could be used in future projects to select yeast best suited for Icewine production. Therefore, the focus of my project was two-fold. Firstly, microarray technology was to be used to identify yeast genes induced or repressed during Icewine fermentation relative to table wine fermentation by comparing the genome-wide expression between these two conditions during the first five days of fermentation. Secondly, differences in gene expression patterns within entire metabolic pathways were to be correlated to yeast cell growth, sugar and nitrogen usage and metabolites produced by the yeast under the two conditions to understand how and why wine yeast respond differently during Icewine fermentation.

1.3. EXPERIMENTAL DESIGN

Differences in gene expression at the genomic level of the commercial wine yeast *Saccharomyces cerevisiae* K1-V1116 fermenting 40°Brix Icewine and 20°Brix diluted juice during the first 5 days of fermentation were compared using cDNA microarrays. Following data analysis, significant changes in gene expression between the two fermentation conditions were interpreted as fold gene induction or repression. These genes were further categorized based on their biological function or participation within specific metabolic pathways using a statistical datamining software package integrated with the *Saccharomyces* genome database (Ashburner *et al.*, 2000; Dwight *et al.*, 2002). The expression of a small subset of genes differentially expressed between fermentation conditions was verified using Northern analysis. To relate the differences in gene expression between juice conditions to juice components consumed during fermentation or metabolites produced by the yeast during fermentation, enzyme assays and HPLC were used to measure metabolite levels throughout the fermentations.

2. LITERATURE REVIEW

2.1. INTRODUCTION TO ICEWINE: PRODUCTION AND CHALLENGES

Icewine is an intensely sweet dessert wine fermented from the juice of grapes frozen naturally on the vine. The first Icewines originated in Germany during the mid-1800's when grapes froze on the vine before harvest thereby producing wines with intense aromas and flavours (Schreiner, 2001). By allowing grapes to freeze on the vine past their normal fall harvest, the berries are subjected to multiple freeze-thaw cycles leading to mechanical and biochemical changes in the berry tissue. Over time, these changes likely contribute to the unique chemical profile of Icewine juice in comparison to grape juice produced from grapes harvested past their normal fall harvest. Today, the successful commercial development of Canadian Icewine into a unique, specialty dessert wine has securely established Canada as a world leader in Icewine production. Production of Canadian Icewines has increased considerably over recent years (Vintners Quality Alliance Ontario, 2001 and 2007) and as a result, Canada has gained international recognition as a premium wine producing country. Since Icewine is considered to have a key role in the ongoing commercial and economic success of the Canadian wine industry, it is essential that strict standards for Icewine production are met to ensure continued wine quality (Vintners Quality Alliance, 1999).

The Canadian wine industry is regulated by the Vintners Quality Alliance (VQA). Both grape growers and winemakers must follow strict rules and regulations implemented by the VQA covering all aspects of Icewine production, from harvest to finished wine (Vintners Quality Alliance, 1999). Of these regulations, temperature of the harvest is critical to the production of an authentic Icewine. The entire harvesting and

pressing process must be carried out at cold temperatures (–8°C or below) with harvests typically occurring once temperatures reach –11°C. These temperatures must be maintained throughout the pressing process without artificial refrigeration to ensure that the frozen water of the berries does not thaw and dilute the juice. As a result, a juice highly concentrated in all soluble solids including sugars, acids and nitrogenous compounds is extracted as the water remains with the grape skins in the form of ice during pressing. According to the VQA regulations, the concentration of soluble solids in Canadian Icewine juice must reach a minimum of 35°Brix following pressing (Vintners Quality Alliance, 1999) with concentrations of solutes in Icewine musts commonly falling within the range of approximately 38 to 42°Brix (Pigeau *et al.*, 2007).

Icewine production presents many challenges to winemakers as the high levels of naturally concentrated soluble solids like fermentable sugars in the juice place commercial wine yeast under extreme hyperosmotic stress as they ferment the juice into wine (Kontkanen *et al.*, 2004). In comparison to table wine fermentation, the increased osmotic stress yeast experience throughout the course of Icewine fermentation elicits changes in yeast metabolism, which can contribute to fermentation difficulties (Pigeau and Inglis, 2005; Pigeau *et al.*, 2007). Icewine fermentations are often slow and require lengthy periods of time to reach desired ethanol concentrations, with increasing ethanol levels placing yeast under additional stress as alcoholic fermentation progresses. Typically, yeast consume about half of the available sugar and nitrogen during Icewine fermentation such that fermentation ends while there is still considerable residual sugar present (Kontkanen *et al.*, 2004; Pigeau and Inglis, 2005), imparting the intense sweetness characteristic of this wine. Typical ethanol levels in commercial Icewines are

reported at 10.2 % (v/v) with an average of 214.7 g L^{-1} residual sugar (Nurgel *et al.*, 2004). Stress induced changes in yeast metabolism can also lead to the production of metabolites that ultimately affect wine quality. Of these metabolites, there are concerns regarding the high levels of acetic acid in Icewine produced by wine yeast as a metabolic response to the high osmotic conditions present during Icewine juice fermentation. Acetic acid at high concentrations can be considered an undesirable organoleptic fault in Icewine as it imparts a vinegar aroma to wine when present above its sensory detection threshold. It is also often associated with wine spoilage.

A recent study by Cliff and Pickering (2006) indicates that acetic acid is only detected in Icewine once it reaches a concentration above 3.185 g L^{-1}, whereas the allowable VQA limit of 2.1 g L^{-1} acetic acid is well below this detection threshold. Furthermore, the average level of acetic acid reported in a survey of 50 Canadian Icewines was only 1.3 g L^{-1} with a range of 0.5 g L^{-1} to 2.3 g L^{-1}, with some wines exceeding the allowable limit (Nurgel *et al.*, 2004). So, there is a concern with understanding and controlling volatile acidity during Icewine fermentations in terms of overall wine quality. Since acetic acid can react with ethanol to form ethyl acetate, which is also considered an oxidation fault described as smelling like nail polish remover, high levels of acetic acid may lead to high levels of ethyl acetate. In fact, in the same survey of 50 commercial Icewines, ethyl acetate levels were reported on average to be 0.24 g L^{-1} (Nurgel *et al.*, 2004), which is very close to (and exceeds) the reported sensory detection threshold for ethyl acetate in Icewine at 0.198 g L^{-1} (Cliff and Pickering, 2006). In addition to concerns of high acetic acid concentrations leading to high ethyl acetate levels, it has also been reported that wines made from Icewine juice that is very

concentrated (above 42°Brix) may lead to levels of acetic acid that surpass allowable limits (Pigeau *et al.*, 2007). Since Icewine quality is key to its success in the global marketplace, the fundamental goal of this research is to further understand how wine yeast respond and adapt to prolonged hyperosmotic stress during Icewine fermentation and how these responses may affect Icewine quality.

2.2. Responding to hyperosmotic stress and osmoadaptation in *S. cerevisiae*

2.2.1. Hyperosmotic stress: cellular effects, consequences and responses

Yeast live in a continually changing environment where the extracellular water activity can fluctuate considerably over the lifetime of the cell. When yeast cells are exposed to hyperosmotic conditions, the immediate effect is the loss of cytosolic water by osmosis driven by the difference in osmotic pressure across the cell membrane. Loss of cytosolic water ultimately leads to changes in cell volume and shape, loss of turgor pressure, compression of the cytoplasm, oxidative damage and changes in metabolism (Blomberg and Adler, 1992; Varela and Mager, 1996; Billi and Potts, 2002). Thus, maintaining intracellular water homeostasis is fundamental for survival.

Osmoadaptation is a cellular survival response used by yeast to adjust to high external osmolarity by re-establishing the osmotic gradient across the plasma membrane. This response is associated with the increased intracellular accumulation of compatible osmolytes to counteract the efflux of water, thereby restoring cell volume and turgor pressure. Glycerol is the main internal osmolyte produced by *S. cerevisiae* under hyperosmotic conditions (reviewed in Nevoigt and Stahl, 1997).

Adaptation to increased osmolarity is a dynamic process dependent on sensing osmotic changes and relaying these changes to initiate appropriate cellular responses

aimed at maintaining normal biological activities in the cell. The principal cellular response in yeast involved in adaptation to hyperosmotic stress is the high osmolarity glycerol (HOG) response (Brewster *et al.*, 1993). Yeast are also capable of invoking a general stress response which also has an important role in cell survival under a range of stress conditions, including exposure to hyperosmolarity (reviewed in Hohmann, 2002). However, the length of the osmoadaptive phase can vary and is dependent on the type and concentration of stress-inducing solute, yeast strain and duration of exposure to osmotic stress (Blomberg *et al.*, 1988). During Icewine juice fermentation, the stresses placed on wine yeast are persistent and continually changing.

2.2.2. Signaling pathways involved in the hyperosmotic stress response

2.2.2.1. The HOG response

Adaptation to hyperosmotic stress in *S. cerevisiae* is controlled, in part, by an osmosensing and signaling system called the HOG (High Osmolarity Glycerol) MAPK (Mitogen-activated protein kinase) pathway. Evidence of a central MAPK-dependent phosphorelay transduction pathway in *S. cerevisiae*, regulating osmotically induced physiological changes in yeast subjected to hyperosmotic stress, was provided by Brewster *et al.* (1993) using osmosensitive mutants. MAPK signal transduction pathways are highly conserved among eukaryotes and participate in a number of central cellular processes including growth, morphogenesis and stress response. In addition to the HOG pathway, there are five other distinct MAPK pathways in *S. cerevisiae*, involved in sporulation, cell integrity, vegetative growth, pseudohyphal development and mating (reviewed in Hohmann, 2002).

The signaling mechanism of the HOG pathway is based on the sequential phosphorylation of three levels of protein kinases: a MAP kinase kinase kinase (MAPKKK), a MAP kinase kinase (MAPKK) and a MAP kinase (MAPK). In general, the MAPKKK activates the MAPKK via phosphorylation of N-terminal serine and threonine residues residing in the kinase domain. The MAPKK subsequently phosphorylates a threonine or serine residue and a tyrosine residue located within the activation loop of the MAPK catalytic domain. Dual phosphorylation of the threonine/serine and tyrosine residues is required for MAPK activation and subsequent translocation into the nucleus where it then activates downstream transcriptional regulatory proteins (Figure 2.1) (reviewed in Hohmann, 2002). These kinases appear to be activated via osmosensors where changes in extracellular osmolarity generate an internal signal that is transmitted to the HOG MAP kinase cascade. In *S. cerevisiae*, two distinct transmembrane protein osmosensors, Sln1p (Ostrander and Gorman, 1999) and Sho1p (Reiser *et al.*, 2000), have been implicated in sensing osmotic stress. Mutations in the genes encoding for Sln1p (Maeda *et al.*, 1994) and Sho1p (Posas and Saito 1997) affect the activity of the HOG pathway thereby placing the osmosensors upstream of all other HOG pathway components.

Although the mechanism of sensing extracellular osmolarity has not been fully elucidated, observations by Tamás *et al.* (2000) suggest that the signal perceived by the osmosensors results from a change in membrane tension due to turgor stress imposed on the cell rather than a change in extracellular water activity. In yeast, both branches of the HOG pathway were reported to be differentially activated in response to different degrees of salt-induced hyperosmotic stress (O'Rourke and Herskowitz, 2004). Following

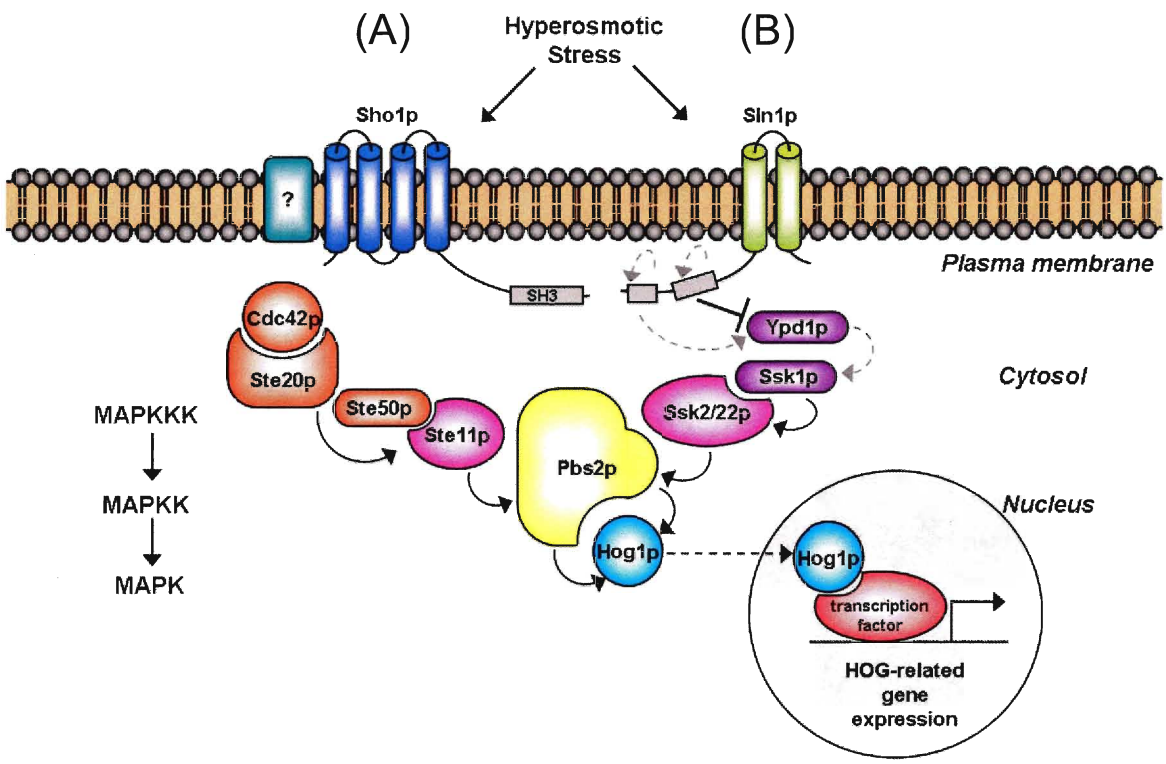

Figure 2.1: The HOG pathway in *S. cerevisiae*. The major components of the high osmolarity glycerol (HOG) pathway including the Sho1p (A) and Sln1p (B) branches are outlined. Solid black arrows indicate associative and phosphorylation events between protein complexes and MAP kinases required for signal transmission under hyperosmotic conditions. Dashed grey arrows indicate phosphotransfer events under normal growth conditions. Adapted from Hohmann (2002) and O'Rourke *et al*. (2002).

transcriptional analysis using microarray technology, O'Rourke and Herskowitz (2004) found that genes associated with the Sln1-branch, but not Sho1p, were induced in yeast exposed to low osmolarity (up to 0.125 M KCl) whereas transcription of genes associated with both branches of the pathways were induced under moderately high hyperosmotic stress (>0.5 M KCl). At higher osmolarities, genes involved in both branches of the HOG pathway as well as the general stress response pathway were involved in the response to hyperosmotic stress.

Central to the HOG pathway are three MAPKKK (Ssk2p, Ssk22p and Ste11p), a MAPKK (Pbs2p) and a MAPK (Hog1p) (reviewed in Hohmann, 2002). The HOG pathway is divided into two independently operating branches, the Sho1p and Sln1p branches, upstream of both Pbs2p and Hog1p (Figure 2.1). Blocking either branch of the pathway still permits phosphorylation and activation of Hog1p upon osmotic shock (Maeda *et al.*, 1995). However, osmosensors Sho1p and Sln1p have very different functional domains and therefore activate different downstream effector proteins within the HOG pathway.

Sho1p contains four transmembrane domains and a cytosolic C-terminal SH3 linker domain (Figure 2.1) (Posas and Saito, 1997). Results from a study by Raitt *et al.* (2000) suggest that Sho1p might not sense osmolarity changes directly, but may instead provide a membrane-bound docking site for Pbs2p via the SH3 linker domain, indicating the possible involvement of a yet unidentified sensor protein or an alternate mechanism for signal transmission through this branch of the HOG pathway. HOG pathway activation by the Sho1p branch relies on the formation of a transient multiprotein osmosignaling complex at the plasma membrane following osmotic shock consisting of

Sho1p, Cdc42p (a GTPase), Ste20p (p21-activated kinase), Ste50p (a SAM domain containing protein), Ste11p (MAPKKK) and Pbs2p (MAPKK) (Reiser *et al.*, 2000; reviewed in O'Rourke *et al.* 2002). The Sho1p branch of the osmosensing HOG pathway and the pseudohyphal development pathway share several MAP kinase components including Sho1p itself (reviewed in Hohmann, 2002). Cdc42p plays a potential role in recruiting the Pbs2p complex to the plasma membrane, as the localization and the physical interaction of Pbs2p with the Sho1p SH3 domain is required for activation of this HOG pathway branch (Reiser *et al.*, 2000). Within the complex, Ste11p is activated by Ste20p (Gustin *et al.*, 1998). Osmostress induced activation of Ste11p is dependent on its association with a putative protein cofactor Ste50p (Posas *et al.*, 1998; Jansen *et al.*, 2001). Activated Ste11p phosphorylates Pbs2p and in turn, Pbs2p phosphorylates cytosolic Hog1p (MAPK) (Posas and Saito, 1998). Phosphorylated Hog1p then translocates into the nucleus (Reiser *et al.*, 1999; Ferrigno *et al.*, 1998). Once in the nucleus, Hog1p regulates the expression of several HOG pathway targeted osmoresponsive genes mediated by its association with several transcriptional regulators.

The Sln1p branch functions as a negative regulator of the HOG pathway under normal growth conditions. Sln1p is comprised of two N-terminal transmembrane domains separated by a loop, an intracellular linker region, a histidine kinase domain and a receiver domain (Figure 2.1) (Ota and Varshavsky, 1993). The transmembrane domains of Sln1p likely function as osmosensors (Ostrander and Gorman, 1999), while the histidine kinase and receiver domains together form a two-component system responsible for relaying signals to two other downstream effector proteins Ypd1p and Ssk1p (West and Stock, 2001). Sln1p-Ypd1p-Ssk1p forms a compact phosphorelay system that

regulates the HOG pathway (Posas *et al.*, 1996). Under normal growth conditions, Sln1p is constitutively activated by autophosphorylation of an internal histidine. The phosphate is intramolecularly transferred to an aspartic acid residue within the receiver domain and in turn, the phosphate is then passed to a histidine residue in Ypd1p. The response regulator, Ssk1p, is the final phosphoacceptor protein in this system. Subsequent transfer of the phosphate group from Ypd1p to Ssk1p deactivates Ssk1p (Posas *et al.*, 1996) consequently preventing activation of the downstream MAPKKs Ssk2p and Ssk22p within the Sln1 branch of the HOG pathway (Posas *et al.*, 1998). Deletion of *SLN1* and/or *YPD1* is lethal due to HOG pathway overactivation (Maeda *et al.*, 1994). Exposure to hyperosmotic stress inhibits the histidine kinase activity of Sln1p thereby disrupting the phosphorelay cascade and thus enabling the binding of dephosphorylated Ssk1p to Ssk2p/Ssk22p (Maeda *et al.*, 1995). Association with dephosphorylated Ssk1p triggers autophosphorylation of Ssk2p/Ssk22p (Posas and Saito, 1998), followed by phosphorylation of Pbs2p and ultimately the activation of Hog1p.

Under hyperosmotic stress, the Sho1p and Sln1p branches of the HOG pathway merge and the activated MAPKK Pbs2p that is shared between branches phosphorylates the cytosolic MAPK Hog1p (Posas and Saito, 1998). Phosphorylated Hog1p then translocates into the nucleus (Figure 2.1) (Ferrigno *et al.*, 1998; Reiser *et al.*, 1999). Once in the nucleus, Hog1p regulates the expression of several osmoresponsive genes mediated by its association with several transcription factors like Hot1p. In turn, the expression of a small subset of HOG pathway targeted genes, including the upregulation of genes encoding for key enzymes involved in glycerol synthesis (*GPD1* and *GPP2*) is affected (Rep *et al.*, 1999; Rep *et al.*, 2000). Yeast cells compensate for the loss of cytosolic water

by accumulating an internal osmolyte, glycerol, through increased biosynthesis when placed under high extracellular osmolarity conditions (Blomberg and Adler, 1989). Mutations in or deletions of Pbs2p or Hog1p cause osmosensitivity in yeast, in addition to reducing intracellular glycerol accumulation (Brewster *et al.*, 1993).

Upon adaptation to hyperosmotic stress, three serine/threonine phosphatases (Ptc1p, Ptc2p and Ptc3p) and two tyrosine phosphatases (Ptp2p and Ptp3p) are upregulated. These phosphatases function to dephosphorylate Hog1p and/or the other MAP kinases in order to deactivate the HOG pathway (Warmka *et al.*, 2001; Jacoby *et al.*, 1997; Wurgler-Murphy *et al.*, 1997). HOG pathway deactivation is necessary once yeast cells return to normal growth conditions since constitutive Hog1p activation in yeast is lethal (Maeda *et al.*, 1993; Jacoby *et al.*, 1997).

2.2.2.2. The general stress response

Yeast can invoke an additional cellular response upon exposure to a broad spectrum of stress conditions including heat shock, nutrient starvation together with oxidative and osmotic stress (reviewed in Hohmann, 2002). Similar to the HOG response, the general stress response ultimately affects the expression of a number of genes which have key roles in protecting yeast cells exposed to multiple stress conditions. Of these general stress-responsive genes, a considerable subset contain stress response elements (STREs) within their promoter regions and their expression is controlled by the transcription factors Msn2p and Msn4p (Martinez-Pastor *et al.*, 1996). Both Msn2p and Msn4p contain DNA-binding zinc finger domains predicted to interact with the core CCCCT sequence within the STRE promoter regions (Martinez-Pastor *et al.*, 1996). Control of STRE targeted gene expression is regulated by cellular localization of

Msn2p/Msn4p through protein kinase A (PKA) activity (Görner *et al.*, 1998). Exposure to various stress conditions like high extracellular osmolarity results in the nuclear translocation of Msn2p and Msn4p, causing the upregulation of stress responsive genes, whereas PKA activity mediates the translocation of Msn2p/Msn4p from the nucleus back to the cytosol (Görner *et al.*, 1998). There is evidence supporting an overlap between the HOG pathway and the general stress response when yeast are subjected to hyperosmotic stress (Schüller *et al.*, 1994; Rep *et al.*, 2000; O'Rourke and Herskowitz, 2004). The simultaneous transcriptional activation of some osmoresponsive genes by both HOG-specific stress signaling and STRE-dependent promoter control may be necessary to ensure an effective stress response.

2.2.2.3. Immediate response to hyperosmotic stress

It has been previously shown that Icewine juice contains concentrated solutes in addition to sugar that increase stress on wine yeast fermenting this juice (Pigeau and Inglis, 2005). Although the concentration of salt present in Icewine juice is largely unknown and has not been measured to date, the presence of salts in this juice could potentially intensify the overall hyperosmotic stress wine yeast face during Icewine fermentation, inducing not only the HOG pathway and the general stress response but also an immediate response.

The uptake and export of ions play an important role during osmoadaptation in essentially all types of organisms (reviewed in Hohmann, 2002). Yeast cells specifically control intracellular sodium and potassium ion homeostasis by actively exporting Na^+ and accumulating K^+ (reviewed in Serrano and Rodriguez-Navarro, 2001; reviewed in Hohmann, 2002). Na^+ and K^+ transport is mediated either by ATP-dependent active

transport or by H^+ antiport systems, which are dependant upon the proton gradients established and maintained by ATPases across both the cytoplasmic and vacuolar membranes (reviewed in Serrano and Rodriguez-Navarro, 2001; reviewed in Hohmann, 2002). Although these mechanisms are particularly important for maintaining ion homeostasis in yeast exposed to salt stress, several ion transporters also have roles in osmotic adaptation and/or are regulated by osmotic stress (reviewed in Hohmann, 2002). Nha1p is a yeast plasma membrane K^+/H^+ and Na^+/H^+ antiporter that increases Na^+ efflux in yeast cells exposed to sodium chloride stress (Proft and Struhl, 2004) and decreases K^+ efflux from cells subjected to sorbitol stress (Kinclova-Zimmermannova and Sychrova, 2006). Maintenance of intracellular ion balance via the expression of *NHA1* may have an integral role in facilitating a yeast cell's ability to mount an immediate response to hyperosmotic stress as activation of *NHA1* may be HOG-dependent (Proft and Struhl, 2004; Kinclova-Zimmermannova and Sychrova, 2006).

2.2.3. Glycerol metabolism in *S. cerevisiae*

Glycerol is a major by-product of yeast alcoholic fermentation, in addition to serving as an internal osmolyte during hyperosmotic stress. During typical alcoholic fermentation, approximately 5% of sugars present in grape juice are not completely converted to ethanol and carbon dioxide, but are diverted towards glycerol biosynthesis (reviewed in Scanes *et al.*, 1998). During table wine fermentations, glycerol biosynthesis in yeast primarily serves to maintain balance between redox equivalents by reoxidizing NADH produced during biomass formation (van Dijken and Scheffers, 1986). Glycerol contributes to the sensory qualities of table wine including taste, viscosity and mouthfeel (reviewed in Scanes *et al.*, 1998). The threshold for perceived sweetness and mouthfeel in

table wine due to the presence of glycerol is 5.2 g L^{-1} and 25.8 g L^{-1}, respectively (Noble and Bursick, 1984). A survey of Canadian Icewines reported an average glycerol concentration of 12.4 g L^{-1} (Nurgel *et al.*, 2004). The contribution of glycerol to the overall perceived sweetness and mouthfeel in Icewine at this concentration is not clear but it is part of an ongoing investigation (Nurgel and Pickering, 2005).

Three main purposes for glycerol production during wine fermentation have been established, two of which are involved in maintaining cytosolic redox balance during the early stages of fermentation and the third is in response to hyperosmotic stress. Glycerol can be synthesized by commercially available, aerobically grown lyophilized wine yeast strains when introduced to an anaerobic grape juice environment. Glycerol is chiefly produced to reestablish the balance in cytosolic redox equivalents within the nicotinamide cofactor system by oxidizing the additional NADH generated during yeast biomass accumulation under anaerobic conditions like those found during table wine fermentation (van Dijken and Scheffers, 1986). Glycerol synthesis also permits yeast to fulfill the demand for oxidized cofactor, NAD^+, in response to the build up of NADH generated in glycolysis when the enzymes associated with alcoholic fermentation that would normally oxidize NADH to NAD^+ are not present in sufficient concentrations to cope with the initial stages of sugar assimilation upon inoculation (reviewed in Bisson, 1993).

2.2.3.1. Glycerol synthesis during hyperosmotic stress

Upon exposure to hyperosmotic stress, water is recruited from the vacuole into the cytoplasm to partially compensate for the sudden loss of cytosolic water by osmosis and the subsequent increase in intracellular osmolarity (Latterich and Watson, 1993;

Mager and Siderius, 2002). This mechanism permits cell survival until yeast begin to accumulate glycerol to adjust to changes in external water activities. Studies involving laboratory yeast strains grown under salt stress have shown that glycerol functions as an internal osmolyte to counterbalance the osmotic pressure placed on cells, and to counteract water loss and help cells resume growth (Blomberg and Adler, 1989; Blomberg and Adler, 1992; Brewster *et al.*, 1993; Blomberg, 2000). Net glycerol accumulation in yeast under hyperosmotic stress may be dependent on a series of events: increased production, decreased catabolism, increased retention by the plasma membrane and/or increased uptake of extracellular glycerol (reviewed in Nevoigt and Stahl, 1997).

In *S. cerevisiae*, glycerol is synthesized from the glycolytic intermediate dihydroxyacetone phosphate (DHAP) in two enzymatic reactions. The first reaction requires the reduction of DHAP to glycerol-3-phosphate along with the simultaneous oxidization of NADH to NAD^+ (Figure 2.2). This rate-limiting step (Remize *et al.*, 2001) in glycerol synthesis is catalyzed by a NAD^+-dependent glycerol-3-phosphate dehydrogenase encoded by the highly homologous genes *GPD1* and *GPD2* (Larsson *et al.*, 1993; Eriksson *et al.*, 1995). The second reaction is completed following the dephosphorylation of glycerol-3-phosphate to glycerol by glycerol-3-phosphatases (*GPP1* and *GPP2*) (Påhlman *et al.*, 2001). This pathway appears to be the sole route identified to date for glycerol production in *S. cerevisiae*.

The genes encoding for the isoforms of glycerol-3-phosphate dehydrogenase and glycerol-3-phosphatase are differentially expressed and appear to be controlled by different physiological triggers. *GPD1* expression is upregulated upon the exposure of cells to hyperosmotic stress and is considered to be the major isoform responsible for

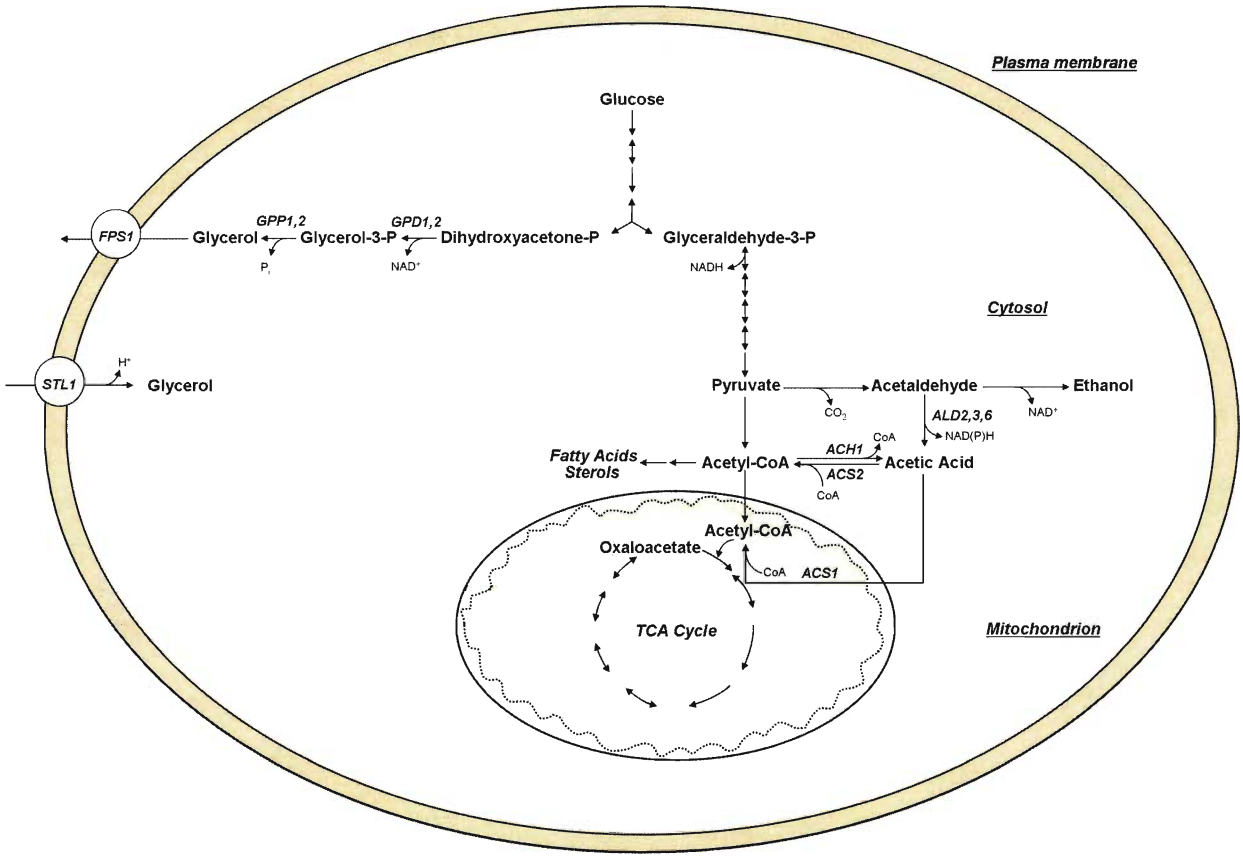

Figure 2.2: Glycerol and acetic acid metabolic pathways in *S. cerevisiae*. The pathways of glycerol and acetic acid metabolism and the genes encoding for enzymes involved in these pathways are illustrated. Metabolic intermediates and cofactors are also depicted. *GPD1,2*- Glycerol-3-phosphate dehydrogenase; *GPP1,2*- Glycerol-3-phosphatase; *FPS1*- glyceroporin channel; *STL1*- glycerol/H^+ symporter; *ALD2,3,6*- aldehyde dehydrogenase; *ACS1,2*- acetyl-CoA synthetase and *ACH1*- acetyl-CoA hydrolase.

glycerol production during the hyperosmotic response by yeast (Larsson *et al.*, 1993; Albertyn *et al.*, 1994a). In comparison, *GPD2* expression is slightly repressed under hyperosmotic conditions but is upregulated in the absence of oxygen (Ansell *et al.*, 1997). Expression of *GPD2* functions to maintain intracellular redox balance under anaerobic conditions (Eriksson *et al.*, 1995; Ansell *et al.*, 1997). The *GPD1* promoter binds Hog1p (Alepuz *et al.*, 2001), yet the HOG pathway was found to exert limited control of *GPD1* expression during table wine fermentations (Remize *et al.*, 2003). The *GPD1* promoter also contains three STREs (Eriksson *et al.*, 2000) indicating that expression is regulated by both the HOG pathway and the general stress response. In contrast, *GPD2* expression is thought to be regulated by the redox state of the cell (Ansell *et al.*, 1997).

GPP1 and *GPP2* are both induced by hyperosmotic conditions such that salt stress induced expression was found to be dependent on HOG pathway activation (Norbeck *et al.*, 1996; Rep *et al.*, 2000; Påhlman *et al.*, 2001). *GPP2* expression is more responsive in yeast exposed to saline stress (Hirayama *et al.*, 1995), whereas *GPP1* expression is found to be less responsive (Norbeck *et al.*, 1996). However, *GPP1* expression exhibits transient upregulation when yeast cells are transferred to anaerobic conditions, while *GPP2* expression remains unaffected (Påhlman *et al.*, 2001). Under hyperosmotic conditions, expression of *GPP2* is independent of the STRE binding general stress response transcription factors Msn2p and Msn4p (Rep *et al.*, 1999) and PKA activity (Norbeck and Blomberg, 2000), while *GPP1* expression is diminished in yeast strains with low PKA activity (Påhlman *et al.*, 2001).

The combination of Gpd1p-Gpp2p activity is proposed to be mainly involved in glycerol production during osmotic stress, whereas the Gpd2p-Gpp1p combination is

associated with balancing the NAD^+/NADH cofactor system under anaerobic conditions (Albertyn *et al.*, 1994b; Ansell *et al.*, 1997; Påhlman *et al.*, 2001). Wine yeast face both anaerobic and osmotic stress during fermentation and either of these factors may control the expression of *GPD* and *GPP* genes. However, the elevated production of glycerol by wine yeast during Icewine fermentation corresponds to an increase of *GPD1* expression (Pigeau and Inglis, 2005) but not of *GPD2* (Pigeau and Inglis, 2007).

Glycerol can be used as a sole carbon source under aerobic conditions. A cytosolic glycerol kinase encoded by *GUT1* (Pavlik *et al.*, 1993) phosphorylates glycerol to form glycerol-3-phosphate and in turn is oxidized to DHAP, which then enters the glycolytic pathway. This reaction is catalyzed by a mitochondrial FAD^+-dependent glycerol-3-phosphate dehydrogenase encoded by *GUT2* (Rønnow and Kielland-Brandt, 1993). Expression of both *GUT1* and *GUT2* is subject to glucose repression and does not appear to be induced by osmotic stress (reviewed in Hohmann, 2002). A decrease in glycerol catabolism in yeast under hyperosmotic stress may be necessary to maintain intracellular glycerol levels.

2.2.3.2. Glycerol retention and uptake

To ensure that the glycerol produced in *S. cerevisiae* upon exposure to hyperosmotic stress is accumulated to offset the osmotic pressure exerted on the plasma membrane, yeast must simultaneously rely on increased glycerol biosynthesis and decreased glycerol export through the plasma membrane. Of the two major glycerol transport systems currently identified in *S. cerevisiae*, one system involves a channel protein belonging to the Major Intrinsic Protein (MIP) family and is encoded by the gene *FPS1* (Van Aelst *et al.*, 1991), as illustrated in Figure 2.2.

The rate of simple diffusion of glycerol through the plasma membrane is low, however membrane permeability to glycerol is reduced even further in osmotically stressed yeast cells (Tamás *et al.*, 1999; Sutherland *et al.*, 1997). There may be a connection between the modification of the fatty acid composition of phospholipids and ergosterol levels in the lipid bilayer of the plasma membrane to reduced permeability to glycerol to regulate transmembrane flux of glycerol (reviewed in Nevoigt and Stahl, 1997; Hohmann, 2002). The main physiological role of Fps1p appears to be exporting glycerol from yeast cells upon hypoosmotic shock or a return to normal growth conditions following hyperosmotic shock, by facilitating passive transport of glycerol across the membrane down a concentration gradient (Van Aelst *et al.*, 1991; Luyten *et al.*, 1995; Sutherland *et al.*, 1997; Oliveira *et al.*, 2003). It has been suggested that Fps1p can transport glycerol in both directions across the membrane (Sutherland *et al.*, 1997; Tamás *et al.*, 1999). However, this channel rapidly closes upon exposure to hyperosmotic stress, thereby controlling the amount of glycerol retained by the cell (Támas *et al.*, 1999). Therefore, it is unlikely that Fps1p would be involved in glycerol uptake in osmotically stressed yeast cells.

It has been shown that deletion mutants lacking Fps1p retain more glycerol than their wild-type counterparts following exposure to salt stress (Luyten *et al.*, 1995). The N-terminal regulatory domain of Fps1p is responsible for controlling channel opening and closing (Támas *et al.*, 1999). Deletion of this domain results in constitutive glycerol export, thereby causing yeast cells to overproduce glycerol in order to counterbalance the loss of cytosolic glycerol (Támas *et al.*, 1999; Remize *et al.*, 2001). Regulation of Fps1p closing upon hyperosmotic stress is still unclear but may require HOG pathway activation

and/or may depend on sensing changes in cytoskeleton architecture (reviewed in Hohmann, 2002).

Osmotolerant yeasts like *Zygosaccharomyces rouxii* actively uptake glycerol against a concentration gradient and it has been suggested that a high affinity glycerol/H^+ symporter uptake system also exists in *S. cerevisiae* (van Zyl *et al.*, 1990; Lages and Lucas, 1997). Active glycerol transport was first proposed to be mediated in *S. cerevisiae* by the putative multi-membrane spanning glycerol uptake proteins Gup1p and Gup2p (Holst *et al.*, 2000). *GUP1* expression was found to be necessary for growth on nonfermentable carbon sources, specifically glycerol as the sole carbon source, while *GUP2* expression was found to be induced by salt stress (Holst *et al.*, 2000). However, a study by Oliveira and Lucas in 2004 revealed that *GUP1* and *GUP2* transcriptional activity was found to be constitutive and not affected by either glucose repression or salt stress in laboratory strains of *S. cerevisiae*. Also, glycerol uptake was also observed in Δ*gup1gup2gut2* deletion mutants grown under salt stress, suggesting the existence of another protein involved in active glycerol uptake in *S. cerevisiae* (Neves *et al.*, 2004). *STL1* was first characterized as encoding a putative sugar transporter-like protein (Nelissen *et al.*, 1997) and its expression was found to be strongly but transiently induced by salt stress and required HOG pathway activation (Rep *et al.*, 2000). *STL1* was also one of the most strongly upregulated genes in wine yeast following a two hour exposure to high sugar stress (Erasmus *et al.*, 2003). Recently, Stl1p (Figure 2.2) has been characterized as a glycerol/H^+ symporter subject to glucose repression in aerobically grown laboratory yeast strains (Ferreira *et al.*, 2005). Active glycerol uptake has not been investigated in osmotically stressed wine yeast strains in the presence of high

concentrations of fermentable sugars. It is not currently known if this is a mechanism that wine yeast utilize during Icewine juice fermentation to combat hyperosmotic stress in order to add to the cytosolic pools of biosynthesized glycerol.

2.2.4. Acetic acid metabolism in *S. cerevisiae*

Fermentation of glucose to ethanol via glycolysis and alcoholic fermentation is a redox neutral process whereby the NADH generated during glycolysis is reoxidized during alcoholic fermentation. Glycerol synthesis is not a redox neutral process so a redox imbalance in the NAD^+/NADH cofactor system is potentially set up while osmotically stressed wine yeast cells are fermenting sugar to ethanol. Yeast are unable to convert reducing equivalents between the NAD^+/NADH and $NADP^+$/NADPH cofactor systems as they lack transhydrogenase activity, so they must rely on alternate metabolic pathways to maintain intracellular redox balance between these cofactor systems (van Dijken and Scheffers, 1986). Acetic acid synthesis has been suggested as a mechanism through which yeast can metabolically reestablish cytosolic redox balance by regenerating NADH from the NAD^+ produced during glycerol biosynthesis in response to salt induced hyperosmotic stress (Blomberg and Adler, 1989; Wang *et al.*, 1998; Navarro-Avino *et al.*, 1999). This pathway involves the oxidation of acetaldehyde to acetic acid catalyzed by an aldehyde dehydrogenase (Figure 2.2).

Of the five aldehyde dehydrogenases known in *S. cerevisiae*, only three are specific to NAD^+ (*ALD2*, *3* and *4*) and may solve the redox imbalance during glycerol production. However, the $NADP^+$-dependent Ald6p was found to be the main aldehyde dehydrogenase responsible for acetic acid production in laboratory *S. cerevisiae* strains fermenting glucose media (Remize *et al.*, 1999; Eglinton *et al.*, 2002), while Ald5p was

also found to contribute to acetic acid biosynthesis during anaerobic growth on glucose (Saint-Prix *et al.*, 2004). Of these two $NADP^+$-dependent isoforms, only *ALD6* was upregulated under salt stress and its expression required HOG pathway activation (Akhtar *et al.*, 1997; Rep *et al.*, 2000). Furthermore, deletion of *ALD6* in wine yeast fermenting synthetic must containing 200 g L^{-1} of sugar, resulted in a decrease in acetic acid production and an increase in the formation of other metabolites, specifically glycerol, succinate and butanediol (Remize *et al.*, 2000). Although it is clear that Ald6p plays a role in acetic acid production during fermentation, its function, if any, in resolving redox imbalance under these hyperosmotic stress conditions where glycerol is made, is not clear due to its cofactor specificity.

Expression of the highly homologous *ALD2* and *ALD3* isoforms was thought to be both subject to osmotic stress induction and regulated by the general stress transcription factors Msn2p and Msn4p (Martinez-Pastor *et al.*, 1996), but only *ALD3* expression was observed to be responsive to salt stress in laboratory yeast strains (Norbeck and Blomberg, 2000). Ald2p activity has been associated with catalyzing the oxidation of 3-aminopropanal to form β-alanine, which is required for pantothenic acid production (White *et al.*, 2003). The contribution of aldehyde dehydrogenase activity to increased acetic acid levels produced by wine yeast strains in the presence of high concentrations of fermentable sugars during Icewine fermentation is not fully understood. In a study by Pigeau and Inglis (2005, 2007), of all the *ALD* genes, only *ALD3* has been found to be more highly expressed during Icewine fermentation in comparison to that found during a table wine fermentation and this increased expression corresponded to an increase in acetic acid in the wine. Although the cytosolic isoform *ALD6* was expressed

throughout Icewine juice fermentation, its expression was not significantly different when compared to dilute juice fermentation.

To date, it is not clear if Ald3p plays a role in the elevated acetic acid production during Icewine fermentation. Studies by Pigeau and Inglis (2005 and 2007) indicate that of all the aldehyde dehydrogenases, only *ALD3* shows an increased expression in Icewine fermentation above that found during the table wine fermentation. However, two recent studies have shown that deletion of *ALD3* from the yeast genome did not reduce acetic acid production (Cordier *et al.*, 2007; Modig *et al.*, 2007). It was also reported that overexpression of *ALD3* in a laboratory yeast strain did not significantly change the amount of acetic acid produced by cells exposed to salt stress (Modig *et al.*, 2007). It is likely that the expression of *ALD3* plays a role in maintaining redox balance and ultimately contributes to elevated acetic acid levels in Icewine (Pigeau and Inglis, 2005), but enzymatic activity of Ald3p has yet to be reported.

2.2.5. Pyruvate dehydrogenase bypass

Acetic acid is an intermediate metabolite of the pyruvate dehydrogenase (PDH) bypass in *S. cerevisiae* leading to the formation of acetyl-CoA from pyruvate (reviewed in Pronk *et al.*, 1996). In this pathway, acetic acid can be converted to acetyl-CoA by acetyl-CoA synthetase. In yeast, two genes (*ACS1* and *ACS2*) have been identified as encoding for proteins associated with acetyl-CoA synthetase activity (Figure 2.2). *ACS1* is the mitochondrial isoform required for respiratory growth on non-fermentable carbon sources and is subject to glucose repression (Kratzer and Schüller, 1995; Van den Berg *et al.*, 1996). *ACS2* is the cytosolic isoform which is constitutively transcribed and is required for growth on glucose under anaerobic conditions (Van den Berg and Steensma,

1995). Coenzyme A can also be regenerated from the hydrolysis of acetyl-CoA by a cytosolic acetyl-CoA hydrolase (*ACH1*) and is required for growth on acetic acid (Lee *et al.*, 1996). The pool of available cytosolic acetyl-CoA produced by the bypass pathway is utilized for a variety of anabolic reactions, including fatty acid and amino acid biosynthesis (reviewed in Pronk *et al.*, 1996). Akamatsu *et al.* (2000) reported that genes encoding for both acetyl-CoA synthetase isoforms (*ACS1/2*) and the acetyl-CoA hydrolase (*ACH1*) were expressed by an *S. cerevisiae* sake yeast strain fermenting sake mash. In the same study, the expression of a cytosolic NAD^+-dependent aldehyde dehydrogenase encoded by either *ALD2* or *ALD3* was also observed. However, the authors were unable to design probes specific for these highly homologous isoforms to make a distinction between *ALD2* and *ALD3* expression during sake fermentation. Akamatsu *et al.* (2000) also reported that the overexpression of *ACS2*, but not *ACS1*, resulted in a four-fold reduction in acetic acid production by yeast during small-scale sake fermentations. So, the results from this study suggest that there may be a connection between aldehyde dehydrogenase and acetyl-CoA synthetase activity on acetic acid production by yeast during fermentation. However, expression of *ACS1/2* and *ACH1* during Icewine juice fermentation has not been investigated to date. Acetic acid metabolism in yeast during fermentation is currently not fully understood, but expression of the genes involved in its synthesis along with its degradation may overall contribute to the acetic acid levels produced by wine yeast as they adapt to prolonged exposure to hyperosmotic stress during the fermentation of Icewine juice.

2.3. GENE EXPRESSION PROFILING IN *S. CEREVISIAE* DURING FERMENTATION

Yeast are subjected to continuous fluctuations in their environment and cells must cope with a variety of stress conditions that can eventually affect cell growth and viability. Survival is dependent on rapid adaptation to extracellular stresses and therefore requires substantial genome-wide changes in gene expression to maintain cell integrity and metabolic activity. Under oenological conditions, wine yeast cells are exposed to multiple and concurrent stress conditions during the fermentation of grape juice. Yeast are predominantly challenged with hyperosmotic stress due to high starting sugar concentrations upon inoculation. As the fermentation process proceeds, yeast must contend with ethanol stress and variations in pH, in addition to nutrient depletion and starvation. The overall change in gene expression in conjunction with the corresponding changes in metabolic activity as they respond and adapt to stress during fermentation can lead to the production of compounds that contribute to the sensory properties of the wine. Studying the initial response of wine yeast to a fermentation condition would not take into account these changes in the environment and the impact on gene expression and metabolism.

Commercial *S. cerevisiae* strains currently used for winemaking are closely related to laboratory yeast strains but display unique physiological characteristics allowing them to be more suitable for wine fermentation. The majority of laboratory yeast strains are either haploid or diploid. Wine yeast strains are commonly diploid, aneuploid and/or polyploid and the genome may contain several chromosomal rearrangements (Bidenne *et al.* 1992; reviewed in Pretorius, 2000). An increase in the expression of genes essential for fermentation through an increase in gene copy number or by other genomic reorganizations may play a role in the metabolic properties of wine

yeasts, such as fermentation efficiency, as well as ethanol and osmotic tolerance (reviewed in Pretorius, 2000). There is evidence that the differences in metabolic activity between laboratory and wine yeast strains under fermentative conditions may influence the metabolites produced (Remize *et al.*, 1999).

Genomic expression profiling using microarray technology can uncover the differences in gene expression patterns in yeast under a number of growth and stress conditions. DNA microarrays can measure the relative transcriptional abundance in every gene in the yeast genome. Several microarray experiments have focused on the initial hyperosmotic stress response of laboratory strains exposed to salt stress and will be further discussed in Section 2.3.1. Genome-wide changes in gene expression associated with the adapted stress response to prolonged exposure to sugar stress during Icewine fermentation and its effect on metabolic activity in yeast is yet unclear.

2.3.1. Gene expression of laboratory yeast strains under salt stress

The genome of *S. cerevisiae* was the first eukaryotic genome to be fully sequenced. The earliest array experiments were performed using this organism, and characterized the genes differentially expressed when laboratory yeast strains were grown under differing nutrient conditions associated with carbon source limitation or the diauxic shift (Wodicka *et al.*, 1997; DeRisi *et al.*, 1997; ter Linde *et al.*, 1999). A number of studies have used either salt or sorbitol to determine the changes in gene expression during the hyperosmotic stress response (Posas *et al.*, 2000; Rep *et al.*, 2000; Yale and Bohnert, 2001, Causton *et al.*, 2001). When yeast cells were subjected to a 30-minute exposure to either salt or sorbitol stress, 5% of the yeast genome (286 genes) was found to be induced under hyperosmotic stress, but the expression of only a few genes was

observed to be solute specific. The expression of 10 genes including *ALD3* was upregulated more strongly by salt stress than by sorbitol. In contrast, 26 genes were more strongly upregulated by sorbitol, including *GPD1*, *STL1* and *ALD6* (Rep *et al.*, 2000).

In addition to the number and degree of differential gene expression changes upon exposure to high osmotic stress, the timing of each response can also be affected by the amount of stress. Posas *et al.* (2000) showed the transcriptional response of yeast exposed to salt stress was time and concentration dependent. When placed under a mild (0.4 M) and brief (10 minute) osmotic shock, yeast cells displayed a rapid but transient transcriptional response where approximately 21% of the yeast genome was upregulated at least three-fold. The number of induced genes decreased ten-fold after 20 minutes. However, a higher sodium chloride concentration (0.8 M) resulted in a delayed response, as the number of genes induced after 10 minutes increased two-fold after 20 minutes. In a similar study, Yale and Bohnert (2001) exposed yeast to 1 M sodium chloride for 10, 30 and 90 minutes. It was observed that the changes in transcript abundance greater than two-fold corresponded to an increase in the number of salt-induced genes expressed over time. Genes associated with the initial osmotic stress response after 10 minutes were connected to nucleotide metabolism. The pattern of gene expression after 90 minutes of adaptation to salt stress changed, as the majority of genes induced were associated with energy generation, nitrogen metabolism, fatty acid biosynthesis and the stress response.

Microarray analysis can also illustrate how gene expression patterns can overlap in response to different stresses. Causton *et al.* (2001) performed a time-course expression profile of laboratory yeast strain under multiple conditions including: heat shock, acid and alkali, oxidative, carbon limitation and osmotic stress. Of the 66% of

genes within the yeast genome differentially expressed between the various stresses, most exhibited similar expression patterns over time. The genes significantly upregulated under most environmental stress conditions were related to carbohydrate metabolism, energy generation and cell stress response. Conversely, genes showing a downregulated response were associated with amino acid metabolism, cell wall maintenance and protein synthesis. However, a small subset 370 of genes was uniquely specific for a given environmental stress.

2.3.2. Gene expression profiling in wine yeast

A number of studies have focused exclusively on the genome-wide transcriptional differences between wine yeast strains fermenting synthetic must simulating table wine conditions (Cavalieri *et al.*, 2000; Hauser *et al.*, 2001) or the differences derived when wine yeast are placed under differing nitrogen conditions during fermentation (Backhus *et al.*, 2001; Marks *et al.*, 2003). A comparison of two wine yeast strains revealed significant differences in gene expression as the cells entered early stationary phase during the fermentation of synthetic must (Zuzuarregui *et al.*, 2006). The expression of over 2000 genes was significantly different between strains. Of those genes, 423 showed at least a two-fold difference in mRNA abundance. These differences were primarily related to genes involved in carbohydrate and nitrogen metabolism, in addition to fatty acid and ergosterol synthesis.

In 2003, Rossignol *et al.* profiled the dynamic gene expression changes of a commercially available wine yeast strain throughout the fermentation of synthetic must as cells adapted to changing nutrient and environmental conditions from early exponential to late stationary phase of growth. The greatest number of genes induced or

repressed in cells occurred upon entry into stationary phase, where the expression of over 1000 genes was significantly different when compared to that at the start of the fermentation. The transcriptional response observed corresponded to the changes in nutrient availability, osmotic and ethanol stress.

Erasmus *et al.* (2003) conducted one of the first transcriptional comparisons involving a wine yeast strain of S. *cerevisiae* exposed to high sugar stress. The transcription of 589 genes changed more than two-fold when yeast were exposed for two hours to Riesling grape juice chaptalized with equal amounts of glucose and fructose to a final concentration of 40% (w/v). However, only the initial response to sugar stress was monitored and this response may not relate directly to the metabolic responses that alter wine quality as the yeast continued to ferment for an additional 400 to 500 hours (Kontkanen *et al.*, 2004; Pigeau and Inglis, 2005). One should also note that although Erasmus *et al.* were trying to mimic the composition of Icewine juice in their study, the growth media used did not accurately reflect the high levels of the other naturally concentrated soluble solids in Icewine juice, such as organic acids and salts, which place commercial wine yeast under additional stress (Pigeau and Inglis, 2005). The response of wine yeast as they adapt to prolonged exposure to high osmotic stress throughout Icewine juice fermentation is still unclear and therefore needs to be addressed.

With the use of microarray analysis, our goal in this project was to identify metabolic pathways more or less active during Icewine fermentation, and how these related to the use of nutrients during the fermentation and the production of yeast metabolites involved in redox balance. In addition to more fully understanding acetic

acid and glycerol metabolism under Icewine conditions, overall sugar and nitrogen utilization could be investigated.

2.4. YEAST SUGAR AND NITROGEN METABOLISM

2.4.1. Sugar Utilization

The conversion of grape juice sugars (glucose and fructose) by *S. cerevisiae* to ethanol is of vital importance to wine production (Bisson, 1993). Glucose and fructose are the primary fermentable sugars in grape juice and they are usually present in equal amounts. Under anaerobic conditions, they are cofermented to ethanol and carbon dioxide by *S. cerevisiae* (Fleet and Heard, 1993). The metabolic intermediates of glycolysis and alcoholic fermentation, along with the genes encoding for enzymes associated with these pathways, are depicted in Figure 2.3. Although fructose is used concurrently with glucose during table wine fermentation, *S. cerevisiae* displays a preference for glucose as a carbon source, such that glucose is typically depleted from the juice first, giving rise to a difference between the amount of glucose and fructose consumed during fermentation (Berthels *et al.*, 2004). Previous studies have shown that yeast fermenting Icewine juice only utilize half of the available fermentable sugars present in the juice and are glucophilic (Kontkanen *et al.*, 2004; Pigeau and Inglis, 2005).

In yeast, transporting sugar across the plasma membrane has been proposed as a rate-limiting step of glycolysis by influencing carbon flux through the glycolytic pathway (reviewed in Kruckeberg and Dickinson, 2004). At present, 20 different genes encoding for hexose transport-related proteins have been identified in *S. cerevisiae* (Wieczorke *et al.*, 1999). Expression of a small number of these transporters has been implicated in playing different roles in sugar uptake during wine fermentation (Luyten *et al.*, 2002).

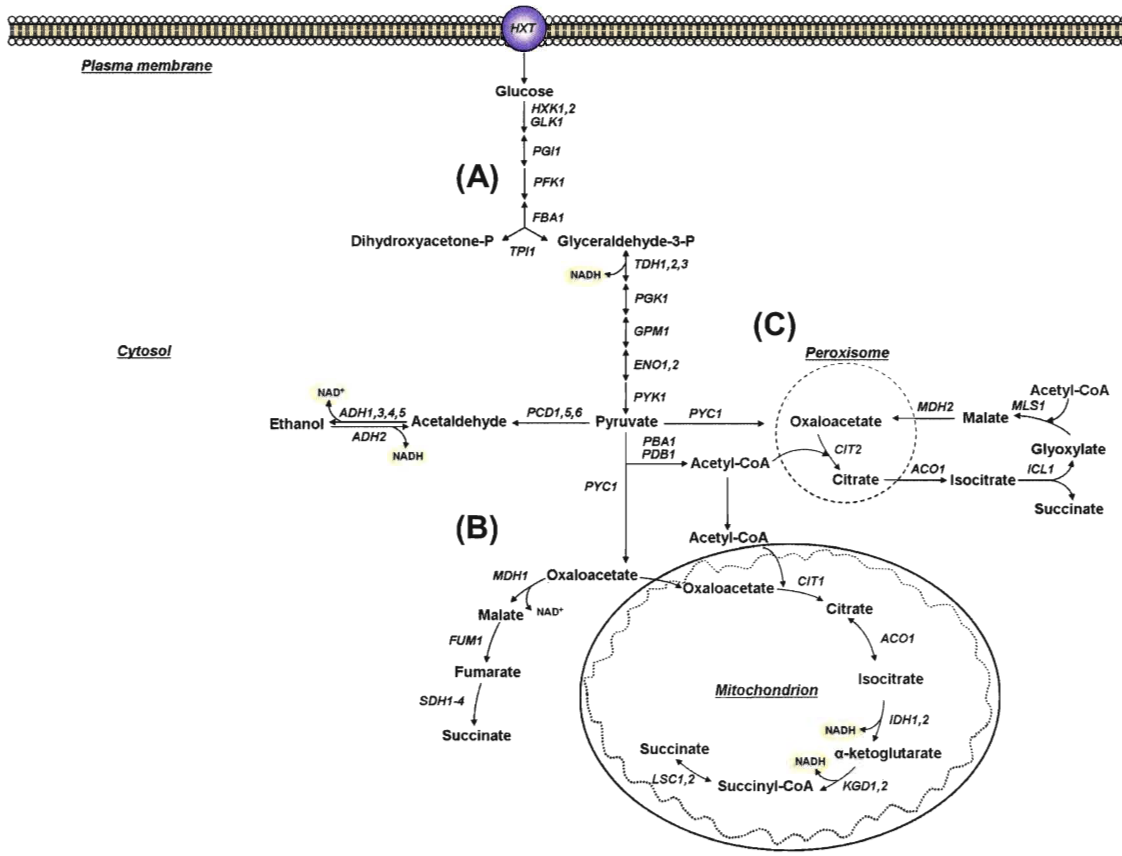

Figure 2.3: Pathways associated with carbohydrate metabolism in *S. cerevisiae*. Illustrated are the metabolic intermediates and the genes associated with (A) glycolysis and alcoholic fermentation, (B) the oxidative and reductive pathways of the tricarboxylic acid (TCA) cycle and (C) the glyoxylate cycle.

There are 18 genes that encode for sugar transporters (*HXT1-17* and *GAL2*) (reviewed in Özcan and Johnston, 1999) and there are two glucose sensors (*SNF3* and *RGT2*) with putative sugar transporter activities (reviewed in Kruckeberg and Dickinson, 2004). Under laboratory conditions, *HXT1-4*, *HXT6* and *HXT7* function as major hexose transporters and deletion of *HXT1-7* abolishes sugar transport altogether in glucose media grown yeast (Reifenberger *et al.*, 1997). Expression of the *HXT* gene family is differentially regulated by the availability of extracellular sugar and all *HXT* gene products have different sugar substrate specificities and affinities. *HXT1* and *HXT3* encode for low affinity transporters expressed in response to glucose levels in excess of 4% (w/v) and were found to play a predominant role in sugar transport in wine yeast fermenting synthetic must (Özcan and Johnston, 1999; Luyten *et al.*, 2002; Perez *et al.*, 2005). *HXT2* and *HXT4* encode for transporters with moderate to low affinity for hexoses. *HXT6* and *HXT7* are associated with high affinity sugar transport in cells under glucose-limited conditions and are repressed by high levels of glucose (Özcan and Johnston, 1999; reviewed in Kruckeberg and Dickinson, 2004). The remaining *HXT* genes (*HXT8-17*) encode for proteins closely related to hexose transporters but it is unclear if they mediate glucose transport, since they are weakly expressed in yeast grown in the presence of differing glucose levels (reviewed in Özcan and Johnston, 1999).

Following transport into the cell, hexoses are phosphorylated by hexokinases upon entry into the glycolytic pathway. *HXK2* is the primary glucose phosphorylating enzyme in yeast growing in conditions of abundant glucose, while the expression of *HXK1* and *GLK1* is required during glucose-limited conditions and is repressed by high glucose conditions (Herrero *et al.*, 1995; Rodriguez *et al.*, 2001). In addition to catalyzing

the first enzymatic reaction of glycolysis, the hexokinases (*HXK1* and *HXK2*) and glucokinase (*GLK1*) may also have key roles in glucose transport in yeast, such that glucose phosphorylation may be required for high affinity glucose uptake (Bisson and Fraenkel, 1983; Bisson and Fraenkel, 1984). *HXK1* and *GLK1* are also responsive to a number of stresses (Gasch *et al.*, 2000). The expression of both genes was induced by salt stress (Posas *et al.*, 2000; Rep *et al.*, 2000; Yale and Bohnert, 2001) and by high sugar stresses (Erasmus *et al.*, 2003). The ability of yeast to ferment hexose sugars is essential for growth and survival under oenological conditions and requires the coupling of glycolysis to alcoholic fermentation to create an energy generating but redox neutral system in the absence of oxygen (van Dijken and Scheffers, 1986).

Pyruvate decarboxylase (*PDC*) and alcohol dehydrogenase (*ADH*) are the key enzymes of alcoholic fermentation. Of the three *PDC* isoforms, *PDC1* is strongly expressed in actively fermenting cells, while conversely, expression of *PDC5* in these same cells cannot be detected (Flikweert *et al.*, 1996; Hohmann and Cederberg, 1990). It has been previously reported that the expression of the minor isoform (*PDC6*) was not involved in glucose fermentation (Hohmann, 1991). However, *PDC6* was strongly upregulated in wine yeast two hours after exposure to high sugar stress but was unaffected by salt stress (Erasmus *et al.*, 2003; Rep *et al.*, 2000). Of the alcohol dehydrogenase isoforms, *ADH1* expression is upregulated in the presence of glucose and is the major cytosolic isoform involved in glucose fermentation (Denis *et al.*, 1983). *ADH2* expression is repressed by glucose and is required for growth on ethanol, while the participation of the other three isoforms (*ADH3-5*) during fermentation has not been fully elucidated (reviewed in Kruckeberg and Dickinson, 2004).

In glycolysis, there is a net production of two ATP molecules by substrate-level phosphorylation and two NADH molecules. Alcoholic fermentation involves the decarboxylation of pyruvate produced during glycolysis to acetaldehyde, which in turn is then reduced to ethanol thereby regenerating NAD^+. Under aerobic conditions, the pyruvate generated via glycolysis can enter the mitochondria and be converted to oxaloacetate and/or acetyl-CoA, which can enter the tricarboxylic acid cycle (TCA). Alternatively, pyruvate can enter the glyoxylate cycle (reviewed in Krukeberg and Dickinson, 2004). In the presence of fermentable sugars, yeast cells downregulate the expression of genes involved in mitochondrial functions, including respiration and the metabolism of alternate carbon sources such as ethanol and acetate through carbon catabolite repression (Gancedo, 1998).

In *S. cerevisiae*, the tricarboxylic acid (TCA) cycle plays a central role in oxidative growth to provide reducing equivalents used by the mitochondrial respiratory chain to produce ATP (van Dijken and Scheffers, 1986). Under anaerobic conditions, the TCA cycle has been proposed to operate in a noncyclic manner and can be divided into two distinct pathways (Figure 2.3): a cytosolic reductive pathway from oxaloacetate resulting in the formation of NAD^+ or FAD and a mitochondrial oxidative pathway starting from α-ketoglutarate but resulting in the production of NADH (Radler, 1993; Camarasa *et al.*, 2003). It is not known if these pathways operate in yeast during fermentation, especially during an Icewine fermentation, but both pathways can lead to succinate production, which is another important organic acid produced by yeast during grape juice fermentation (Radler, 1993). The glyoxylate cycle typically operates in yeast during respiratory growth, especially when glucose is exhausted and yeast begin to grow

on C-2 compounds like acetate (reviewed in Krukeberg and Dickinson, 2004). This cycle is important for the formation of four carbon metabolic intermediates that can feed into the TCA cycle (reviewed in Krukeberg and Dickinson, 2004). No studies to date have examined the expression profiles of genes associated with sugar metabolism in wine yeast fermenting Icewine juice and correlated these expression patterns to the rate of sugar utilization during fermentation.

2.4.2. Nitrogen Utilization

The metabolism of amino acids in yeast is dependent on their initial uptake from the growth medium. Paulsen *et al.* (1998) listed several genes encoding for proteins with amino acid transporting activity as part of a larger study involving the categorization of a number of putative and established transporters encoded in the yeast genome. In 1999, Regenberg *et al.* extensively investigated and subsequently described the substrate specificity of 15 identified amino acid permeases. Based on their results and those from other studies, some transporters are general, such as Gap1p and Agp1p, since they display broad substrate specificity by transporting all amino acids and other nitrogenous compounds across the yeast membrane. Some transporters are class-specific and exhibit narrower substrate specificity, for example, Bap2p and Bap3p, both of which are specific for transporting branched chain amino acids. Although class-specific amino acid transporters have a higher affinity for their preferred amino acid substrates than the general carriers, regulation of the expression of genes encoding for all amino acid transporters is dependent in part on available extracellular nitrogen sources (Regenberg *et al.*, 1999).

The availability and composition of nitrogen-containing compounds in grape juice can affect yeast metabolism during fermentation and ultimately the sensory characteristics of the final wine, by influencing the production of a number of aroma and spoilage compounds (Monteiro and Bisson, 1991a; reviewed in Boulton *et al.*, 1998). Grape juice contains a variety of nitrogenous compounds, which is dependent on grape variety and time of harvest (Kluba *et al.*, 1978). Ammonium ions and amino acids are the two main sources of yeast-assimilable nitrogen (YAN) compounds in grape juice, with ammonium ions making up a large percentage (up to 40%) of the total YAN. Proline and arginine are the most common nitrogenous compounds present in juice (35-60% of total amino acid content) (Beltran *et al.*, 2004; reviewed in Boulton *et al.*, 1998). However, yeast are not able to utilize proline during fermentation and so, it is important to exclude proline when determining YAN in juice. The other major nitrogen species found in unfermented grape juice are alanine, γ-aminobutyrate (GABA), glutamate, glutamine, serine and threonine (reviewed in Boulton *et al.*, 1998). High concentrations of GABA present in the juice may possibly be formed in grape postharvest (reviewed in Boulton *et al.*, 1998). GABA is among the major nitrogen sources present in grape juice that can be used by yeast as a nitrogen source during fermentation of grape juice (Monteiro and Bisson, 1991a). GABA is a non-protein amino acid, which plays a number of important roles in eukaryotic systems, including oxidative stress tolerance in *S. cerevisiae* (reviewed in Shelp *et al.*, 1999; Coleman *et al.*, 2001). Previous studies have shown that GABA may be used as a compatible osmolyte in plants subjected to salt stress (reviewed in Shelp *et al.*, 1999). Glutamate can be decarboxylated by a glutamate decarboxylase to synthesize GABA and in turn, GABA can be degraded to form succinate in a two step

reaction. No studies to date have reported on the utilization of various nitrogen sources like GABA during Icewine fermentation and how this may relate to reduced rates of fermentation and biomass accumulation.

S. cerevisiae is able to use different nitrogen sources for growth but shows selectivity towards preferred nitrogen sources like ammonia and glutamine by repressing the genes encoding for enzymes required for the utilization of poorer nitrogen sources like ornithine, GABA, allantoin and urea. A mechanism, referred to as nitrogen catabolite repression (NCR), is invoked (reviewed in Magasanik and Kaiser, 2002). Amino acids have three distinct fates in *S. cerevisiae*: direct incorporation within biosynthetic pathways, conversion to a related compound for subsequent biosynthesis, or degradation, releasing nitrogen either as a free ammonium ion or as bound nitrogen via a transamination reaction (reviewed in Boulton *et al.*, 1998). Past studies have established that *S. cerevisiae* shows selectivity towards the uptake and utilization of different nitrogen sources (Monteiro and Bisson, 1991a and 1991b). Compounds considered as good sources of nitrogen are the ammonium ion, glutamate and glutamine, all of which are specifically depleted from the medium first before poorer sources of nitrogen, like arginine, asparagine, aspartate, urea and GABA, are taken up (reviewed in Cooper,1982; Boulton *et al.*, 1998). Despite high concentrations of nitrogen compounds in the starting juice, yeast fermenting Icewine juice take up approximately half of the available amino acids (Kontkanen *et al.*, 2004; Pigeau and Inglis, 2005). Therefore, it is unclear if differences exist in the usage of individual amino acids by yeast during an Icewine fermentation compared to a table wine fermentation.

Previous studies by Pigeau and Inglis (2005 and 2007) showed that there were clear differences the rates of sugar consumption, nitrogen utilization, glycerol and acetic acid production by wine yeast during the first week of Icewine juice fermentation relative to a diluted Icewine juice fermentation. However, there have been no studies published to date that have compared the transcriptomic differences associated with wine yeast during Icewine fermentation compared to a table wine fermentation. To understand how and why wine yeast respond differently during Icewine fermentation, the focus of my project was to identify and compare these differences in *S. cerevisiae* using cDNA microarray technology, during the first five days of fermentation. Differences in gene expression patterns on a genomic level were correlated to yeast cell growth, sugar consumption, nitrogen usage and metabolites produced by the yeast under the two fermentation conditions.

3. MATERIALS AND METHODS

3.1. YEAST STRAINS

The commercial wine yeast strain used for fermentations, *Saccharomyces cerevisiae* K1-V1116, was provided by Lallemand Inc. (Montrèal, QC, Canada). Yeast strains used for the validation of DNA probe specificities for Northern analysis were deletion mutants (Δ*ACS1*, Δ*ACS2* and Δ*STL1*) of the parental strains of *S. cerevisiae* S228C BY4742 (MATα his3Δ1 leu2Δ0 lys2Δ0 ura3Δ0) and BY4743 (MATα his3Δ1 leu2Δ0 lys2Δ0 met15Δ0 ura3Δ0) obtained from Open Biosystems (Huntsville, AL, USA).

3.2. MEDIA

To validate the specificity of DNA probes prior to Northern analysis, parental and deletion mutant yeast strains were grown under inducing and non-inducing conditions specific for the expression of the gene under investigation. All deletion mutants were grown with 200 μg mL^{-1} Geneticin (G418) (Sigma; Oakville, ON, Canada) For *STL1* probe validation, yeast cells were grown aerobically overnight in YPD medium (1% yeast extract, 2% peptone, 2% dextrose) at 30°C with shaking at 150 rpm. Osmotic stress was induced in the cells following the addition 5 M sodium chloride to a final concentration of 0.7 M NaCl and using a 30 minute exposure time prior to RNA isolation as described by Rep *et al.* (2000). For *ACS1* probe validation, yeast cells were grown aerobically for three days in YPD medium at 30°C with shaking at 150 rpm prior to RNA isolation. For *ACS2* probe validation, yeast cells were grown anaerobically at 30°C for two days in a modified YPD medium containing 4% dextrose.

3.3. ICEWINE JUICE PREPARATION AND COMPOSITIONAL ANALYSIS

Vidal Icewine juice was kindly provided by Inniskillin Wines (Niagara-on-the-Lake, ON. Canada). The juice was filtered through a series of coarse, medium and fine pore-size pads using a Bueno Vino Mini Jet filter system (Vineco; St. Catharines, ON, Canada). The juice was then sterile-filtered through a 0.22 μm membrane cartridge filter (Millipore; Etobicoke, ON, Canada) into sterile 1L bottles. The sterile juice was stored at -40°C prior to the fermentation experiments. Two fermentation conditions were used to investigate the osmotic stress response of wine yeast using this juice. One condition required that the Icewine juice remained undiluted at 40.1°Brix prior to fermentation and the other condition required the dilution of the Icewine juice to 20.2°Brix using sterile distilled water (RiOs-16; Millipore).

The initial Icewine juice was assessed for soluble solids, titratable acidity (T.A.), pH and total nitrogen content prior to inoculation and fermentation (Table 3.1). All analyses were performed in duplicate. Soluble solids of the starting unfermented juices were determined with an ABBE bench top refractometer (American Optical). The titratable acidity of the initial juices was determined using the method outlined by Zoecklein *et al.* (1996). The pH of the initial juices was measured using a Corning pH meter (model 445) first calibrated to pH 4.0, pH 7.0 and pH 10.0. Yeast assimilable amino acid nitrogen (YAN) levels were determined using the *O*-phthaldialdehyde (NOPA) assay described by Dukes and Butzke (1998). Ammonia nitrogen in the initial juice was determined in duplicate using the ammonia enzyme assay kit from Megazyme (Bray Co., Wicklow, Ireland).

Table 3.1: Icewine juice parameters.

Parameter	Value*
Soluble solids	40.2°Brix
Reducing sugars	447.7 ± 8.5 g L^{-1}
Glucose	193.0 ± 4.6 g L^{-1}
Fructose	254.7 ± 4.1 g L^{-1}
pH	3.6 ± 0.2
Titratable acidity (TA)	6.8 ± 0.2 g L^{-1} Tartaric acid
Assimilable amino acid nitrogen	388.1 ± 5.5 mg N L^{-1}
Ammonia nitrogen	38.6 ± 3.2 mg N L^{-1}
Glycerol	1.9 ± 0.2 g L^{-1}
Acetic Acid	0.03 ± 0.00 g L^{-1}
Succinate	0.05 ± 0.01 g L^{-1}

*Represents mean values ± standard deviation of three independent replicate Icewine juice samples with tests performed in duplicate (n=6).

3.4. STARTER CULTURE PREPARATION AND INOCULATION

Starter cultures were prepared with the commercial yeast *Saccharomyces cerevisiae* K1-V1116 by using step-wise acclimation method. In a sterile 250 mL Erlenmeyer flask, 5.0 g of dehydrated yeast was rehydrated in 50 mL of sterile, 40°C distilled water for 15 min with gentle swirling every 5 min to encourage aeration. To acclimatize the yeast to the growth medium, 50 mL of sterile diluted Icewine juice diluted to 20°Brix was added aseptically to the rehydrated yeast and the starter culture was incubated at 25°C for 1 h in a water bath, swirling every 30 min. An additional 50 mL of undiluted Icewine juice was introduced to the starter culture achieving a final juice concentration of approximately 20°Brix. The starter culture was incubated at 20°C for 2 h and the culture was aerated by periodically swirling the flask every 30 min. A sample of the starter culture was examined for actively budding yeast cells under 40× magnification using a light microscope prior to inoculation. In sterile 0.5 L fermentation vessels fitted with air locks, 7.5 mL of the starter culture was used to inoculate 0.5 L each of Icewine juice (40°Brix) and diluted Icewine juice (20°Brix), reaching a final yeast inoculation rate of 0.5 g (dry weight) L^{-1}.

3.5. FERMENTATION AND METABOLITE ANALYSIS

Fermentations were carried out at 17°C and were monitored daily for the first week and then every other day thereafter for sugar consumption, biomass production and cell population. Fermentations were allowed to continue until approximately 200 g L^{-1} of sugar was consumed by the yeast. All fermentations were performed in triplicate. Yeast biomass accumulation was determined using a filter retention assay. A 5 mL sample from each fermentation condition was removed and passed through a sterile, preweighed 0.45 µm cellulose nitrate membrane filter under a vacuum. The undiluted filtrate was sterile-filtered through a 0.22µm syringe filter before being stored at -30°C until metabolite analysis was performed. Filters were washed twice with deionized water and dried at 60°C for 2 days. Filters were then reweighed and biomass was determined as the difference in mass. Total cell concentrations were determined in duplicate using a haemocytometer under 40× magnification with a light microscope. Fermentation samples were diluted with 0.1 M potassium phosphate buffer (pH 7.0) prior to counting. Reducing sugar (glucose and fructose), glycerol, acetaldehyde and acetic acid levels, in samples taken from both the starting and the fermenting juices, were determined in duplicate using enzyme assay kits from Megazyme. Succinate concentrations in the finished wines were also determined in duplicate using an enzyme kit from Megazyme. Changes in yeast assimilable amino acid nitrogen levels were followed throughout the fermentations using the NOPA assay and measurements were performed in duplicate. Ethanol levels in the final wines were determined in triplicate using a Hewlett-Packard 5890 gas chromatograph with a 30 m × 0.32 mm (5%) phenyl methyl silicone column. All samples were diluted 10-fold prior to analysis and contained 1% (v/v) n-butanol as an internal

standard. XL Stat v7.1 (Addinsoft; NY., USA) was used for data analysis. Significant differences in metabolite levels were determined using a two-tailed paired t-test.

3.6. RNA Extraction

The RNA extraction protocol used in this study was adapted from the protocol used by Pigeau and Inglis (2005). Juice sample volumes up to 50 mL were removed directly from the fermentation vessels and to the samples 0.01 mg mL^{-1} cyclohexamide was added prior to centrifugation. The cells were pelleted at 3800 *g* for 5 min at 4°C using a Sorvall RC 5C plus centrifuge (Sorvall; Newtown, CT, USA). The cells were resuspended in 10 mL of DEPC-treated distilled water and were pelleted as before. On ice, cells were resuspended in 375 µL of extraction buffer (0.1 M NaCl, 10 mM Tris-Cl (pH 8.0), 1 mM EDTA (pH 8.0) and 5% Triton X-100) and 250 µL phenol/chloroform/isoamyl alcohol (PCI). Following the of addition 300 mg of glass beads, the suspension was vortexed at 2500 rpm for 6 min to lyse the cells. After vortexing, 6 µL of 20% (w/v) SDS was added and the mixture was left to stand on ice for 1 h. The mixture was centrifuged at 16000 *g* in a Sorvall RMC-14 centrifuge for 20 min at 4°C. To precipitate the RNA, 15 µL of 5 M NaCl and 1250 µL absolute ethanol was added to the supernatant. The solution was allowed to sit at -30°C for 2 h prior to centrifugation at 16000 *g* for 20 min at 4°C. The resulting RNA pellet was resuspended in 50 µL of DEPC-treated distilled water and stored at -80°C until use. RNA concentration was determined spectrophotometrically at 260 nm. RNA extracted from yeast cells fermenting the Icewine and diluted Icewine juice was subsequently used for microarray and Northern analysis.

3.7. MICROARRAY ANALYSIS

3.7.1. Reverse transcription and hybridization

Total RNA (30 ug) isolated from yeast was purified using the RNeasy Minelute Cleanup Kit (Qiagen; Mississauga, ON, Canada). An aliquot of purified RNA was sent to the Microarray Centre of the University Health Network in Toronto, ON, Canada (http:// www.microarrays.ca/) to assess RNA quality and purity using an Agilent 2100 Bioanalyzer. RNA samples not showing degradation were used to generate fluorescently labeled cDNA for subsequent microarray analysis. Yeast 6.4Kv6 cDNA microarray slides were purchased from The Microarray Center. The slides contain 6240 characterized and unknown yeast ORFs spotted in duplicate, together with positive and negative control spots. cDNA copies of the RNA transcripts obtained from yeast fermenting dilute juice or Icewine juice were generated using a modified direct labeling protocol provided by The Microarray Center. One microarray hybridization experiment was performed per fermentation replicate. Cyanine dyes were obtained from Perkin-Elmer (Boston, MA, USA). Fluorescently-labeled first-strand cDNA probes were synthesized from 20 μg of total purified RNA in a 40 μL reaction mix containing: 8.0 μL of 5X first strand buffer (Invitrogen; Burlington, ON, Canada), 2.0 μL 100 pmole μL^{-1} AncT primer (5' T20VN 3'), 3.0 μL of 6.67 mM each of dATP, dGTP and dTTP; 1.0 μL 2 mM dCTP, 4.0 μL 0.1 M DTT, 5.0 μL of 5 ng artificial Arabidopsis transcript, 1.0 μL 1 mM cyanine 3-dCTP (Cy3, diluted Icewine juice samples) or cyanine 5-dCTP (Cy5, Icewine juice samples). The reaction mixture was first incubated at 65°C for 5 min and then cooled to 55°C for an additional 5 min to denature the RNA and anneal the AncT primer. Reverse transcription was initiated following the addition of 2 μL of Superscript III reverse transcriptase

(Invitrogen) and the reactions were incubated at 55°C for 2 h. The reaction was stopped by adding 4 μL of 50 mM EDTA (pH 8.0) and the RNA templates were hydrolyzed by adding 2 μL of 10 N NaOH to the reaction, followed by an incubation at 65°C for 20 min. The reaction was then neutralized by adding 4 μL of 5 M acetic acid. The labeled cDNA probes were pooled and purified using the CyScribe GFX Purification Kit (Amersham Biosciences; Piscataway, NJ, USA) and concentrated to a final volume of 5 μL by evaporation under vacuum using a Savant DNA110 Speed Vac. The concentrated probe was added to 80 μL of rehydrated DIG Easy Hyb (Roche) containing 5 μL of calf thymus tRNA and 5 μL yeast tRNA. The solution was heated to 65°C for 2 min and then allowed to fully cool to room temperature. The solution was applied to a yeast microarray slide covered with a Lifterslip (ErieScientific; Portsmouth, NH, USA). The slides were placed in a hybridization chamber overnight at 37°C. Following hybridization, the slides were briefly dipped in a 1× SSC solution to remove the Lifterslips. The slides were then washed three times in 1× SSC solution containing 0.1 % (w/v) SDS in 15 min intervals at 50°C with occasional agitation. After the washes were complete, the slides were briefly rinsed in 1× SSC followed by a second rinse in 0.1× SSC. The slides were dried by centrifugation at 40 *g* in a Sorvall RC 5C plus centrifuge for 10 min.

3.7.2. Image acquisition and data analysis

The slides were scanned using a PerkinElmer ScanArray Lite confocal laser scanner with excitation/emission wavelengths of 550 nm/570 nm for Cy3 and 649 nm/670 nm for Cy5. A preliminary scan was performed at a resolution of 50 μm to adjust laser power and photomultiplier tube (PMT) settings using the Line Scan tool until the fluorescent signal intensity of the Arabidopsis control spots was equal in each dye

channel. A final scan was performed at a resolution of 10 μm. For each dye channel, the fluorescent gene spot signal intensities were stored as separate 16-bit grayscale TIFF image files and were quantified with ScanArray Express software v3.0 (PerkinElmer) using the adaptive spot finding method. The background-adjusted signal intensities were calculated by subtracting the median local background intensity from the median signal intensity per gene spot. The adjusted signal intensities were then normalized by the Lowess (locally weighted linear regression) method. Gene spots having a normalized signal-to-background value less than 500 units were flagged and removed from subsequent analysis. Poor quality spots were flagged manually by the user and were also removed from the dataset. Of those gene spots passing the quality criteria, normalized gene expression values were reported as $\log_2$ transformed median Cy3 and Cy5 signal intensity values and exported as a tab delimited text data file in Microsoft Excel 2000 (Microsoft Corporation; Redmond, WA, USA). The text files were imported into GeneMaths XT v.1.5 (Applied Maths; Austin, TX, USA), which is a microarray statistical and datamining software package. A paired t-test was performed to determine significant differences in median Cy3 and Cy5 signal intensity values for each gene spot. From these values, the Cy5/Cy3 signal intensity ratios were calculated to determine fold differences in gene expression change between fermentation conditions. Gene spots passing the paired t-test ($P \leq 0.05$) and showing at least a two-fold change in the level of expression between fermentation conditions were subjected to datamining. GeneMaths can link directly to the *Saccharomyces* Genome Database (SGD) (http://www.yeastgenome.org/). Additional information using the Gene Ontology (GO) Slim term annotations for each gene in the yeast genome catalogued by the SGD was

retrieved and assigned to the appropriate genes within data sets (Ashburner *et al.*, 2000; Dwight *et al.*, 2002). These annotations provided information on the product of a given gene, such as its biological process, molecular function, cellular component and biochemical pathway association within the yeast cell.

3.8. Validation of microarray results using Northern Analysis

3.8.1. DNA Probe Design

DNA probes for *STL1*, *ACS1* and *ACS2* were designed by the author against regions of low homology to related genes and gene sequences were obtained using the BLAST analysis search tool from the *Saccharomyces* Genome Database (SGD). Forward and reverse primers for each gene were designed to amplify these regions using PCR. PCR was carried out in a PTC-200 DNAEngine thermocycler (MJ Research; Waltham, MA, USA) using the following parameters: 30 cycles of 94°C for 40 s, 55°C for 60 s and 72°C for 90 s. The probe sequences are summarized in Table 3.2. The *STL1* primers (forward and reverse) amplified a 550 bp fragment, the *ACS1* primers amplified a 300 bp fragment and the *ACS2* primers amplified a 250 bp fragment. The DNA probe for *ALD3* was previously designed by Pigeau and Inglis in 2005. The primers for *ALD3* amplified a 259 bp fragment. The forward *ITS1* primer and the reverse *ITS4* primer, designed by Esteve-Zarzoso *et al.* (1999), amplified a DNA fragment size of 850 bp. The PCR products were run on a 1% (w/v) agarose gel to verify probe size and were visualized under UV light using a BioRad Gel-doc 1000 system and accompanying software. Probes were purified with a Qiagen QIAquick gel extraction kit.

Table 3.2: Primer sequences used for Northern analysis probe design

Probe	Sequence
STL1	FWD 5'-TCAAAGGCAAATTTATAAGCAGAAC-3' REV 5'-CCAAAATCAATCCAATAAGCAATCA-3'
ACS1	FWD 5'-CAAAACTAGAAGAACAGTCAAGTGA-3' REV 5'-CTGCCCGTTTTAGGGTCTGGGATGA-3'
ACS2	FWD 5'-TTTATGAAGCTCACAACGTAAAGGC-3' REV 5'-ATGTCTGTCAACACAATTGTATGAT-3'
ALD3	FWD 5'TGGTTATGGTTCCGTTGTGGGGAAA-3' REV 5'-AAACTCTTGAGTTTGCAGTGCAGAT-3'
ITS1 *ITS4*	FWD 5'-TCCGTAGGTGAACCTGCGG -3' REV 5'-TCCTCCGCTTATTGATATGC -3'

3.8.2. Northern Analysis

Unpurified (50 μg) total RNA samples extracted from one fermentation trial were electrophoresed at 95 V for 4.5 h in a 1.25% (w/v) agarose gel containing 18% (v/v) formaldehyde and blotted onto a positively charged nylon membrane (Boehringer Mannheim; Darmstadt, Germany) using capillary transfer. RNA was cross-linked to the membrane using a Hoefer UVC 500 UV crosslinker (Hoefer, Inc.; CA, USA). Probes were labeled with [α-^{32}P]-dATP (Perkin Elmer) using a Boehringer Mannheim random primed labeling kit and 20 ng of labeled probe was hybridized to the bound RNA following an overnight incubation at 42°C in 50 mL of hybridization solution containing 5× SSC, 5× Denhardt's solution, 1% (v/v) SDS, 50% (v/v) formamide and 0.1 mg mL^{-1} sheared salmon sperm DNA. The membrane was washed twice with 50 mL volumes of 2× SSC containing 0.1% (v/v) SDS for 20 min at room temperature and washed twice with 50 mL volumes of 0.2× SSC, also containing 0.1% (v/v) SDS, for 15 min at 50°C. The probed membrane was exposed to a Fujifilm phosphorimaging screen for up to seven days and the screen was scanned using a Fujifilm FLA-3000 phosphorimager with a 633

nm helium-neon laser. The subsequent images were quantified with Fujifilm Image Gauge software (v.4.0). Gene expression levels were normalized to the signal intensities derived from a rDNA region spanning the 5.8S rRNA gene and flanking internal transcribed spacers (ITS) 1 and 2.

3.9. Measuring amino acid concentration using HPLC

Individual primary amino acids, including γ-aminobutyrate (GABA) and imino acids (proline), in Icewine and diluted Icewine juice samples were separated and quantified using the Agilent 1100 Series HPLC following their conversion to their respective *O*-phthaldialdehyde (OPA) and 9-fluorenylmethyl chloroformate (FMOC) derivatives. Juice samples were diluted with water prior to preparing the derivatization reactions using the Agilent 1313A autosampler according to the manufacturer's instructions. 0.5 μL of each derivatized sample was injected into a 4.6 × 150 mm, 3.5 μm ZORBAX Eclipse-AAA column. The OPA- and FMOC-derivatized amino acids were detected at 340 nm using a G1315A Fluorescence Detector (FLD). The concentration of each amino acid present per juice sample was determined in singlet for each of the three fermentation replicates and expressed in mg N L^{-1}.

4. RESULTS AND DISCUSSION

4.1. MICROARRAY ANALYSIS OVERVIEW

4.1.1. Results - Microarray

The genomic expression profiles of the commercial wine yeast *Saccharomyces cerevisiae* K1-V1116 fermenting Icewine juice were compared to those generated by yeast cells fermenting diluted Icewine juice using cDNA microarray analysis. All fermentations were carried out in triplicate and one microarray experiment was performed for each of the days examined per fermentation replicate. The expression of approximately 6240 open reading frames (ORFs) in yeast was compared between juice conditions during the first five days of fermentation which corresponded to the start of the early exponential growth phase until cells entered to early stationary phase. Gene expression was considered to be significantly up- or downregulated in the Icewine juice condition if the difference in gene expression passed a paired t-test ($P \leq 0.05$) and showed at least a two-fold change in the level of expression between fermentation conditions. A small fraction of the number of genes within the yeast genome displayed significant changes in expression in response to the fermentation of Icewine juice (Table 4.1.1). Of these genes, the vast majority showed a difference in expression between juice conditions resulting in an up- or downregulation of less than five-fold in the Icewine juice fermentation. The total number of up- and downregulated genes was approximately equivalent on day two of the fermentations. The total number of genes downregulated was slightly higher than those upregulated for each of the remaining fermentation days analyzed (Table 4.1.1). The total number of genes differentially expressed in yeast

Table 4.1.1: Distribution of the differentially expressed genes in *S. cerevisiae* fermenting Icewine juice and dilute Icewine juice.

Expression	Fold Change*	Number of Genes			
		Day 2	Day 3	Day 4	Day 5
Upregulated	2 to <5	120	80	115	37
	≥5 to <10	9	13	21	11
	≥10	1	6	12	5
	Total upregulated	130	99	148	53
Downregulated	2 to <5	120	131	154	55
	≥5 to <10	19	12	24	9
	≥10	6	1	3	8
	Total downregulated	145	144	181	72
Total		275	243	329	125

*Significantly different as determined by a paired t-test ($P \leq 0.05$)

between fermentation conditions reached a maximum on day four (329 genes) which represents about 5% of the genome. The total number began to decline on day five (125 genes) as cells entered stationary phase (section 4.2.1.1.).

Genes were also characterized according to Gene Ontology (GO) Slim terms of the *Saccharomyces* genome database (SGD). Those genes identified as being differentially expressed at least two-fold between fermentation conditions were grouped together into broad categories based on common biological gene function within the yeast cell. Table 4.1.2 lists the distribution of the genes differentially expressed in yeast fermenting Icewine juice based on their 2007 GO Slim biological function annotations. The number of gene expression changes was transient and occurred at a low frequency throughout the early stages of the Icewine fermentation for genes associated with GO Slim categories related to cell growth and reproduction. This category included cellular functions related to budding, cytokinesis, morphogenesis and sporulation (Table 4.1.2). In contrast, a greater number of yeast genes whose expression was significantly affected by fermentation of Icewine juice and consistently displayed overall up- or downregulation throughout the first five days of fermentation could be divided into seven main biological categories as illustrated in Figure 4.1.1. When the number of genes differentially expressed more than two-fold between fermentation conditions was divided by the total number of genes either up- or downregulated from days two to five of the fermentations in each GO Slim category, it was found that the overall expression of genes associated with the generation of precursor metabolites and energy, lipid metabolism, amino acid metabolism, carbohydrate metabolism and transport were expressed to a lesser degree in yeast fermenting Icewine juice relative to cells fermenting the dilute

Table 4.1.2: Distribution of GO Slim terms for differentially expressed genes in *S. cerevisiae* fermenting Icewine juice.

GO Slim Term	Day 2		Day 3		Day 4		Day 5	
	Up	Down	Up	Down	Up	Down	Up	Down
amino acid and derivative metabolism	8	17	10	10	8	14	4	6
carbohydrate metabolism	14	11	8	24	7	30	7	9
cell budding	0	1	0	2	0	2	0	2
cell cycle	6	6	4	7	9	8	2	3
cell homeostasis	1	1	2	6	2	6	1	6
cell wall organization and biogenesis	3	3	3	7	6	9	1	6
cellular respiration	6	2	0	17	0	25	1	2
conjugation	1	2	1	4	1	4	0	0
cytokinesis	0	1	0	1	1	1	1	2
cytoskeleton organization and biogenesis	0	1	0	2	1	3	1	3
DNA metabolism	20	4	4	8	9	11	2	2
electron transport	2	1	0	13	0	12	0	1
generation of precursor metabolites and energy	19	16	6	49	5	53	7	17
lipid metabolism	6	21	4	2	3	11	0	1
meiosis	2	5	3	5	6	5	2	0
membrane organization and biogenesis	3	2	0	1	1	2	0	0
morphogenesis	2	2	1	4	3	4	0	5
nuclear organization and biogenesis	0	2	0	0	0	0	0	0
organelle organization and biogenesis	11	9	9	12	25	18	3	7
other	7	11	6	6	12	11	8	4
protein biosynthesis	20	9	11	6	5	11	2	7
protein catabolism	2	3	1	1	1	2	1	3
protein modification	7	8	4	8	10	11	1	2
pseudohyphal growth	1	0	1	0	2	1	0	1
response to stress	10	12	15	12	18	14	12	12
ribosome biogenesis and assembly	0	1	4	1	16	1	2	2
RNA metabolism	3	5	5	5	15	5	3	5
signal transduction	0	6	2	1	2	3	2	0
sporulation	0	5	2	3	2	3	2	3
transcription	6	2	5	6	14	7	4	2
transport	18	28	13	25	17	31	5	13
unknown	16	19	22	23	32	29	6	7
vesicle-mediated transport	2	5	3	3	5	7	2	3
vitamin metabolism	7	7	2	2	5	4	2	2

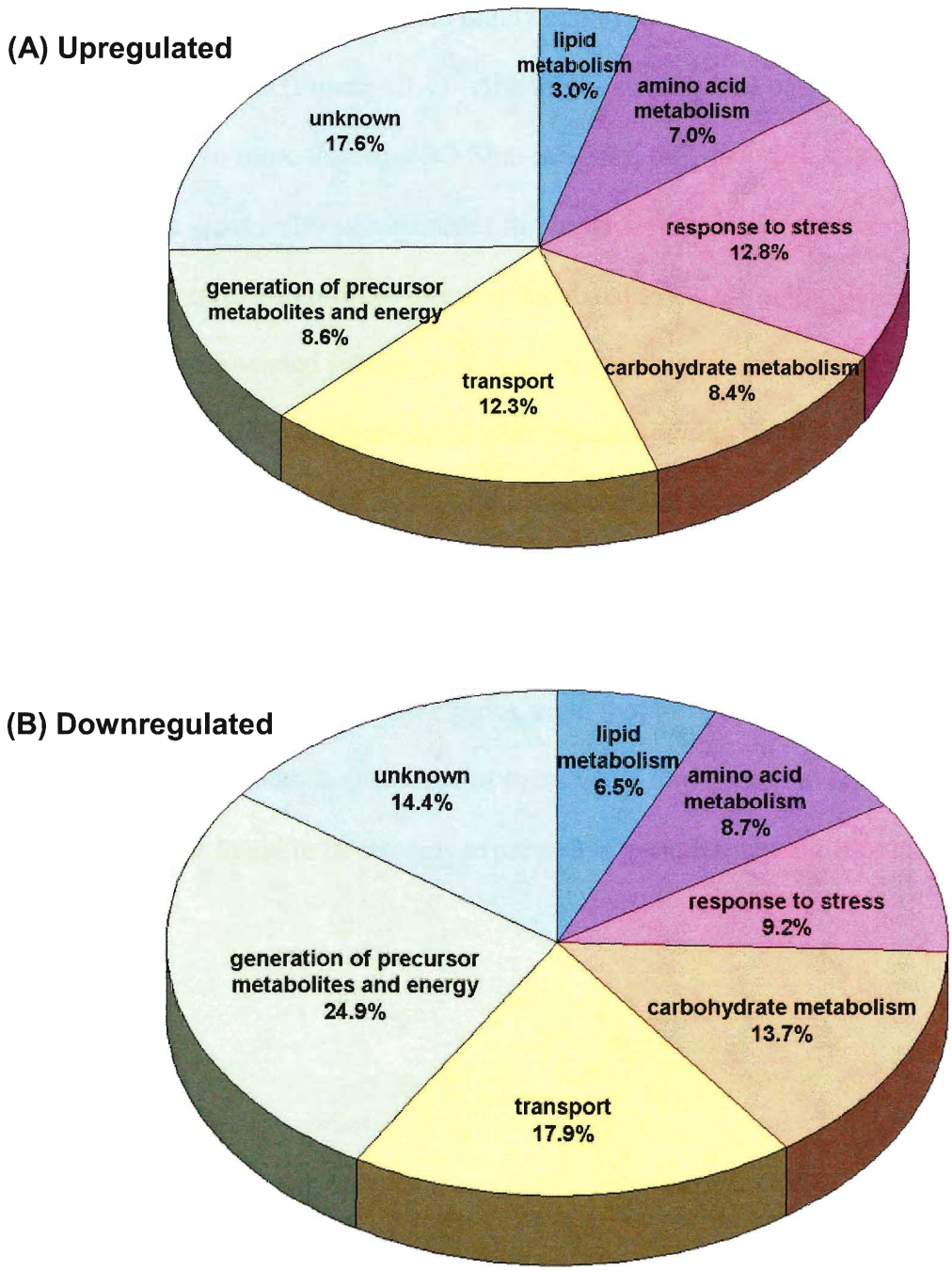

Figure 4.1.1: The major Gene Ontology (GO) Slim term categories containing genes differentially expressed in *S. cerevisiae* fermenting Icewine juice. The overall percentage of genes associated with each of the GO Slim categories containing genes that were found to be (A) upregulated or (B) downregulated in yeast fermenting Icewine juice.

juice. In contrast, more genes involved with the response to stress and those with unknown function were found to be more highly expressed on days two to five of the Icewine juice fermentation (Figure 4.1.1). Although a small subset of these genes may have been annotated to more than one GO Slim category, only their primary biological function within the yeast cell was considered for this calculation. A more detailed description of the expression profiles of genes annotated to the six major GO Slim categories and their associated subcategories will be presented in subsequent sections. Very few genes were up- or downregulated more than ten-fold in the Icewine juice condition, which represents less than 5% of the total number of genes differently expressed between fermentations (Table 4.1.1). Table 4.1.3 lists the genes with changes in expression calculated to be more than ten-fold between juice conditions on one or more days of the fermentations. Of these genes, eight that were upregulated more than ten-fold were associated with the response to stress while four genes having no known function to date were found to be strongly expressed in yeast fermenting Icewine juice.

Table 4.1.3: Genes up- or downregulated more than 10-fold in *S. cerevisiae* fermenting Icewine juice.

ORF	Gene	Description	GO Slim Category
Upregulated			
YCR010C	ADY2	acetate transporter	transport
YMR169C	ALD3	aldehyde dehydrogenase	response to stress
YHR053C	CUP1-1	metallothionein; copper ion binding	response to stress
YHR055C	CUP1-2	metallothionein; copper ion binding	response to stress
YIL053W	GPP1	glycerol-3-phosphatase	response to stress
YER062C	GPP2	glycerol-3-phosphatase	response to stress
YOL151W	GRE2	oxidoreductase activity	response to stress
YNL036W	NCE103	carbonate dehydratase	response to stress
YGR159C	NSR1	rRNA processing	RNA metabolism
YJR095W	SFC1	succinate-fumarate transporter	transport
YMR175W	SIP18	phospholipid binding	response to stress
YHR139C	SPS100	spore wall maturation protein	sporulation
YDR536W	STL1	glycerol proton symporter	transport
YBR281C		unknown	unknown
YGL157W		unknown	unknown
YHR087W		unknown	unknown
YOL150C		unknown	unknown
Downregulated			
YAL054C	ACS1	acetyl-CoA synthetase	generation of metabolites and energy
YLR153C	ACS2	acetyl-CoA synthetase	generation of metabolites and energy
YGR204W	ADE3	formate-tetrahydrofolate ligase	other
YDR384C	ATO3	ammonium transporter	transport
YBL101C	ECM21	unknown	cell wall organization and biogenesis
YMR212C	EFR3	unknown	morphogenesis
YGR254W	ENO1	enolase	carbohydrate metabolism
YPL281C	ERR2	phosphopyruvate hydratase activity	unknown
YOR388C	FDH1	formate dehydrogenase	vitamin metabolism
YPL275W	FDH2	formate dehydrogenase	other
YKR002W	PAP1	polynucleotide adenylyltransferase	RNA metabolism
YGR087C	PDC6	pyruvate decarboxylase	carbohydrate metabolism
YBR229C	ROT2	alpha-glucosidase	cell wall organization and biogenesis
YLR410W	VIP1	unknown	cytoskeleton organization and biogenesis
YIL057C		unknown	unknown
YPL276W		unknown	unknown

4.1.2. Discussion - Microarray Overview

Past genomic profiling studies have extensively investigated the impact of salt and sorbitol-induced hyperosmotic stress on the transcriptome of laboratory strains of *S. cerevisiae* (Posas *et al.*, 2000; Rep *et al.*, 2000; Yale and Bohnert, 2001). A large scale microarray study revealed that the expression of a substantial group of nearly 900 genes is affected when yeast are challenged with a variety of environmental stresses, including hypo- and hyperosmotic stress, oxidative stress and nutrient depletion (Gasch *et al.*, 2000). Causton *et al.* (2000) found that 10% of genes within the yeast genome affected by transient stress respond in a similar manner and are expressed collectively under many different stress conditions. Genes that are induced or repressed by stress and are within this "common environmental response" or CER group are involved in carbohydrate metabolism, the generation of energy, response to reactive oxygen species, response to stress, ion homeostasis and protein synthesis. The results from the microarray data obtained in the present study revealed that 2-5% of genes within the genome of the commercial wine yeast K1-V1116 were differentially expressed between Icewine and diluted Icewine juice fermentation conditions. The bulk of these genes are involved in carbohydrate metabolism, transport and amino acid and lipid metabolism. The majority of genes that also demonstrated a difference in transcriptional response between fermentation conditions are associated with the generation of precursor metabolites and energy which were observed to be downregulated in cells fermenting Icewine juice while a greater proportion of genes associated with the response to stress, including osmotic stress, were more highly expressed relative to the table wine fermentation. In contrast to the transcriptional response of laboratory yeast strains to individual, transient

environmental stresses (Gasch *et al.*, 2000; Causton *et al.*, 2001), wine yeast cells under oenological conditions are faced with a continually changing environment and must adapt accordingly to several simultaneous stresses. In has been previously shown that solutes in Icewine juice in addition to sugar place yeast under incredible hyperosmotic stress during fermentation (Kontkanen *et al.*, 2004; Pigeau and Inglis, 2005). The transcriptional response by a wine yeast strain to stress under fermentative conditions is likely to be drastically different from that of an aerobically grown laboratory strain (reviewed in Pretorius, 2000). Only 28 out of the 186 genes induced in a laboratory yeast strain briefly exposed to salt and sorbitol hyperosmotic stress (Rep *et al.*, 2000) were found to be similarly induced in wine yeast during the first five days of Icewine juice fermentation relative to table wine fermentation. These genes were associated with the metabolism of glycerol and amino acids, maintaining redox balance and responding to cell stress. However, a number of genes induced under salt and/or sorbitol stress but not during Icewine fermentation were associated with gene functional categories related to signal transduction, proteolysis, vacuolar biogenesis in addition to trehalose and glycogen metabolism. The initial stresses of high osmotic pressure and low pH, coupled with the additional stress from ethanol as the fermentation progresses are involved in wine yeast stress response during fermentation and have been monitored at the transcriptomic level (Perez-Torrado *et al.*, 2002; Rossignol *et al.*, 2003). Gene expression profiling studies involving the adapted stress response of a wine yeast strain fermenting synthetic grape juice or the initial stress response to high sugar stress within a chaptalized grape juice environment similarly identified a large subset of genes differentially expressed under fermentative conditions that were associated with nutrient metabolism, transport and

response to stress (Rossignol *et al.*, 2003; Erasmus *et al.*, 2003). In a 2008 study by Marks *et al.*, transcriptional analysis of the stress response of a commercially available wine yeast strain throughout table wine fermentation identified a group of 223 highly expressed genes. This gene group was later designated as the fermentation stress response (FSR) and genes within this group were subsequently categorized based on their GO biological annotations. From the FSR, only 11 genes in my study induced throughout table wine fermentation were also found to be similarly expressed during Icewine fermentation. However, the majority of FSR genes expressed in the study by Marks *et al.* (2008) were associated with GO biological process categories that were not part of the majority of genes differentially expressed between Icewine and diluted juice fermentations. Of the FSR genes, the highly represented GO categories identified during table wine fermentation included genes encoding for uncharacterized proteins (28%), organelle organization and biogenesis (15%), protein modification processes (13%) and RNA metabolic processes (12%). However, FSR genes related to stress response (11%) and transport (18%) were also expressed during fermentation. In agreement with this study, genes involved with the response to stress and transport were found to be highly expressed during Icewine juice fermentation relative to the dilute juice fermentation. However, unlike the results reported in Marks *et al.* study, the majority of genes differentially expressed between Icewine and dilute juice fermentations were associated with the generation of precursor metabolites and energy, lipid metabolism, amino acid metabolism and carbohydrate metabolism.

The microarray experiments have clearly provided a wealth of information on the transcriptional differences associated with a commercial wine yeast strain (K1-V1116)

fermenting Icewine and diluted Icewine juice. Following statistical and biological gene function analysis, the resulting gene expression profile patterns were used in this study as a starting point to identify metabolic pathways related to the use of nutrients and the production of yeast metabolites that were significantly up- or downregulated during Icewine fermentation. Based on these results, a more detailed analysis of the key genes associated with these pathways will be discussed in subsequent chapters of this thesis. Transcriptional differences of genes linked to sugar and amino acid metabolism will be correlated to yeast cell growth and nutrient uptake in Sections 4.2 and 4.3. Also, the transcriptional differences in glycerol and acetic acid transport and metabolism related genes identified through microarray analysis and verified with Northern analysis will be correlated to differences in glycerol and acetic acid production in Sections 4.4 and 4.5. Section 4.6 will focus on the changes in expression of a number of stress response genes observed throughout the first five days of Icewine juice fermentation.

4.2. Carbohydrate Metabolism

4.2.1. Results - Carbohydrate Metabolism

4.2.1.1. Yeast Cell Growth

The high level of osmotic stress placed on fermenting yeast due to the presence of concentrated solutes in Icewine juice had an overall negative impact on cell growth. In comparison to the diluted Icewine juice fermentation condition, increased extracellular osmotic pressure exerted on yeast cells fermenting Icewine juice contributed to decreased cell size and biomass accumulation, as well as lengthened the duration of the lag phase and increased the time elapsed before yeast cells began to actively bud and proliferate

(Figures 4.2.1 and 4.2.2). Icewine juice fermenting cells were visibly smaller in size due to the loss of cytosolic water and turgor pressure compared to their diluted Icewine juice fermenting counterparts up to 96 h into the fermentations (Figure 4.2.1). Up to this 48 h timepoint, cells fermenting Icewine juice were not actively budding and remained in late lag phase, while cells fermenting the dilute juice were rapidly budding and had already reached midexponential growth phase (Figure 4.2.2A). Yeast cell growth in both juice conditions reached stationary phase approximately 120 h into the fermentations. The diluted fermentation achieved a peak cell concentration of 1.1×10^8 cells mL^{-1}, whereas the high sugar fermentation accumulated a cell concentration of 6.4×10^7 cells mL^{-1} (Figure 4.2.2A). This corresponded to a 2-fold higher peak biomass accumulation in the dilute juice fermentation in comparison to the Icewine juice fermentation, which also showed an overall slower rate of biomass accumulation (Figure 4.2.2B). These results agree with previous observations demonstrating that yeast subjected to increasing levels of osmotic stress have diminished cell volume and delayed budding (Blomberg and Adler, 1992).

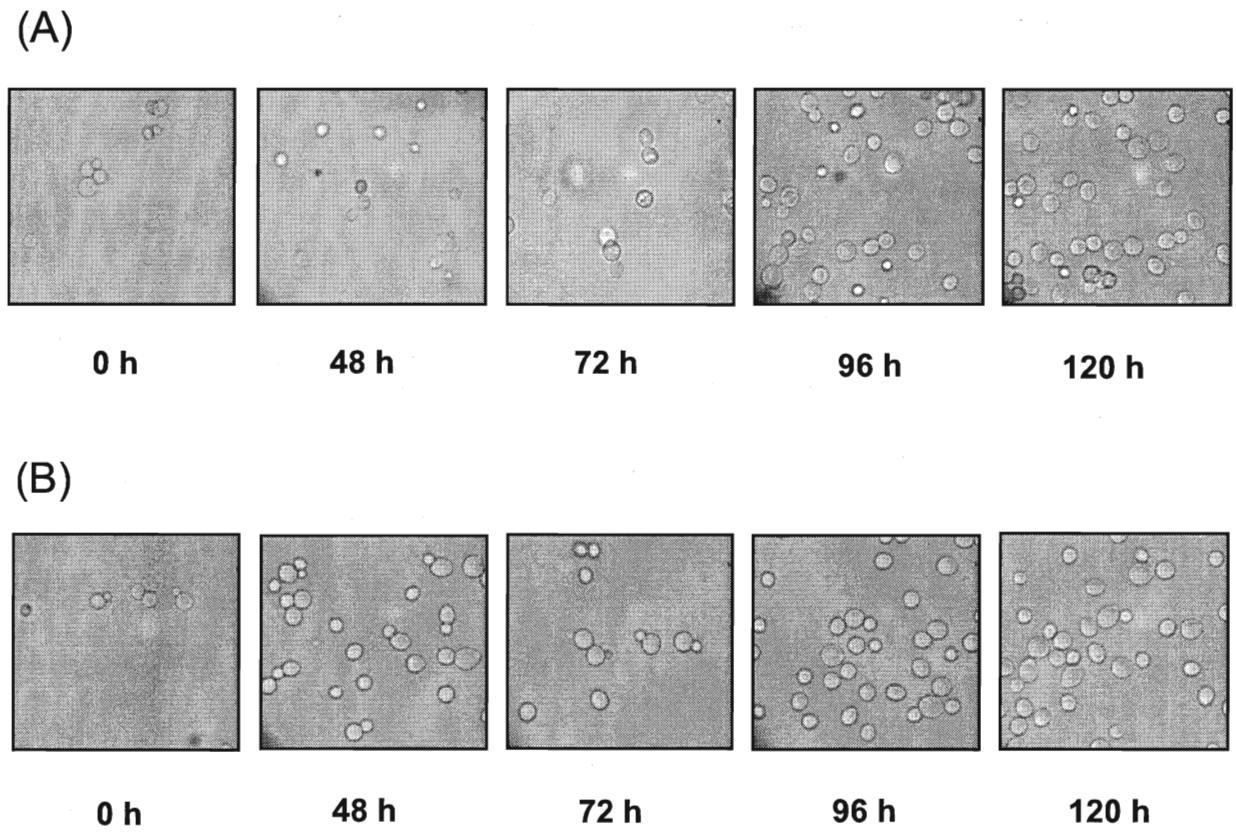

Figure 4.2.1.: Yeast cell morphology during fermentation. Yeast cells fermenting Icewine juice (A) and diluted Icewine juice (B) were visualized daily under 40× magnification.

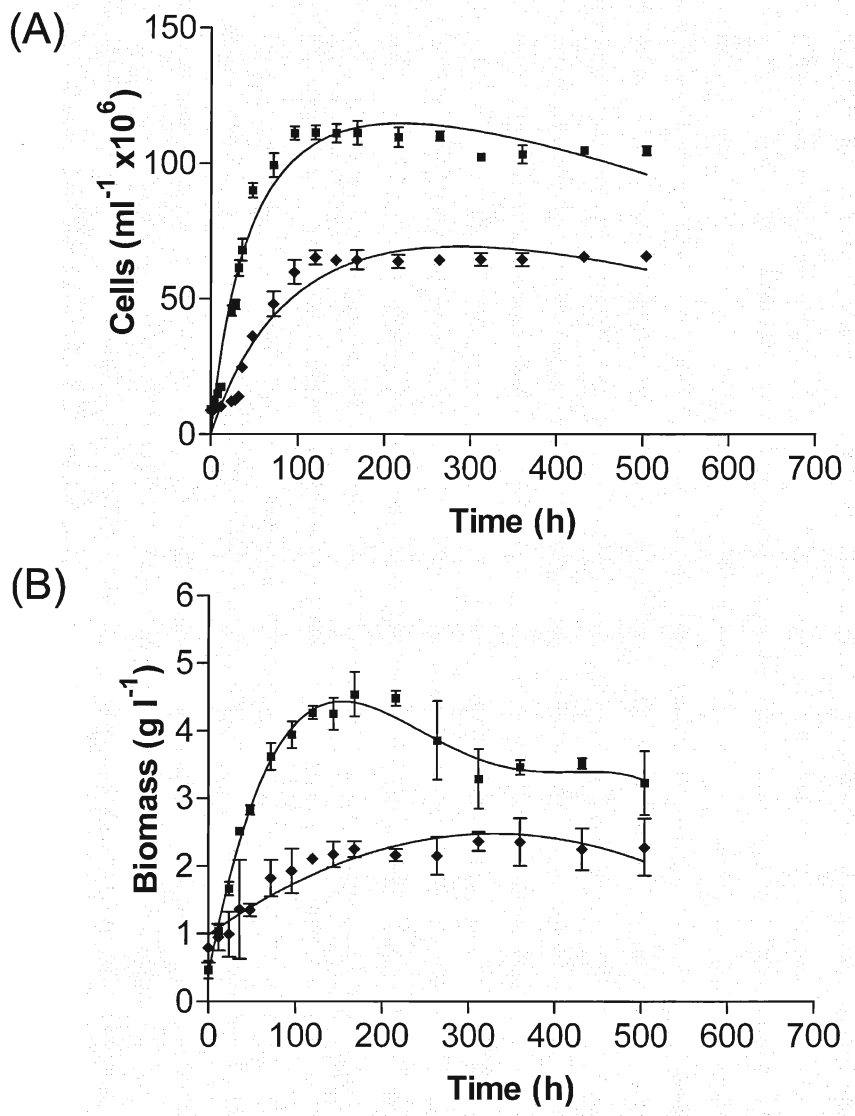

Figure 4.2.2.: Yeast cell growth and biomass accumulation. Fermentations of Icewine juice (♦) and diluted Icewine juice (■) were monitored daily for total cell counts (A) and biomass accumulation (B). The values represent the average ± standard deviation of the mean of triplicate fermentations.

4.2.1.2. Sugar Consumption

At the start of the fermentations, there was approximately twice the amount of total sugar present in Icewine juice when compared to the diluted juice (Figure 4.2.3A). Of the reducing sugars, the unfermented Icewine and diluted juices had a lower initial glucose concentration in comparison to the fructose concentration prior to inoculation (Figures 4.2.3B and C). At the end of the fermentations, only about half of the available fermentable sugars were consumed by Icewine juice fermenting yeast in twice the amount of time it took the dilute juice cells to consume the same amount of sugar (Figure 4.2.3A). When comparing the fermentation rate between juice conditions, the high concentration of sugar and other solutes in the Icewine juice appeared to impede the ability of yeast to ferment this juice. There was a slight lag in the rate of sugar consumption during the first 48 h of the Icewine juice fermentation. The reducing sugar concentration steadily declined throughout the duration of the Icewine juice fermentation with yeast only consuming 187.8 ± 2.8 g L^{-1} of the 447.7 ± 8.5 g L^{-1} of available sugars in 576 h. In comparison, the dilute juice fermenting cells demonstrated a considerably faster fermentation rate consuming 186.8 g ± 3.1 L^{-1} of sugar in 216 h and ultimately consuming all available reducing sugars (221.9 ± 0.6 g L^{-1}) in 312 h (Figure 4.2.3A). Additionally, there was a difference in the amount of glucose and fructose consumed by yeast between fermentation conditions. Approximately 2.5-fold more fructose (183.9 ± 0.3 g L^{-1}) remained unfermented compared to glucose (73.9 ± 0.8 g L^{-1}) in 576 h by yeast in the Icewine juice condition (Figures 4.2.3B and C). In contrast, all of the available glucose and fructose was consumed at the end of the dilute juice fermentation. Furthermore, yeast cells in both Icewine and diluted juice displayed a clear difference in

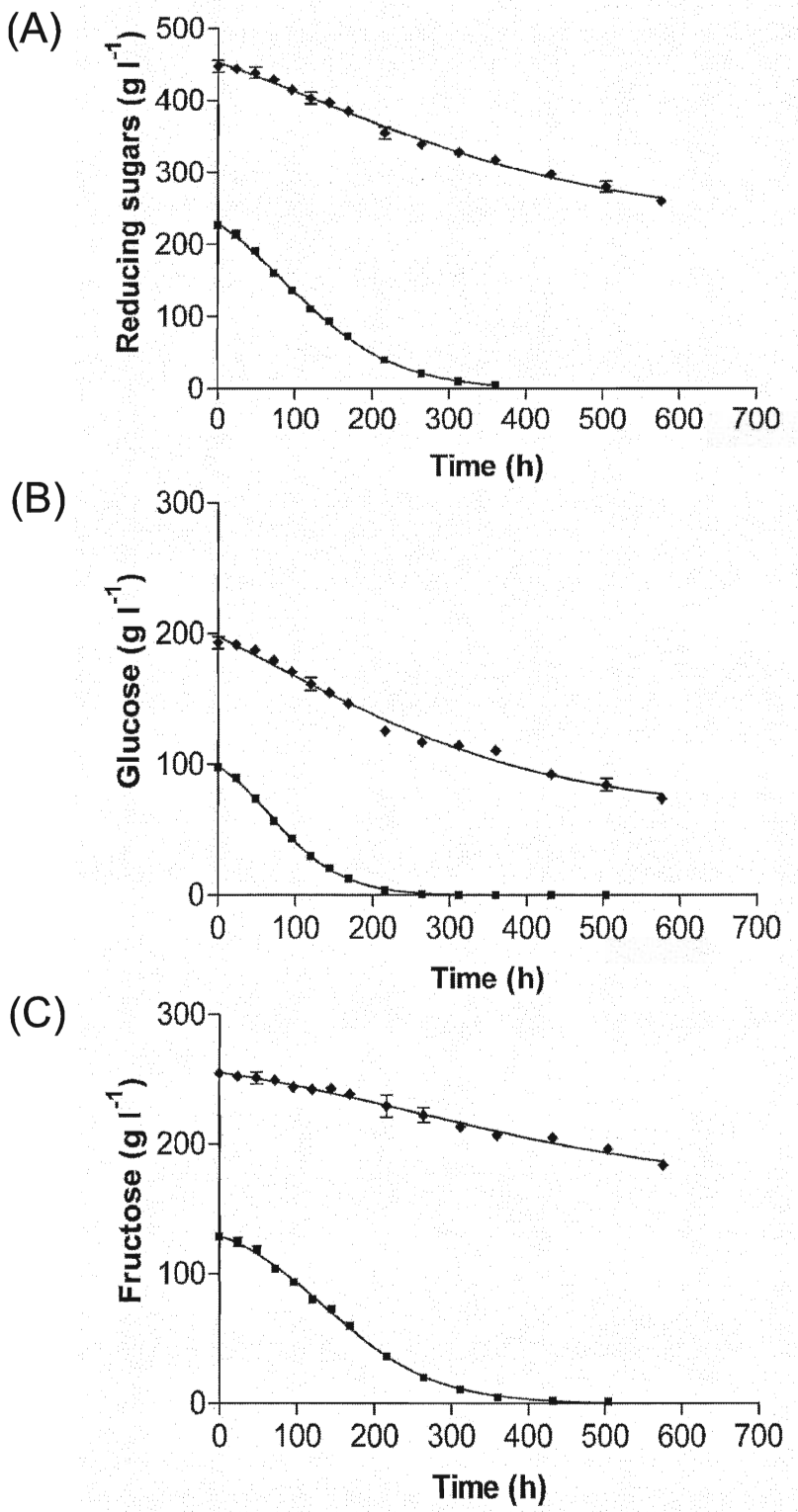

Figure 4.2.3: Yeast sugar consumption. Fermentations of Icewine juice (♦) and diluted Icewine juice (■) were monitored daily for total reducing sugars (A), glucose (B) and fructose (C) throughout the course of the fermentations. Fermentations were performed in triplicate with measurements performed in duplicate. The mean values ± standard deviation are shown.

the fermentation rates of both reducing sugars. Under both fermentation conditions, yeast appeared to preferentially take up glucose since the fermentation rate of glucose was faster than that of fructose (Figures 4.2.3B and C).

4.2.1.3. Gene expression profiles for carbohydrate metabolism

Expression of the genes encoding for proteins involved in carbohydrate metabolism were highly expressed in both fermentation conditions. From the microarray results, the routes of carbohydrate metabolism in *S. cerevisiae* containing genes that were differentially expressed between fermentation conditions are illustrated in Figure 4.2.4. Upon entry into the cell, hexoses such as glucose and fructose are converted to pyruvate via glycolysis. Pyruvate is then further metabolized to either ethanol and CO_2 by alcoholic fermentation (Figure 4.2.4A) or to oxaloacetate and/or acetyl-CoA, which can enter the tricarboxylic acid cycle (TCA) (Figure 4.2.4B). Alternatively, pyruvate can enter the glyoxylate cycle (Figure 4.2.4C). All of these pathways were evaluated in fermenting yeast using microarray technology.

4.2.1.3.1. Glycolysis and alcoholic fermentation

The first step of glycolysis is the transport of sugar molecules into the yeast cell. The sugar transporter gene family encodes for the largest family of transporters in *S. cerevisiae*. In the yeast genome, there are 20 genes identified as belonging to the *HXT* family that encode for hexose transporters (Luyten *et al.*, 2002). Six *HXT* genes were observed to be differentially expressed between fermentation conditions and all were downregulated up to nine-fold throughout the Icewine juice fermentation (Table 4.4). Both *HXT8* and *HXT10* (putative hexose transporters) were expressed at the same level in

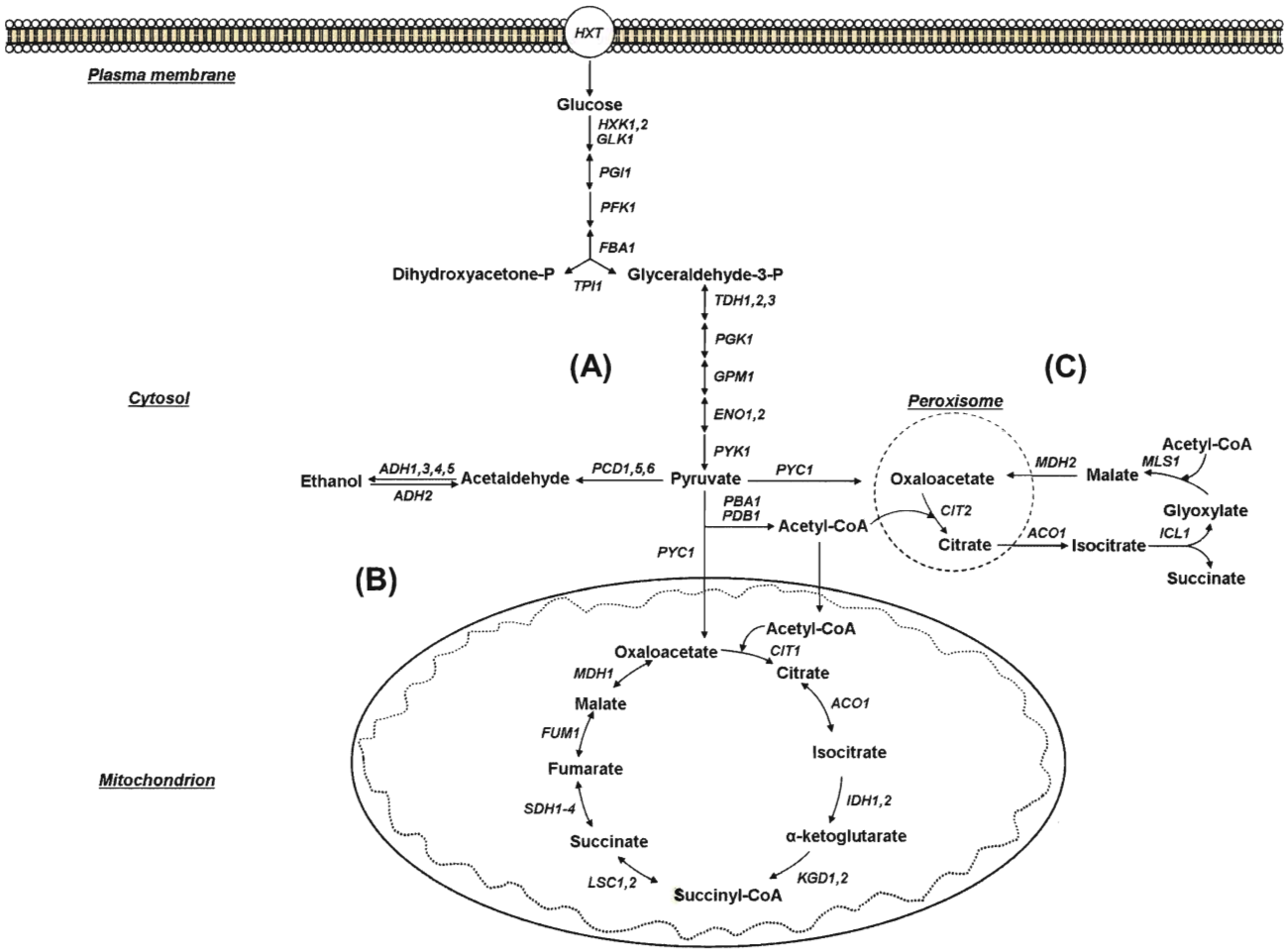

Figure 4.2.4: The pathways involved in carbohydrate metabolism differentially expressed in *S. cerevisiae* between fermentation conditions. Illustrated are the metabolic intermediates and the genes associated with (A) glycolysis and alcoholic fermentation, (B) the tricarboxylic acid (TCA) cycle and (C) the glyoxylate cycle.

both fermentation conditions on day two, along with *HXT5* (moderate affinity glucose transporter) on days three and four. The rate of sugar consumption by dilute juice fermenting cells increased considerably after day two in comparison to Icewine juice fermenting cells, which maintain a slower but steady rate of sugar consumption as seen in Figure 4.2.3A. This observation corresponded to the degree of *HXT* downregulation in Icewine juice fermenting yeast, along with a general downregulation in the genes associated with carbohydrate metabolism (Table 4.2.1).

The large majority of genes involved in the glycolytic pathway and alcoholic fermentation were differentially expressed between fermentation conditions. However, genes specifically encoding for enzymes responsible for catalyzing the energy generating, rate-limiting steps in glycolysis all showed a relatively lower fold expression in yeast under the Icewine juice condition compared to the dilute juice fermentation after day two, as recorded in Table 4.2.1. This was the case for *HXK2* (2.9-fold) encoding for hexokinase II, which catalyzes the first irreversible enzymatic step in glycolysis by transferring a phosphate group from ATP to a hexose molecule. Both hexokinase isoforms (*HXK1* and *HXK2*) were strongly downregulated in the Icewine condition relative to the dilute condition; 6.6- and 9.5-fold on day five of the fermentations, respectively. *GLK1* encodes for a glucokinase, which participates in the phosphorylation of glucose only, and it was observed to be differentially expressed in yeast between juice conditions but was expressed at a significantly higher level on day five of the Icewine juice fermentation. *PFK1* encodes for the α-subunit of phosphofructokinase, which catalyzes the second irreversible and unidirectional reaction of the glycolytic pathway, where fructose-6-phosphate is phosphorylated to form the six carbon intermediate

Table 4.2.1: Expression profile of the genes involved in carbohydrate metabolism.

ORF	Gene	Description	Fold Change*			
			Day 2	Day 3	Day 4	Day 5
Monosaccharide Transport						
YHR094C	HXT1	low affinity glucose transporter	-	-2.4	-4.8	-4.6
YHR092C	HXT4	moderate affinity glucose transporter	-	-2.9	-5.7	-7.8
YHR096C	HXT5	moderate affinity glucose transporter	-2.2	•	•	-4.2
YJL214W	HXT8	putative hexose transporter	•	-2.4	-2.9	×
YFL011W	HXT10	putative hexose transporter	-	-3.9	-9.3	×
YIL171W	HXT12	putative hexose transporter	•	-2.2	-4.4	×
Glycolysis and Alcoholic Fermentation						
YFR053C	HXK1	hexokinase I	×	-	-2.5	-6.6
YGL253W	HXK2	hexokinase II	+2.9	-2.2	-2.7	-9.5
YCL040W	GLK1	glucokinase	•	+	+	+2.4
YBR196C	PGI1	glucose-6-phosphate isomerase	•	×	×	×
YGR240C	PFK1	phosphofructokinase	•	-5.7	-5.9	×
YKL060C	FBA1	aldolase	+	-4.0	-3.4	•
YDR050C	TPI1	triose-phosphate isomerase	+	-4.4	-3.3	•
YJL052W	TDH1	glyceraldehyde-3-phosphate dehydrogenase	•	-6.7	-4.7	•
YJR009C	TDH2	glyceraldehyde-3-phosphate dehydrogenase	•	-6.0	-3.2	-2.6
YGR192C	TDH3	glyceraldehyde-3-phosphate dehydrogenase	•	-6.7	-5.5	-6.6
YCR012W	PGK1	phosphoglycerate kinase	+	-7.2	-6.7	-6.6
YKL152C	GPM1	phosphoglycerate mutase	+5.4	-4.1	-3.1	-
YGR254W	ENO1	enolase	+2.8	-12.2	-11.6	-13.6
YHR174W	ENO2	enolase	+2.5	-8.6	-7.0	-4.0
YAL038W	PYK1	pyruvate kinase	+2.4	-3.5	-3.4	•
YLR044C	PDC1	pyruvate decarboxylase	+2.4	-4.7	-5.4	-3.9
YLR134W	PDC5	pyruvate decarboxylase	+2.2	-4.4	-5.9	•
YGR087C	PDC6	pyruvate decarboxylase	+2.2	-4.5	-6.7	-10.1
YOL086C	ADH1	alcohol dehydrogenase (cytosolic)	-	-4.6	-6.5	-3.2
YMR303C	ADH2	alcohol dehydrogenase (cytosolic)	-2.2	-4.4	-6.4	-4.9
YMR083W	ADH3	alcohol dehydrogenase (mitochondrial)	-2.0	-3.2	•	-3.6
YGL256W	ADH4	alcohol dehydrogenase (mitochondrial)	+2.0	×	×	×
YBR145W	ADH5	alcohol dehydrogenase (cytosolic)	×	-4.3	-4.9	•
TCA Cycle						
YER178W	PDA1	pyruvate dehydrogenase	-	-2.3	-2.4	•
YBR221C	PDB1	pyruvate dehydrogenase	•	-	-	•
YGL062W	PYC1	pyruvate carboxylase	-2.3	-	-2.4	+2.4
YNR001C	CIT1	citrate synthase (mitochondrial)	-2.3	-	-2.3	•
YLR304C	ACO1	aconitase	•	-	-2.0	-7.3
YNL037C	IDH1	isocitrate dehydrogenase	+	-	-	-2.0
YOR136W	IDH2	isocitrate dehydrogenase	+2.4	-	•	•
YIL125W	KGD1	α-ketoglutarate dehyrogenase	•	•	-2.0	×
YDR148C	KGD2	α-ketoglutarate dehyrogenase	•	-	-2.2	•
YOR142W	LSC1	succinyl-CoA ligase	•	×	-2.5	×
YGR244C	LSC2	succinyl-CoA ligase	•	-2.8	-3.2	•
YKL148C	SDH1	succinate dehydrogenase	×	-2.8	-3.7	×
YLL041C	SDH2	succinate dehydrogenase	•	-2.7	-2.4	•
YKL141W	SDH3	succinate dehydrogenase	•	-2.5	-2.2	•
YDR178W	SDH4	succinate dehydrogenase	•	×	×	×
YPL262W	FUM1	fumarate hydratase	×	-3.4	-3.1	×
YKL085W	MDH1	malate dehydrogenase (mitochondrial)	+	-2.4	-2.9	•
Glyoxylate Cycle						
YCR005C	CIT2	citrate synthase (peroxisomal)	-6.4	+2.1	+	+4.7
YER065C	ICL1	isocitrate lyase	-4.1	+2.3	•	+9.3
YNL117W	MLS1	malate synthase	-7.1	+	•	×
YOL126C	MDH2	malate dehydrogenase	-2.2	+	•	•

*Significantly different as determined by a paired t-test ($P \leq 0.05$)

The level of gene expression changes in *S. cerevisiae* fermenting Icewine juice in comparison to gene expression changes in *S. cerevisiae* fermenting dilute Icewine juice are shown as either positive (+ fold upregulation) or negative (-fold downregulation) values. A plus sign (+) or minus sign (-) alone indicates significant difference in gene expression but less than a 2-fold change; • indicates no significant difference in gene expression; × indicates no expression was detected.

fructose-1,6-bisphosphate. The difference in *PFK1* expression between fermentation conditions was nearly six-fold on days three and four. Pyruvate kinase (*PYK1*) catalyzes the final and irreversible reaction of glycolysis, which involves the transfer of energy stored in phosphoenolpyruvate to ADP to form ATP. *PYK1* was upregulated on day two of the Icewine juice fermentation but was downregulated approximately three-fold on days three and four. Reduced expression of the genes involved in these three key glycolytic reactions by yeast fermenting Icewine juice also corresponded to an overall decreased rate of reducing sugar consumption throughout this fermentation, as illustrated in Figure 4.2.3.

The expression of additional genes associated with all the other steps of glycolysis and alcoholic fermentation, including those that are redox reactive, followed the same trend (Table 4.2.1). For example, Glyceraldehyde-3-phosphate dehydrogenase is encoded by three highly homologous genes (*TDH1*, *TDH2* and *TDH3*) and the gene product participates in the reversible redox reactive conversion of glyceraldehyde-3-phosphate to 1,3-bisphosphoglycerate, resulting in the formation of NADH. The expression of all three isoforms was strongly reduced up to 6.7-fold on days three and four in the Icewine juice condition relative to the dilute juice condition.

Pyruvate metabolism represents a central branch point in carbohydrate metabolism in yeast since it can either: (1) follow a reductive route, where it is decarboxylated to acetaldehyde and in turn be further reduced to ethanol by alcoholic fermentation; or (2) follow an oxidative route to form oxaloacetate and/or acetyl-CoA, both of which can enter the TCA cycle (Pronk *et al.*, 1996) (Figure 4.2.4). The fermentative route consists of two enzymatic reactions, the first of which is catalyzed by

pyruvate decarboxylase. *PDC1*, *PDC5* and *PDC6* encode for three isozymes of pyruvate decarboxylase, which catalyze the decarboxylation of pyruvate to acetaldehyde. All three *PDC* isoforms were expressed approximately two-fold higher in those yeast cells fermenting Icewine juice on day two. On days three and four, these isoforms were increasingly downregulated in the Icewine juice condition. By day five, the difference in expression of the major isoform (*PDC1*) was ten-fold between fermentations.

The second step of alcoholic fermentation is the reduction of acetaldehyde to ethanol, which regenerates oxidized cofactor, NAD^+. This reaction is catalyzed by alcohol dehydrogenases and the cytosolic isoforms (*ADH1*, *ADH2* and *ADH5*), together with the mitochondrial isoform (*ADH3*), were for the most part downregulated throughout the first few days of the Icewine fermentation (Table 4.2.1). A minor mitochondrial isoform encoded by the gene *ADH4* showed a two-fold increase in expression in yeast fermenting Icewine juice on day two, but no expression of this gene was detected in either fermentation condition on subsequent days. The higher expression of all three *PDC* isoforms on day two of the Icewine juice fermentation, combined with the general downregulation of *ADH* expression, possibly corresponds to the spike in acetaldehyde levels measured early on in the Icewine fermentation, along with lowered ethanol levels measured at the end of the fermentation (see Section 4.5.1.1).

4.2.1.3.2. TCA and glyoxylate cycles

RNA expression signals for the genes involved in the TCA cycle were detected using the microarrays (Table 4.2.1), allowing for the expression profile of these genes to be compared between fermentation conditions. In general, the expression of genes associated with the TCA cycle was at least two-fold lower on days three and four during

the Icewine juice fermentation condition compared to the dilute juice fermentation. Two of the five genes that encode for subunits of the pyruvate dehydrogenase enzyme complex (*PDA1* and *PDB1*), which catalyzes the conversion of pyruvate to acetyl-CoA and the formation of NADH, were weakly downregulated in Icewine juice fermenting cells. The two genes encoding for both subunits of NAD^+-dependent isocitrate dehydrogenase (*IDH1* and *IDH2*), which is responsible for catalyzing the oxidative decarboxylation of isocitrate to α-ketoglutarate, were differentially expressed between fermentation conditions. The TCA cycle intermediate α-ketoglutarate formed in this reaction then can be used for other metabolic reactions such as glutamate biosynthesis. Expression of the genes encoding for subunits of α-ketoglutarate dehydrogenase (*KGD1* and *KGD2*), succinyl-CoA ligase (*LSC1* and *LSC2*), as well as the subunits of the succinate dehydrogenase enzyme complex (*SDH1-4*), were lower at least two-fold on days three and four of the Icewine fermentation relative to the dilute juice fermentation. Malate dehydrogenase (*MDH1*) either catalyzes the final reaction of the oxidative branch of the TCA cycle, thereby producing reduced cofactor (NADH), or catalyzes the first reaction of the reductive branch, which generates oxidized cofactor (NAD^+). The expression of this gene followed a similar pattern established by the other genes of the TCA cycle during the Icewine juice fermentation.

Despite the fact that the expression of genes encoding for enzymes of the glyoxylate cycle, such as isocitrate lyase (*ICL1*) and malate synthase (*MLS1*), have been reported in the past to be subject to glucose repression (reviewed in Krukeberg and Dickinson, 2004), expression signals were detected for these genes associated with this pathway in yeast under both fermentation conditions, even in the presence of high

concentrations glucose still remaining in the fermenting juice (see Figure 4.2.3). A 4.1- and 7.1-fold lower expression of *ICL1* and *MLS1*, respectively, was observed in Icewine juice fermenting yeast on day two compared to dilute juice fermenting yeast (Table 4.2.1). The genes encoding for peroxisomal citrate synthase (*CIT2*) and cytosolic malate dehydrogenase (*MDH2*) followed a similar trend. Aconitase (encoded by *ACO1*) is located both in the mitochondrion and in the cytosol. *ACO1* can also participate in the continuation of the glyoxylate cycle by reforming isocitrate from citrate. On day two, no significant difference in *ACO1* expression was observed between fermentations. However, increased expression levels of *CIT2* and *ICL1* were observed on days three and five of the Icewine juice fermentation.

4.2.2. Discussion - Sugar Metabolism

Glucose and fructose are the primary fermentable sugars in grape juice cofermented to generate ethanol and carbon dioxide (Fleet and Heard, 1993). Although fructose is used concurrently with glucose during table wine fermentation, *S. cerevisiae* can be described as glucophilic such that glucose is typically depleted from the juice first, giving rise to a difference between the rate of glucose and fructose consumed during fermentation (Berthels *et al.*, 2004). Under both the Icewine and dilute juice conditions, it was observed that the rate of fructose fermentation by yeast lagged behind the rate of glucose fermentation (Figure 4.2.3). However, this difference in hexose fermentation was more extensive in the Icewine juice condition. The variability between the rates of hexose utilization by *S. cerevisiae* during wine fermentation was found to be both strain dependent and is also influenced by ethanol and assimilable nitrogen levels in the must (Berthels *et al.*, 2004).

The expression profile of glycolytic and alcoholic fermentation genes from the microarray data generated in this study revealed that osmotically stressed wine yeast fermenting Icewine juice undergo a specific transcriptional change in sugar metabolism over time in response to the presence of high concentrations of fermentable sugars and this change in expression appears to slow sugar consumption rates. Sugar uptake by yeast cells has been proposed as a rate-limiting step of glycolysis (reviewed in Kruckeberg and Dickinson, 2004). Of the 20 genes encoding for different hexose transport-related proteins identified in *S. cerevisiae* (Wieczorke *et al.*, 1999), only a small subset of these were found to be differently expressed by yeast between the Icewine and diluted juice fermentation conditions (Table 4.2.1). Contrary to our results, microarray analysis has shown that *HXT5* is upregulated in laboratory yeast strains under several stress conditions including salt-induced osmotic stress (Hirayama *et al.*, 1995; Posas *et al.*, 2000; Rep *et al.*, 2000; Gasch *et al.*, 2000) and *HXT5* expression was also upregulated in wine yeast two hours after exposure to high sugar stress (Erasmus *et al.*, 2003). However, these responses are the initial responses of the yeast just hours after exposure to stress. The expression of six *HXT* genes, including HXT5 (*HXT1*, *4*, *5*, *8*, *10* and *12*), was found to be downregulated more than two-fold in *S. cerevisiae* on days three to five of the Icewine juice fermentation. The downregulation of the *HXT* sugar transporter genes in yeast early on in Icewine fermentation may contribute to the reduced sugar consumption rate, by controlling the rate of sugar transported across the plasma membrane in the presence of over 400 g L^{-1} of fermentable sugars in the starting juice. Also, the downregulation of these genes may also be in response to the downregulation of genes associated with glycolysis and alcoholic fermentation, since many factors affect the number of sugar

transporters occupying the plasma membrane of wine yeast cells and their affinities for hexoses. These factors include stage and rate of cell growth, nutrient availability and rate of carbon flux through the glycolytic pathway, in addition to extracellular sugar concentration (reviewed in Pretorius, 2000). The overall reduced sugar consumption rate observed in the Icewine fermentation is also in agreement with the reduction in expression of the gene encoding the rate-limiting step of glycolysis, phosphofructokinase (Table 4.2.1). Although on day two, several genes involved in the glycolytic pathway were expressed at relatively higher levels in yeast fermenting Icewine juice compared to the dilute juice, these same genes in addition to those associated with alcoholic fermentation, were significantly downregulated between fermentation conditions after day two, in agreement with the lower sugar consumption rate observed during the Icewine fermentation.

The relatively higher expression level of many of the glycolytic genes in the Icewine condition on day two of the fermentation may be related to glycerol production as opposed to ethanol production. In this study, *HXK2* and *GLK1* were significantly upregulated in wine yeast on separate days of Icewine fermentation (Table 4.2.1), but this is in opposition to the downregulation of the hexose transporters. It was previously shown by Singh and Norton (1991) that changes in yeast metabolism were induced during the adaptation of a laboratory strain of *S. cerevisiae* exposed to salt stress over an 8 h period. When exponentially growing yeast were transferred to a growth medium containing 8% (w/v) NaCl, it was found that the rates of ethanol production and glucose consumption in these stressed cells were reduced more than two-fold over those for yeast not exposed to salt. Intracellular measurements of glycolytic intermediates revealed an

accumulation of sugar phosphates associated with the upper half of the glycolytic pathway, which occurred in yeast 3 to 4 h after the transfer to salt. The decreased expression of glyceraldehyde-3-phosphate dehydrogenase (*TDH*) isoforms observed in wine yeast fermenting Icewine juice support this finding (Table 4.2.1), in that this reduced expression may separate the metabolic intermediate pools of the upper and lower halves of the glycolytic pathway and allow for the accumulation of triose phosphates, specifically DHAP, which is required for glycerol synthesis in response to osmotic stress. Both DHAP and NADH are substrates required for glycerol formation and therefore, cells need to replenish the intracellular pools of these substrates during osmoadaptation to allow glycerol synthesis to continue under hyperosmotic stress.

The increase in *PDC* expression and decrease in *ADH* expression on day two of the Icewine fermentation (Table 4.2.1) may facilitate the redirection of carbon towards acetaldehyde production for acetic acid biosynthesis and away from the more redox unfavourable pathway involving alcohol production, while osmotically stressed wine yeast cells are fermenting sugar in addition to synthesizing glycerol. Interestingly, acetaldehyde production significantly increased in the Icewine condition on day two of the fermentation (Figure 4.5.1).

Yeast cells downregulate the expression of genes involved in mitochondrial functions, including respiration and the metabolism of alternate carbon sources, such as ethanol and acetate, through carbon catabolite repression in the presence of fermentable sugars (Gancedo, 1998). It has been previously established, through genomic expression profiling using microarray analysis, that the genes associated with aerobic energy generation are induced upon a shift from glucose fermentation to respiratory growth

(Gasch *et al.*, 2000; Causton *et al.*, 2001). However, genes encoding for proteins involved in the TCA cycle, respiration and gluconeogenesis were still expressed but at very low levels during the fermentation of synthetic must containing 200 g L^{-1} sugar (Rossignol *et al.*, 2003). In my study, the genes associated with the TCA cycle and the glyoxylate cycle were detected on the microarrays, and further, were differentially expressed between fermentation conditions (Table 4.2.1). Residual activity of TCA enzymes is maintained during fermentation to supply metabolic precursors to biosynthetic pathways (such as amino acid synthesis), but this activity results in the production of organic acids such as citrate, malate and succinate (Radler, 1993; Camarasa *et al.*, 2003). The TCA cycle has been proposed to operate in a noncyclic fashion under anaerobic conditions and can be divided into two pathways: a cytosolic reductive pathway from oxaloacetate forming NAD^+ or FAD, and a NADH forming mitochondrial oxidative pathway beginning at α-ketoglutarate (Radler, 1993; Camarasa *et al.*, 2003). Although it is unclear what pathway operates in yeast during wine fermentation, or even if the pathways are operative, genes of the TCA cycle were expressed at significantly lower levels most prominently on day four of the Icewine juice fermentation (Table 4.2.1). So it is unlikely that either pathway (reductive or oxidative) has an impact on the cytosolic redox balance of Icewine juice cells during the first five days of fermentation. Genes associated with the glyoxylate cycle were downregulated on day two, but *CIT2* (peroxisomal citrate synthase) and *ICL1* (isocitrate lyase) were strongly upregulated as the Icewine fermentation progressed. Interestingly, the reaction catalyzed by Icl1p results in the production of both glyoxylate and succinate. So, the glyoxylate cycle may be another pathway, in addition to the oxidative and reductive pathways of the TCA cycle, which potentially contributes to

succinate production by yeast during fermentation. Under osmotic stress, the glyoxylate cycle may partially function to recycle metabolic intermediates. This pathway may also involve shuttling two carbon acetyl units in the form of acetyl-CoA between metabolites if acetyl-CoA is not being used for other anabolic reactions like amino acid synthesis (see Section 4.3), in response to a decreased availability of acetyl-CoA. The expression of the genes encoding for both acetyl-CoA synthetases (*ACS1* and *ACS2*) were found to be significantly lower in Icewine juice fermenting yeast compared to their dilute juice counterparts (refer to Figure 4.5.4) and will be further discussed in the context of acetic acid metabolism in Section 4.5.

4.3. Nitrogen Metabolism

4.3.1. Results- Nitrogen Metabolism

4.3.1.1. Amino acid composition and nitrogen utilization

Initially, there was approximately twice the amount of assimilable nitrogen in the unfermented Icewine juice (388.1 ± 5.5 mg N L^{-1}) compared to the diluted juice (184.7 ± 10.7 mg N L^{-1}) (Figure 4.3.1A). Yeast fermenting Icewine juice also displayed a slower rate of nitrogen uptake compared to the dilute juice fermenting cells (Figure 4.3.1A). Using the *O*-phthaldialdehyde (NOPA) assay to measure total nitrogen content in the fermenting juices, it appeared that yeast under both juice conditions only took up nitrogen during the first five days of the fermentations (Figure 4.3.1A) corresponding to entry into stationary phase. At this timepoint, dilute juice fermenting yeast cells had depleted nearly all of the pool of assimilable amino acids (Figure 4.3.1A) whereas the Icewine juice fermenting cells utilized only 20% (78.9 ± 2.5 mg N L^{-1}) of available amino acid nitrogen

present in the juice. Although the starting concentration of ammonia present in the unfermented Icewine juice was approximately two-fold higher than the concentration in the diluted Icewine juice (Figure 4.3.1B), the rate of ammonia uptake by Icewine juice fermenting cells lagged behind yeast cells fermenting the diluted juice.

The results presented here clearly show differences in both the rate and degree of total amino acid nitrogen utilization between fermentation conditions. However, information on the differences in the usage of individual amino acids by commercial wine yeast during fermentation, especially yeast under hyperosmotic stress, is very limited. The NOPA assay cannot be used to quantify individual amino acids in a wine sample. This assay is based on the derivatization of all primary amino groups to their corresponding isoindole counterparts, thereby excluding proline, in order to spectrophotometrically measure the total yeast assimilable nitrogen (YAN) levels present in a sample (Dukes and Butzke, 1998). In past studies, HPLC was used by Sanders and Ough (1985) and by Monteiro and Bisson (1991a and 1991b) to separate and quantify individual amino acids present in unfermented grape musts, using the *O*-phthaldialdehyde (OPA) derivatives of amino acids, and to determine the patterns of amino acid utilization by two commercial wine yeast strains. Therefore, in this study, HPLC was used to measure the changes in the uptake of individual amino acids, including GABA and proline by yeast during Icewine and diluted juice fermentations.

The distribution of amino acids in the unfermented Icewine juice is shown in Figure 4.3.2. Of the amino acids identified and quantified using HPLC, four amino acids, cysteine, lysine, methionine and tyrosine, were not detected in the initial Icewine and diluted juices and in the samples collected throughout the duration of the fermentations.

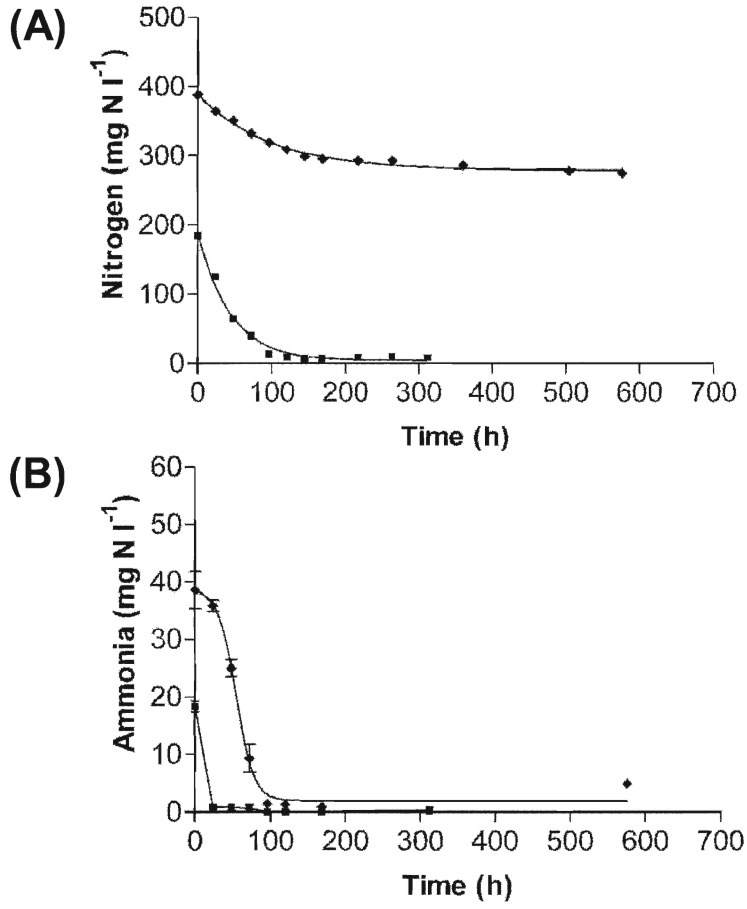

Figure 4.3.1: Yeast nitrogen utilization. Fermentations of Icewine juice (♦) and diluted Icewine juice (■) were monitored daily for total nitrogen utilization (A) and ammonia (B) throughout the course of the fermentations. Fermentations were performed in triplicate with measurements performed in duplicate. The mean values ± standard deviation were calculated but some error bars are smaller than the symbols representing each fermentation condition.

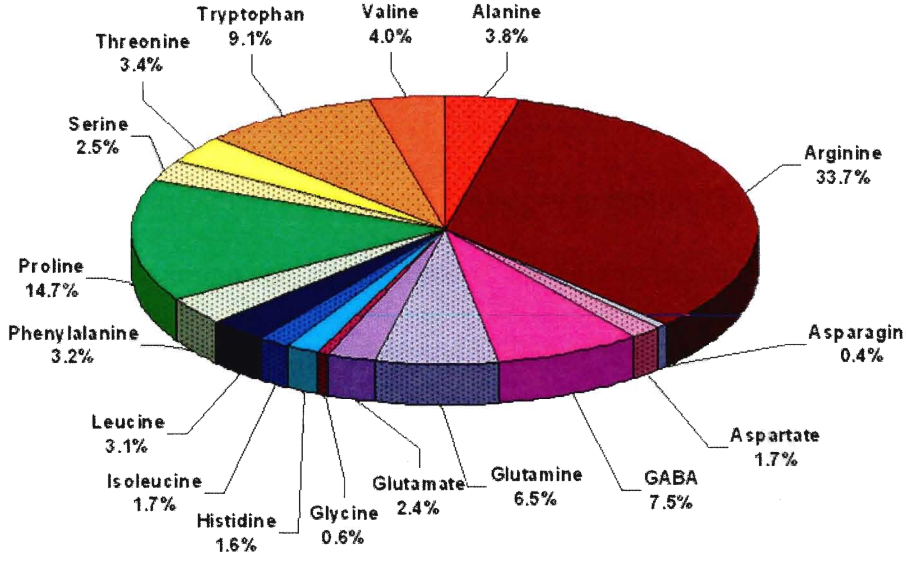

Figure 4.3.2: Distribution of amino acids in unfermented Icewine juice. The percentage of each amino acid present in the initial juice is shown.

The remaining amino acids shown in Figure 4.3.2 and listed in Tables 4.3.1 and 4.3.2 were quantified using HPLC. Although at the start of the fermentations, the diluted Icewine juice contained half the amount of each amino acid in comparison to the undiluted and unfermented Icewine juice, the percent contribution of each amino acid to the total YAN content was approximately equivalent between juices (Tables 4.3.1 and 4.3.2). Arginine and proline were the predominant amino acids present in Icewine juice. The initial arginine concentration of 1535 mg L^{-1} (122.8 mg N L^{-1}) represented 33.7% of the total amino acids measured, while the contribution of the initial proline concentration of 668 mg L^{-1} to the overall amino acid content in the juice was 14.7% at the start of the fermentation. However, proline does not contribute to YAN under anaerobic conditions. Considerable concentrations of GABA, tryptophan and glutamine were also present in the starting Icewine juice, such that each nitrogen compound was found to be 7.5% and 9.1% and 6.5% of the YAN nitrogen in the juice, respectively (Table 4.3.1). Branched chain amino acids leucine, isoleucine and valine occupied a smaller portion of the total amino acids measured (less than 10% combined). Glycine made up only 0.6% of the amino acids measured. In addition to the amino acids measured, ammonia also made up a considerable portion of the YAN (nearly 10%).

Regarding the distribution of amino acid nitrogen present in the Icewine juice 168 h post-inoculation where amino acid uptake ceased, the bulk of the amino acids remaining were arginine, proline, tryptophan and GABA (Figure 4.3.3). This timepoint (168 h) was used to compare the differences in amino acid usage, as it represents the stage where yeast cells under both fermentation conditions have almost ceased nitrogen uptake and it also represents the time before cells lyse and release their intracellular

Table 4.3.1: Amino acids present in unfermented Icewine juice and finished wine.

	Juice			Wine		
Amino Acid	mg L^{-1}	mg N L^{-1}	% Total YAN	mg L^{-1}	mg N L^{-1}	% Total YAN
Alanine	173.6 ± 16.4	27.3 ± 2.6	6.6	113.5 ± 4.0	17.8 ± 0.6	6.4
Arginine	1535.2 ± 20.1	122.8 ± 1.6	29.5	1273.1 ± 29.0	101.9 ± 10.3	36.6
Asparagine	20.35 ± 1.7	2.1 ± 0.2	0.5	13.5 ± 1.5	1.4 ± 0.2	0.5
Aspartate	76.5 ± 6.5	8.0 ± 0.7	1.9	48.9 ± 4.6	5.1 ± 0.5	1.8
GABA	343.1 ± 13.0	46.7 ± 1.8	11.2	319.6 ± 49.1	43.5 ± 6.7	15.6
Glutamate	109.6 ± 9.2	10.4 ± 0.9	2.5	95.7 ± 11.0	9.1 ± 1.0	3.3
Glutamine	298.1 ± 22.5	28.3 ± 2.1	6.8	202.9 ± 20.0	19.3 ± 1.9	6.9
Glycine	29.5 ± 1.2	5.5 ± 0.2	1.3	14.3 ± 1.5	2.7 ± 0.3	1.0
Histidine	72.6 ± 4.1	6.5 ± 0.4	1.6	45.3 ± 6.6	4.1 ± 0.6	1.5
Isoleucine	78.7 ± 7.0	8.4 ± 0.8	2.0	0.0 ± 0.0	0.0 ± 0.0	0.0
Leucine	139.7 ± 5.6	15.0 ± 0.6	3.6	23.6 ± 7.9	2.5 ± 0.8	0.9
Phenylalanine	145.6 ± 18.0	12.4 ± 1.5	3.0	109.6 ± 10.8	9.3 ± 0.9	3.3
Proline	668.2 ± 15.1	-	-	674.0 ± 57.0	-	-
Serine	114.9 ± 5.3	15.3 ± 0.7	3.7	54.0 ± 5.6	7.2 ± 0.7	2.6
Threonine	152.7 ± 7.4	18.0 ± 0.9	4.3	68.7 ± 19.7	8.1 ± 2.3	2.9
Tryptophan	416.2 ± 18.6	28.7 ± 1.3	6.9	383.5 ± 36.2	26.5 ± 2.5	9.5
Valine	180.1 ± 14.2	21.6 ± 1.7	5.2	122.3 ± 16.1	14.7 ± 1.9	5.5
Total amino acid	4554.7 ± 84.4	377.1 ± 9.6		3557.5 ± 342.0	273.2 ± 27.1	
Ammonia	49.2 ± 3.2	38.6 ± 3.2	9.3	6.2 ± 0.5	4.9 ± 0.5	1.8
Total YAN		**415.7**	100		**278.1**	100

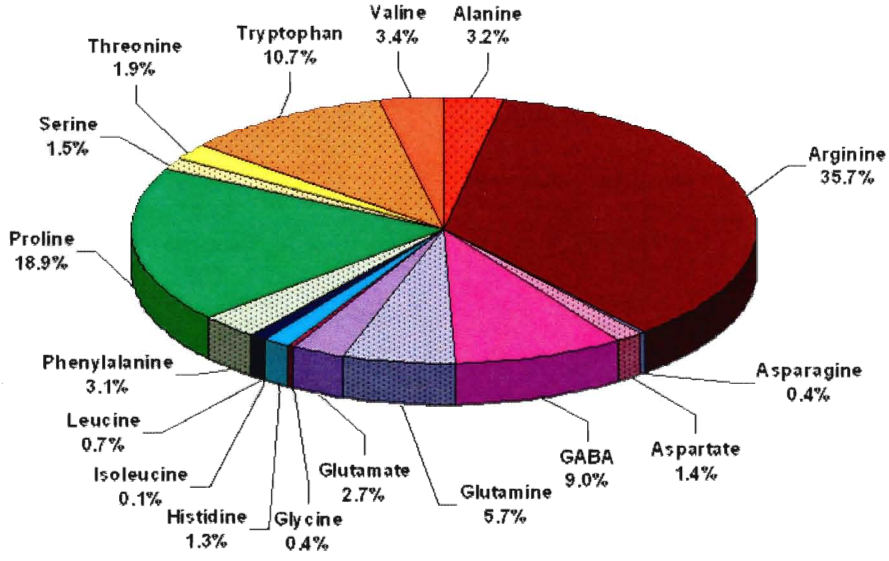

Figure 4.3.3: Distribution of amino acids in Icewine juice 168 h post-inoculation.

Table 4.3.2: Amino acids present in unfermented diluted Icewine juice and finished wine.

	Juice			Wine		
Amino Acid	mg L^{-1}	mg N L^{-1}	% Total YAN	mg L^{-1}	mg N L^{-1}	% Total YAN
Alanine	61.2 ± 12.0	9.6 ± 1.9	5.8	0.6 ± 3.2	0.1 ± 0.5	2.8
Arginine	592.9 ± 34.5	47.3 ± 2.8	28.7	0.1 ± 2.7	0.0 ± 0.2	0.0
Asparagine	7.0 ± 0.7	0.7 ± 0.1	0.4	0.0 ± 0.6	0.0 ± 0.1	0.0
Aspartate	29.2 ± 2.1	3.1 ± 0.2	1.9	0.5 ± 0.9	0.1 ± 0.1	2.8
GABA	136.9 ± 8.2	18.6 ± 1.1	11.3	0.0 ± 0.0	0.0 ± 0.0	0.0
Glutamate	42.1 ± 4.2	4.0 ± 0.4	2.4	0.0 ± 1.8	0.0 ± 0.1	0.0
Glutamine	117.6 ± 3.8	11.2 ± 0.4	6.8	0.0 ± 0.0	0.0 ± 0.0	0.0
Glycine	7.4 ± 0.5	1.4 ± 0.1	0.9	1.0 ± 0.6	0.2 ± 0.1	5.6
Histidine	26.5 ± 3.2	2.4 ± 0.3	1.5	2.9 ± 1.9	0.3 ± 0.2	8.3
Isoleucine	32.0 ± 6.5	3.4 ± 0.7	2.1	0.0 ± 0.0	0.0 ± 0.1	0.0
Leucine	53.5 ± 2.6	5.7 ± 0.3	3.5	0.0 ± 0.0	0.0 ± 0.8	0.0
Phenylalanine	57.4 ± 11.2	4.9 ± 1.0	3.0	0.9 ± 1.9	0.1 ± 0.2	2.8
Proline	304.7 ± 16.0	-	-	281.9 ± 8.4	-	-
Serine	43.5 ± 2.5	5.8 ± 0.3	3.5	2.2 ± 0.5	0.3 ± 0.1	8.3
Threonine	58.5 ± 3.9	6.9 ± 0.5	4.2	4.3 ± 2.4	0.5 ± 0.3	13.9
Tryptophan	170.7 ± 14.7	11.8 ± 1.0	7.2	3.6 ± 0.9	0.3 ± 0.1	8.3
Valine	70.4 ± 5.5	8.5 ± 0.7	5.2	14.3 ± 3.3	1.7 ± 0.4	47.2
Total amino acid	1811.2 ± 98.3	145.3 ± 8.3		310.0 ± 28.0	3.6 ± 2.2	
Ammonia	24.7 ± 1.7	19.3 ± 1.7	11.7	0.0 ± 0.0	0.0 ± 0.0	0.0
Total YAN		**164.6**	100		**3.6**	100

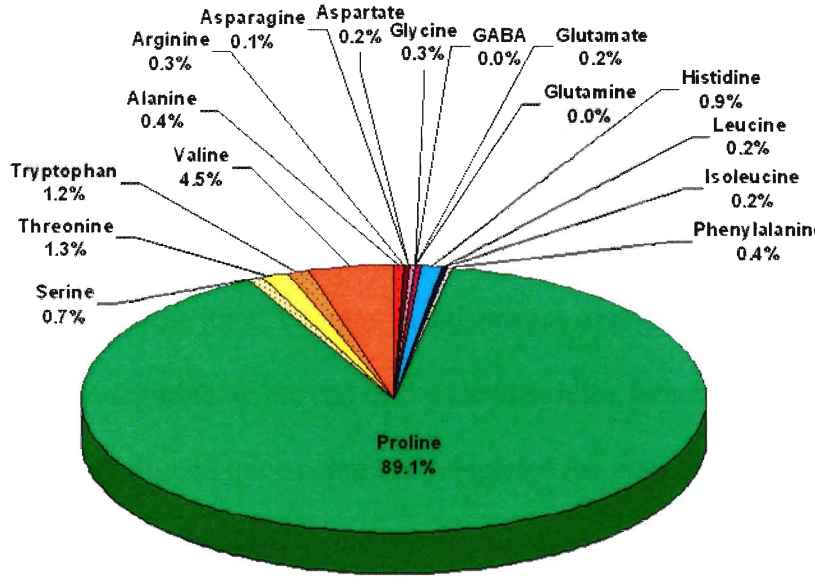

Figure 4.3.4: Distribution of amino acids in diluted Icewine juice 168 h post-inoculation.

contents into the finished wines, thereby skewing the results. Even though yeast fermenting Icewine juice failed to take up a substantial amount of each available amino acid, branched chain amino acids, leucine and isoleucine, were the only amino acids nearly or completely depleted in the juice (Table 4.3.1). In contrast, proline constituted nearly 90% of the amino acids still present in the diluted juice up to this timepoint with the residual amino acid concentrations making up the difference, individually ranging between 0-3.8% (Figure 4.3.4). In conjunction with the differences in the concentration of individual amino acids found in the finished wines compared to the starting concentrations in the initial juices, there were also obvious differences in the rate and degree of amino acid uptake over time between fermentation conditions. These results are presented in Tables 4.3.3 and 4.3.4, both of which illustrate the remaining percentage of each amino acid measured in the fermenting Icewine and diluted juices over time. Rapid uptake of amino acid nitrogen by yeast in the diluted juice condition was observed to occur 24 h into the fermentation, with near or complete depletion of the available amino acid pool by 48 to 72 h. In general, more than 50% of asparagine, aspartate, glutamine, isoleucine, leucine, serine and threonine were depleted in this juice condition after one day following inoculation. In contrast, uptake of amino acids occurred at a much slower rate by yeast fermenting Icewine juice. Despite the abundance of arginine, yeast took up only 10% of the available arginine by the end of the Icewine juice fermentation. However, yeast fermenting diluted juice completely depleted the pool of available arginine 96 h into the fermentation. GABA did not appear to be appreciably taken up by yeast fermenting Icewine juice. Conversely, by 48 h, nearly 20% of GABA was taken up

Table 4.3.3: Amino acid utilization over time by yeast fermenting Icewine juice.*

	Time (hrs)						
	0	24	48	72	96	120	168
Amino Acid							
Alanine	100.0	101.5	98.5	81.3	73.6	66.3	65.7
Arginine	100.0	99.9	97.5	93.5	90.0	84.3	82.9
Asparagine	100.0	97.8	83.5	74.1	71.7	59.3	66.4
Aspartate	100.0	96.2	88.2	82.5	76.3	64.8	64.1
GABA	100.0	103.0	98.6	100.1	102.8	97.3	93.1
Glutamate	100.0	103.1	103.5	100.4	96.9	89.1	87.4
Glutamine	100.0	97.2	88.2	87.9	77.2	69.6	68.0
Glycine	100.0	53.0	50.7	47.8	43.7	46.8	48.3
Histidine	100.0	96.1	82.9	79.2	70.5	62.4	62.4
Isoleucine	100.0	85.1	58.4	46.3	28.2	14.7	0.0
Leucine	100.0	84.4	56.7	44.4	30.6	19.9	16.9
Phenylalanine	100.0	93.8	85.3	88.4	81.2	69.3	76.0
Proline	100.0	104.4	101.5	102.0	99.3	99.1	101.0
Serine	100.0	95.6	81.1	73.5	62.5	49.4	47.1
Threonine	100.0	88.9	78.4	75.8	61.4	51.4	45.2
Tryptophan	100.0	106.7	103.8	93.5	96.0	88.1	92.0
Valine	100.0	97.8	93.0	85.2	77.8	72.3	68.0

* Shows the percentage of amino acids remaining in the juice relative to their starting concentrations.

Table 4.3.4: Amino acid utilization over time by yeast fermenting diluted Icewine juice.*

	Time (hrs)						
	0	24	48	72	96	120	168
Amino Acid							
Alanine	100.0	74.6	8.6	7.0	1.5	1.7	0.4
Arginine	100.0	92.9	37.3	2.2	0.2	0.4	0.0
Asparagine	100.0	22.5	0.0	0.0	0.0	0.0	0.0
Aspartate	100.0	40.0	0.0	3.2	1.7	1.7	1.6
GABA	100.0	101.4	82.0	84.1	28.6	0.0	0.0
Glutamate	100.0	76.7	2.8	0.0	0.0	0.0	0.0
Glutamine	100.0	38.2	0.8	1.2	0.0	0.0	0.0
Glycine	100.0	107.9	69.2	79.9	15.8	19.2	13.1
Histidine	100.0	77.7	11.1	3.1	9.7	12.6	10.6
Isoleucine	100.0	20.3	2.7	3.0	3.0	0.8	0.5
Leucine	100.0	22.5	1.1	0.0	0.0	1.3	0.0
Phenylalanine	100.0	89.1	3.3	3.5	0.3	1.0	1.4
Proline	100.0	110.5	46.9	51.9	69.4	72.4	92.6
Serine	100.0	22.6	6.0	6.7	3.5	5.7	5.0
Threonine	100.0	20.9	5.6	5.8	2.8	4.4	7.1
Tryptophan	100.0	114.4	121.2	126.6	29.0	5.3	2.1
Valine	100.0	79.5	33.6	36.7	21.9	24.6	20.2

* Shows the percentage of amino acids remaining in the juice relative to their starting concentrations.

by yeast fermenting diluted juice and by 120 h, all of the available GABA pool was exhausted.

With respect to the individual amino acids measured throughout the Icewine juice fermentation condition, approximately 90-100% of arginine, GABA, glutamate and tryptophan remained in the juice upon entry into stationary phase. So, 10% or less of each nitrogen compound was taken up by the yeast by the end of the fermentation. In the same fermentation condition, only 20-40% of alanine, asparagine, aspartate, glutamine, histidine and valine were taken up by yeast up to this timepoint. More than 50% of leucine, isoleucine, phenylalanine, serine, threonine and glycine were taken up by yeast by the end of the fermentation, coinciding with a lack of expression of corresponding permease genes, which will be further illustrated in subsequent sections. However, with respect to the individual amino acids measured in the diluted juice condition, there was a slight increase in glycine (less than 10%) and a more considerable increase in tryptophan (nearly 25%) over the first three days of fermentation before uptake at 96 h. There also seems to be a decrease in proline pools from days two to four even though yeast cannot use proline under fermentative conditions. Due to the large differences in nitrogen uptake between fermentation conditions, the results from the microarray experiments presented in the following section will try to correlate the changes in the expression of genes associated with nitrogen metabolism and transport to the patterns of amino acid uptake.

4.3.1.2. Gene expression profiles for nitrogen transport and metabolism

It has already been shown that Icewine juice fermenting cells consume only half of the amino acid nitrogen available to them, in comparison to dilute Icewine juice fermenting cells (Figure 4.3.1). *S. cerevisiae* is able to use different nitrogen sources for

growth but shows selectivity towards preferred nitrogen sources, like ammonia and glutamine. Repression the genes encoding for enzymes required for the utilization of poorer nitrogen sources, like ornithine, γ-aminobutyrate (GABA), allantoin and urea is invoked by a mechanism referred to as nitrogen catabolite repression (NCR) (reviewed in Magasanik and Kaiser, 2002).

The expression of yeast genes involved in nitrogen metabolism during Icewine juice fermentation was also profiled using microarray analysis (Table 4.3.5). Only four genes associated with amino acid catabolism showed significant differential expression between juice conditions. Expression of some of the genes encoding for enzymes involved in multiple amino acid biosynthesis pathways followed a similar trend. The expression of the majority of genes downregulated on day two of the Icewine juice conditions could be detected in either fermentation condition by day five.

On day two, several genes encoding for amino acid and polyamine transporters with variable substrate affinities and specificities were expressed (*AGP1*, *GNP1*, *HIP1*, *TPO2* and *TPO5*) but there was no significant difference in expression (Table 4.3.5). There was a two-fold increase in expression of the genes associated with glutamine (*GNP1*), proline (*PUT4*) and spermine (*TPO2*) transport on day three, as well as basic amino acid transport (*RHB1*) on day four of the Icewine juice fermentation. *DIP5* encodes for a dicarboxylic amino acid permease that exhibits a broad substrate specificity range, which includes glutamate (Regenberg *et al.*, 1999). *DIP5* expression was 4.7-fold lower on day two of the Icewine juice fermentation relative to the dilute juice fermentation, and corresponded to lowered expression of *GDH2* (glutamate dehydrogenase), which is involved in glutamate utilization. Expression of the GABA-

Table 4.3.5: Changes in the expression profile of genes involved in amino acid metabolism.

ORF	Gene	Description	Fold Change*			
			Day 2	Day 3	Day 4	Day 5
Nitrogen Transport						
YCL025C	AGP1	broad range amino acid permease	•	•	-2.4	•
YBR132C	AGP2	broad range amino acid permease	•	•	•	×
YNR002C	ATO2	ammonium transporter	-6.0	•	•	•
YDR384C	ATO3	ammonium transporter	-26.1	×	×	×
YBR068C	BAP2	branched chain amino acid permease	-	+	+	+2.0
YDR046C	BAP3	branched chain amino acid permease	-2.0	×	×	×
YEL063C	CAN1	basic amino acid permease	-	×	×	×
YPL265W	DIP5	dicarboxylic amino acid permease	-4.7	•	-	•
YKR039W	GAP1	general amino acid permease	×	×	-6.0	×
YDR508C	GNP1	high affinity glutamine permease	•	+2.1	+	×
YGR191W	HIP1	basic amino acid permease	•	×	-2.5	×
YNL142W	MEP2	ammonium permease	•	-	-7.1	×
YOR348C	PUT4	proline permease	-	+2.9	+	×
YCR027C	RHB1	basic amino acid permease	+	×	+2.4	×
YGR138C	TPO2	spermine transporter	•	+2.3	•	×
YOR273C	TPO4	spermine transporter	-3.0	×	×	×
YKL174C	TPO5	putative polyamine transporter	•	-3.9	-2.1	×
YDL210W	UGA4	GABA-specific permease	×	×	-2.1	×
Amino Acid Biosynthesis and Utilization						
YFL030W	AGX1	alanine-glyoxylate transaminase	•	-3.9	-6.9	×
YOL058W	ARG1	argininosuccinate synthase	-2.1	×	-5.9	×
YJL088W	ARG3	ornithine carbamoyltransferase	-2.1	+3.4	+3.0	×
YHR018C	ARG4	argininosuccinate lyase	-2.9	×	-	×
YGL202W	ARO8	aromatic-amino-acid transaminase	+	•	-2.8	×
YHR137W	ARO9	aromatic-amino-acid transaminase	+	+	+3.2	•
YDR380W	ARO10	similar to pyruvate decarboxylase	-	-2.8	×	×
YHR208W	BAT1	branched-chain-amino-acid transaminase	-	-	•	×
YJR148W	BAT2	branched-chain-amino-acid transaminase	-2.8	-2.4	-2.6	×
YPL111W	CAR1	arginase	+3.1	•	•	•
YOR303W	CPA1	carbamoyl-phosphate synthase	•	+4.1	×	×
YAL012W	CYS3	cystathionine gamma-lyase	+2.5	×	+2.5	×
YBR208C	DUR1,2	urea amidolyase	•	×	×	×
YMR250W	GAD1	glutamate decarboxylase	-	×	•	×
YOR375C	GDH1	glutamate dehydrogenase	-	•	•	-5.3
YDL215C	GDH2	glutamate dehydrogenase	-2.5	-	-2.2	×
YAL062W	GDH3	glutamate dehydrogenase	-3.7	•	-	•
YPR035W	GLN1	glutamine synthetase	×	-	-	-4.3
YDL171C	GLT1	glutamate synthase	-	•	-	×
YJR139C	HOM6	homoserine dehydrogenase	-	×	-2.2	×
YJR016C	ILV3	dihydroxy-acid dehydratase	•	-3.0	-3.1	-3.0
YLR355C	ILV5	ketol-acid reductoisomerase	-2.1	•	•	×
YNL104C	LEU4	2-isopropylmalate synthase	-5.5	•	•	×
YOR108W	LEU9	2-isopropylmalate synthase	-5.9	•	•	×
YDL182W	LYS20	homocitrate synthase	-	+	+	+3.5
YER091C	MET6	homocysteine methyltransferase	-2.4	•	•	×
YER023W	PRO3	pyrroline-5-carboxylate reductase	•	-2.7	-2.4	•
YGR208W	SER2	phosphoserine phosphatase	+2.4	×	×	×
YER081W	SER3	phosphoglycerate dehydrogenase	+2.7	+2.0	•	×
YDL168W	SFA1	long-chain alcohol dehydrogenase	+	+3.1	+3.4	×
YDL080C	THI1	alpha-ketoisocaproate decarboxylase	+2.2	×	×	×
YGR019W	UGA1	GABA transaminase	×	×	•	×
YBR006W	UGA2	succinate semialdehyde dehydrogenase	×	×	•	×
Nitrogen Metabolism Regulation						
YFL021W	GAT1	transcription factor	+3.7	+2.6	+5.9	+3.7
YGL195W	GCN4	transcription factor	•	-	-2.0	+2.5
YDL170W	UGA3	activator of GABA catabolic genes	×	+	+	×

*Significantly different as determined by a paired t-test ($P \leq 0.05$)

The level of gene expression changes in *S. cerevisiae* fermenting Icewine juice in comparison to gene expression changes in *S. cerevisiae* fermenting dilute Icewine juice are shown as either positive (+ fold upregulation) or negative (-fold downregulation) values. A plus sign (+) or minus sign (-) alone indicates significant difference in gene expression but less than a 2-fold change; • indicates no significant difference in gene expression; × indicates no expression was detected.

specific permease *UGA4* was approximately two-fold higher on day four of the dilute juice fermentation, corresponding to an increase of GABA uptake by these yeast cells (Table 4.3.5). However, the genes involved in both GABA synthesis (*GAD1*) and catabolism (*UGA1* and *UGA2*) were expressed at the same level between fermentation conditions also on day four. Additionally, genes encoding for ammonium ion transporters (*ATO2*, *ATO3* and *MEP2*) were similarly downregulated in the Icewine juice condition.

All pathways for nitrogen utilization converge into a common set of reactions involving glutamate and glutamine metabolism, which acts as a hub for further amino acid biosynthesis (Figure 4.3.5). Two $NADP^+$-dependent glutamate dehydrogenase isoforms (*GDH1* and *GDH3*) both displayed significantly lower expression during the Icewine juice fermentation compared to the dilute juice fermentation. The enzymes encoded by these isoforms generate glutamate from ammonia and the TCA cycle intermediate α-ketoglutarate. Conversely, *GDH2* catalyzes the reverse reaction, forming NADH and NH_4^+ in the process. *GDH2* was also significantly downregulated in yeast two-fold on days two and four of the Icewine juice fermentation. *GLN1* (glutamine synthase) and *GLT1* (glutamate synthase) are involved in the production and degradation of glutamine, respectively. *GLN1* was downregulated four-fold on day five of the Icewine juice fermentation, while *GLT1* showed a significant difference in expression between juice conditions but a less than two-fold difference change was observed. Genes encoding for some of the enzymes involved in the leucine, serine, valine and lysine biosynthetic pathways that require glutamate exhibited differential expression between juice conditions. Within the leucine biosynthetic pathway, *ILV5* (ketol-acid reductoisomerase) and *ILV3* (dihydroxy-acid dehydratase) catalyze the two step

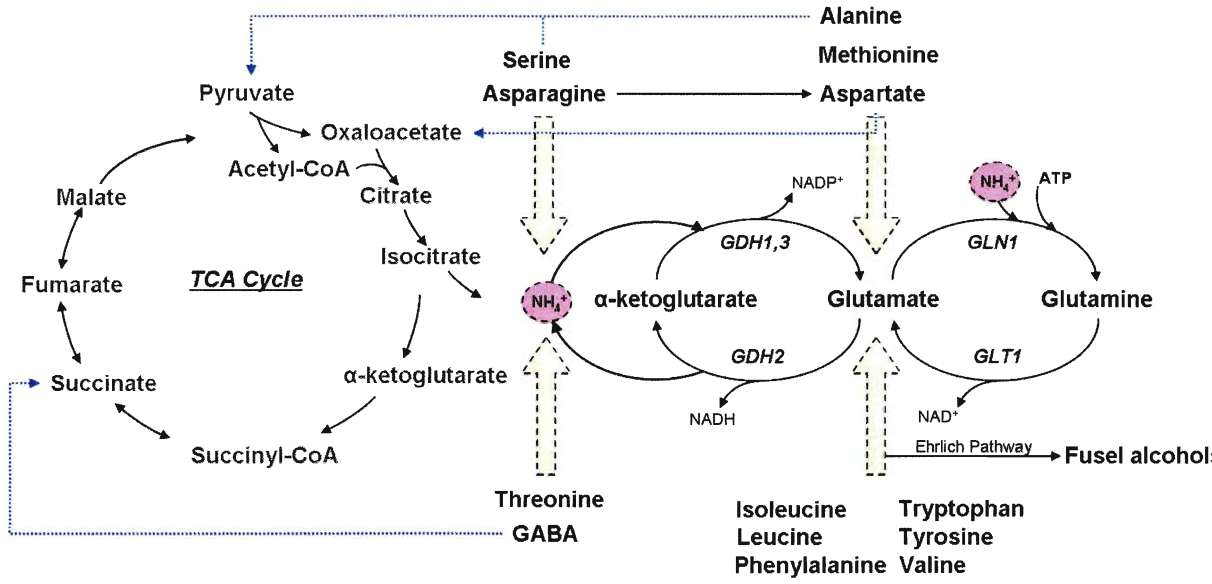

Figure 4.3.5: The central pathways of nitrogen metabolism in *S. cerevisiae*. Illustrated are the main routes associated with amino acid utilization involving deamination and transamination reactions leading to glutamate and/or ammonium ion formation (green arrows). Dashed blue lines represent pathways for the resulting carbon end products that feed into the TCA cycle. The genes associated with the enzymes involved in glutamate and glutamine metabolism are also shown (Adapted from Magasanik and Kaiser, 2002 and Godard *et al*., 2007).

conversion of α-acetolactate to 2,3-dihydroxyisovalerate and finally to α-ketoisovalerate. Expression of both *ILV3* and *ILV5* was observed to be at least two-fold lower in Icewine juice fermenting cells. *BAT2* (branched chain amino acid transaminase) followed a similar trend (Table 4.3.5). This transaminase catalyzes the conversion of one of the intermediates of the leucine biosynthetic pathway (α-ketoisovalerate) to valine, while regenerating α-ketoglutarate from glutamate (Figure 4.3.6). *LEU4* and *LEU9* both encode for isoenzymes (2-isopropylmalate synthase) involved in the conversion of α-ketoisovalerate to α-isopropylmalate, also within the leucine biosynthetic pathway. This reaction requires the utilization of an acetyl unit from acetyl-CoA, but the expression of both *LEU4* and *LEU9* was significantly reduced five-fold on day two of the Icewine juice in comparison to the dilute juice fermentation. The serine biosynthetic pathway involves a total of three enzymatic reactions and requires glutamate, but only two of the three genes associated with this pathway were differentially expressed between juice conditions.

Alternatively, the branched chain amino acids (isoleucine, leucine and valine) can enter a common pathway and be catabolized within a series of deamination, decarboxylation and reduction reactions catalyzed by shared enzymes to form higher (fusel) alcohols, as shown in Figure 4.3.6. The enzyme encoded by *SER3* (phosphoglycerate dehydrogenase) functions to convert the glycolytic intermediate 3-phosphoglycerate to 3-phosphohydroxypyruvate, while generating NADH in the process. Expression of this gene along with the expression of *SER2* (phosphoserine phosphatase), which dephosphorylates 3-phosphoserine to form serine, were found to be higher in yeast during Icewine juice fermentation as compared to the dilute juice fermentation.

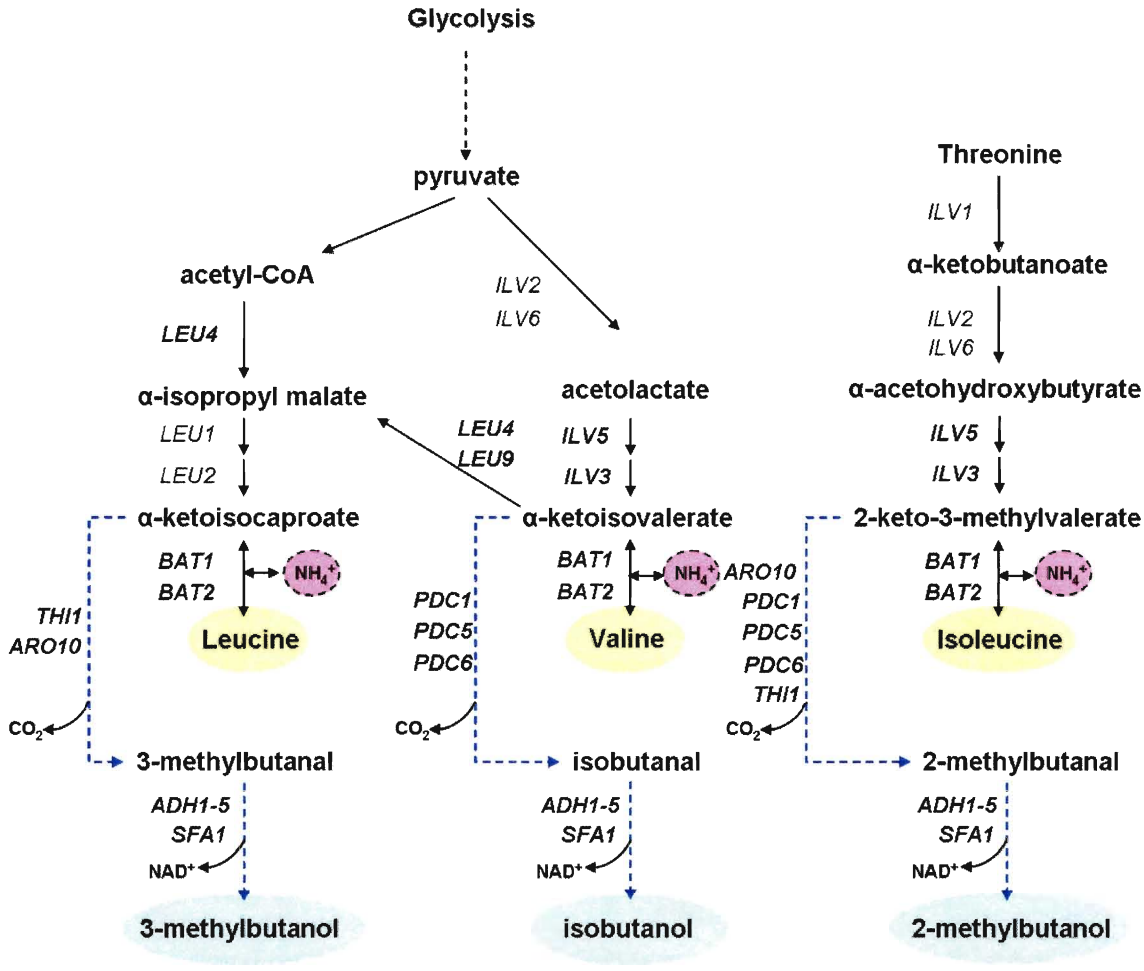

Figure 4.3.6: The pathways of branched chain amino acid metabolism in *S. cerevisiae*. Illustrated are the main routes associated with branched chain amino acid biosynthesis. Dashed blue lines represent pathways for fusel alcohol formation. Genes encoding for enzymes involved in these pathways are also shown and those in bold represent genes differentially expressed between fermentation conditions. (Adapted from Marks *et al.*, 2003).

The genes involved in arginine metabolism were also found to be differentially expressed between juice conditions (Table 4.3.5). *CAR1* (arginase), which is involved in the catabolism of arginine to ornithine and urea, was expressed three-fold higher in yeast fermenting Icewine juice on day two, but no significant difference in the expression of this gene was observed between juice conditions after this timepoint. However, arginine can be synthesized from glutamine and/or ornithine directly. The expression of three genes, whose products are involved in arginine synthesis from ornithine, was approximately two-fold higher on day two of the dilute juice fermentation compared to the Icewine juice fermentation (Table 4.3.5). In this pathway, ornithine is converted to citrulline via an ornithine carbamoyl transferase (*ARG3*). Citrulline is in turn converted into L-argininosuccinate by an argininosuccinate synthase and the last reaction is catalyzed by an argininosuccinate lyase (*ARG4*), which ultimately forms arginine. Alternatively, *CPA1* encodes for a carbamoyl phosphate synthase that serves to generate carbamoyl phosphate from glutamine. This intermediate is necessary for completing the downstream reaction catalyzed by ornithine carbamoyl transferase. *CPA1* was upregulated four-fold on day three of the Icewine juice fermentation while *ARG3* was similarly upregulated on days three and four. Genes involved in the biosynthesis of aromatic amino acids (*ARO8* and *ARO9*), cysteine (*CYS3*), homoserine (*HOM6*), lysine (*LYS20*), methionine (*MET6*) and proline (*PRO3*) were also differentially expressed between fermentation conditions (Table 4.3.5).

Nitrogen metabolism is tightly regulated in *S. cerevisiae*. Both *GAT1* and *GCN4* are transcriptional activators associated with the activation of a large number of NCR-sensitive genes connected with the transport and catabolism of nonpreferential amino

acids during nitrogen starvation. *GAT1* was more highly expressed throughout the Icewine juice fermentation and showed a nearly six-fold increase in expression on day four relative to the other fermentation condition (Table 4.3.5). Under Icewine fermentation conditions, *GCN4* was downregulated on days three and four but upregulated 2.5-fold on day five.

4.3.2. Discussion - Nitrogen Metabolism

4.3.2.1. Amino acid content of Icewine juice

The nitrogenous composition of Icewine juice has not been previously reported. In grape juice used for table wine production, ammonium ions and amino acids are the two main sources of yeast assimilable nitrogen compounds with ammonium ions taking up a large percentage (up to 40%) of the total YAN. Although proline and arginine are the most common nitrogenous compounds present in juice (35-60% of total amino acid content) (Beltran *et al.*, 2004; reviewed in Boulton *et al.*, 1998), proline is normally not metabolized during fermentation and must be excluded from YAN calculations. The concentrations of ammonium, proline and arginine measured in Icewine juice used in this study did fall into these projected ranges, however, it was also found that the aromatic amino acid tryptophan contributed to nearly 10% of the total amino acid content. Furthermore, like GABA, high levels of tryptophan present in the Icewine juice may be a result of subjecting the grapes from which this juice was derived to multiple freeze-thaw cycles thereby concentrating and eventually changing the juice's nitrogen profile over time.

The results presented in this study has demonstrated that despite the abundance of amino acids, osmotically stressed yeast in Icewine juice struggled to utilize both good

and poor sources of nitrogen throughout the fermentation compared to their diluted juice fermenting counterparts. In the following sections, these differences in amino acid utilization by yeast between fermentation conditions will be related to differences in the expression of genes associated with amino acid transport and metabolism.

4.3.2.2. General amino acid transport

The microarray transcription profiles of three general amino acid permeases (*AGP1*, *AGP2* and *GAP1*) revealed that these genes were expressed in yeast under Icewine and diluted juice conditions up to day five of the fermentations. In general, there was no significant difference in the expression of broad range amino acid permeases *AGP1* and *AGP2* between yeast exposed to high osmotic conditions and in the presence of non-limiting nitrogen sources compared to those under less osmotically stressful but increasingly nitrogen-limiting conditions. The expression of *AGP2* was previously observed to be downregulated by salt and sorbitol induced osmotic stress (Lee *et al.*, 2002). Also, the expression level of *AGP2* was found to be 10-fold lower than the more highly expressed general permeases (*GAP1* and *AGP1*) in laboratory yeast strains grown under nitrogen limiting conditions on minimal media (Schreve and Garrett, 2004). Despite these observations, *AGP2* was still expressed in wine yeast under both fermentative conditions in my study. *GAP1* also encodes a general amino acid permease that governs the uptake of all naturally occurring L-amino acids and other nitrogenous compounds including polyamines and GABA. But, its expression is subject to NCR thereby facilitating the transport of poorer sources in the absence of optimal nitrogen sources like glutamate and glutamine (Stanbrough and Magasanik, 1995; Regenberg *et al.*, 1999; reviewed in Boulton *et al.*, 1998; ter Schure *et al.*, 2000). In my study, it was

observed that the expression of *GAP1* was only detected on day four of the fermentations but it was expressed at much lower levels in the Icewine condition in conjunction with *AGP1*. The relatively higher expression of *GAP1* in the dilute juice condition versus the Icewine juice condition corresponds to a timepoint when nitrogen levels in the diluted juice had become extremely limiting and preferable amino acids had been completely depleted. In comparison, Icewine juice fermenting cells still had access to preferable nitrogen sources like glutamate and glutamine up to this timepoint. The lower expression of genes encoding for broad specificity amino acid transporters like *AGP1* and *GAP1* may indicate a necessity for yeast to have a tighter control over the rate of amino acid transport into the cell under Icewine fermentation conditions where high concentrations of amino acids, in addition to sugar and other solutes, contribute to the overall hyperosmotic environment. In a study by Norbeck and Blomberg (1998), uptake of methionine, leucine and histidine was found to be greatly reduced in laboratory yeast strains grown the presence of sodium chloride compared to strains grown without salt. They proposed that reduced amino acid uptake in salt stressed yeast cells was due to a lack of the expression of high affinity amino acid transporter-encoding genes and/or by the dissipation of the proton gradient across the plasma membrane. Amino acid uptake in yeast is generally driven by proton motive force (reviewed in Boulton *et al.*, 1998) and dissipation of the proton gradient may negatively impact yeast cells' ability to import amino acids. This latter point will be further discussed in Section 4.4 in the context of the glycerol/H^+ symporter *STL1* which was found to be highly expressed during Icewine fermentation. Exposure to high osmotic stress and expression of low activity and low

affinity bulk amino acid transporters like *AGP2*, may also contribute to the overall reduction in amino acids taken up by yeast fermenting Icewine juice.

4.3.2.3. Specific amino acid uptake and metabolism

The branched chain amino acids (leucine, isoleucine and valine) combined contributed to less than 10% of the total amino acid content in the initial Icewine juice. Interestingly, of all the amino acids present, only leucine and isoleucine were completely depleted from this juice at the end of the fermentation. Uptake of leucine and isoleucine by yeast fermenting Icewine juice corresponded to a relative increase in *BAP2* expression up to day five. *BAP2* along with its isoform *BAP3* are closely related to *AGP1* and are capable of transporting branched chain and aromatic amino acids (Regenberg *et al.*, 1999). It is unclear why yeast fermenting Icewine juice would favour the uptake of leucine and isoleucine in the presence preferential nitrogen sources (glutamate and glutamine) whose concentrations remained relatively high in the juice until the end of the fermentation. However, the microarray data showed a small subset of genes associated with leucine and isoleucine biosynthesis that were either downregulated in yeast fermenting Icewine juice relative to those fermenting dilute juice or were expressed, but showed no significant difference between fermentation conditions. If not being actively synthesized by yeast, the influx of leucine and isoleucine transported into the cells may be diverted to other pathways such as protein synthesis or fusel alcohol production via the Ehrlich pathway.

During all fermentations, small amounts of higher (fusel) alcohols can be formed from the transamination products of branched chain and aromatic amino acids. However, fusel alcohol synthesis usually occurs during the later stages of fermentation following

the period of rapid amino acid uptake (reviewed in Boulton *et al.*, 1998). During fusel alcohol synthesis, amino acids are first transaminated to their corresponding α-ketoacids and in turn, α-ketoglutarate accepts an ammonia group to form glutamate (Figure 4.3.6). In the second step, the α-ketoacid is decarboxylated to produce an aldehyde. The final reaction of this redox reactive pathway involves the reduction of the aldehyde by an alcohol dehydrogenase and formation of a fusel alcohol. This pathway allows nitrogen in the form of ammonia to be retrieved (Dickinson, 2004). Dickinson *et al.* (2003) presented evidence that the final step of fusel alcohol formation via the conversion of an aldehyde to a fusel alcohol could be performed by any of the five *ADH* genes and *SFA1* (formaldehyde dehydrogenase). Although not measured in the fermenting juices, fusel alcohols may have been formed early on in the Icewine fermentation as a consequence of the upregulation of the pyruvate decarboxylases (*PDC1,5* and *6*) (Table 4.2.1) along with the decarboxylase encoded by *THI1* and the dehydrogenase encoded by *SFA1* (Table 4.3.5). If Icewine fermenting yeast are able to produce fusel alcohols, these cells would have likely been limited at the beginning of this pathway due to the relative downregulation of the transaminase encoding genes *BAT1* and *BAT2*. Furthermore, since this pathway is redox reactive, the production of NAD^+ in a cell which may already be in cytosolic redox imbalance, would potentially place additional stress on yeast cells fermenting Icewine juice.

Fusel alcohol production is one of many pathways involving the recycling of an ammonia group from another amino acid to form glutamate. Both glutamate and glutamine are important amino group donors in the biosynthesis of amino acids and other nitrogen containing compounds (reviewed in Boulton *et al.*, 1998; Magasanik and Kaiser,

2002). It has been shown in this study that Icewine juice fermenting cells fail to take up a large proportion of the available glutamate and glutamine present in the juice. A small number of glutamate and glutamine-specific transporters have been identified in yeast. *DIP5* encodes for a glutamate transporter which is also capable of transporting glutamine, aspartate and asparagine (Regenberg *et al.*, 1999). From the microarray data, *DIP5* was not found to be expressed at the same degree in Icewine juice fermenting cells as compared to dilute juice fermenting cells. *GNP1* encodes for a transporter capable of transporting glutamine (Regenberg *et al.*, 1999) but was found to be more highly expressed in yeast during Icewine fermentation. Glutamate and glutamine transport is also mediated by *GAP1* (Regenberg *et al.*, 1999). Generally, the slower rate of uptake of glutamate and glutamine by Icewine fermenting yeast cells corresponds to an overall downregulation of genes encoding for carriers responsible for their transport. These amino acids may also be competing with each other for available transporters potentially driving down their ability to be taken up by the cell even further. A decrease in glutamate and glutamine uptake also corresponds to the downregulation of glutamate metabolism genes. The formation of glutamate from α-ketoglutarate involves the enzymatic activity of glutamate dehydrogenases encoded by *GDH1* and *GDH3* (Figure 4.3.5). The expression of *GDH1* and *GDH3* was reported to be dependent on carbon source by DeLuna *et al.*, (2001). Gdh3p activity was found to be glucose repressed in yeast but activity increased on non-fermentable carbon sources like ethanol whereas Gpdh1p activity contributed to glutamate formation during exponential growth and in the presence of high glucose concentrations. However, expression of both *GDH* isoforms during Icewine and diluted juice fermentation seem to be independent of the availability

of glucose. There are two routes for the catabolic production of glutamate from glutamine via enzymes encoded by *GDH2* or *GLT1*/*GLN1* (Figure 4.3.5). However, in the presence of glutamate and glutamine, both *GDH1* and *GDH2* are subject to NCR (reviewed in ter Schure *et al.*, 2000). *GDH3*, and to a lesser extent *GDH2*, were upregulated in wine yeast cells briefly exposed to high sugar stress (Erasmus *et al.*, 2003). This was not the case in our study since yeast were placed under prolonged exposure to hyperosmotic stress during Icewine fermentation. The depletion of both glutamate and glutamine in the diluted juice condition, together with the probable lifting of NCR by day two of the fermentation, could account for the increase expression of these genes compared to yeast fermenting Icewine juice.

Proline and arginine were the predominant amino acids measured in Icewine juice. Yeast cannot use proline as a source of nitrogen in anaerobic conditions (reviewed in Boulton *et al.*, 1998). Under aerobic conditions, yeast can degrade proline to glutamate since the first enzymatic step in the proline catabolic pathway occurs in the mitochondrion and is catalyzed by a proline oxidase (encoded by *PUT1*). The second and last step of the proline degradation pathway is catalyzed by a dehydrogenase (*PUT2*) (reviewed in Boulton *et al.*, 1998). Proline utilization is also subject to NCR (reviewed in Boulton *et al.*, 1998; Magasanik and Kaiser, 2002). As expected, proline was not utilized or metabolized by yeast fermenting either Icewine or diluted Icewine juices and the microarray data supports these observations since none of the genes involved in proline catabolism were expressed under either fermentation condition. In addition to proline, *PUT4* can facilitate the import of alanine and glycine (Regenberg *et al.*, 1999) and GABA (Andre *et al.*, 1993). Although *PUT4* expression is regulated transcriptionally by

NCR thereby preventing proline utilization if better nitrogen compounds are present (ter Schure *et al.*, 2000), this gene was found to be expressed in Icewine juice fermenting cells up to three-fold higher than that found in the dilute condition. *PUT4* upregulation could be correlated to an increased uptake of glycine by cells in Icewine juice compared to those in diluted juice. But, increased glycine uptake may be associated with amino acid transporters other that *PUT4*. Elevated *PUT4* expression may also be attributed to the hyperosmotic stress imposed on yeast cells fermenting Icewine juice as this gene was reported to be upregulated by both brief high salt- and sugar-induced hyperosmotic stress (Posas *et al.*, 2000; Rep *et al.*, 2000; Erasmus *et al.*, 2003). Proline uptake by diluted juice fermenting yeast may be a result of cells being relieved of NCR as the fermentation progressed but they were unable to use it as a nitrogen source under anaerobic conditions.

Arginine transport is mediated by *GAP1* in addition to the arginine-specific permease *CAN1* (Regenberg *et al.*, 1999). Downregulation of both transporters by Icewine juice fermenting cells may have lead to an overall reduction in arginine uptake. Despite these observations the expression of *CAR1*, which encodes an NCR-sensitive arginase responsible for degrading arginine to ornithine and urea, was significantly higher on day two in the Icewine juice condition. In contrast, three genes associated with arginine biosynthesis (*ARG1*, *3* and *4*) were concurrently downregulated. The higher expression of *CAR1* in yeast during Icewine fermentation may be in response to hyperosmotic stress since this gene was strongly upregulated more than 25-fold in sorbitol-stressed laboratory yeast strain (Rep *et al.*, 2000). The activity of urea amidolyase (encoded by *DUR1,2*) can further metabolize urea to ammonia and carbon dioxide. The microarray results show that *DUR1,2* was expressed only on day two but

there was no significant difference in expression between fermentation conditions. Since urea was not measured in the fermenting juices in this study it would be impossible to conclude if increased expression of *CAR1* and lack of expression of *DUR1,2* by Icewine fermenting cells lead to increased urea levels in the wine. Ornithine can be further degraded to form polyamine precursors of spermine, spermidine and putrescine (reviewed in Boulton *et al.*, 1998). Although the genes involved in spermine, spermidine and putrescine biosynthesis (*SPE1-4*) were not expressed in yeast fermenting either Icewine or diluted juice the polyamine exporters (*TPO2*, *4* and *5*) were downregulated in Icewine fermenting cells. Polyamines are required for yeast growth (reviewed in Boulton *et al.*, 1998) however it is unclear whether wine yeast utilize polyamines during fermentation, especially those under Icewine fermentation conditions where yeast growth is limited.

GABA also made up a considerable percentage of the available nitrogen measured in Icewine juice as expected, since GABA is among the major nitrogen sources present in grape juice (Monteiro and Bisson, 1991a). GABA transport in yeast is mediated by the GABA-specific permease *UGA4* (Andre *et al.*, 1993) in addition to *GAP1* and *PUT4*. No appreciable GABA appeared to be taken up by Icewine fermenting yeast. Typically, yeast do not use all available GABA due to the effects of NCR (Monteiro and Bisson, 1991b). However, yeast fermenting diluted juice did uptake GABA but only after approximately 120 mg N L^{-1} of amino acid nitrogen had already been taken up from the juice. This possibly indicated that cells were being relieved of NCR. An increase in *GAP1* and *UGA4* expression in conjunction with lifting of NCR may be correlated to a substantial increase in GABA uptake after day three by yeast in

the diluted juice condition where nearly all the amino acids had already been depleted from the fermenting juice. *UGA1* encodes a 4-aminobutyrate aminotransferase that deaminates GABA to succinate semialdehyde which in turn, is converted to succinate by the $NADP^+$-dependent succinate semialdehyde dehydrogenase (SSADH) encoded by *UGA2* (Ramos *et al.*, 1985). In the presence of good nitrogen sources, *UGA1* is also subject to NCR (reviewed in ter Schure *et al.*, 2000). As seen in Table 4.5.1, there was no significant difference in the concentration of succinate found in the finished wines. Since the genes involved in the GABA degradation pathway were generally not expressed in yeast under both juice conditions, it is unlikely that this pathway contributes to succinate production during the first five days of the fermentations. Day four of the fermentations seems to be a key timepoint for GABA transport and metabolism. Although the genes involved in its synthesis and degradation were expressed on day four, no significant difference was found between fermentation conditions. In the presence of GABA, expression of *UGA1* and *UGA2* is induced which is mediated by the transcriptional activator Uga3p (Vissers *et al.*, 1989). Interestingly, *UGA3* was upregulated in the Icewine juice condition. Expression of *GAD1* and *UGA2* are also upregulated under conditions of oxidative stress (Coleman *et al.*, 2001). In 2003, Erasmus *et al.* also found that exposure to brief sugar stress upregulated the expression of GABA metabolism genes in wine yeast. Even though Icewine juice fermenting cells took up approximately 7% of the available GABA present in the juice, expression of genes associated with GABA metabolism may be attributed to the general stress response by yeast. Previous studies have shown that GABA may act as a compatible osmolyte in plants subjected to salt stress (reviewed in Shelp *et al.*, 1999). Based on the gene profiling data and amino acid

usage results presented in our current study, it is unlikely that *S. cerevisiae* uses GABA for osmoregulation during Icewine juice fermentation.

4.4. GLYCEROL METABOLISM

4.4.1. Results- Glycerol Metabolism

4.4.1.1. Glycerol Production

The concentration of extracellular glycerol measured during both the Icewine and diluted juice fermentations was found to increase over time, yet there was little difference in the rate of glycerol production by yeast as a function of time between fermentation conditions over the first 120 h (Figure 4.4.1A). Following this timepoint, glycerol production subsequently continued to increase over time in the Icewine juice fermentation resulting in a final glycerol concentration of 11.95 ± 0.16 g L^{-1}, while the rate of glycerol production plateaued in the dilute juice fermentation leading to a final glycerol concentration of 6.30 ± 0.19 g L^{-1} (Table 4.4.1). This represents a significant 1.9-fold increase in glycerol production by yeast fermenting Icewine juice compared to the dilute juice after subtracting the initial glycerol concentration in the starting juices. Since the rates of sugar consumption differed greatly between fermentation conditions (Figure 4.2.3) and glycerol is a byproduct of sugar metabolism, the amount of glycerol produced was plotted against sugar consumed to compare the rate of glycerol production as a function of sugar consumed (Figure 4.4.1B). Although Icewine juice fermenting yeast consumed less sugar over time, more glycerol was released by these cells throughout the fermentation after an equal amount of sugar was consumed in comparison to the dilute juice fermenting yeast.

Table 4.4.1: Glycerol produced by *S. cerevisiae* following the consumption of 187 g L^{-1} of sugar.

Fermentation	Initial reducing sugar in juice* ($g\ L^{-1}$)	Final reducing sugar in wine* ($g\ L^{-1}$)	Total sugar consumed ($g\ L^{-1}$)	Glycerol produced* ($g\ L^{-1}$)
Icewine juice	447.7 ± 8.5	259.9 ± 2.8	187.8 ± 2.8	11.95 ± 0.16
Dilute Icewine juice	226.7 ± 4.1	39.9 ± 3.1	186.8 ± 3.1	6.30 ± 0.19

* Values within the same column are significantly different as determined by a paired t-test ($P \leq 0.05$)

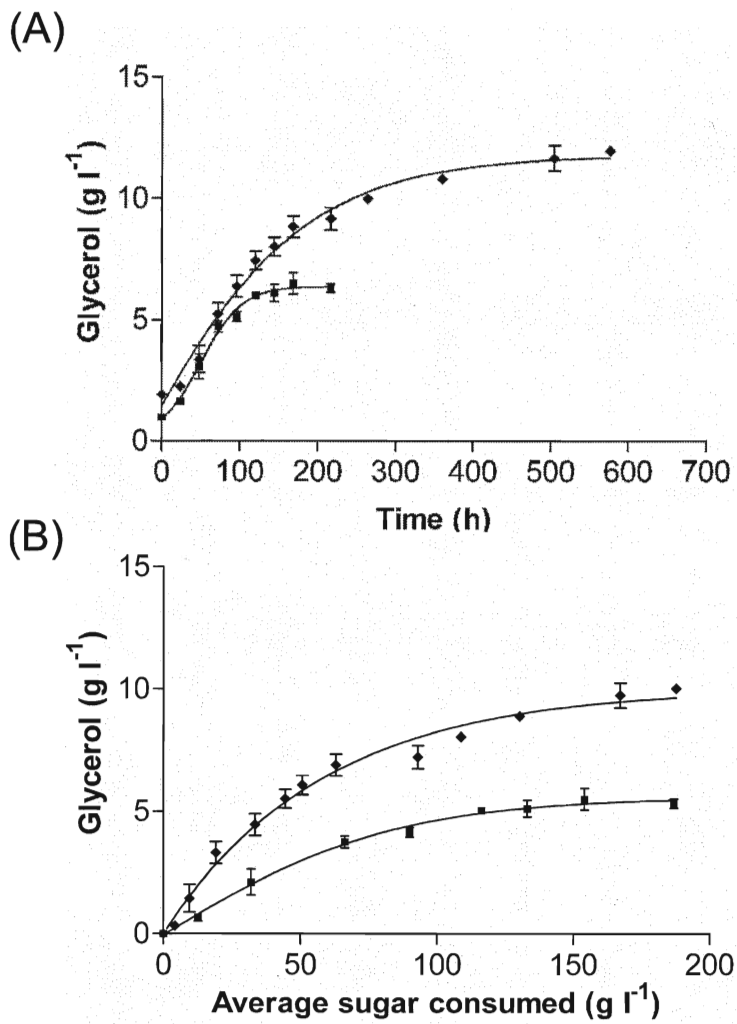

Figure 4.4.1: Yeast glycerol production. The concentration of extracellular glycerol (A) was measured in duplicate throughout the course of the fermentations of Icewine juice (♦) and diluted Icewine juice (■) and was plotted as a function of sugar consumed (B). The values represent the average ± standard deviation of the mean of triplicate fermentations.

4.4.1.2. Gene expression profiles (Microarrays)- Glycerol metabolism and transport

The genes involved in glycerol synthesis were generally more highly expressed in yeast fermenting Icewine juice. Both *GPD1* and *GPD2* encode for NAD^+-dependent glycerol-3-phosphate dehydrogenase isoenzymes that catalyze the first redox reactive and rate-limiting step in glycerol synthesis (Larsson *et al.*, 1993; Eriksson *et al.*, 1995; Remize *et al.*, 2001). However, only *GPD1* showed significant differential expression between fermentation conditions (Table 4.4.2). *GPD1* was upregulated four-fold on day three, but the fold difference in the expression of this gene between the Icewine and dilute juice conditions peaked on day four (6.6-fold). Although *GPD2* was found to be expressed during days two and three of the fermentations, there was little to no significant difference in its expression between juice conditions. By day five, the expression of both *GPD* isoforms could not be detected using the cDNA microarrays for all three replicate fermentations. Both glycerol-3-phosphatase isoforms (*GPP1* and *GPP2*) were observed to have similar expression patterns throughout the Icewine juice fermentation (Table 4.4.2). *GPP1* and *GPP2* were strongly expressed in the Icewine condition relative to the dilute juice condition. The fold change in the expression of *GPP1* and *GPP2* between fermentation conditions peaked on day four. After which, the level of upregulation for these genes began to decline by day five in comparison to the dilute juice fermentation. Also seen in Table 4.2.2, two genes encoding for enzymes responsible for catalyzing the conversion of glycerol back into the glycolytic intermediate DHAP (*GUT1* and *GUT2*) were found to be expressed at the same level between fermentation conditions on day two. However, the expression of both genes was significantly lower by 2.4-fold on day three of the Icewine juice fermentation compared

to the dilute juice fermentation. Increased expression of glycerol synthesis genes along with decreased expression of glycerol catabolism genes during the early stages of Icewine juice fermentation corresponds to increased levels of glycerol produced by these yeast (Figures 4.4.1A and B).

Accumulation of glycerol under hyperosmotic stress is also dependent on the yeast cell's ability to retain it within the cytoplasm. *FPS1* encodes for a glyceroporin channel that passively facilitates the export of glycerol (Van Aelst *et al.*, 1991; Luyten *et al.*, 1995; Sutherland *et al.*, 1997; Oliveira *et al.*, 2003). *FPS1* was expressed at the same level between fermentation conditions on day two (Table 4.4.2). After day two, the expression of *FPS1* could not be detected in yeast fermenting either juice. In contrast, *STL1* which encodes for a putative glycerol/H^+ symporter (Ferreira *et al.*, 2005), was one of the most strongly upregulated genes identified in yeast fermenting Icewine juice (Table 4.2.2). This was intriguing since the expression of *STL1* was previously found to be transiently induced under salt stress (Rep *et al.*, 2000) and subject to glucose repression (Ferreira *et al.*, 2005). Throughout the Icewine juice fermentation, the fold change in *STL1* expression increased and ultimately peaked on day five (25.6-fold) as compared to the dilute juice fermentation.

Table 4.4.2: Expression profile of the genes involved in glycerol metabolism.

ORF	Gene	Description	Fold Change*			
			Day 2	Day 3	Day 4	Day 5
Glycerol						
YDL022W	GPD1	glycerol-3-phosphate dehydrogenase	+	+4.3	+6.6	×
YOL059W	GPD2	glycerol-3-phosphate dehydrogenase	+	•	×	×
YIL053W	GPP1	glycerol-3-phosphatase	+3.1	+8.7	+12.3	+3.5
YER062C	GPP2	glycerol-3-phosphatase	+3.0	+9.3	+14.0	+4.7
YHL032C	GUT1	glycerol kinase	•	-2.4	-5.4	×
YIL155C	GUT2	glycerol-3-phosphate dehydrogenase	•	-2.4	×	×
YLL043W	FPS1	glycerol channel	•	×	×	×
YDR536W	STL1	glycerol proton symporter	+11.5	+11.9	+18.9	+25.6

*Significantly different as determined by a paired t-test ($P \leq 0.05$)
The level of gene expression changes in *S. cerevisiae* fermenting Icewine juice in comparison to gene expression changes in *S. cerevisiae* fermenting dilute Icewine juice are shown as either positive (+ fold upregulation) or negative (-fold downregulation) values. A plus sign (+) or minus sign (-) alone indicates significant difference in gene expression but less than a 2-fold change; • indicates no significant difference in gene expression; × indicates no expression was detected.

4.4.1.3. Gene expression profiles (Northerns)- Glycerol

From the microarray data, the expression profile of the gene *STL1* (glycerol/H^+ symporter) was shown to be highly upregulated in yeast fermenting Icewine juice. Since this gene displayed a greater than ten-fold change in expression between fermentation conditions, it was decided that the expression of *STL1* in yeast under Icewine and diluted juice fermentation conditions required validation using Northern analysis. However, it was necessary to validate the specificity of the DNA probe designed exclusively for *STL1*.

Salt induced hyperosmotic stress was used for *STL1* probe validation since *STL1* had been previously shown to be strongly induced in laboratory yeast strains exposed to saline stress (Rep *et al.*, 2000). Figure 4.4.2 shows that under salt stress the *STL1* probe was specific to detect the expression of *STL1* in the commercial wine yeast strain of *S. cerevisiae* K1-V1116 in addition to the laboratory strain BY4742. A weak signal was detected in the *STL1* deletion mutant (Δ*STL1*) under inductive conditions, however, this signal was 17- and 11-fold lower than the signal generated from either the wine yeast or the laboratory yeast strains, respectively. This signal may be attributed to background noise from the blot as there was no visible band observed on the Northern.

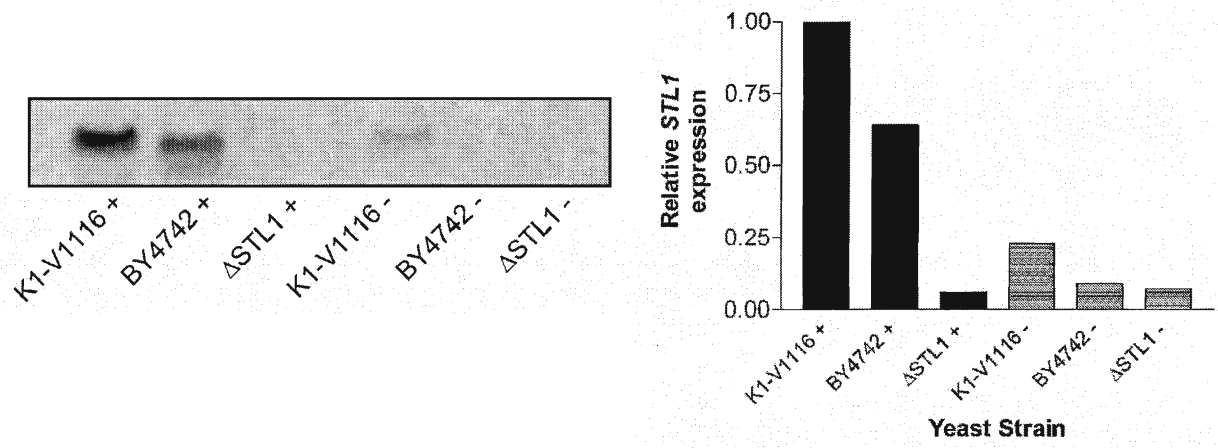

Figure 4.4.2: Probe specificity for *STL1* validation Northern blots. Yeast cultures were induced (+) or not induced (-) with salt prior to RNA isolation. Expression profiles of the blot following hybridization of ^{32}P-labeled DNA probes specific for *STL1* to RNA isolated from the commercial wine yeast strain (K1-V1116), parent yeast strain (BY4742) and knockout yeast strain (Δ*STL1*).

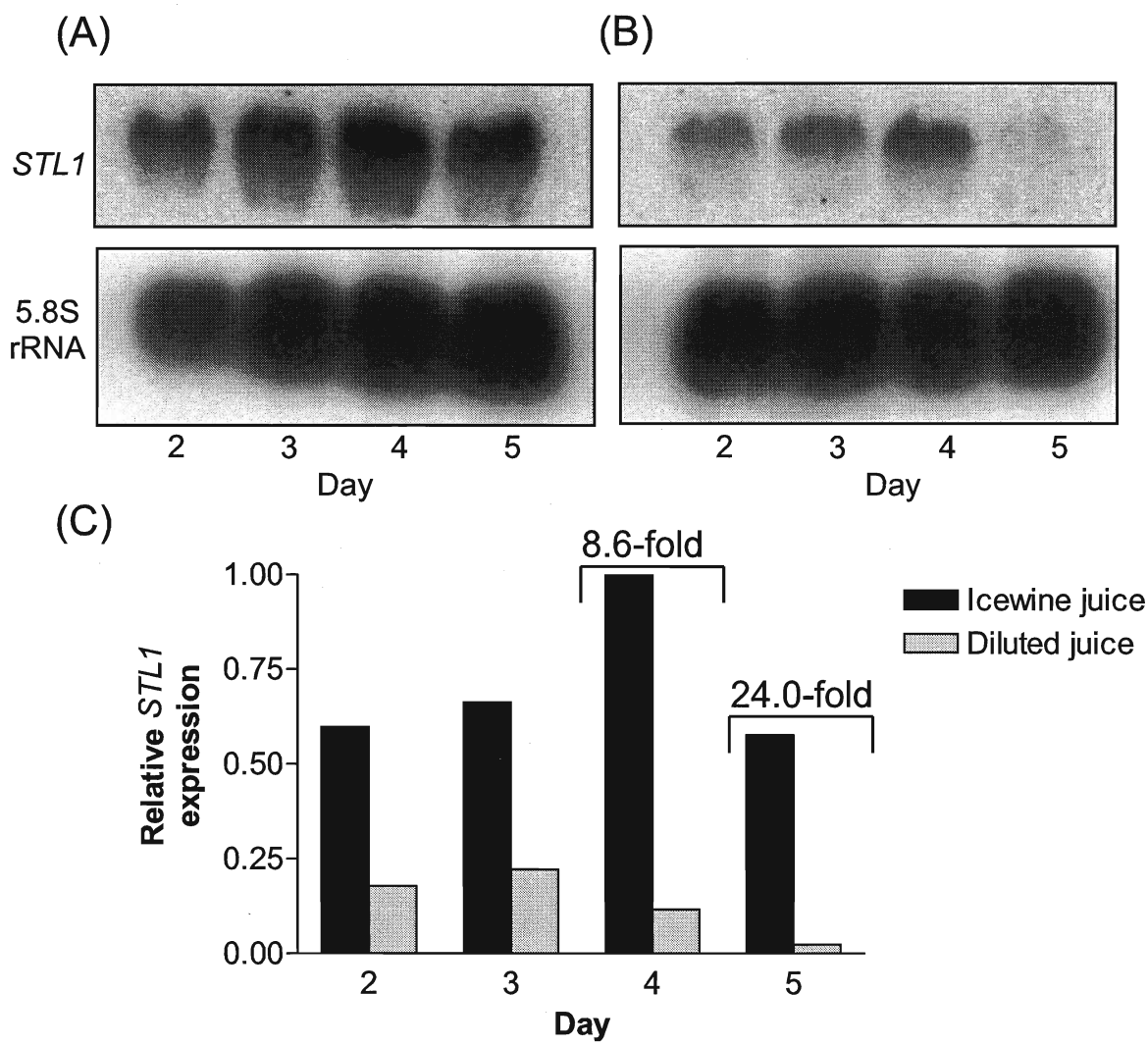

Figure 4.4.3: Expression of *STL1* during fermentation. The expression profiles of *STL1* from yeast fermenting Icewine juice (A) and diluted Icewine juice (B) using Northern analysis. 5.8S ribosomal RNA was used as a loading control. (C) Comparison of the relative levels of *STL1* expression between fermentation conditions.

The relative gene expression profile of *STL1* during Icewine and dilute wine fermentation is depicted in Figure 4.4.3. From the Northern blot, *STL1* was expressed throughout both fermentation conditions but to a much greater extent in yeast fermenting Icewine juice. The signal intensity for *STL1* peaked on day four of the Icewine juice fermentation in comparison to the signal intensity of the dilute juice fermentation, representing a 8.6-fold difference in expression. However, the relative fold difference in *STL1* expression peaked on day five between fermentation conditions giving rise to a 24-fold increase in *STL1* expression in Icewine juice fermenting cells similar to that found with the microarrays.

4.4.2. Discussion - Glycerol metabolism and transport

The combination of Gpd1p-Gpp2p activity is proposed to be mainly involved in glycerol production during osmotic stress, while the Gpd2p-Gpp1p combination is connected with balancing the NAD^+/NADH cofactor system under anaerobic conditions (Albertyn *et al.*, 1994b; Ansell *et al.*, 1997; Påhlman *et al.*, 2001). Wine yeast face both anaerobic and osmotic stress during Icewine fermentation, so either or both of these factors may control the expression of genes associated with glycerol synthesis.

At the start of fermentation, glycerol is produced in response to the excess NADH generated during yeast cell biomass formation and its synthesis acts to restore redox balance by reoxidizing reduced cofactor (van Dijken and Scheffers, 1986). However, the fermentation of Icewine juice results in a reduction in biomass formation but an increase in glycerol production. The microarray results obtained in the present study showed that the expression of *GPD2* did not significantly differ between Icewine and dilute juice fermentation conditions and therefore *GPD2* does not appear to be contributing to the

increased glycerol levels found in the Icewine fermentation. Since *GPD2* expression would not be required for glycerol production to restore the cytosolic pool of NAD^+ since biomass formation is diminished, the elevated production of glycerol in wine yeast during Icewine fermentation corresponded to an upregulation of *GPD1* expression. These microarray results are in agreement with studies by Pigeau and Inglis (2005 and 2007), in which the increase in *GPD1* expression as measured by Northern analysis, but not *GPD2* expression, over time in wine yeast fermenting Icewine juice compared to dilute juice corresponded to elevated glycerol levels produced throughout the fermentation. From our study, it appears that glycerol synthesis is also dependent on both glycerol-3-phosphatase isoforms during Icewine juice fermentation as *GPP1* and *GPP2* were observed to be strongly expressed. The expression of *GUT1* (glycerol kinase) and *GUT2* (glycerol-3-phosphate dehydrogenase) is subject to glucose repression and does not appear to be induced by osmotic stress (reviewed in Hohmann, 2002). However, both glycerol catabolizing genes were more highly expressed on day three of the dilute juice fermentation in which over 160 g L^{-1} of fermentable sugars remained in the juice up to this timepoint. The osmotic stress imposed on yeast by high concentrations of sugars is dynamic since the extracellular osmotic pressure exerted on cells decreases as they take up and eventually ferment the sugar. An increase in *GUT1* and *GUT2* may be a reflection of the decreasing osmotic stress in the dilute juice condition and a lower demand for high intracellular glycerol levels by yeast fermenting this juice in comparison to the Icewine juice fermenting cells.

To ensure that the glycerol produced in *S. cerevisiae* upon exposure to hyperosmotic stress is accumulated to offset the osmotic pressure exerted on the plasma

membrane, yeast must regulate glycerol export through the plasma membrane. *FPS1* encodes for a glyceroporin channel that functions as a glycerol exporter. Once yeast cells return to normal growth conditions following osmotic shock, Fps1p facilitates passive transport of glycerol across the membrane down a concentration gradient (Van Aelst *et al.*, 1991; Luyten *et al.*, 1995; Sutherland *et al.*, 1997; Oliveira *et al.*, 2003). However, this channel rapidly closes when yeast are exposed to hyperosmotic stress (Támas *et al.*, 1999), thereby controlling the amount of glycerol retained by the cell. No expression of this gene could be detected in yeast fermenting either Icewine or diluted juice after day two. Although measurable, there was no significant difference in the expression of this gene between fermentation conditions. Despite the lack of *FPS1* expression, extracellular glycerol levels measured in the fermenting juices increased steadily over the days subject to microarray analysis. It is possible that *FPS1* expression was below the detection level of microarray analysis, or a number of glyceroporin channels had already occupied the yeast plasma membrane early on during the fermentations such that *FPS1* expression was no longer required after day two. It is also likely that the glycerol released by yeast cells into the fermenting juices occurred by simple diffusion across the plasma membrane. However, rate of glycerol diffusion across the membrane is generally low and membrane permeability to glycerol is reduced even further in osmotically stressed yeast cells (Tamás *et al.*, 1999; Sutherland *et al.*, 1997).

Active glycerol uptake via a glycerol/H+ symporter (Stl1p) may be occurring in *S. cerevisiae* during Icewine juice fermentation. *STL1* was one of the most strongly expressed genes identified in yeast fermenting Icewine juice. Expression of this gene was previously found to be transiently induced in laboratory yeast strains under salt stress

(Rep *et al.*, 2000) and is reported to be subject to glucose repression (Ferreira *et al.*, 2005). However, in agreement with our study, *STL1* was one of the most strongly upregulated genes in wine yeast following a two hour exposure to high sugar stress (Erasmus *et al.*, 2003). A comparison of the expression profiles of this gene throughout the Icewine juice and dilute juice fermentations using both microarray and Northern analysis showed a considerable differential increase in *STL1* expression in yeast fermenting Icewine juice. This ultimately resulted in a peak 25-fold increase in *STL1* expression on day five of the fermentation relative to the level in the dilute juice condition. The roles of Fps1p and Stl1p in glycerol transport in the presence of high concentrations of fermentable sugars during Icewine fermentation are unclear. Osmotolerant yeast species like *Zygosaccharomyces rouxii* are capable of actively importing glycerol against a concentration gradient into the cell in the presence of salt-induced hyperosmotic stress (van Zyl *et al.*, 1990). Active glycerol uptake is a mechanism yeast can use to increase intracellular glycerol concentrations under hyperosmotic stress and it has been suggested that a high affinity glycerol/H^+ symporter uptake system also exists in *S. cerevisiae* (Lages and Lucas, 1997). The use of Stl1p by yeast for glycerol uptake during Icewine juice fermentation may contribute to limited cell growth by dissipating the proton gradient across the plasma membrane in an energy dependent manner. Many yeast amino acid transport systems are proton symports (reviewed in Boulton *et al.*, 1998; Horák, 1986) therefore any disturbance in the proton gradient across the cell membrane may negatively influence amino acid uptake. It has been shown in Section 4.3 that the rate and degree of amino acid uptake by yeast fermenting Icewine juice is far lower than that of dilute juice fermenting cells. However

if yeast cells are using Stl1p to actively take up glycerol in the Icewine juice condition, then the increased influx of protons into the cytoplasm may ultimately hinder active amino acid uptake. The ability to excrete excess protons is an important regulatory factor for amino acid uptake in yeast in addition to preventing cytoplasm acidification and cell death (reviewed in Boulton *et al.*, 1998).

4.5. ACETIC ACID METABOLISM

4.5.1. Results - Acetic Acid Metabolism

4.5.1.1. Acetic Acid Production

Since acetaldehyde is the precursor to acetic acid, extracellular acetaldehyde and acetic acid levels were both measured throughout the fermentations. The rate of acetaldehyde production increased rapidly in the Icewine juice fermentation and reached a maximum concentration of 0.13 ± 0.01 g L^{-1} in 96 h (Figure 4.5.1A). This corresponds to a 5.5-fold difference in acetaldehyde concentration between juice conditions at this timepoint. Acetaldehyde levels then quickly declined eventually leading to a significant 1.5-fold increase in acetaldehyde concentration at the end of the Icewine juice fermentation in comparison to the end of the fermentation of the diluted juice. Similar trends were observed when the amount of acetaldehyde released into the juice was plotted against sugar consumed (Figure 4.5.1B).

The rate of extracellular acetic acid released into the fermenting juices greatly differed between fermentation conditions (Figure 4.5.1C). Acetic acid was produced and released at a faster rate and to a greater extent during the first five days of the Icewine juice fermentation in comparison to the dilute juice condition. The rate slowed down and

Table 4.5.1: Metabolites produced by *S. cerevisiae* following the consumption of 187 g L^{-1} of sugar.

Fermentation	Acetaldehyde* ($g\ L^{-1}$)	Acetic Acid* ($g\ L^{-1}$)	Succinate ($g\ L^{-1}$)	Ethanol* % (v/v)
Icewine juice	0.05 ± 0.00	1.40 ± 0.03	0.68 ± 0.05	11.5 ± 0.8
Dilute Icewine juice	0.03 ± 0.00	0.14 ± 0.01	0.64 ± 0.01	14.4 ± 0.2

* Values within the same column are significantly different as determined by a paired t-test ($P \leq 0.05$)

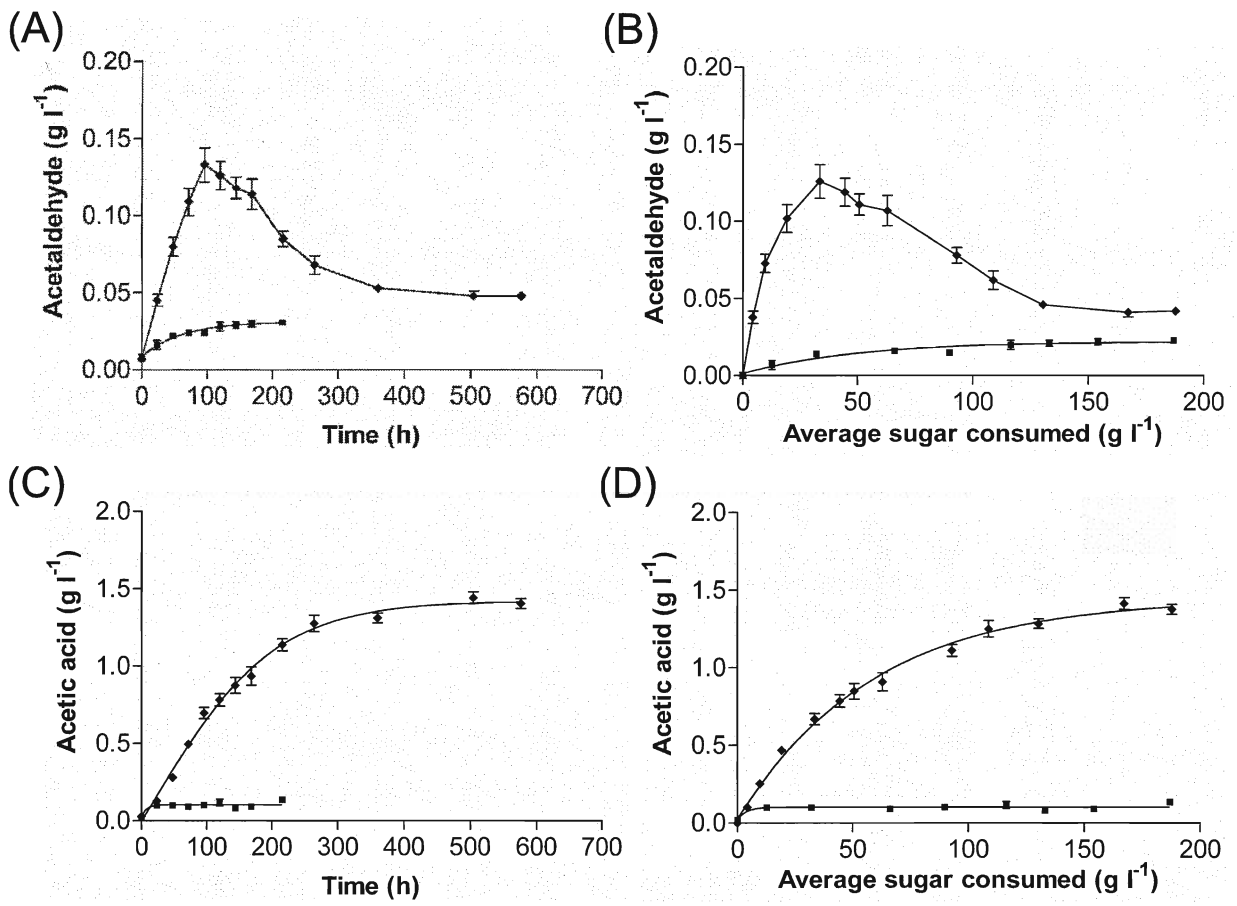

Figure 4.5.1: Yeast acetaldehyde and acetic acid production. Acetaldehyde (A) and acetic acid (C) were measured in duplicate throughout the course of the fermentations of Icewine juice (♦) and diluted Icewine juice (■). Acetaldehyde (B) and acetic acid (D) were plotted as a function of sugar consumed. The values represent the average ± standard deviation of the mean of triplicate fermentations.

eventually plateaued after 300 h of fermentation resulting in a final extracellular acetic acid concentration of 1.40 ± 0.03 g L^{-1} (Table 4.5.1). In contrast, acetic acid was produced at a slower rate up to 48 h into the dilute juice fermentation with the extracellular acetic acid concentration remaining constant at 0.14 ± 0.01 g L^{-1} until the end of the fermentation. Wine yeast fermenting Icewine juice produced 10-fold more acetic acid than yeast fermenting the diluted juice after approximately 187 g L^{-1} of sugar was consumed (Figure 4.5.1.D).

In contrast to the measured levels of glycerol, acetaldehyde and acetic acid produced by Icewine juice fermenting yeast, these cells produced significantly less ethanol than the dilute juice cells by the end of the fermentations when 187 g L^{-1} of sugar was consumed (Table 4.5.1). A decrease in ethanol production by osmotically stressed yeast cells fermenting Icewine juice may indicate a change in the metabolic flux of hexose sugars through glycolysis and alcoholic fermentation. Carbon derived from sugar metabolism is possibly being diverted away from ethanol synthesis and towards the production of other metabolites for necessary survival and adaptation to hyperosmotic stress.

4.5.1.2. Gene expression profiles for acetic acid and fatty acid metabolism

Of the five genes encoding for aldehyde dehydrogenases identified in *S. cerevisiae*, only *ALD3* encoding for a cytosolic NAD^+-dependent aldehyde dehydrogenase was differentially expressed for three of the four fermentation days examined (Table 4.5.2). *ALD3* was strongly expressed on day two of the Icewine juice fermentation relative to the dilute condition. The differential expression of this gene continued to increase as the fermentation progressed whereupon the relative fold change

Table 4.5.2: Expression profile of the genes involved in acetic acid metabolism.

ORF	Gene	Description	Fold Change*			
			Day 2	Day 3	Day 4	Day 5
Acetic acid						
YAL054C	ACS1	acetyl-CoA synthetase	-19.0	•	•	×
YLR153C	ACS2	acetyl-CoA synthetase	-4.8	-3.6	-11.2	×
YBL015W	ACH1	acetyl-CoA hydrolase	-5.2	-2.3	-2.9	+2.4
YCR010C	ADY2	acetate transporter	-13.9	+3.2	+5.6	+14.1
YMR170C	ALD2	aldehyde dehydrogenase	•	•	+2.2	×
YMR169C	ALD3	aldehyde dehydrogenase	+8.4	+9.7	+14.6	×
YOR374W	ALD4	aldehyde dehydrogenase (mitochondrial)	-6.2	•	•	•
YER073W	ALD5	aldehyde dehydrogenase (mitochondrial)	-4.4	•	•	×
YPL061W	ALD6	aldehyde dehydrogenase	-2.4	+	•	•

*Significantly different as determined by a paired t-test ($P \leq 0.05$)
The level of gene expression changes in *S. cerevisiae* fermenting Icewine juice in comparison to gene expression changes in *S. cerevisiae* fermenting dilute Icewine juice are shown as either positive (+ fold upregulation) or negative (-fold downregulation) values. A plus sign (+) or minus sign (-) alone indicates significant difference in gene expression but less than a 2-fold change; • indicates no significant difference in gene expression; × indicates no expression was detected.

in *ALD3* expression peaked on day four (14.6-fold) of the Icewine juice fermentation. In contrast both mitochondrial *ALD* isoforms (*ALD4* and *ALD5*) along with the cytosolic $NADP^+$-dependent isoform (*ALD6*) were expressed up to six-fold lower in yeast fermenting Icewine juice relative to the dilute condition (Table 4.5.2). The expression level of these three genes was not significantly different between fermentation conditions after day two. *ALD2* encodes for an additional cytosolic NAD^+-dependent aldehyde dehydrogenase and was found to be transiently upregulated in yeast on day four of the Icewine juice fermentation. *ADY2* encodes for a protein that has been proposed to function as an acetate permease (Paiva *et al.*, 2004). *ADY2* expression was found to be far lower (13.9-fold) on day two of the Icewine fermentation relative to the dilute condition. As the fermentation progressed, however, *ADY2* expression increased over that found in the dilute condition where the fold change in expression of *ADY2* eventually peaked on day five (14.1-fold).

The genes encoding for two acetyl-CoA synthetases (*ACS1* and *ACS2*), which are involved in the generation of acetyl-CoA from acetic acid were two of the most strongly downregulated genes in yeast fermenting Icewine juice in comparison to the expression level in the dilute juice condition (Table 4.5.2). The mitochondrial isoform (*ACS1*) was downregulated 19-fold on day two while the cytosolic isoform (*ACS2*) was downregulated throughout the Icewine juice fermentation with the relative fold downregulation for *ACS2* peaking on day four (11-fold). Expression of both *ACS* isoforms could not be detected after day four in either fermentation condition. Acetic acid and coenzyme A (CoA) can also be regenerated through the hydrolysis of acetyl-CoA by an acetyl-CoA hydrolase (encoded by *ACH1*). The expression profile of *ACH1* was

similar to that of *ACS2*, however, *ACH1* was found to be expressed 2.4-fold higher on day five of the Icewine juice fermentation. Increased *ALD3* expression in conjunction with decreased expression of both acetyl-CoA synthetase isoforms may have contributed to the increased acetaldehyde and acetic acid levels produced by Icewine juice fermenting yeast compared to those fermenting diluted juice (Figure 4.5.1).

A considerable number of genes in *S. cerevisiae* associated with lipid and sterol metabolism, which involves the input or production of acetyl-CoA, displayed noticeably similar expression patterns in yeast under the Icewine juice condition. The expression of the vast majority of genes involved in fatty acid metabolism, phospholipid and ergosterol synthesis were relatively higher at least two-fold on day two of the dilute juice fermentation as shown in Table 4.5.3. However, as yeast continued to ferment both Icewine and diluted juices, the expression of many of these genes could not be detected in either juice condition (Table 4.5.3). In addition to fatty acids, phospholipids and sterols are important membrane components and genes involved in phospholipid and sterol metabolism were also found to be differentially expressed between fermentation conditions.

Four genes encoding for enzymes associated with phosphatidic acid metabolism showed a two-fold difference in expression (*LPP1*, *SLC1*, *AYR1* and *OPI3*). Downregulation of the ergosterol synthesis (*ERG*) genes also corresponds to the downregulation of the *ACS* (acetyl-CoA synthetase) genes. The products of the *ACS* genes can function to supply acetyl-CoA units required for ergosterol synthesis. Ergosterol is the primary sterol in yeast and one of its primary functions is to maintain

Table 4.5.3: Expression profile of the genes involved in lipid metabolism.

ORF	Gene	Description	Fold Change*			
			Day 2	Day 3	Day 4	Day 5
Fatty Acid Metabolism						
YML042W	CAT2	carnitine O-acetyltransferase	-4.4	•	×	×
YDR256C	CTA1	catalase	•	×	+2.1	×
YLR284C	ECI1	dodecenoyl-CoA delta-isomerase	-4.2	×	×	×
YBR026C	ETR1	enoyl-[acyl-carrier protein] reductase	-3.1	×	-2.5	×
YIL009W	FAA3	long-chain-fatty-acid-CoA ligase	-2.2	×	×	×
YMR246W	FAA4	long-chain-fatty-acid-CoA ligase	-2.1	×	×	×
YKL182W	FAS1	S-malonyltransferase	-4.1	×	×	×
YKR009C	FOX2	3-hydroxyacyl-CoA dehydrogenase	-2.3	×	×	×
YNL009W	IDP3	isocitrate dehydrogenase	-2.0	-	-2.8	×
YIL160C	POT1	acetyl-CoA C-acyltransferase	-2.1	×	•	×
YGL205W	POX1	acyl-CoA oxidase	-2.5	×	×	×
YPL147W	PXA1	fatty acid transport	-2.0	×	×	×
YNL202W	SPS19	2,4-dienoyl-CoA reductase	-3.5	×	×	×
YAR035W	YAT1	carnitine O-acetyltransferase	-7.2	×	×	×
YER024W	YAT2	carnitine O-acetyltransferase	-4.6	+2.7	+2.3	+3.1
Phospholipid Metabolism						
YIL124W	AYR1	acylglycerone-phosphate reductase	-2.2	×	-	×
YMR162C	DNF3	phospholipid-translocating ATPase	-4.1	×	×	×
YDR503C	LPP1	phosphatidate phosphatase	+2.4	×	×	×
YJR073C	OPI3	methylene-fatty-acyl-phospholipid synthase	-2.1	-2.1	-	×
YNL231C	PDR16	phosphatidylinositol transporter	+2.1	×	×	×
YDL052C	SLC1	1-acylglycerol-3-phosphate O-acyltransferase	+2.2	×	×	×
Sterol Metabolism						
YGR175C	ERG1	squalene monooxygenase	-2.1	×	-2.0	×
YML008C	ERG6	sterol 24-C-methyltransferase	-2.5	×	•	×
YPL028W	ERG10	acetyl-CoA C-acetyltransferase	-2.1	×	-4.3	×
YHR007C	ERG11	sterol 14-demethylase	-2.1	-2.2	-2.2	×
YML075C	HMG1	hydroxymethylglutaryl-CoA reductase	-3.7	×	×	×
YHR001W	OSH7	oxysterol binding	-2.0	×	•	×
YDR213W	UPC2	sterol biosynthesis transcription factor	+2.6	×	×	×

*Significantly different as determined by a paired t-test ($P \leq 0.05$)

The level of gene expression changes in *S. cerevisiae* fermenting Icewine juice in comparison to gene expression changes in *S. cerevisiae* fermenting dilute Icewine juice are shown as either positive (+ fold upregulation) or negative (-fold downregulation) values. A plus sign (+) or minus sign (-) alone indicates significant difference in gene expression but less than a 2-fold change; • indicates no significant difference in gene expression; × indicates no expression was detected.

membrane fluidity (Schweizer, 2004). In general, the ergosterol (*ERG*) synthesis genes found to be differentially expressed between conditions were downregulated approximately two-fold on days two and four (Table 4.5.3). *ERG10* is involved in the first reaction of the ergosterol biosynthetic pathway. *ERG10* encodes for a thiolase that catalyzes the condensation of two acetyl-CoA molecules to form acetoacetyl-CoA. Hydroxymethylglutaryl-CoA (HMG-CoA) reductase (encoded by *HMG1*) which catalyzes the reduction of HMG-CoA to mevalonate showed a four-fold lower differential expression in Icewine juice only on day two of the fermentation. Ergosterol synthesis requires oxygen and of the three other *ERG* genes (*ERG1*, *ERG6* and *ERG11*) that were less highly expressed in yeast under the Icewine juice condition, *ERG1* encodes for squalene monooxygenase which catalyzes the first oxidation reaction of the ergosterol biosynthetic pathway.

The main pathway of fatty acid degradation in *S. cerevisiae* is through β-oxidation, a process which occurs exclusively within the peroxisomes and oxygen is required for this process (reviewed in Hiltunen *et al.*, 2003) (Figure 4.5.2). The end result of the β-oxidation pathway is the formation of acetyl-CoA units which in turn can be used for biosynthetic reactions. Since the peroxisomal membrane is essentially impermeable to small molecules like cofactors and acetyl-CoA (van Roermund *et al.*, 1995), transport of larger molecules like fatty acids into peroxisomes is dependent on their conversion into acyl-CoA esters via fatty acid-CoA ligases (*FAA3* and *FAA4*). Import of these activated esters into the peroxisomal matrix is mediated by a membrane bound transporter protein encoded by the gene *PXA1*. Together, these three genes involved in fatty acid activation and transport were relatively downregulated

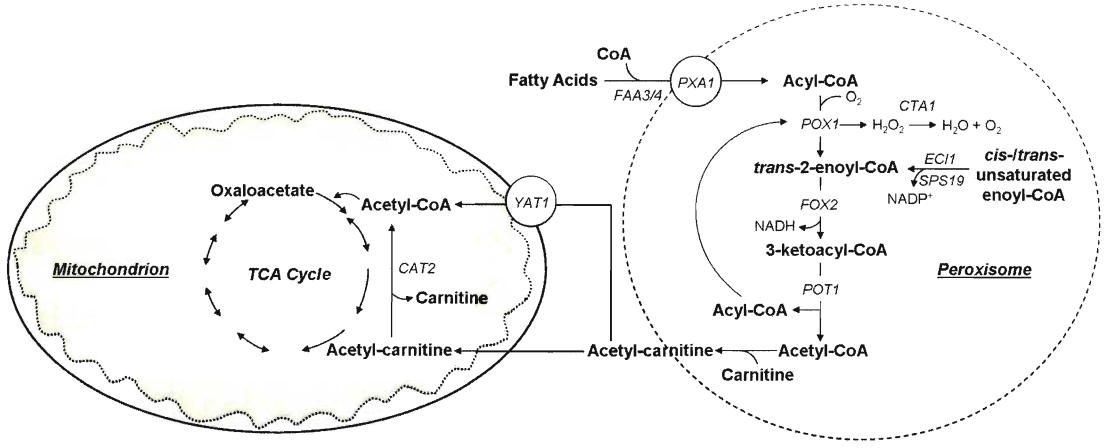

Figure 4.5.2: The central pathway of fatty acid β-oxidation in *S. cerevisiae*. Illustrated are the major metabolites generated within the main route of peroxisomal β-oxidation of fatty acids in yeast. The genes associated with the enzymes involved in fatty acid degradation are also shown. (Adapted from Hiltunen *et al.*, 2003).

approximately two-fold on day two of the Icewine fermentation (Table 4.5.3).

A large group of genes associated with β-oxidation pathway were more highly expressed in yeast on day two of the dilute juice fermentation compared to the Icewine juice fermentation (Table 4.5.3). This group included genes like *POX1*, which encodes a peroxisomal acyl-CoA oxidase that catalyzes the first (and rate-limiting) reaction of the β-oxidation process by converting the acyl-CoA ester to *trans*-2-enoyl-CoA (Figure 4.5.2). The H_2O_2 generated by this oxygen consuming reaction is removed through its decomposition to water and oxygen by a peroxisomal catalase A (*CTA1*). There was no significant difference in the expression of *CTA1* between juice conditions on day two. *ECI1* (an isomerase) and *SPS19* (a $NADP^+$-dependent reductase) both can participate in the β-oxidation of unsaturated enoyl-CoAs. Activity of the peroxisomal isocitrate dehydrogenase (*IDP3*) can regenerate NADPH thereby maintaining the peroxisomal $NADP^+$/NADPH cofactor pool. The last two enzymatic steps of the β-oxidation pathway involves *FOX2* and *POT1* which generates acetyl-CoA and a shortened acyl-CoA ester which then reenters the β-oxidation cycle.

Export of acetyl-CoA from the peroxisome is completed by its conjugation to carnitine via carnitine acetyl transferases encoded by three genes (*CAT2*, *YAT1* and *YAT2*) (Swiegers *et al.*, 2001). All three genes were more highly expressed in the dilute juice condition relative to the Icewine juice condition on day two of the fermentations. However, *YAT2* was more highly expressed in Icewine juice fermenting yeast after day two. Acetyl-CoA transported to the mitochondrion through this mechanism can enter the TCA cycle or be used towards other biosynthetic pathways.

4.5.1.3. Gene expression profiles (Northerns)- Acetic acid

Along with *STL1*, the gene expression profiles of *ACS1* and *ACS2* (mitochondrial and cytosolic acetyl-CoA synthetases) generated from the microarray data were found to be highly expressed in yeast fermenting diluted Icewine juice and had also showed a greater than ten-fold change in expression between fermentation conditions. The expression profile of these two genes in addition to the NAD^+-dependent aldehyde dehydrogenase *ALD3* was further validated using Northern analysis. The specificity of the DNA probes designed for *ACS1* and *ACS2* required validation prior to monitoring the expression of these selected genes throughout the first five days of Icewine and diluted Icewine juice fermentations. The DNA probe for *ALD3* was found to be specific for this gene and had been previously validated by Pigeau and Inglis (2005).

ACS1 and *ACS2* share 66% sequence homology but induction of each gene is triggered by different metabolic conditions in yeast. Respiratory growth and glucose limitation was used to induce *ACS1* expression (Van den Berg *et al.*, 1996) while anaerobic growth conditions were used to induce *ACS2* expression (Van den Berg and Steensma, 1995). Under aerobic conditions, the *ACS1* probe was found to be specific for its target gene as the probe bound to the RNA from the Δ*ACS2* strain but not to the RNA from the Δ*ACS1* strain (Figure 4.5.3A). Under anaerobic conditions, the *ACS2* probe generated a strong signal from the wine yeast strain, the parent strain and the Δ*ACS1* strain. A weak signal for the Δ*ACS2* strain was detected. This weak signal may have been due to high background signal by failure to remove non-specific probe binding during the membrane washing procedure (Figure 4.5.3B). Thus, the DNA probes designed for *ACS1* and *ACS2* appear to be specific for their targets.

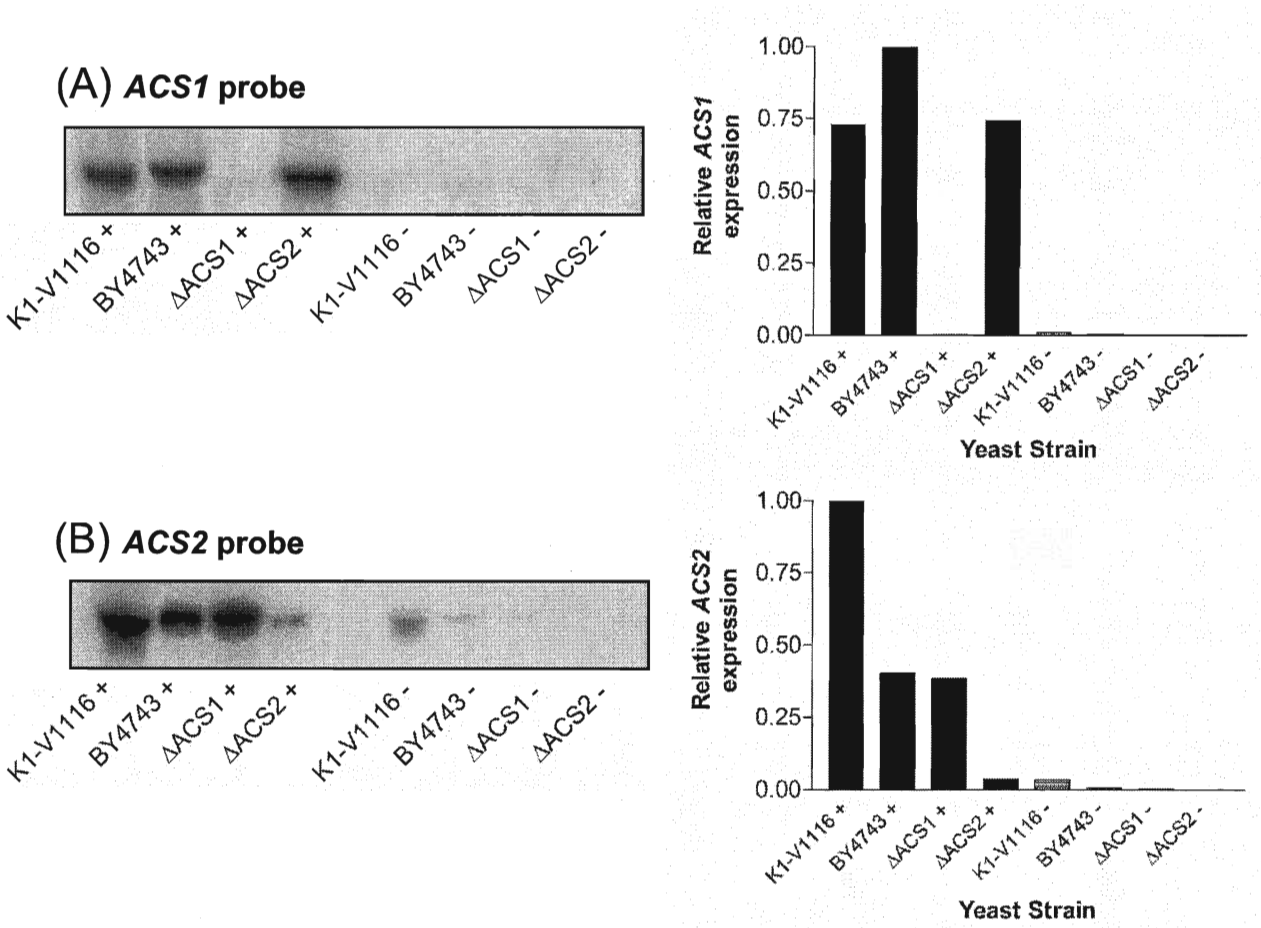

Figure 4.5.3: *ACS1* and *ACS2* probe specificity for validation Northern blots. Yeast cultures were induced to express *ACS1* under aerobic conditions (+) or not induced (-) under anaerobic conditions (A) or were induced to express *ACS2* under anaerobic conditions (+) or not induced (-) under aerobic conditions (B). Expression profiles of the blots following hybridization of ^{32}P-labeled DNA probes specific for *ACS1* and *ACS2* to RNA isolated from the commercial wine yeast strain (K1-V1116), parent yeast strains (BY4742 and BY4743) and knockout yeast strains (Δ*ACS1* and Δ*ACS2*) are shown. Relative gene expression is also shown in the bar graphs.

The relative gene expression profiles for *ACS1*/*ACS2* and *ALD3* are depicted in Figures 4.5.4 and 4.5.5, respectively. The Northern expression profile shows that the relative signal intensity of *ACS1* was 29-fold higher in yeast fermenting the dilute juice on day two of the fermentations. As both fermentations progressed, *ACS1* was weakly expressed at approximately the same level between fermentation conditions. The relative level of *ACS2* expression increased in the dilute juice condition over time until day four and at this timepoint, a 13.2-fold difference in *ACS2* expression between fermentation conditions was observed. By day five, there was no difference in *ACS2* expression. *ALD3* was also expressed throughout both fermentations and the relative difference in peak fold expression occurred on day four of the Icewine juice fermentation giving rise to a 16-fold increase in *ALD3* expression.

The fold changes in expression for this small subset of genes determined from Northern analysis was similar to the results obtained from the microarray analysis. However, the magnitude in fold changes differed slightly between gene expression techniques but the trends were the same. Also, expression of *ACS1*, *ACS2* and *ALD3* was weak but measurable on day five of the fermentations using Northern analysis but no expression could be detected in either juice condition on this day using microarray analysis.

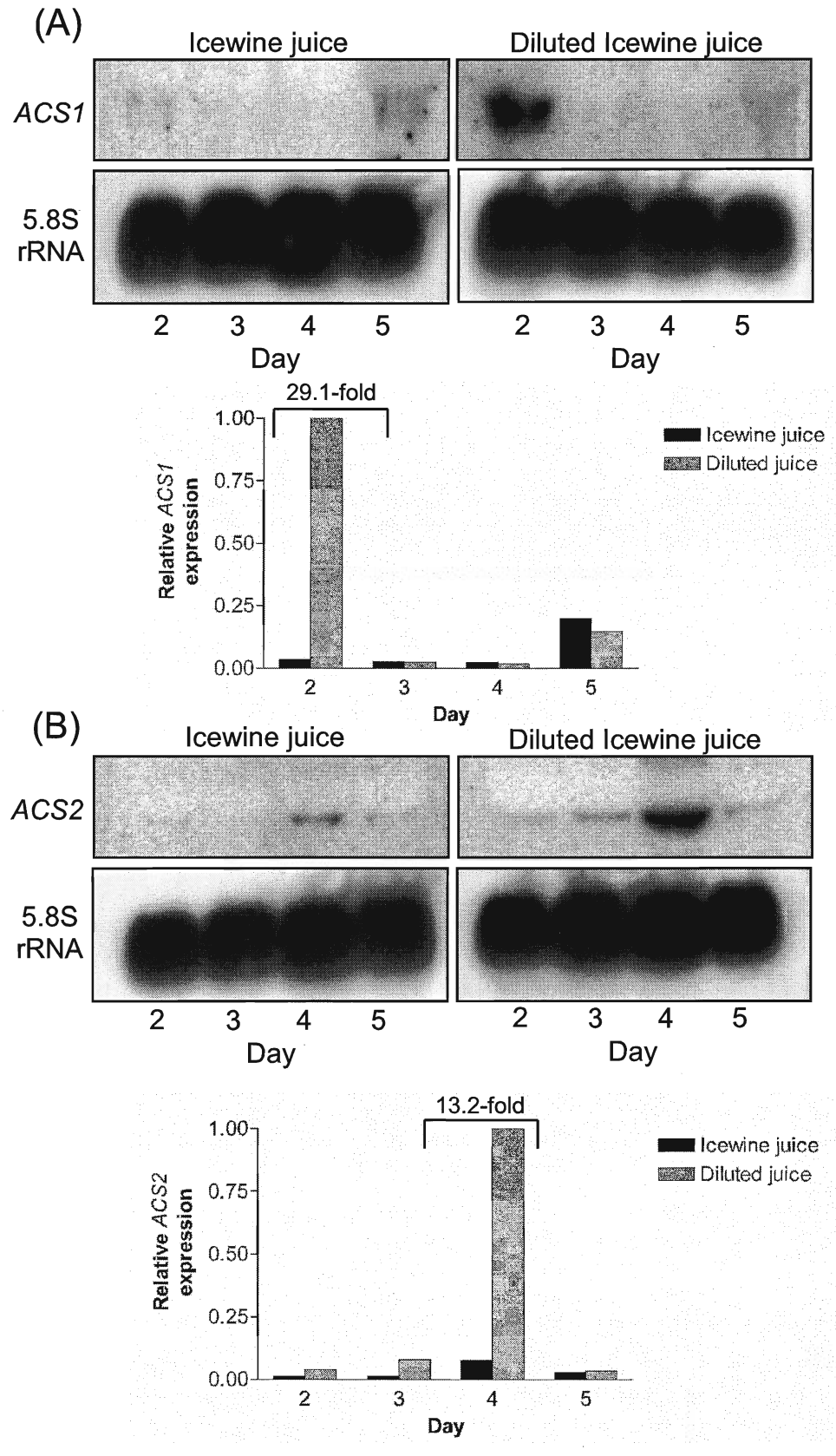

Figure 4.5.4: Expression of *ACS1* and *ACS2* during fermentation. Expression profiles of *ACS1* (A) and *ACS2* (B) from yeast fermenting Icewine juice and diluted Icewine juice using Northern analysis. 5.8S ribosomal RNA was used as a loading control. Relative gene expression between fermentation conditions is illustrated in the bar graphs.

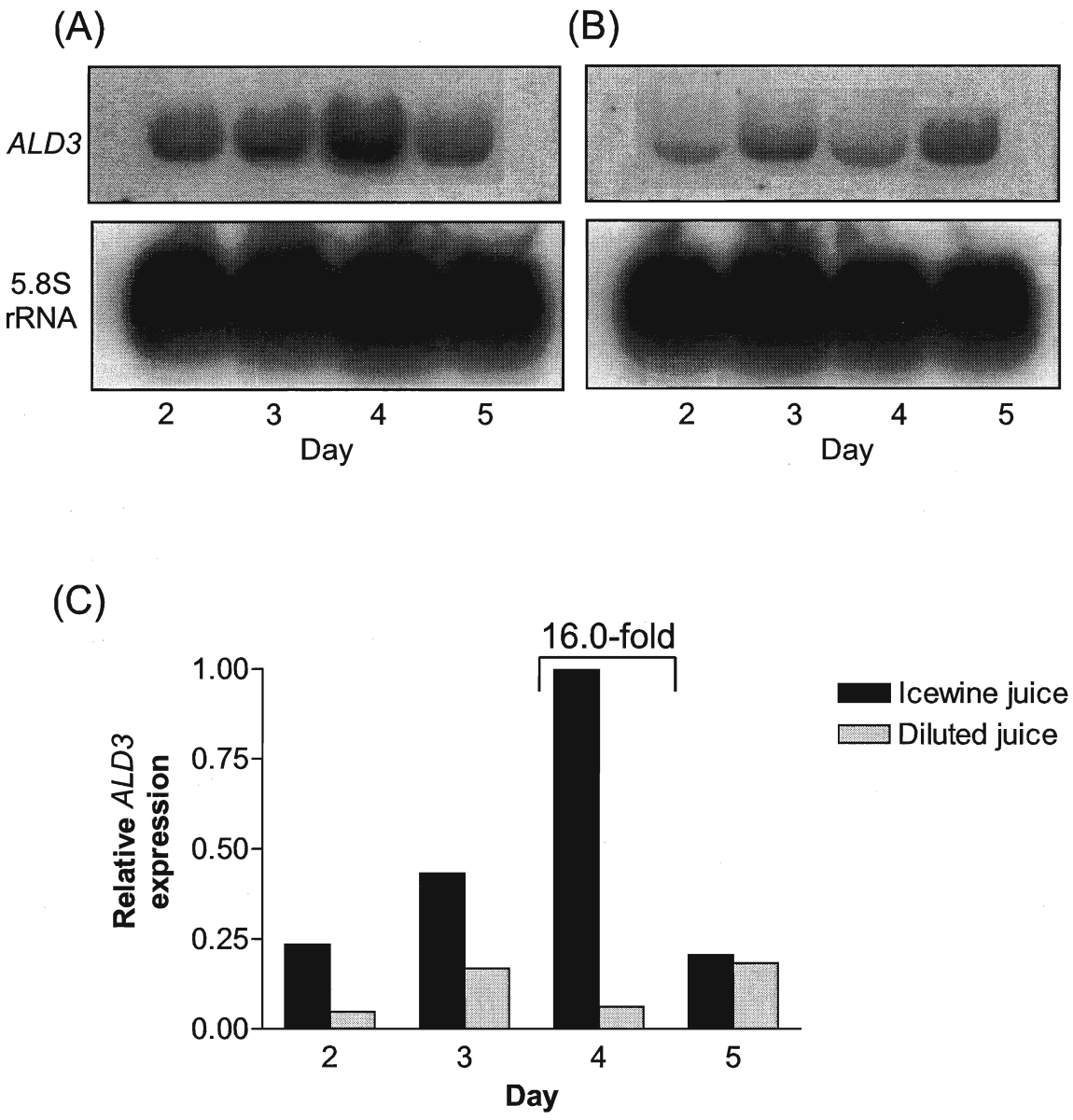

Figure 4.5.5: Expression of *ALD3* during fermentation. The expression profiles of *ALD3* from yeast fermenting Icewine juice (A) and diluted Icewine juice (B) using Northern analysis. 5.8S ribosomal RNA was used as a loading control. (C) Comparison of the relative levels of *ALD3* expression between fermentation conditions.

4.5.2. Discussion- Acetic acid Metabolism

During alcoholic fermentation, acetic acid is synthesized in *S. cerevisiae* via the cytosolic pyruvate dehydrogenase (PDH) bypass which reroutes the pyruvate produced during glycolysis away from the PDH reaction that converts pyruvate to acetyl-CoA and towards aldehyde dehydrogenase forming acetic acid. Acetic acid synthesis has been suggested as a mechanism through which yeast can reestablish cytosolic redox balance by regenerating NADH from the NAD^+ produced during glycerol biosynthesis in response to salt induced hyperosmotic stress (Blomberg and Adler, 1989; Wang *et al.*, 1998; Navarro-Avino *et al.*, 1999). Of the five genes encoding for aldehyde dehydrogenases identified in *S. cerevisiae*, upregulation of *ALD3* and *ALD6* has been associated with increased acetic acid production in osmotically stressed cells (Blomberg and Adler, 1989; Miralles and Serrano, 1995; Navarro-Avino *et al.*, 1999; Norbeck and Blomberg, 2000). However, both isoforms differ in their cofactor requirement with Ald3p being specific for NAD^+ and Ald6p being specific for $NADP^+$. Due to the differences in cofactor requirement between these two *ALD* isoforms, the function of the $NADP^+$-dependent dehydrogenase in maintaining redox balance in yeast under hyperosmotic stress is unclear as they lack transhydrogenase activity to convert reducing equivalents between the NAD^+/NADH and $NADP^+$/NADPH cofactors systems (van Dijken and Scheffers, 1986; Meaden *et al.*, 1997; Navarro-Avino *et al.*, 1999). The expression of several aldehyde dehydrogenase isoforms have been implicated in acetic acid production during table wine fermentation. However, the results from the microarray data from this study in addition to the Northern analysis results from previous studies by Pigeau and Inglis (2005 and 2007) shows that it is likely that the upregulation of the NAD^+-dependent *ALD3*

isoform contributes to the increased levels of acetic acid in Icewine. Northern analysis verified the microarray results showing that *ALD3* was also expressed throughout both fermentation conditions, however its expression was significantly greater in the Icewine juice condition with the largest fold difference in expression occurring 96 h into the Icewine juice fermentation. Also from the microarray results, the other aldehyde dehydrogenase isoforms were observed to be expressed but the expression level of these genes was not significantly different between fermentation conditions after day two.

Expression of the mitochondrial aldehyde dehydrogenase isoforms encoded by *ALD4* and *ALD5* together with the cytosolic $NADP^+$-dependent isoform encoded by *ALD6* were found to contribute to acetic acid production in wine yeast strains fermenting 20% (w/v) glucose media similar to conditions found in a table wine fermentation (Remize *et al.*, 2000; Saint-Prix *et al.*, 2004). Based on these results, these three Aldp isoforms along with the cytosolic NAD^+-dependent isoform Ald2p, likely contributed to acetic acid production in yeast during diluted Icewine juice fermentation, but their roles in the increased acetic acid synthesis and redox balancing in Icewine juice fermenting cells may be only minor. However, Erasmus *et al.* (2003) reported a significant upregulation of *ALD2*, *ALD3*, *ALD4* and *ALD6* expression in wine yeast following a 2 h exposure to 40% (w/v) sugar stress using microarray analysis. Their results may reflect a transient transcriptional response of *ALD* expression upon exposure to high sugar levels. The results from our study reflect the adapted response of wine yeast to prolonged exposure to high osmotic stress during the early stages of Icewine juice fermentation. Similar to the results reported by Pigeau and Inglis in 2005 and 2007, our microarray data indicate that the aldehyde dehydrogenases encoded by *ALD2*, *4*, *5* and *6* were not

differentially expressed between the high and low sugar stress fermentation conditions, thereby indicating that these isoforms likely do not contribute to the elevated levels acetic acid produced during Icewine fermentation. From the microarray data, both mitochondrial isoforms (encoded by *ALD4* and *ALD5*) along with the cytosolic $NADP^+$-dependent isoform (*ALD6*) were actually found to be significantly downregulated in Icewine juice fermenting cells on day two which would further limit their contribution to acetic acid production.

Elevated acetic acid production by Icewine juice fermenting yeast may also be implicated in the inactivation of the plasma membrane aquaglyceroporin Fps1p. In industrial *S. cerevisiae* strains used in the food industry, resistance and adaptation to weak acid stress involves the loss of Fps1p that passively facilitates the uptake of acetic acid (reviewed in Mollapour *et al.*, 2008). Acetic acid is small enough to gain entry into yeast cells through Fps1p by passive diffusion but when glucose repressed cells are confronted with high levels of acetic acid, the sudden influx of this weak acid through Fps1p can transiently activate Hog1p via the Sln1p branch of the HOG pathway (Mollapour and Piper, 2007; reviewed in Mollapour *et al.*, 2008). Hog1p in turn, phosphorylates Fps1p, therefore targeting Fps1p for endocytosis and degradation within the vacuole (Mollapour and Piper, 2007; reviewed in Mollapour *et al.*, 2008). High levels of acetic acid can initiate apoptosis in yeast cells so removing Fps1p may be part of an essential process to protect cells against apoptotic cell death when challenged with acetic acid (Giannattasio *et al.*, 2005; reviewed in Mollapour *et al.*, 2008). It is unknown if these events occur in yeast fermenting Icewine juice. By day two, the Icewine fermenting cells have already produced a considerable amount of acetic acid compared to the dilute juice

cells. Additionally from the microarray data, *FPS1* was found to be expressed by yeast under both fermentation conditions on day two but this channel rapidly closes upon exposure to hyperosmotic stress to control the amount of glycerol retained by the cell (Támas *et al.*, 1999). Activity of Fps1p in yeast during fermentation may be subject to a number of controls including high osmotic pressure and the presence of acetic acid but further research is necessary to clearly define its role during Icewine fermentation.

Since acetic acid is an intermediate of the PDH bypass in *S. cerevisiae*, acetic acid can be converted to acetyl-CoA via an ATP-dependent reaction catalyzed by an acetyl-CoA synthetase encoded by two isoforms, *ACS1* and *ACS2*. The bypass may have an important role in contributing to the cytosolic pool of acetyl-CoA which is required for lipid, sterol and amino acid synthesis (reviewed in Pronk *et al.*, 1996). *ACS1* encodes for the mitochondrial isozyme while *ACS2* encodes for the cytosolic acetyl-CoA synthetase. Although *ACS1* expression is required for respiratory growth on nonfermentable carbon sources and is glucose repressed (van den Berg *et al.*, 1996), it was strongly expressed in yeast on day two of the dilute juice fermentation. An increase in mitochondrial acetyl-CoA reserves may correspond to an increase in its consumption in other metabolic pathways. Genes associated with the TCA cycle were more highly expressed in dilute juice fermenting cells and an increase in *ACS1* expression may be required to replenish acetyl-CoA. The fatty acid β-oxidation pathway results in the formation of acetyl-CoA so an increase in the expression of genes associated with this pathway in dilute juice fermenting yeast cells may reflect a need for an increase in acetyl-CoA production. Since the rate of yeast biomass accumulation was faster in the dilute juice condition compared to the rate observed in the Icewine juice condition (see Section 4.2.1.), increased

production acetyl-CoA in yeast during dilute juice fermentation may have been required to support increased cell growth and reproduction.

However, the isoenzyme encoded by *ACS2* is required for fermentative growth on glucose (van den Berg and Steensma, 1995). *ACS2* was significantly downregulated up to day four of the Icewine fermentation. A decreased demand for cytosolic acetyl-CoA during Icewine fermentation corresponds to a decrease in the expression of genes involved in other metabolic pathways requiring the input of acetyl units such as lipid and ergosterol synthesis. Since yeast cells accumulate twice the biomass when fermenting dilute juice in comparison to the fermentation of Icewine juice, these cells would have an increased metabolic need for lipid and ergosterol synthesis. A wine yeast strain overexpressing *ACS2* did not result in reduced acetic acid levels (Remize *et al.*, 2000), however a reduction in acetic acid in sake yeast overexpressing *ACS2* was reported by Akamatsu *et al.* (2000). So, increased synthesis of acetyl-CoA by Acs2p from the acetic acid produced by yeast fermenting dilute juice may have resulted in the lower acetic acid levels found in this juice. But, the combination of increased *ALD3* expression together with decreased *ACS1/2* expression in osmotically stressed yeast cells during Icewine fermentation may have ultimately contributed to the elevated acetic acid levels measured in the final wine. Acetyl-CoA can also be converted back to acetic acid in a reaction catalyzed by an acetyl-CoA hydrolase encoded by *ACH1*. *ACH1* was more highly expressed in yeast fermenting dilute juice up to day four. The expression of this gene may be involved in regulating the cytosolic acetyl-CoA pools.

S. cerevisiae is able to use acetic acid as sole carbon source under aerobic conditions and the plasma membrane protein encoded by *ADY2* was identified as a

putative acetate transporter (Paiva *et al.*, 2004). Transport analyses of a Δ*ady2* laboratory yeast strain demonstrated that this gene mediates acetate transport which is crucial for growth on acetic acid. *ADY2* was strongly upregulated more than ten-fold in Icewine juice fermenting cells. After day two, the extracellular acetic acid levels increased considerably in the Icewine fermentation condition corresponding to an increase in the expression of this gene. It is not known if this transporter is capable of exporting acetic acid from the cell especially in wine yeast under fermentative conditions. But, due to the low concentration of acetic acid in the initial Icewine juice, the concentration gradient across the yeast plasma membrane would favour acetic acid export.

4.6. Additional transcriptome responses during Icewine fermentation

4.6.1. Results - additional transcriptome responses

4.6.1.1. Stress Responsive Genes

Significant fold-changes in the expression of a number of stress response genes in wine yeast were observed throughout the first five days of Icewine juice fermentation, particularly genes associated with heat shock, osmotic and oxidative stress (Table 4.6.1). Upon exposure, the expression of several yeast genes is regulated by stress with a large proportion of them responding in a related manner to many types of stresses (Causton *et al.*, 2001; Gasch *et al.*, 2000). There were six genes encoding for heat shock proteins that were found to be differentially expressed between fermentation conditions. Typically, heat shock proteins function as molecular chaperones that facilitate protein refolding and/or maintain protein conformation in yeast subject to heat-induced stress (Dawes, 2004). Of these genes, *HSP12* was strongly expressed throughout the Icewine juice fermentation with the greatest fold difference (8.9-fold) occurring on day five of the

Table 4.6.1: Expression profile of the genes involved in responding to stress.

ORF	Gene	Description	Fold Change*			
			Day 2	Day 3	Day 4	Day 5
Heat Shock						
YOR020C	HSP10	mitochondrial chaperonin	+	-	-	+2.4
YFL014W	HSP12	cytosolic heat shock protein	+4.7	+3.8	+8.5	+8.9
YBR072W	HSP26	cytosolic heat shock protein	-3.0	•	•	•
YCR021C	HSP30	plasma membrane heat shock protein	-3.5	•	-	•
YPL240C	HSP82	ATPase activity	•	•	•	-2.9
YBL075C	SSA3	ATPase activity	-	-	-2.1	-5.1
Osmotic Stress **						
YMR169C	ALD3	aldehyde dehydrogenase	+8.4	+9.7	+14.6	×
YDL022W	GPD1	glycerol-3-phosphate dehydrogenase	+	+4.3	+6.6	×
YIL053W	GPP1	glycerol-3-phosphatase	+3.1	+8.7	+12.3	+3.5
YER062C	GPP2	glycerol-3-phosphatase	+3.0	+9.3	+14.0	+4.7
YPL223C	GRE1	unknown function	+2.1	+2.7	+6.7	+7.5
YOL151W	GRE2	oxidoreductase activity	×	+13.7	+24.9	+6.1
YHR104W	GRE3	aldo-keto reductase activity	+2.9	+2.5	+2.7	•
YMR175W	SIP18	phospholipid binding	•	+2.1	+4.7	+25.4
Oxidative Stress						
YGR088W	CTT1	catalase	+3.0	+2.0	+3.6	•
YKL026C	GPX1	glutathione peroxidase	•	-2.3	×	×
YBR244W	GPX2	glutathione peroxidase	-	-2.1	-2.1	•
YIR037W	HYR1	glutathione peroxidase	-	-2.2	-2.3	•
YNL036W	NCE103	carbonate dehydratase	+	+2.8	+5.1	+13.8
YJR104C	SOD1	copper-zinc superoxide dismutase	-2.6	•	•	•
YHR008C	SOD2	manganese superoxide dismutase	-	-2.7	-2.1	•
YML028W	TSA1	thioredoxin peroxidase	•	-2.9	-2.6	-3.0
YDR453C	TSA2	thioredoxin peroxidase	×	-3.0	-2.3	-2.0
Response to Metal Ion						
YHR053C	CUP1-1	metallothionein; copper ion binding	•	+14.4	+15.4	+6.7
YHR055C	CUP1-2	metallothionein; copper ion binding	•	+13.4	+15.3	+6.2
Response to Stimulus						
YML070W	DAK1	dihydroxyacetone kinase	•	+2.3	+2.7	×
YOL053C	DDR2	DNA damage responsive	+2.0	•	+2.6	+3.6
YHR044C	DOG1	2-deoxyglucose-6-phosphate phosphatase	+7.3	×	×	×
YHR043C	DOG2	2-deoxyglucose-6-phosphate phosphatase	+9.2	×	+2.4	×
YML004C	GLO1	glyoxylase	+	+2.1	+3.2	•

*Significantly different as determined by a paired t-test ($P \leq 0.05$)
The level of gene expression changes in *S. cerevisiae* fermenting Icewine juice in comparison to gene expression changes in *S. cerevisiae* fermenting dilute Icewine juice are shown as either positive (+ fold upregulation) or negative (-fold downregulation) values. A plus sign (+) or minus sign (-) alone indicates significant difference in gene expression but less than a 2-fold change; • indicates no significant difference in gene expression; × indicates no expression was detected.
***GPD1*, *GPP1*, *GPP2* and *ALD3* are also included in this subcategory and further discussed in Sections 4.4 and 4.5

fermentation despite being reported as subject to glucose repression (de Groot *et al.*, 2000). The expression of the majority of heat shock encoding genes profiled using microarray analysis were found to be transiently downregulated at least three-fold on day two in the Icewine condition relative to the dilute condition (Table 4.6.1). This included *HSP26* which encodes for a small cytosolic heat shock protein and *HSP30* which encodes for protein possibly involved in H^+ homeostasis (Dawes, 2004). *HSP12* and *HSP26* expression had been previously found to be induced in laboratory yeast strains under salt-induced osmotic stress (Rep *et al.*, 2000; Yale and Bohnert, 2001). *HSP82* encodes for a plasma membrane-bound protein with ATPase activity (Richter *et al.*, 2002) and expression of this gene was observed to be nearly three-fold higher on day five of the dilute Icewine juice fermentation. *SSA3* encodes for a protein that belongs to the *HSP70* family of ATP-binding chaperones which functions to prevent the aggregation of unfolded proteins (Dawes, 2004). *SSA3* expression was induced under salt stress (Rep *et al.*, 2000) but its expression was significantly reduced more than two-fold on days four and five of the Icewine juice fermentation.

According to the GO Slim functional category of genes associated with the response to stress within the *Saccharomyces* genome database (SGD), a number of these genes are further divided into subcategories including the response to osmotic stress. The genes involved in glycerol (*GPD1*, *GPP1* and *GPP2*) and acetic acid (*ALD3*) synthesis fall into this category and their expression profiles have been previously described in Sections 4.4 and 4.5. From the microarray data, the genes associated with the osmotic response appeared to be expressed early during the Icewine juice fermentation and restricted to only a few responsive genes. The strongly osmoresponsive genes (*GRE1*,

GRE2, *GRE3* and *SIP18*) were induced in yeast on day two of the Icewine juice fermentation and maintained higher expression levels throughout the days examined in comparison to the expression levels of these genes in yeast fermenting the dilute juice (Table 4.6.1). Both *GRE1* and *SIP18* encode for hydrophilin-like proteins and expression of these genes was found to be upregulated in laboratory yeast strains under desiccation stress (Garay-Arroyo *et al.*, 2000; Singh *et al.*, 2005). The fold difference in *GRE1* (7.5-fold) and *SIP18* (25.4-fold) expression peaked on day five of the Icewine juice fermentation. Expression of all three *GRE* isoforms was found to be induced by osmotic and other stresses (Garay-Arroyo and Covarrubias, 1999). *GRE2* encodes for a protein with oxidoreductase activity while *GRE3* expression is associated with methylglyoxal metabolism (Garay-Arroyo and Covarrubias, 1999; Aguilera and Prieto, 2001). *GRE2* was more highly expressed in the Icewine juice cells than *GRE3*. *GRE2* was identified as being one of the mostly highly upregulated genes (25-fold) identified in yeast fermenting Icewine juice (Table 4.6.1).

The genes associated with responding to oxidative stress were predominantly less highly expressed during Icewine juice fermentation compared to the dilute juice fermentation by approximately two-fold on days three and four of the fermentations. This expression profile was characterized by the downregulation of genes known to be associated with reactive oxygen species defense and superoxide radical detoxification such as the superoxide dismutases (*SOD1* and *SOD2*), glutathione peroxidases (*GPX1*, *GPX2* and *HYR1*) and the thioredoxin peroxidases (*TSA1* and *TSA2*). However, cytosolic catalase T (*CTT1*) which is involved in dissipating H_2O_2 into water and oxygen (Dawes, 2004; reviewed in Hohmann, 2002) was highly expressed from days two to four of the

Icewine juice fermentation relative to the dilute juice fermentation. *CTT1* expression is regulated by the general stress transcription factors Msn2p and Msn4p (Martinez-Pastor *et al.*, 1996; reviewed in Hohmann, 2002). *NCE103* encodes for a carbonate dehydratase and expression of this gene is typically weak under anaerobic conditions (Götz *et al.*, 1999). However, *NCE103* was found to be strongly expressed on day five of the Icewine juice fermentation (Table 4.6.1).

Genes encoding for copper ion binding metallothionein proteins (*CUP1-1* and *CUP1-2*) were two of the most strongly expressed genes in yeast fermenting Icewine juice. In yeast, these proteins function as copper ion scavengers in response to metal ion stress (Dawes, 2004) but under Icewine juice fermentation conditions both isoforms were expressed more than ten-fold higher on days three and four compared to the dilute fermentation (Table 4.6.1).

The response to stimulus is a broad category encompassing a subset of genes expressed under a variety of stress conditions also including osmotic and oxidative stresses. Of these genes, two of them associated with glycerol degradation (*DAK1*) and methylglyoxal metabolism (*GLO1*) exhibited differential expression between fermentation conditions (Table 4.6.1). *DAK1* encodes for a dihydroxyacetone kinase that functions to phosphorylate dihydroxyacetone to form DHAP at the expense of one ATP molecule (reviewed in Blomberg, 2000). This gene was expressed just over two-fold greater on day two in the Icewine juice when compared to the dilute juice fermentation. *GLO1* encodes an enzyme (glyoxylase I) involved in the first step in the methylglyoxal degradation pathway that ultimately forms lactic acid in the presence of glutathione (Inoue and Kimura, 1995). The difference in *GLO1* expression was at least two-fold

higher on days three and four of Icewine juice fermentation relative to the dilute juice fermentation. Two genes encoding for putative 2-deoxyglucose-6-phosphate phosphatases (*DOG1* and *DOG2*) were strongly but transiently expressed on day two of the Icewine fermentation (Table 4.6.1).

4.6.1.2. Transport Responses

Several genes associated with transport of small molecules and ions in *S. cerevisiae* were differentially expressed between fermentation conditions. Transport protein encoding genes were significantly up- or downregulated up to day four of the Icewine juice fermentation and by day five, no expression of these genes could be detected in either fermentation condition (Table 4.6.2).

The *ENA* gene family encodes for plasma membrane Na^+-ATPase pumps mediating the active efflux of sodium from the cytoplasm (reviewed in Hohmann, 2002). *ENA1* expression was found to be induced in response to salt stress in laboratory yeast (Posas *et al.*, 2000) however three *ENA* isoforms were strongly expressed in yeast fermenting Icewine juice compared to yeast fermenting dilute juice. Also, genes involved in iron transport (*FIT1*, *FIT2* and *FTR1*) were relatively more highly expressed early on in the Icewine juice fermentation. Three genes encoding for organic acid transporters in yeast (*DIC1*, *JEN1* and *SFC1*) were found to be less highly expressed on day two of the Icewine juice fermentation. However, the difference in *SFC1* (mitochondrial succinate-fumarate antiporter) expression was more than ten-fold on day five of the fermentations (Table 4.6.2). The role of *SFC1* in yeast during Icewine fermentation is unclear since its expression is required for aerobic growth on ethanol and acetate (Fernández *et al.*, 1994; Palmieri *et al.*, 1997).

Table 4.6.2: Expression profile of the genes involved in transport.

ORF	Gene	Description	Fold Change*			
			Day 2	Day 3	Day 4	Day 5
Ion Transport						
YFL050C	ALR2	magnesium cation transporter	×	+	+3.0	×
YDR040C	ENA1	sodium ion transporter	•	+3.5	+5.0	×
YDR039C	ENA2	sodium ion transporter	-2.0	+3.9	+4.7	×
YDR038C	ENA5	sodium ion transporter	•	+3.0	×	×
YDR534C	FIT1	siderophore transporter	+2.3	×	×	×
YOR382W	FIT2	siderophore transporter	+6.5	×	×	×
YER145C	FTR1	high affinity iron permease	•	+4.7	×	×
YJR077C	MIR1	phosphate transporter	+	-2.2	-2.8	•
YER053C	PIC2	phosphate transporter	+	-	-2.3	-2.0
YNL055C	POR1	phosphate transporter	•	-4.6	-3.4	-2.6
YGL255W	ZRT1	high affinity zinc ion transporter	-6.9	×	×	×
YLR130C	ZRT2	low affinity zinc ion transporter	-3.0	×	×	×
Organic Acid Transport						
YLR348C	DIC1	dicarboxylic acid transporter	-2.3	×	×	×
YKL217W	JEN1	lactate and pyuvate permease	-2.0	•	-2.4	×
YJR095W	SFC1	mitochondrial succinate-fumarate transporter	-3.4	+	•	+11.4

*Significantly different as determined by a paired t-test ($P \leq 0.05$)

The level of gene expression changes in *S. cerevisiae* fermenting Icewine juice in comparison to gene expression changes in *S. cerevisiae* fermenting dilute Icewine juice are shown as either positive (+ fold upregulation) or negative (-fold downregulation) values. A plus sign (+) or minus sign (-) alone indicates significant difference in gene expression but less than a 2-fold change; • indicates no significant difference in gene expression; × indicates no expression was detected.

4.6.2. Discussion – additional transcriptome responses

The high osmotic pressure yeast encountered during Icewine fermentation elicited the upregulation of a number of genes categorized as stress responsive according to the Gene Ontology (GO) Slim term annotations of the *Saccharomyces* genome database (SGD) (Ashburner *et al.*, 2000; Dwight *et al.*, 2002). The expression of many of these genes encode for proteins and enzymes that are primarily involved with the protection of yeast cells against osmotic and oxidative damage upon exposure to salt, oxidizing agents and other environmental stimuli (Gasch *et al.*, 2000; Rep *et al.*, 2000; Causton *et al.*, 2001). In order to select and/or design yeast strains better suited to Icewine fermentations, identifying which genes that are characteristically expressed during the adaptive stress response of commercial wine yeast under extended hyperosmotic stress throughout Icewine fermentation is of great interest.

Of the genes annotated by the SGD as responsive to osmotic stress, *SIP18* was one of the mostly highly expressed genes by yeast fermenting Icewine juice compared to yeast fermenting dilute juice. *SIP18* was one of four novel genes found to be inducible upon salt stress, and expression of this gene was found to be Hog1p-dependent (Miralles and Serrano, 1995). *SIP18* was also found to be upregulated four-fold in a wine yeast strain exposed to high sugar stress compared to nonstressed cells (Erasmus *et al.*, 2003). Rossignol *et al.* (2003) reported that *SIP18* was strongly expressed in a commercial wine strain throughout the fermentation of synthetic grape must containing 200 g L^{-1} sugar with maximum *SIP18* expression occurring at the stationary growth phase. In agreement with the findings of Rossignol *et al.* (2003), the peak difference in *SIP18* expression occurred when Icewine and diluted juice fermenting cells entered early stationary phase.

The function of *SIP18* (salt induced protein) in response to hyperosmotic stress has not been fully elucidated but there is evidence that this gene putatively encodes for a hydrophilin (Garay-Arroyo *et al.*, 2000).

The hydrophilins are part of a broad class of proteins which include plant late embryogenesis abundant (*LEA*) proteins that are implicated in providing desiccation tolerance to plants under water-limiting conditions (Baker *et al.*, 1988; Garay-Arroyo *et al.*, 2000). *LEA*-like proteins have been identified in fungi and they appear to be involved in pathways that respond to osmotic stress and desiccation (Garay-Arroyo *et al.*, 2000; Singh *et al.*, 2005). These hydrophilic proteins are structurally characterized by high glycine contents and contain many charged amino acid residues (Bray, 1997; Garay-Arroyo *et al.*, 2000). Microarray analysis of the response of a laboratory strain of *S. cerevisiae* to desiccation and subsequent rehydration under minimal glucose conditions showed that *SIP18* was found to be strongly expressed in conjunction with another gene, *GRE1* (Singh *et al.*, 2005). In *S. cerevisiae*, 12 hydrophilin-encoding genes have been identified within the genome (Garay-Arroyo *et al.*, 2000). Of these, three (*SIP18*, *HSP12* and *GRE1*) have been previously reported to be induced in yeast exposed to osmotic stress (Miralles and Serrano, 1995; Varela *et al.*, 1992; Garay-Arroyo and Covarrubias, 1999).

Both *HSP12* and *GRE1* were also observed to be upregulated in yeast under high sugar stress and during alcoholic fermentation (Erasmus *et al.*, 2003; Rossignol *et al.*, 2003). *HSP12* is a member of the heat shock protein family (Dawes, 2004) and is typically upregulated under in yeast under a variety of stress conditions including heat shock and salt stress (Gasch *et al.*, 2000; Rep *et al.*, 2000; Causton *et al.*, 2001).

Although *HSP12* expression was shown to be subject to glucose repression (de Groot *et al.*, 2000), our microarray data indicated that the fold-change in expression of both *HSP12* and *GRE1* was higher during the first five days of Icewine juice fermentation compared to dilute juice fermentation. Both *HSP12* and *GRE1* were additionally observed to be upregulated in wine yeast during high sugar stress and alcoholic fermentation (Erasmus *et al.*, 2003; Rossignol *et al.*, 2003). Singh *et al.* (2005) proposed that in desiccated yeast that have not biosynthesized or accumulated sufficient amounts of glycerol or trehalose required for survival during desiccation, the Sip18p protein could function as a compatible solute. It has been clearly shown in previous studies that yeast synthesize and accumulate glycerol as a compatible osmolyte in response to osmotic stress (reviewed in Nevoigt and Stahl, 1997). In our present study, yeast fermenting Icewine juice also produced glycerol in response to high concentrations of solutes present in the juice (Section 4.3.1). Although yeast cells experience loss of cytosolic water and reduced turgor pressure upon exposure to osmotic stress (Blomberg and Adler, 1992; Varela and Mager, 1996; Blomberg and Adler, 2002; Billi and Potts, 2002), it is unknown if hydrophilins have a role in protecting wine yeast cells against hyperosmotic stress during Icewine fermentation.

As previously stated, *GRE1* was highly expressed in yeast fermenting Icewine juice but the microarray data also showed that two other genes, *GRE2* and *GRE3* followed the same trend. *GRE1*, *GRE2* and *GRE3* were all reported to be responsive to sorbitol-induced osmotic stress and other stresses including ionic, oxidative and heat stress (Garay-Arroyo and Covarrubias, 1999). *GRE1* and *GRE2* were also upregulated in a laboratory yeast strain in response to desiccation but the expression of these genes

declined upon yeast rehydration (Singh *et al.*, 2005). Of the *GRE* genes, only *GRE2* was significantly upregulated in wine yeast under high sugar stress 2 h post inoculation (Erasmus *et al.*, 2003). Expression of all three *GRE* genes are under control of the HOG-pathway but activation *GRE1* and *GRE3* upon stress is also mediated by the general stress response STRE-transcription factors Msn2p and Msn4p (Garay-Arroyo and Covarrubias, 1999). Amino acid sequence analysis revealed that *GRE2* encodes for a protein with similarity to a plant $NADP^+$-dependent dihydroflavonol-4-reductase while *GRE3* encodes for a NADPH-dependent keto-aldose reductase highly related to fungal xylose-reductases (Garay-Arroyo and Covarrubias, 1999). There is evidence that the aldose reductase encoded by *GRE3* has a key role in the methylglyoxal detoxification pathway in yeast (Aguilera and Prieto, 2001). Both *GRE2* and *GRE3* encode for putative enzymes involved in redox reactive pathways so they could possibly participate in maintaining intracellular redox balance in the $NADP^+$/NADPH cofactor system if an imbalance exists during osmotic stress. However, the function of the *GRE* genes in wine yeast fermenting Icewine juice is unknown. *ALD6*, which encodes for a $NADP^+$-dependent aldehyde dehydrogenase, was found to be expressed by yeast fermenting both Icewine and diluted Icewine juice (see Table 4.5.2 in Section 4.5). Ald6p was found to be the main aldehyde dehydrogenase responsible for acetic acid production in laboratory *S. cerevisiae* strains fermenting glucose media (Remize *et al.*, 1999; Eglinton *et al.*, 2002). In addition, *ALD6* expression was found to be both upregulated under salt stress and dependent on HOG pathway activation (Akhtar *et al.*, 1997; Rep *et al.*, 2000). However, the function of Ald6p, if any, in maintaining redox balance under these hyperosmotic stress conditions during glycerol biosynthesis is not clear due to its cofactor specificity. However, Ald6p

activity in yeast may be partially responsible for the increased acetic acid produced during Icewine fermentation and may have a role in maintaining redox balance in the $NADP^+$/NADPH cofactor system in order to offset the $NADP^+$ generated by Gre3p during fermentation.

Expression of genes associated with responding to reactive oxygen species and superoxide radical detoxification- superoxide dismutases (*SOD1* and *SOD2*), glutathione peroxidases (*GPX1*, *GPX2* and *HYR1*) and the thioredoxin peroxidases (TSA1 and *TSA2*)- were for the most part lower in yeast during Icewine juice fermentation compared to those fermenting dilute juice. The expression of many genes encoding proteins and enzymes involved in oxidative damage defense and in redox metabolism is activated under a variety of stress conditions (Causton *et al.*, 2001; reviewed in Hohmann, 2002). One of which, cytosolic catalase T (*CTT1*), was upregulated during in yeast fermenting high sugar grape juice (Erasmus *et al.*, 2003). *CTT1* is involved in H_2O_2 dissipation (Dawes, 2004) and this gene was also found to be upregulated during Icewine juice fermentation. Activation of *CTT1* expression is mediated by the Hog1p and the general stress response transcription factors Msn2p/Msn4p (Martinez-Pastor *et al.*, 1996; reviewed in Hohmann, 2002). Hohmann (2002) proposed that the response to oxidative stress is partially activated in yeast upon exposure to various stress conditions. When yeast are under stress, oxidative metabolism is stimulated leading to enhanced intracellular production of reactive oxygen species. However, it is unknown if expression of oxidative defense genes in yeast cells fermenting diluted juice compared to those fermenting Icewine juice actually corresponds to an increase in the generation of reactive oxygen species under anaerobic conditions.

Genes encoding enzymes involved in methylglyoxal (MG) detoxification, *GLO1* (glyoxylase I) and *GRE3* (aldose reductase) were also more highly expressed in yeast fermenting Icewine juice. Expression of *GLO1* has been found to be induced in laboratory yeast strains under salt and sorbitol stress (Inoue *et al.*, 1998). Methylglyoxal (2-oxoaldehyde) is a highly reactive cytotoxic by-product derived from dihydroxyacetone phosphate (DHAP) following the spontaneous dephosphorylation of endiolate phosphate formed from the interconversion of the glycolytic triose phosphate intermediates DHAP and glyceraldehyde-3-phosphate (Inoue *et al.*, 1998; Aguilera and Prieto, 2001; Margarida *et al.*, 2001; Aguilera *et al.*, 2005). Up to 0.3% of glucose consumed in exponentially growing yeast cells is converted to methylglyoxal (Margarida *et al.*, 2001). There are two routes of methylglyoxal detoxification in yeast. The first route involves Glo1p which requires glutathione to convert methylglyoxal to S-D-lactoylglutathione and Glo2p (glyoxylase II) catalyzes the hydrolysis of the thioester forming D-lactate and regenerating glutathione (Margarida *et al.*, 2001). *GLO2* was not found to be expressed by yeast under either fermentation condition. In the alternate pathway, Gre3p catalyzes the NADPH-dependent conversion of methylglyoxal to 1-2 propanediol (Aguilera *et al.*, 2005). Intracellular methylglyoxal levels have been shown to transiently increase upon brief hyperosmotic shock (Aguilera and Prieto, 2001). *GLO1*, but not *GRE3*, was upregulated in wine yeast under high sugar stress (Erasmus *et al.*, 2003). It is not known if yeast cells accumulate methylglyoxal when exposed to prolonged hyperosmotic stress such as during Icewine fermentation. Enhanced methylglyoxal formation should result if a proportional increase in the rate of carbon flux through glycolysis also occurs (Aguilera and Prieto, 2001). But, we observed that sugar uptake and the expression of glycolytic

genes are greatly reduced in yeast during Icewine fermentation compared to dilute juice fermentation. Upregulation of *GLO1* and *GRE3* in these cells may only be in response to the higher osmotic pressure placed on yeast in Icewine juice compared to those in diluted juice and not due to an accumulation of methylglyoxal. However, methylglyoxal accumulation in Icewine fermenting yeast could occur as a consequence of an increased demand for DHAP required for glycerol synthesis. This demand would favour the redirection of triose phosphates formed during glycolysis towards DHAP production and away from glyceraldehyde-3-phosphate thereby increasing the chances of methylglyoxal formation.

Of the several genes associated with transport of small molecules and ions in *S. cerevisiae* that were differentially expressed between fermentation conditions, the genes encoding for magnesium, sodium and iron transporters were upregulated in Icewine juice fermenting yeast. The uptake or export of ions plays an important role during osmoadaptation in all types of organisms including yeast (reviewed in Hohmann, 2002). The *ENA* gene family encodes for plasma membrane Na^+-ATPase pumps mediating the efflux of sodium from the cytoplasm (reviewed in Hohmann, 2002). *ENA1* expression was found to be induced in response to salt stress in laboratory yeast (Posas *et al.*, 2000) and expression during osmotic stress is Hog1p-dependent (reviewed in Hohmann, 2002). Two *ENA* isoforms (*ENA2* and *ENA5*) were upregulated in sugar-stressed wine yeast (Erasmus *et al.*, 2003) however our microarray results revealed that three *ENA* isoforms were strongly upregulated in yeast fermenting Icewine juice. Additionally, genes encoding for the copper ion binding metallothionein proteins (*CUP1-1* and *CUP1-2*) were observed to be strongly expressed during Icewine fermentation. The

metallothioneins can function as antioxidants in yeast under oxidative stress conditions in addition to acting as scavengers for metal ions thereby protecting cells against copper toxicity (Dawes, 2004). It has been previously shown that Icewine juice contains concentrated solutes in addition to sugar that increases stress on wine yeast fermenting this juice (Pigeau and Inglis, 2005). Although the concentrations of salt and metal ions present in Icewine juice has not been measured to date, their presence could potentially intensify the overall hyperosmotic stress wine yeast face during Icewine fermentation and initiate other stress responses if they disrupt intracellular ion homeostasis during fermentation.

5. OVERALL DISCUSSION AND FUTURE DIRECTIONS

The successful commercial development of Canadian Icewine into a unique specialty dessert wine has garnered Canada international recognition as a world leader in Icewine production. Although the high concentrations of naturally concentrated solutes in the juice ultimately contribute to the intense flavours and aromas characteristic of this wine, the hyperosmotic nature of the juice places commercial wine yeast under considerable stress as they ferment the juice into wine (Kontkanen *et al.*, 2004; Pigeau and Inglis, 2005, Pigeau *et al.*, 2007). In this study, the high osmotic stress experienced by the commercial wine yeast *Saccharomyces cerevisiae* K1-V1116 throughout the course of Icewine fermentation elicited changes in cell growth and metabolism which correlated to several fermentation difficulties including reduced biomass accumulation and fermentation rate, reduced nutrient uptake and increased production of potentially undesirable metabolites like acetic acid that could ultimately affect the quality of the finished wine. With the use of microarray analysis, we further bridged the gap between the genome-wide transcriptional response of wine yeast as they adapt to prolonged exposure to high osmotic stress to changes within metabolic pathways associated with sugar and nitrogen and the production of yeast metabolites throughout Icewine juice fermentation. Typically throughout table wine fermentations, yeast growth is restricted by carbon and nitrogen source availability, but more frequently by nitrogen source limitation. Despite the fact that the Icewine juice contained approximately twice the amount of both sugar and nitrogen in comparison to the diluted Icewine juice, only about half the amount of available reducing sugars and amino acid nitrogen was ultimately consumed by the Icewine juice fermenting yeast. Based on these results, sugar and

nitrogen availability was not a contributing factor to the impaired cell growth exhibited by Icewine juice fermenting cells. However, the osmotic stress due to the overall abundance of concentrated sugar and nitrogen in addition to other solutes in the juice hindered the ability of the wine yeast to ferment this juice. In 2005, a study by Pigeau and Inglis demonstrated that yeast fermenting chaptalized diluted Icewine juice, which contained equal amounts of fermentable sugars as the undiluted Icewine juice but half the amounts of all other soluble solids, were able to generate more biomass and consume more sugar than Icewine juice fermenting cells. This further indicated that in addition to sugar, other solutes concentrated in the juice affects the overall fermentative capacity of wine yeast. Using microarray and Northern analysis, we also identified the expression of a glycerol/H^+ symporter (*STL1*) which was highly upregulated in yeast fermenting Icewine juice along with the expression of two acetyl-CoA synthetase isoforms (*ACS1* and *2*) which were greatly downregulated. The expression patterns of these genes potentially contribute to decreased cell viability and increased acetic acid production demonstrated by yeast fermenting Icewine juice.

The concentrated solutes in the Icewine juice increased the osmotic stress placed on yeast cells was manifested in a longer lag phase and fewer actively budding cells at the start of the fermentation. Yeast fermenting Icewine juice did not reach the same cell concentration or accumulate the same amount of biomass compared to cells fermenting diluted Icewine juice. Since there were high concentrations of residual sugar and nitrogenous compounds measured in Icewine, reduced biomass formation was not due to limited nutrient availability. The gene profiling data clearly indicated that genes associated with sugar and amino acid uptake and metabolism were predominantly

downregulated during the exponential growth phase of Icewine fermenting yeast correlating to an overall decrease in the rate of sugar and nitrogen utilization compared to yeast fermenting diluted juice. Despite the high concentrations of fermentable sugars present in the juice, many of the genes associated with sugar metabolism that were not highly expressed in yeast under the Icewine condition were involved in glycolysis and the TCA cycle. Decreased or lack of expression of the genes associated with ATP-generating metabolic pathways could contribute to impaired cell growth by limiting the amount of energy produced during Icewine fermentation that is normally required for optimal cell division and growth under anaerobic conditions. It also appears that the high osmotic stress yeast encounter during Icewine fermentation impedes amino acid uptake. In the dilute juice condition, over 90% of assimilable amino acids and ammonia were taken up after five days of the fermentation compared to only 28% in the Icewine juice condition. Reduced amino acid uptake coupled with a decrease in the expression of amino acid biosynthetic genes may also further impair cell growth and contribute nitrogen deficiencies that typically lead to sluggish fermentation rates (Monteiro and Bisson, 1991a).

Reduced biomass formation during Icewine fermentation may also be a consequence of diverting sugar away from cell growth and towards glycerol and acetic acid production as part of the yeast stress response to prolonged exposure to high osmotic conditions. The microarray results showed that the genes within the glycerol and acetic acid metabolic pathways were significantly upregulated in yeast fermenting Icewine juice and an increase in the expression of these genes corresponded to elevated levels of both metabolites found in the wine. Wine yeast face both anaerobic and osmotic stress during

Icewine fermentation and either of these factors may control the transcriptional response of genes associated with glycerol synthesis. Glycerol production by osmotically stressed yeast has been correlated to an increased expression of the NAD^+-dependent glycerol-3-phosphate dehydrogenase (*GPD1*) in order to balance the external osmotic pressure (Larsson *et al.*, 1993; Albertyn *et al.*, 1994a; Blomberg, 2000). *GPD1* was found to upregulated during Icewine fermentation however *GPD2* was not expressed after day three by yeast under both fermentation conditions. *GPD2* isoform has been reported to serve a role in maintaining redox balance under anaerobic conditions by oxidizing excess NADH generated during biomass formation (van Dijken and Scheffers, 1986; Ansell *et al.*, 1997). In agreement with the results of Pigeau and Inglis (2005 and 2007) *GPD2*, unlike *GPD1,* does not appear to contribute to the elevated glycerol found in the wine. Both isoforms of glycerol-3-phosphatase (*GPP1* and *GPP2*) were more strongly expressed during Icewine fermentation. *GPP1* and *GPP2* are both induced by osmotic stress in a HOG pathway dependent manner (Norbeck *et al.*, 1996; Rep *et al.*, 2000; Påhlman *et al.*, 2001) but *GPP2* expression was found to be more responsive to salt stress (Hirayama *et al.*, 1995) whereas *GPP1* expression was found to be transiently upregulated under anaerobic conditions (Påhlman *et al.*, 2001). Although the rate-limiting step in glycerol synthesis is catalyzed by glycerol-3-phosphate dehydrogenase (Larsson *et al.*, 1993; Eriksson *et al.*, 1995; Remize *et al.*, 2001), both isoforms were highly expressed in yeast in the presence of high concentrations of fermentable sugars, and the increased expression appears to be required for glycerol synthesis during Icewine fermentation.

Active glycerol uptake via a glycerol/H^+ symporter (Stl1p) may be occurring in *S. cerevisiae* during Icewine juice fermentation. *STL1* was one of the most strongly expressed genes identified in yeast fermenting Icewine juice. *STL1* expression has been previously described as salt-induced and glucose repressed in laboratory yeast strains (Rep *et al.*, 2000; Ferreira *et al.*, 2005). However, results from this thesis study showed *STL1* was one of the most highly upregulated genes in wine yeast. Similar results were found when wine yeast were briefly exposed to high sugar stress (Erasmus *et al.*, 2003). Using both microarray and Northern analysis in our study, an expression profile comparison of this gene throughout the Icewine juice and dilute juice fermentations resulted in a relative 25-fold difference in *STL1* expression between juice conditions on day five of the fermentations.

The use of Stl1p by yeast for glycerol uptake during Icewine juice fermentation may contribute to limited cell growth by dissipating the plasma membrane proton gradient in an energy dependent manner. Protons that enter the cell must be excreted to prevent acidification of the cytoplasm and cell death but proton export requires the activity of several plasma membrane ATPases (reviewed in Boulton *et al.*, 1998). This extra energy expenditure to maintain the proton gradient may also further disadvantage yeast during Icewine fermentation. Reduced expression of ATPase encoding genes like *HSP82* may decrease the ability of yeast cells to regulate intracellular proton concentrations during Icewine fermentation. Disruption in the proton motive force necessary to import amino acids through the dissipation of the plasma membrane proton gradient may also be potentially responsible for reduced amino acid uptake observed in Icewine juice fermenting cells.

Although expression of *STL1* is HOG pathway dependent (reviewed in Hohmann, 2002) and it appears that *STL1* expression is induced upon prolonged exposure to high sugar stress during Icewine fermentation, upregulation of *STL1* in yeast does not necessarily mean that its protein product is functional during Icewine fermentation. Future studies involving [^{14}C]glycerol transport assays in wine yeast fermenting Icewine and diluted Icewine juice in the presence and absence of a chemical protonophore will help to determine if yeast cells are actively taking up glycerol during Icewine fermentation.

Additionally from the microarray data, upregulation of the aldehyde dehydrogenase isoform *ALD3* appears to have a key role in acetic acid formation and maintaining redox balance during glycerol synthesis in yeast during Icewine fermentation. The production of acetic acid by Ald3p can resupply the cytosolic NADH required to support increased glycerol production in Icewine fermenting yeast cells in response to the high extracellular osmotic pressure. Erasmus *et al.* (2003) reported the upregulation of *ALD2*, *ALD3*, *ALD4* and *ALD6* in wine yeast briefly exposed to high sugar stress. However, our microarray results were in agreement with the findings by Pigeau and Inglis (2005 and 2007) whereby the upregulation of *ALD3* during Icewine fermentation in conjunction with a lack of differential expression of the other aldehyde dehydrogenase isoforms (*ALD2*, *4*, *5* and *6*) between fermentation conditions corresponded to a considerable fold increase in acetic acid production by Icewine fermenting yeast. Expression of the mitochondrial aldehyde dehydrogenase isoforms *ALD4* and *ALD5* together with the cytosolic $NADP^+$-dependent isoform *ALD6* were found to contribute to acetic acid production in wine yeast strains fermenting 20% (w/v)

glucose media similar to conditions found in a table wine fermentation (Remize *et al.*, 2000; Saint-Prix *et al.*, 2004). HOG-dependent upregulation of *ALD3* and *ALD6* has been associated with increased acetic acid production in osmotically stressed cells (Blomberg and Adler, 1989; Miralles and Serrano, 1995; Navarro-Avino *et al.*, 1999; Norbeck and Blomberg, 2000). However *ALD3* encodes for a cytosolic NAD^+-dependent aldehyde dehydrogenase (Navarro-Avino *et al.*, 1999) while *ALD6* encodes for a cytosolic $NADP^+$-dependent isoform (Meaden *et al.*, 1997) thus the redox balancing role of Ald6p during Icewine fermentation is not clear since yeast lack a transhydrogenase to convert between reducing equivalents (van Dijken and Scheffers, 1986). Even though we have transcriptional evidence of *ALD3* contributing to the elevated acetic acid levels generated by yeast fermenting Icewine juice, enzyme assays would clarify which cytosolic aldehyde dehydrogenase contributes to acetic acid production.

Acetic acid can be the substrate of acetyl-CoA synthetase which catalyzes the formation of acetyl-CoA from acetate and coenzyme A. Two acetyl-CoA synthetase isoenzymes exist in *S. cerevisiae* and the cytosolic isoenzyme encoded by *ACS2* is necessary for growth on glucose by yeast under anaerobic conditions (van den Berg and Steensma 1995) while *ACS1* is the glucose repressible mitochondrial isoform required for respiratory growth on non-fermentable carbon sources (Kratzer and Schüller, 1995; Van den Berg *et al.*, 1996). A cytosolic supply of acetyl-CoA is required for lipid, sterol and amino acid biosynthesis such that yeast can utilize the cytosolic pyruvate dehydrogenase bypass to generate cytosolic acetyl-CoA (reviewed in Pronk *et al.* 1996). Acetic acid is an intermediate of the bypass in *S. cerevisiae* and it can be converted to acetyl-CoA via an ATP-dependent reaction catalyzed by acetyl-CoA synthetase. The bypass may have an

important role in contributing to the cytosolic pool of acetyl-CoA which is required for lipid, sterol and amino acid synthesis (reviewed in Pronk *et al.*, 1996).

The microarray expression profiles of the acetyl-CoA synthetases which were successfully verified by Northern analysis showed that both *ACS* isoforms were strongly downregulated in yeast cells fermenting Icewine juice compared to their diluted juice fermenting counterparts. Downregulation of *ACS2* during Icewine fermentation corresponded to the downregulation of genes involved in other metabolic pathways requiring the input of acetyl units such as lipid, ergosterol and amino acid synthesis. Yeast cells fermenting dilute juice accumulate twice the biomass than those fermenting Icewine juice therefore demonstrating that less osmotically stressed cells have a metabolic need for increased various biosynthetic reactions and depend on replenishing the pool of available cytosolic acetyl-CoA. The combination of increased *ALD3* expression together with the decrease in *ACS1/2* expression in osmotically stressed yeast cells during Icewine fermentation may ultimately contribute to the elevated acetic acid levels measured in the wine. A reduction in acetyl-CoA formation from acetate by *ACS2* may be a contributing factor to the elevated acetic acid levels measured in Icewine. A reduction in acetic acid in sake yeast overexpressing *ACS2* was reported by Akamatsu *et al.* (2000) but a wine yeast strain also overexpressing *ACS2* did not result in reduced acetic acid levels (Remize *et al.*, 2000). It is unclear if increased expression of *ACS2* during the diluted juice fermentation contributes to increased acetic acid catabolism and therefore lower levels of acetic acid released into the wine. It is also not known if increasing *ACS2* expression in a wine yeast strain during Icewine fermentation would promote increased acetic acid catabolism. Since *ACS1* is expressed during respiratory

growth and is glucose repressed (van den Berg *et al.* 1996) it is unlikely that it would have an influence on increased acetic acid production during Icewine fermentation.

The gene profiling data also revealed the upregulation of a number of stress response genes including those involved in redox reactive metabolic pathways (*GRE1, 2* and *3*) and those related to oxidative stress (*CTT1*). The expression of these genes have been found to be upregulated under numerous stress conditions (Gasch *et al.*, 2000; Causton *et al.*, 2001; Rossignol *et al.*, 2003; Erasmus *et al.*, 2003), their importance to yeast under Icewine fermentations conditions clearly needs to be further investigated. A large-scale transcriptomic study by Marks *et al.* (2008) revealed that over 200 genes were highly induced by a wine yeast strain throughout the fermentation of grape juice and were categorized into their own group termed the fermentation stress response (FSR). The expression of a number of these genes affected by the stresses imposed on yeast cells during fermentation were associated with transport, response to stress but the vast majority of them are of unknown function and still have not been characterized. The microarray data generated in our study can be further mined to identify additional genes that may be uniquely up- or downregulated in response to Icewine fermentation and specifically those used to cope with high sugar stress conditions. Ando *et al.* (2006) used a collection of deletion mutants to identify genes required for tolerance to high sucrose stress in Baker's yeast. Of the 273 osmosensitive deletion mutants, 269 showed cross-sensitivities to high concentrations of sodium chloride and sorbitol. However, four genes associated with purine biosynthesis and intracellular ATP accumulation were found to be necessary for sucrose stress tolerance. Thus, the stress response of wine yeast to concentrated solutes present in Icewine juice may differ from the responses observed

with other osmotic stresses, especially since the wine yeast are also present in an anaerobic environment. These characteristic responses could possibly involve the activation of Icewine-specific genes or entire metabolic pathways not identified to date. It would also be of importance to identify the transcriptional responses of genes that are expressed constitutively or not affected during Icewine fermentation in addition to the expression of genes required for adaptation to the changing physiological and metabolic conditions faced by yeast cells during alcoholic fermentation. This would facilitate a greater understanding of the overall response of *S. cerevisiae* to Icewine fermentation thereby improving our ability to select for or design strains better suited to these fermentations.

6. CONCLUSIONS

With the use of microarray analysis, this thesis project has demonstrated that the hyperosmotic stress experienced by the commercial wine yeast *Saccharomyces cerevisiae* K1-V1116 during the first five days of Icewine fermentation compared to table wine fermentation evoked transcriptional changes on a genomic level. These differences in gene expression ultimately lead to differences in yeast cell growth and metabolism. During Icewine fermentation, yeast were observed to experience several fermentation difficulties including decreased biomass accumulation, decreased nutrient uptake and increased production of metabolites like glycerol and acetic acid. Despite the fact that the Icewine juice contained approximately twice the amount of both sugar and nitrogen in comparison to the diluted Icewine juice, only half the amount of available reducing sugars and amino acid nitrogen was utilized by the Icewine juice fermenting yeast. Based on these results, sugar and nitrogen availability was not a contributing factor to the

impaired cell growth exhibited by Icewine juice fermenting cells. However, the osmotic stress due to the overall abundance of concentrated sugar and nitrogen in addition to other solutes in the juice hindered the ability of the wine yeast to ferment this juice. This study also identified the expression of a glycerol/H^+ symporter (*STL1*) which was one of the most highly expressed genes in yeast fermenting Icewine juice along with the expression of two acetyl-CoA synthetase isoforms (*ACS1* and *2*) which were greatly downregulated. The expression patterns of these genes potentially contributed to decreased cell viability and increased acetic acid production demonstrated by yeast fermenting Icewine juice. The results presented in this study has further bridged the gap between the transcriptional response of wine yeast as they adapt to prolonged exposure to hyperosmotic stress to changes within metabolic pathways associated with sugar and nitrogen and the production of yeast metabolites throughout Icewine juice fermentation thereby improving our ability to select for yeast strains better suited to these fermentations.

LITERATURE CITED

Aguilera, J. and Prieto, J.A. (2001) The *Saccharomyces cerevisiae* aldose reductase is implied in the metabolism of methylglyoxal in response to stress conditions. *Curr Genet* **39**:273-283.

Aguilera, J., Rodríguez-Vargas, S. and Prieto, J.A. (2005) The HOG MAP kinase pathway is required for the induction of methylglyoxal-responsive genes and determines methylglyoxal resistance in *Saccharomyces cerevisiae*. *Mol Microbiol* **56**:228-239.

Akamatsu, S., Kamiya, H., Yamashita, N., Motoyoshi, T., Goto-Yamamoto, N., Ishikawa, T., Okazaki, N. and Nishimura, A. (2000) Effects of aldehyde dehydrogenase and acetyl-CoA synthetase on acetate formation in sake mash. *J Biosci Bioeng* **90**:555-560.

Akhtar, N., Blomberg, A. and Adler, L. (1997) Osmoregulation and protein expression in a *pbs2Δ* mutant of *Saccharomyces cerevisiae* during adaptation to hypersaline stress. *FEBS Lett* **403**:173-180.

Albertyn, J., Hohmann, S. and Prior, B.A. (1994a) Characterization of the osmotic-stress response in *Saccharomyces cerevisiae*: osmotic stress and glucose repression regulate glycerol-3-phosphate dehydrogenase independently. *Curr Genet* **25**:12-18.

Albertyn, J., Hohmann, S., Thevelein, J.M. and Prior, B.A. (1994b) *GPD1*, which encodes glycerol-3-phosphate dehydrogenase, is essential for growth under osmotic stress *Saccharomyces cerevisiae*, and its expression is regulated by the high-osmolarity glycerol response pathway. *Mol Cell Biol* **14**:4135-4144.

Alepuz, P.M., Jovanovic, A., Reiser, V. and Ammerer, G. (2001) Stress-Induced MAP Kinase Hog1 Is Part of Transcription Activation Complexes. *Mol Cell* **7**:767–777.

Andre, B., Hein, C., Grenson, M. and Jauniaux, J.C. (1993) Cloning and expression of the *UGA4* gene coding for the inducible GABA-specific transport protein of *Saccharomyces cerevisiae*. *Mol Gen Genet* **237**:17-25.

Ando, A., Tanaka, F., Murata, Y., Takagi, H. and Shima, J. (2006) Identification and classification of genes required for tolerance to high-sucrose stress by genome-wide screening of *Saccharomyces cerevisiae*. *FEMS Yeast Res* **6**:249-267.

Ansell, R., Granath, K., Hohmann, S., Thevelein, J.M. and Adler, L. (1997) The two isoenzymes for yeast NAD^+-dependent glycerol 3-phosphate dehydrogenase encoded by *GPD1* and *GPD2* have distinct roles in osmoadaptation and redox regulation. *EMBO J* **16**:2179-2187.

Ashburner, M., Ball, C.A., Blake, J.A., Botstein, D., Butler, H., Cherry, J. M., Davis, A.P., Dolinski, K., Dwight, S.S., Eppig, J.T., Harris, M.A., Hill, D.P., Issel-Tarver, L., Kasarskis, A., Lewis, S., Matese, J.C., Richardson, J.E., Ringwald, M., Rubin, G.M. and Sherlock, G. (2000) Gene Ontology: tool for the unification of biology. *Nature Genet* **25**:25-29.

Backhus, L.E., DeRisi, J., Brown, P.O. and Bisson, L.F. (2001) Functional genomic analysis of a commercial wine strain of *Saccharomyces cerevisiae* under differing nitrogen conditions. *FEMS Yeast Res* **1**:111-125.

Baker, J., Steele, C. and Dure, L. (1988) Sequence and characterization of 6 *Lea* proteins and their genes from cotton. *Plant Mol Biol* **11**:277-291.

Beltran, G., Novo, M., Rozès, M., Mas, A. and Guillamón, J.M. (2004) Nitrogen catabolite repression in *Saccharomyces cerevisiae* during wine fermentation. *FEMS Yeast Res* **4**:625-632.

Bidenne, C., Blondin, B., Dequin, S. and Vezinhet, E. (1992) Analysis of the chromosomal DNA polymorphism of wine strains of *Saccharomyces cerevisiae. Curr Genet* **22**:1-7

Berthels, N.J., Otero, R.R.C., Bauer, F.F., Thevelein, J.M. and Pretorius, I.S. (2004) Discrepancy in glucose and fructose utilisation during fermentation by *Saccharomyces cerevisiae* wine yeast strains. *FEMS Yeast Res* **4**:683-689.

Billi, D. and Potts, M. (2002) Life and death of dried prokaryotes. *Res Microbiol* **153**:7-12.

Bisson, L.F. (1993) Yeasts - Metabolism of sugars. In *Wine Microbiology and Biotechnology* Fleet, G.H. (Ed.) pp. 55-75. Switzerland: Harwood Academic Publishers.

Bisson, L.F. and Fraenkel, D.G. (1983) Involvement of kinases in glucose and fructose uptake by *Saccharomyces cerevisiae. Proc Natl Acad Sci USA* **80**:1730-1734.

Bisson, L.F. and Fraenkel, D.G. (1984) Expression of Kinase-Dependent Glucose Uptake in *Saccharomyces cerevisiae. J Bacteriol* **159**:1013-1017.

Blomberg, A. (2000) Metabolic surprises in *Saccharomyces cerevisiae* during adaptation to saline conditions: questions, some answers and a model. *FEMS Microbiol Lett* **182**:1-8.

Blomberg, A. and Adler, L. (1989) Roles of glycerol and glycerol-3-phosphate dehydrogenase (NAD^+) in acquired osmotolerance of *Saccharomyces cerevisiae. J Bacteriol* **171**:1087-1092.

Blomberg, A. and Adler, L. (1992) Physiology of osmotolerance in fungi. *Adv Microb Physiol* **33**:145–212

Blomberg, A., Larsson, C. and Gustafsson, L. (1988) Microcalorimetric monitoring of growth of *Saccharomyces cerevisiae*: Osmotolerance in relation to physiological state. *J Bacteriol* **170**:4562-4568.

Boulton, R.B., Singleton, V.L., Bisson, L.F. and Kunkee, R.E. (1998) *Principles and practices of winemaking*. Maryland: Aspen Publishers, Inc.

Bray, E.A. (1997) Plant responses to water deficit. *Trends Plant Sci* **2**:48-54.

Brewster, J.L., de Valoir, T., Dwyer, N.D.,Winter, E. and Gustin, M.C. (1993) An osmosensing signal transduction pathway in yeast. *Science* **259**: 1760-1763.

Camarasa, C., Grivet, J. and Dequin, S. (2003) Investigation by ^{13}C-NMR and tricarboxylic acid (TCA) deletion mutant analysis of pathways for succinate formation in *Saccharomyces cerevisiae* during anaerobic fermentation. *Microbiology* **149**:2669-2678.

Causton, H.C., Ren, B., Koh, S.S., Harbison, C.T., Kanin, E., Jennings, E.G., Lee, T.I., True, H.L., Lander, E.S. and Young, R.A. (2001) Remodeling of yeast genome expression in response to environmental changes. *Mol Biol Cell* **12**:323–337.

Cavalieri, D., Townsend, J.P. and Hartl, D.L. (2000) Manifold anomalies in gene expression in a vineyard isolate of *Saccharomyces cerevisiae* revealed by DNA microarray analysis. *Proc Natl Acad Sci USA* **97**:12369-12374.

Cliff, M.A. and Pickering, G.J. (2006) Determination of odour detection thresholds for acetic acid and ethyl acetate in Ice wine. *J Wine Res* **17**:45-52.

Coleman, S.T., Fang, T.K., Rovinsky, S.A., Turano, F.J. and Moye-Rowley, W.S. (2001) Expression of a glutamate decarboxylase homologue is required for normal oxidative stress tolerance in *Saccharomyces cerevisiae*. *J Biol Chem* **276**:244-250.

Cooper, T.G. (1982) Nitrogen metabolism in *Saccharomyces cerevisiae*. In *The Molecular Biology of the Yeast Saccharomyces: Metabolism and Gene Expression*. Strathern, J.N., Jones, E.W. and Broach, J.R. (Eds.) pp 39-99. New York: Cold Spring Harbor Laboratory.

Cordier, H., Mendes, F., Vasconcelos, I. and François, J.M. (2007) A metabolic and genomic study of engineered *Saccharomyces cerevisiae* strains for high glycerol production. *Metab Eng* **9**:364-378.

Dawes, I.W. (2004) Stress responses. In *The Metabolism and Molecular Physiology of Saccharomyces cerevisiae* Dickinson, J.R. and Schweizer, M. (Eds.) pp. 376-413. New York: CRC Press.

de Groot, E., Bebelman, J., Mager, W.H. and Planta, R. J. (2000) Very low amounts of glucose cause repression of the stress-responsive gene *HSP12* in *Saccharomyces cerevisiae*. *Microbiology* **146**:367-375.

Denis, C.L., Ferguson, J. and Young, E.T. (1983) mRNA levels for the fermentative alcohol dehydrogenase of *Saccharomyces cerevisiae* decrease upon growth on a nonfermentable carbon source. *J Biol Chem* **258**:1165-1171.

DeRisi, J.L., Iyer, V.R. and Brown, P.O. (1997) Exploring the metabolic and genetic control of gene expression on a genomic scale. *Science* **278**:680–686.

Dickinson, J.R., Salgado, L. and Hewlins, M. (2003) The catabolism of amino acids to long chain and complex alcohols in *Saccharomyces cerevisiae*. *J Biol Chem* **278**:8028-8034.

Dickinson, J.R. (2004) Nitrogen metabolism. *In The Metabolism and Molecular Physiology of Saccharomyces cerevisiae* Dickinson, J.R. and Schweizer, M. (Eds.) pp. 104-116. New York: CRC Press.

DeLuna, A., Avendano, A., Riego, L. and González, A. (2001) NADP-glutamate dehydrogenase isoenzymes of *Saccharomyces cerevisiae*. *J Biol Chem* **276**:43775-43783.

Dukes, B.C. and Butzke, C.E. (1998) Rapid determination of primary amino acids in grape juice using an *o*-Phthaldialdehyde/N-Acetyl-L-Cysteine spectrophotometric assay. *Am J Enol Vitic* **49**:125-134.

Dwight, S.S., Harris, M.A., Dolinski, K., Ball, C.A., Binkley, G., Christie, K.R., Fisk, D.G., Issel-Tarver, L., Schroeder, M., Sherlock, G., Sethuraman, A., Weng, S., Botstein, D. and Cherry, M. (2002) *Saccharomyces* Genome Database (SGD) provides secondary gene annotation using the Gene Ontology (GO). *Nucleic Acids Res* **30**:69-72

Eglinton, J.M., Heinrich, A.J., Pollnitz, A.P., Langridge, P., Henschke, P.A. and de Barros Lopes, M. (2002) Decreasing acetic acid accumulation by a glycerol overproducing strain of *Saccharomyces cerevisiae* by deleting the *ALD6* aldehyde dehydrogenase gene. *Yeast* **19**:295-301.

Erasmus, D.J., van der Merwe, G.K. and van Vuuren, H.J.J. (2003) Genome-wide expression analyses: Metabolic adaptation of *Saccharomyces cerevisiae* to high sugar stress. *FEMS Yeast Res* **3**:375-399.

Eriksson, P., André, L., Ansell, R., Blomberg, A. and Adler, L. (1995) Cloning and characterization of *GPD2*, a second gene encoding *sn*-glycerol 3-phosphate dehydrogenase (NAD^+) in *Saccharomyces cerevisiae*, and its comparison with *GPD1*. *Mol Microbiol* **17**:95-107.

Eriksson, P., Alipour, H., Adler, L. and Blomberg, A. (2000) Rap1p-binding sites in the *Saccharomyces cerevisiae* GPD1 promoter are involved in its response to NaCl. *J Biol Chem* **275**:29368–29376.

Esteve-Zarzoso, B., Belloc h, C., Uruburu, F. and Querol, A. (1999) Identification of yeasts by RFLP analysis of the 5.8S rRNA gene and the two ribosomal internal transcribed spacers. *Int J Syst Bacteriol* **49**: 329–337.

Fernández, M., Fernández, E. and Rodicio, R. (1994) *ACR1*, a gene encoding a protein related to mitochondrial carriers, is essential for acetyl-CoA synthetase activity in *Saccharomyces cerevisiae*. *Mol Gen Genet* **242**:727-735.

Ferreira, C., van Voorst, F., Martins, A., Neves, L., Oliveira, R., Kielland-Brandt, M.C., Lucas, C. and Brandt, A. (2005) A member of the sugar transporter family, Stl1p is the glycerol/H^+ symporter in *Saccharomyces cerevisiae*. *Mol Biol Cell* **16**:2068-2076.

Ferrigno, P., Posas, F., Koepp, D., Saito, H. and Silver, P.A. (1998) Regulated nucleo/cytoplasmic exchange of HOG1 MAPK requires the importin β homologs NMD5 and XPO1. *EMBO J* **17**:5606–5614.

Fleet, G.H. and Heard, G.M (1993) Yeasts- Growth during Fermentation. In *Wine Microbiology and Biotechnology* Fleet, G.H. (Ed.) pp. 27-54. Switzerland: Harwood Academic Publishers.

Flikweert, M.T., van der Zanden, L., Janssen, W.M., Steensma, H.Y., van Dijken, J.P. and Pronk, J.T. (1996) Pyruvate decarboxylase: an indispensable enzyme for growth of *Saccharomyces cerevisiae* on glucose. *Yeast* **12**:247-257.

Gancedo, J.M. (1998) Yeast carbon catabolite repression. *Microbiol Mol Biol Rev* **62**:334-361.

Garay-Arroyo, A. and Covarrubias, A.A. (1999) Three genes whose expression is induced by stress in *Saccharomyces cerevisiae*. *Yeast* **15**:879-892.

Garay-Arroyo, A., Colmenero-Flores, J.M., Garciarrubio, A. and Covarrubias, A.A. (2000) Highly hydrophilic proteins in prokaryotes and eukaryotes are common during conditions of water deficit. *J Biol Chem* **275**:5668-5674.

Gasch, A.P., Spellman, P.T., Kao, C.M., Carmel-Harel, O., Eisen, M.B., Storz, G., Botstein, D. and Brown, P.O. (2000) Genomic Expression Programs in the Response of Yeast Cells to Environmental Changes. *Mol Biol Cell* **11**:4241–4257.

Giannattasio, S., Guaragnella, N., Corte-Real, M., Passarellac, S. and Marra, E. (2005) Acid stress adaptation protects *Saccharomyces cerevisiae* from acetic acid-induced programmed cell death. *Gene* **354**:94-98.

Godard, P., Urrestarazu, A., Vissers, S., Kontos, K., Bontempi, G., van Helden, J. and André, B. (2007) Effect of 21 different nitrogen sources on global gene expression in the yeast *Saccharomyces cerevisiae*. *Mol Cell Biol* **27**:3065-3086.

Görner, W., Durchschlag, E., Martinez-Pastor, M.T., Estruch, F., Ammerer, G., Hamilton, B., Ruis, H. and Schüller, C. (1998) Nuclear localization of the C_2H_2 zinc finger protein Msn2p is regulated by stress and protein kinase A activity. *Gene Dev* **12**:586–597.

Götz, R., Gnann, A. and Zimmerman, F.K. (1999) Deletion of the carbonic anhydrase-like gene *NCE103* of the yeast *Saccharomyces cerevisiae* causes an oxygen-sensitive growth defect. *Yeast* **15**:855-864.

Gustin, M.C., Albertyn, J., Alexander, M. and Davenport, K. (1998) MAP Kinase Pathways in the yeast *Saccharomyces cerevisiae*. *Microbiol Mol Biol Rev* **62**:1264–1300.

Hauser, N.C., Fellenberg, K., Gil, R., Bastuck, S., Hoheisel, J.D. and Pérez-Ortin, J.E. (2001) Whole genome analysis of a wine yeast strain. *Comp Funct Genom* **2**:69-79.

Herrero, P., Galindez, J., Ruiz, N., Martinez-Campa, C. and Moreno, F. (1995) Transcriptional regulation of the *Saccharomyces cerevisiae HXK1*, *HXK2* and *GLK1* genes. *Yeast* **11**:137-144.

Hiltunen, J.K., Mursula, A.M., Rottensteiner, H., Wierenga, R.K., Kastaniotis, A.J. and Gurvitz, A. (2003) The biochemistry of peroxisomal β-oxidation in the yeast *Saccharomyces cerevisiae*. *FEMS Microbiol Rev* **27**:35-64.

Hirayama, T., Maeda, T., Saito, H. and Shinozaki, K. (1995) Cloning and characterization of seven cDNAs for hyperosmolarity-responsive (*HOR*) genes of *Saccharomyces cerevisiae*. *Mol Gen Genet* **249**:127–138.

Hohmann, S. (1991) *PCD6*, a weakly expressed pyruvate decarboxylase gene from yeast, is activated when fused spontaneously under the control of the *PDC1* promoter. *Curr Genet* **20**:373-378.

Hohmann, S. and Cederberg, H. (1990) Autoregulation may control the expression of yeast pyruvate decarboxylase structural genes *PDC1* and *PDC5*. *Eur J Biochem* **188**:615-621.

Hohmann, S. (2002) Osmotic stress signaling and osmoadaptation in yeasts. *Microbiol Mol Biol Rev* **66**:300-372.

Holst, B., Lunde, C., Lages, F., Oliveira, R., Lucas, C. and Kielland-Brandt, M.C. (2000) *GUP1* and its close homologue *GUP2*, encoding multimembrane-spanning proteins involved in active glycerol uptake in *Saccharomyces cerevisiae*. *Mol Microbiol* **37**:108-124.

Horák, J. (1986) Amino acid transport in eucaryotic microorganisms. *Biochim Biophys Acta* **864**:223-256.

Inoue, Y. and Kimura, A. (1995) Methylglyoxal and regulation of its metabolism in microorganisms. *Adv Microb Physiol* **37**:177-227.

Inoue, Y., Tsujimoto, Y. and Kimura, A. (1998) Expression of the glyoxalase I gene of *Saccharomyces cerevisiae* is regulated by high osmolarity glycerol mitogen-activated protein kinase pathway in osmotic stress response. *J Biol Chem* **273**:2977-2983.

Jacoby, T., Flanagan, H., Faykin, A., Seto, A.G., Mattison, C. and Ota, I. (1997) Two protein-tyrosine phosphatases inactivate the osmotic stress response pathway in yeast by targeting the mitogen-activated protein kinase, Hog1. *J Biol Chem* **272**:17749–17755.

Jansen, G., Buhring, F., Hollenberg, C.P. and Ramezani Rad, M. (2001) Mutations in the SAM domain of STE50 differentially influence the MAP kinase-mediated pathways for mating, filamentous growth and osmotolerance in *Saccharomyces cerevisiae. Mol Genet Genom* **265**:102–117.

Kinclova-Zimmermannova, O. and Sychrova, H. (2006) Functional study of the Nha1p C-terminus: involvement in cell response to changes in external osmolarity. *Curr Genet* **49**:229-236.

Kluba, R.M., Mattick, L.R. and Hackler, L.R. (1978) Changes in the free and total amino acid composition of several *Vitis labruscana* grape varieties during maturation. *Am J Enol Vitic* **29**:102-111.

Kontkanen, D., Inglis, D.L., Pickering, G.J. and Reynolds, A. (2004) Effect of yeast inoculation rate, acclimatization and nutrient addition on Icewine fermentation. *Am J Enol Vitic* **55**:363-370.

Kratzer, S. and Schüller, H. (1995) Carbon source-dependent regulation of the acetyl-coenzyme A synthetase-encoding gene *ACS1* from *Saccharomyces cerevisiae. Gene* **161**:75-79.

Krukeberg, A.L. and Dickinson, J.R. (2004) Carbon metabolism. In *The Metabolism and Molecular Physiology of Saccharomyces cerevisiae* Dickinson, J.R. and Schweizer, M. (Eds.) pp. 42-103. New York: CRC Press.

Lages, F. and Lucas, C. (1997) Contribution to the physiological characterization of glycerol active uptake in *Saccharomyces cerevisiae. Biochim Biophys Acta* **1322**:8-18.

Larsson, K., Ansell, R., Eriksson, P. and Adler, L. (1993) A gene encoding *sn*-glycerol 3-phosphate dehydrogenase (NAD^+) complements an osmosensitive mutant of *Saccharomyces cerevisiae. Mol Microbiol* **10**:1101-1111.

Latterich, M. and Watson, M.D. (1993) Evidence for a dual osmoregulatory mechanism in the yeast *Saccharomyces cerevisiae*. *Biochem Biophys Res Commun* **191**:1111–1117.

Lee, F., Lin, L. and Smith, J.A. (1996) Acetyl-CoA hydrolase involved in acetate utilization in *Saccharomyces cerevisiae*. *Biochim Biophys Acta* **1297**:99-104.

Lee, J., Lee, B., Shin, D., Kwak, S., Bahk, J.D., Lim, C.O. and Yun, D. (2002) Carnitine uptake by *AGP2* in yeast *Saccharomyces cerevisiae* is dependent on Hog1 MAP kinase pathway *Mol Cells* **13**:407-412.

Luyten, K., Albertyn, J., Skibbe, W.F., Prior, B.A., Ramos, J., Thevelein, J.M. and Hohmann, S. (1995) Fps1, a yeast member of the MIP family of channel proteins, is a facilitator for glycerol uptake and efflux and is inactive under osmotic stress. *EMBO J* **14**:1360-1371.

Luyten, K., Riou, C. and Blondin, B. (2002) The hexose transporters of *Saccharomyces cerevisiae* play different roles during enological fermentation. *Yeast* **19**:713-726.

Maeda, T., Tsai, A.Y.M. and Saito, H. (1993) Mutations in a protein tyrosine phosphatase gene (PTP2) and a protein serine/threonine phosphatase gene (PTC1) cause a synthetic growth defect in *Saccharomyces cerevisiae*. *Mol Cell Biol* **13**:5408–5417.

Maeda, T., Wurgler-Murphy, S.M. and Saito, H. (1994) A two-component system that regulates an osmosensing MAP kinase cascade in yeast. *Nature* **369**:242-245.

Maeda, T., Takekawa, M. and Saito, H. (1995) Activation of yeast PBS2 MAPKK by MAPKKKs or by binding of an SH3-containing osmosensor. *Science* **269**:554-558.

Magasanik, B. and Kaiser, C.A. (2002) Nitrogen regulation in *Saccharomyces cerevisiae*. *Gene* **290**:1-18.

Mager, W.H. and Siderius, M. (2002) Novel insights into the osmotic stress response of yeast. *FEMS Yeast Res* **2**:251-257.

Margarida, A., Cordeiro, C., Ponces Freire, A. (2001) In situ analysis of methylglyoxal metabolism in *Saccharomyces cerevisiae*. *FEBS Lett* **499**:41-44.

Marks, V.D., van der Merwe, G.K. and van Vuuren, H.J.J. (2003) Transcriptional profiling of wine yeast in fermenting grape juice: regulatory effect of diammonium phosphate. *FEMS Yeast Res* **3**:269-287.

Marks, V.D., Ho Sui, S.J., Erasmus, D., van der Merwe, G.K., Brumm, J., Wasserman, W.W., Bryan, J. and van Vuuren, H.J.J. (2008) Dynamics of the yeast transcriptome during wine fermentation reveals a novel fermentation stress response. *FEMS Yeast Res* **8**:35-52.

Martinez-Pastor, M.T., Marchler, G., Schüller, C., Marchler-Bauer, A., Ruis, H. and Estruch, F. (1996) The *Saccharomyces cerevisiae* zinc finger proteins Msn2p and Msn4p are required for transcriptional induction through the stress-response element (STRE). *EMBO J* **15**:2227–2235.

Meaden, P., Dickinson, F., Mifsud, A., Tessier, W., Westwater, J., Bussey, H. and Midgley, M. (1997) The *ALD6* gene of *Saccharomyces cerevisiae* encodes a cytosolic, Mg^{2+}-activated acetaldehyde dehydrogenase. *Yeast* **13**:1319-1327.

Miralles, V.J. and Serrano, R. (1995) A genomic locus in *Saccharomyces cerevisiae* with four genes up-regulated by osmotic stress. *Mol Microbiol* **17**:653-662.

Modig, T., Granath, K., Adler, L. and Lidén, G. (2007) Anaerobic glycerol production by *Saccharomyces cerevisiae* strains under hyperosmotic stress. *Appl Microbiol and Biotechnol* **75**:289-296.

Mollapour, M. and Piper, P.W. (2007) Hog1 mitogen-activated protein kinase phosphorylation targets the yeast Fps1 aquaglycerolporin for endocytosis, thereby rendering cells resistant to acetic acid. *Mol Cell Biol* **27**:6446-6556.

Mollapour, M., Shepherd, A. and Piper, P.W. (2008) Novel stress responses facilitate *Saccharomyces cerevisiae* in the presence of the monocarboxylate preservatives. *Yeast* **25**:169-177.

Monteiro, F.F. and Bisson, L.F. (1991a) Biological assay of nitrogen content of grape juice and prediction of sluggish fermentations. *Am J Enol Vitic* **42**:47-57.

Monteiro, F.F. and Bisson, L.F. (1991b) Amino acid utilization and urea formation during vinification fermentations. *Am J Enol Vitic* **42**:199-208.

Navarro-Avino, J.P., Prasad, R., Miralles, V.J., Benito, R.M. and Serrano, R. (1999) A proposal for nomenclature of aldehyde dehydrogenases in *Saccharomyces cerevisiae* and characterization of the stress-inducible *ALD2* and *ALD3*. *Yeast* **15**:829-842.

Nelissen, B., de Wachter, R. and Goffeau, A. (1997) Classification of all putative permeases and other membrane plurispanners of the major facilitator superfamily encoded by the complete genome of *Saccharomyces cerevisiae*. *FEMS Microbiol Rev* **21**:113–134.

Neves, L., Lages, F. and Lucas, C. (2004) New insights on glycerol transport in *Saccharomyces cerevisiae*. *FEBS Lett* **565**:160-162.

Nevoigt, E. and Stahl, U. (1997) Osmoregulation and glycerol metabolism in the yeast *Saccharomyces cerevisiae*. *FEMS Microbiol Rev* **21**:231-241.

Noble, A.C. and Bursick, G.F. (1984) The contribution of glycerol to perceived viscosity and sweetness in white wine. *Am J Enol Vitic* **35**:110-112.

Norbeck, J. and Blomberg, A. (1998) Amino acid uptake is strongly affected during exponential growth of *Saccharomyces cerevisiae* in 0.7 M NaCl medium. *FEMS Microbiol Lett* **158**:121-126.

Norbeck, J. and Blomberg, A. (2000) The level of cAMP-dependent protein kinase A activity strongly affects osmotolerance and osmo-instigated gene expression changes in *Saccharomyces cerevisiae*. *Yeast* **16**:121-137.

Norbeck, J., Påhlman, A., Akhtar, N., Blomberg, A. and Adler, L. (1996) Purification and characterization of two isoenzymes of DL-glycerol-3-phosphatase from *Saccharomyces cerevisiae*. *J Biol Chem* **271**:13875-13881.

Nurgel, C., Pickering, G.J. and Inglis, D.L. (2004) Sensory and chemical characteristics of Canadian ice wines. *J Sci Food Agr* **84**:1675–1684.

Nurgel, C. and Pickering, G.J. (2005) Contribution of glycerol, ethanol and sugar to the perception of viscosity and density elicited by model white wines. *J Texture Stud* **36**:303-323.

Oliveira, R., Lages, F., Silva-Graça, M. and Lucas, C. (2003) Fps1p channel is the mediator of the major part of glycerol passive diffusion in *Saccharomyces cerevisiae*: artifacts and re-definitions. *Biochim Biophys Acta* **1613**: 57-71.

Oliveira, R. and Lucas, C. (2004) Expression studies of *GUP1* and *GUP2*, genes involved in glycerol active transport in *Saccharomyces cerevisiae*, using semi-quantitative RT-PCR. *Curr Genet* **46**:140-146.

O'Rourke, S., Herskowitz, I. and O'Shea, E.K. (2002) Yeast go the whole HOG for the hyperosmotic stress response. *Trends Genet* **18**:405-412.

O'Rourke, S.M. and Herskowitz, I. (2004) Unique and redundant roles for HOG MAPK pathway components as revealed by whole-genome expression analysis. *Mol Biol Cell* **15**:532-542.

Ostrander, D.B. and Gorman, J.A. (1999) The extracellular domain of the *Saccharomyces cerevisiae* Sln1p membrane osmolarity sensor is necessary for kinase activity. *J Bacteriol* **181**:2527–2534.

Ota, I.M. and Varshavsky, A. (1993) A yeast protein similar to bacterial two-component regulators. *Science* **262**:566–569.

Özcan, S. and Johnston, M. (1999) Function and Regulation of Yeast Hexose Transporters. *Microbiol Mol Biol Rev* **63**:554-569.

Påhlman, A., Granath, K., Ansell, R., Hohmann, S. and Adler, L. (2001) The yeast glycerol 3-phosphatases Gpp1p and Gpp2p are required for glycerol biosynthesis and differentially involved in the cellular responses to osmotic, anaerobic and oxidative stress. *J Biol Chem* **276**:3555-3563.

Paiva, S., Devaux, F., Barbosa, S., Jacq, C. and Casal, M. (2004) Ady2p is essential for the acetate permease activity in the yeast *Saccharomyces cerevisiae*. *Yeast* **21**:201–210.

Palmieri, L., Lasorsa, F.M., De Palma, A., Palmieri, F., Runswick, M.J. and Walker, J.E. (1997) Identication of the yeast *ACR1* gene product as a succinate-fumarate transporter essential for growth on ethanol or acetate. *FEBS Lett* **417**:114-118.

Paulsen, I.T., Sliwinski, M.K., Nelissen, B., Goffeau, A. and Saier, M.H. (1998) Unified inventory of established and putative transporters encoded within the complete genome of *Saccharomyces cerevisiae*. *FEBS Lett* **430**:116-125.

Pavlik, P., Simon, M., Schuster, T. and Ruis, H. (1993) The glycerol kinase (*GUT1*) gene of *Saccharomyces cerevisiae*: cloning and characterization. *Curr Genet* **24**:21–25.

Perez, M., Luyten, K., Michel, R., Riou, C. and Blondin, B. (2005) Analysis of *Saccharomyces cerevisiae* hexose carrier expression during wine fermentation: both low- and high-affinity Hxt transporters are expressed. *FEMS Yeast Res* **5**:351-361.

Perez-Torrado, R., Carrasco, P., Aranda, A., Gimeno-Alcañiza, J., Pérez-Ortína, J.E., Matallana, E. and del Olmo, M. (2002) Study of the first hours of microvinification by the use of osmotic stress-response genes as probes. *Syst Appl Microbiol* **25**:153–161.

Pigeau, G.M. and Inglis, D.L. (2005) Upregulation of ALD3 and GPD1 in *Saccharomyces cerevisiae* during Icewine fermentation. *J Appl Microbiol* **99**:112–125.

Pigeau, G.M. and Inglis, D.L. (2007) Response of wine yeast (*Saccharomyces cerevisiae*) aldehyde dehydrogenases to acetaldehyde stress during Icewine fermentation. *J Appl Microbiol* **103**:1576-1586.

Pigeau, G.M., Bozza, E., Kaiser, K. and Inglis, D.L. (2007) Concentration effect of Riesling Icewine juice on yeast performance and wine acidity. *J Appl Microbiol* **103**:1691-1698.

Posas, F., Wurgler-Murphy, S.M., Maeda, T., Witten, E.A., Thai, T.C. and Saito, H. (1996) Yeast HOG1 MAP kinase cascade is regulated by a multistep phosphorelay mechanism in the SLN1-YPD1-SSK1 "two-component" osmosensor. *Cell* **86**:865–875.

Posas, F. and Saito, H. (1997) Osmotic activation of the HOG MAP kinase pathway via Ste11p MAPKKK: scaffold role of Pbs2p MAPKK. *Science* **276**:1702–1705.

Posas, F. and Saito, H. (1997) Osmotic activation of the HOG MAP kinase pathway via Ste11p MAPKKK: scaffold role of Pbs2p MAPKK. *Science* **276**:1702-1705.

Posas, F. and Saito, H. (1998) Activation of the yeast SSK2 MAP kinase kinase kinase by the SSK1 two-component response regulator. *EMBO J* **17**:1385-1394.

Posas, F., Takekawa, M. and Saito, H. (1998) Signal transduction by MAP kinase cascades in budding yeast. *Curr Opin Microbiol* **1**:175-182.

Posas, F., Chambers, J.R., Heyman, J.A., Hoeffler, J.P., de Nadal, E. and Ariño, J. (2000) The Transcriptional Response of Yeast to Saline Stress. *J Biol Chem* **275**:17249-17255.

Pretorius, I.S. (2000) Tailoring wine yeast for the new millennium: novel approaches to the ancient art of winemaking. *Yeast* **16**:675-729.

Proft, M. and Struhl, K. (2004) MAP kinase-mediated stress relief that precedes and regulates the timing of transcriptional induction. *Cell* **118**:351–361.

Pronk, J.T., Steensma, H.Y. and van Dijken, J.P. (1996) Pyruvate metabolism in *Saccharomyces cerevisiae*. *Yeast* **12**:1607-1633.

Radler, F. (1993) Yeasts - Metabolism of organic acids. In *Wine Microbiology and Biotechnology* Fleet, G.H. (Ed.) pp. 165-182. Switzerland: Harwood Academic Publishers.

Raitt, D.C., Posas, F. and Saito, H. (2000) Yeast Cdc42 GTPase and Ste20 PAK-like kinase regulate Sho1-dependent activation of the Hog1 MAPK pathway. *EMBO J* **19**:4623-4631.

Ramos, F., El Guezzar, M., Grenson, M. and Wiame, J. (1985) Mutations affecting the enzymes involved in the utilization of 4-aminobutyric acid as nitrogen source by the yeast *Saccharomyces cerevisiae*. *Eur J Biochem* **149**:401-404.

Regenberg, B., During-Olsen, L., Kielland-Brandt, M.C. and Holmberg, S. (1999) Substrate specificity and gene expression of the amino-acid permeases in *Saccharomyces cerevisiae*. *Curr Genet* **36**:317-328.

Reifenberger, E., Boles, E. and Ciriacy, M. (1997) Kinetic characterization of individual hexose transporters of *Saccharomyces cerevisiae* and their relation to the triggering mechanisms of glucose repression. *Eur J Biochem* **245**:324–333.

Reiser, V., Ruis, H. and Ammerer, G. (1999) Kinase activity-dependent nuclear export opposes stress-induced nuclear accumulation and retention of Hog1 mitogen-activated protein kinase in the budding yeast *Saccharomyces cerevisiae*. *Mol Biol Cell* **10**:1147–1161.

Reiser, V., Salah, S.M. and Ammerer, G. (2000) Polarized localization of yeast Pbs2 depends on osmostress, the membrane protein Sho1 and Cdc42. *Nat Cell Biol* **2**:620-627.

Remize, F., Roustan, J.L., Sablayrolles, J.M., Barre, P. and Dequin, S. (1999) Glycerol overproduction by engineered *Saccharomyces cerevisiae* wine yeast leads to substantial changes in by-product formation and to a stimulation of fermentation rate in stationary phase. *Appl Environ Microbiol* **65**:143-149.

Remize, F., Andrieu, E. and Dequin, S. (2000) Engineering of the pyruvate dehydrogenase bypass in *Saccharomyces cerevisiae*: role of the cytosolic Mg^{2+} and mitochondrial K^{+} acetaldehyde dehydrogenases Ald6p and Ald4p in acetate formation during alcoholic fermentation. *Appl Environ Microbiol* **66**:3151-3159.

Remize, F., Barnavon, L. and Dequin, S. (2001) Glycerol export and glycerol-3-phosphate dehydrogenase, but not glycerol phosphatase, are rate limiting for glycerol production in *Saccharomyces cerevisiae*. *Metabol Eng* **3**:301-312.

Remize, F., Cambon, B., Barnavon, L. and Dequin, S. (2003) Glycerol formation during wine fermentation is mainly linked to Gpd1p and is only partially controlled by the HOG pathway. *Yeast* **20**:1243-1253.

Rep, M., Albertyn, J., Thevelein, J.M., Prior, B.A. and Hohmann, S. (1999) Different signalling pathways contribute to the control of GPD1 expression by osmotic stress in *Saccharomyces cerevisiae*. *Microbiol* **145**:715–727.

Rep, M., Krantz, M., Thevelein, J.M. and Hohmann, S. (2000) The Transcriptional Response of *Saccharomyces cerevisiae* to Osmotic Shock. *J Biol Chem* **275**: 8290–8300.

Richter, K., Reinstein, J. and Buchner, J. (2002) N-terminal residues regulate the catalytic efficiency of the Hsp90 ATPase cycle. *J Biol Chem* **277**:44905-44910.

Rodriguez, A., De La Cera, T., Herrero, P. and Moreno, F. (2001) The hexokinase 2 protein regulates the expression of the *GLK1*, *HXK1* and *HXK2* genes of *Saccharomyces cerevisiae*. *Biochem J* **355**:625-631.

Rønnow, B. and Kielland-Brandt, M. (1993) *GUT2*, a gene for mitochondrial glycerol 3-phosphate dehydrogenase of *Saccharomyces cerevisiae*. *Yeast* **9**:1121–1130.

Rossignol, T., Dulau, L., Julien, A. and Blondin, B. (2003) Genome-wide monitoring of wine yeast gene expression during alcoholic fermentation. *Yeast* **20**:1369-1385.

Saint-Prix, F., Bönquist, L. and Dequin, S. (2004) Functional analysis of the *ALD* gene family of *Saccharomyces cerevisiae* during anaerobic growth on glucose: the $NADP^{+}$-dependent Ald6p and Ald5p isoforms play a major role in acetate formation. *Microbiol* **150**:2209-2220.

Sanders, E.M. and Ough, C.S. (1985) Determination of Free Amino Acids in Wine by HPLC. *Am J Enol Vitic* **36**:1:43-46

Scanes, K.T., Hohmann, S. and Prior, B.A. (1998) Glycerol production by the yeast *Saccharomyces cerevisiae* and its relevance to wine: a review. *S Afr J Enol Vitic* **19**:17-24.

Schreiner, J. (2001) Icewine: The complete story. pp. 18-25. Toronto: Warwick Publishing Inc.

Schreve, J.L. and Garrett, J.M. (2004) Yeast Agp2p and Agp3 function as amino acid permeases in poor nutrient conditions. *Biochem Biophys Res Commun* **313**:745-751.

Schüller, G., Brewster, J.L., Alexander, M.R., Gustin, M.C. and Ruis, H. (1994) The HOG pathway controls osmotic regulation of transcription via the stress response element (STRE) of the *Saccharomyces cerevisiae* CTT1 gene. *EMBO J* **13**:4382–4389.

Schweizer, M. (2004) Lipids and membranes. In *The Metabolism and Molecular Physiology of Saccharomyces cerevisiae* Dickinson, J.R. and Schweizer, M. (Eds.) pp. 140-223. New York: CRC Press.

Serrano, R. and Rodriguez-Navarro, A. (2001) Ion homeostasis during salt stress in plants. *Curr Opin Cell Biol* **13**:399–404.

Shelp, B.J., Bown, A.W. and McLean, M.D. (1999) Metabolism and functions of gamma-aminobutyric acid. *Trends Plant Sci* **4**:446-452.

Singh, K.K. and Norton, R.S. (1991) Metabolic changes induced during adaptation of *Saccharomyces cerevisiae* to a water stress. *Arch Microbiol* **156**:38-42.

Singh, J., Kumar, D., Ramakrishnan, N., Singhal, V., Jervis, J., Garst, J.F., Slaughter, S.M., DeSantis, A.M., Potts, M. and Helm, R.F. (2005) Transcriptional response of *Saccharomyces cerevisiae* to desiccation and rehydration. *Appl Env Microbiol* **71**:8752–8763

Stanbrough, M. and Magasanik, B. (1995) Transcriptional and posttranslational regulation of the general acid permease of *Saccharomyces cerevisiae*. *J Bacteriol* **177**:94-102.

Sutherland, F.C.W., Lages, F., Lucas, C., Luyten, K., Albertyn, J., Hohmann, S., Prior, B.A. and Kilian, S.G. (1997) Characteristics of Fps1-Dependent and -Independent Glycerol Transport in *Saccharomyces cerevisiae*. *J Bacteriol* **179**:7790–7795.

Swiegers, J.H., Dippenaar, N., Pretorius, I.S. and Bauer, F.F. (2001) Carnitine-dependent metabolic activities in *Saccharomyces cerevisiae*: three carnitine acetyltransferases are essential in a carnitine-dependent strain. *Yeast* **18**:585-595.

Tamás, M.J., Luyten, K., Sutherland, F.C.W., Hernandez, A., Albertyn, J., Valadi, H., Li, H., Prior, B.A., Kilian, S.G., Ramos, J., Gustafsson, L., Thevelein, J.M. and Hohmann, S. (1999) Fps1p controls the accumulation and release of the compatible solute glycerol in yeast osmoregulation. *Mol Microbiol* **31**:1087-1104.

Tamás, M.J., Rep, M., Thevelein, J.M. and Hohmann, S. (2000) Stimulation of the yeast high osmolarity glycerol (HOG) pathway: evidence for a signal generated by a change in turgor rather than by water stress. *FEBS Lett* **472**:159-165.

ter Linde, J.J.M., Liang, H., Davis, R.W., Steensma, H.Y., van Dijken, J.P. and Pronk, J.T. (1999) Genome-wide transcriptional analysis of aerobic and anaerobic chemostat cultures of *Saccharomyces cerevisiae*. *J Bacteriol* **181**:7409-7413.

ter Schure, E.G., van Riel, N.A.W. and Verrips, C.T. (2000) The role of ammonia metabolism in nitrogen catabolite repression in *Saccharomyces cerevisiae*. *FEMS Microbiol Rev* **24**:67-83.

Van Aelst, L., Hohmann, S., Zimmermann, F.K., Jans, A.W.H. and Thevelein, J.M. (1991) A yeast homologue of the bovine lens fibre MIP gene family complements the growth defect of a *Saccharomyces cerevisiae* mutant on fermentable sugars but not its defect in glucose-induced RAS-mediated cAMP signaling. *EMBO J* **10**:2095-2104.

van den Berg, M.A. and Steensma, H.Y. (1995) *ACS2*, a *Saccharomyces cerevisiae* gene encoding acetyl-coenzyme A synthetase, essential for growth on glucose. *Eur J Biochem* **231**:704-713.

van den Berg, M.A., de Jong-Gubbels, P., Kortland, C.J., van Dijken, J.P., Pronk, J.T. and Steensma, H.Y. (1996) The two acetyl-coenzyme A synthetases of *Saccharomyces cerevisiae* differ with respect to kinetic properties and transcriptional regulation. *J Biol Chem* **271**:28953-28959.

van Dijken, J. and Sheffers, W. (1986) Redox balances in the metabolism of sugars by yeasts. *FEMS Microbiol Rev* **32**:199-224.

van Roermund, C.W., Elgersma, Y., Singh, N., Wanders, R.J. and Tabak, H.F. (1995) The membrane of peroxisomes in *Saccharomyces cerevisiae* is impermeable to NAD(H) and acetyl-CoA under *in vivo* conditions. *EMBO J* **14**:3480-3486.

van Zyl, P.J., Kilian, S.G. and Prior, B.A. (1990) The role of an active mechanism in glycerol accumulation during osmoregulation by *Zygosaccharomyces rouxii*. *Appl Microbiol Biotechnol* **34**:231-235.

Varela J.C.S., van Beekvelt, C., Planta, R.J. and Mager, W.H. (1992) Osmostress-induced changes in yeast gene expression. *Mol Microbiol* **6**:2183-2190

Varela, J.C.S. and Mager, W.H. (1996) Response of *Saccharomyces cerevisiae* to changes in external osmolarity. *Microbiology* **142**: 721-731.

Vintners Quality Alliance (VQA) Act (1999) Vintners Quality Alliance Act. Ontario Regulation 406/00.

Vintners Quality Alliance Ontario (2001) Annual Report. Vintners Quality Alliance. Toronto, Ontario.

Vintners Quality Alliance Ontario (2007) Annual Report. Vintners Quality Alliance. Toronto, Ontario.

Vissers, S., Andre, B., Muyldermans, F. and Grenson, M. (1989) Positive and negative regulatory elements control the expression of the *UGA4* gene coding for the inducible 4-aminobutyric-acid-specific permease in *Saccharomyces cerevisiae*. *Eur J Biochem* **181**:357-61.

Wang, X., Mann, C.J., Bai, Y., Ni, L. and Weiner, H. (1998) Molecular cloning, characterization, and potential roles of cytosolic and mitochondrial aldehyde dehydrogenases in ethanol metabolism in *Saccharomyces cerevisiae*. *J Bacteriol* **1480**:822-830.

Warmka, J., Hanneman, J., Lee, J., Amin, D. and Ota, I. (2001) Ptc1, a type 2C Ser/Thr phosphatase, inactivates the HOG pathway by dephosphorylating the mitogen-activated protein kinase Hog1. *Mol Cell Biol* **21**:51–60.

West, A.H. and Stock, A.M. (2001) Histidine kinases and response regulator proteins in two-component signaling systems. *Trends Biochem Sci* **26**:369–376.

White, W.H., Skatrud, P.L., Xue, Z. and Toyn, J.H. (2003) Specialization of function among aldehyde dehydrogenases: the *ALD2* and *ALD3* genes are required for β-alanine biosynthesis in *Saccharomyces cerevisiae*. *Genetics* **163**:69-77.

Wieczorke, R., Krampe, S., Weierstall, T., Freidel, K., Hollenberg, C.P. and Boles, E. (1999) Concurrent knock-out of at least 20 transporter genes is required to block uptake of hexoses in *Saccharomyces cerevisiae*. *FEBS Lett* **464**:123-128.

Wodicka, L., Dong, H., Mittmann, M., Ho, M. and Lockhart, D.J. (1997) Genome-wide expression monitoring in *Saccharomyces cerevisiae*. *Nat Biotechnol* **15**:1359-1367.

Wurgler-Murphy, S.M., Maeda, T., Witten, E.A. and Saito, H. (1997) Regulation of the *Saccharomyces cerevisiae* Hog1 mitogen-activated protein kinase by the Ptp2 and Ptp3 protein tyrosine phosphatases. *Mol Cell Biol* **17**:1289–1297.

Yale, J. and Bohnert, H.J. (2001) Transcript Expression in *Saccharomyces cerevisiae* at High Salinity. *J Biol Chem* **276**:15996-16007.

Zoecklein, B.W., Fugelsang, K.C. and Gump, B.H. (1996) Laboratory Procedures. *In Wine Analysis and Production*. pp. 474–477. New York: Chapman and Hall, International Thomson Publishing.

Zuzuarregui, A., Monteoliva, L., Gil, C. and del Olmo, M. (2006) Transcriptomic and proteomic approach for understanding the molecular basis of adaptation of *Saccharomyces cerevisiae* to wine fermentation. *Appl Environ Microbiol* **72**:836-847.

APPENDIX I RAW MICROARRAY DATA

Table 1: Raw microarray data for fermentation day two.

ORF ID	Gene Name	Gene Function	Avg Log_2 Ratio	Fold Change	T-test
YDR384C	ATO3	ammonium transporter	-4.7080	-26.1	0.000218073
YAL054C	ACS1	acetate-CoA ligase	-4.2472	-19.0	0.00136708
YOR388C	FDH1	formate dehydrogenase	-3.9233	-15.2	0.00112218
YPL276W		formate dehydrogenase	-3.9048	-15.0	0.0018313
YIL057C		unknown	-3.8852	-14.8	0.000269461
YCR010C	ADY2	ammonium transporter	-3.7943	-13.9	0.000531308
YPL275W	FDH2	formate dehydrogenase	-3.4663	-11.1	0.00099206
YJL152W			-3.1458	-8.9	0.000432178
YOR100C	CRC1	carnitine:acyl carnitine antiporter	-3.1388	-8.8	0.207383
YPR002W	PDH1	unknown	-3.0130	-8.1	0.000701407
YAR037W			-2.9253	-7.6	0.00359492
YGR236C	SPG1	unknown	-2.8983	-7.5	0.000121819
YAR035W	YAT1	carnitine O-acetyltransferase	-2.8412	-7.2	0.00131289
YNL117W	MLS1	malate synthase	-2.8367	-7.1	0.00327977
YJL153C	INO1	inositol-3-phosphate synthase	-2.8182	-7.1	0.00723627
YGL255W	ZRT1	high affinity zinc uptake transporter	-2.7940	-6.9	0.0145379
YIR031C	DAL7	malate synthase	-2.7370	-6.7	0.00173296
YMR107W	SPG4	unknown	-2.7080	-6.5	0.00169631
YHR139C	SPS100	unknown	-2.6807	-6.4	0.000117484
YCR005C	CIT2	citrate (Si)-synthase	-2.6782	-6.4	0.00406735
YOR374W	ALD4	aldehyde dehydrogenase	-2.6317	-6.2	0.0107259
YMR118C		unknown	-2.5947	-6.0	0.00108584
YNR002C	ATO2	ammonium transporter	-2.5923	-6.0	8.52408E-05
YOR108W	LEU9	2-isopropylmalate synthase	-2.5578	-5.9	0.000410554
YOR230W	WTM1	transcription corepressor	-2.5483	-5.8	0.00397148
YNL104C	LEU4	2-isopropylmalate synthase	-2.4547	-5.5	0.0014671
YBL015W	ACH1	acetyl-CoA hydrolase	-2.3808	-5.2	0.00598072
YKR097W	PCK1	phosphoenolpyruvate carboxykinase	-2.3562	-5.1	0.00160329
YKL187C		unknown	-2.3010	-4.9	0.00213718
YLR153C	ACS2	acetate-CoA ligase	-2.2760	-4.8	0.00197593
YPL265W	DIP5	amino acid transporter	-2.2202	-4.7	0.00815705
YER024W	YAT2	carnitine O-acetyltransferase	-2.2080	-4.6	0.00638496
YLR377C	FBP1	fructose-bisphosphatase	-2.1493	-4.4	0.00168549
YER073W	ALD5	3-chloroallyl aldehyde dehydrogenase	-2.1482	-4.4	1.08085E-05
YML042W	CAT2	carnitine O-acetyltransferase	-2.1473	-4.4	0.000981853
YLR284C	ECI1	dodecenoyl-CoA delta-isomerase	-2.0637	-4.2	0.00124702
YER065C	ICL1	isocitrate lyase	-2.0530	-4.1	0.0022822
YKL182W	FAS1	[acyl-carrier protein] S-malonyltransferase *	-2.0425	-4.1	0.00282861
YCR028C	FEN2	pantothenate transporter	-2.0362	-4.1	0.00153978
YMR162C	DNF3	phospholipid-translocating ATPase	-2.0222	-4.1	0.00603812
YGR205W		ATP binding	-1.8952	-3.7	0.00389137
YPL274W	SAM3	S-adenosylmethionine transporter	-1.8845	-3.7	0.0110817
YCR033W	SNT1	NAD-dependent histone deacetylase *	-1.8798	-3.7	0.00195978
YKL095W	YJU2	unknown	-1.8765	-3.7	0.0167637
YML075C	HMG1	hydroxymethylglutaryl-CoA reductase (NADPH)	-1.8725	-3.7	0.040413
YAL062W	GDH3	glutamate dehydrogenase	-1.8695	-3.7	0.00747882
YCR035C	RRP43	3'-5'-exoribonuclease	-1.8692	-3.7	0.00149969
YCR050C			-1.8357	-3.6	0.000974659
YCR021C	HSP30	unknown	-1.8237	-3.5	0.00169245
YOR243C	PUS7	pseudouridine synthase	-1.8205	-3.5	0.0128418
YAL009W	SPO7	unknown	-1.8122	-3.5	0.00558326
YNL202W	SPS19	2,4-dienoyl-CoA reductase (NADPH)	-1.8025	-3.5	0.00130246
YJR095W	SFC1	succinate:fumarate antiporter	-1.7818	-3.4	0.000114951
YLR331C			-1.7783	-3.4	0.00372839
YPR006C	ICL2	methylisocitrate lyase	-1.7735	-3.4	0.000791573
YBR050C	REG2	protein phosphatase type 1 regulator	-1.7712	-3.4	0.00222256
YDR161W		unknown	-1.7522	-3.4	0.00168643
YPL036W	PMA2	hydrogen-exporting ATPase , phosphorylative mechanism	-1.7505	-3.4	0.00103896
YJL043W		unknown	-1.7497	-3.4	0.00722442
YBR026C	ETR1	enoyl-[acyl-carrier protein] reductase	-1.7342	-3.3	0.00442948
YDL049C	KNH1	unknown	-1.6668	-3.2	0.00182923
YHR185C	PFS1	unknown	-1.6512	-3.1	0.00120209
YIR038C	GTT1	glutathione transferase	-1.6492	-3.1	9.55407E-05
YIR040C			-1.6405	-3.1	0.0122417
YNL173C	MDG1	unknown	-1.6380	-3.1	0.00548629
YLR164W		unknown	-1.6185	-3.1	0.000293696
YLR371W	ROM2	signal transducer *	-1.6180	-3.1	0.075157
YOL083W		unknown	-1.5882	-3.0	0.000994279
YLR130C	ZRT2	low-affinity zinc ion transporter	-1.5797	-3.0	0.0102896

Table 1: continued.

ORF ID	Gene Name	Gene Function	Avg Log_2 Ratio	Fold Change	T-test
YIR036C		unknown	-1.5775	-3.0	0.0075153
YOR273C	TPO4	spermine transporter	-1.5768	-3.0	0.0477474
YGL145W	TIP20	unknown	-1.5640	-3.0	0.00343406
YBR072W	HSP26	unfolded protein binding	-1.5610	-3.0	0.00139315
YHR018C	ARG4	argininosuccinate lyase	-1.5507	-2.9	0.03339
YBR067C	TIP1	structural constituent of cell wall*	-1.5468	-2.9	0.00537742
YGR271W	SLH1	RNA helicase	-1.5133	-2.9	0.00143023
YKL050C		unknown	-1.5112	-2.9	0.000526195
YPL004C	LSP1	protein kinase	-1.4955	-2.8	0.00346151
YGR146C		unknown	-1.4940	-2.8	0.00641131
YDL232W	OST4	protein binding	-1.4845	-2.8	0.0198544
YJR148W	BAT2	branched-chain-amino-acid transaminase	-1.4750	-2.8	0.0146444
YJL039C	NUP192	structural constituent of nuclear pore	-1.4678	-2.8	0.0344339
YBL013W	FMT1	methionyl-tRNA formyltransferase	-1.4555	-2.7	0.0120324
YMR085W		unknown	-1.4387	-2.7	0.0656791
YDR438W		unknown	-1.4293	-2.7	0.00396554
YKR076W	ECM4	unknown	-1.4290	-2.7	0.00661339
YAL043C	PTA1	RNA binding	-1.4202	-2.7	0.00367684
YDR111C	ALT2	transaminase	-1.4067	-2.7	0.00859708
YJL085W	EXO70	protein binding	-1.4025	-2.6	0.00894946
YBR222C	PCS60	AMP binding	-1.3972	-2.6	0.00133507
YOR290C	SNF2	general RNA polymerase II transcription factor	-1.3777	-2.6	0.061678
YJR104C	SOD1	copper, zinc superoxide dismutase	-1.3720	-2.6	0.00125702
YMR006C	PLB2	lysophospholipase	-1.3660	-2.6	0.0152239
YMR041C		unknown	-1.3607	-2.6	0.0627898
YLL053C		unknown	-1.3583	-2.6	0.12105
YMR031C		unknown	-1.3423	-2.5	0.0204176
YNL014W	HEF3	ATPase *	-1.3380	-2.5	0.000928258
YPL278C		unknown	-1.3358	-2.5	0.000933247
YFL006W			-1.3337	-2.5	0.00970652
YLR283W		unknown	-1.3327	-2.5	0.00560181
YIL136W	OM45	unknown	-1.3317	-2.5	0.00925432
YOR342C		unknown	-1.3288	-2.5	0.0217426
YML008C	ERG6	sterol 24-C-methyltransferase	-1.3130	-2.5	0.00512992
YGL205W	POX1	acyl-CoA oxidase	-1.3047	-2.5	0.00114115
YNL208W		unknown	-1.3030	-2.5	0.0108054
YDL215C	GDH2	glutamate dehydrogenase	-1.2965	-2.5	0.00240171
YDR385W	EFT2	translation elongation factor	-1.2947	-2.5	0.00958742
YBR094W		unknown	-1.2908	-2.4	0.0118839
YER091C	MET6	5-methyltetrahydropteroyltriglutamate-homocysteine S-met	-1.2880	-2.4	0.0012232
YOR101W	RAS1	GTPase	-1.2768	-2.4	0.0246678
YDR319C		unknown	-1.2712	-2.4	0.00046448
YPL061W	ALD6	3-chloroallyl aldehyde dehydrogenase	-1.2535	-2.4	0.0103137
YDL085W	NDE2	NADH dehydrogenase	-1.2443	-2.4	0.00672484
YGR247W	CPD1	2',3'-cyclic-nucleotide 3'-phosphodiesterase	-1.2383	-2.4	0.00429145
YGR008C	STF2	unknown	-1.2238	-2.3	0.00971904
YAL067C	SEO1	transporter	-1.2233	-2.3	0.00757927
YPL113C		oxidoreductase	-1.2220	-2.3	0.0205914
YGR154C	GTO1	unknown	-1.2203	-2.3	0.0372931
YGR056W	RSC1	unknown	-1.2193	-2.3	0.00918573
YLR389C	STE23	metallopeptidase	-1.2183	-2.3	0.00519147
YLR267W	BOP2	unknown	-1.2130	-2.3	0.00069634
YNR001C	CIT1	citrate (Si)-synthase	-1.2120	-2.3	0.00125313
YEL028W			-1.2077	-2.3	0.0106174
YGL062W	PYC1	pyruvate carboxylase	-1.2017	-2.3	0.00807525
YGR161C	RTS3	protein phosphatase type 2A	-1.1925	-2.3	0.00124208
YKR009C	FOX2	3-hydroxyacyl-CoA dehydrogenase	-1.1897	-2.3	0.0332398
YLR348C	DIC1	dicarboxylic acid transporter	-1.1777	-2.3	0.00787494
YGL196W		unknown	-1.1738	-2.3	0.0163304
YER124C	DSE1	unknown	-1.1725	-2.3	0.0582102
YJL163C		unknown	-1.1620	-2.2	0.0160042
YIL124W	AYR1	acylglycerone-phosphate reductase	-1.1532	-2.2	0.000707662
YER121W			-1.1497	-2.2	0.00201393
YAR042W	SWH1	phosphatidylinositol binding	-1.1483	-2.2	0.0384143
YMR214W	SCJ1	chaperone binding	-1.1378	-2.2	0.00542857
YGR086C	PIL1	protein kinase	-1.1333	-2.2	0.00138338
YAR040C			-1.1330	-2.2	0.013239
YMR072W	ABF2	DNA binding	-1.1308	-2.2	0.0142121
YIL009W	FAA3	long-chain-fatty-acid-CoA ligase	-1.1298	-2.2	0.0118662

Table 1: continued.

ORF ID	Gene Name	Gene Function	Avg Log_2 Ratio	Fold Change	T-test
YOL126C	MDH2	L-malate dehydrogenase	-1.1280	-2.2	0.00466172
YMR303C	ADH2	alcohol dehydrogenase	-1.1158	-2.2	0.0242276
YPL246C	RBD2	unknown	-1.1157	-2.2	0.0158778
YHR096C	HXT5	glucose transporter	-1.1155	-2.2	0.031484
YMR315W		unknown	-1.1118	-2.2	0.0450408
YDR497C	ITR1	myo-inositol transporter	-1.1070	-2.2	0.00777437
YOR133W	EFT1	translation elongation factor	-1.1047	-2.2	0.0332233
YPR150W			-1.1033	-2.1	0.0116281
YOL058W	ARG1	argininosuccinate synthase	-1.0945	-2.1	0.0134545
YGR052W	FMP48	kinase	-1.0840	-2.1	0.00176231
YIL160C	POT1	acetyl-CoA C-acyltransferase	-1.0828	-2.1	0.0255099
YMR246W	FAA4	long-chain-fatty-acid-CoA ligase	-1.0808	-2.1	0.00450923
YEL060C	PRB1	serine-type endopeptidase	-1.0758	-2.1	0.0232746
YJR073C	OPI3	phosphatidyl-N-methylethanolamine N-methyltransferase	-1.0692	-2.1	0.00285444
YJL045W		succinate dehydrogenase	-1.0680	-2.1	0.0377457
YOL110W	SHR5	protein-cysteine S-palmitoleyltransferase	-1.0673	-2.1	0.0170142
YHR007C	ERG11	sterol 14-demethylase	-1.0665	-2.1	0.0151038
YOR373W	NUD1	structural constituent of cytoskeleton	-1.0662	-2.1	0.0256083
YBR046C	ZTA1	unknown	-1.0640	-2.1	0.00188264
YER084W			-1.0623	-2.1	0.000970999
YNL057W			-1.0615	-2.1	0.0259222
YLR355C	ILV5	ketol-acid reductoisomerase	-1.0612	-2.1	0.00223063
YDL046W	NPC2	unknown	-1.0610	-2.1	0.00236527
YMR191W	SPG5	unknown	-1.0607	-2.1	0.00187758
YGR175C	ERG1	squalene monooxygenase *	-1.0603	-2.1	0.0279659
YPL028W	ERG10	acetyl-CoA C-acetyltransferase	-1.0572	-2.1	0.0327046
YJL088W	ARG3	ornithine carbamoyltransferase	-1.0455	-2.1	0.0143854
YMR152W	YIM1	unknown	-1.0428	-2.1	0.0119463
YOL053C-A			-1.0337	-2.0	0.0101263
YJL067W			-1.0325	-2.0	0.0457892
YNL115C		unknown	-1.0318	-2.0	0.00478682
YNL195C		unknown	-1.0278	-2.0	0.0280353
YPL147W	PXA1	ATPase , coupled to transmembrane movement of substanc	-1.0272	-2.0	0.0185403
YEL071W	DLD3	D-lactate dehydrogenase	-1.0162	-2.0	0.0501081
YKL217W	JEN1	lactate transporter	-1.0117	-2.0	0.0502041
YMR160W		unknown	-1.0105	-2.0	0.0206442
YBL016W	FUS3	MAP kinase	-1.0055	-2.0	0.0239609
YIL047C	SYG1	unknown	-1.0007	-2.0	0.0106308
YLR369W	SSQ1	unfolded protein binding	-0.9982	-2.0	0.164697
YDR039C	ENA2	ATPase , coupled to transmembrane movement of ions, phc	-0.9973	-2.0	0.0332456
YNL009W	IDP3	isocitrate dehydrogenase	-0.9895	-2.0	0.0191983
YMR083W	ADH3	alcohol dehydrogenase	-0.9872	-2.0	0.0232675
YDR046C	BAP3	amino acid transporter	-0.9850	-2.0	0.0161152
YCR004C	YCP4	electron carrier	-0.9833	-2.0	0.00378332
YHR001W	OSH7	oxysterol binding	-0.9828	-2.0	0.0115582
YMR251W-A	HOR7	unknown	-0.9800	-2.0	0.00778365
YGL184C	STR3	cystathionine beta-lyase	-0.9758	-2.0	0.000968937
YMR297W	PRC1	carboxypeptidase C	-0.9695	-2.0	0.00983392
YIL177C		helicase	-0.9693	-2.0	0.00539022
YLR081W	GAL2	glucose transporter	-0.9660	-2.0	0.0561172
YOR229W	WTM2	transcription corepressor	-0.9615	-1.9	0.0126279
YLR320W	MMS22	unknown	-0.9605	-1.9	0.0182108
YPR139C	VPS66	unknown	-0.9583	-1.9	0.00745739
YMR056C	AAC1	ATP:ADP antiporter	-0.9543	-1.9	0.0320628
YJL026W	RNR2	ribonucleoside-diphosphate reductase	-0.9527	-1.9	0.00274444
YHR208W	BAT1	branched-chain-amino-acid transaminase	-0.9523	-1.9	0.0278678
YDR033W	MRH1	unknown	-0.9478	-1.9	0.0036846
YGL156W	AMS1	alpha-mannosidase	-0.9452	-1.9	0.0352944
YDL073W		unknown	-0.9368	-1.9	0.0480045
YHR092C	HXT4	glucose transporter	-0.9333	-1.9	0.0327426
YJR008W		unknown	-0.9323	-1.9	0.00354344
YBL075C	SSA3	ATPase *	-0.9300	-1.9	0.0127402
YHR215W	PHO12	acid phosphatase	-0.9293	-1.9	0.00354773
YIL115C	NUP159	structural molecule	-0.9272	-1.9	0.00832438
YOL086C	ADH1	alcohol dehydrogenase	-0.9160	-1.9	0.0153947
YLR467W	YRF1-5	DNA helicase	-0.9117	-1.9	0.0144548
YOR375C	GDH1	glutamate dehydrogenase	-0.9117	-1.9	0.0909276
YOR348C	PUT4	L-proline permease	-0.9108	-1.9	0.0414861
YJR107W		lipase	-0.9088	-1.9	0.121761

Table 1: continued.

ORF ID	Gene Name	Gene Function	Avg Log_2 Ratio	Fold Change	T-test
YDL182W	LYS20	homocitrate synthase	-0.9077	-1.9	0.000343853
YIL166C		transporter	-0.8972	-1.9	0.0112094
YDL173W		unknown	-0.8942	-1.9	0.00417624
YCR047C	BUD23	S-adenosylmethionine-dependent methyltransferase	-0.8927	-1.9	0.0126782
YPL049C	DIG1	DNA binding	-0.8923	-1.9	0.0125409
YGR180C	RNR4	ribonucleoside-diphosphate reductase	-0.8910	-1.9	0.0207537
YLR327C	TMA10	unknown	-0.8853	-1.8	0.00970216
YCL004W(1)			-0.8823	-1.8	0.0139477
YIR002C	MPH1	RNA helicase	-0.8813	-1.8	0.00902535
YLL052C	AQY2	water channel	-0.8812	-1.8	0.0206034
YLR174W	IDP2	isocitrate dehydrogenase	-0.8795	-1.8	0.019632
YMR195W	ICY1	unknown	-0.8792	-1.8	0.00503988
YFR036W-A			-0.8792	-1.8	0.0451375
YDR032C	PST2	unknown	-0.8775	-1.8	0.00213569
YBR144C			-0.8765	-1.8	0.0428772
YOR095C	RKI1	ribose-5-phosphate isomerase	-0.8748	-1.8	0.00791865
YPR010C	RPA135	DNA-directed RNA polymerase	-0.8745	-1.8	0.0288493
YMR116C	ASC1	unknown	-0.8728	-1.8	0.0020079
YIL119C	RPI1	small GTPase regulator	-0.8722	-1.8	0.0277949
YIL033C	BCY1	cAMP-dependent protein kinase	-0.8713	-1.8	0.0576105
YKL199C			-0.8675	-1.8	0.0202703
YKL033W		unknown	-0.8670	-1.8	0.0244836
YJL219W	HXT9	glucose transporter	-0.8655	-1.8	0.0332624
YJL130C	URA2	carbamoyl-phosphate synthase (glutamine-hydrolyzing) *	-0.8623	-1.8	0.0180221
YFR044C		unknown	-0.8602	-1.8	0.0224477
YHR094C	HXT1	glucose transporter	-0.8542	-1.8	0.0336488
YMR139W	RIM11	protein serine/threonine kinase	-0.8488	-1.8	0.29394
YOR054C	VHS3	phosphopantothenoylcysteine decarboxylase	-0.8488	-1.8	0.0502112
YBR068C	BAP2	amino acid transporter	-0.8447	-1.8	0.00322697
YLR414C		unknown	-0.8437	-1.8	0.00244411
YOL153C		unknown	-0.8388	-1.8	0.0439778
YER084W-A			-0.8360	-1.8	0.221601
YFL011W	HXT10	glucose transporter	-0.8352	-1.8	0.002615
YAL056W	GPB2	signal transducer	-0.8345	-1.8	0.0003491
YIR039C	YPS6	aspartic-type endopeptidase	-0.8338	-1.8	0.0522286
YMR250W	GAD1	glutamate decarboxylase	-0.8335	-1.8	0.0295853
YNL008C	ASI3	ubiquitin-protein ligase	-0.8330	-1.8	0.0218619
YIR037W	HYR1	thioredoxin peroxidase	-0.8285	-1.8	0.00356745
YIL170W	HXT12	unknown	-0.8280	-1.8	0.0527226
YOR031W	CRS5	copper ion binding	-0.8278	-1.8	0.00849453
YNL239W	LAP3	transcription regulator	-0.8267	-1.8	0.104249
YMR164C	MSS11	specific RNA polymerase II transcription factor	-0.8260	-1.8	0.0892817
YML118W	NGL3	endonuclease	-0.8248	-1.8	0.00521392
YPL103C	FMP30	unknown	-0.8238	-1.8	0.0799272
YKL057C	NUP120	structural molecule	-0.8182	-1.8	0.172077
YBR025C		unknown	-0.8165	-1.8	0.00703013
YGL017W	ATE1	arginyltransferase	-0.8155	-1.8	0.0192379
YBR054W	YRO2	unknown	-0.8132	-1.8	0.0395992
YGR130C		unknown	-0.8085	-1.8	0.0177596
YNL134C		alcohol dehydrogenase	-0.8077	-1.8	0.0099102
YBR083W	TEC1	specific RNA polymerase II transcription factor	-0.8068	-1.7	0.0207251
YPL062W			-0.8052	-1.7	0.10305
YJL225C		helicase	-0.8017	-1.7	0.0174451
YKL005C	BYE1	transcriptional elongation regulator	-0.8017	-1.7	0.0042893
YER138C			-0.8013	-1.7	0.113771
YLL066W-A			-0.7983	-1.7	0.0394687
YPL254W	HFI1	transcription coactivator *	-0.7972	-1.7	0.189492
YHL034C	SBP1	RNA binding	-0.7935	-1.7	0.000827879
YML010W-B			-0.7923	-1.7	0.124338
YPL264C		unknown	-0.7920	-1.7	0.000450074
YLR306W	UBC12	NEDD8 conjugating enzyme	-0.7910	-1.7	0.000975033
YNR050C	LYS9	saccharopine dehydrogenase	-0.7850	-1.7	0.00158771
YJR139C	HOM6	homoserine dehydrogenase	-0.7848	-1.7	0.0133602
YPR012W			-0.7787	-1.7	0.0489419
YLR356W		unknown	-0.7785	-1.7	0.0226944
YLL020C			-0.7768	-1.7	0.00430602
YOL123W	HRP1	RNA binding	-0.7747	-1.7	0.0259376
YLL016W	SDC25	Ras guanyl-nucleotide exchange factor	-0.7745	-1.7	0.00764971
YDR038C	ENA5	ATPase , coupled to transmembrane movement of ions, phc	-0.7725	-1.7	0.0714362

Table 1: continued.

ORF ID	Gene Name	Gene Function	Avg Log_2 Ratio	Fold Change	T-test
YPL109C		unknown	-0.7715	-1.7	0.025346
YNL200C		unknown	-0.7687	-1.7	0.0135264
YAR018C	KIN3	protein kinase	-0.7663	-1.7	0.0126639
YMR318C	ADH6	alcohol dehydrogenase	-0.7657	-1.7	0.0238493
YMR206W		unknown	-0.7625	-1.7	0.00165901
YDR300C	PRO1	glutamate 5-kinase	-0.7597	-1.7	0.0259768
YOL065C	INP54	inositol-polyphosphate 5-phosphatase	-0.7592	-1.7	0.0063353
YMR251W	GTO3	unknown	-0.7585	-1.7	0.14233
YKL197C	PEX1	ATPase	-0.7573	-1.7	0.146408
YOR184W	SER1	phosphoserine transaminase	-0.7538	-1.7	0.250373
YBR286W	APE3	aminopeptidase	-0.7537	-1.7	0.0292206
YBL113W-A			-0.7518	-1.7	0.0448722
YNL268W	LYP1	basic amino acid transporter	-0.7517	-1.7	0.0364305
YOR336W	KRE5	UDP-glucose:glycoprotein glucosyltransferase	-0.7507	-1.7	0.0484315
YBR244W	GPX2	glutathione peroxidase	-0.7505	-1.7	0.00137412
YIR015W	RPR2	ribonuclease P	-0.7500	-1.7	0.0316138
YBL042C	FUI1	uridine transporter	-0.7498	-1.7	0.000486736
YDL169C	UGX2	unknown	-0.7495	-1.7	0.00759826
YCR056W			-0.7452	-1.7	0.0252701
YOL147C	PEX11	unknown	-0.7450	-1.7	0.041068
YLR214W	FRE1	ferric-chelate reductase	-0.7440	-1.7	0.00501358
YPR173C	VPS4	ATPase	-0.7410	-1.7	0.0300097
YBL014C	RRN6	RNA polymerase I transcription factor	-0.7378	-1.7	0.0319721
YPL119C	DBP1	RNA helicase	-0.7348	-1.7	0.263192
YMR110C	HFD1	3-chloroallyl aldehyde dehydrogenase	-0.7338	-1.7	0.00668068
YJL042W	MHP1	structural constituent of cytoskeleton	-0.7317	-1.7	0.00112377
YGR155W	CYS4	cystathionine beta-synthase	-0.7302	-1.7	0.00020141
YDL171C	GLT1	glutamate synthase (NADH)	-0.7295	-1.7	0.0297633
YPL018W	CTF19	protein binding	-0.7293	-1.7	0.298707
YNL246W	VPS75	unknown	-0.7287	-1.7	0.00399544
YOL018C	TLG2	v-SNARE *	-0.7280	-1.7	0.236142
YBR139W		serine hydrolase *	-0.7277	-1.7	0.0186737
YBR020W	GAL1	galactokinase	-0.7275	-1.7	0.030461
YKL157W	APE2	leucyl aminopeptidase	-0.7245	-1.7	0.0142352
YEL063C	CAN1	basic amino acid transporter	-0.7240	-1.7	0.0502109
YNL015W	PBI2	endopeptidase inhibitor	-0.7208	-1.6	0.0767774
YMR019W	STB4	DNA binding	-0.7207	-1.6	0.0519094
YMR114C		unknown	-0.7203	-1.6	0.0150624
YCR011C	ADP1	ATPase , coupled to transmembrane movement of substanc	-0.7202	-1.6	0.0508017
YHR074W	QNS1	hydrolase , acting on carbon-nitrogen (but not peptide) bon	-0.7202	-1.6	0.120026
YCL049C		unknown	-0.7200	-1.6	0.00646251
YEL058W	PCM1	phosphoacetylglucosamine mutase	-0.7187	-1.6	0.00194544
YCRX02C			-0.7187	-1.6	0.0384456
YPR025C	CCL1	general RNA polymerase II transcription factor	-0.7162	-1.6	0.0412672
YLR450W	HMG2	hydroxymethylglutaryl-CoA reductase (NADPH)	-0.7160	-1.6	0.154623
YGR141W	VPS62	unknown	-0.7150	-1.6	0.0198467
YLL002W	RTT109	unknown	-0.7147	-1.6	0.00725145
YBR265W	TSC10	oxidoreductase	-0.7138	-1.6	0.00954183
YPL186C	UIP4	unknown	-0.7137	-1.6	0.0223697
Q0110	BI2	nuclease	-0.7120	-1.6	0.0261979
YDR015C			-0.7098	-1.6	0.0546078
YMR102C		unknown	-0.7095	-1.6	0.0849514
YNL270C	ALP1	basic amino acid transporter	-0.7075	-1.6	0.0330172
YBR053C		unknown	-0.7068	-1.6	0.00179155
YEL011W	GLC3	1,4-alpha-glucan branching enzyme	-0.7062	-1.6	0.00120619
YNL307C	MCK1	glycogen synthase kinase	-0.7058	-1.6	0.034878
YLR460C		unknown	-0.7040	-1.6	0.0528768
YER130C		unknown	-0.7030	-1.6	0.0164337
YDL078C	MDH3	L-malate dehydrogenase	-0.7028	-1.6	0.0198745
YDL222C	FMP45	unknown	-0.7027	-1.6	0.00370794
YER172C	BRR2	RNA splicing factor	-0.7022	-1.6	0.0715497
YJL116C	NCA3	unknown	-0.6948	-1.6	0.0499002
YNL168C	FMP41	unknown	-0.6930	-1.6	0.0106248
YPR013C		unknown	-0.6927	-1.6	0.00832789
YMR108W	ILV2	acetolactate synthase *	-0.6835	-1.6	0.0118143
YAL055W	PEX22	unknown	-0.6795	-1.6	0.0141397
YIL071C	PCI8	unknown	-0.6792	-1.6	0.00119162
YMR119W-A			-0.6772	-1.6	0.00780916
YCR093W	CDC39	3'-5'-exoribonuclease	-0.6765	-1.6	0.00752911

Table 1: continued.

ORF ID	Gene Name	Gene Function	Avg Log_2 Ratio	Fold Change	T-test
YJR112W	NNF1	unknown	-0.6753	-1.6	0.00507128
YLR143W		unknown	-0.6752	-1.6	0.0924621
YNL280C	ERG24	delta14-sterol reductase	-0.6750	-1.6	0.133412
YOR165W	SEY1	unknown	-0.6742	-1.6	0.112196
YCRX15W			-0.6735	-1.6	0.0498245
YKL123W			-0.6733	-1.6	0.0326957
YBR131W	CCZ1	guanyl-nucleotide exchange factor	-0.6727	-1.6	0.0176449
YFR024C-A	LSB3	unknown	-0.6717	-1.6	0.0190464
YBR080C	SEC18	ATPase	-0.6697	-1.6	0.00238185
YBL067C	UBP13	ubiquitin-specific protease	-0.6693	-1.6	0.008725
YNL067W	RPL9B	structural constituent of ribosome	-0.6690	-1.6	0.0126196
YDR129C	SAC6	protein binding	-0.6660	-1.6	0.0821353
YPL037C	EGD1	unfolded protein binding	-0.6647	-1.6	0.0293449
YHR097C		unknown	-0.6608	-1.6	0.0185694
YLR438W	CAR2	ornithine-oxo-acid transaminase	-0.6593	-1.6	0.0153655
YGR067C		unknown	-0.6565	-1.6	0.023154
YER178W	PDA1	pyruvate dehydrogenase	-0.6545	-1.6	0.0220401
YHR072W	ERG7	lanosterol synthase	-0.6535	-1.6	0.0129567
YOL103W	ITR2	myo-inositol transporter	-0.6495	-1.6	0.121942
YKR084C	HBS1	unknown	-0.6488	-1.6	0.000758252
YPR080W	TEF1	translation elongation factor	-0.6478	-1.6	0.166537
YOR040W	GLO4	hydroxyacylglutathione hydrolase	-0.6477	-1.6	0.111901
YPL134C	ODC1	intracellular transporter	-0.6463	-1.6	0.00333852
YML072C	TCB3	lipid binding	-0.6462	-1.6	0.0119512
YPL074W	YTA6	ATPase	-0.6455	-1.6	0.0791675
YJL172W	CPS1	Gly-X carboxypeptidase	-0.6432	-1.6	0.0579268
YGL059W		protein kinase	-0.6397	-1.6	0.0254145
YCR062W			-0.6383	-1.6	0.000857556
YEL016C	NPP2	nucleoside-triphosphatase *	-0.6383	-1.6	0.110499
YGL055W	OLE1	stearoyl-CoA 9-desaturase	-0.6365	-1.6	0.0514347
YDR247W	VHS1	protein kinase	-0.6360	-1.6	0.102614
YGL161C	YIP5	Rab GTPase binding	-0.6357	-1.6	0.0342868
YDR160W	SSY1	amino acid binding	-0.6303	-1.5	0.0671155
YER020W	GPA2	GTPase	-0.6288	-1.5	0.00348378
YLR237W	THI7	thiamin transporter	-0.6282	-1.5	0.0478375
YCL013W			-0.6278	-1.5	0.00123192
YDR506C		unknown	-0.6273	-1.5	0.132163
YDR246W	TRS23	unknown	-0.6272	-1.5	0.0978044
YDL179W	PCL9	cyclin-dependent protein kinase	-0.6263	-1.5	0.0274064
YNL321W		unknown	-0.6262	-1.5	0.107064
YNR016C	ACC1	acetyl-CoA carboxylase *	-0.6242	-1.5	0.0356062
YJR130C	STR2	cystathionine gamma-synthase	-0.6238	-1.5	0.00401844
YNL093W	YPT53	GTPase	-0.6232	-1.5	0.10927
YLR178C	TFS1	lipid binding	-0.6230	-1.5	0.00316436
YER103W	SSA4	ATPase *	-0.6228	-1.5	0.0342273
YIL094C	LYS12	homoisocitrate dehydrogenase	-0.6215	-1.5	0.0524943
YFR047C	BNA6	nicotinate-nucleotide diphosphorylase (carboxylating)	-0.6182	-1.5	0.0108959
YGR134W	CAF130	unknown	-0.6155	-1.5	0.0326339
YOL165C	AAD15	aryl-alcohol dehydrogenase	-0.6135	-1.5	0.0442084
YDL200C	MGT1	methylated-DNA-[protein]-cysteine S-methyltransferase	-0.6120	-1.5	0.0588737
YMR238W	DFG5	mannosidase	-0.6108	-1.5	0.0255659
YCR086W	CSM1	unknown	-0.6107	-1.5	0.0445425
YJL147C		unknown	-0.6090	-1.5	0.00069081
YFR041C	ERJ5	unknown	-0.6088	-1.5	0.00303969
YLR093C	NYV1	v-SNARE	-0.6087	-1.5	0.00229792
YDL239C	ADY3	protein binding	-0.6072	-1.5	0.0512154
YPR003C		unknown	-0.6070	-1.5	0.0254132
YBR097W	VPS15	protein serine/threonine kinase	-0.6068	-1.5	0.171751
YLR205C	HMX1	heme binding	-0.6057	-1.5	0.00028184
YML010W-A			-0.6057	-1.5	0.11892
YPR133C	SPN1	RNA polymerase II transcription elongation factor	-0.6028	-1.5	0.00158878
YMR106C	YKU80	RNA binding	-0.6020	-1.5	0.0711883
YKL117W	SBA1	chaperone binding	-0.6017	-1.5	0.0136933
YIL158W		unknown	-0.5998	-1.5	0.00198558
YHL010C		nuclear localization sequence binding	-0.5982	-1.5	0.0633709
YOR019W		unknown	-0.5952	-1.5	0.0734784
YJR039W		unknown	-0.5950	-1.5	0.0469764
YKL210W	UBA1	ubiquitin activating enzyme	-0.5945	-1.5	0.00132668
YDR179W-A		unknown	-0.5945	-1.5	0.0388303

Table 1: continued.

ORF ID	Gene Name	Gene Function	Avg Log_2 Ratio	Fold Change	T-test
YPR108W	RPN7	structural molecule	-0.5937	-1.5	0.0188019
YCR102C		unknown	-0.5933	-1.5	0.00549815
YPR015C		unknown	-0.5923	-1.5	0.0167209
YOL062C	APM4	unknown	-0.5915	-1.5	0.149685
YOR304W	ISW2	ATPase	-0.5913	-1.5	0.0275905
YDR433W			-0.5913	-1.5	0.0854852
YJR099W	YUH1	ubiquitin-specific protease	-0.5910	-1.5	0.00976385
YIL046W	MET30	protein binding	-0.5898	-1.5	0.112747
YPR082C	DIB1	RNA splicing factor	-0.5887	-1.5	0.0189485
YDR249C		unknown	-0.5885	-1.5	0.0414751
YDR358W	GGA1	ubiquitin binding	-0.5880	-1.5	0.00056417
YDL185W	TFP1	hydrogen-transporting ATPase , rotational mechanism*	-0.5880	-1.5	0.0597065
YAR071W	PHO11	acid phosphatase	-0.5878	-1.5	0.00744237
YGR256W	GND2	phosphogluconate dehydrogenase	-0.5865	-1.5	0.0455373
YPL154C	PEP4	endopeptidase *	-0.5850	-1.5	0.0292443
YOR192C		transporter	-0.5837	-1.5	0.00113163
YJR066W	TOR1	protein binding	-0.5820	-1.5	0.0123851
YJR131W	MNS1	mannosyl-oligosaccharide 1,2-alpha-mannosidase	-0.5807	-1.5	0.00633896
YLR058C	SHM2	glycine hydroxymethyltransferase	-0.5807	-1.5	0.0883191
YHR008C	SOD2	manganese superoxide dismutase	-0.5795	-1.5	0.00554771
YGL164C	YRB30	protein binding	-0.5788	-1.5	0.00457977
YDL032W			-0.5767	-1.5	0.0595341
YLR088W	GAA1	GPI-anchor transamidase	-0.5762	-1.5	0.0886485
YMR258C		unknown	-0.5760	-1.5	0.000731584
YDR285W	ZIP1	chromatin binding	-0.5750	-1.5	0.0192479
YGR121C	MEP1	ammonium transporter	-0.5723	-1.5	0.0646348
YJL132W		unknown	-0.5707	-1.5	0.0178218
YOR175C		O-acyltransferase	-0.5707	-1.5	0.0125068
YGL245W	GUS1	glutamate-tRNA ligase	-0.5705	-1.5	0.0476166
YPR053C			-0.5700	-1.5	0.036026
YPL230W		unknown	-0.5697	-1.5	0.165868
YLR401C	DUS3	tRNA dihydrouridine synthase	-0.5692	-1.5	0.114528
YDR406W	PDR15	ATPase , coupled to transmembrane movement of substanc	-0.5678	-1.5	0.161776
YNR059W	MNT4	alpha-1,3-mannosyltransferase	-0.5677	-1.5	0.182102
YML133C		helicase	-0.5668	-1.5	0.128108
YOR356W		oxidoreductase	-0.5665	-1.5	0.249975
YAR014C	BUD14	protein phosphatase type 1 regulator	-0.5660	-1.5	0.0107293
YLR120C	YPS1	aspartic-type endopeptidase	-0.5657	-1.5	0.0716904
YPL232W	SSO1	t-SNARE	-0.5645	-1.5	0.250982
YDL199C		unknown	-0.5638	-1.5	0.0701341
YBR214W	SDS24	unknown	-0.5633	-1.5	0.0245915
YOL082W	ATG19	protein binding	-0.5623	-1.5	0.000890104
YIL093C	RSM25	structural constituent of ribosome	-0.5602	-1.5	0.156624
YLR365W			-0.5560	-1.5	0.0871798
YJL070C		unknown	-0.5557	-1.5	0.00281013
YPL256C	CLN2	cyclin-dependent protein kinase	-0.5548	-1.5	0.183438
YJL186W	MNN5	alpha-1,2-mannosyltransferase	-0.5547	-1.5	0.0550634
YCR045C		serine-type peptidase	-0.5542	-1.5	0.0264241
Q0105	COB	ubiquinol-cytochrome-c reductase	-0.5542	-1.5	0.0669248
YAR043C			-0.5518	-1.5	0.040718
YOR259C	RPT4	ATPase *	-0.5517	-1.5	0.0198706
YKL020C	SPT23	DNA binding	-0.5515	-1.5	0.142356
YLR173W		unknown	-0.5507	-1.5	0.071563
YLR219W	MSC3	unknown	-0.5490	-1.5	0.077245
YLR337W			-0.5488	-1.5	0.121434
YLR084C	RAX2	unknown	-0.5488	-1.5	0.0751995
YMR038C	CCS1	superoxide dismutase copper chaperone	-0.5482	-1.5	0.0136339
YNL135C	FPR1	peptidyl-prolyl cis-trans isomerase	-0.5472	-1.5	0.00331367
YJL164C	TPK1	protein serine/threonine kinase	-0.5472	-1.5	0.0462802
YBL108W			-0.5465	-1.5	0.0387518
YDL144C		unknown	-0.5463	-1.5	0.0163463
YIL082W			-0.5457	-1.5	0.00657654
YJR009C	TDH2	glyceraldehyde-3-phosphate dehydrogenase	-0.5440	-1.5	0.447956
YJL024C	APS3	unknown	-0.5402	-1.5	0.00762379
YKL144C	RPC25	DNA-directed RNA polymerase	-0.5398	-1.5	0.224644
YOR215C		unknown	-0.5393	-1.5	0.0124647
YBR243C	ALG7	UDP-N-acetylglucosamine-dolichyl-phosphate N-acetylglu	-0.5392	-1.5	0.0021535
YHR136C	SPL2	enzyme inhibitor	-0.5380	-1.5	0.0230976
YML065W	ORC1	ATPase *	-0.5367	-1.5	0.0471695

Table 1: continued.

ORF ID	Gene Name	Gene Function	Avg Log_2 Ratio	Fold Change	T-test
YDL218W		unknown	-0.5367	-1.5	0.0116372
YIL055C		unknown	-0.5363	-1.5	0.0862143
YBR118W	TEF2	translation elongation factor	-0.5360	-1.4	0.0939697
YPR032W	SRO7	unknown	-0.5360	-1.4	0.0133945
YKR067W	GPT2	glycerol-3-phosphate O-acyltransferase	-0.5353	-1.4	0.012607
YLL032C		unknown	-0.5327	-1.4	0.00509479
YGL153W	PEX14	protein binding	-0.5327	-1.4	0.107384
YDL086W		carboxymethylenebutenolidase	-0.5312	-1.4	0.0251987
YBR069C	TAT1	amino acid transporter	-0.5292	-1.4	8.83079E-05
YBR280C		unknown	-0.5273	-1.4	0.00187071
YER023W	PRO3	pyrroline-5-carboxylate reductase	-0.5263	-1.4	0.025616
YBR092C	PHO3	acid phosphatase	-0.5255	-1.4	0.0417088
YNL170W			-0.5253	-1.4	0.175941
YKR049C	FMP46	oxidoreductase	-0.5240	-1.4	0.0619188
YCRX18C			-0.5223	-1.4	0.0791725
YMR262W		unknown	-0.5222	-1.4	0.00984903
Q0075	AI5_BETA	unknown	-0.5197	-1.4	0.0989434
YPL193W	RSA1	unknown	-0.5192	-1.4	0.139014
YBR093C	PHO5	acid phosphatase *	-0.5188	-1.4	0.0818423
YMR052C-A			-0.5187	-1.4	0.0704699
YAL036C	RBG1	GTP binding	-0.5187	-1.4	0.0896977
YDR417C			-0.5183	-1.4	0.252248
YNL212W	VID27	unknown	-0.5167	-1.4	0.0611748
YIL083C		phosphopantothenate--cysteine ligase	-0.5155	-1.4	0.0512875
YLR117C	CLF1	protein binding	-0.5148	-1.4	0.00842562
YOR285W		unknown	-0.5145	-1.4	0.0897088
YLR070C	XYL2	D-xylulose reductase	-0.5133	-1.4	0.0887707
YPR104C	FHL1	transcription factor	-0.5132	-1.4	0.20462
YJR106W	ECM27	unknown	-0.5127	-1.4	0.0295507
YJL143W	TIM17	protein transporter	-0.5127	-1.4	0.220021
YJL076W	NET1	rDNA binding	-0.5123	-1.4	0.000427566
YAL044C	GCV3	glycine dehydrogenase	-0.5103	-1.4	0.143108
YJL210W	PEX2	protein binding	-0.5100	-1.4	0.00431764
YGL002W	ERP6	unknown	-0.5078	-1.4	0.00854339
YIL112W	HOS4	NAD-dependent histone deacetylase *	-0.5077	-1.4	0.013199
YNL163C	RIA1	GTPase	-0.5077	-1.4	0.0706703
YMR129W	POM152	structural molecule	-0.5065	-1.4	0.119404
YMR301C	ATM1	ATPase , coupled to transmembrane movement of substanc	-0.5062	-1.4	0.222795
YCR088W	ABP1	protein binding	-0.5060	-1.4	0.033444
YDL126C	CDC48	ATPase	-0.5055	-1.4	0.0979334
YHL034W-A			-0.5050	-1.4	0.0825645
YMR054W	STV1	hydrogen-transporting ATPase , rotational mechanism	-0.5048	-1.4	0.0371778
YCR032W	BPH1	unknown	-0.5042	-1.4	0.00446393
YDL125C	HNT1	hydrolase *	-0.5040	-1.4	0.0293068
YER169W	RPH1	specific transcriptional repressor	-0.5033	-1.4	0.0804288
YMR086W		unknown	-0.5010	-1.4	0.117261
YGR031C-A			-0.5008	-1.4	0.127507
YOR251C		thiosulfate sulfurtransferase	-0.4997	-1.4	0.0109806
YPR149W	NCE102	unknown	-0.4990	-1.4	0.0186356
YPL218W	SAR1	GTPase	-0.4972	-1.4	0.11647
YNL159C	ASI2	unknown	-0.4970	-1.4	0.0175164
YPR121W	THI22	phosphomethylpyrimidine kinase	-0.4957	-1.4	0.112944
YJL041W	NSP1	structural molecule	-0.4953	-1.4	0.145725
YBR043C	QDR3	multidrug efflux pump	-0.4938	-1.4	0.0159107
YLR411W	CTR3	copper uptake transporter	-0.4935	-1.4	0.0517532
YBR027C			-0.4935	-1.4	0.0798947
YOR317W	FAA1	long-chain-fatty-acid-CoA ligase	-0.4932	-1.4	0.0126549
YKL103C	LAP4	aminopeptidase I	-0.4928	-1.4	0.00656555
YLR305C	STT4	1-phosphatidylinositol 4-kinase	-0.4907	-1.4	0.106349
YMR168C	CEP3	DNA bending *	-0.4903	-1.4	0.034848
YGL047W	ALG13	N-acetylglucosaminyldiphosphodolichol N-acetylglucosami	-0.4893	-1.4	0.00410846
YOR390W		unknown	-0.4890	-1.4	0.0191167
YBR143C	SUP45	translation release factor	-0.4887	-1.4	0.0665569
YBL112C		unknown	-0.4852	-1.4	0.141422
YPR204W		DNA helicase	-0.4845	-1.4	0.0994032
YPL259C	APM1	clathrin binding	-0.4837	-1.4	0.0289903
YPR008W	HAA1	specific RNA polymerase II transcription factor	-0.4835	-1.4	0.170798
YGR266W		unknown	-0.4835	-1.4	0.0707942
YJL092W	HPR5	DNA helicase	-0.4835	-1.4	0.107225

Table 1: continued.

ORF ID	Gene Name	Gene Function	Avg Log_2 Ratio	Fold Change	T-test
YOL145C	CTR9	RNA polymerase II transcription elongation factor	-0.4830	-1.4	0.0954519
YDL174C	DLD1	D-lactate dehydrogenase	-0.4830	-1.4	0.0514905
YIR003W		unknown	-0.4827	-1.4	0.013127
YBR126C	TPS1	alpha,alpha-trehalose-phosphate synthase (UDP-forming)	-0.4822	-1.4	0.100145
YAL053W	FLC2	unknown	-0.4820	-1.4	0.0185939
YJR159W	SOR1	L-iditol 2-dehydrogenase	-0.4813	-1.4	0.0415122
YER104W	RTT105	unknown	-0.4805	-1.4	0.110018
YKL168C	KKQ8	protein kinase	-0.4800	-1.4	0.0687454
YJL156C	SSY5	amino acid binding	-0.4797	-1.4	0.0941579
YEL045C			-0.4793	-1.4	0.017107
YNL042W	BOP3	unknown	-0.4790	-1.4	0.218752
YNL329C	PEX6	ATPase	-0.4762	-1.4	0.0764895
YIL068C	SEC6	protein binding	-0.4755	-1.4	0.0509458
YGL022W	STT3	dolichyl-diphosphooligosaccharide-protein glycotransferase	-0.4752	-1.4	0.358289
YDL245C	HXT15	glucose transporter	-0.4750	-1.4	0.127009
YMR061W	RNA14	RNA binding	-0.4738	-1.4	0.0183702
YPR064W			-0.4732	-1.4	0.0128985
YJL017W			-0.4730	-1.4	0.0485984
YJR094W-A	RPL43B	structural constituent of ribosome	-0.4730	-1.4	0.0610702
YLR043C	TRX1	thiol-disulfide exchange intermediate	-0.4728	-1.4	0.134268
YDR177W	UBC1	ubiquitin conjugating enzyme	-0.4717	-1.4	0.00314272
YDR452W	PPN1	endopolyphosphatase	-0.4717	-1.4	0.00551443
YER060W	FCY21	cytosine-purine permease	-0.4715	-1.4	0.108139
YJL038C		unknown	-0.4710	-1.4	0.100531
YGL190C	CDC55	protein phosphatase type 2A	-0.4700	-1.4	0.0940218
YLR430W	SEN1	ATP-dependent RNA helicase	-0.4695	-1.4	0.121147
YMR165C	PAH1	phosphatidate phosphatase	-0.4690	-1.4	0.100722
YJR126C	VPS70	unknown	-0.4682	-1.4	0.0249087
YIL165C		unknown	-0.4682	-1.4	0.0870425
YGR187C	HGH1	unknown	-0.4680	-1.4	0.0805572
YMR028W	TAP42	protein binding	-0.4670	-1.4	0.021618
YKR095W	MLP1	ribonucleoprotein binding	-0.4658	-1.4	0.179188
YMR253C		unknown	-0.4647	-1.4	0.0353179
YGL117W		unknown	-0.4617	-1.4	0.0369442
YDR219C	MFB1	protein binding	-0.4617	-1.4	0.129003
YOL129W	VPS68	unknown	-0.4613	-1.4	0.0118574
YGL113W	SLD3	chromatin binding	-0.4607	-1.4	0.152581
YOR069W	VPS5	protein transporter	-0.4605	-1.4	0.0382584
YLR181C	VTA1	unknown	-0.4602	-1.4	0.0282043
YER035W	EDC2	RNA binding	-0.4595	-1.4	0.0145424
YFR026C		unknown	-0.4568	-1.4	0.041594
YBR150C	TBS1	unknown	-0.4567	-1.4	0.0419611
YER044C	ERG28	protein binding	-0.4560	-1.4	0.0423537
YJL048C	UBX6	unknown	-0.4552	-1.4	0.154123
YJL109C	UTP10	snoRNA binding	-0.4538	-1.4	0.139538
YNR055C	HOL1	transporter	-0.4538	-1.4	0.250811
YKL198C	PTK1	protein kinase	-0.4535	-1.4	0.150575
YPR030W	CSR2	unknown	-0.4532	-1.4	0.0712164
YDR504C	SPG3	unknown	-0.4522	-1.4	0.0907874
YKL171W		protein kinase	-0.4517	-1.4	0.172418
YDL097C	RPN6	structural molecule	-0.4488	-1.4	0.55625
YCR049C			-0.4487	-1.4	0.0193044
YER152C		unknown	-0.4477	-1.4	0.129653
YJL111W	CCT7	unfolded protein binding	-0.4472	-1.4	0.0712587
YDL094C			-0.4470	-1.4	0.084454
YMR040W	YET2	unknown	-0.4468	-1.4	0.00702652
YDR354W	TRP4	anthranilate phosphoribosyltransferase	-0.4462	-1.4	0.205888
YBR056W		unknown	-0.4462	-1.4	0.047543
YGR148C	RPL24B	structural constituent of ribosome*	-0.4455	-1.4	0.00613356
YLL044W			-0.4455	-1.4	0.130872
YKR099W	BAS1	RNA polymerase II transcription factor	-0.4448	-1.4	0.23014
YOR002W	ALG6	transferase , transferring hexosyl groups	-0.4442	-1.4	0.0486861
YHR029C	YHI9	unknown	-0.4432	-1.4	0.0151874
YBR208C	DUR1,2	allophanate hydrolase *	-0.4425	-1.4	0.0451659
YLL042C	ATG10	APG12 conjugating enzyme	-0.4423	-1.4	0.0536761
YGR026W		unknown	-0.4422	-1.4	0.0962748
YPR160W	GPH1	glycogen phosphorylase	-0.4403	-1.4	0.129606
YPL226W	NEW1	ATPase *	-0.4400	-1.4	0.0484021
YBR241C		unknown	-0.4395	-1.4	0.0628322

Table 1: continued.

ORF ID	Gene Name	Gene Function	Avg Log_2 Ratio	Fold Change	T-test
YCL039W	GID7	unknown	-0.4393	-1.4	0.0120231
YOR257W	CDC31	structural constituent of cytoskeleton	-0.4393	-1.4	0.0116983
YCRX13W			-0.4392	-1.4	0.053636
YPL135W	ISU1	protein binding	-0.4388	-1.4	0.0137557
YKR106W		transporter	-0.4387	-1.4	0.1718
YDR094W			-0.4385	-1.4	0.13269
YNL066W	SUN4	glucosidase	-0.4383	-1.4	0.0675842
YNL288W	CAF40	unknown	-0.4382	-1.4	0.09862
YLR304C	ACO1	aconitate hydratase	-0.4375	-1.4	0.317796
YIL090W	ICE2	unknown	-0.4372	-1.4	0.0491991
YCLX06C			-0.4372	-1.4	0.131869
YEL032W	MCM3	chromatin binding	-0.4352	-1.4	0.0664749
YGL121C	GPG1	signal transducer	-0.4348	-1.4	0.0307259
YDR180W	SCC2	unknown	-0.4347	-1.4	0.00701108
YHL050C		helicase	-0.4345	-1.4	0.0142224
YMR011W	HXT2	glucose transporter	-0.4338	-1.4	0.000672935
YIR026C	YVH1	protein tyrosine phosphatase *	-0.4335	-1.4	0.0717492
YPL277C		unknown	-0.4322	-1.3	0.000202168
YNL238W	KEX2	serine-type endopeptidase	-0.4322	-1.3	0.325006
YOR162C	YRR1	specific RNA polymerase II transcription factor	-0.4317	-1.3	0.00379771
YPR014C			-0.4305	-1.3	0.224391
YER135C			-0.4302	-1.3	0.0369493
YGR224W	AZR1	azole transporter	-0.4298	-1.3	0.0816517
YBR036C	CSG2	enzyme regulator	-0.4297	-1.3	0.111793
YOR008C	SLG1	transmembrane receptor	-0.4295	-1.3	0.00608226
YHR146W	CRP1	DNA binding	-0.4293	-1.3	0.0820957
YPL260W		unknown	-0.4292	-1.3	0.206985
YLR422W		unknown	-0.4290	-1.3	0.12454
YHR217C			-0.4290	-1.3	0.057322
YLR403W	SFP1	transcription factor	-0.4280	-1.3	0.0664659
YMR009W	ADI1	oxidoreductase	-0.4268	-1.3	0.0113855
YER152W-A			-0.4263	-1.3	0.476486
YMR136W	GAT2	transcription factor	-0.4260	-1.3	0.0599794
YPL105C		unknown	-0.4238	-1.3	0.0450218
YGR030C	POP6	ribonuclease P *	-0.4227	-1.3	0.123354
YGL229C	SAP4	protein serine/threonine phosphatase	-0.4227	-1.3	0.210173
YDR435C	PPM1	C-terminal protein carboxyl methyltransferase	-0.4223	-1.3	0.017329
YDR458C		unknown	-0.4220	-1.3	0.0496971
YDR135C	YCF1	bilirubin transporter	-0.4213	-1.3	0.0178295
YOL020W	TAT2	aromatic amino acid transporter	-0.4203	-1.3	0.0608652
YHR193C	EGD2	unfolded protein binding	-0.4197	-1.3	0.0131244
YJL019W	MPS3	unknown	-0.4193	-1.3	0.0193792
YPR119W	CLB2	cyclin-dependent protein kinase	-0.4193	-1.3	0.0622373
YGL080W	FMP37	unknown	-0.4182	-1.3	0.238567
YOR118W		unknown	-0.4178	-1.3	0.0194561
YKR050W	TRK2	potassium ion transporter	-0.4178	-1.3	0.133554
YDR070C	FMP16	unknown	-0.4178	-1.3	0.0459416
YDL016C			-0.4177	-1.3	0.0336167
YGL125W	MET13	structural constituent of ribosome*	-0.4148	-1.3	0.0382414
YJR049C	UTR1	NADH kinase	-0.4148	-1.3	0.108827
YLR212C	TUB4	structural constituent of cytoskeleton	-0.4133	-1.3	0.102901
YDL019C	OSH2	oxysterol binding	-0.4132	-1.3	0.317286
YPL241C	CIN2	unknown	-0.4122	-1.3	0.0694184
YMR205C	PFK2	6-phosphofructokinase	-0.4110	-1.3	0.0300246
YGL146C		unknown	-0.4103	-1.3	0.0423687
YGL056C	SDS23	unknown	-0.4100	-1.3	0.0889102
YHL032C	GUT1	glycerol kinase	-0.4097	-1.3	0.0430023
YOR296W		unknown	-0.4093	-1.3	0.111869
YOR005C	DNL4	DNA ligase (ATP)	-0.4087	-1.3	0.427535
YPR111W	DBF20	protein serine/threonine kinase	-0.4085	-1.3	0.216799
YBR047W	FMP23	unknown	-0.4080	-1.3	0.0758466
YEL020C		unknown	-0.4075	-1.3	0.0634133
YDR381W	YRA1	RNA binding	-0.4072	-1.3	0.112742
YKL036C			-0.4070	-1.3	0.0473712
YJL021C			-0.4067	-1.3	0.0339177
YOR015W			-0.4065	-1.3	0.034166
YCL069W	VBA3	basic amino acid permease	-0.4065	-1.3	0.0939933
YMR193C-A			-0.4062	-1.3	0.170668
YLR231C	BNA5	kynureninase	-0.4062	-1.3	0.0201093

Table 1: continued.

ORF ID	Gene Name	Gene Function	Avg Log_2 Ratio	Fold Change	T-test
YHR219W		unknown	-0.4060	-1.3	0.0114355
YLL019C	KNS1	protein serine/threonine kinase	-0.4057	-1.3	0.0525125
YNL055C	POR1	voltage-gated ion-selective channel	-0.4053	-1.3	0.000681334
YDL090C	RAM1	protein farnesyltransferase	-0.4053	-1.3	0.0163692
YMR294W	JNM1	structural constituent of cytoskeleton	-0.4033	-1.3	0.0320005
YMR156C	TPP1	polynucleotide 3'-phosphatase	-0.4027	-1.3	0.0155728
YIL114C	POR2	voltage-gated ion-selective channel	-0.4022	-1.3	0.118164
YEL035C	UTR5	unknown	-0.4022	-1.3	0.0931454
YCL033C		protein-methionine-R-oxide reductase	-0.4013	-1.3	0.0416362
YCR043C		unknown	-0.4013	-1.3	0.12404
YDR093W	DNF2	phospholipid-translocating ATPase	-0.4008	-1.3	0.0682648
YML059C	NTE1	hydrolase *	-0.4005	-1.3	0.0720435
YKR046C	PET10	unknown	-0.4003	-1.3	0.0351939
YGR178C	PBP1	unknown	-0.4002	-1.3	0.26864
YIL146C	ECM37	unknown	-0.3990	-1.3	0.0281309
YIL173W	VTH1	signal sequence binding	-0.3988	-1.3	0.0046866
YOR063W	RPL3	structural constituent of ribosome	-0.3987	-1.3	0.0332418
YEL046C	GLY1	threonine aldolase	-0.3985	-1.3	0.0326248
YLR286C	CTS1	endochitinase	-0.3975	-1.3	0.0145287
YBL072C	RPS8A	structural constituent of ribosome	-0.3972	-1.3	0.146455
YHR120W	MSH1	ATP binding	-0.3972	-1.3	0.11787
YNR056C	BIO5	permease	-0.3970	-1.3	0.201742
YGL026C	TRP5	tryptophan synthase	-0.3970	-1.3	0.216121
YNL245C	CWC25	unknown	-0.3958	-1.3	0.100959
YOR386W	PHR1	deoxyribodipyrimidine photo-lyase	-0.3957	-1.3	0.0923783
YDR221W	GTB1	alpha-glucosidase	-0.3952	-1.3	0.256941
YGL020C	GET1	unknown	-0.3945	-1.3	0.0485926
YGL123W	RPS2	structural constituent of ribosome	-0.3943	-1.3	0.00716124
YGR230W	BNS1	unknown	-0.3940	-1.3	0.217864
YMR004W	MVP1	unknown	-0.3938	-1.3	0.0710217
YBR177C	EHT1	serine hydrolase	-0.3937	-1.3	0.0193988
YNL139C	RLR1	DNA binding	-0.3923	-1.3	0.212095
YIL086C			-0.3920	-1.3	0.126133
YNL020C	ARK1	protein serine/threonine kinase	-0.3915	-1.3	0.00441007
YOR071C		transporter	-0.3910	-1.3	0.0207143
YMR306W	FKS3	1,3-beta-glucan synthase	-0.3908	-1.3	0.12844
YGL031C	RPL24A	structural constituent of ribosome*	-0.3905	-1.3	0.0210776
YPR051W	MAK3	peptide alpha-N-acetyltransferase	-0.3892	-1.3	0.01282
YGL134W	PCL10	cyclin-dependent protein kinase	-0.3890	-1.3	0.0825362
YNL025C	SSN8	general RNA polymerase II transcription factor	-0.3888	-1.3	0.00675383
YBR074W		metalloendopeptidase	-0.3883	-1.3	0.0210965
YDR232W	HEM1	5-aminolevulinate synthase	-0.3880	-1.3	0.0214868
YJR036C	HUL4	ubiquitin-protein ligase	-0.3877	-1.3	0.0582429
YCR057C	PWP2	snoRNA binding	-0.3872	-1.3	0.103727
YNL113W	RPC19	DNA-directed RNA polymerase	-0.3867	-1.3	0.0122487
YGR110W		unknown	-0.3867	-1.3	0.0942809
YKR010C	TOF2	unknown	-0.3865	-1.3	0.0590761
YHL015W	RPS20	structural constituent of ribosome	-0.3862	-1.3	0.0396134
YJL015C			-0.3860	-1.3	0.0625249
YOR206W	NOC2	unknown	-0.3855	-1.3	0.0966049
YPL019C	VTC3	unknown	-0.3855	-1.3	0.213552
YHR155W	YSP1	unknown	-0.3853	-1.3	0.000390112
YOL015W	IRC10	unknown	-0.3853	-1.3	0.0130453
YBL048W			-0.3850	-1.3	0.0300682
YGR044C	RME1	specific transcriptional repressor	-0.3847	-1.3	0.121294
YCR070W			-0.3845	-1.3	0.0157626
YDR130C	FIN1	unknown	-0.3835	-1.3	0.0467969
YLL024C	SSA2	ATPase *	-0.3832	-1.3	0.17181
YOL075C		ATPase , coupled to transmembrane movement of substanc	-0.3830	-1.3	0.375379
YDR030C	RAD28	unknown	-0.3827	-1.3	0.11101
YLR096W	KIN2	protein kinase	-0.3827	-1.3	0.0345304
YLR101C			-0.3817	-1.3	0.211039
YLR149C		unknown	-0.3807	-1.3	0.0435502
YCR079W		phosphoprotein phosphatase	-0.3807	-1.3	0.16315
YER064C		unknown	-0.3805	-1.3	0.123981
YNL218W	MGS1	ATPase *	-0.3798	-1.3	0.249181
YJR047C	ANB1	translation initiation factor	-0.3798	-1.3	0.0321636
YDL223C	HBT1	unknown	-0.3798	-1.3	0.0913413
YGR133W	PEX4	ubiquitin conjugating enzyme	-0.3797	-1.3	0.0420709

Table 1: continued.

ORF ID	Gene Name	Gene Function	Avg Log_2 Ratio	Fold Change	T-test
YMR155W		unknown	-0.3795	-1.3	0.0297039
YIL151C		unknown	-0.3793	-1.3	0.0826828
YLL048C	YBT1	ATPase , coupled to transmembrane movement of substanc	-0.3790	-1.3	0.148646
YDR488C	PAC11	microtubule motor *	-0.3788	-1.3	0.0181579
YLL056C		unknown	-0.3787	-1.3	0.0986739
YDR255C	RMD5	unknown	-0.3765	-1.3	0.0107499
YLR046C		unknown	-0.3762	-1.3	0.0308213
YPR098C		unknown	-0.3758	-1.3	0.182261
YLR004C		transporter	-0.3758	-1.3	0.166659
YJL214W	HXT8	glucose transporter	-0.3758	-1.3	0.0182851
YKL213C	DOA1	ubiquitin binding	-0.3753	-1.3	0.212179
YLR281C		unknown	-0.3753	-1.3	0.0953294
YPR112C	MRD1	snoRNA binding	-0.3752	-1.3	0.332033
YHR053C	CUP1-1	copper ion binding	-0.3748	-1.3	0.0818693
YDR286C		unknown	-0.3742	-1.3	0.167057
YFR009W	GCN20	ATPase	-0.3740	-1.3	0.041979
YJL050W	MTR4	ATP-dependent RNA helicase	-0.3733	-1.3	0.117821
YKL112W	ABF1	DNA binding	-0.3732	-1.3	0.140515
YNL311C	SKP2	protein binding	-0.3730	-1.3	0.162079
YOR109W	INP53	inositol-polyphosphate 5-phosphatase	-0.3730	-1.3	0.103584
YJR002W	MPP10	unknown	-0.3725	-1.3	0.0935528
YCL029C	BIK1	microtubule binding	-0.3725	-1.3	0.149847
YAL017W	PSK1	protein serine/threonine kinase	-0.3723	-1.3	0.00339556
YEL013W	VAC8	protein binding	-0.3717	-1.3	0.0590419
YJL044C	GYP6	GTPase activator	-0.3717	-1.3	0.0957658
YML048W-A			-0.3710	-1.3	0.211523
YER110C	KAP123	protein carrier	-0.3697	-1.3	0.085444
YEL067C			-0.3693	-1.3	0.0814103
YBL001C	ECM15	unknown	-0.3693	-1.3	0.0301314
YEL018C-A			-0.3690	-1.3	0.219798
YDR464W	SPP41	unknown	-0.3690	-1.3	0.0662367
YIL045W	PIG2	protein phosphatase type 1 regulator	-0.3687	-1.3	0.00277491
YNL271C	BNI1	cytoskeletal regulator	-0.3683	-1.3	0.0397408
YPL115C	BEM3	signal transducer *	-0.3682	-1.3	0.26892
YJR084W	CSN12	unknown	-0.3680	-1.3	0.0573032
YBR221C	PDB1	pyruvate dehydrogenase	-0.3673	-1.3	0.00295331
YKL131W			-0.3672	-1.3	0.309144
YIR010W	DSN1	unknown	-0.3670	-1.3	0.0920181
YMR071C	TVP18	unknown	-0.3667	-1.3	0.105491
YPL080C			-0.3663	-1.3	0.275041
YJR061W		unknown	-0.3663	-1.3	0.148606
YDL238C	GUD1	hydrolase , acting on carbon-nitrogen (but not peptide) bon	-0.3662	-1.3	0.0237509
YJR044C	VPS55	unknown	-0.3658	-1.3	0.0182088
YER033C	ZRG8	unknown	-0.3655	-1.3	0.100425
YBR270C	BIT2	unknown	-0.3655	-1.3	0.0146778
YDR036C	EHD3	3-hydroxyisobutyryl-CoA hydrolase	-0.3653	-1.3	0.0225316
YBR084W	MIS1	formate-tetrahydrofolate ligase *	-0.3652	-1.3	0.118197
YKL002W	DID4	protein binding	-0.3652	-1.3	0.147969
YLR095C	IOC2	protein binding	-0.3650	-1.3	0.0790264
YBR049C	REB1	RNA polymerase II transcription factor	-0.3648	-1.3	0.031966
YLR297W		unknown	-0.3648	-1.3	0.0477301
YNL099C	OCA1	protein tyrosine phosphatase	-0.3648	-1.3	0.0157561
YOR302W		translation regulator	-0.3647	-1.3	0.109012
YGL019W	CKB1	protein kinase	-0.3645	-1.3	0.223894
YJL027C		unknown	-0.3643	-1.3	0.000625393
YGL180W	ATG1	protein serine/threonine kinase	-0.3643	-1.3	0.196206
YCR026C	NPP1	nucleoside-triphosphatase *	-0.3643	-1.3	0.0910544
YDL043C	PRP11	RNA binding	-0.3635	-1.3	0.187732
YOL068C	HST1	NAD-dependent histone deacetylase *	-0.3635	-1.3	0.0669284
YOR377W	ATF1	alcohol O-acetyltransferase	-0.3633	-1.3	0.0506751
YML115C	VAN1	mannosyltransferase	-0.3628	-1.3	0.0858051
YNL047C	SLM2	phosphoinositide binding	-0.3623	-1.3	0.115462
YOR389W		unknown	-0.3620	-1.3	0.347217
YGR032W	GSC2	1,3-beta-glucan synthase	-0.3615	-1.3	0.102087
YGL147C	RPL9A	structural constituent of ribosome	-0.3613	-1.3	0.0266679
YPR027C		unknown	-0.3612	-1.3	0.0389922
YIL154C	IMP2'	transcription coactivator	-0.3612	-1.3	0.0337666
YER114C	BOI2	phospholipid binding	-0.3608	-1.3	0.261809
YBR125C	PTC4	protein phosphatase type 2C	-0.3602	-1.3	0.00616517

Table 1: continued.

ORF ID	Gene Name	Gene Function	Avg Log_2 Ratio	Fold Change	T-test
YBL049W	MOH1	unknown	-0.3602	-1.3	0.00186263
YJL094C	KHA1	potassium:hydrogen antiporter	-0.3600	-1.3	0.168465
YIR020C			-0.3595	-1.3	0.171964
YGL195W	GCN1	unknown	-0.3593	-1.3	0.2328
YFR040W	SAP155	protein serine/threonine phosphatase	-0.3588	-1.3	0.200062
YGL149W			-0.3587	-1.3	0.0303589
YIL078W	THS1	threonine-tRNA ligase	-0.3587	-1.3	0.0608405
YLR466W	YRF1-4	DNA helicase	-0.3580	-1.3	0.230476
YCL001W	RER1	unknown	-0.3578	-1.3	0.130139
YKR054C	DYN1	motor	-0.3578	-1.3	0.0243847
YDR114C			-0.3573	-1.3	0.25864
YER126C	NSA2	unknown	-0.3563	-1.3	0.125991
YBR302C	COS2	unknown	-0.3562	-1.3	0.353745
YJL087C	TRL1	2',3'-cyclic-nucleotide 3'-phosphodiesterase *	-0.3557	-1.3	0.15026
YER164W	CHD1	ATPase *	-0.3547	-1.3	0.339312
YAL064W		unknown	-0.3547	-1.3	0.0305268
YOR173W	DCS2	unknown	-0.3542	-1.3	0.181664
YNL103W	MET4	transcription coactivator	-0.3540	-1.3	0.00229351
YGR270W	YTA7	ATPase	-0.3533	-1.3	0.0281176
YLR220W	CCC1	manganese ion transporter	-0.3525	-1.3	0.080686
YKR081C	RPF2	rRNA binding	-0.3513	-1.3	0.0568543
YAL010C	MDM10	unknown	-0.3507	-1.3	0.000520101
YNL194C		unknown	-0.3505	-1.3	0.114887
YLR172C	DPH5	diphthine synthase	-0.3502	-1.3	0.0386634
YJL034W	KAR2	ATPase *	-0.3498	-1.3	0.0953108
YKR028W	SAP190	protein serine/threonine phosphatase	-0.3488	-1.3	0.0233924
YNR062C		unknown	-0.3485	-1.3	0.11698
YGR268C	HUA1	unknown	-0.3478	-1.3	0.110137
YIR007W		unknown	-0.3477	-1.3	0.00633846
YGL045W	RIM8	unknown	-0.3473	-1.3	0.361064
YMR198W	CIK1	microtubule motor	-0.3470	-1.3	0.0889176
YJR025C	BNA1	3-hydroxyanthranilate 3,4-dioxygenase	-0.3467	-1.3	0.034792
YIL174W		unknown	-0.3467	-1.3	0.0408922
YLR357W	RSC2	unknown	-0.3462	-1.3	0.0704888
YOL025W	LAG2	unknown	-0.3460	-1.3	0.153501
YLR406C	RPL31B	structural constituent of ribosome	-0.3455	-1.3	0.424517
YHR026W	PPA1	hydrogen-transporting ATPase , rotational mechanism	-0.3453	-1.3	0.000658306
YDR040C	ENA1	ATPase , coupled to transmembrane movement of ions, phc	-0.3452	-1.3	0.0573736
YLR247C		helicase	-0.3448	-1.3	0.0604129
YPL087W	YDC1	ceramidase	-0.3438	-1.3	0.0427593
YGL028C	SCW11	glucan 1,3-beta-glucosidase	-0.3438	-1.3	0.0161148
YML103C	NUP188	structural molecule	-0.3433	-1.3	0.0702357
YDR128W		unknown	-0.3433	-1.3	0.0264648
YBR129C	OPY1	unknown	-0.3430	-1.3	0.0340172
YEL012W	UBC8	ubiquitin conjugating enzyme	-0.3430	-1.3	0.032993
YJL190C	RPS22A	structural constituent of ribosome	-0.3427	-1.3	0.0309105
YCR030C	SYP1	unknown	-0.3425	-1.3	0.00612528
YNL189W	SRP1	protein carrier	-0.3418	-1.3	0.155534
YPL003W	ULA1	NEDD8 activating enzyme	-0.3408	-1.3	0.0551799
YML049C	RSE1	U2 snRNA binding	-0.3407	-1.3	0.117339
YGR033C	TIM21	unknown	-0.3405	-1.3	0.394495
YPL196W	OXR1	unknown	-0.3403	-1.3	0.123484
YOR289W		unknown	-0.3395	-1.3	0.00946276
YFR024C			-0.3393	-1.3	0.193063
YKR048C	NAP1	protein binding	-0.3367	-1.3	0.256456
YGL104C	VPS73	unknown	-0.3365	-1.3	0.181702
YBL037W	APL3	unknown	-0.3362	-1.3	0.36038
YCL034W	LSB5	unknown	-0.3362	-1.3	0.110745
YBR206W			-0.3350	-1.3	0.16347
YNL255C	GIS2	unknown	-0.3345	-1.3	0.113514
YNL273W	TOF1	unknown	-0.3345	-1.3	0.0420212
YCR061W		unknown	-0.3342	-1.3	0.0100186
YBR295W	PCA1	ATPase , coupled to transmembrane movement of ions, phc	-0.3337	-1.3	0.0899295
YER132C	PMD1	unknown	-0.3333	-1.3	0.0230068
YLR079W	SIC1	protein binding	-0.3332	-1.3	0.146741
YIL130W	ASG1	unknown	-0.3330	-1.3	0.0302388
YBL023C	MCM2	chromatin binding	-0.3330	-1.3	0.357925
YJL150W			-0.3328	-1.3	0.338089
YPR022C		unknown	-0.3323	-1.3	0.010152

Table 1: continued.

ORF ID	Gene Name	Gene Function	Avg Log_2 Ratio	Fold Change	T-test
YDR150W	NUM1	tubulin binding	-0.3322	-1.3	0.329595
YNL339C	YRF1-6	DNA helicase	-0.3308	-1.3	0.135011
YBR184W		unknown	-0.3305	-1.3	0.0735225
YGL096W	TOS8	transcription factor	-0.3300	-1.3	0.028522
YCR046C	IMG1	structural constituent of ribosome	-0.3300	-1.3	0.155281
YPR023C	EAF3	histone acetyltransferase	-0.3288	-1.3	0.253674
YIR033W	MGA2	transcriptional activator	-0.3287	-1.3	0.252323
YNL064C	YDJ1	chaperone regulator	-0.3282	-1.3	0.0987389
YGR284C	ERV29	unknown	-0.3280	-1.3	0.144333
YDR334W	SWR1	helicase	-0.3277	-1.3	0.338694
YOR253W	NAT5	peptide alpha-N-acetyltransferase	-0.3273	-1.3	0.376428
YCR024C-A	PMP1	enzyme regulator	-0.3268	-1.3	0.0436619
YLR441C	RPS1A	structural constituent of ribosome	-0.3268	-1.3	0.000738866
YLL045C	RPL8B	structural constituent of ribosome	-0.3267	-1.3	0.075163
YIR022W	SEC11	signal peptidase	-0.3267	-1.3	0.0228676
YLR028C	ADE16	IMP cyclohydrolase *	-0.3265	-1.3	0.731278
YOR221C	MCT1	[acyl-carrier protein] S-malonyltransferase	-0.3250	-1.3	0.107038
YOR056C	NOB1	protein binding	-0.3238	-1.3	0.0649157
YOR164C		unknown	-0.3233	-1.3	0.0459013
YDR267C	CIA1	unknown	-0.3228	-1.3	0.0736498
YMR148W		unknown	-0.3222	-1.3	0.146561
YER090W	TRP2	anthranilate synthase	-0.3222	-1.3	0.239247
YEL077C		helicase	-0.3222	-1.3	0.0230515
YOR226C	ISU2	unknown	-0.3222	-1.3	0.26995
YKR058W	GLG1	glycogenin glucosyltransferase	-0.3218	-1.2	0.00460518
YHR015W	MIP6	RNA binding	-0.3218	-1.2	0.144614
YKL093W	MBR1	unknown	-0.3217	-1.2	0.00156233
YLR170C	APS1	clathrin binding	-0.3213	-1.2	0.137038
YIL121W	QDR2	multidrug efflux pump	-0.3208	-1.2	0.115464
YCR069W(1)			-0.3203	-1.2	0.0464665
YDL087C	LUC7	mRNA binding	-0.3197	-1.2	0.195616
YJL058C	BIT61	unknown	-0.3195	-1.2	0.425197
YOL149W	DCP1	mRNA binding	-0.3192	-1.2	0.0292123
YIL087C		unknown	-0.3190	-1.2	0.149801
YJL068C		S-formylglutathione hydrolase	-0.3190	-1.2	0.0641067
YML057W	CMP2	calcium-dependent protein serine/threonine phosphatase	-0.3190	-1.2	0.286472
YDR304C	CPR5	peptidyl-prolyl cis-trans isomerase	-0.3187	-1.2	0.167846
YKR066C	CCP1	cytochrome-c peroxidase	-0.3187	-1.2	0.069421
YLR278C		unknown	-0.3185	-1.2	0.171956
YMR138W	CIN4	GTP binding	-0.3177	-1.2	0.203049
YLL055W		ion transporter	-0.3177	-1.2	0.281899
YJL215C			-0.3177	-1.2	0.373016
YGL008C	PMA1	hydrogen-exporting ATPase , phosphorylative mechanism	-0.3173	-1.2	0.427074
YCL012W			-0.3173	-1.2	0.38203
YGL252C	RTG2	transcription regulator	-0.3172	-1.2	0.253311
YPL039W		unknown	-0.3168	-1.2	0.190561
YHR213W		unknown	-0.3163	-1.2	0.127817
YLR013W	GAT3	transcription factor	-0.3143	-1.2	0.224647
YJL018W			-0.3142	-1.2	0.240913
YLR007W	NSE1	unknown	-0.3133	-1.2	0.0763403
YJR103W	URA8	CTP synthase	-0.3130	-1.2	0.0488268
YMR026C	PEX12	protein binding	-0.3127	-1.2	0.222365
YOR307C	SLY41	unknown	-0.3125	-1.2	0.120842
YJL212C	OPT1	oligopeptide transporter	-0.3123	-1.2	0.0175854
YJR074W	MOG1	Ran GTPase binding	-0.3117	-1.2	0.0057921
YOL119C	MCH4	transporter	-0.3113	-1.2	0.0459738
YBR148W	YSW1	unknown	-0.3112	-1.2	0.0098082
YPL216W		unknown	-0.3103	-1.2	0.429185
YGR119C	NUP57	structural molecule	-0.3103	-1.2	0.0849686
YJL188C			-0.3102	-1.2	0.154474
YDL172C			-0.3100	-1.2	0.315286
YPR069C	SPE3	spermidine synthase	-0.3098	-1.2	0.11871
YDL221W			-0.3095	-1.2	0.258251
YMR119W	ASI1	ubiquitin-protein ligase	-0.3095	-1.2	0.0904633
YLR127C	APC2	protein binding	-0.3095	-1.2	0.00337982
YER115C	SPR6	unknown	-0.3095	-1.2	0.0457322
YOL115W	PAP2	polynucleotide adenylyltransferase *	-0.3093	-1.2	0.216002
YBR232C			-0.3093	-1.2	0.0533928
YNL317W	PFS2	RNA binding	-0.3088	-1.2	0.241934

Table 1: continued.

ORF ID	Gene Name	Gene Function	Avg Log_2 Ratio	Fold Change	T-test
YLR208W	SEC13	structural molecule	-0.3085	-1.2	0.0143548
YGR117C		unknown	-0.3085	-1.2	0.0653263
YEL041W	YEF1	NADH kinase	-0.3083	-1.2	0.0261819
YML105C	SEC65	unknown	-0.3078	-1.2	0.1293
YDL132W	CDC53	structural molecule *	-0.3075	-1.2	0.254634
YNL040W		unknown	-0.3070	-1.2	0.297549
YCL017C	NFS1	cystathionine gamma-lyase *	-0.3062	-1.2	0.0663081
YPR011C		transporter	-0.3060	-1.2	0.325417
YNL331C	AAD14	aryl-alcohol dehydrogenase	-0.3058	-1.2	0.102079
YAL008W	FUN14	unknown	-0.3048	-1.2	0.0436598
YJL028W			-0.3047	-1.2	0.21731
YHR158C	KEL1	unknown	-0.3045	-1.2	0.0207596
YNL032W	SIW14	protein tyrosine phosphatase	-0.3043	-1.2	0.185659
YMR244W		unknown	-0.3032	-1.2	0.191666
YKR064W		unknown	-0.3030	-1.2	0.0511864
YCL021W			-0.3030	-1.2	0.0797907
YMR284W	YKU70	RNA binding	-0.3027	-1.2	0.107959
YAL063C	FLO9	mannose binding	-0.3020	-1.2	0.0230551
YDR034C	LYS14	transcriptional activator	-0.3012	-1.2	0.279172
YMR167W	MLH1	DNA binding	-0.3012	-1.2	0.363348
YOR116C	RPO31	DNA-directed RNA polymerase	-0.3010	-1.2	0.216505
YPL279C		unknown	-0.3008	-1.2	0.172261
YJR033C	RAV1	unknown	-0.2998	-1.2	0.270695
YDR118W	APC4	protein binding	-0.2995	-1.2	0.267451
YBR271W		S-adenosylmethionine-dependent methyltransferase	-0.2987	-1.2	0.218152
YLR036C		unknown	-0.2987	-1.2	0.141137
YIL088C	AVT7	transporter	-0.2980	-1.2	0.117921
YCR029C-A			-0.2977	-1.2	0.119231
YDR313C	PIB1	ubiquitin-protein ligase	-0.2973	-1.2	0.144972
YLR188W	MDL1	ATPase *	-0.2973	-1.2	0.148506
YBR023C	CHS3	chitin synthase	-0.2972	-1.2	0.240613
YJR143C	PMT4	dolichyl-phosphate-mannose-protein mannosyltransferase	-0.2968	-1.2	0.1268
YLR091W		unknown	-0.2967	-1.2	0.11262
YHR102W	KIC1	kinase	-0.2965	-1.2	0.269345
YMR035W	IMP2	peptidase *	-0.2965	-1.2	0.2329
YGL244W	RTF1	RNA polymerase II transcription elongation factor	-0.2960	-1.2	0.196771
YHR191C	CTF8	unknown	-0.2958	-1.2	0.267098
YLR150W	STM1	DNA binding	-0.2957	-1.2	0.0116584
YMR066W	SOV1	unknown	-0.2955	-1.2	0.505338
YNL048W	ALG11	alpha-1,2-mannosyltransferase	-0.2955	-1.2	0.16061
YHR012W	VPS29	unknown	-0.2953	-1.2	0.288983
YPR095C	SYT1	ARF guanyl-nucleotide exchange factor	-0.2947	-1.2	0.0952162
YGR244C	LSC2	succinate-CoA ligase (ADP-forming)	-0.2945	-1.2	0.168096
YJL200C	ACO2	aconitate hydratase	-0.2942	-1.2	0.204212
YFL057C	AAD16	aryl-alcohol dehydrogenase	-0.2938	-1.2	0.00211918
YEL075W-A			-0.2938	-1.2	0.00463365
YMR104C	YPK2	protein kinase	-0.2938	-1.2	0.441384
YGR012W		cysteine synthase	-0.2935	-1.2	0.0704522
YNL140C			-0.2933	-1.2	0.00989018
YOR053W			-0.2932	-1.2	0.1043
YNL144C		unknown	-0.2922	-1.2	0.289503
YLR083C	EMP70	transporter	-0.2922	-1.2	0.0267471
YDR498C	SEC20	v-SNARE	-0.2922	-1.2	0.0698801
YNL258C	DSL1	unknown	-0.2915	-1.2	0.153289
YBR038W	CHS2	chitin synthase	-0.2912	-1.2	0.134516
YKL212W	SAC1	inositol or phosphatidylinositol phosphatase	-0.2910	-1.2	0.192238
YHR088W	RPF1	rRNA primary transcript binding	-0.2908	-1.2	0.209599
YKR042W	UTH1	unknown	-0.2905	-1.2	0.0138391
YDL096C			-0.2903	-1.2	0.360037
YEL033W			-0.2903	-1.2	0.0126113
YDR191W	HST4	DNA binding	-0.2897	-1.2	0.0354186
YGR031W		unknown	-0.2893	-1.2	0.479593
YJL060W	BNA3	arylformamidase	-0.2892	-1.2	0.105514
YPL114W			-0.2885	-1.2	0.126682
YPL283C	YRF1-7	DNA helicase	-0.2878	-1.2	0.266183
YHL019C	APM2	clathrin binding	-0.2870	-1.2	0.359133
YDR432W	NPL3	mRNA binding	-0.2870	-1.2	0.163522
YLR298C	YHC1	mRNA binding	-0.2860	-1.2	0.275848
YIL075C	RPN2	endopeptidase *	-0.2855	-1.2	0.0323434

Table 1: continued.

ORF ID	Gene Name	Gene Function	Avg Log_2 Ratio	Fold Change	T-test
YIL125W	KGD1	oxoglutarate dehydrogenase	-0.2850	-1.2	0.145096
YNL116W	DMA2	unknown	-0.2845	-1.2	0.0612135
YLR165C	PUS5	pseudouridylate synthase	-0.2842	-1.2	0.110067
YPR182W	SMX3	RNA splicing factor	-0.2837	-1.2	0.126484
YBR240C	THI2	transcriptional activator	-0.2837	-1.2	0.12723
YJL095W	BCK1	MAP kinase	-0.2837	-1.2	0.0360289
YGR051C			-0.2833	-1.2	0.282056
YHR055C	CUP1-2	copper ion binding	-0.2828	-1.2	0.145946
YGR272C		unknown	-0.2827	-1.2	0.160985
YLR133W	CKI1	choline kinase	-0.2825	-1.2	0.258537
YMR299C	DYN3	motor	-0.2825	-1.2	0.0732341
YPL002C	SNF8	protein binding	-0.2822	-1.2	0.142638
YPL248C	GAL4	transcriptional activator	-0.2817	-1.2	0.148514
YKL188C	PXA2	ATPase , coupled to transmembrane movement of substanc	-0.2815	-1.2	0.130443
YER162C	RAD4	damaged DNA binding	-0.2812	-1.2	0.0490349
YLR263W	RED1	protein binding	-0.2810	-1.2	0.26412
YPL255W	BBP1	structural constituent of cytoskeleton	-0.2805	-1.2	0.390277
YFL056C	AAD6	aryl-alcohol dehydrogenase	-0.2802	-1.2	0.403613
YKL160W	ELF1	RNA polymerase II transcription elongation factor	-0.2800	-1.2	0.0373281
YLR062C			-0.2797	-1.2	0.164426
YKL179C	COY1	unknown	-0.2795	-1.2	0.333529
YNR072W	HXT17	glucose transporter	-0.2795	-1.2	0.254371
YDL247W	MPH2	carbohydrate transporter	-0.2787	-1.2	0.0749303
YGL114W		oligopeptide transporter	-0.2782	-1.2	0.0282769
YER097W			-0.2777	-1.2	0.206894
YHR143W	DSE2	glucan 1,3-beta-glucosidase	-0.2775	-1.2	0.0648855
YPL195W	APL5	protein binding	-0.2763	-1.2	0.20459
YGR046W		unknown	-0.2760	-1.2	0.0714618
YDR448W	ADA2	transcription coactivator	-0.2758	-1.2	0.197634
YOR110W	TFC7	RNA polymerase III transcription factor	-0.2758	-1.2	0.116424
YGR053C		unknown	-0.2757	-1.2	0.24044
YBR225W		unknown	-0.2757	-1.2	0.0331226
YNL072W	RNH201	ribonuclease H	-0.2753	-1.2	0.0304125
YBR019C	GAL10	UDP-glucose 4-epimerase	-0.2747	-1.2	0.144732
YML089C			-0.2742	-1.2	0.0298623
YDL194W	SNF3	receptor *	-0.2738	-1.2	0.17203
YML085C	TUB1	structural constituent of cytoskeleton	-0.2737	-1.2	0.198223
YDR477W	SNF1	AMP-activated protein kinase	-0.2733	-1.2	0.268546
YDR439W	LRS4	unknown	-0.2732	-1.2	0.29128
YDR233C	RTN1	unknown	-0.2730	-1.2	0.000750613
YPL033C		unknown	-0.2730	-1.2	0.153332
YPR047W	MSF1	phenylalanine-tRNA ligase	-0.2728	-1.2	0.107901
YOL044W	PEX15	unknown	-0.2723	-1.2	0.14747
YFL048C	EMP47	unknown	-0.2717	-1.2	0.0820216
YHR075C	PPE1	structural constituent of ribosome*	-0.2717	-1.2	0.113036
YBL051C	PIN4	unknown	-0.2713	-1.2	0.127455
YOR197W	MCA1	caspase	-0.2712	-1.2	0.0943845
YNL007C	SIS1	unfolded protein binding	-0.2712	-1.2	0.196744
YJL185C		unknown	-0.2710	-1.2	0.0217942
YBR219C		unknown	-0.2708	-1.2	0.124366
YBL104C		unknown	-0.2707	-1.2	0.197818
Q0140(1)			-0.2707	-1.2	0.141678
YMR271C	URA10	orotate phosphoribosyltransferase	-0.2705	-1.2	0.0404899
YLR350W	ORM2	unknown	-0.2703	-1.2	0.0341071
YFR001W	LOC1	mRNA binding	-0.2703	-1.2	0.187593
YJL149W		unknown	-0.2698	-1.2	0.188421
YLR373C	VID22	unknown	-0.2690	-1.2	0.0736018
YMR143W	RPS16A	structural constituent of ribosome	-0.2688	-1.2	0.000614648
YDR172W	SUP35	translation release factor	-0.2688	-1.2	0.457449
YGL150C	INO80	ATPase *	-0.2687	-1.2	0.0351436
YHR079C	IRE1	protein serine/threonine kinase	-0.2687	-1.2	0.444175
YIL054W			-0.2677	-1.2	0.0593568
YNR013C	PHO91	phosphate transporter	-0.2675	-1.2	0.432888
YER144C	UBP5	ubiquitin-specific protease	-0.2675	-1.2	0.0653402
YBR123C	TFC1	RNA polymerase III transcription factor	-0.2670	-1.2	0.0248508
YLR399C	BDF1	transcription regulator	-0.2670	-1.2	0.00886552
YML086C	ALO1	D-arabinono-1,4-lactone oxidase	-0.2668	-1.2	0.427595
YPR024W	YME1	ATP-dependent peptidase	-0.2667	-1.2	0.0419777
YOR018W	ROD1	unknown	-0.2667	-1.2	0.0374907

Table 1: continued.

ORF ID	Gene Name	Gene Function	Avg Log_2 Ratio	Fold Change	T-test
YKL026C	GPX1	glutathione peroxidase	-0.2658	-1.2	0.0373404
YJR146W			-0.2655	-1.2	0.0868322
YPL084W	BRO1	intracellular transporter	-0.2650	-1.2	0.0688557
YBL079W	NUP170	structural molecule	-0.2645	-1.2	0.115582
YOR291W		unknown	-0.2645	-1.2	0.273591
YEL017W	GTT3	unknown	-0.2643	-1.2	0.0220221
YIL108W		metalloendopeptidase	-0.2642	-1.2	0.324628
YPR185W	ATG13	protein binding	-0.2638	-1.2	0.313024
YBR180W	DTR1	multidrug transporter	-0.2632	-1.2	0.104528
YDR436W	PPZ2	protein serine/threonine phosphatase	-0.2632	-1.2	0.126736
YNL237W	YTP1	unknown	-0.2632	-1.2	0.250947
YLR378C	SEC61	protein transporter	-0.2630	-1.2	0.0174894
YJR135C	MCM22	protein binding	-0.2627	-1.2	0.107988
YLR464W		unknown	-0.2625	-1.2	0.0894882
YCL052C	PBN1	mannosyltransferase	-0.2623	-1.2	0.0618867
YDR157W			-0.2620	-1.2	0.2262
YGL241W	KAP114	protein carrier	-0.2618	-1.2	0.217246
YKL015W	PUT3	specific RNA polymerase II transcription factor	-0.2618	-1.2	0.0342445
YJL176C	SWI3	general RNA polymerase II transcription factor	-0.2618	-1.2	0.0275564
YLR129W	DIP2	snoRNA binding	-0.2615	-1.2	0.289882
YDL184C	RPL41A	structural constituent of ribosome	-0.2610	-1.2	0.314721
YPL222W	FMP40	unknown	-0.2608	-1.2	0.0572508
YER151C	UBP3	ubiquitin-specific protease	-0.2608	-1.2	0.0833568
YML019W	OST6	dolichyl-diphosphooligosaccharide-protein glycotransferase	-0.2603	-1.2	0.0412345
YJR123W	RPS5	structural constituent of ribosome	-0.2598	-1.2	0.0326675
YLL018C	DPS1	RNA binding	-0.2595	-1.2	0.0149096
YLR449W	FPR4	peptidyl-prolyl cis-trans isomerase	-0.2592	-1.2	0.265286
YCR063W	BUD31	unknown	-0.2590	-1.2	0.0322333
YDL116W	NUP84	structural molecule	-0.2588	-1.2	0.488018
YEL034W	HYP2	protein binding	-0.2587	-1.2	0.0214605
YDR390C	UBA2	SUMO activating enzyme	-0.2587	-1.2	0.107489
YCR075C	ERS1	L-cystine transporter	-0.2583	-1.2	0.345851
YNL297C	MON2	guanyl-nucleotide exchange factor	-0.2573	-1.2	0.158648
YAL022C	FUN26	nucleoside transporter	-0.2573	-1.2	0.154617
YMR008C	PLB1	lysophospholipase	-0.2567	-1.2	0.128139
YNR019W	ARE2	sterol O-acyltransferase	-0.2567	-1.2	0.0135564
YDL027C		unknown	-0.2565	-1.2	0.182748
YMR279C		unknown	-0.2563	-1.2	0.376012
YGL084C	GUP1	O-acyltransferase	-0.2560	-1.2	0.00135456
YJL069C	UTP18	unknown	-0.2560	-1.2	0.0607718
YIL099W	SGA1	glucan 1,4-alpha-glucosidase	-0.2558	-1.2	0.166555
YGR122W		unknown	-0.2553	-1.2	0.232435
YML063W	RPS1B	structural constituent of ribosome	-0.2550	-1.2	0.00160181
YJL020C	BBC1	myosin I binding	-0.2547	-1.2	0.15365
YOL016C	CMK2	calcium- and calmodulin-dependent protein kinase	-0.2547	-1.2	0.00048993
YLR394W	CST9	DNA binding	-0.2547	-1.2	0.68103
YBR127C	VMA2	hydrogen-transporting ATPase , rotational mechanism	-0.2543	-1.2	0.0112857
YHR150W	PEX28	unknown	-0.2535	-1.2	0.14774
YLR213C	CRR1	hydrolase , acting on carbon-nitrogen (but not peptide) bon	-0.2533	-1.2	0.0455935
YLL028W	TPO1	spermine transporter	-0.2532	-1.2	0.271141
YIL126W	STH1	ATPase *	-0.2532	-1.2	0.101753
YPL045W	VPS16	unknown	-0.2530	-1.2	0.0211698
YLR222C	UTP13	snoRNA binding	-0.2528	-1.2	0.193564
YLR324W	PEX30	unknown	-0.2523	-1.2	0.489549
YML128C	MSC1	unknown	-0.2523	-1.2	0.266155
YJL101C	GSH1	glutamate-cysteine ligase	-0.2522	-1.2	0.00156114
YDR195W	REF2	RNA binding	-0.2522	-1.2	0.173436
YLR102C	APC9	protein binding	-0.2520	-1.2	0.103975
YKL104C	GFA1	glutamine-fructose-6-phosphate transaminase (isomerizing)	-0.2520	-1.2	0.288859
YOR380W	RDR1	transcription factor	-0.2512	-1.2	0.11804
YOL081W	IRA2	Ras GTPase activator	-0.2512	-1.2	0.00885719
YKR057W	RPS21A	structural constituent of ribosome	-0.2510	-1.2	0.171322
YMR153W	NUP53	structural molecule	-0.2502	-1.2	0.367126
YML001W	YPT7	GTPase	-0.2500	-1.2	0.121734
YLL026W	HSP104	chaperone binding	-0.2500	-1.2	0.258573
YGR209C	TRX2	thiol-disulfide exchange intermediate	-0.2495	-1.2	0.154526
YOR152C		unknown	-0.2495	-1.2	0.220141
YOR104W	PIN2	unknown	-0.2495	-1.2	0.00179944
YMR015C	ERG5	C-22 sterol desaturase	-0.2493	-1.2	0.0319063

Table 1: continued.

ORF ID	Gene Name	Gene Function	Avg Log_2 Ratio	Fold Change	T-test
YKL215C		unknown	-0.2492	-1.2	0.41864
YEL044W	IES6	unknown	-0.2490	-1.2	0.0626487
YLR076C			-0.2490	-1.2	0.16775
YAR009C			-0.2485	-1.2	0.0969267
YDR424C	DYN2	microtubule motor	-0.2483	-1.2	0.219492
YMR047C	NUP116	structural molecule	-0.2482	-1.2	0.520856
YIL107C	PFK26	6-phosphofructo-2-kinase	-0.2482	-1.2	0.0170721
YIL164C	NIT1	nitrilase	-0.2478	-1.2	0.261048
YIL171W		unknown	-0.2475	-1.2	0.120696
YJL131C		unknown	-0.2475	-1.2	0.0212596
YDR248C		unknown	-0.2472	-1.2	0.232051
YLR340W	RPP0	structural constituent of ribosome	-0.2468	-1.2	0.00877985
YHR171W	ATG7	APG12 activating enzyme *	-0.2468	-1.2	0.161572
YCRX07W			-0.2468	-1.2	0.0810165
YIL002C	INP51	inositol-polyphosphate 5-phosphatase	-0.2455	-1.2	0.171141
YDL234C	GYP7	Rab GTPase activator	-0.2455	-1.2	0.057663
YPL050C	MNN9	mannosyltransferase	-0.2452	-1.2	0.0274268
YPL042C	SSN3	general RNA polymerase II transcription factor	-0.2450	-1.2	0.0493595
YMR140W	SIP5	unknown	-0.2448	-1.2	0.273744
YKL076C			-0.2442	-1.2	0.0465207
YBR104W	YMC2	transporter	-0.2438	-1.2	0.0904243
YHL025W	SNF6	general RNA polymerase II transcription factor	-0.2438	-1.2	0.331243
YDR075W	PPH3	protein phosphatase type 2A	-0.2437	-1.2	0.15949
YBR204C		serine hydrolase	-0.2435	-1.2	0.0679402
YMR181C		unknown	-0.2435	-1.2	0.44701
YML031W	NDC1	structural constituent of cytoskeleton	-0.2433	-1.2	0.0654127
YJL019W(1)			-0.2427	-1.2	0.18281
YBR138C		unknown	-0.2425	-1.2	0.0809029
YDL203C	ACK1	unknown	-0.2420	-1.2	0.363991
YDR254W	CHL4	DNA binding	-0.2417	-1.2	0.126545
YOR282W			-0.2410	-1.2	0.0744311
YOR001W	RRP6	3'-5'-exoribonuclease	-0.2410	-1.2	0.260877
YHL009W-B			-0.2407	-1.2	0.25337
YJL029C	VPS53	protein binding	-0.2405	-1.2	0.0826482
YFR031C-A	RPL2A	structural constituent of ribosome	-0.2405	-1.2	0.130493
YLR169W			-0.2402	-1.2	0.0600343
YLR029C	RPL15A	structural constituent of ribosome*	-0.2402	-1.2	0.153211
YCRX08W			-0.2402	-1.2	0.019306
YLR463C			-0.2400	-1.2	0.469446
YLR080W	EMP46	glycoprotein binding	-0.2395	-1.2	0.0869459
YOR329C	SCD5	protein binding	-0.2395	-1.2	0.300737
YML052W	SUR7	unknown	-0.2392	-1.2	0.178489
YDR010C			-0.2387	-1.2	0.35756
YMR236W	TAF9	general RNA polymerase II transcription factor	-0.2383	-1.2	0.261216
YMR233W		unknown	-0.2383	-1.2	0.0724573
YNL061W	NOP2	S-adenosylmethionine-dependent methyltransferase *	-0.2380	-1.2	0.0521716
YIL167W	SDL1	L-serine ammonia-lyase	-0.2378	-1.2	0.152492
YLR336C	SGD1	unknown	-0.2373	-1.2	0.367347
YPL161C	BEM4	unknown	-0.2373	-1.2	0.0437026
YDR308C	SRB7	RNA polymerase II transcription mediator	-0.2370	-1.2	0.0643722
YDR205W	MSC2	cation:cation antiporter	-0.2367	-1.2	0.16205
YOL155C		glucosidase	-0.2367	-1.2	0.262301
YGR193C	PDX1	protein binding	-0.2365	-1.2	0.0026172
YJL123C		unknown	-0.2363	-1.2	0.0973195
YJL204C	RCY1	protein binding	-0.2363	-1.2	0.144429
YDL075W	RPL31A	structural constituent of ribosome	-0.2360	-1.2	0.197413
YDR159W	SAC3	protein binding	-0.2355	-1.2	0.214276
YFR014C	CMK1	calmodulin-dependent protein kinase	-0.2355	-1.2	0.0162826
YDR023W	SES1	serine-tRNA ligase	-0.2355	-1.2	0.0630756
YDR411C	DFM1	unknown	-0.2353	-1.2	0.445655
YNL091W	NST1	unknown	-0.2352	-1.2	0.101224
YAL029C	MYO4	microfilament motor	-0.2347	-1.2	0.442965
YJR003C		unknown	-0.2347	-1.2	0.0628078
YGR143W	SKN1	glucosidase	-0.2343	-1.2	0.511969
YER141W	COX15	oxidoreductase	-0.2343	-1.2	0.369236
YAL013W	DEP1	transcription regulator	-0.2342	-1.2	0.0499822
YER056C	FCY2	cytosine-purine permease	-0.2340	-1.2	0.192632
YCRX11W			-0.2338	-1.2	0.147816
YNL293W	MSB3	Rab GTPase activator	-0.2338	-1.2	0.099886

Table 1: continued.

ORF ID	Gene Name	Gene Function	Avg Log_2 Ratio	Fold Change	T-test
YHR126C		unknown	-0.2337	-1.2	0.045413
YMR027W		unknown	-0.2337	-1.2	0.153094
YJR124C		unknown	-0.2332	-1.2	0.320303
YDR007W	TRP1	phosphoribosylanthranilate isomerase	-0.2330	-1.2	0.249427
YPL243W	SRP68	signal sequence binding	-0.2328	-1.2	0.314728
YDR257C	SET7	unknown	-0.2318	-1.2	0.207816
YGR125W		unknown	-0.2315	-1.2	0.119398
YPR156C	TPO3	spermine transporter	-0.2310	-1.2	0.322995
YDL140C	RPO21	DNA-directed RNA polymerase	-0.2310	-1.2	0.19293
YKL028W	TFA1	general RNA polymerase II transcription factor	-0.2308	-1.2	0.403845
YPL257W		unknown	-0.2308	-1.2	0.0519107
YKL053W			-0.2307	-1.2	0.0269436
YHR050W	SMF2	di-, tri-valent inorganic cation transporter	-0.2305	-1.2	0.0986259
YER060W-A	FCY22	cytosine-purine permease	-0.2305	-1.2	0.24289
YCR107W	AAD3	aryl-alcohol dehydrogenase	-0.2302	-1.2	0.164833
YER176W	ECM32	DNA helicase	-0.2295	-1.2	0.0259928
YNL323W	LEM3	phospholipid-translocating ATPase	-0.2295	-1.2	0.0200659
YCR085W			-0.2293	-1.2	0.299004
YOR151C	RPB2	DNA-directed RNA polymerase	-0.2292	-1.2	0.07438
YDR229W	IVY1	phospholipid binding	-0.2292	-1.2	0.0379493
YOL087C		unknown	-0.2292	-1.2	0.119349
YLR112W			-0.2288	-1.2	0.142866
YDR491C			-0.2287	-1.2	0.261307
YDL095W	PMT1	dolichyl-phosphate-mannose-protein mannosyltransferase	-0.2285	-1.2	0.00453395
YNL267W	PIK1	1-phosphatidylinositol 4-kinase	-0.2282	-1.2	0.264012
YJL117W	PHO86	unknown	-0.2278	-1.2	0.0356406
YER029C	SMB1	RNA splicing factor	-0.2278	-1.2	0.13411
YBL063W	KIP1	structural constituent of cytoskeleton*	-0.2275	-1.2	0.0721784
YMR283C	RIT1	transferase , transferring pentosyl groups	-0.2273	-1.2	0.161925
YGL005C	COG7	unknown	-0.2270	-1.2	0.359984
YDL131W	LYS21	homocitrate synthase	-0.2268	-1.2	0.0523713
YPL245W		unknown	-0.2267	-1.2	0.0454598
YAL037W		unknown	-0.2257	-1.2	0.0056484
YLR187W	SKG3	unknown	-0.2255	-1.2	0.00387435
YNL041C	COG6	unknown	-0.2255	-1.2	0.249376
YNL305C		unknown	-0.2242	-1.2	0.110952
YBR121C	GRS1	glycine-tRNA ligase	-0.2242	-1.2	0.0784277
YNL216W	RAP1	DNA binding	-0.2238	-1.2	0.582078
YNR008W	LRO1	phospholipid:diacylglycerol acyltransferase	-0.2238	-1.2	0.306257
YDR141C	DOP1	unknown	-0.2237	-1.2	0.11779
YLR022C	SDO1	unknown	-0.2235	-1.2	0.0481293
YOR324C	FRT1	unknown	-0.2235	-1.2	0.276188
YPR163C	TIF3	translation initiation factor	-0.2228	-1.2	0.374347
YBL073W			-0.2227	-1.2	0.136236
YLL067C		helicase	-0.2225	-1.2	0.260464
YDR154C			-0.2223	-1.2	0.443918
YLR386W	VAC14	enzyme activator	-0.2218	-1.2	0.670444
YNL223W	ATG4	microtubule binding	-0.2215	-1.2	0.177088
YNL249C	MPA43	unknown	-0.2213	-1.2	0.247201
YDR245W	MNN10	alpha-1,6-mannosyltransferase	-0.2213	-1.2	0.265929
YIL128W	MET18	RNA polymerase II transcription factor	-0.2213	-1.2	0.286136
YAL058W	CNE1	unfolded protein binding	-0.2210	-1.2	0.345723
YDR155C	CPR1	peptidyl-prolyl cis-trans isomerase	-0.2197	-1.2	0.272882
YDR107C		unknown	-0.2197	-1.2	0.225775
YER117W	RPL23B	structural constituent of ribosome	-0.2195	-1.2	0.0581939
YPL025C			-0.2192	-1.2	0.130259
YHR192W		unknown	-0.2187	-1.2	0.190976
YJL052W	TDH1	glyceraldehyde-3-phosphate dehydrogenase	-0.2185	-1.2	0.702105
YFL018C	LPD1	glycine dehydrogenase	-0.2185	-1.2	0.147204
YNL102W	POL1	alpha DNA polymerase	-0.2183	-1.2	0.0300448
YBR256C	RIB5	riboflavin synthase	-0.2182	-1.2	0.159044
YGL016W	KAP122	protein carrier	-0.2180	-1.2	0.259761
YPL201C	YIG1	unknown	-0.2177	-1.2	0.15187
YOR044W		unknown	-0.2175	-1.2	0.481068
YJR045C	SSC1	ATPase *	-0.2175	-1.2	0.276815
YJL181W		unknown	-0.2167	-1.2	0.133913
YJL083W	TAX4	unknown	-0.2165	-1.2	0.11638
YIR017C	MET28	DNA binding	-0.2163	-1.2	0.0207469
YDL150W	RPC53	DNA-directed RNA polymerase	-0.2163	-1.2	0.150158

Table 1: continued.

ORF ID	Gene Name	Gene Function	Avg Log_2 Ratio	Fold Change	T-test
YNL056W	OCA2	unknown	-0.2162	-1.2	0.0942471
YCR051W		unknown	-0.2160	-1.2	0.403227
YGL257C	MNT2	alpha-1,3-mannosyltransferase	-0.2155	-1.2	0.0547978
YPL200W	CSM4	unknown	-0.2153	-1.2	0.39695
YOL125W		unknown	-0.2153	-1.2	0.405998
YPL262W	FUM1	fumarate hydratase	-0.2152	-1.2	0.236443
YGR231C	PHB2	unknown	-0.2148	-1.2	0.00187986
YMR092C	AIP1	protein binding	-0.2147	-1.2	0.292137
YPL055C	LGE1	unknown	-0.2143	-1.2	0.470635
YML058W	SML1	enzyme inhibitor	-0.2142	-1.2	0.0839627
YKR027W	BCH2	unknown	-0.2140	-1.2	0.11813
YDL178W	DLD2	actin binding	-0.2132	-1.2	0.267848
YIL159W	BNR1	cytoskeletal protein binding	-0.2132	-1.2	0.0804846
YJL113W			-0.2130	-1.2	0.0520398
YPR017C	DSS4	guanyl-nucleotide exchange factor	-0.2128	-1.2	0.344965
YPL100W	ATG21	phosphoinositide binding	-0.2118	-1.2	0.331224
YGL142C	GPI10	mannosyltransferase	-0.2118	-1.2	0.182593
YNL162W	RPL42A	structural constituent of ribosome	-0.2113	-1.2	0.168983
YPL120W	VPS30	unknown	-0.2110	-1.2	0.46631
YBR223C	TDP1	tyrosyl-DNA phosphodiesterase	-0.2108	-1.2	0.227007
YPL249C	GYP5	Rab GTPase activator	-0.2107	-1.2	0.0873048
YER155C	BEM2	signal transducer *	-0.2105	-1.2	0.385583
YKR018C		unknown	-0.2105	-1.2	0.403198
YOL093W	TRM10	tRNA (guanine) methyltransferase	-0.2103	-1.2	0.148813
YGL065C	ALG2	glycolipid mannosyltransferase	-0.2102	-1.2	0.483334
YKL075C		unknown	-0.2102	-1.2	0.214572
YLR018C	POM34	unknown	-0.2098	-1.2	0.302181
YGL208W	SIP2	AMP-activated protein kinase	-0.2098	-1.2	0.155246
YER069W	ARG5,6	N-acetyl-gamma-glutamyl-phosphate reductase *	-0.2097	-1.2	0.153587
YDR198C	RKM2	unknown	-0.2092	-1.2	0.352641
YPL263C	KEL3	unknown	-0.2083	-1.2	0.189924
YDR239C		unknown	-0.2082	-1.2	0.0510936
YDR317W	HIM1	unknown	-0.2080	-1.2	0.131023
YLR353W	BUD8	unknown	-0.2072	-1.2	0.30901
YOR256C	TRE2	unknown	-0.2070	-1.2	0.330804
YJL023C	PET130	unknown	-0.2067	-1.2	0.0228948
YFL042C		unknown	-0.2060	-1.2	0.223268
YPR031W	NTO1	unknown	-0.2055	-1.2	0.341158
YNL012W	SPO1	phospholipase	-0.2050	-1.2	0.282462
YER175C	TMT1	trans-aconitate 3-methyltransferase	-0.2050	-1.2	0.353242
YHL020C	OPI1	transcription corepressor	-0.2048	-1.2	0.197546
YMR302C	YME2	exonuclease	-0.2048	-1.2	0.0712404
YMR121C	RPL15B	structural constituent of ribosome*	-0.2043	-1.2	0.0988629
YML033W			-0.2040	-1.2	0.154901
YBR269C	FMP21	unknown	-0.2040	-1.2	0.0967279
YCR052W	RSC6	unknown	-0.2038	-1.2	0.145826
YOR209C	NPT1	nicotinate phosphoribosyltransferase	-0.2037	-1.2	0.525355
YDR022C	CIS1	unknown	-0.2033	-1.2	0.0556651
YIL113W	SDP1	MAP kinase	-0.2028	-1.2	0.000606035
YCR106W	RDS1	DNA binding	-0.2027	-1.2	0.000620939
YNL290W	RFC3	ATPase *	-0.2023	-1.2	0.069327
YLR384C	IKI3	RNA polymerase II transcription elongation factor	-0.2022	-1.2	0.222151
YAR029W		unknown	-0.2022	-1.2	0.51015
YJR137C	ECM17	sulfite reductase (NADPH)	-0.2018	-1.2	0.271362
YHR164C	DNA2	ATP-dependent DNA helicase	-0.2018	-1.2	0.127563
YNR007C	ATG3	APG8 conjugating enzyme	-0.2017	-1.2	0.279633
YOL073C		unknown	-0.2013	-1.1	0.073663
YLR431C	ATG23	unknown	-0.2012	-1.1	0.527273
YPR026W	ATH1	alpha,alpha-trehalase	-0.2010	-1.1	0.434043
YDR533C	HSP31	unfolded protein binding	-0.2007	-1.1	0.433214
YBR198C	TAF5	general RNA polymerase II transcription factor	-0.2007	-1.1	0.0946451
YNR047W		protein kinase	-0.2005	-1.1	0.232978
YLL041C	SDH2	succinate dehydrogenase	-0.2003	-1.1	0.0204958
YBR200W	BEM1	protein binding	-0.2003	-1.1	0.355777
YHR124W	NDT80	transcription factor	-0.2002	-1.1	0.561575
YJL191W	RPS14B	structural constituent of ribosome*	-0.1992	-1.1	0.0196037
YFL004W	VTC2	unknown	-0.1990	-1.1	0.131676
YIL030C	SSM4	ubiquitin-protein ligase	-0.1990	-1.1	0.0311752
YIL042C		kinase	-0.1988	-1.1	0.624707

Table 1: continued.

ORF ID	Gene Name	Gene Function	Avg Log_2 Ratio	Fold Change	T-test
YNR071C		unknown	-0.1987	-1.1	0.014146
YJL055W		unknown	-0.1983	-1.1	0.218068
YDR103W	STE5	MAP-kinase	-0.1982	-1.1	0.0622573
YNL182C	IPI3	unknown	-0.1982	-1.1	0.327416
YLR367W	RPS22B	structural constituent of ribosome	-0.1980	-1.1	0.304604
YNL086W		unknown	-0.1978	-1.1	0.414778
YAR044W			-0.1978	-1.1	0.181802
YIL153W	RRD1	protein phosphatase type 2A regulator	-0.1977	-1.1	0.446439
YLR413W		unknown	-0.1973	-1.1	0.14924
YGL077C	HNM1	choline transporter	-0.1972	-1.1	0.346969
YLR056W	ERG3	C-5 sterol desaturase	-0.1972	-1.1	0.110014
YOR185C	GSP2	GTPase	-0.1972	-1.1	0.00874084
YDL083C	RPS16B	structural constituent of ribosome	-0.1968	-1.1	0.18014
YNL111C	CYB5	electron carrier	-0.1965	-1.1	0.0125685
YER102W	RPS8B	structural constituent of ribosome	-0.1963	-1.1	0.0685175
YGR024C	THG1	tRNA guanylyltransferase	-0.1963	-1.1	0.0844974
YGL140C		unknown	-0.1960	-1.1	0.677868
YCR089W	FIG2	unknown	-0.1960	-1.1	0.202286
YDR063W		unknown	-0.1957	-1.1	0.43149
YDR514C		unknown	-0.1955	-1.1	0.00173328
YGR157W	CHO2	phosphatidylethanolamine N-methyltransferase	-0.1952	-1.1	0.0104341
YKL006W	RPL14A	structural constituent of ribosome*	-0.1950	-1.1	0.0137289
YMR042W	ARG80	DNA binding	-0.1945	-1.1	0.400391
YAL005C	SSA1	ATPase *	-0.1938	-1.1	0.0705759
YCL011C	GBP2	RNA binding	-0.1937	-1.1	0.194575
YIR032C	DAL3	ureidoglycolate hydrolase	-0.1937	-1.1	0.264595
YIR013C	GAT4	transcription factor	-0.1935	-1.1	0.652147
YHR039C	MSC7	unknown	-0.1932	-1.1	0.00617729
YPL118W	MRP51	structural constituent of ribosome	-0.1923	-1.1	0.146772
YDL060W	TSR1	ribonucleoprotein binding	-0.1920	-1.1	0.525278
YJL207C	LAA1	unknown	-0.1913	-1.1	0.24327
YDR110W	FOB1	rDNA binding	-0.1912	-1.1	0.519262
YKL204W	EAP1	eukaryotic initiation factor	-0.1908	-1.1	0.349033
YBR168W	PEX32	unknown	-0.1907	-1.1	0.0685203
YNL052W	COX5A	cytochrome-c oxidase	-0.1905	-1.1	0.00785718
YLR241W		unknown	-0.1903	-1.1	0.162437
YJL071W	ARG2	amino-acid N-acetyltransferase	-0.1902	-1.1	0.295536
YDR418W	RPL12B	structural constituent of ribosome	-0.1900	-1.1	0.0668711
YBR218C	PYC2	pyruvate carboxylase	-0.1898	-1.1	0.0669744
YOR219C	STE13	aminopeptidase	-0.1895	-1.1	0.0384164
YDL113C	ATG20	lipid binding	-0.1893	-1.1	0.185725
YPL005W	AEP3	unknown	-0.1888	-1.1	0.298119
YPR087W			-0.1888	-1.1	0.0253101
YEL056W	HAT2	H3/H4 histone acetyltransferase	-0.1885	-1.1	0.0988706
YNL082W	PMS1	DNA binding	-0.1883	-1.1	0.614609
YDR342C	HXT7	glucose transporter	-0.1883	-1.1	0.0173234
YJL198W	PHO90	phosphate transporter	-0.1883	-1.1	0.196866
YER037W	PHM8	unknown	-0.1882	-1.1	0.159415
YDR144C	MKC7	aspartic-type signal peptidase	-0.1873	-1.1	0.516103
YBL005W-B			-0.1873	-1.1	0.0699958
YOL063C	CRT10	unknown	-0.1870	-1.1	0.432888
YDR087C	RRP1	unknown	-0.1868	-1.1	0.192172
YHR129C	ARP1	structural constituent of cytoskeleton	-0.1867	-1.1	0.14652
YGR221C	TOS2	unknown	-0.1863	-1.1	0.0837577
YGL167C	PMR1	calcium-transporting ATPase *	-0.1853	-1.1	0.569547
YJR051W	OSM1	fumarate reductase (NADH)	-0.1852	-1.1	0.298732
YOR322C	LDB19	unknown	-0.1845	-1.1	0.384461
YPL048W	CAM1	translation elongation factor	-0.1842	-1.1	0.146357
YDR024W			-0.1840	-1.1	0.107408
YDR057W	YOS9	sugar binding	-0.1838	-1.1	0.335856
YPL174C	NIP100	protein binding	-0.1837	-1.1	0.125331
YNL156C	NSG2	unknown	-0.1832	-1.1	0.0276688
YFR002W	NIC96	structural molecule	-0.1832	-1.1	0.479515
YDR519W	FPR2	peptidyl-prolyl cis-trans isomerase	-0.1832	-1.1	0.232466
YDL128W	VCX1	calcium ion transporter	-0.1828	-1.1	0.0191666
YGR210C		unknown	-0.1828	-1.1	0.430335
YLL051C	FRE6	ferric-chelate reductase	-0.1825	-1.1	0.0248889
YGR118W	RPS23A	structural constituent of ribosome	-0.1825	-1.1	0.20151
YAL049C		unknown	-0.1823	-1.1	0.120851

Table 1: continued.

ORF ID	Gene Name	Gene Function	Avg Log_2 Ratio	Fold Change	T-test
YDR301W	CFT1	RNA binding	-0.1823	-1.1	0.362748
YFR051C	RET2	protein binding	-0.1822	-1.1	0.614975
YBR263W	SHM1	glycine hydroxymethyltransferase	-0.1820	-1.1	0.0704646
YKR004C	ECM9	unknown	-0.1808	-1.1	0.187982
YOL070C		unknown	-0.1808	-1.1	0.611163
YHR184W	SSP1	unknown	-0.1807	-1.1	0.205008
YOR080W	DIA2	DNA replication origin binding	-0.1805	-1.1	0.102328
YHR207C	SET5	unknown	-0.1805	-1.1	0.175472
YHR089C	GAR1	RNA binding	-0.1802	-1.1	0.254382
YNL204C	SPS18	unknown	-0.1798	-1.1	0.362832
YLR005W	SSL1	general RNA polymerase II transcription factor	-0.1798	-1.1	0.393944
YBR217W	ATG12	protein tag	-0.1797	-1.1	0.189485
YJR005W	APL1	unknown	-0.1797	-1.1	0.0916489
YGL160W		oxidoreductase	-0.1797	-1.1	0.269812
YBR190W			-0.1793	-1.1	0.160566
YGL078C	DBP3	ATP-dependent RNA helicase	-0.1790	-1.1	0.668114
YJL202C			-0.1790	-1.1	0.543677
YJL057C	IKS1	unknown	-0.1787	-1.1	0.122885
YKL146W	AVT3	neutral amino acid transporter	-0.1787	-1.1	0.466741
YOR172W	YRM1	specific RNA polymerase II transcription factor	-0.1785	-1.1	0.657443
YGL159W		unknown	-0.1785	-1.1	0.490604
YDR505C	PSP1	unknown	-0.1783	-1.1	0.000011021
YPR188C	MLC2	myosin II binding	-0.1780	-1.1	0.0613593
YLR316C	TAD3	tRNA specific adenosine deaminase	-0.1777	-1.1	0.335402
YDR122W	KIN1	protein kinase	-0.1775	-1.1	0.366255
YIR016W		unknown	-0.1772	-1.1	0.128747
YNL098C	RAS2	GTPase	-0.1770	-1.1	0.309857
YNL026W	SAM50	unknown	-0.1770	-1.1	0.331834
YGL144C	ROG1	lipase	-0.1765	-1.1	0.230924
YFL068W		unknown	-0.1765	-1.1	0.482891
YLR078C	BOS1	v-SNARE	-0.1763	-1.1	0.646854
YNL209W	SSB2	ATPase *	-0.1762	-1.1	0.28421
YLR069C	MEF1	translation elongation factor	-0.1755	-1.1	0.444866
YDR009W	GAL3	protein binding	-0.1752	-1.1	0.401443
YDR284C	DPP1	phosphatidate phosphatase *	-0.1750	-1.1	0.415261
YER145C	FTR1	iron ion transporter	-0.1750	-1.1	0.683138
YDR119W		unknown	-0.1748	-1.1	0.0589274
YHR138C		endopeptidase inhibitor	-0.1742	-1.1	0.0384909
YPR117W		unknown	-0.1742	-1.1	0.312816
YEL076C		unknown	-0.1740	-1.1	0.399054
YKR047W			-0.1735	-1.1	0.207979
YCRX05W			-0.1733	-1.1	0.178291
YGR242W			-0.1723	-1.1	0.415747
YER074W	RPS24A	structural constituent of ribosome	-0.1723	-1.1	0.286989
YKL006C-A	SFT1	v-SNARE	-0.1723	-1.1	0.207603
YOL078W	AVO1	unknown	-0.1722	-1.1	0.0127619
YDL124W		alpha-keto amide reductase *	-0.1718	-1.1	0.149378
YER011W	TIR1	structural constituent of cell wall	-0.1715	-1.1	0.454998
YML007W	YAP1	transcription factor	-0.1715	-1.1	0.0305475
YLL008W	DRS1	ATP-dependent RNA helicase	-0.1713	-1.1	0.306329
YHR028C	DAP2	dipeptidyl-peptidase and tripeptidyl-peptidase	-0.1712	-1.1	0.192277
YNL095C		unknown	-0.1710	-1.1	0.373872
YLL029W		unknown	-0.1710	-1.1	0.394528
YNL241C	ZWF1	glucose-6-phosphate 1-dehydrogenase	-0.1710	-1.1	0.000651512
YMR213W	CEF1	RNA splicing factor	-0.1708	-1.1	0.505728
YML121W	GTR1	GTPase	-0.1700	-1.1	0.535884
YJR017C	ESS1	peptidyl-prolyl cis-trans isomerase *	-0.1695	-1.1	0.0942642
YEL062W	NPR2	channel regulator	-0.1695	-1.1	0.541517
YML114C	TAF8	RNA polymerase II transcription factor	-0.1690	-1.1	0.563205
YDR261C	EXG2	glucan 1,3-beta-glucosidase	-0.1690	-1.1	0.481691
YKR094C	RPL40B	structural constituent of ribosome*	-0.1690	-1.1	0.233029
YER054C	GIP2	protein phosphatase regulator	-0.1688	-1.1	0.135282
YPL266W	DIM1	rRNA (adenine-N6,N6-)-dimethyltransferase	-0.1687	-1.1	0.403424
YOR168W	GLN4	glutamine-tRNA ligase	-0.1685	-1.1	0.0676644
YBL035C	POL12	alpha DNA polymerase	-0.1683	-1.1	0.206414
YCL056C		unknown	-0.1680	-1.1	0.0996936
YML109W	ZDS2	unknown	-0.1680	-1.1	0.61398
YKL127W	PGM1	phosphoglucomutase	-0.1673	-1.1	0.143154
YIL082W-A			-0.1672	-1.1	0.218595

Table 1: continued.

ORF ID	Gene Name	Gene Function	Avg Log_2 Ratio	Fold Change	T-test
YJR155W	AAD10	aryl-alcohol dehydrogenase	-0.1672	-1.1	0.411299
YKL038W	RGT1	DNA binding	-0.1670	-1.1	0.253924
YDL029W	ARP2	structural constituent of cytoskeleton*	-0.1670	-1.1	0.260656
YLR006C	SSK1	enzyme activator *	-0.1668	-1.1	0.0652506
YGR237C		unknown	-0.1667	-1.1	0.646357
YNL301C	RPL18B	structural constituent of ribosome	-0.1663	-1.1	0.0604157
YCR031			-0.1663	-1.1	0.0528392
YGR055W	MUP1	L-methionine porter	-0.1662	-1.1	0.348708
YFL030W	AGX1	alanine-glyoxylate transaminase	-0.1662	-1.1	0.467607
YER125W	RSP5	ubiquitin-protein ligase	-0.1660	-1.1	0.011421
YPL160W	CDC60	leucine-tRNA ligase	-0.1658	-1.1	0.483143
YFR056C			-0.1658	-1.1	0.143967
YML079W		unknown	-0.1655	-1.1	0.357011
YPL228W	CET1	polynucleotide 5'-phosphatase	-0.1655	-1.1	0.583975
YGL079W		unknown	-0.1652	-1.1	0.538476
YDR256C	CTA1	catalase	-0.1652	-1.1	0.0211351
YOR207C	RET1	DNA-directed RNA polymerase	-0.1648	-1.1	0.436541
YOL109W	ZEO1	unknown	-0.1648	-1.1	0.0374093
YKR072C	SIS2	phosphopantothenoylcysteine decarboxylase	-0.1648	-1.1	0.413038
YGR263C		unknown	-0.1648	-1.1	0.20384
YOL026C	MIM1	unknown	-0.1647	-1.1	0.210557
YLR037C	DAN2	unknown	-0.1647	-1.1	0.242491
YCRX20C			-0.1645	-1.1	0.380218
YDL014W	NOP1	methyltransferase	-0.1645	-1.1	0.107702
YML117W-A			-0.1643	-1.1	0.391433
YCL061C	MRC1	unknown	-0.1643	-1.1	0.21952
YOR098C	NUP1	protein binding	-0.1642	-1.1	0.407653
YKL097W-A			-0.1635	-1.1	0.127224
YPR103W	PRE2	endopeptidase	-0.1632	-1.1	0.303018
YBR188C	NTC20	RNA splicing factor	-0.1630	-1.1	0.232823
YOR326W	MYO2	microfilament motor	-0.1630	-1.1	0.573711
YJR083C	ACF4	unknown	-0.1628	-1.1	0.270647
YNL130C	CPT1	diacylglycerol cholinephosphotransferase	-0.1625	-1.1	0.1984
YCRX04W			-0.1623	-1.1	0.213715
YDR434W	GPI17	GPI-anchor transamidase	-0.1615	-1.1	0.27259
YIL097W	FYV10	unknown	-0.1612	-1.1	0.317394
YDR125C	ECM18	unknown	-0.1612	-1.1	0.0848058
YBR157C	ICS2	unknown	-0.1610	-1.1	0.051735
YPL233W	NSL1	unknown	-0.1607	-1.1	0.516377
YDR307W		unknown	-0.1607	-1.1	0.409325
YGL101W		unknown	-0.1603	-1.1	0.0730395
YLR097C	HRT3	protein binding	-0.1600	-1.1	0.544836
YDR104C	SPO71	unknown	-0.1600	-1.1	0.0860873
YOR078W	BUD21	snoRNA binding	-0.1600	-1.1	0.558052
YAL059W	ECM1	unknown	-0.1600	-1.1	0.332912
YLR190W	MMR1	unknown	-0.1595	-1.1	0.217316
YMR099C		unknown	-0.1590	-1.1	0.162635
YER077C		unknown	-0.1588	-1.1	0.0806498
YNR053C	NOG2	GTPase	-0.1588	-1.1	0.678687
YGL067W	NPY1	NAD+ diphosphatase	-0.1588	-1.1	0.35436
YER095W	RAD51	recombinase	-0.1585	-1.1	0.613685
YBR115C	LYS2	L-aminoadipate-semialdehyde dehydrogenase	-0.1583	-1.1	0.213266
YPL085W	SEC16	structural molecule	-0.1582	-1.1	0.724429
YBR005W	RCR1	unknown	-0.1582	-1.1	0.274733
YER143W	DDI1	SNARE binding	-0.1580	-1.1	0.434764
YPR129W	SCD6	RNA binding	-0.1575	-1.1	0.493044
YGR145W	ENP2	unknown	-0.1573	-1.1	0.375207
YDR134C		unknown	-0.1572	-1.1	0.693514
YOR223W		unknown	-0.1572	-1.1	0.345942
YJL168C	SET2	histone methyltransferase *	-0.1562	-1.1	0.310537
YLR162W		unknown	-0.1560	-1.1	0.670529
YJL218W		acetyltransferase	-0.1560	-1.1	0.0773773
YNL219C	ALG9	mannosyltransferase	-0.1560	-1.1	0.18093
YLR429W	CRN1	protein binding	-0.1557	-1.1	0.194577
YOR293W	RPS10A	structural constituent of ribosome	-0.1557	-1.1	0.222946
YDL050C			-0.1552	-1.1	0.20359
YLR396C	VPS33	ATP binding	-0.1545	-1.1	0.327105
YOL117W	RRI2	unknown	-0.1542	-1.1	0.359962
YCR053W	THR4	threonine synthase	-0.1542	-1.1	0.079656

Table 1: continued.

ORF ID	Gene Name	Gene Function	Avg Log_2 Ratio	Fold Change	T-test
YBR140C	IRA1	Ras GTPase activator	-0.1540	-1.1	0.458754
YDR192C	NUP42	structural molecule	-0.1538	-1.1	0.00553585
YMR202W	ERG2	C-8 sterol isomerase	-0.1532	-1.1	0.171855
YPL020C	ULP1	cysteine-type peptidase *	-0.1532	-1.1	0.0052059
YCL019W			-0.1530	-1.1	0.0104307
YPL181W	CTI6	transcription factor	-0.1528	-1.1	0.0727742
YGL227W	VID30	unknown	-0.1528	-1.1	0.158456
YML035C	AMD1	AMP deaminase	-0.1525	-1.1	0.200459
YFL034W		unknown	-0.1523	-1.1	0.402388
YDL134C-A			-0.1522	-1.1	0.459258
YKL061W		unknown	-0.1520	-1.1	0.375097
YCL060C			-0.1518	-1.1	0.466136
YER019C-A	SBH2	protein transporter	-0.1510	-1.1	0.344397
YDL170W	UGA3	transcription factor	-0.1510	-1.1	0.175256
YPR056W	TFB4	general RNA polymerase II transcription factor	-0.1510	-1.1	0.408277
YML010W	SPT5	RNA polymerase II transcription elongation factor	-0.1510	-1.1	0.150946
YCR103C			-0.1508	-1.1	0.692309
YAL023C	PMT2	dolichyl-phosphate-mannose-protein mannosyltransferase	-0.1507	-1.1	0.0514421
YCL028W	RNQ1	unknown	-0.1507	-1.1	0.218445
YJL008C	CCT8	unfolded protein binding	-0.1507	-1.1	0.422893
YCL062W			-0.1502	-1.1	0.33935
YBL039C	URA7	CTP synthase	-0.1500	-1.1	0.00835407
YKL191W	DPH2	unknown	-0.1498	-1.1	0.52146
YJL079C	PRY1	unknown	-0.1495	-1.1	0.108335
YJL142C			-0.1490	-1.1	0.167029
YJL197W	UBP12	ubiquitin-specific protease	-0.1490	-1.1	0.174864
YGR199W	PMT6	dolichyl-phosphate-mannose-protein mannosyltransferase	-0.1487	-1.1	0.658009
YJR091C	JSN1	mRNA binding	-0.1478	-1.1	0.53689
YCR074C			-0.1477	-1.1	0.254702
YBR176W	ECM31	3-methyl-2-oxobutanoate hydroxymethyltransferase	-0.1477	-1.1	0.340126
YOR112W		unknown	-0.1477	-1.1	0.638027
YEL065W	SIT1	siderophore-iron (ferrioxamine) uptake transporter	-0.1472	-1.1	0.536128
YGL105W	ARC1	tRNA binding	-0.1472	-1.1	0.419087
YGR009C	SEC9	t-SNARE	-0.1470	-1.1	0.473314
YJL194W	CDC6	protein binding	-0.1470	-1.1	0.506294
YEL034C-A			-0.1468	-1.1	0.0600568
YJL103C		unknown	-0.1467	-1.1	0.182308
YML067C	ERV41	unknown	-0.1465	-1.1	0.510663
YMR264W	CUE1	protein binding	-0.1462	-1.1	0.0622459
YPL013C	MRPS16	structural constituent of ribosome	-0.1457	-1.1	0.58588
YAL028W	FRT2	unknown	-0.1453	-1.1	0.502288
YGL198W	YIP4	Rab GTPase binding	-0.1453	-1.1	0.320778
YPL244C	HUT1	UDP-galactose transporter	-0.1452	-1.1	0.719539
YIL069C	RPS24B	structural constituent of ribosome	-0.1450	-1.1	0.114642
YNL085W	MKT1	nuclease	-0.1447	-1.1	0.783931
YKR082W	NUP133	structural molecule	-0.1445	-1.1	0.58851
YDL091C	UBX3	unknown	-0.1443	-1.1	0.252958
YKL205W	LOS1	tRNA binding	-0.1440	-1.1	0.114825
YPR058W	YMC1	transporter	-0.1438	-1.1	0.0191705
YHL001W	RPL14B	structural constituent of ribosome*	-0.1432	-1.1	0.0227286
YBR197C		unknown	-0.1432	-1.1	0.165258
YKL058W	TOA2	general RNA polymerase II transcription factor	-0.1430	-1.1	0.126217
YDR463W	STP1	transcription factor	-0.1425	-1.1	0.211949
YDL134C	PPH21	protein phosphatase type 2A	-0.1423	-1.1	0.239603
YHR004C	NEM1	unknown	-0.1422	-1.1	0.51864
YER186W-A			-0.1418	-1.1	0.696071
YDL180W		unknown	-0.1415	-1.1	0.319678
YBR298C	MAL31	alpha-glucoside:hydrogen symporter	-0.1413	-1.1	0.240859
YER101C	AST2	unknown	-0.1410	-1.1	0.0800624
YKR005C		unknown	-0.1410	-1.1	0.743751
YKR055W	RHO4	GTPase *	-0.1408	-1.1	0.120538
YER063W	THO1	unknown	-0.1407	-1.1	0.280179
YKL140W	TGL1	lipase *	-0.1405	-1.1	0.18071
YGL162W	SUT1	transcription factor	-0.1403	-1.1	0.553877
YEL015W	EDC3	unknown	-0.1402	-1.1	0.507748
YDL188C	PPH22	protein phosphatase type 2A	-0.1402	-1.1	0.206989
YML029W	USA1	unknown	-0.1397	-1.1	0.260129
YOR084W		lipase	-0.1397	-1.1	0.4144
YIL109C	SEC24	protein binding	-0.1397	-1.1	0.0170902

Table 1: continued.

ORF ID	Gene Name	Gene Function	Avg Log_2 Ratio	Fold Change	T-test
YMR154C	RIM13	cysteine-type endopeptidase	-0.1395	-1.1	0.312268
YPL065W	VPS28	protein binding	-0.1393	-1.1	0.244121
YDL040C	NAT1	peptide alpha-N-acetyltransferase	-0.1392	-1.1	0.116916
YHR056C	RSC30	DNA binding	-0.1392	-1.1	0.552839
YML054C	CYB2	L-lactate dehydrogenase	-0.1390	-1.1	0.160074
YER119C	AVT6	amino acid transporter	-0.1390	-1.1	0.321395
YJL220W			-0.1387	-1.1	0.502612
YLR048W	RPS0B	structural constituent of ribosome	-0.1387	-1.1	0.122979
YKR089C	TGL4	triacylglycerol lipase	-0.1382	-1.1	0.104015
YHR042W	NCP1	electron carrier	-0.1382	-1.1	0.42079
YDR124W		unknown	-0.1375	-1.1	0.663955
YER045C	ACA1	specific RNA polymerase II transcription factor	-0.1373	-1.1	0.517027
YHR218W		unknown	-0.1362	-1.1	0.47965
YKL164C	PIR1	structural constituent of cell wall	-0.1362	-1.1	0.0145756
YGR206W		unknown	-0.1355	-1.1	0.25151
YJL144W		unknown	-0.1352	-1.1	0.365825
YPR183W	DPM1	transferase , transferring glycosyl groups*	-0.1352	-1.1	0.145994
YBR224W			-0.1350	-1.1	0.162801
YDR303C	RSC3	DNA binding	-0.1348	-1.1	0.0107748
YOR327C	SNC2	v-SNARE	-0.1348	-1.1	0.279553
YDR210W		unknown	-0.1347	-1.1	0.027591
YNL174W			-0.1343	-1.1	0.274503
YGL234W	ADE5,7	phosphoribosylamine-glycine ligase *	-0.1343	-1.1	0.614681
YOL133W	HRT1	protein binding	-0.1338	-1.1	0.41228
YBR052C	RFS1	unknown	-0.1337	-1.1	0.534689
YHL033C	RPL8A	structural constituent of ribosome	-0.1335	-1.1	0.125305
YDL066W	IDP1	isocitrate dehydrogenase	-0.1328	-1.1	0.231345
YER160C			-0.1327	-1.1	0.599519
YDL149W	ATG9	unknown	-0.1327	-1.1	0.507524
YML082W		carbon-sulfur lyase	-0.1325	-1.1	0.367651
YBR134W			-0.1322	-1.1	0.0899691
YGR168C		unknown	-0.1322	-1.1	0.561527
YDR006C	SOK1	unknown	-0.1315	-1.1	0.0861411
YLL022C	HIF1	unknown	-0.1315	-1.1	0.50235
YGR010W	NMA2	nicotinate-nucleotide adenylyltransferase	-0.1313	-1.1	0.0718076
YBR081C	SPT7	structural molecule	-0.1313	-1.1	0.288386
YDR012W	RPL4B	structural constituent of ribosome	-0.1312	-1.1	0.18938
YKR098C	UBP11	ubiquitin-specific protease	-0.1310	-1.1	0.677098
YKR070W		unknown	-0.1308	-1.1	0.402678
YDL042C	SIR2	NAD-dependent histone deacetylase (H3-K14 specific)*	-0.1308	-1.1	0.551522
YOR032C	HMS1	transcription factor	-0.1305	-1.1	0.0376045
YMR196W		unknown	-0.1303	-1.1	0.0124299
YML068W	ITT1	unknown	-0.1303	-1.1	0.33264
YNR051C	BRE5	unknown	-0.1302	-1.1	0.410234
YBR090C		unknown	-0.1300	-1.1	0.182789
YNL092W		S-adenosylmethionine-dependent methyltransferase	-0.1297	-1.1	0.525087
YCRX16C			-0.1295	-1.1	0.110964
YGR248W	SOL4	6-phosphogluconolactonase	-0.1295	-1.1	0.281456
YKR003W	OSH6	oxysterol binding	-0.1295	-1.1	0.594147
YER136W	GDI1	Rab GDP-dissociation inhibitor	-0.1290	-1.1	0.607331
YKR031C	SPO14	phospholipase D	-0.1288	-1.1	0.362785
YLR189C	ATG26	sterol 3-beta-glucosyltransferase	-0.1288	-1.1	0.130953
YOL113W	SKM1	protein serine/threonine kinase	-0.1287	-1.1	0.079073
YOR294W	RRS1	unknown	-0.1282	-1.1	0.156294
YPL224C	MMT2	unknown	-0.1282	-1.1	0.111812
YPL040C	ISM1	isoleucine-tRNA ligase	-0.1282	-1.1	0.487183
YCL003W			-0.1282	-1.1	0.310555
YOR351C	MEK1	protein serine/threonine kinase	-0.1278	-1.1	0.492191
YJL195C			-0.1273	-1.1	0.429607
YOR367W	SCP1	protein binding	-0.1273	-1.1	0.419922
YPL190C	NAB3	poly(A) binding	-0.1265	-1.1	0.317702
YGR197C	SNG1	unknown	-0.1260	-1.1	0.579721
YIL021W	RPB3	DNA-directed RNA polymerase	-0.1260	-1.1	0.201332
YBR230C	OM14	unknown	-0.1258	-1.1	0.235694
YMR131C	RRB1	unknown	-0.1258	-1.1	0.522484
YFR038W	IRC5	helicase	-0.1257	-1.1	0.561434
YKR087C	OMA1	metalloendopeptidase	-0.1252	-1.1	0.477111
YLL043W	FPS1	transporter	-0.1250	-1.1	0.316211
YJL179W	PFD1	unfolded protein binding	-0.1248	-1.1	0.234553

Table 1: continued.

ORF ID	Gene Name	Gene Function	Avg Log_2 Ratio	Fold Change	T-test
YJR111C		unknown	-0.1245	-1.1	0.652085
YHR194W	MDM31	unknown	-0.1243	-1.1	0.53552
YHR168W	MTG2	GTPase *	-0.1240	-1.1	0.664784
YDL164C	CDC9	DNA ligase (ATP)	-0.1240	-1.1	0.19217
YIL079C	AIR1	unknown	-0.1240	-1.1	0.752631
YFL005W	SEC4	GTPase	-0.1240	-1.1	0.27207
YDR346C	SVF1	unknown	-0.1237	-1.1	0.379918
YDR292C	SRP101	GTP binding	-0.1237	-1.1	0.166305
YNR065C	YSN1	unknown	-0.1235	-1.1	0.35304
YGL233W	SEC15	protein binding	-0.1235	-1.1	0.692571
YNL294C	RIM21	unknown	-0.1227	-1.1	0.73693
YBR041W	FAT1	long-chain-fatty-acid-CoA ligase *	-0.1227	-1.1	0.546734
YDR005C	MAF1	unknown	-0.1220	-1.1	0.616001
YHR073W	OSH3	oxysterol binding	-0.1217	-1.1	0.542836
YHR019C	DED81	ATP binding	-0.1217	-1.1	0.558466
YMR247C	RKR1	unknown	-0.1212	-1.1	0.284673
YCL038C	ATG22	unknown	-0.1212	-1.1	0.383753
YDR512C	EMI1	unknown	-0.1210	-1.1	0.0791264
YOR142W	LSC1	succinate-CoA ligase (ADP-forming)	-0.1208	-1.1	0.250671
YAL020C	ATS1	unknown	-0.1208	-1.1	0.51629
YPL121C	MEI5	unknown	-0.1207	-1.1	0.432727
YPL124W	SPC29	structural constituent of cytoskeleton	-0.1205	-1.1	0.120549
YOL048C		unknown	-0.1202	-1.1	0.382193
YPR127W		unknown	-0.1200	-1.1	0.451897
YJL065C	DLS1	unknown	-0.1198	-1.1	0.483416
Q0070	AI5_ALPHA	endonuclease	-0.1197	-1.1	0.456487
YKL010C	UFD4	ubiquitin-protein ligase	-0.1193	-1.1	0.587727
YPR115W		unknown	-0.1192	-1.1	0.663059
YBR255W		unknown	-0.1182	-1.1	0.488223
YDL093W	PMT5	dolichyl-phosphate-mannose-protein mannosyltransferase	-0.1178	-1.1	0.284084
YPR122W	AXL1	metalloendopeptidase	-0.1178	-1.1	0.397162
YIR001C	SGN1	poly(A) binding	-0.1178	-1.1	0.449523
YGR279C	SCW4	glucosidase	-0.1178	-1.1	0.0277105
YAR002C-A	ERP1	unknown	-0.1173	-1.1	0.701653
YDR222W		unknown	-0.1172	-1.1	0.68272
YGL133W	ITC1	unknown	-0.1172	-1.1	0.15743
YHL035C	VMR1	ATPase , coupled to transmembrane movement of substanc	-0.1168	-1.1	0.00621729
YGR081C	SLX9	unknown	-0.1167	-1.1	0.634225
YHL047C	ARN2	siderophore-iron transporter	-0.1165	-1.1	0.59923
YDR466W	PKH3	protein kinase	-0.1165	-1.1	0.0988444
YLR109W	AHP1	thioredoxin peroxidase	-0.1162	-1.1	0.129314
YDR167W	TAF10	general RNA polymerase II transcription factor	-0.1160	-1.1	0.554085
YLL058W		cystathionine gamma-synthase	-0.1157	-1.1	0.782135
YMR068W	AVO2	unknown	-0.1155	-1.1	0.415312
YJL106W	IME2	protein kinase	-0.1153	-1.1	0.664707
YMR310C		unknown	-0.1152	-1.1	0.627971
YBR296C	PHO89	sodium:inorganic phosphate symporter	-0.1152	-1.1	0.79518
YCL061C(1)			-0.1152	-1.1	0.401777
YDR051C		unknown	-0.1148	-1.1	0.415071
YIL026C	IRR1	protein binding	-0.1145	-1.1	0.288713
YHR151C		unknown	-0.1145	-1.1	0.143917
YKL031W			-0.1138	-1.1	0.573415
YHR130C			-0.1137	-1.1	0.334166
YGR043C		transaldolase	-0.1135	-1.1	0.419885
YPL081W	RPS9A	structural constituent of ribosome	-0.1133	-1.1	0.528172
YJL089W	SIP4	specific RNA polymerase II transcription factor	-0.1133	-1.1	0.256606
YLL003W	SFI1	unknown	-0.1132	-1.1	0.816836
YNR046W	TRM112	zinc ion binding	-0.1130	-1.1	0.40181
YIL142W	CCT2	unfolded protein binding	-0.1113	-1.1	0.0189217
YGL021W	ALK1	protein serine/threonine kinase	-0.1112	-1.1	0.581939
YGL025C	PGD1	RNA polymerase II transcription mediator	-0.1110	-1.1	0.578863
YMR308C	PSE1	protein carrier	-0.1110	-1.1	0.801939
YDR168W	CDC37	unfolded protein binding	-0.1107	-1.1	0.54073
YKR026C	GCN3	translation initiation factor	-0.1107	-1.1	0.70457
YCR023C		unknown	-0.1103	-1.1	0.503026
YIR027C	DAL1	allantoinase	-0.1100	-1.1	0.35964
YBR179C	FZO1	GTPase	-0.1098	-1.1	0.0903247
YDR199W			-0.1097	-1.1	0.612925
YHR052W	CIC1	protein binding	-0.1095	-1.1	0.71155

Table 1: continued.

ORF ID	Gene Name	Gene Function	Avg Log_2 Ratio	Fold Change	T-test
YNL318C	HXT14	galactose transporter	-0.1090	-1.1	0.561886
YOR334W	MRS2	magnesium ion transporter	-0.1090	-1.1	0.475746
YDL220C	CDC13	single-stranded DNA binding	-0.1085	-1.1	0.626707
YLR039C	RIC1	guanyl-nucleotide exchange factor	-0.1083	-1.1	0.406453
YJL213W		unknown	-0.1083	-1.1	0.0221943
YOR030W	DFG16	unknown	-0.1082	-1.1	0.706998
YDR132C		unknown	-0.1080	-1.1	0.396707
YIL066C	RNR3	ribonucleoside-diphosphate reductase	-0.1080	-1.1	0.519733
YGR149W		unknown	-0.1078	-1.1	0.58802
YBR287W	ZSP1	unknown	-0.1073	-1.1	0.55854
YJR075W	HOC1	alpha-1,6-mannosyltransferase *	-0.1070	-1.1	0.705919
YPL219W	PCL8	cyclin-dependent protein kinase	-0.1070	-1.1	0.417464
YDL115C	IWR1	unknown	-0.1065	-1.1	0.225728
YIR012W	SQT1	unknown	-0.1065	-1.1	0.396582
YNR031C	SSK2	MAP kinase	-0.1065	-1.1	0.641207
YGR194C	XKS1	xylulokinase	-0.1060	-1.1	0.552747
YPL107W		unknown	-0.1057	-1.1	0.459986
YKL185W	ASH1	specific transcriptional repressor	-0.1057	-1.1	0.467262
YFL007W	BLM10	proteasome activator	-0.1055	-1.1	0.640187
YML102W	CAC2	transcription regulator	-0.1053	-1.1	0.385734
YOR204W	DED1	RNA helicase	-0.1053	-1.1	0.394536
YOR252W	TMA16	unknown	-0.1052	-1.1	0.589433
YCL042W		unknown	-0.1052	-1.1	0.412876
YJR086W	STE18	GTPase	-0.1050	-1.1	0.37391
YCL002C		unknown	-0.1047	-1.1	0.502632
YOL163W		transporter	-0.1047	-1.1	0.483146
YCL068C		unknown	-0.1047	-1.1	0.417229
YER076C		unknown	-0.1043	-1.1	0.545744
YAL061W		oxidoreductase	-0.1040	-1.1	0.580307
YFL054C		transporter	-0.1038	-1.1	0.552908
YCR099C		unknown	-0.1038	-1.1	0.710152
YMR222C	FSH2	serine hydrolase	-0.1038	-1.1	0.732189
YJL064W			-0.1035	-1.1	0.41045
YDR499W	LCD1	protein binding	-0.1035	-1.1	0.490138
YLL039C	UBI4	protein tag*	-0.1032	-1.1	0.414639
YNL059C	ARP5	unknown	-0.1028	-1.1	0.540652
YDR121W	DPB4	epsilon DNA polymerase	-0.1028	-1.1	0.122586
YBR066C	NRG2	transcriptional repressor	-0.1028	-1.1	0.395035
YBL086C		unknown	-0.1025	-1.1	0.626178
Q0140	VAR1	structural constituent of ribosome	-0.1025	-1.1	0.165831
YGL166W	CUP2	ligand-regulated transcription factor	-0.1025	-1.1	0.406585
YDR193W			-0.1023	-1.1	0.562171
YIL147C	SLN1	osmosensor *	-0.1022	-1.1	0.262349
YCR076C		unknown	-0.1020	-1.1	0.429321
YER119C-A			-0.1020	-1.1	0.619839
YGR241C	YAP1802	clathrin binding	-0.1012	-1.1	0.561593
YPR081C	GRS2	glycine-tRNA ligase	-0.1010	-1.1	0.219001
YDR490C	PKH1	protein kinase	-0.1010	-1.1	0.443309
YDR419W	RAD30	eta DNA polymerase	-0.1008	-1.1	0.846298
YFL026W	STE2	mating-type alpha-factor	-0.1007	-1.1	0.615022
YJL157C	FAR1	cyclin-dependent protein kinase	-0.1003	-1.1	0.719177
YCRX17W			-0.1002	-1.1	0.566506
YER036C	ARB1	ATPase , coupled to transmembrane movement of substanc	-0.1000	-1.1	0.598631
YOR330C	MIP1	gamma DNA-directed DNA polymerase	-0.0998	-1.1	0.737422
YPL090C	RPS6A	structural constituent of ribosome	-0.0997	-1.1	0.162503
YEL068C			-0.0993	-1.1	0.629579
YHR197W	RIX1	unknown	-0.0993	-1.1	0.645877
YDL015C	TSC13	oxidoreductase	-0.0990	-1.1	0.548753
YPR021C	AGC1	L-glutamate transporter	-0.0990	-1.1	0.338194
YDR478W	SNM1	ribonuclease MRP	-0.0990	-1.1	0.316946
YAL048C	GEM1	GTPase	-0.0988	-1.1	0.687986
YGL023C	PIB2	phosphatidylinositol binding	-0.0988	-1.1	0.446593
YFR054C			-0.0985	-1.1	0.313029
YEL054C	RPL12A	structural constituent of ribosome	-0.0982	-1.1	0.137389
YDR460W	TFB3	general RNA polymerase II transcription factor	-0.0978	-1.1	0.208248
YNR030W	ALG12	alpha-1,6-mannosyltransferase	-0.0977	-1.1	0.172108
YEL002C	WBP1	dolichyl-diphosphooligosaccharide-protein glycotransferase	-0.0977	-1.1	0.481781
YDR196C		dephospho-CoA kinase	-0.0972	-1.1	0.763823
YAL042W	ERV46	unknown	-0.0970	-1.1	0.650228

Table 1: continued.

ORF ID	Gene Name	Gene Function	Avg Log_2 Ratio	Fold Change	T-test
YJL134W	LCB3	sphingosine-1-phosphate phosphatase	-0.0970	-1.1	0.620955
YPL191C		unknown	-0.0968	-1.1	0.600678
YPL139C	UME1	transcription corepressor	-0.0965	-1.1	0.4321
YGR214W	RPS0A	structural constituent of ribosome	-0.0960	-1.1	0.41406
YKR021W		unknown	-0.0958	-1.1	0.723693
YDR275W	BSC2	unknown	-0.0957	-1.1	0.150502
YJL080C	SCP160	RNA binding	-0.0957	-1.1	0.328908
YIR014W		unknown	-0.0953	-1.1	0.655018
YAL016W	TPD3	protein phosphatase type 2A	-0.0953	-1.1	0.353189
YNL186W	UBP10	ubiquitin-specific protease	-0.0953	-1.1	0.330683
YER017C	AFG3	ATPase *	-0.0952	-1.1	0.501967
YAL021C	CCR4	3'-5'-exoribonuclease	-0.0950	-1.1	0.460238
YGR167W	CLC1	structural molecule	-0.0948	-1.1	0.600349
YER108C			-0.0947	-1.1	0.593368
YNL071W	LAT1	dihydrolipoyllysine-residue acetyltransferase	-0.0945	-1.1	0.660212
YHR003C		unknown	-0.0942	-1.1	0.349251
YHR131C		unknown	-0.0942	-1.1	0.119275
YIL155C	GUT2	glycerol-3-phosphate dehydrogenase	-0.0942	-1.1	0.552905
YIL102C		unknown	-0.0938	-1.1	0.454619
YDR483W	KRE2	alpha-1,2-mannosyltransferase	-0.0933	-1.1	0.157579
YLR009W	RLP24	unknown	-0.0933	-1.1	0.365664
YJR021C	REC107	unknown	-0.0932	-1.1	0.461811
YOR141C	ARP8	unknown	-0.0927	-1.1	0.624924
YML003W		unknown	-0.0927	-1.1	0.60556
YBL069W	AST1	unknown	-0.0918	-1.1	0.453725
YPL060C-A		protein binding	-0.0915	-1.1	0.0892925
YDR240C	SNU56	mRNA binding	-0.0915	-1.1	0.740086
YER079W		unknown	-0.0912	-1.1	0.666715
YOL038W	PRE6	endopeptidase	-0.0910	-1.1	0.0454698
YKR088C	TVP38	unknown	-0.0910	-1.1	0.378549
YJL056C	ZAP1	DNA binding	-0.0907	-1.1	0.725004
YDR325W	YCG1	unknown	-0.0905	-1.1	0.512063
YHR132C	ECM14	metalloendopeptidase	-0.0897	-1.1	0.607188
YKL124W	SSH4	unknown	-0.0892	-1.1	0.4995
YGL186C	TPN1	vitamin transporter	-0.0892	-1.1	0.56691
YLR206W	ENT2	clathrin binding	-0.0888	-1.1	0.566322
YDL005C	MED2	RNA polymerase II transcription mediator	-0.0882	-1.1	0.210473
YBR275C	RIF1	protein binding	-0.0880	-1.1	0.694292
YJR006W	HYS2	delta DNA polymerase *	-0.0878	-1.1	0.466511
YJL145W	SFH5	phosphatidylinositol transporter	-0.0877	-1.1	0.737913
YBR227C	MCX1	unfolded protein binding	-0.0873	-1.1	0.201705
YOR036W	PEP12	t-SNARE	-0.0873	-1.1	0.815163
YJL158C	CIS3	structural constituent of cell wall	-0.0870	-1.1	0.552086
YDR227W	SIR4	histone binding	-0.0870	-1.1	0.68597
YDR388W	RVS167	cytoskeletal protein binding	-0.0863	-1.1	0.337839
YBR024W	SCO2	thioredoxin peroxidase	-0.0863	-1.1	0.649241
YNL214W	PEX17	protein binding	-0.0862	-1.1	0.752375
YBR236C	ABD1	mRNA (guanine-N7-)-methyltransferase	-0.0855	-1.1	0.0825306
YOR283W		unknown	-0.0853	-1.1	0.42211
YOR335C	ALA1	alanine-tRNA ligase	-0.0853	-1.1	0.560501
YKL065C	YET1	unknown	-0.0852	-1.1	0.0141304
YLR025W	SNF7	protein binding	-0.0848	-1.1	0.756184
YNR067C	DSE4	glucan 1,3-beta-glucosidase	-0.0847	-1.1	0.356448
YER098W	UBP9	ubiquitin-specific protease	-0.0843	-1.1	0.62841
YHR057C	CPR2	peptidyl-prolyl cis-trans isomerase	-0.0842	-1.1	0.387437
YDL109C		unknown	-0.0842	-1.1	0.654916
YHR182W		unknown	-0.0842	-1.1	0.633753
YML022W	APT1	adenine phosphoribosyltransferase	-0.0842	-1.1	0.125272
YJR114W			-0.0840	-1.1	0.576313
YPR088C	SRP54	signal sequence binding	-0.0838	-1.1	0.723875
YLR330W	CHS5	unknown	-0.0837	-1.1	0.247817
YMR076C	PDS5	structural molecule	-0.0837	-1.1	0.560107
YBR158W	AMN1	protein binding	-0.0837	-1.1	0.350479
YGL207W	SPT16	RNA polymerase II transcription elongation factor	-0.0835	-1.1	0.363243
YJL036W	SNX4	lipid binding	-0.0833	-1.1	0.0747348
YKL129C	MYO3	microfilament motor	-0.0832	-1.1	0.577019
YLR433C	CNA1	calcium-dependent protein serine/threonine phosphatase	-0.0832	-1.1	0.474033
YCR069W	CPR4	peptidyl-prolyl cis-trans isomerase	-0.0832	-1.1	0.407747
YOR099W	KTR1	alpha-1,2-mannosyltransferase	-0.0830	-1.1	0.692675

Table 1: continued.

ORF ID	Gene Name	Gene Function	Avg Log_2 Ratio	Fold Change	T-test
YPR088C	SRP54	signal sequence binding	-0.0838	-1.1	0.723875
YLR330W	CHS5	unknown	-0.0837	-1.1	0.247817
YMR076C	PDS5	structural molecule	-0.0837	-1.1	0.560107
YBR158W	AMN1	protein binding	-0.0837	-1.1	0.350479
YGL207W	SPT16	RNA polymerase II transcription elongation factor	-0.0835	-1.1	0.363243
YJL036W	SNX4	lipid binding	-0.0833	-1.1	0.0747348
YKL129C	MYO3	microfilament motor	-0.0832	-1.1	0.577019
YLR433C	CNA1	calcium-dependent protein serine/threonine phosphatase	-0.0832	-1.1	0.474033
YCR069W	CPR4	peptidyl-prolyl cis-trans isomerase	-0.0832	-1.1	0.407747
YOR099W	KTR1	alpha-1,2-mannosyltransferase	-0.0830	-1.1	0.692675
YIL161W		unknown	-0.0825	-1.1	0.299947
YER031C	YPT31	GTPase	-0.0825	-1.1	0.524133
YIL061C	SNP1	mRNA binding	-0.0823	-1.1	0.630719
YIR025W	MND2	unknown	-0.0818	-1.1	0.123731
YDR080W	VPS41	Rab guanyl-nucleotide exchange factor	-0.0810	-1.1	0.614169
YDR120C	TRM1	tRNA (guanine-N2-)-methyltransferase	-0.0810	-1.1	0.601546
YOR176W	HEM15	ferrochelatase	-0.0807	-1.1	0.0104136
YHR002W	LEU5	coenzyme A transporter	-0.0805	-1.1	0.741839
YMR150C	IMP1	peptidase *	-0.0805	-1.1	0.281257
YPR143W	RRP15	unknown	-0.0805	-1.1	0.0625195
YGL076C	RPL7A	structural constituent of ribosome	-0.0800	-1.1	0.259775
YGL038C	OCH1	alpha-1,6-mannosyltransferase *	-0.0797	-1.1	0.515338
YAL051W	OAF1	DNA binding	-0.0797	-1.1	0.46412
YKL068W	NUP100	structural molecule	-0.0797	-1.1	0.518192
YNL126W	SPC98	structural constituent of cytoskeleton	-0.0795	-1.1	0.677532
YBL068W	PRS4	ribose phosphate diphosphokinase	-0.0795	-1.1	0.399251
YDR485C	VPS72	unknown	-0.0795	-1.1	0.490134
YGL261C	PAU11	unknown	-0.0792	-1.1	0.746785
YKL142W	MRP8	structural constituent of ribosome	-0.0792	-1.1	0.522486
YMR295C		unknown	-0.0792	-1.1	0.0874288
YNR029C		unknown	-0.0792	-1.1	0.750417
YIL156W	UBP7	ubiquitin-specific protease	-0.0790	-1.1	0.471508
YDR214W	AHA1	chaperone activator	-0.0788	-1.1	0.536494
YDR228C	PCF11	protein binding	-0.0788	-1.1	0.415821
YDR178W	SDH4	succinate dehydrogenase	-0.0783	-1.1	0.532243
YJR090C	GRR1	protein binding	-0.0782	-1.1	0.301653
YNL044W	YIP3	unknown	-0.0780	-1.1	0.433749
YOR090C	PTC5	protein phosphatase type 2C	-0.0780	-1.1	0.418865
YLR259C	HSP60	single-stranded DNA binding	-0.0780	-1.1	0.711928
YNL022C		unknown	-0.0778	-1.1	0.781413
YBR192W	RIM2	transporter	-0.0777	-1.1	0.383125
YDR408C	ADE8	phosphoribosylglycinamide formyltransferase	-0.0773	-1.1	0.239948
YMR120C	ADE17	IMP cyclohydrolase *	-0.0770	-1.1	0.545417
YNL049C	SFB2	unknown	-0.0767	-1.1	0.388245
YCR067C	SED4	unknown	-0.0763	-1.1	0.878061
YJL033W	HCA4	ATP-dependent RNA helicase	-0.0762	-1.1	0.674849
YOR350C	MNE1	unknown	-0.0762	-1.1	0.745499
YGR184C	UBR1	ubiquitin-protein ligase	-0.0755	-1.1	0.586155
YLL064C	PAU18	unknown	-0.0752	-1.1	0.0922036
YHR115C	DMA1	unknown	-0.0752	-1.1	0.512706
YNL338W			-0.0750	-1.1	0.757544
YLR461W	PAU4	unknown	-0.0748	-1.1	0.603761
YKR096W		unknown	-0.0747	-1.1	0.267379
YJL170C	ASG7	unknown	-0.0742	-1.1	0.685283
YIL038C	NOT3	3'-5'-exoribonuclease	-0.0742	-1.1	0.714739
YIL137C	TMA108	metalloendopeptidase	-0.0742	-1.1	0.365396
YLR021W		unknown	-0.0738	-1.1	0.732806
YIL058W			-0.0732	-1.1	0.706899
YIR006C	PAN1	protein binding	-0.0730	-1.1	0.279951
YDR276C	PMP3	unknown	-0.0728	-1.1	0.496391
YGL048C	RPT6	ATPase *	-0.0727	-1.1	0.566183
YGL248W	PDE1	3',5'-cyclic-AMP phosphodiesterase	-0.0723	-1.1	0.779259
YDL044C	MTF2	RNA binding	-0.0720	-1.1	0.810227
YOR245C	DGA1	diacylglycerol O-acyltransferase	-0.0718	-1.1	0.436354
YPL057C	SUR1	mannosyltransferase *	-0.0712	-1.1	0.592684
YJR023C			-0.0710	-1.1	0.31534
YBL026W	LSM2	RNA binding	-0.0708	-1.1	0.201151
YHR016C	YSC84	unknown	-0.0708	-1.1	0.704123
YIL051C	MMF1	unknown	-0.0707	-1.1	0.611708

Table 1: continued.

ORF ID	Gene Name	Gene Function	Avg Log_2 Ratio	Fold Change	T-test
YCR006C			-0.0707	-1.1	0.603686
YGR019W	UGA1	4-aminobutyrate transaminase	-0.0707	-1.1	0.547897
YOR355W	GDS1	unknown	-0.0707	-1.1	0.592982
YMR216C	SKY1	protein kinase	-0.0702	-1.0	0.812541
YKR001C	VPS1	GTPase	-0.0698	-1.0	0.790657
YBR245C	ISW1	ATPase	-0.0697	-1.0	0.529826
YGR218W	CRM1	protein carrier	-0.0695	-1.0	0.488509
YMR285C	NGL2	endoribonuclease	-0.0692	-1.0	0.552782
YLR198C			-0.0683	-1.0	0.635873
YDR142C	PEX7	peroxisome targeting sequence binding	-0.0682	-1.0	0.159493
YKL032C	IXR1	DNA binding	-0.0678	-1.0	0.336766
YIR035C		unknown	-0.0677	-1.0	0.794106
YJR134C	SGM1	unknown	-0.0670	-1.0	0.793626
YCL022C			-0.0670	-1.0	0.74836
YDR003W	RCR2	unknown	-0.0668	-1.0	0.528346
YLR436C	ECM30	unknown	-0.0667	-1.0	0.764871
YMR163C		unknown	-0.0667	-1.0	0.677302
YBR205W	KTR3	mannosyltransferase	-0.0667	-1.0	0.465679
YJR015W		unknown	-0.0667	-1.0	0.786448
YIL091C		RNA helicase	-0.0663	-1.0	0.566556
YJL074C	SMC3	ATPase	-0.0658	-1.0	0.72267
YBR234C	ARC40	structural constituent of cytoskeleton	-0.0658	-1.0	0.329258
YAL014C	SYN8	SNAP receptor	-0.0653	-1.0	0.538265
YGR005C	TFG2	general RNA polymerase II transcription factor	-0.0650	-1.0	0.739137
YBR209W			-0.0648	-1.0	0.23019
YML061C	PIF1	DNA helicase	-0.0645	-1.0	0.80414
YCR081W	SRB8	RNA polymerase II transcription mediator	-0.0645	-1.0	0.268712
YIL118W	RHO3	GTPase *	-0.0643	-1.0	0.581101
YGL112C	TAF6	general RNA polymerase II transcription factor	-0.0642	-1.0	0.769054
YNL302C	RPS19B	structural constituent of ribosome	-0.0642	-1.0	0.212852
YCL025C	AGP1	amino acid transporter	-0.0642	-1.0	0.141827
YPL096W	PNG1	peptide-N4-(N-acetyl-beta-glucosaminyl)asparagine amidas	-0.0642	-1.0	0.74358
YDR296W	MHR1	transcription regulator	-0.0642	-1.0	0.790316
YBR260C	RGD1	Rho GTPase activator	-0.0640	-1.0	0.599352
YPL138C	SPP1	histone lysine N-methyltransferase (H3-K4 specific)	-0.0640	-1.0	0.37735
YLL007C		unknown	-0.0640	-1.0	0.707012
YIL080W		protein binding	-0.0638	-1.0	0.213685
YHR118C	ORC6	DNA replication origin binding	-0.0638	-1.0	0.759624
YNL058C		unknown	-0.0637	-1.0	0.667642
YOR211C	MGM1	GTPase	-0.0637	-1.0	0.756564
YDR479C	PEX29	unknown	-0.0635	-1.0	0.714359
YIL120W	QDR1	multidrug transporter	-0.0633	-1.0	0.419906
YEL027W	CUP5	hydrogen ion transporter	-0.0633	-1.0	0.57829
YDR520C		unknown	-0.0632	-1.0	0.0981678
YER159C	BUR6	transcription corepressor	-0.0632	-1.0	0.589858
YGR200C	ELP2	RNA polymerase II transcription elongation factor	-0.0630	-1.0	0.636785
YDL077C	VAM6	Rab guanyl-nucleotide exchange factor	-0.0628	-1.0	0.642508
YLR061W	RPL22A	structural constituent of ribosome	-0.0625	-1.0	0.568171
YJR054W		unknown	-0.0623	-1.0	0.821618
YLR266C	PDR8	DNA binding	-0.0622	-1.0	0.735361
YNL197C	WHI3	RNA binding	-0.0620	-1.0	0.0354348
YNL230C	ELA1	transcriptional elongation regulator	-0.0620	-1.0	0.472669
YPL102C			-0.0618	-1.0	0.770348
YER142C	MAG1	alkylbase DNA N-glycosylase	-0.0617	-1.0	0.663885
YPR134W	MSS18	unknown	-0.0617	-1.0	0.877084
YLR344W	RPL26A	structural constituent of ribosome*	-0.0615	-1.0	0.529548
YGL083W	SCY1	unknown	-0.0608	-1.0	0.165426
YJL016W		unknown	-0.0602	-1.0	0.0949792
YDR387C		permease	-0.0598	-1.0	0.736849
YFR029W	PTR3	amino acid binding	-0.0597	-1.0	0.716968
YIL016W	SNL1	chaperone regulator	-0.0593	-1.0	0.687521
YDR106W	ARP10	structural constituent of cytoskeleton	-0.0590	-1.0	0.375597
YPR101W	SNT309	protein binding	-0.0588	-1.0	0.464079
YIL139C	REV7	zeta DNA polymerase	-0.0583	-1.0	0.636454
YDL167C	NRP1	unknown	-0.0583	-1.0	0.688413
YDL204W	RTN2	unknown	-0.0582	-1.0	0.561918
YIL018W	RPL2B	structural constituent of ribosome	-0.0580	-1.0	0.467008
YDR271C			-0.0577	-1.0	0.568474
YBR300C			-0.0575	-1.0	0.727731

Table 1: continued.

ORF ID	Gene Name	Gene Function	Avg Log_2 Ratio	Fold Change	T-test
YCR055C			-0.0575	-1.0	0.66127
YDR508C	GNP1	amino acid transporter	-0.0572	-1.0	0.639641
YNL330C	RPD3	histone deacetylase	-0.0568	-1.0	0.670249
YIL084C	SDS3	protein binding	-0.0563	-1.0	0.571722
YBL006C	LDB7	unknown	-0.0562	-1.0	0.517844
YHR084W	STE12	transcription factor	-0.0560	-1.0	0.797162
YPL093W	NOG1	GTP binding	-0.0558	-1.0	0.708988
YOL108C	INO4	DNA binding	-0.0557	-1.0	0.807595
YML110C	COQ5	2-hexaprenyl-6-methoxy-1,4-benzoquinone methyltransfera	-0.0557	-1.0	0.438954
YJR132W	NMD5	protein carrier	-0.0555	-1.0	0.550784
YOL049W	GSH2	glutathione synthase	-0.0553	-1.0	0.834448
YJL167W	ERG20	dimethylallyltranstransferase *	-0.0552	-1.0	0.504351
YNR060W	FRE4	ferric-chelate reductase	-0.0552	-1.0	0.699472
YNL035C		unknown	-0.0550	-1.0	0.901154
YLR131C	ACE2	transcriptional activator	-0.0550	-1.0	0.827293
YJL199C			-0.0550	-1.0	0.33007
YDR223W	CRF1	transcriptional repressor	-0.0550	-1.0	0.627539
YFL035C			-0.0550	-1.0	0.743481
YLR200W	YKE2	tubulin binding	-0.0550	-1.0	0.922733
YFL002C	SPB4	ATP-dependent RNA helicase	-0.0548	-1.0	0.698917
YMR080C	NAM7	ATP-dependent RNA helicase	-0.0547	-1.0	0.658536
YKL145W	RPT1	ATPase *	-0.0543	-1.0	0.780687
YBR281C		unknown	-0.0540	-1.0	0.754943
YLR362W	STE11	MAP kinase	-0.0538	-1.0	0.628554
YDR194C	MSS116	RNA splicing factor	-0.0537	-1.0	0.594011
YPR042C	PUF2	mRNA binding	-0.0532	-1.0	0.740833
YOR010C	TIR2	unknown	-0.0532	-1.0	0.33762
YPL240C	HSP82	ATPase , coupled	-0.0528	-1.0	0.656215
YHL029C	OCA5	unknown	-0.0523	-1.0	0.44933
YDR538W	PAD1	carboxy-lyase	-0.0523	-1.0	0.828355
YIL143C	SSL2	general RNA polymerase II transcription factor	-0.0517	-1.0	0.732884
YBR239C		unknown	-0.0513	-1.0	0.763219
YDR062W	LCB2	serine C-palmitoyltransferase	-0.0508	-1.0	0.128936
YBL024W	NCL1	tRNA (cytosine-5-)-methyltransferase	-0.0508	-1.0	0.445493
YOL120C	RPL18A	structural constituent of ribosome	-0.0507	-1.0	0.581717
YDR415C		unknown	-0.0507	-1.0	0.408703
YKL184W	SPE1	ornithine decarboxylase	-0.0507	-1.0	0.904162
YPR033C	HTS1	histidine-tRNA ligase	-0.0507	-1.0	0.688431
YGR250C		RNA binding	-0.0503	-1.0	0.78522
YLR253W		unknown	-0.0503	-1.0	0.79846
YJL099W	CHS6	unknown	-0.0503	-1.0	0.509136
YAL024C	LTE1	guanyl-nucleotide exchange factor	-0.0502	-1.0	0.84551
YAL031C	GIP4	unknown	-0.0502	-1.0	0.327453
YDL025C		protein kinase	-0.0500	-1.0	0.715289
YOR123C	LEO1	RNA polymerase II transcription elongation factor	-0.0498	-1.0	0.761871
YNR038W	DBP6	ATP-dependent RNA helicase	-0.0497	-1.0	0.85949
YDR052C	DBF4	protein serine/threonine kinase	-0.0497	-1.0	0.368072
YJL209W	CBP1	mRNA binding	-0.0495	-1.0	0.717052
YGR174C	CBP4	unknown	-0.0495	-1.0	0.494709
YMR241W	YHM2	DNA binding	-0.0493	-1.0	0.822219
YGR267C	FOL2	GTP cyclohydrolase I	-0.0492	-1.0	0.723074
YEL038W	UTR4	unknown	-0.0488	-1.0	0.822115
YBL050W	SEC17	soluble NSF attachment protein	-0.0487	-1.0	0.763212
YDR055W	PST1	unknown	-0.0487	-1.0	0.645496
YPR091C		unknown	-0.0483	-1.0	0.653785
YOR111W		unknown	-0.0482	-1.0	0.529584
YOR014W	RTS1	protein phosphatase type 2A	-0.0478	-1.0	0.634223
YDR209C			-0.0478	-1.0	0.726479
YHR009C		unknown	-0.0478	-1.0	0.780936
YMR045C			-0.0473	-1.0	0.596718
YKL224C	PAU16	unknown	-0.0458	-1.0	0.643853
YJR065C	ARP3	structural constituent of cytoskeleton*	-0.0458	-1.0	0.805372
YPL097W	MSY1	tyrosine-tRNA ligase	-0.0458	-1.0	0.856857
YBR095C	RXT2	unknown	-0.0455	-1.0	0.758017
YJL120W			-0.0452	-1.0	0.744544
YLR311C			-0.0450	-1.0	0.832563
YPR083W	MDM36	unknown	-0.0448	-1.0	0.880933
YPL229W		unknown	-0.0447	-1.0	0.73406
YLR107W	REX3	3'-5' exonuclease	-0.0447	-1.0	0.744217

Table 1: continued.

ORF ID	Gene Name	Gene Function	Avg Log_2 Ratio	Fold Change	T-test
YBR193C	MED8	RNA polymerase II transcription mediator	-0.0445	-1.0	0.66091
YDL240W	LRG1	Rho GTPase activator	-0.0443	-1.0	0.88954
YDR169C	STB3	unknown	-0.0443	-1.0	0.738794
YLR027C	AAT2	aspartate transaminase	-0.0443	-1.0	0.836396
YNL243W	SLA2	protein binding	-0.0438	-1.0	0.693871
YLR087C	CSF1	unknown	-0.0427	-1.0	0.813665
YCR077C	PAT1	unknown	-0.0425	-1.0	0.32749
YPL269W	KAR9	unknown	-0.0425	-1.0	0.754015
YBR279W	PAF1	RNA polymerase II transcription elongation factor	-0.0425	-1.0	0.797614
YLR277C	YSH1	RNA binding	-0.0423	-1.0	0.744149
YML126C	ERG13	hydroxymethylglutaryl-CoA synthase	-0.0422	-1.0	0.692601
YGL030W	RPL30	structural constituent of ribosome	-0.0418	-1.0	0.77923
YBL085W	BOI1	phospholipid binding	-0.0417	-1.0	0.849995
YKR101W	SIR1	DNA binding	-0.0415	-1.0	0.843167
YHL014C	YLF2	GTP binding	-0.0413	-1.0	0.821546
YNR006W	VPS27	protein binding	-0.0412	-1.0	0.70028
YDR175C	RSM24	structural constituent of ribosome	-0.0412	-1.0	0.831344
YML093W	UTP14	snoRNA binding	-0.0412	-1.0	0.830397
YHR165C	PRP8	RNA splicing factor	-0.0408	-1.0	0.688679
YHL002W	HSE1	protein binding	-0.0405	-1.0	0.208205
YDL047W	SIT4	protein serine/threonine phosphatase	-0.0405	-1.0	0.758653
YOL064C	MET22	3'(2'),5'-bisphosphate nucleotidase	-0.0398	-1.0	0.899443
YDR037W	KRS1	lysine-tRNA ligase	-0.0395	-1.0	0.573149
YFL009W	CDC4	protein binding	-0.0392	-1.0	0.811173
YLR223C	IFH1	transcription factor	-0.0390	-1.0	0.413213
YGL135W	RPL1B	structural constituent of ribosome	-0.0387	-1.0	0.472007
YJR115W		unknown	-0.0385	-1.0	0.813272
YHR032W		unknown	-0.0385	-1.0	0.881959
YOR278W	HEM4	uroporphyrinogen-III synthase	-0.0383	-1.0	0.801465
YHR157W	REC104	unknown	-0.0382	-1.0	0.625552
YLR152C		unknown	-0.0380	-1.0	0.567681
YKL108W	SLD2	unknown	-0.0377	-1.0	0.76919
YCL064C	CHA1	L-serine ammonia-lyase *	-0.0375	-1.0	0.627189
YDR369C	XRS2	protein binding	-0.0373	-1.0	0.771616
YCR084C	TUP1	general transcriptional repressor	-0.0373	-1.0	0.692725
YLR456W		unknown	-0.0373	-1.0	0.920594
YAL011W	SWC3	unknown	-0.0368	-1.0	0.629277
YDR309C	GIC2	small GTPase regulator	-0.0365	-1.0	0.696474
YNL226W			-0.0365	-1.0	0.910752
YFR049W	YMR31	structural constituent of ribosome	-0.0363	-1.0	0.755133
YIL036W	CST6	specific RNA polymerase II transcription factor	-0.0363	-1.0	0.685682
YER156C		unknown	-0.0358	-1.0	0.837611
YLR094C	GIS3	unknown	-0.0357	-1.0	0.428858
YBL106C	SRO77	unknown	-0.0353	-1.0	0.809037
YIL005W	EPS1	protein disulfide isomerase	-0.0352	-1.0	0.767351
YNL199C	GCR2	transcriptional activator	-0.0352	-1.0	0.676969
YNL004W	HRB1	RNA binding	-0.0348	-1.0	0.871035
YLR258W	GSY2	glycogen (starch) synthase	-0.0348	-1.0	0.508692
YGR192C	TDH3	glyceraldehyde-3-phosphate dehydrogenase	-0.0348	-1.0	0.906233
YBR006W	UGA2	succinate-semialdehyde dehydrogenase	-0.0348	-1.0	0.827324
YDR264C	AKR1	protein-cysteine S-palmitoleyltransferase	-0.0343	-1.0	0.782456
YLR345W		6-phosphofructo-2-kinase	-0.0333	-1.0	0.402839
YGL259W	YPS5	aspartic-type endopeptidase	-0.0332	-1.0	0.886959
YBR272C	HSM3	unknown	-0.0328	-1.0	0.801052
YER038C	KRE29	unknown	-0.0327	-1.0	0.880421
YFR031C	SMC2	ATPase *	-0.0325	-1.0	0.847582
YJL066C	MPM1	unknown	-0.0325	-1.0	0.825287
YHL017W		unknown	-0.0318	-1.0	0.738255
YLR115W	CFT2	RNA binding	-0.0315	-1.0	0.864786
YBL005W	PDR3	DNA binding	-0.0315	-1.0	0.877363
YLR249W	YEF3	translation elongation factor	-0.0315	-1.0	0.826874
YGR029W	ERV1	thiol oxidase	-0.0315	-1.0	0.910451
YDR016C	DAD1	structural constituent of cytoskeleton	-0.0312	-1.0	0.711208
YHR203C	RPS4B	structural constituent of ribosome	-0.0312	-1.0	0.565359
YML074C	FPR3	peptidyl-prolyl cis-trans isomerase	-0.0312	-1.0	0.551524
YCLX11W			-0.0310	-1.0	0.775965
YMR058W	FET3	ferroxidase	-0.0308	-1.0	0.705061
YDR451C	YHP1	DNA binding	-0.0308	-1.0	0.89077
YDR341C		arginine-tRNA ligase	-0.0307	-1.0	0.857252

Table 1: continued.

ORF ID	Gene Name	Gene Function	Avg Log_2 Ratio	Fold Change	T-test
YDL035C	GPR1	G-protein coupled receptor	-0.0307	-1.0	0.235418
YEL021W	URA3	orotidine-5'-phosphate decarboxylase	-0.0303	-1.0	0.656666
YJR110W	YMR1	phosphoric monoester hydrolase *	-0.0303	-1.0	0.857032
YER173W	RAD24	DNA clamp loader	-0.0302	-1.0	0.819899
YKL178C	STE3	mating-type a-factor	-0.0297	-1.0	0.811775
YDL155W	CLB3	cyclin-dependent protein kinase	-0.0290	-1.0	0.789163
YDR011W	SNQ2	xenobiotic-transporting ATPase	-0.0283	-1.0	0.512959
YDR312W	SSF2	rRNA binding	-0.0282	-1.0	0.8547
YDR082W	STN1	protein binding	-0.0280	-1.0	0.810832
YPR036W	VMA13	hydrogen-transporting ATPase , rotational mechanism	-0.0280	-1.0	0.840109
YPL272C		unknown	-0.0278	-1.0	0.902439
YBR226C			-0.0277	-1.0	0.92866
YDL076C	RXT3	unknown	-0.0270	-1.0	0.629982
YBR189W	RPS9B	structural constituent of ribosome	-0.0268	-1.0	0.86549
YPL032C	SVL3	unknown	-0.0267	-1.0	0.897005
YMR125W	STO1	mRNA binding	-0.0267	-1.0	0.782313
YDR170C	SEC7	ARF guanyl-nucleotide exchange factor	-0.0267	-1.0	0.680173
YPL053C	KTR6	mannosylphosphate transferase	-0.0265	-1.0	0.876311
YJR088C		unknown	-0.0263	-1.0	0.763243
YER068W	MOT2	3'-5'-exoribonuclease *	-0.0262	-1.0	0.909695
YLR352W		unknown	-0.0257	-1.0	0.894795
YBR075W			-0.0255	-1.0	0.91607
YDR471W	RPL27B	structural constituent of ribosome	-0.0255	-1.0	0.806729
YER005W	YND1	nucleoside-diphosphatase	-0.0255	-1.0	0.799056
YLR454W	FMP27	unknown	-0.0252	-1.0	0.818101
YNL314W	DAL82	transcriptional activator	-0.0252	-1.0	0.876213
YDL229W	SSB1	ATPase *	-0.0247	-1.0	0.876287
YDL038C		unknown	-0.0247	-1.0	0.859105
YOR006C		unknown	-0.0245	-1.0	0.848252
YLL027W	ISA1	unknown	-0.0243	-1.0	0.0889849
YCR018C	SRD1	unknown	-0.0240	-1.0	0.882025
YHR086W	NAM8	RNA binding	-0.0238	-1.0	0.905254
YER018C	SPC25	structural constituent of cytoskeleton	-0.0238	-1.0	0.940266
YLR002C	NOC3	protein binding	-0.0237	-1.0	0.918626
YDR404C	RPB7	DNA-directed RNA polymerase	-0.0235	-1.0	0.870546
YPL203W	TPK2	protein serine/threonine kinase	-0.0233	-1.0	0.849897
YBR086C	IST2	unknown	-0.0233	-1.0	0.620594
YER016W	BIM1	structural constituent of cytoskeleton	-0.0232	-1.0	0.895782
YGL090W	LIF1	structural molecule	-0.0230	-1.0	0.873865
YPL067C		unknown	-0.0228	-1.0	0.739484
YLR055C	SPT8	transcription cofactor	-0.0225	-1.0	0.480433
YKR038C	KAE1	metalloendopeptidase *	-0.0222	-1.0	0.884817
YDL177C		unknown	-0.0222	-1.0	0.888284
YGR243W	FMP43	unknown	-0.0222	-1.0	0.779583
YDR211W	GCD6	translation initiation factor	-0.0218	-1.0	0.975059
YFL003C	MSH4	DNA binding	-0.0213	-1.0	0.909779
YHR030C	SLT2	MAP kinase	-0.0212	-1.0	0.816458
YFL044C	OTU1	ubiquitin-specific protease	-0.0212	-1.0	0.739483
YLR447C	VMA6	hydrogen-transporting ATPase , rotational mechanism	-0.0207	-1.0	0.84532
YJL061W	NUP82	structural molecule	-0.0205	-1.0	0.699444
YDL197C	ASF2	unknown	-0.0205	-1.0	0.88636
YER183C	FAU1	5-formyltetrahydrofolate cyclo-ligase	-0.0202	-1.0	0.835756
YDR242W	AMD2	amidase	-0.0202	-1.0	0.79376
YGL188C			-0.0193	-1.0	0.914519
YHR202W		unknown	-0.0192	-1.0	0.566001
YPR004C		electron carrier	-0.0187	-1.0	0.780857
YBR031W	RPL4A	structural constituent of ribosome	-0.0185	-1.0	0.556407
YGL215W	CLG1	cyclin-dependent protein kinase	-0.0183	-1.0	0.844932
YBL092W	RPL32	structural constituent of ribosome	-0.0183	-1.0	0.901405
YDR492W	IZH1	metal ion binding	-0.0182	-1.0	0.591465
YIL089W		unknown	-0.0178	-1.0	0.892496
YJR142W		unknown	-0.0177	-1.0	0.872164
YKL116C	PRR1	receptor signaling protein serine/threonine kinase	-0.0175	-1.0	0.913189
YPL070W	MUK1	unknown	-0.0175	-1.0	0.89165
YIL129C	TAO3	unknown	-0.0173	-1.0	0.85467
YJL160C		unknown	-0.0170	-1.0	0.851012
YOR155C	ISN1	IMP 5'-nucleotidase	-0.0165	-1.0	0.89266
YMR087W		phosphoric monoester hydrolase	-0.0163	-1.0	0.966298
YDL119C		transporter	-0.0163	-1.0	0.725175

Table 1: continued.

ORF ID	Gene Name	Gene Function	Avg Log_2 Ratio	Fold Change	T-test
YML028W	TSA1	thioredoxin peroxidase	-0.0163	-1.0	0.853232
YNL247W		cysteine-tRNA ligase	-0.0163	-1.0	0.914835
YMR182C	RGM1	RNA polymerase II transcription factor	-0.0160	-1.0	0.92509
YEL043W		unknown	-0.0160	-1.0	0.933527
YMR211W	DML1	structural molecule	-0.0160	-1.0	0.905066
YIL123W	SIM1	unknown	-0.0158	-1.0	0.820533
YDR422C	SIP1	AMP-activated protein kinase	-0.0157	-1.0	0.965271
YFL019C			-0.0148	-1.0	0.951163
YOR149C	SMP3	alpha-1,2-mannosyltransferase	-0.0147	-1.0	0.750432
YBL041W	PRE7	endopeptidase	-0.0147	-1.0	0.867584
YHR117W	TOM71	protein transporter	-0.0145	-1.0	0.935168
YLR334C			-0.0143	-1.0	0.934978
YOR362C	PRE10	endopeptidase	-0.0142	-1.0	0.881543
YPL214C	THI6	hydroxyethylthiazole kinase	-0.0142	-1.0	0.882508
YER099C	PRS2	ribose phosphate diphosphokinase	-0.0140	-1.0	0.833864
YHR183W	GND1	phosphogluconate dehydrogenase	-0.0140	-1.0	0.885177
YER118C	SHO1	osmosensor	-0.0138	-1.0	0.463847
YKL029C	MAE1	malic enzyme	-0.0138	-1.0	0.63547
YKL039W	PTM1	unknown	-0.0135	-1.0	0.888301
YBR220C		unknown	-0.0130	-1.0	0.707317
YDR076W	RAD55	protein binding	-0.0128	-1.0	0.896876
YGL052W			-0.0128	-1.0	0.961485
YDR537C			-0.0125	-1.0	0.908935
YNR048W		phospholipid-translocating ATPase	-0.0123	-1.0	0.966898
YBR178W			-0.0122	-1.0	0.948954
YKL094W	YJU3	serine hydrolase	-0.0113	-1.0	0.926478
YLR246W	ERF2	protein-cysteine S-palmitoleyltransferase	-0.0113	-1.0	0.834724
YGR007W	MUQ1	ethanolamine-phosphate cytidylyltransferase	-0.0110	-1.0	0.780634
YCL076W			-0.0108	-1.0	0.937906
YOL150C			-0.0107	-1.0	0.979358
YIR008C	PRI1	alpha DNA polymerase	-0.0105	-1.0	0.917847
YCL010C	SGF29	unknown	-0.0102	-1.0	0.960243
YBL011W	SCT1	glycerol-3-phosphate O-acyltransferase	-0.0102	-1.0	0.931716
YPR016C	TIF6	unknown	-0.0097	-1.0	0.94569
YLR343W	GAS2	1,3-beta-glucanosyltransferase	-0.0095	-1.0	0.935365
YMR032W	HOF1	cytoskeletal protein binding	-0.0087	-1.0	0.982998
YFL021C-A			-0.0087	-1.0	0.902364
YOL009C	MDM12	unknown	-0.0087	-1.0	0.951285
YBL082C	ALG3	alpha-1,3-mannosyltransferase	-0.0085	-1.0	0.961397
YKL186C	MTR2	protein binding	-0.0085	-1.0	0.946552
YCL040W	GLK1	glucokinase	-0.0083	-1.0	0.954952
YDR108W	GSG1	unknown	-0.0083	-1.0	0.936945
YPR050C			-0.0083	-1.0	0.768144
YMR100W	MUB1	unknown	-0.0080	-1.0	0.965812
YMR036C	MIH1	protein tyrosine phosphatase	-0.0080	-1.0	0.969095
YPL079W	RPL21B	structural constituent of ribosome	-0.0080	-1.0	0.962126
YOR396W		helicase	-0.0078	-1.0	0.969009
YGL010W		unknown	-0.0078	-1.0	0.964464
YIL067C		unknown	-0.0067	-1.0	0.987825
YNL029C	KTR5	mannosyltransferase	-0.0065	-1.0	0.950516
YKL141W	SDH3	succinate dehydrogenase	-0.0065	-1.0	0.972882
YLR077W	FMP25	unknown	-0.0065	-1.0	0.986181
YML116W	ATR1	multidrug efflux pump	-0.0063	-1.0	0.954845
YHR160C	PEX18	protein binding	-0.0063	-1.0	0.968018
YGL003C	CDH1	enzyme activator	-0.0063	-1.0	0.976939
YAL030W	SNC1	v-SNARE	-0.0062	-1.0	0.949962
YPL235W	RVB2	ATPase *	-0.0057	-1.0	0.724514
YNL053W	MSG5	prenylated protein tyrosine phosphatase	-0.0057	-1.0	0.92569
YJL053W	PEP8	unknown	-0.0055	-1.0	0.986169
YER100W	UBC6	ubiquitin conjugating enzyme	-0.0055	-1.0	0.956651
YGL228W	SHE10	unknown	-0.0053	-1.0	0.904817
YEL030W	ECM10	unknown	-0.0048	-1.0	0.986114
YGL194C	HOS2	NAD-dependent histone deacetylase *	-0.0047	-1.0	0.989816
YOL091W	SPO21	structural molecule	-0.0047	-1.0	0.994736
YLR375W	STP3	unknown	-0.0047	-1.0	0.984555
YJR089W	BIR1	unknown	-0.0045	-1.0	0.989651
YDR526C			-0.0045	-1.0	0.988068
YER026C	CHO1	CDP-diacylglycerol-serine O-phosphatidyltransferase	-0.0043	-1.0	0.961849
YDL013W	HEX3	DNA binding	-0.0040	-1.0	0.907154

Table 1: continued.

ORF ID	Gene Name	Gene Function	Avg Log_2 Ratio	Fold Change	T-test
YLR167W	RPS31	structural constituent of ribosome*	-0.0038	-1.0	0.953089
YGL119W	ABC1	unknown	-0.0037	-1.0	0.986921
YDR207C	UME6	DNA binding	-0.0037	-1.0	0.959383
YOR196C	LIP5	lipoic acid synthase	-0.0035	-1.0	0.977437
YNR069C	BSC5	unknown	-0.0033	-1.0	0.974219
YHR140W		unknown	-0.0030	-1.0	0.974017
YER089C	PTC2	protein phosphatase type 2C	-0.0028	-1.0	0.987311
YEL023C		unknown	-0.0027	-1.0	0.9757
YNL101W	AVT4	neutral amino acid transporter	-0.0027	-1.0	0.962791
YJL084C		cyclin binding	-0.0023	-1.0	0.966938
YDR259C	YAP6	RNA polymerase II transcription factor	-0.0022	-1.0	0.981948
YCL008C	STP22	protein binding	-0.0020	-1.0	0.987755
YKL220C	FRE2	ferric-chelate reductase	-0.0020	-1.0	0.987206
YBR181C	RPS6B	structural constituent of ribosome	-0.0018	-1.0	0.985355
YBR248C	HIS7	imidazoleglycerol-phosphate synthase	-0.0017	-1.0	0.98545
YOR039W	CKB2	protein kinase	-0.0015	-1.0	0.9952
YMR201C	RAD14	damaged DNA binding	-0.0013	-1.0	0.996328
YLR148W	PEP3	protein binding	-0.0010	-1.0	0.99211
YBL101C	ECM21	unknown	-0.0010	-1.0	0.977996
YAL025C	MAK16	unknown	-0.0008	-1.0	0.984468
YDR197W	CBS2	unknown	-0.0003	-1.0	0.997697
YNL167C	SKO1	RNA polymerase II transcription factor	-0.0003	-1.0	0.996755
YIL009C-A	EST3	telomerase	-0.0002	-1.0	0.998196
YDR069C	DOA4	endopeptidase *	-0.0002	-1.0	0.997927
YCRX19W			-0.0002	-1.0	0.995345
YFL049W	SWP82	transcriptional activator	0.0002	1.0	0.999866
YGR038W	ORM1	unknown	0.0017	1.0	0.990929
YHL003C	LAG1	sphingosine N-acyltransferase	0.0017	1.0	0.992478
YJL193W		unknown	0.0017	1.0	0.992934
YHR010W	RPL27A	structural constituent of ribosome	0.0022	1.0	0.982863
YGR282C	BGL2	glucan 1,3-beta-glucosidase	0.0023	1.0	0.961234
YDL214C	PRR2	receptor signaling protein serine/threonine kinase	0.0025	1.0	0.914954
YGL054C	ERV14	unknown	0.0027	1.0	0.983101
YGL004C	RPN14	unknown	0.0027	1.0	0.982868
YFL046W	FMP32	unknown	0.0027	1.0	0.976357
YPL035C			0.0028	1.0	0.980972
YAR020C	PAU7	unknown	0.0032	1.0	0.977324
YGR162W	TIF4631	translation initiation factor	0.0035	1.0	0.96052
YEL076W-C			0.0038	1.0	0.976404
YBR124W			0.0040	1.0	0.986923
YBR175W	SWD3	histone lysine N-methyltransferase (H3-K4 specific)	0.0047	1.0	0.977356
YJL129C	TRK1	potassium ion transporter	0.0047	1.0	0.941221
YBR078W	ECM33	unknown	0.0047	1.0	0.801488
YMR115W	FMP24	unknown	0.0053	1.0	0.865852
YFL017C	GNA1	glucosamine 6-phosphate N-acetyltransferase	0.0053	1.0	0.977619
YBL058W	SHP1	protein phosphatase type 1 regulator	0.0055	1.0	0.981329
YNR033W	ABZ1	4-amino-4-deoxychorismate synthase	0.0055	1.0	0.959059
YHR006W	STP2	specific RNA polymerase II transcription factor	0.0058	1.0	0.989157
YMR204C	INP1	unknown	0.0058	1.0	0.95237
YPL131W	RPL5	structural constituent of ribosome*	0.0058	1.0	0.899598
YIL110W		S-adenosylmethionine-dependent methyltransferase	0.0060	1.0	0.982015
YJL100W	LSB6	1-phosphatidylinositol 4-kinase	0.0063	1.0	0.971512
YGL151W	NUT1	unknown	0.0068	1.0	0.897142
YGR144W	THI4	unknown	0.0070	1.0	0.961283
YNL151C	RPC31	DNA-directed RNA polymerase	0.0072	1.0	0.959531
YMR325W	PAU19	unknown	0.0082	1.0	0.934866
YCR101C		unknown	0.0083	1.0	0.96852
YJL072C	PSF2	unknown	0.0083	1.0	0.964802
YEL022W	GEA2	ARF guanyl-nucleotide exchange factor	0.0085	1.0	0.948783
YOR092W	ECM3	ATPase	0.0090	1.0	0.971739
YFR039C		unknown	0.0092	1.0	0.725848
YGR077C	PEX8	peroxisome targeting sequence binding	0.0093	1.0	0.918307
YLL049W	LDB18	unknown	0.0093	1.0	0.965144
YLR289W	GUF1	GTPase	0.0095	1.0	0.962573
YKR063C	LAS1	unknown	0.0097	1.0	0.809164
YPL083C	SEN54	tRNA-intron endonuclease	0.0097	1.0	0.953372
YCR019W	MAK32	unknown	0.0098	1.0	0.958434
YKL091C		unknown	0.0098	1.0	0.920954
YIL003W	CFD1	ATPase	0.0100	1.0	0.64238

Table 1: continued.

ORF ID	Gene Name	Gene Function	Avg Log_2 Ratio	Fold Change	T-test
YPL038W	MET31	DNA binding	0.0100	1.0	0.947141
YGR278W	CWC22	unknown	0.0103	1.0	0.772344
YBR159W	IFA38	ketoreductase	0.0105	1.0	0.949024
YBR229C	ROT2	alpha-glucosidase	0.0108	1.0	0.923785
YPR054W	SMK1	MAP kinase	0.0112	1.0	0.935499
YLR089C	ALT1	transaminase	0.0113	1.0	0.911161
YPR065W	ROX1	specific transcriptional repressor *	0.0115	1.0	0.941161
YML026C	RPS18B	structural constituent of ribosome	0.0117	1.0	0.797332
YDL237W		unknown	0.0118	1.0	0.941923
YJL049W		unknown	0.0118	1.0	0.926511
YER055C	HIS1	ATP phosphoribosyltransferase	0.0120	1.0	0.96253
YHR054C		unknown	0.0122	1.0	0.866992
YGL192W	IME4	mRNA methyltransferase	0.0123	1.0	0.960502
YLR381W	CTF3	protein binding	0.0130	1.0	0.915219
YDL142C	CRD1	cardiolipin synthase	0.0133	1.0	0.648914
YOL132W	GAS4	1,3-beta-glucanosyltransferase	0.0135	1.0	0.968147
YPR055W	SEC8	protein binding	0.0135	1.0	0.92908
YMR064W	AEP1	unknown	0.0143	1.0	0.407033
YBR273C	UBX7	unknown	0.0148	1.0	0.8991
YKR044W	UIP5	unknown	0.0150	1.0	0.860043
YGL128C	CWC23	unknown	0.0155	1.0	0.924011
YLR388W	RPS29A	structural constituent of ribosome	0.0158	1.0	0.902194
YBR051W			0.0158	1.0	0.989968
YNL023C	FAP1	transcription factor	0.0170	1.0	0.911849
YNL169C	PSD1	phosphatidylserine decarboxylase	0.0170	1.0	0.958885
YJR064W	CCT5	unfolded protein binding	0.0172	1.0	0.549699
YLR015W	BRE2	transcription regulator	0.0173	1.0	0.955263
YJL177W	RPL17B	structural constituent of ribosome	0.0180	1.0	0.895936
YLR410W	VIP1	unknown	0.0182	1.0	0.853617
YLR288C	MEC3	DNA binding	0.0182	1.0	0.852004
YHL040C	ARN1	siderophore-iron transporter	0.0185	1.0	0.83389
YGR211W	ZPR1	protein binding	0.0187	1.0	0.911054
YKL021C	MAK11	unknown	0.0188	1.0	0.829758
YCRX21C			0.0188	1.0	0.769287
YJL159W	HSP150	structural constituent of cell wall	0.0192	1.0	0.541174
YBR016W		unknown	0.0192	1.0	0.931148
YML077W	BET5	unknown	0.0195	1.0	0.896553
YIL168W		L-serine ammonia-lyase	0.0197	1.0	0.960346
YDR277C	MTH1	unknown	0.0198	1.0	0.712504
YKR024C	DBP7	ATP-dependent RNA helicase	0.0198	1.0	0.851759
YPL086C	ELP3	RNA polymerase II transcription elongation factor	0.0203	1.0	0.700191
YLR067C	PET309	translation regulator	0.0203	1.0	0.68054
YML071C	COG8	unknown	0.0205	1.0	0.899939
YCL016C	DCC1	unknown	0.0212	1.0	0.790765
YPR097W		unknown	0.0212	1.0	0.837848
YCL009C	ILV6	enzyme regulator	0.0213	1.0	0.434225
YDL138W	RGT2	receptor *	0.0217	1.0	0.845873
YGR288W	MAL13	transcription factor	0.0218	1.0	0.679269
YOL032W	OPI10	unknown	0.0220	1.0	0.868077
YHR214W		unknown	0.0220	1.0	0.81766
YML100W	TSL1	enzyme regulator	0.0220	1.0	0.89818
YKL166C	TPK3	protein serine/threonine kinase	0.0225	1.0	0.804767
YLR075W	RPL10	structural constituent of ribosome	0.0225	1.0	0.800051
YDR330W	UBX5	unknown	0.0228	1.0	0.908215
YOL112W	MSB4	Rab GTPase activator	0.0230	1.0	0.895016
YMR142C	RPL13B	structural constituent of ribosome	0.0230	1.0	0.49292
YKL040C	NFU1	unknown	0.0232	1.0	0.848228
YOR238W		unknown	0.0233	1.0	0.937095
YDL166C	FAP7	nucleoside-triphosphatase	0.0233	1.0	0.890104
YLR347C	KAP95	protein carrier	0.0235	1.0	0.840648
YGR217W	CCH1	calcium channel	0.0237	1.0	0.84024
YGL081W		unknown	0.0238	1.0	0.775623
YNL112W	DBP2	RNA helicase	0.0238	1.0	0.661468
YLL004W	ORC3	DNA replication origin binding	0.0240	1.0	0.887808
YDR182W	CDC1	unknown	0.0242	1.0	0.877942
YLR066W	SPC3	signal peptidase	0.0247	1.0	0.230894
YBR057C	MUM2	unknown	0.0248	1.0	0.767094
YKL022C	CDC16	protein binding	0.0252	1.0	0.743003
YOR097C		unknown	0.0255	1.0	0.934471

Table 1: continued.

ORF ID	Gene Name	Gene Function	Avg Log_2 Ratio	Fold Change	T-test
YDR131C		protein binding	0.0260	1.0	0.915824
YOR193W	PEX27	unknown	0.0263	1.0	0.680639
YKL049C	CSE4	centromeric DNA binding	0.0265	1.0	0.931872
YNR058W	BIO3	adenosylmethionine-8-amino-7-oxononanoate transaminase	0.0267	1.0	0.73044
YCR072C	RSA4	unknown	0.0268	1.0	0.684291
YGR249W	MGA1	unknown	0.0273	1.0	0.894769
YJL081C	ARP4	chromatin binding	0.0275	1.0	0.784925
YMR256C	COX7	cytochrome-c oxidase	0.0275	1.0	0.903989
YNL016W	PUB1	mRNA binding	0.0280	1.0	0.786195
YLR270W	DCS1	hydrolase , acting on acid anhydrides, in phosphorus-contai	0.0280	1.0	0.734285
YOR125C	CAT5	unknown	0.0280	1.0	0.812534
YMR230W	RPS10B	structural constituent of ribosome	0.0282	1.0	0.784171
YPL122C	TFB2	general RNA polymerase II transcription factor	0.0282	1.0	0.639985
YDL033C	SLM3	tRNA (5-methylaminomethyl-2-thiouridylate)-methyltransf	0.0283	1.0	0.923466
YBR211C	AME1	unknown	0.0285	1.0	0.846335
YDR102C			0.0285	1.0	0.767122
YNR035C	ARC35	structural molecule	0.0287	1.0	0.755131
YPR067W	ISA2	unknown	0.0287	1.0	0.892851
YKL135C	APL2	clathrin binding	0.0290	1.0	0.795939
YMR200W	ROT1	unknown	0.0292	1.0	0.760418
YCR041W			0.0293	1.0	0.683209
YCL045C		unknown	0.0293	1.0	0.626402
YNL176C		unknown	0.0293	1.0	0.867167
YFL064C		unknown	0.0295	1.0	0.904342
YDR450W	RPS18A	structural constituent of ribosome	0.0297	1.0	0.581783
YKR014C	YPT52	GTPase	0.0297	1.0	0.508974
YDR230W			0.0297	1.0	0.602258
YCL065W			0.0300	1.0	0.847089
YDR518W	EUG1	protein disulfide isomerase	0.0303	1.0	0.820679
YML030W		unknown	0.0308	1.0	0.13709
YOL057W		metalloendopeptidase	0.0308	1.0	0.878971
YEL029C	BUD16	unknown	0.0310	1.0	0.863763
YBL057C	PTH2	aminoacyl-tRNA hydrolase	0.0310	1.0	0.859699
YDR021W	FAL1	ATP-dependent RNA helicase	0.0310	1.0	0.795597
YFL024C	EPL1	histone acetyltransferase	0.0312	1.0	0.885992
YGR191W	HIP1	L-histidine transporter	0.0312	1.0	0.623334
YDR321W	ASP1	asparaginase	0.0315	1.0	0.782034
YJL115W	ASF1	transcription regulator	0.0315	1.0	0.879222
YBL087C	RPL23A	structural constituent of ribosome	0.0318	1.0	0.176756
YPR005C	HAL1	unknown	0.0320	1.0	0.894193
YDR208W	MSS4	1-phosphatidylinositol-4-phosphate 5-kinase	0.0320	1.0	0.678057
YBR001C	NTH2	alpha,alpha-trehalase	0.0323	1.0	0.838192
YBR163W	DEM1	unknown	0.0323	1.0	0.667708
YGL108C		unknown	0.0325	1.0	0.932601
YKR037C	SPC34	structural constituent of cytoskeleton	0.0330	1.0	0.384864
YJR014W	TMA22	RNA binding	0.0333	1.0	0.553566
YGL223C	COG1	unknown	0.0337	1.0	0.914697
YDR133C			0.0338	1.0	0.87363
YOR096W	RPS7A	structural constituent of ribosome	0.0338	1.0	0.836781
YBR235W		ion transporter	0.0345	1.0	0.794652
YMR313C	TGL3	triacylglycerol lipase	0.0345	1.0	0.807244
YLR421C	RPN13	endopeptidase	0.0348	1.0	0.723852
YGR196C	FYV8	unknown	0.0350	1.0	0.891246
YEL049W	PAU2	unknown	0.0352	1.0	0.474199
YBL027W	RPL19B	structural constituent of ribosome	0.0352	1.0	0.00875076
YKL211C	TRP3	anthranilate synthase *	0.0353	1.0	0.817613
YKR078W		protein transporter	0.0355	1.0	0.921548
YDR020C		unknown	0.0355	1.0	0.697937
YMR276W	DSK2	protein binding	0.0357	1.0	0.55471
YGR163W	GTR2	GTPase	0.0357	1.0	0.874576
YDR017C	KCS1	inositol or phosphatidylinositol kinase	0.0357	1.0	0.889864
YOR220W	WSP1	unknown	0.0358	1.0	0.732431
YOL019W		unknown	0.0362	1.0	0.761237
YGR264C	MES1	methionine-tRNA ligase	0.0365	1.0	0.884875
YLR392C		unknown	0.0365	1.0	0.83436
YER048C	CAJ1	chaperone regulator	0.0367	1.0	0.342318
YGR232W	NAS6	unknown	0.0368	1.0	0.858467
YLR242C	ARV1	unknown	0.0370	1.0	0.440339
YDL065C	PEX19	protein binding	0.0370	1.0	0.746451

Table 1: continued.

ORF ID	Gene Name	Gene Function	Avg Log_2 Ratio	Fold Change	T-test
YLL031C	GPI13	transferase , transferring phosphorus-containing groups	0.0372	1.0	0.857006
YNL138W	SRV2	cytoskeletal protein binding	0.0372	1.0	0.126351
YDR484W	VPS52	protein binding	0.0377	1.0	0.791187
YJL141C	YAK1	protein kinase	0.0380	1.0	0.325906
YDR183W	PLP1	GTPase inhibitor	0.0382	1.0	0.838822
YML112W	CTK3	cyclin-dependent protein kinase	0.0383	1.0	0.89062
YKR020W	VPS51	protein binding	0.0383	1.0	0.638897
YHR077C	NMD2	protein binding	0.0387	1.0	0.839633
YER148W	SPT15	DNA binding	0.0387	1.0	0.839561
YIL176C	PAU14	unknown	0.0388	1.0	0.73136
YBR135W	CKS1	protein kinase	0.0388	1.0	0.505092
YHR001W-A	QCR10	ubiquinol-cytochrome-c reductase	0.0392	1.0	0.769979
YNR076W	PAU6	unknown	0.0392	1.0	0.792688
YDR127W	ARO1	3-dehydroquinate dehydratase *	0.0393	1.0	0.766315
YBR213W	MET8	ferrochelatase *	0.0395	1.0	0.804685
YJL091C	GWT1	unknown	0.0397	1.0	0.625225
YAR074C			0.0397	1.0	0.779955
YGL210W	YPT32	GTPase	0.0403	1.0	0.228714
YIL017W			0.0405	1.0	0.652588
YHR210C		unknown	0.0405	1.0	0.625477
YKL206C	ADD66	unknown	0.0405	1.0	0.78834
YBR288C	APM3	unknown	0.0408	1.0	0.638011
YER056C-A	RPL34A	structural constituent of ribosome	0.0417	1.0	0.860541
YEL005C	VAB2	protein binding	0.0417	1.0	0.759062
YPL198W	RPL7B	structural constituent of ribosome	0.0417	1.0	0.860632
YOL069W	NUF2	structural constituent of cytoskeleton	0.0418	1.0	0.769603
YGL111W	NSA1	unknown	0.0420	1.0	0.847127
YER042W	MXR1	protein-methionine-S-oxide reductase	0.0420	1.0	0.705487
YLR234W	TOP3	DNA topoisomerase type I	0.0422	1.0	0.848958
YHL036W	MUP3	L-methionine transporter	0.0422	1.0	0.690519
YDL231C	BRE4	unknown	0.0422	1.0	0.721389
YJL030W	MAD2	unknown	0.0422	1.0	0.366983
YCR008W	SAT4	protein kinase	0.0422	1.0	0.0918535
YJR016C	ILV3	dihydroxy-acid dehydratase	0.0423	1.0	0.461489
YNL215W	IES2	unknown	0.0427	1.0	0.15267
YBL003C	HTA2	DNA binding	0.0430	1.0	0.675361
YKL176C	LST4	protein transporter	0.0430	1.0	0.070922
YBR167C	POP7	ribonuclease P *	0.0435	1.0	0.44425
YDR315C	IPK1	inositol or phosphatidylinositol kinase	0.0440	1.0	0.754089
YKL034W	TUL1	ubiquitin-protein ligase	0.0440	1.0	0.58028
YDL084W	SUB2	protein binding	0.0440	1.0	0.658628
YML124C	TUB3	structural constituent of cytoskeleton	0.0442	1.0	0.836215
YBR212W	NGR1	RNA binding	0.0448	1.0	0.63668
YJL180C	ATP12	unfolded protein binding	0.0450	1.0	0.795626
YDR025W	RPS11A	structural constituent of ribosome	0.0453	1.0	0.755357
YOR061W	CKA2	protein kinase	0.0453	1.0	0.36483
YDR004W	RAD57	protein binding	0.0455	1.0	0.351499
YPL282C	PAU22	unknown	0.0460	1.0	0.713519
YJR145C	RPS4A	structural constituent of ribosome	0.0462	1.0	0.707526
YCR024C	SLM5	asparagine-tRNA ligase	0.0462	1.0	0.563609
YDL216C	RRI1	metalloendopeptidase	0.0463	1.0	0.793798
YHR013C	ARD1	peptide alpha-N-acetyltransferase	0.0463	1.0	0.622674
YGL197W	MDS3	unknown	0.0463	1.0	0.666317
YOR132W	VPS17	unknown	0.0463	1.0	0.563151
YOL128C	YGK3	glycogen synthase kinase	0.0465	1.0	0.262505
YDR224C	HTB1	DNA binding	0.0465	1.0	0.771997
YIL071W			0.0472	1.0	0.44109
YFL008W	SMC1	ATPase *	0.0472	1.0	0.136363
YLR099C	ICT1	unknown	0.0472	1.0	0.821152
YMR016C	SOK2	transcription factor	0.0473	1.0	0.754306
YGR262C	BUD32	protein serine/threonine kinase	0.0475	1.0	0.800796
YML106W	URA5	orotate phosphoribosyltransferase	0.0475	1.0	0.527079
YGL035C	MIG1	specific RNA polymerase II transcription factor	0.0480	1.0	0.798228
YCR048W	ARE1	sterol O-acyltransferase	0.0480	1.0	0.821126
YJR151C	DAN4	unknown	0.0482	1.0	0.680507
YPR019W	CDC54	chromatin binding	0.0483	1.0	0.700098
YLR426W		unknown	0.0490	1.0	0.760096
YDR148C	KGD2	dihydrolipoyllysine-residue succinyltransferase	0.0490	1.0	0.554161
YIL013C	PDR11	ATPase , coupled to transmembrane movement of substanc	0.0493	1.0	0.91236

Table 1: continued.

ORF ID	Gene Name	Gene Function	Avg Log_2 Ratio	Fold Change	T-test
YLL025W	PAU17	unknown	0.0495	1.0	0.810281
YOR267C	HRK1	protein kinase	0.0500	1.0	0.857649
YDR061W		ATPase , coupled to transmembrane movement of substanc	0.0507	1.0	0.652089
YER167W	BCK2	unknown	0.0508	1.0	0.710259
YCL005W	LDB16	unknown	0.0510	1.0	0.106253
YLR163C	MAS1	mitochondrial processing peptidase	0.0512	1.0	0.799011
YPR093C	ASR1	unknown	0.0512	1.0	0.740813
YDL058W	USO1	unknown	0.0515	1.0	0.72163
YNL006W	LST8	protein binding	0.0522	1.0	0.770075
YFL067W		unknown	0.0523	1.0	0.0332627
YIL152W		unknown	0.0523	1.0	0.655281
YER093C	TSC11	protein binding	0.0525	1.0	0.680729
YOR143C	THI80	thiamin diphosphokinase	0.0527	1.0	0.778965
YLR351C	NIT3	hydrolase , acting on carbon-nitrogen (but not peptide) bon	0.0528	1.0	0.503414
YPL022W	RAD1	DNA binding	0.0530	1.0	0.801398
YOR148C	SPP2	unknown	0.0533	1.0	0.732447
YBR276C	PPS1	protein tyrosine/threonine phosphatase	0.0533	1.0	0.321266
YOL161C	PAU20	unknown	0.0537	1.0	0.695709
YDR474C			0.0543	1.0	0.659719
YMR242C	RPL20A	structural constituent of ribosome	0.0547	1.0	0.716096
YMR105C	PGM2	phosphoglucomutase	0.0548	1.0	0.580892
YFR019W	FAB1	1-phosphatidylinositol-3-phosphate 5-kinase	0.0550	1.0	0.501533
YFR015C	GSY1	glycogen (starch) synthase	0.0552	1.0	0.550496
YCR104W	PAU3	unknown	0.0557	1.0	0.424407
YMR220W	ERG8	phosphomevalonate kinase	0.0558	1.0	0.902766
YLR260W	LCB5	D-erythro-sphingosine kinase	0.0562	1.0	0.663162
YJL078C	PRY3	unknown	0.0562	1.0	0.652513
YDR147W	EKI1	choline kinase	0.0562	1.0	0.684737
YJL121C	RPE1	ribulose-phosphate 3-epimerase	0.0562	1.0	0.361005
YMR189W	GCV2	glycine dehydrogenase	0.0565	1.0	0.00685438
YLL050C	COF1	protein binding	0.0567	1.0	0.404432
YMR243C	ZRC1	di-, tri-valent inorganic cation transporter	0.0567	1.0	0.481262
YPR029C	APL4	clathrin binding	0.0568	1.0	0.887749
YLR325C	RPL38	structural constituent of ribosome	0.0568	1.0	0.551469
YIL150C	MCM10	chromatin binding	0.0570	1.0	0.355852
YOR320C	GNT1	acetylglucosaminyltransferase	0.0572	1.0	0.294937
YBL019W	APN2	phosphodiesterase I *	0.0573	1.0	0.53149
YJL140W	RPB4	DNA-directed RNA polymerase	0.0577	1.0	0.493736
YOR043W	WHI2	phosphatase activator	0.0578	1.0	0.525622
YMR194W	RPL36A	structural constituent of ribosome*	0.0580	1.0	0.238934
YOR250C	CLP1	RNA binding	0.0580	1.0	0.884374
YMR088C	VBA1	basic amino acid permease	0.0583	1.0	0.849485
YOR246C		oxidoreductase	0.0583	1.0	0.118339
YOR332W	VMA4	hydrogen-transporting ATPase , rotational mechanism	0.0583	1.0	0.617465
YJL014W	CCT3	unfolded protein binding	0.0587	1.0	0.455095
YNL266W			0.0590	1.0	0.6418
YDR068W	DOS2	unknown	0.0592	1.0	0.64928
YBR161W	CSH1	mannosyltransferase *	0.0593	1.0	0.684661
YMR261C	TPS3	enzyme regulator	0.0593	1.0	0.0444578
YPL023C	MET12	methylenetetrahydrofolate reductase (NADPH)	0.0593	1.0	0.807659
YOL027C	MDM38	unknown	0.0598	1.0	0.453741
YBR133C	HSL7	protein-arginine N-methyltransferase	0.0598	1.0	0.135992
YJL013C	MAD3	unknown	0.0600	1.0	0.483097
YDR162C	NBP2	unknown	0.0605	1.0	0.706345
YFL065C		unknown	0.0610	1.0	0.694884
YPR102C	RPL11A	structural constituent of ribosome	0.0613	1.0	0.0491071
YNL119W	NCS2	unknown	0.0617	1.0	0.739047
YIL095W	PRK1	protein serine/threonine kinase	0.0620	1.0	0.520303
YOR359W	VTS1	RNA binding	0.0620	1.0	0.272477
YMR218C	TRS130	unknown	0.0625	1.0	0.647464
YHR188C	GPI16	GPI-anchor transamidase	0.0633	1.0	0.642159
YIR041W	PAU15	unknown	0.0633	1.0	0.624994
YDR109C		kinase	0.0635	1.0	0.492814
YPL149W	ATG5	unknown	0.0635	1.0	0.676752
YLR342W	FKS1	1,3-beta-glucan synthase	0.0638	1.0	0.782619
YGL137W	SEC27	unknown	0.0638	1.0	0.764248
YDR105C	TMS1	unknown	0.0640	1.0	0.268727
YCL030C	HIS4	phosphoribosyl-ATP diphosphatase *	0.0640	1.0	0.583129
YCR097WA			0.0642	1.0	0.685302

Table 1: continued.

ORF ID	Gene Name	Gene Function	Avg Log_2 Ratio	Fold Change	T-test
YKL046C	DCW1	mannosidase	0.0643	1.0	0.754956
YJL035C	TAD2	tRNA specific adenosine deaminase	0.0643	1.0	0.376867
YJL139C	YUR1	mannosyltransferase	0.0647	1.0	0.551196
YJL127C	SPT10	histone acetyltransferase	0.0648	1.0	0.286744
YOR383C	FIT3	unknown	0.0650	1.0	0.579344
YKL047W		unknown	0.0652	1.0	0.83548
YGL085W		unknown	0.0653	1.0	0.46591
YBR112C	CYC8	transcription coactivator *	0.0655	1.0	0.122959
YDL010W		unknown	0.0658	1.0	0.499612
YOR144C	ELG1	unknown	0.0658	1.0	0.851304
YOR089C	VPS21	GTPase	0.0660	1.0	0.543415
YER181C			0.0667	1.0	0.594153
YKL122C	SRP21	signal sequence binding	0.0668	1.0	0.447795
YOR103C	OST2	dolichyl-diphosphooligosaccharide-protein glycotransferase	0.0670	1.0	0.690893
YGR102C		unknown	0.0672	1.0	0.197037
YPL044C			0.0673	1.0	0.799545
YER082C	UTP7	snoRNA binding	0.0675	1.0	0.450726
YNL259C	ATX1	copper chaperone	0.0675	1.0	0.671987
YPR079W	MRL1	signal sequence binding	0.0675	1.0	0.827861
YDR091C	RLI1	ATPase *	0.0677	1.0	0.560033
YNL225C	CNM67	structural constituent of cytoskeleton	0.0677	1.0	0.718632
YER109C	FLO8	specific RNA polymerase II transcription factor	0.0678	1.0	0.483187
YNL254C		unknown	0.0678	1.0	0.699391
YMR255W	GFD1	unknown	0.0680	1.0	0.485423
YML073C	RPL6A	structural constituent of ribosome*	0.0680	1.0	0.361732
YBR102C	EXO84	protein binding	0.0682	1.0	0.495793
YBR058C	UBP14	ubiquitin-specific protease	0.0682	1.0	0.782692
YBL102W	SFT2	unknown	0.0687	1.0	0.611863
YER186C		unknown	0.0688	1.0	0.672433
YIL017C	VID28	unknown	0.0688	1.0	0.813693
YGR070W	ROM1	signal transducer *	0.0693	1.0	0.764803
YGL092W	NUP145	structural molecule	0.0695	1.0	0.831691
YHL002C-A			0.0697	1.0	0.00904149
YDR372C	VPS74	unknown	0.0700	1.0	0.13573
YKL048C	ELM1	protein serine/threonine kinase	0.0708	1.1	0.412275
YPL273W	SAM4	homocysteine S-methyltransferase	0.0710	1.1	0.586741
YER004W	FMP52	unknown	0.0710	1.1	0.653063
YDR263C	DIN7	nuclease	0.0713	1.1	0.22303
YDL176W		unknown	0.0713	1.1	0.696016
YLR144C	ACF2	glucan 1,3-beta-glucosidase	0.0717	1.1	0.748828
YHL042W		unknown	0.0717	1.1	0.39104
YPL071C		unknown	0.0718	1.1	0.286152
YDR516C	EMI2	unknown	0.0725	1.1	0.571553
YGR132C	PHB1	unknown	0.0732	1.1	0.325858
YDR428C		unknown	0.0732	1.1	0.657755
YLR233C	EST1	RNA binding	0.0735	1.1	0.810466
YKL051W	SFK1	unknown	0.0738	1.1	0.214504
YBR079C	RPG1	translation initiation factor	0.0742	1.1	0.283855
YAL019W	FUN30	unknown	0.0742	1.1	0.69321
YDL112W	TRM3	tRNA (guanosine) methyltransferase	0.0747	1.1	0.29187
YIL134W	FLX1	FAD transporter	0.0748	1.1	0.67789
YLR301W		unknown	0.0752	1.1	0.656596
YOR027W	STI1	unfolded protein binding	0.0755	1.1	0.549152
YDR060W	MAK21	unknown	0.0755	1.1	0.117159
YLR312C		unknown	0.0755	1.1	0.437697
YDL063C		unknown	0.0758	1.1	0.318933
YBR231C	SWC5	unknown	0.0762	1.1	0.475621
YER046W	SPO73	unknown	0.0763	1.1	0.445665
YBR017C	KAP104	nuclear localization sequence binding	0.0763	1.1	0.651697
YPL217C	BMS1	GTP binding	0.0765	1.1	0.586416
YGL063W	PUS2	tRNA-pseudouridine synthase	0.0767	1.1	0.693064
YPL234C	TFP3	hydrogen-transporting ATPase , rotational mechanism	0.0767	1.1	0.524751
YIL148W	RPL40A	structural constituent of ribosome*	0.0770	1.1	0.1342
YLR177W		unknown	0.0770	1.1	0.772262
YDL064W	UBC9	SUMO conjugating enzyme	0.0773	1.1	0.20966
YPL179W	PPQ1	protein serine/threonine phosphatase	0.0775	1.1	0.435543
YMR300C	ADE4	amidophosphoribosyltransferase	0.0777	1.1	0.601431
YBR247C	ENP1	snoRNA binding	0.0778	1.1	0.452546
YCR100C		unknown	0.0778	1.1	0.647394

Table 1: continued.

ORF ID	Gene Name	Gene Function	Avg Log_2 Ratio	Fold Change	T-test
YGR112W	SHY1	unfolded protein binding	0.0782	1.1	0.338026
YMR033W	ARP9	general RNA polymerase II transcription factor	0.0782	1.1	0.737167
YGR049W	SCM4	unknown	0.0785	1.1	0.436405
YLR215C	CDC123	unknown	0.0785	1.1	0.646919
YKR062W	TFA2	general RNA polymerase II transcription factor	0.0785	1.1	0.0699522
YNL178W	RPS3	structural constituent of ribosome	0.0785	1.1	0.499495
YMR289W	ABZ2	unknown	0.0787	1.1	0.632771
YLR047C	FRE8	oxidoreductase	0.0790	1.1	0.840524
YGR186W	TFG1	general RNA polymerase II transcription factor	0.0795	1.1	0.801059
YMR077C	VPS20	protein binding	0.0797	1.1	0.0991138
YKR071C	DRE2	unknown	0.0798	1.1	0.414462
YCR015C		unknown	0.0800	1.1	0.502485
YIL048W	NEO1	phospholipid-translocating ATPase *	0.0807	1.1	0.346581
YMR074C		unknown	0.0810	1.1	0.54994
YDR294C	DPL1	sphinganine-1-phosphate aldolase	0.0815	1.1	0.526139
YBR237W	PRP5	RNA splicing factor	0.0815	1.1	0.236781
YLR408C		unknown	0.0818	1.1	0.731278
YPR043W	RPL43A	structural constituent of ribosome	0.0822	1.1	0.195287
YDL196W			0.0822	1.1	0.472237
YGL181W	GTS1	unknown	0.0823	1.1	0.420337
YHL049C		unknown	0.0827	1.1	0.454649
YOR312C	RPL20B	structural constituent of ribosome	0.0827	1.1	0.0348962
YHR078W		unknown	0.0828	1.1	0.182504
YHR011W	DIA4	serine-tRNA ligase	0.0833	1.1	0.0705088
YKL222C		unknown	0.0835	1.1	0.693354
YJR013W	GPI14	mannosyltransferase	0.0837	1.1	0.607683
YGL009C	LEU1	3-isopropylmalate dehydratase	0.0838	1.1	0.79821
YDR185C		unknown	0.0845	1.1	0.353996
YCL073C		transporter	0.0848	1.1	0.549888
YMR060C	SAM37	protein binding	0.0848	1.1	0.669086
YOR117W	RPT5	ATPase *	0.0850	1.1	0.690479
YBR238C		unknown	0.0852	1.1	0.371894
YPL144W		unknown	0.0852	1.1	0.354544
YHR201C	PPX1	exopolyphosphatase	0.0855	1.1	0.322964
YKL207W		unknown	0.0857	1.1	0.550222
YDR101C	ARX1	unknown	0.0865	1.1	0.597683
YIL011W	TIR3	unknown	0.0867	1.1	0.161438
YER049W	TPA1	unknown	0.0868	1.1	0.623126
YDL141W	BPL1	biotin-[acetyl-CoA-carboxylase] ligase *	0.0870	1.1	0.252365
YOR272W	YTM1	unknown	0.0870	1.1	0.252762
YKL162C		unknown	0.0872	1.1	0.367748
YMR069W	NAT4	peptide alpha-N-acetyltransferase	0.0872	1.1	0.679046
YBR216C	YBP1	unknown	0.0872	1.1	0.478932
YGR258C	RAD2	single-stranded DNA specific endodeoxyribonuclease	0.0873	1.1	0.579613
YCL018W	LEU2	3-isopropylmalate dehydrogenase	0.0878	1.1	0.0434134
YBR110W	ALG1	beta-1,4-mannosyltransferase	0.0880	1.1	0.360102
YPL095C	EEB1	unknown	0.0882	1.1	0.506272
YOL039W	RPP2A	structural constituent of ribosome	0.0887	1.1	0.181571
YER184C		unknown	0.0888	1.1	0.661686
YDL224C	WHI4	RNA binding	0.0888	1.1	0.445724
YDR293C	SSD1	RNA binding	0.0892	1.1	0.428122
YIL022W	TIM44	protein transporter	0.0892	1.1	0.70065
YDR487C	RIB3	3,4-dihydroxy-2-butanone-4-phosphate synthase	0.0893	1.1	0.0209302
YER179W	DMC1	single-stranded DNA binding	0.0893	1.1	0.626534
YDL189W	RBS1	unknown	0.0895	1.1	0.11124
YIL135C	VHS2	unknown	0.0895	1.1	0.352168
YJR079W		unknown	0.0897	1.1	0.70391
YDR019C	GCV1	glycine dehydrogenase	0.0898	1.1	0.77012
YDR137W	RGP1	guanyl-nucleotide exchange factor	0.0898	1.1	0.667073
YPL098C	MGR2	unknown	0.0900	1.1	0.535491
YML051W	GAL80	transcription corepressor	0.0903	1.1	0.191366
YGL178W	MPT5	mRNA binding	0.0905	1.1	0.769038
YDL088C	ASM4	structural molecule	0.0907	1.1	0.488145
YBR044C	TCM62	unfolded protein binding	0.0908	1.1	0.606928
YDR258C	HSP78	ATPase *	0.0910	1.1	0.0854136
YCL032W	STE50	protein kinase	0.0913	1.1	0.576846
YGR111W		unknown	0.0915	1.1	0.254635
YNL127W	FAR11	unknown	0.0915	1.1	0.484484
YGL172W	NUP49	structural molecule	0.0920	1.1	0.676493

Table 1: continued.

ORF ID	Gene Name	Gene Function	Avg Log_2 Ratio	Fold Change	T-test
YER010C		unknown	0.0922	1.1	0.579126
YOR270C	VPH1	hydrogen-transporting ATPase , rotational mechanism	0.0922	1.1	0.574421
YFL033C	RIM15	protein kinase	0.0923	1.1	0.085125
YGL139W	FLC3	unknown	0.0923	1.1	0.581172
YMR239C	RNT1	ribonuclease III	0.0927	1.1	0.762863
YKR008W	RSC4	unknown	0.0927	1.1	0.637762
YML113W	DAT1	AT DNA binding	0.0927	1.1	0.317989
YLR201C	COQ9	unknown	0.0930	1.1	0.238061
YJR011C		unknown	0.0935	1.1	0.454217
YPL220W	RPL1A	structural constituent of ribosome	0.0937	1.1	0.307226
YIL050W	PCL7	cyclin-dependent protein kinase	0.0938	1.1	0.566823
YOL072W	THP1	protein binding	0.0938	1.1	0.370865
YGL066W	SGF73	structural molecule *	0.0940	1.1	0.036297
YPL152W	RRD2	protein phosphatase type 2A regulator	0.0940	1.1	0.120268
YLR068W	FYV7	unknown	0.0942	1.1	0.704986
YDL236W	PHO13	alkaline phosphatase *	0.0942	1.1	0.170029
YOL012C	HTZ1	chromatin binding	0.0948	1.1	0.283158
YDR356W	SPC110	structural constituent of cytoskeleton	0.0950	1.1	0.580334
YDR427W	RPN9	structural molecule	0.0950	1.1	0.381451
YER013W	PRP22	RNA splicing factor	0.0952	1.1	0.522285
YBR278W	DPB3	epsilon DNA polymerase	0.0952	1.1	0.66785
YJL004C	SYS1	unknown	0.0955	1.1	0.759446
YBR250W		unknown	0.0955	1.1	0.03594
YMR133W	REC114	unknown	0.0960	1.1	0.544977
Q0045	COX1	cytochrome-c oxidase	0.0960	1.1	0.637676
YCR091W	KIN82	protein kinase	0.0962	1.1	0.493797
YKR029C	SET3	NAD-dependent histone deacetylase *	0.0963	1.1	0.339699
YNR066C		unknown	0.0963	1.1	0.652778
YLR310C	CDC25	Ras guanyl-nucleotide exchange factor	0.0963	1.1	0.0336884
YPL133C	RDS2	transcription factor	0.0965	1.1	0.640981
YML014W	TRM9	tRNA (uridine) methyltransferase	0.0967	1.1	0.161281
YHR169W	DBP8	ATP-dependent RNA helicase	0.0970	1.1	0.115755
YLR003C		unknown	0.0972	1.1	0.697762
YMR282C	AEP2	unknown	0.0975	1.1	0.574056
YPR048W	TAH18	unknown	0.0975	1.1	0.561827
YGL189C	RPS26A	structural constituent of ribosome	0.0977	1.1	0.49197
YJR105W	ADO1	adenosine kinase	0.0977	1.1	0.468926
YMR291W		protein kinase	0.0977	1.1	0.639081
YDR074W	TPS2	trehalose-phosphatase	0.0980	1.1	0.126764
YBR301W	DAN3	unknown	0.0980	1.1	0.650155
YPL208W	RKM1	protein-lysine N-methyltransferase	0.0980	1.1	0.334358
YKL121W		unknown	0.0982	1.1	0.46047
YDL211C		unknown	0.0983	1.1	0.601651
YDR531W		pantothenate kinase	0.0985	1.1	0.195369
YGR294W	PAU12	unknown	0.0985	1.1	0.130403
YFL027C	GYP8	Rab GTPase activator	0.0987	1.1	0.607376
YIR034C	LYS1	saccharopine dehydrogenase	0.0988	1.1	0.58791
YBR029C	CDS1	phosphatidate cytidylyltransferase	0.0988	1.1	0.0414334
YFL038C	YPT1	GTPase	0.0988	1.1	0.513632
YPR099C			0.0990	1.1	0.575795
YMR186W	HSC82	unfolded protein binding	0.0992	1.1	0.274954
YOR195W	SLK19	unknown	0.0992	1.1	0.833194
YBL034C	STU1	structural constituent of cytoskeleton	0.0992	1.1	0.844424
YDL104C	QRI7	metalloendopeptidase	0.0995	1.1	0.204384
YMR134W		unknown	0.0997	1.1	0.367815
YPL178W	CBC2	RNA cap binding	0.1003	1.1	0.0571149
YFL028C	CAF16	ATPase	0.1005	1.1	0.736906
YDR164C	SEC1	SNARE binding	0.1005	1.1	0.557822
YGR216C	GPI1	UDP-glycosyltransferase	0.1007	1.1	0.50966
YOL006C	TOP1	DNA topoisomerase type I	0.1007	1.1	0.405039
YPL143W	RPL33A	structural constituent of ribosome	0.1012	1.1	0.435448
YLR273C	PIG1	protein phosphatase type 1 regulator	0.1015	1.1	0.310524
YBL007C	SLA1	protein binding	0.1017	1.1	0.563892
YBR089W			0.1020	1.1	0.0155459
YMR223W	UBP8	ubiquitin-specific protease	0.1025	1.1	0.673637
YLR279W			0.1030	1.1	0.574652
YAR027W	UIP3	unknown	0.1032	1.1	0.131823
YHR098C	SFB3	unknown	0.1032	1.1	0.193573
YNL087W	TCB2	unknown	0.1033	1.1	0.630482

Table 1: continued.

ORF ID	Gene Name	Gene Function	Avg Log_2 Ratio	Fold Change	T-test
YHR161C	YAP1801	clathrin binding	0.1037	1.1	0.290656
YHL011C	PRS3	ribose phosphate diphosphokinase	0.1037	1.1	0.0660632
YFR042W		unknown	0.1037	1.1	0.766893
YJL093C	TOK1	potassium channel	0.1038	1.1	0.10765
YBR113W			0.1038	1.1	0.181183
YPL153C	RAD53	protein threonine/tyrosine kinase	0.1040	1.1	0.725589
YOR009W	TIR4	unknown	0.1042	1.1	0.648487
YNL080C		unknown	0.1047	1.1	0.100427
YBR195C	MSI1	transcription regulator	0.1047	1.1	0.485527
YKL180W	RPL17A	structural constituent of ribosome	0.1048	1.1	0.112591
YGR150C		unknown	0.1050	1.1	0.562377
YPR152C	URN1	unknown	0.1052	1.1	0.529878
YMR091C	NPL6	unknown	0.1053	1.1	0.016653
YOL088C	MPD2	protein disulfide isomerase	0.1055	1.1	0.275261
YLR147C	SMD3	RNA splicing factor	0.1055	1.1	0.0530108
YDR298C	ATP5	structural molecule *	0.1055	1.1	0.570317
YER034W		unknown	0.1057	1.1	0.417125
YFR028C	CDC14	phosphoprotein phosphatase	0.1060	1.1	0.823634
YDR352W		unknown	0.1060	1.1	0.395957
YBR152W	SPP381	protein binding	0.1060	1.1	0.656622
YBR283C	SSH1	protein transporter	0.1060	1.1	0.669242
YDL007W	RPT2	ATPase *	0.1062	1.1	0.0547079
YKR091W	SRL3	unknown	0.1065	1.1	0.181936
YNL096C	RPS7B	structural constituent of ribosome	0.1072	1.1	0.0348401
YLR398C	SKI2	RNA helicase	0.1077	1.1	0.672459
YNR021W		unknown	0.1078	1.1	0.0966738
YMR161W	HLJ1	chaperone regulator	0.1080	1.1	0.385789
YPR107C	YTH1	RNA binding	0.1080	1.1	0.47814
YGR041W	BUD9	unknown	0.1080	1.1	0.733979
YMR212C	EFR3	unknown	0.1082	1.1	0.46249
YDL081C	RPP1A	structural constituent of ribosome	0.1083	1.1	0.139958
YKL165C	MCD4	unknown	0.1083	1.1	0.744045
YOR323C	PRO2	glutamate-5-semialdehyde dehydrogenase	0.1083	1.1	0.404042
YOR275C	RIM20	unknown	0.1090	1.1	0.518349
YIL006W	YIA6	transporter	0.1090	1.1	0.321675
YLR272C	YCS4	unknown	0.1092	1.1	0.262957
YCR059C	YIH1	unknown	0.1095	1.1	0.296258
YNL133C	FYV6	unknown	0.1100	1.1	0.0698388
YER041W	YEN1	single-stranded DNA specific endodeoxyribonuclease	0.1103	1.1	0.444506
YGL100W	SEH1	structural molecule	0.1108	1.1	0.659628
YGL044C	RNA15	RNA binding	0.1110	1.1	0.440088
YGL131C	SNT2	DNA binding	0.1115	1.1	0.728825
YDL051W	LHP1	RNA binding	0.1115	1.1	0.60111
YKR075C		unknown	0.1115	1.1	0.268586
YDL009C			0.1117	1.1	0.656888
YMR277W	FCP1	phosphoprotein phosphatase *	0.1117	1.1	0.338533
YBR154C	RPB5	DNA-directed RNA polymerase	0.1118	1.1	0.501093
YLR280C			0.1120	1.1	0.202865
YPL267W	ACM1	unknown	0.1122	1.1	0.661205
YPL094C	SEC62	protein binding	0.1122	1.1	0.631389
YOL013C	HRD1	ubiquitin-protein ligase	0.1128	1.1	0.258275
YHR082C	KSP1	protein serine/threonine kinase	0.1128	1.1	0.783873
YOL054W	PSH1	unknown	0.1128	1.1	0.215513
YGR239C	PEX21	protein binding	0.1130	1.1	0.72442
YGR280C	PXR1	unknown	0.1132	1.1	0.574029
YNL121C	TOM70	protein transporter	0.1132	1.1	0.367403
YJL126W	NIT2	hydrolase , acting on carbon-nitrogen (but not peptide) bon	0.1133	1.1	0.554981
YDR262W		unknown	0.1138	1.1	0.198983
YML104C	MDM1	structural constituent of cytoskeleton	0.1138	1.1	0.785894
YDL153C	SAS10	snoRNA binding	0.1142	1.1	0.512859
YPL063W	TIM50	unknown	0.1143	1.1	0.545651
YHR108W	GGA2	ubiquitin binding	0.1145	1.1	0.572836
YDR188W	CCT6	unfolded protein binding	0.1145	1.1	0.49423
YKL098W		unknown	0.1145	1.1	0.402327
YBL032W	HEK2	mRNA binding	0.1147	1.1	0.562439
YER123W	YCK3	casein kinase	0.1148	1.1	0.146617
YLR199C		unknown	0.1148	1.1	0.070085
YJR128W			0.1148	1.1	0.537542
YAL035W	FUN12	GTPase *	0.1153	1.1	0.109083

Table 1: continued.

ORF ID	Gene Name	Gene Function	Avg Log_2 Ratio	Fold Change	T-test
YCL054W	SPB1	rRNA (uridine-2'-O-)-methyltransferase *	0.1155	1.1	0.503113
YKL004W	AUR1	inositol phosphoceramide synthase	0.1158	1.1	0.561091
YBR258C	SHG1	histone lysine N-methyltransferase (H3-K4 specific)	0.1163	1.1	0.100662
YMR208W	ERG12	mevalonate kinase	0.1165	1.1	0.216129
YML095C	RAD10	single-stranded DNA binding	0.1167	1.1	0.101069
YKR083C	DAD2	structural constituent of cytoskeleton	0.1167	1.1	0.0839237
YBL101W-B			0.1167	1.1	0.504111
YNR003C	RPC34	DNA-directed RNA polymerase	0.1170	1.1	0.0551875
YDL082W	RPL13A	structural constituent of ribosome	0.1173	1.1	0.267745
YLR154C	RNH203	ribonuclease H	0.1175	1.1	0.3495
YPR086W	SUA7	general RNA polymerase II transcription factor	0.1180	1.1	0.521669
YGL001C	ERG26	C-3 sterol dehydrogenase	0.1180	1.1	0.293019
YOR280C	FSH3	serine hydrolase	0.1183	1.1	0.256269
YDR340W			0.1192	1.1	0.273447
YDR136C			0.1193	1.1	0.591126
YLR333C	RPS25B	structural constituent of ribosome	0.1193	1.1	0.284028
YLR313C	SPH1	cytoskeletal regulator	0.1195	1.1	0.448867
YDR449C	UTP6	snoRNA binding	0.1198	1.1	0.388719
YOL051W	GAL11	RNA polymerase II transcription mediator	0.1200	1.1	0.606222
YJL128C	PBS2	MAP kinase	0.1202	1.1	0.628837
YOR157C	PUP1	endopeptidase	0.1205	1.1	0.11702
YFL037W	TUB2	structural constituent of cytoskeleton	0.1208	1.1	0.345192
YHR166C	CDC23	protein binding	0.1210	1.1	0.185775
YOL084W	PHM7	unknown	0.1212	1.1	0.662521
YPR145W	ASN1	asparagine synthase (glutamine-hydrolyzing)	0.1213	1.1	0.802176
YDL129W		unknown	0.1218	1.1	0.60064
YER128W		unknown	0.1223	1.1	0.00573564
YAL032C	PRP45	transcriptional activator	0.1225	1.1	0.310836
YLR191W	PEX13	protein binding	0.1235	1.1	0.485826
YDL074C	BRE1	ubiquitin-protein ligase	0.1238	1.1	0.48786
YPL140C	MKK2	MAP kinase	0.1240	1.1	0.688968
YHR177W		unknown	0.1243	1.1	0.360452
YLR210W	CLB4	cyclin-dependent protein kinase	0.1247	1.1	0.076248
YEL053C	MAK10	peptide alpha-N-acetyltransferase	0.1250	1.1	0.185465
YPL239W	YAR1	unknown	0.1250	1.1	0.162251
YBL046W	PSY4	unknown	0.1252	1.1	0.425641
YDL031W	DBP10	ATP-dependent RNA helicase	0.1258	1.1	0.173824
YNL157W	IGO1	unknown	0.1258	1.1	0.152728
YBR003W	COQ1	trans-hexaprenyltranstransferase	0.1260	1.1	0.506417
YIL007C	NAS2	unknown	0.1265	1.1	0.315869
YLR228C	ECM22	RNA polymerase II transcription factor	0.1267	1.1	0.24262
YDL190C	UFD2	ubiquitin conjugating enzyme	0.1268	1.1	0.0742965
YJL002C	OST1	dolichyl-diphosphooligosaccharide-protein glycotransferase	0.1277	1.1	0.517673
YIL169C		unknown	0.1282	1.1	0.600069
YBL033C	RIB1	cyclohydrolase	0.1283	1.1	0.0602846
YBR111C	YSA1	phosphoribosyl-ATP diphosphatase	0.1285	1.1	0.123213
YOL158C	ENB1	ferric-enterobactin transporter	0.1287	1.1	0.491319
YDL137W	ARF2	GTPase	0.1288	1.1	0.0891944
YGL122C	NAB2	poly(A) binding	0.1290	1.1	0.338914
YLR317W			0.1292	1.1	0.0329692
YKR079C	TRZ1	purine nucleotide binding	0.1292	1.1	0.264391
YMR304C-A			0.1295	1.1	0.137957
YBL081W		unknown	0.1297	1.1	0.194578
YJR030C		unknown	0.1298	1.1	0.0414806
YLL062C	MHT1	homocysteine S-methyltransferase	0.1303	1.1	0.644286
YGL018C	JAC1	chaperone binding	0.1308	1.1	0.729041
YJR031C	GEA1	ARF guanyl-nucleotide exchange factor	0.1308	1.1	0.569886
YGL221C	NIF3	unknown	0.1308	1.1	0.147054
YLR440C	SEC39	unknown	0.1310	1.1	0.0588094
YEL018W	EAF5	unknown	0.1312	1.1	0.605228
YDR269C			0.1313	1.1	0.193176
YFR018C		unknown	0.1313	1.1	0.110047
YMR044W	IOC4	protein binding	0.1315	1.1	0.630978
YLR360W	VPS38	unknown	0.1317	1.1	0.153893
YFL042C(1)			0.1317	1.1	0.154369
YHR005C	GPA1	GTPase	0.1318	1.1	0.424583
YDR100W	TVP15	unknown	0.1320	1.1	0.370396
YBR164C	ARL1	GTPase	0.1327	1.1	0.0427965
YLL013C	PUF3	mRNA binding	0.1327	1.1	0.208463

Table 1: continued.

ORF ID	Gene Name	Gene Function	Avg Log_2 Ratio	Fold Change	T-test
YBR136W	MEC1	protein kinase	0.1327	1.1	0.478742
YKL214C	YRA2	RNA binding	0.1328	1.1	0.546143
YER189W		unknown	0.1330	1.1	0.559705
YOR394W	PAU21	unknown	0.1330	1.1	0.364599
YCL004W	PGS1	CDP-diacylglycerol-glycerol-3-phosphate 3-phosphatidyltra	0.1333	1.1	0.538722
YDL030W	PRP9	RNA binding	0.1333	1.1	0.420907
Q0065	AI4	endonuclease	0.1335	1.1	0.550689
YMR197C	VTI1	v-SNARE	0.1337	1.1	0.18774
YHR135C	YCK1	casein kinase	0.1337	1.1	0.288841
YDR443C	SSN2	general RNA polymerase II transcription factor	0.1338	1.1	0.0916875
YEL037C	RAD23	protein binding	0.1340	1.1	0.358748
YPR191W	QCR2	ubiquinol-cytochrome-c reductase	0.1340	1.1	0.118421
YNL298W	CLA4	protein serine/threonine kinase	0.1345	1.1	0.595546
YBL098W	BNA4	kynurenine 3-monooxygenase	0.1347	1.1	0.153824
YOR059C		unknown	0.1350	1.1	0.0949166
YAR007C	RFA1	single-stranded DNA binding	0.1352	1.1	0.20586
YDL061C	RPS29B	structural constituent of ribosome	0.1355	1.1	0.0872979
YDR203W			0.1360	1.1	0.182824
YMR293C		amidase	0.1365	1.1	0.140582
YAL068C	PAU8	unknown	0.1368	1.1	0.405266
YCR020C	PET18	unknown	0.1368	1.1	0.224054
YLL036C	PRP19	RNA splicing factor	0.1372	1.1	0.340738
YLR323C	CWC24	unknown	0.1372	1.1	0.475044
YER161C	SPT2	DNA binding	0.1375	1.1	0.139997
YER075C	PTP3	protein tyrosine phosphatase	0.1377	1.1	0.0634348
YML102C-A			0.1378	1.1	0.528052
YBR242W		unknown	0.1383	1.1	0.358679
YHR067W	HTD2	3-hydroxyacyl-[acyl-carrier protein] dehydratase	0.1385	1.1	0.711139
YDR496C	PUF6	specific transcriptional repressor	0.1387	1.1	0.0849547
YCR066W	RAD18	ubiquitin conjugating enzyme *	0.1392	1.1	0.336428
YKR002W	PAP1	polynucleotide adenylyltransferase	0.1393	1.1	0.12771
YJL162C	JJJ2	unknown	0.1398	1.1	0.256489
YFR030W	MET10	sulfite reductase (NADPH)	0.1400	1.1	0.608248
YDL183C		unknown	0.1400	1.1	0.338239
YBR207W	FTH1	iron ion transporter	0.1402	1.1	0.272778
YDR535C			0.1407	1.1	0.451928
YFL020C	PAU5	unknown	0.1407	1.1	0.512559
YMR272C	SCS7	oxidoreductase	0.1410	1.1	0.541139
YER061C	CEM1	fatty-acid synthase	0.1412	1.1	0.281065
YLR359W	ADE13	adenylosuccinate lyase	0.1412	1.1	0.541508
YOR106W	VAM3	t-SNARE	0.1413	1.1	0.508981
YBL105C	PKC1	protein kinase	0.1413	1.1	0.376838
YIL172C		glucosidase	0.1413	1.1	0.0936326
YCR082W	AHC2	unknown	0.1420	1.1	0.232784
YCR090C		unknown	0.1420	1.1	0.243995
YDR088C	SLU7	RNA splicing factor	0.1423	1.1	0.399517
YLR395C	COX8	cytochrome-c oxidase	0.1423	1.1	0.272628
YMR175W	SIP18	phospholipid binding	0.1428	1.1	0.425012
YBR233W	PBP2	unknown	0.1432	1.1	0.408402
YGR034W	RPL26B	structural constituent of ribosome*	0.1437	1.1	0.175154
YML024W	RPS17A	structural constituent of ribosome	0.1440	1.1	0.400271
YDR077W	SED1	structural constituent of cell wall	0.1442	1.1	0.0491482
YGR003W	CUL3	protein binding	0.1442	1.1	0.00275001
YCR095C	OCA4	unknown	0.1442	1.1	0.151949
YMR237W	BCH1	unknown	0.1445	1.1	0.290032
YNL084C	END3	protein binding	0.1447	1.1	0.15514
YDR306C		protein binding	0.1450	1.1	0.0659009
YEL059W			0.1450	1.1	0.650518
YGR212W	SLI1	N-acetyltransferase	0.1452	1.1	0.704562
YDL159W	STE7	MAP kinase	0.1453	1.1	0.485021
YNL069C	RPL16B	structural constituent of ribosome*	0.1453	1.1	0.176655
YKR053C	YSR3	sphingosine-1-phosphate phosphatase	0.1455	1.1	0.445431
YCR044C	PER1	unknown	0.1457	1.1	0.032751
YDR090C		unknown	0.1457	1.1	0.228858
YDR453C	TSA2	thioredoxin peroxidase	0.1463	1.1	0.216189
YDR287W		inositol-1(or 4)-monophosphatase	0.1463	1.1	0.456887
YBR035C	PDX3	pyridoxamine-phosphate oxidase	0.1465	1.1	0.205745
YDL001W	RMD1	unknown	0.1467	1.1	0.491882
YNL094W	APP1	unknown	0.1470	1.1	0.481346

Table 1: continued.

ORF ID	Gene Name	Gene Function	Avg Log_2 Ratio	Fold Change	T-test
YOR126C	IAH1	hydrolase , acting on ester bonds	0.1470	1.1	0.180527
YER019W	ISC1	phospholipase C	0.1470	1.1	0.360717
YCL014W(1)			0.1475	1.1	0.599441
YOR091W	TMA46	unknown	0.1478	1.1	0.016444
YDR465C	RMT2	protein-arginine N-methyltransferase	0.1480	1.1	0.512471
YCR014C	POL4	beta DNA polymerase	0.1482	1.1	0.178999
YGR042W		unknown	0.1487	1.1	0.40785
YMR014W	BUD22	unknown	0.1488	1.1	0.594856
YLR448W	RPL6B	structural constituent of ribosome*	0.1492	1.1	0.285884
YLR443W	ECM7	unknown	0.1493	1.1	0.744632
YKL054C	DEF1	unknown	0.1493	1.1	0.304704
YGL236C	MTO1	unknown	0.1493	1.1	0.44651
YNR052C	POP2	3'-5'-exoribonuclease	0.1495	1.1	0.0901193
YBL052C	SAS3	histone acetyltransferase *	0.1497	1.1	0.62486
YLR238W	FAR10	unknown	0.1498	1.1	0.275035
YEL004W	YEA4	UDP-N-acetylglucosamine transporter	0.1500	1.1	0.375419
YKR022C	NTR2	unknown	0.1503	1.1	0.514403
YNL149C	PGA2	unknown	0.1507	1.1	0.00900468
YDR456W	NHX1	monovalent inorganic cation transporter	0.1508	1.1	0.381317
YHL038C	CBP2	RNA splicing factor	0.1508	1.1	0.484607
YLR240W	VPS34	protein kinase	0.1515	1.1	0.151736
YIL104C	SHQ1	unknown	0.1517	1.1	0.536381
YJR068W	RFC2	DNA clamp loader *	0.1518	1.1	0.285315
YPR124W	CTR1	copper uptake transporter	0.1520	1.1	0.643434
YNL152W		phospholipid binding	0.1523	1.1	0.584724
YKR092C	SRP40	unfolded protein binding	0.1525	1.1	0.373049
YPR037C	ERV2	thiol oxidase	0.1527	1.1	0.379644
YDL072C	YET3	unknown	0.1528	1.1	0.423548
YKL007W	CAP1	actin filament binding	0.1528	1.1	0.345026
YIR018W	YAP5	RNA polymerase II transcription factor	0.1528	1.1	0.289688
YDR243C	PRP28	RNA splicing factor	0.1528	1.1	0.0768341
YML119W		unknown	0.1530	1.1	0.284889
YPR061C	JID1	unknown	0.1530	1.1	0.0236308
YBL036C		alanine racemase *	0.1532	1.1	0.357397
YER021W	RPN3	unknown	0.1532	1.1	0.1174
YDR361C	BCP1	unknown	0.1537	1.1	0.0211505
YBR002C	RER2	prenyltransferase *	0.1538	1.1	0.725365
YDR310C	SUM1	transcriptional repressor	0.1548	1.1	0.37048
YOR239W	ABP140	S-adenosylmethionine-dependent methyltransferase *	0.1548	1.1	0.312529
YOR025W	HST3	DNA binding	0.1548	1.1	0.301654
YKL019W	RAM2	protein farnesyltransferase *	0.1550	1.1	0.297034
YCL048W	SPS22	unknown	0.1553	1.1	0.503054
YER001W	MNN1	alpha-1,3-mannosyltransferase	0.1553	1.1	0.103183
YEL076C-A		unknown	0.1557	1.1	0.221497
YNL206C	RTT106	unknown	0.1558	1.1	0.169254
YGR040W	KSS1	MAP kinase	0.1560	1.1	0.216823
YGR240C	PFK1	6-phosphofructokinase	0.1562	1.1	0.11625
YDL012C		unknown	0.1567	1.1	0.081968
YLR065C		unknown	0.1568	1.1	0.257181
YMR075W	RCO1	unknown	0.1572	1.1	0.160801
YBR128C	ATG14	unknown	0.1575	1.1	0.326089
YOR288C	MPD1	protein disulfide isomerase	0.1575	1.1	0.589195
YLR435W	TSR2	unknown	0.1578	1.1	0.0166818
YER107C	GLE2	structural molecule	0.1582	1.1	0.414265
YDL067C	COX9	cytochrome-c oxidase	0.1590	1.1	0.225618
YKL216W	URA1	dihydroorotate dehydrogenase	0.1590	1.1	0.359024
YLR299W	ECM38	protein-glutamine gamma-glutamyltransferase	0.1592	1.1	0.0204593
YMR144W		unknown	0.1598	1.1	0.222308
YIL175W		unknown	0.1598	1.1	0.57123
YER043C	SAH1	adenosylhomocysteinase	0.1602	1.1	0.228393
YHR195W	NVJ1	protein binding	0.1602	1.1	0.166609
YER014W	HEM14	protoporphyrinogen oxidase	0.1603	1.1	0.116793
YDR311W	TFB1	general RNA polymerase II transcription factor	0.1603	1.1	0.134742
YKL013C	ARC19	structural molecule	0.1607	1.1	0.191698
YBR274W	CHK1	protein kinase	0.1608	1.1	0.11033
YLR145W	RMP1	unknown	0.1610	1.1	0.36634
YGR203W		protein tyrosine phosphatase *	0.1613	1.1	0.203448
YHR076W	PTC7	protein phosphatase type 2C	0.1617	1.1	0.239947
YDL233W		unknown	0.1617	1.1	0.0213597

Table 1: continued.

ORF ID	Gene Name	Gene Function	Avg Log_2 Ratio	Fold Change	T-test
YER066W		unknown	0.1618	1.1	0.416982
YLR196W	PWP1	unknown	0.1620	1.1	0.397123
YOL052C	SPE2	adenosylmethionine decarboxylase	0.1622	1.1	0.11487
YPL210C	SRP72	signal sequence binding	0.1623	1.1	0.634838
YIR023W	DAL81	specific RNA polymerase II transcription factor	0.1625	1.1	0.37432
YIL077C		unknown	0.1627	1.1	0.22355
YBR249C	ARO4	3-deoxy-7-phosphoheptulonate synthase	0.1633	1.1	0.301179
YLR405W	DUS4	tRNA dihydrouridine synthase	0.1633	1.1	0.405922
YBR191W	RPL21A	structural constituent of ribosome	0.1633	1.1	0.320859
YOR308C	SNU66	RNA splicing factor	0.1635	1.1	0.403565
YGR201C		unknown	0.1647	1.1	0.501478
YDR444W		unknown	0.1648	1.1	0.397247
YMR097C	MTG1	GTPase	0.1653	1.1	0.0950438
YNR018W		unknown	0.1653	1.1	0.0247463
YOL004W	SIN3	histone deacetylase	0.1660	1.1	0.409466
YDL056W	MBP1	DNA binding	0.1662	1.1	0.412157
YER057C	HMF1	unknown	0.1662	1.1	0.29538
YIL001W		unknown	0.1665	1.1	0.612778
YJL223C	PAU1	unknown	0.1667	1.1	0.169025
YER122C	GLO3	ARF GTPase activator	0.1670	1.1	0.458502
YNL264C	PDR17	phosphatidylinositol transporter	0.1670	1.1	0.0993254
YJL136C	RPS21B	structural constituent of ribosome	0.1672	1.1	0.162568
YPL099C	FMP14	unknown	0.1675	1.1	0.491244
YOR113W	AZF1	DNA binding	0.1675	1.1	0.053153
YPL088W		aryl-alcohol dehydrogenase	0.1675	1.1	0.130449
YGL071W	RCS1	transcription factor	0.1677	1.1	0.477391
YIL065C	FIS1	unknown	0.1678	1.1	0.176653
YHR199C	FMP34	unknown	0.1680	1.1	0.117084
YPR187W	RPO26	DNA-directed RNA polymerase	0.1685	1.1	0.204089
YCR105W	ADH7	alcohol dehydrogenase	0.1687	1.1	0.0830892
YIL043C	CBR1	cytochrome-b5 reductase	0.1688	1.1	0.0367232
YMR192W	GYL1	protein binding	0.1690	1.1	0.40146
YGR101W	PCP1	peptidase	0.1692	1.1	0.50063
YPR072W	NOT5	3'-5'-exoribonuclease	0.1692	1.1	0.58087
YLR261C			0.1697	1.1	0.636401
YIL039W		unknown	0.1700	1.1	0.0329626
YHR017W	YSC83	unknown	0.1702	1.1	0.0372833
YMR052W	FAR3	unknown	0.1703	1.1	0.542139
YPL059W	GRX5	thiol-disulfide exchange intermediate	0.1703	1.1	0.320115
YDR279W	RNH202	ribonuclease H	0.1705	1.1	0.447241
YBR107C	IML3	unknown	0.1705	1.1	0.602537
YOR003W	YSP3	peptidase	0.1708	1.1	0.298875
YIL019W	FAF1	unknown	0.1708	1.1	0.28448
YGR128C	UTP8	snoRNA binding	0.1710	1.1	0.0728068
YDR327W			0.1710	1.1	0.147889
YDL243C	AAD4	aryl-alcohol dehydrogenase	0.1712	1.1	0.225989
YNL003C	PET8	S-adenosylmethionine transporter	0.1712	1.1	0.337357
YPR106W	ISR1	protein kinase	0.1715	1.1	0.252978
YDR152W	GIR2	unknown	0.1715	1.1	0.380794
YNL011C		unknown	0.1715	1.1	0.231544
YEL064C	AVT2	transporter	0.1717	1.1	0.446737
YOL030W	GAS5	1,3-beta-glucanosyltransferase	0.1717	1.1	0.177334
YLR382C	NAM2	mRNA binding	0.1722	1.1	0.149685
YLL001W	DNM1	GTPase	0.1728	1.1	0.109521
YDL099W	BUG1	unknown	0.1730	1.1	0.294758
YML050W		unknown	0.1732	1.1	0.356024
YOR391C	HSP33	unfolded protein binding	0.1735	1.1	0.156141
YBR166C	TYR1	prephenate dehydrogenase	0.1737	1.1	0.0193129
YBR259W		unknown	0.1747	1.1	0.23908
YDR454C	GUK1	guanylate kinase	0.1747	1.1	0.209716
YGL097W	SRM1	signal transducer	0.1747	1.1	0.368711
YAR003W	SWD1	histone lysine N-methyltransferase (H3-K4 specific)	0.1752	1.1	0.23003
YPL101W	ELP4	RNA polymerase II transcription elongation factor	0.1753	1.1	0.344681
YDL143W	CCT4	unfolded protein binding	0.1755	1.1	0.544732
YKL175W	ZRT3	zinc ion transporter	0.1755	1.1	0.423098
YDL181W	INH1	enzyme inhibitor	0.1758	1.1	0.0270924
YDR495C	VPS3	unknown	0.1762	1.1	0.336126
YKL163W	PIR3	structural constituent of cell wall	0.1762	1.1	0.0809432
YJL073W	JEM1	unfolded protein binding	0.1762	1.1	0.109618

Table 1: continued.

ORF ID	Gene Name	Gene Function	Avg Log_2 Ratio	Fold Change	T-test
YMR166C		transporter	0.1762	1.1	0.465635
YML038C	YMD8	nucleotide-sugar transporter	0.1765	1.1	0.405977
YMR020W	FMS1	amine oxidase	0.1767	1.1	0.444654
YDL206W		unknown	0.1767	1.1	0.0698194
YDL146W	LDB17	unknown	0.1777	1.1	0.402632
YML055W	SPC2	protein binding	0.1777	1.1	0.147956
YML018C		unknown	0.1777	1.1	0.710491
YGR014W	MSB2	osmosensor	0.1783	1.1	0.535058
YPR062W	FCY1	cytosine deaminase	0.1785	1.1	0.135592
YKL025C	PAN3	poly(A)-specific ribonuclease	0.1787	1.1	0.52356
YJL165C	HAL5	protein kinase	0.1787	1.1	0.0704927
YGR083C	GCD2	translation initiation factor	0.1790	1.1	0.632362
YGR185C	TYS1	tyrosine-tRNA ligase	0.1790	1.1	0.101729
YBR073W	RDH54	DNA-dependent ATPase *	0.1795	1.1	0.319776
YNR032W	PPG1	protein phosphatase type 2A	0.1802	1.1	0.289962
YOR261C	RPN8	unknown	0.1807	1.1	0.0713078
YLR256W	HAP1	specific RNA polymerase II transcription factor	0.1808	1.1	0.103615
YMR265C		unknown	0.1808	1.1	0.256657
YLR092W	SUL2	sulfate transporter	0.1810	1.1	0.393825
YBR048W	RPS11B	structural constituent of ribosome	0.1813	1.1	0.168943
YHR153C	SPO16	unknown	0.1813	1.1	0.432357
YNL076W	MKS1	transcriptional repressor	0.1815	1.1	0.481046
YHR031C	RRM3	DNA helicase	0.1818	1.1	0.335263
YOR070C	GYP1	Rab GTPase activator	0.1823	1.1	0.0348458
YNL027W	CRZ1	transcription factor	0.1823	1.1	0.0808546
YKL018W	SWD2	histone lysine N-methyltransferase (H3-K4 specific)	0.1825	1.1	0.406908
YIL064W		S-adenosylmethionine-dependent methyltransferase	0.1835	1.1	0.170483
YHR133C	NSG1	protein binding	0.1837	1.1	0.105198
YLR287C		unknown	0.1838	1.1	0.435417
YDR376W	ARH1	NADPH-adrenodoxin reductase	0.1840	1.1	0.26118
YPL183C		unknown	0.1843	1.1	0.572302
YJL203W	PRP21	RNA binding	0.1845	1.1	0.416913
YIL127C		unknown	0.1847	1.1	0.177489
YML066C	SMA2	unknown	0.1848	1.1	0.681611
YGR169C	PUS6	pseudouridylate synthase	0.1848	1.1	0.558649
YDL154W	MSH5	unknown	0.1850	1.1	0.0226532
YDR215C			0.1855	1.1	0.548794
YCR058C			0.1857	1.1	0.0256472
YBR215W	HPC2	transcription regulator	0.1857	1.1	0.120199
YPL034W		unknown	0.1860	1.1	0.772794
YMR311C	GLC8	enzyme activator	0.1862	1.1	0.295748
YMR322C	SNO4	unfolded protein binding	0.1862	1.1	0.432987
YPL213W	LEA1	RNA splicing factor	0.1863	1.1	0.100498
YMR098C		unknown	0.1865	1.1	0.265559
YDR542W	PAU10	unknown	0.1867	1.1	0.262998
YBR063C		unknown	0.1868	1.1	0.143337
YBR285W		unknown	0.1872	1.1	0.0711402
YOR171C	LCB4	D-erythro-sphingosine kinase	0.1872	1.1	0.180416
YKR059W	TIF1	translation initiation factor	0.1875	1.1	0.166134
YBR253W	SRB6	RNA polymerase II transcription mediator	0.1885	1.1	0.440593
YKL189W	HYM1	unknown	0.1887	1.1	0.240389
YDR212W	TCP1	unfolded protein binding	0.1887	1.1	0.553483
YHR216W	IMD2	IMP dehydrogenase	0.1897	1.1	0.356608
YDL207W	GLE1	unknown	0.1897	1.1	0.104677
YNL160W	YGP1	unknown	0.1902	1.1	0.0411112
YOR205C	FMP38	unknown	0.1905	1.1	0.0141179
YDR423C	CAD1	RNA polymerase II transcription factor	0.1910	1.1	0.664048
YNL287W	SEC21	unknown	0.1912	1.1	0.252102
YER009W	NTF2	Ran GTPase binding	0.1912	1.1	0.314015
YGR255C	COQ6	ubiquinone biosynthesis monooxygenase	0.1912	1.1	0.304234
YGR286C	BIO2	biotin synthase	0.1915	1.1	0.155083
YJR119C		unknown	0.1917	1.1	0.639129
YNL090W	RHO2	GTPase *	0.1917	1.1	0.233709
YGR198W		transferase	0.1918	1.1	0.197213
YKL201C	MNN4	unknown	0.1923	1.1	0.626439
YDR288W	NSE3	DNA binding	0.1935	1.1	0.177183
YNL062C	GCD10	tRNA binding	0.1935	1.1	0.0723126
YKR068C	BET3	unknown	0.1937	1.1	0.222498
YML131W		unknown	0.1938	1.1	0.0895904

Table 1: continued.

ORF ID	Gene Name	Gene Function	Avg Log_2 Ratio	Fold Change	T-test
YDR338C		unknown	0.1940	1.1	0.290121
YBL099W	ATP1	hydrogen-transporting ATP synthase , rotational mechanism	0.1940	1.1	0.0538191
YJL010C	NOP9	RNA binding	0.1943	1.1	0.163332
YLR020C	YEH2	sterol esterase	0.1952	1.1	0.0119782
YIL062C	ARC15	structural molecule *	0.1952	1.1	0.347166
YNR049C	MSO1	unknown	0.1955	1.1	0.206031
YBR077C	SLM4	phosphatidylinositol-3,4-bisphosphate binding	0.1957	1.1	0.142525
YDR383C	NKP1	unknown	0.1958	1.1	0.262588
YDR500C	RPL37B	structural constituent of ribosome	0.1972	1.1	0.408698
YDR365C	ESF1	RNA binding	0.1973	1.1	0.440112
YAR002W	NUP60	structural constituent of nuclear pore	0.1975	1.1	0.00669003
YPR199C	ARR1	RNA polymerase II transcription factor	0.1975	1.1	0.0310066
YDR143C	SAN1	ubiquitin-protein ligase	0.1982	1.1	0.0396306
YBR261C		S-adenosylmethionine-dependent methyltransferase	0.1983	1.1	0.0473883
YCL036W	GFD2	unknown	0.1983	1.1	0.251213
YPL206C		glycerophosphodiester phosphodiesterase	0.1985	1.1	0.0894852
YOR120W	GCY1	aldo-keto reductase	0.1987	1.1	0.305555
YDL102W	CDC2	delta DNA polymerase *	0.1988	1.1	0.355927
YKR013W	PRY2	unknown	0.1990	1.1	0.501651
YPR110C	RPC40	DNA-directed RNA polymerase	0.1992	1.1	0.157473
YHR020W		proline-tRNA ligase	0.1992	1.1	0.312284
YOR122C	PFY1	actin monomer binding	0.1995	1.1	0.0886395
YBL080C	PET112	unknown	0.1998	1.1	0.278379
YGL094C	PAN2	poly(A)-specific ribonuclease	0.2000	1.1	0.345
YER171W	RAD3	general RNA polymerase II transcription factor	0.2003	1.1	0.482323
YJR133W	XPT1	xanthine phosphoribosyltransferase	0.2005	1.1	0.0262605
YMR070W	MOT3	DNA binding	0.2005	1.1	0.00594312
YKL172W	EBP2	unknown	0.2007	1.1	0.187262
YPL068C		unknown	0.2013	1.1	0.343503
YIL105C	SLM1	phosphoinositide binding	0.2017	1.2	0.0844178
YPL211W	NIP7	unknown	0.2017	1.2	0.13289
YOR349W	CIN1	beta-tubulin binding	0.2018	1.2	0.611145
YHL039W		unknown	0.2023	1.2	0.0691562
YCR060W	TAH1	chaperone binding	0.2023	1.2	0.0452439
YDR382W	RPP2B	structural constituent of ribosome	0.2023	1.2	0.104016
YOR166C		unknown	0.2025	1.2	0.228483
YLL023C		unknown	0.2027	1.2	0.148691
YCR094W	CDC50	phospholipid-translocating ATPase	0.2027	1.2	0.275728
YIL157C	FMP35	unknown	0.2028	1.2	0.00442258
YMR145C	NDE1	NADH dehydrogenase	0.2032	1.2	0.181511
YIR030C	DCG1	unknown	0.2033	1.2	0.451877
YGL191W	COX13	enzyme regulator	0.2033	1.2	0.148849
YPR180W	AOS1	SUMO activating enzyme	0.2038	1.2	0.241394
YCL027W	FUS1	unknown	0.2040	1.2	0.283427
YAR073W			0.2042	1.2	0.395782
YNR045W	PET494	translation regulator	0.2042	1.2	0.211323
YBR108W		unknown	0.2043	1.2	0.000884059
YKL041W	VPS24	protein binding	0.2047	1.2	0.459616
YLR110C	CCW12	unknown	0.2047	1.2	0.173838
YCLX05C			0.2052	1.2	0.386081
YBL020W	RFT1	oligosaccharide transporter	0.2052	1.2	0.150556
YMR128W	ECM16	RNA helicase	0.2057	1.2	0.0371025
YMR244C-A		unknown	0.2057	1.2	0.0980733
YDR480W	DIG2	transcription factor	0.2063	1.2	0.553812
YMR081C	ISF1	unknown	0.2063	1.2	0.049114
YLR185W	RPL37A	structural constituent of ribosome	0.2065	1.2	0.53856
YDR368W	YPR1	oxidoreductase	0.2065	1.2	0.0905739
YLR216C	CPR6	unfolded protein binding	0.2067	1.2	0.150434
YOR287C		unknown	0.2068	1.2	0.3349
YDR394W	RPT3	ATPase *	0.2072	1.2	0.09225
YKL045W	PRI2	alpha DNA polymerase	0.2075	1.2	0.195764
YLL065W			0.2083	1.2	0.175184
YOR319W	HSH49	RNA binding	0.2083	1.2	0.172456
YMR273C	ZDS1	protein binding	0.2083	1.2	0.128618
YGR072W	UPF3	unknown	0.2085	1.2	0.0940925
YHR142W	CHS7	unknown	0.2087	1.2	0.315467
YMR010W		unknown	0.2088	1.2	0.364446
YER092W	IES5	unknown	0.2088	1.2	0.216276
YOL036W		unknown	0.2090	1.2	0.233145

Table 1: continued.

ORF ID	Gene Name	Gene Function	Avg Log_2 Ratio	Fold Change	T-test
YFL052W		DNA binding	0.2095	1.2	0.0119911
YCL059C	KRR1	unknown	0.2097	1.2	0.211965
YDR416W	SYF1	unknown	0.2100	1.2	0.402752
YNL253W	TEX1	unknown	0.2107	1.2	0.49864
YDL053C	PBP4	unknown	0.2107	1.2	0.105205
YDR086C	SSS1	protein transporter	0.2110	1.2	0.235194
YIR024C		unknown	0.2110	1.2	0.0107576
YBR142W	MAK5	ATP-dependent RNA helicase	0.2110	1.2	0.274612
YLR370C	ARC18	structural constituent of cytoskeleton	0.2112	1.2	0.021731
YGL095C	VPS45	unfolded protein binding	0.2113	1.2	0.103886
YLR052W	IES3	unknown	0.2115	1.2	0.55265
YPL011C	TAF3	general RNA polymerase II transcription factor	0.2115	1.2	0.452451
YLR387C	REH1	unknown	0.2118	1.2	0.249962
YMR049C	ERB1	unknown	0.2118	1.2	0.287832
YIL073C	SPO22	unknown	0.2118	1.2	0.288363
YKR074W		unknown	0.2120	1.2	0.573312
YFR027W	ECO1	acetyltransferase	0.2122	1.2	0.47313
YGR079W		unknown	0.2122	1.2	0.624995
YEL074W			0.2123	1.2	0.00527358
YBR228W	SLX1	5'-flap endonuclease	0.2123	1.2	0.052611
YOL098C		metalloendopeptidase	0.2127	1.2	0.6106
YKL156W	RPS27A	structural constituent of ribosome	0.2130	1.2	0.254447
YEL059C-A	SOM1	unknown	0.2130	1.2	0.230481
YLR166C	SEC10	protein binding	0.2130	1.2	0.486565
YDR078C	SHU2	unknown	0.2132	1.2	0.427389
YDR501W	PLM2	transcription factor	0.2132	1.2	0.456581
YER131W	RPS26B	structural constituent of ribosome	0.2133	1.2	0.0268335
YHR039BC			0.2137	1.2	0.0938629
YKL079W	SMY1	motor	0.2137	1.2	0.362943
YMR203W	TOM40	protein transporter	0.2140	1.2	0.17831
YBR187W		unknown	0.2148	1.2	0.212924
YJR109C	CPA2	carbamoyl-phosphate synthase (glutamine-hydrolyzing)	0.2148	1.2	0.147469
YDR302W	GPI11	phosphoethanolamine N-methyltransferase	0.2153	1.2	0.0635946
YLR276C	DBP9	ATP-dependent RNA helicase	0.2160	1.2	0.106734
YJL138C	TIF2	translation initiation factor	0.2162	1.2	0.363416
YLR442C	SIR3	histone binding	0.2162	1.2	0.600477
YDR447C	RPS17B	structural constituent of ribosome	0.2165	1.2	0.047969
YGL185C		oxidoreductase	0.2165	1.2	0.313809
YGR135W	PRE9	endopeptidase	0.2173	1.2	0.0929783
YLR425W	TUS1	Rho guanyl-nucleotide exchange factor	0.2175	1.2	0.144708
YGR153W		unknown	0.2175	1.2	0.473033
YAL041W	CDC24	signal transducer *	0.2175	1.2	0.362508
YJR067C	YAE1	unknown	0.2180	1.2	0.663165
YNL125C	ESBP6	transporter	0.2180	1.2	0.231364
YCL057W	PRD1	metalloendopeptidase *	0.2185	1.2	0.151149
YDR073W	SNF11	general RNA polymerase II transcription factor	0.2188	1.2	0.137427
YML053C		unknown	0.2188	1.2	0.335272
YNL010W		unknown	0.2190	1.2	0.0600224
YGL262W		unknown	0.2192	1.2	0.254889
YCR065W	HCM1	specific RNA polymerase II transcription factor	0.2192	1.2	0.230375
YDR266C		unknown	0.2192	1.2	0.134242
YDL212W	SHR3	unfolded protein binding	0.2197	1.2	0.293455
YER188W			0.2197	1.2	0.183911
YNL308C	KRI1	unknown	0.2197	1.2	0.052621
YML120C	NDI1	NADH dehydrogenase	0.2197	1.2	0.243432
YAL046C		unknown	0.2197	1.2	0.345238
YHR123W	EPT1	ethanolaminephosphotransferase	0.2203	1.2	0.126889
YJR012C		unknown	0.2205	1.2	0.0856618
YOL094C	RFC4	DNA clamp loader *	0.2208	1.2	0.0917365
YNL079C	TPM1	actin lateral binding	0.2210	1.2	0.182341
YOR213C	SAS5	acetyltransferase *	0.2212	1.2	0.034141
YCR054C	CTR86	unknown	0.2215	1.2	0.138037
YMR312W	ELP6	RNA polymerase II transcription elongation factor	0.2218	1.2	0.561995
YGL091C	NBP35	ATPase	0.2220	1.2	0.409986
YDR065W		unknown	0.2222	1.2	0.593805
YIL052C	RPL34B	structural constituent of ribosome	0.2223	1.2	0.133539
YDR067C	OCA6	unknown	0.2225	1.2	0.268057
YPR137W	RRP9	snoRNA binding	0.2227	1.2	0.265159
YDR043C	NRG1	DNA binding	0.2228	1.2	0.141086

Table 1: continued.

ORF ID	Gene Name	Gene Function	Avg Log_2 Ratio	Fold Change	T-test
YBR132C	AGP2	amino acid transporter	0.2228	1.2	0.070194
YGR251W		unknown	0.2228	1.2	0.162678
YHR152W	SPO12	unknown	0.2232	1.2	0.0569875
YOL001W	PHO80	cyclin-dependent protein kinase	0.2233	1.2	0.107034
YKL174C	TPO5	polyamine transporter	0.2233	1.2	0.202898
YNL038W	GPI15	UDP-glycosyltransferase	0.2237	1.2	0.40345
YAR031W	PRM9	unknown	0.2240	1.2	0.145567
YDR054C	CDC34	ubiquitin conjugating enzyme	0.2242	1.2	0.00100987
YBR130C	SHE3	mRNA binding	0.2243	1.2	0.196419
YDR165W	TRM82	protein binding	0.2253	1.2	0.474287
YBR264C	YPT10	GTPase *	0.2255	1.2	0.058086
YLR059C	REX2	3'-5' exonuclease	0.2257	1.2	0.553452
YPR084W		unknown	0.2260	1.2	0.289684
YGL103W	RPL28	structural constituent of ribosome*	0.2262	1.2	0.0353955
YGR188C	BUB1	protein binding	0.2262	1.2	0.168036
YAR015W	ADE1	phosphoribosylaminoimidazolesuccinocarboxamide synthas	0.2265	1.2	0.322197
YOR203W			0.2265	1.2	0.119555
YDR236C	FMN1	riboflavin kinase	0.2268	1.2	0.530411
YLR100W	ERG27	3-keto sterol reductase	0.2272	1.2	0.147638
YOL097C	WRS1	tryptophan-tRNA ligase	0.2277	1.2	0.44715
YER094C	PUP3	endopeptidase	0.2283	1.2	0.264687
YMR235C	RNA1	Ran GTPase activator	0.2288	1.2	0.289632
YKL069W		unknown	0.2288	1.2	0.0346682
YNL141W	AAH1	adenine deaminase	0.2290	1.2	0.25245
YCRX12W			0.2300	1.2	0.249624
YEL075C		unknown	0.2305	1.2	0.0369989
YCR097WB			0.2312	1.2	0.212512
YDL148C	NOP14	snoRNA binding	0.2312	1.2	0.0426437
YJR056C		unknown	0.2317	1.2	0.373123
YGL148W	ARO2	chorismate synthase *	0.2318	1.2	0.0740175
YNL229C	URE2	transcription corepressor *	0.2320	1.2	0.379889
YJR007W	SUI2	translation initiation factor	0.2320	1.2	0.168411
YDR421W	ARO80	specific RNA polymerase II transcription factor	0.2322	1.2	0.408847
YML056C	IMD4	IMP dehydrogenase	0.2328	1.2	0.253595
YBL095W		unknown	0.2332	1.2	0.0912774
YER051W	JHD1	histone demethylase (H3-K36 specific)	0.2332	1.2	0.31391
Q0060	AI3	endonuclease	0.2335	1.2	0.00218623
YHR125W			0.2335	1.2	0.448389
YKL126W	YPK1	protein serine/threonine kinase	0.2343	1.2	0.0489144
YJR144W	MGM101	DNA binding	0.2348	1.2	0.165467
YBR289W	SNF5	general RNA polymerase II transcription factor	0.2348	1.2	0.0054577
YPR028W	YOP1	protein binding	0.2352	1.2	0.0367908
YKR043C		unknown	0.2357	1.2	0.213975
YMR320W			0.2358	1.2	0.617323
YGL237C	HAP2	transcriptional activator	0.2358	1.2	0.0216083
YGL110C	CUE3	unknown	0.2362	1.2	0.309886
YGL243W	TAD1	tRNA specific adenosine deaminase	0.2365	1.2	0.364074
YOL067C	RTG1	transcription coactivator	0.2365	1.2	0.115311
YJR127C	RSF2	transcription factor	0.2365	1.2	0.0070084
YKL125W	RRN3	RNA polymerase I transcription factor	0.2367	1.2	0.24365
YDR261W-A			0.2372	1.2	0.196379
YCL050C	APA1	bis(5'-nucleosyl)-tetraphosphatase	0.2375	1.2	0.187713
YLR194C		structural constituent of cell wall	0.2375	1.2	0.00752993
YNL207W	RIO2	protein kinase	0.2380	1.2	0.286799
YPL146C	NOP53	rRNA binding	0.2385	1.2	0.27512
YLR209C	PNP1	purine-nucleoside phosphorylase	0.2387	1.2	0.471536
YOR321W	PMT3	dolichyl-phosphate-mannose-protein mannosyltransferase	0.2388	1.2	0.363515
YDL192W	ARF1	GTPase	0.2393	1.2	0.0132416
YOR369C	RPS12	structural constituent of ribosome	0.2397	1.2	0.70685
YEL025C		unknown	0.2398	1.2	0.0393382
YIL092W		unknown	0.2400	1.2	0.116198
YOR128C	ADE2	phosphoribosylaminoimidazole carboxylase	0.2400	1.2	0.331973
YDL193W	NUS1	prenyltransferase	0.2402	1.2	0.308976
YOR299W	BUD7	unknown	0.2413	1.2	0.0632771
YER146W	LSM5	RNA binding	0.2413	1.2	0.293464
YJL206C-A			0.2417	1.2	0.473818
YNL001W	DOM34	unknown	0.2417	1.2	0.0676259
YNR010W	CSE2	RNA polymerase II transcription mediator	0.2420	1.2	0.347888
YKL056C	TMA19	unknown	0.2425	1.2	0.00992914

Table 1: continued.

ORF ID	Gene Name	Gene Function	Avg Log_2 Ratio	Fold Change	T-test
YEL042W	GDA1	guanosine-diphosphatase *	0.2427	1.2	0.386283
YFR010W	UBP6	ubiquitin-specific protease	0.2430	1.2	0.0131737
YDR425W	SNX41	protein transporter	0.2440	1.2	0.290291
YBR284W		unknown	0.2442	1.2	0.19127
YGL040C	HEM2	porphobilinogen synthase	0.2443	1.2	0.0599176
YAR008W	SEN34	tRNA-intron endonuclease	0.2443	1.2	0.00634203
YGR229C	SMI1	unknown	0.2453	1.2	0.154132
YGR105W	VMA21	unknown	0.2457	1.2	0.13219
YEL007W		unknown	0.2462	1.2	0.0422219
YOR004W	UTP23	unknown	0.2462	1.2	0.480456
YMR217W	GUA1	GMP synthase (glutamine-hydrolyzing)	0.2463	1.2	0.417866
YJL124C	LSM1	RNA binding	0.2465	1.2	0.0799271
YNL166C	BNI5	unknown	0.2468	1.2	0.0145426
YOR194C	TOA1	general RNA polymerase II transcription factor	0.2472	1.2	0.0327548
YMR112C	MED11	RNA polymerase II transcription mediator	0.2475	1.2	0.301758
YFR045W		transporter	0.2492	1.2	0.253317
YCR038C	BUD5	signal transducer *	0.2497	1.2	0.077876
YMR314W	PRE5	endopeptidase	0.2502	1.2	0.127937
YJL183W	MNN11	alpha-1,6-mannosyltransferase	0.2503	1.2	0.158975
YOR340C	RPA43	DNA-directed RNA polymerase	0.2508	1.2	0.376509
YNL118C	DCP2	mRNA binding	0.2515	1.2	0.241346
YBL078C	ATG8	microtubule binding	0.2515	1.2	0.127693
YKL030W			0.2518	1.2	0.101663
YHR127W		unknown	0.2518	1.2	0.0873626
YER025W	GCD11	translation initiation factor	0.2523	1.2	0.0939522
YKR090W	PXL1	protein binding	0.2525	1.2	0.190128
YOL017W	ESC8	unknown	0.2525	1.2	0.21091
YIL025C			0.2528	1.2	0.020315
YHR206W	SKN7	transcription factor	0.2532	1.2	0.224089
YBL083C			0.2533	1.2	0.0765923
YKL193C	SDS22	enzyme regulator	0.2535	1.2	0.11416
YKR012C			0.2545	1.2	0.418796
YFR016C		unknown	0.2548	1.2	0.132335
YDL105W	NSE4	unknown	0.2550	1.2	0.173526
YDL135C	RDI1	signal transducer *	0.2552	1.2	0.0586848
YLR017W	MEU1	S-methyl-5-thioadenosine phosphorylase	0.2553	1.2	0.0523499
YJR001W	AVT1	neutral amino acid transporter	0.2565	1.2	0.0367596
YPL058C	PDR12	xenobiotic-transporting ATPase *	0.2565	1.2	0.189859
YMR240C	CUS1	protein binding	0.2567	1.2	0.133366
YLR118C		palmitoyl-(protein) hydrolase	0.2575	1.2	0.0105155
YLR341W	SPO77	unknown	0.2577	1.2	0.338439
YDR359C	VID21	unknown	0.2577	1.2	0.324662
YML080W	DUS1	tRNA dihydrouridine synthase	0.2577	1.2	0.485112
YBL054W		unknown	0.2578	1.2	0.383595
YCR037C	PHO87	inorganic phosphate transporter	0.2578	1.2	0.300373
YDL106C	PHO2	transcription factor	0.2580	1.2	0.0348297
YDR190C	RVB1	ATPase *	0.2583	1.2	0.144528
YHR048W		drug transporter	0.2587	1.2	0.531096
YER168C	CCA1	tRNA adenylyltransferase	0.2588	1.2	0.0189504
YNL074C	MLF3	unknown	0.2592	1.2	0.158077
YOL040C	RPS15	structural constituent of ribosome	0.2593	1.2	0.0260094
YDR395W	SXM1	protein carrier	0.2598	1.2	0.0992076
YPL017C		S-adenosylmethionine-dependent methyltransferase	0.2600	1.2	0.792581
YDR469W	SDC1	histone lysine N-methyltransferase (H3-K4 specific)	0.2602	1.2	0.00888136
YOR269W	PAC1	unknown	0.2602	1.2	0.314412
YCR087W			0.2603	1.2	0.0461912
YDR366C		unknown	0.2605	1.2	0.0711693
YKL012W	PRP40	RNA binding	0.2607	1.2	0.165549
YPR203W		unknown	0.2608	1.2	0.162637
YHR090C	YNG2	enzyme activator	0.2612	1.2	0.00951868
YGR096W	TPC1	transporter	0.2615	1.2	0.552549
YPR090W			0.2623	1.2	0.00706889
YGR276C	RNH70	3'-5' exonuclease	0.2633	1.2	0.155812
YJL187C	SWE1	protein kinase	0.2635	1.2	0.0525705
YPR063C		unknown	0.2642	1.2	0.0222418
YOR186W		unknown	0.2642	1.2	0.106565
YDL059C	RAD59	protein binding	0.2643	1.2	0.0787789
YNL123W	NMA111	serine-type peptidase	0.2643	1.2	0.158907
YGR106C		unknown	0.2643	1.2	0.000763048

Table 1: continued.

ORF ID	Gene Name	Gene Function	Avg Log_2 Ratio	Fold Change	T-test
YBL009W		protein serine/threonine kinase	0.2643	1.2	0.211382
YBR297W	MAL33	transcription factor	0.2655	1.2	0.245612
YPL270W	MDL2	ATPase , coupled to transmembrane movement of substanc	0.2655	1.2	0.134359
YBR292C			0.2655	1.2	0.364644
YML034W	SRC1	unknown	0.2658	1.2	0.307617
YDR153C	ENT5	clathrin binding	0.2668	1.2	0.0978425
YOR310C	NOP58	unknown	0.2683	1.2	0.173681
YKL181W	PRS1	ribose phosphate diphosphokinase	0.2685	1.2	0.122701
YDR363W	ESC2	unknown	0.2687	1.2	0.00376801
YDR184C	ATC1	unknown	0.2690	1.2	0.11266
YKL155C	RSM22	structural constituent of ribosome	0.2695	1.2	0.112748
YOR343W-A			0.2695	1.2	0.0992868
YPL199C		unknown	0.2697	1.2	0.0222173
YGL231C		unknown	0.2698	1.2	0.0461556
YFL039C	ACT1	structural constituent of cytoskeleton	0.2700	1.2	0.113005
YMR170C	ALD2	3-chloroallyl aldehyde dehydrogenase	0.2708	1.2	0.335334
YHR172W	SPC97	structural constituent of cytoskeleton	0.2715	1.2	0.00437957
YDR071C	PAA1	aralkylamine N-acetyltransferase *	0.2717	1.2	0.111615
YDL110C	TMA17	unknown	0.2720	1.2	0.243543
YFL066C		unknown	0.2722	1.2	0.0590227
YDR364C	CDC40	RNA splicing factor	0.2725	1.2	0.240535
YML094W	GIM5	tubulin binding	0.2727	1.2	0.507227
YDL036C	PUS9	tRNA-pseudouridine synthase	0.2728	1.2	0.347938
YMR158W	MRPS8	structural constituent of ribosome	0.2728	1.2	0.0357293
YOL077C	BRX1	rRNA primary transcript binding	0.2732	1.2	0.258736
YDR237W	MRPL7	structural constituent of ribosome	0.2733	1.2	0.191539
YDR282C		unknown	0.2738	1.2	0.183089
YNR023W	SNF12	general RNA polymerase II transcription factor	0.2738	1.2	0.345581
YLR193C		unknown	0.2740	1.2	0.178595
YNL252C	MRPL17	structural constituent of ribosome	0.2742	1.2	0.0310491
YPL258C	THI21	phosphomethylpyrimidine kinase	0.2743	1.2	0.175314
YIL024C		unknown	0.2745	1.2	0.0113285
YCLX10C			0.2747	1.2	0.362386
YDR324C	UTP4	snoRNA binding	0.2747	1.2	0.175598
YKL209C	STE6	ATPase , coupled to transmembrane movement of substanc	0.2748	1.2	0.198467
YPR162C	ORC4	DNA replication origin binding	0.2752	1.2	0.684754
YDL103C	QRI1	UDP-N-acetylglucosamine diphosphorylase	0.2757	1.2	0.0108105
YCR009C	RVS161	cytoskeletal protein binding	0.2758	1.2	0.11788
YOL106W			0.2760	1.2	0.155653
YBR004C	GPI18	mannosyltransferase	0.2760	1.2	0.0305271
YFR048W	RMD8	unknown	0.2762	1.2	0.0340041
YOR163W	DDP1	diphosphoinositol-polyphosphate diphosphatase	0.2765	1.2	0.175881
YDL195W	SEC31	structural molecule	0.2767	1.2	0.195066
YER047C	SAP1	ATPase	0.2773	1.2	0.181525
YMR043W	MCM1	DNA binding	0.2777	1.2	0.235303
YLR383W	SMC6	unknown	0.2782	1.2	0.306265
YDR072C	IPT1	transferase , transferring phosphorus-containing groups	0.2782	1.2	0.252582
YIR009W	MSL1	RNA binding	0.2782	1.2	0.0323755
YOR064C	YNG1	histone acetyltransferase	0.2787	1.2	0.0494563
YDL002C	NHP10	unknown	0.2790	1.2	0.223141
YDL057W		unknown	0.2792	1.2	0.0067468
YDL186W		unknown	0.2795	1.2	0.0292376
YLR248W	RCK2	protein serine/threonine kinase	0.2795	1.2	0.0249379
YOR281C	PLP2	GTPase inhibitor	0.2798	1.2	0.692365
YLR151C	PCD1	pyrophosphatase	0.2800	1.2	0.354762
YJR100C		unknown	0.2805	1.2	0.10521
YLR175W	CBF5	pseudouridylate synthase	0.2807	1.2	0.161506
YDR238C	SEC26	unknown	0.2810	1.2	0.0429732
YKL080W	VMA5	hydrogen-transporting ATPase , rotational mechanism	0.2812	1.2	0.130258
YGR234W	YHB1	nitric oxide reductase	0.2817	1.2	0.106908
YDR473C	PRP3	RNA splicing factor	0.2822	1.2	0.0489397
YOR316C	COT1	di-, tri-valent inorganic cation transporter	0.2825	1.2	0.0859813
YLR455W		unknown	0.2827	1.2	0.116735
YFL047W	RGD2	Rho GTPase activator	0.2828	1.2	0.0133458
YDL225W	SHS1	structural constituent of cytoskeleton	0.2830	1.2	0.101705
YBR109C	CMD1	protein binding	0.2830	1.2	0.0795603
YGR137W			0.2832	1.2	0.0829099
YDR163W	CWC15	unknown	0.2835	1.2	0.179771
YMR030W	RSF1	unknown	0.2838	1.2	0.0764922

Table 1: continued.

ORF ID	Gene Name	Gene Function	Avg Log_2 Ratio	Fold Change	T-test
YJR085C		unknown	0.2842	1.2	0.063361
YLR229C	CDC42	GTPase *	0.2843	1.2	0.0488772
YGR074W	SMD1	RNA splicing factor	0.2845	1.2	0.28898
YDL108W	KIN28	general RNA polymerase II transcription factor	0.2845	1.2	0.237734
YIL116W	HIS5	histidinol-phosphate transaminase	0.2847	1.2	0.00934731
YJL222W	VTH2	signal sequence binding	0.2853	1.2	0.0252787
YDR045C	RPC11	DNA-directed RNA polymerase	0.2853	1.2	0.041639
YAR019C	CDC15	protein kinase	0.2855	1.2	0.273523
YIL004C	BET1	v-SNARE	0.2855	1.2	0.0786559
YDR468C	TLG1	v-SNARE *	0.2857	1.2	0.0897131
YPL165C	SET6	unknown	0.2858	1.2	0.486303
YBR155W	CNS1	unfolded protein binding	0.2858	1.2	0.0649887
YNL337W			0.2860	1.2	0.114855
YLR420W	URA4	dihydroorotase	0.2860	1.2	0.0240395
YDR058C	TGL2	triacylglycerol lipase	0.2868	1.2	0.122623
YIL096C		unknown	0.2872	1.2	0.215658
YBR071W		unknown	0.2875	1.2	0.290717
YDL068W			0.2878	1.2	0.149483
YDR097C	MSH6	DNA binding	0.2897	1.2	0.0608023
YLR104W		unknown	0.2898	1.2	0.0816736
YNL260C		unknown	0.2902	1.2	0.151976
YEL019C	MMS21	SUMO ligase	0.2908	1.2	0.0563927
YER085C		unknown	0.2913	1.2	0.089874
YCR007C		unknown	0.2918	1.2	0.196194
YER071C		unknown	0.2927	1.2	0.0893787
YNL002C	RLP7	rRNA binding	0.2930	1.2	0.181953
YOL003C	PFA4	protein-cysteine S-palmitoleyltransferase	0.2930	1.2	0.0812157
YGL179C	TOS3	protein kinase	0.2932	1.2	0.138669
YHR162W		unknown	0.2933	1.2	0.0851827
YNL065W	AQR1	monocarboxylic acid transporter	0.2933	1.2	0.212312
YLR432W	IMD3	IMP dehydrogenase	0.2935	1.2	0.290719
YFR006W		X-Pro aminopeptidase	0.2937	1.2	0.0226186
YBL040C	ERD2	HDEL sequence binding	0.2938	1.2	0.0312894
YDR543C			0.2942	1.2	0.233374
YJL122W	ALB1	unknown	0.2945	1.2	0.1925
YMR176W	ECM5	unknown	0.2947	1.2	0.144141
YDL201W	TRM8	protein binding	0.2948	1.2	0.302221
YML101C	CUE4	unknown	0.2953	1.2	0.0523719
YOR311C	HSD1	unknown	0.2958	1.2	0.12189
YJL005W	CYR1	adenylate cyclase	0.2960	1.2	0.180368
YDR365W-A			0.2968	1.2	0.188724
YER039C	HVG1	unknown	0.2973	1.2	0.182631
YNL147W	LSM7	RNA binding	0.2973	1.2	0.0275838
YHR170W	NMD3	protein binding	0.2973	1.2	0.191785
YJR082C	EAF6	unknown	0.2975	1.2	0.213894
YGR252W	GCN5	histone acetyltransferase *	0.2985	1.2	0.480719
YNL083W	SAL1	transporter	0.2988	1.2	0.217947
YGR028W	MSP1	ATPase	0.3008	1.2	0.150702
YDL165W	CDC36	3'-5'-exoribonuclease	0.3010	1.2	0.333445
YCR042C	TAF2	general RNA polymerase II transcription factor	0.3013	1.2	0.0534277
YOL042W	NGL1	endonuclease	0.3020	1.2	0.060534
YMR263W	SAP30	histone deacetylase	0.3025	1.2	0.0207154
YDL213C	NOP6	unknown	0.3037	1.2	0.041178
YDL217C	TIM22	protein transporter	0.3040	1.2	0.511644
YBR082C	UBC4	ubiquitin conjugating enzyme	0.3050	1.2	0.0192093
YBR156C	SLI15	protein kinase	0.3058	1.2	0.0397654
YDL226C	GCS1	actin binding	0.3060	1.2	0.00732041
YLR293C	GSP1	GTPase	0.3062	1.2	0.0663701
YHL031C	GOS1	v-SNARE	0.3065	1.2	0.10777
YMR288W	HSH155	mRNA binding	0.3067	1.2	0.456591
YLR227C	ADY4	structural molecule	0.3067	1.2	0.0881128
YNL183C	NPR1	kinase	0.3070	1.2	0.382339
YBR137W		unknown	0.3078	1.2	0.0516986
YIL027C	KRE27	unknown	0.3083	1.2	0.0359658
YKR061W	KTR2	mannosyltransferase	0.3083	1.2	0.0162137
YDR056C		unknown	0.3088	1.2	0.0200136
YMR079W	SEC14	phosphatidylinositol transporter	0.3095	1.2	0.100294
YPL060W	LPE10	magnesium ion transporter	0.3095	1.2	0.0244191
YDR084C	TVP23	unknown	0.3095	1.2	0.0297584

Table 1: continued.

ORF ID	Gene Name	Gene Function	Avg Log_2 Ratio	Fold Change	T-test
YAR023C		unknown	0.3095	1.2	0.137216
YMR275C	BUL1	protein binding	0.3097	1.2	0.140026
YBR257W	POP4	ribonuclease P *	0.3098	1.2	0.0131032
YLR180W	SAM1	methionine adenosyltransferase	0.3102	1.2	0.146012
YER006W	NUG1	GTPase	0.3103	1.2	0.151331
YGL116W	CDC20	enzyme activator	0.3107	1.2	0.10693
YHR200W	RPN10	endopeptidase	0.3108	1.2	0.0186369
YAL015C	NTG1	DNA-(apurinic or apyrimidinic site) lyase *	0.3112	1.2	0.00146686
YBL076C	ILS1	isoleucine-tRNA ligase	0.3112	1.2	0.188992
YLR309C	IMH1	unknown	0.3118	1.2	0.228186
YDR189W	SLY1	SNARE binding	0.3120	1.2	0.358734
YBR246W		unknown	0.3135	1.2	0.0506469
YLR380W	CSR1	phosphatidylinositol transporter	0.3137	1.2	0.219645
YMR259C		unknown	0.3142	1.2	0.0811376
YFL031W	HAC1	transcription factor	0.3143	1.2	0.15147
YBR011C	IPP1	inorganic diphosphatase	0.3147	1.2	0.0847703
YBR203W	COS111	unknown	0.3148	1.2	0.0659107
YOR239W(1)			0.3152	1.2	0.436596
YOR244W	ESA1	histone acetyltransferase	0.3153	1.2	0.146922
YFL025C	BST1	carboxylic ester hydrolase	0.3158	1.2	0.298488
YDL130W	RPP1B	structural constituent of ribosome	0.3168	1.2	0.120698
YER088C	DOT6	unknown	0.3172	1.2	0.0456176
YBL022C	PIM1	ATP-dependent peptidase	0.3172	1.2	0.049749
YNL313C		unknown	0.3183	1.2	0.554478
YML016C	PPZ1	protein serine/threonine phosphatase	0.3187	1.2	0.0339913
YIL103W	DPH1	unknown	0.3190	1.2	0.0440198
YGL126W	SCS3	unknown	0.3192	1.2	0.186075
YHL021C	FMP12	unknown	0.3195	1.2	0.0944435
YLR243W		signal sequence binding	0.3197	1.2	0.0187408
YNR027W	BUD17	unknown	0.3198	1.2	0.209163
YMR309C	NIP1	translation initiation factor	0.3200	1.2	0.106909
YOR048C	RAT1	5'-3' exoribonuclease	0.3203	1.2	0.00405686
YBR165W	UBS1	unknown	0.3203	1.2	0.00691753
YIL028W			0.3205	1.2	0.181484
YKL119C	VPH2	unknown	0.3207	1.2	0.464783
YLR368W	MDM30	unknown	0.3208	1.2	0.234646
YJR052W	RAD7	DNA binding	0.3210	1.2	0.0507301
YAR066W		unknown	0.3220	1.3	0.277759
YOL090W	MSH2	ATPase *	0.3228	1.3	0.173821
YPL207W	TYW1	unknown	0.3235	1.3	0.368234
YCL066W	HMLALPHA1	transcription coactivator	0.3235	1.3	0.444371
YER012W	PRE1	endopeptidase	0.3240	1.3	0.0115158
YHR154W	RTT107	unknown	0.3242	1.3	0.0250395
YJL006C	CTK2	cyclin-dependent protein kinase	0.3242	1.3	0.465752
YDR034C-C			0.3248	1.3	0.00148546
YLR291C	GCD7	translation initiation factor	0.3252	1.3	0.213169
YNR075W	COS10	unknown	0.3255	1.3	0.105745
YIL138C	TPM2	actin lateral binding	0.3257	1.3	0.153284
YDR047W	HEM12	uroporphyrinogen decarboxylase	0.3257	1.3	0.0167387
YEL024W	RIP1	ubiquinol-cytochrome-c reductase	0.3267	1.3	0.0137258
YGL060W	YBP2	unknown	0.3268	1.3	0.0483485
YNL073W	MSK1	lysine-tRNA ligase	0.3270	1.3	0.0441222
YOL061W	PRS5	ribose phosphate diphosphokinase	0.3275	1.3	0.00448467
YLR303W	MET17	cysteine synthase *	0.3277	1.3	0.0929698
YMR210W		unknown	0.3282	1.3	0.244544
YJL112W	MDV1	unknown	0.3285	1.3	0.00071224
YMR267W	PPA2	inorganic diphosphatase	0.3290	1.3	0.104133
YNL263C	YIF1	unknown	0.3290	1.3	0.00195159
YBL045C	COR1	ubiquinol-cytochrome-c reductase	0.3298	1.3	0.0531117
YNL284C-A			0.3303	1.3	0.113605
YKL064W	MNR2	magnesium ion transporter	0.3305	1.3	0.0660159
YNL106C	INP52	inositol-polyphosphate 5-phosphatase	0.3305	1.3	0.264571
YMR215W	GAS3	1,3-beta-glucanosyltransferase	0.3305	1.3	0.15332
YOL127W	RPL25	structural constituent of ribosome*	0.3308	1.3	0.0984725
YGR057C	LST7	protein transporter	0.3315	1.3	0.249987
YNL154C	YCK2	casein kinase	0.3317	1.3	0.0456629
YLR019W	PSR2	phosphoprotein phosphatase	0.3317	1.3	0.0234776
YPR165W	RHO1	GTPase *	0.3317	1.3	0.163847
YBR199W	KTR4	mannosyltransferase	0.3323	1.3	0.162804

Table 1: continued.

ORF ID	Gene Name	Gene Function	Avg Log_2 Ratio	Fold Change	T-test
YML011C	RAD33	unknown	0.3330	1.3	0.282426
YCL024W	KCC4	protein kinase	0.3337	1.3	0.0558064
YDR502C	SAM2	methionine adenosyltransferase	0.3337	1.3	0.0322586
YLR195C	NMT1	glycylpeptide N-tetradecanoyltransferase	0.3340	1.3	0.0724227
YCL037C	SRO9	RNA binding	0.3342	1.3	0.211033
YIL020C	HIS6	1-(5-phosphoribosyl)-5-[(5-phosphoribosylamino)methylid	0.3343	1.3	0.0961617
YOR276W	CAF20	translation regulator	0.3348	1.3	0.0793003
YLR256W-A			0.3350	1.3	0.152657
YGR245C	SDA1	unknown	0.3357	1.3	0.509982
YPL194W	DDC1	unknown	0.3360	1.3	0.446199
YBR034C	HMT1	protein-arginine N-methyltransferase	0.3372	1.3	0.0100556
YPL009C		unknown	0.3372	1.3	0.285743
YGR277C		pantetheine-phosphate adenylyltransferase	0.3377	1.3	9.26074E-05
YBR293W	VBA2	multidrug transporter	0.3377	1.3	0.102285
YNL054W-A			0.3395	1.3	0.0759197
YNR015W	SMM1	tRNA dihydrouridine synthase	0.3397	1.3	0.487621
YKL099C	UTP11	snoRNA binding	0.3400	1.3	0.229313
YDR336W		unknown	0.3407	1.3	0.269227
YDR064W	RPS13	structural constituent of ribosome	0.3408	1.3	0.0417386
YJL161W	FMP33	unknown	0.3412	1.3	0.160599
YNR074C	AIF1	oxidoreductase	0.3412	1.3	0.152855
YNL050C		unknown	0.3413	1.3	0.0712413
YDR083W	RRP8	methyltransferase	0.3417	1.3	0.153002
YPR045C		unknown	0.3420	1.3	0.327041
YJL110C	GZF3	transcription factor	0.3422	1.3	0.245413
YDL198C	GGC1	guanine nucleotide transporter	0.3425	1.3	0.0371653
YNL142W	MEP2	ammonium transporter	0.3428	1.3	0.0610554
YNL110C	NOP15	unknown	0.3430	1.3	0.229352
YNL180C	RHO5	GTPase	0.3440	1.3	0.0248899
YMR178W		unknown	0.3442	1.3	0.0126728
YDL028C	MPS1	protein threonine/tyrosine kinase	0.3460	1.3	0.0722155
YOR047C	STD1	protein kinase	0.3462	1.3	0.301447
YDL045C	FAD1	FMN adenylyltransferase	0.3463	1.3	0.0154089
YLR074C	BUD20	unknown	0.3465	1.3	0.0329259
YKR025W	RPC37	DNA-directed RNA polymerase	0.3472	1.3	0.0586111
YNL181W		oxidoreductase	0.3473	1.3	0.0774725
YMR298W	LIP1	sphingosine N-acyltransferase	0.3475	1.3	0.0671655
YER137C		unknown	0.3478	1.3	0.134993
YOR007C	SGT2	unknown	0.3478	1.3	0.112838
YAR028W		unknown	0.3480	1.3	0.110732
YLR038C	COX12	cytochrome-c oxidase	0.3495	1.3	0.375377
YML097C	VPS9	guanyl-nucleotide exchange factor	0.3510	1.3	0.100685
YHR211W	FLO5	mannose binding	0.3510	1.3	0.20237
YLR060W	FRS1	phenylalanine-tRNA ligase	0.3512	1.3	0.0252629
YBR196C	PGI1	glucose-6-phosphate isomerase	0.3520	1.3	0.169196
YFL023W	BUD27	unknown	0.3523	1.3	0.125296
YPR109W		unknown	0.3527	1.3	0.0115682
YGL115W	SNF4	protein kinase	0.3530	1.3	0.0479353
YHR091C	MSR1	arginine-tRNA ligase	0.3535	1.3	0.277625
YNL251C	NRD1	RNA binding	0.3537	1.3	0.294214
YLR335W	NUP2	structural molecule	0.3545	1.3	0.212291
YNL220W	ADE12	adenylosuccinate synthase	0.3545	1.3	0.153954
YDR089W		unknown	0.3547	1.3	0.265498
YGR138C	TPO2	spermine transporter	0.3552	1.3	0.00530685
YNL309W	STB1	transcriptional activator	0.3553	1.3	0.326359
YJL118W		unknown	0.3553	1.3	0.171763
YGR058W		unknown	0.3558	1.3	0.181036
YFR004W	RPN11	endopeptidase	0.3578	1.3	0.00633033
YER027C	GAL83	AMP-activated protein kinase	0.3582	1.3	0.0759152
YMR005W	TAF4	RNA polymerase II transcription factor	0.3585	1.3	0.0781685
YKL088W		purine nucleotide binding	0.3585	1.3	0.164433
YOL144W	NOP8	unknown	0.3588	1.3	0.465894
YHR106W	TRR2	thioredoxin-disulfide reductase	0.3590	1.3	0.0814045
YOL043C	NTG2	DNA-(apurinic or apyrimidinic site) lyase *	0.3592	1.3	0.127536
YGL029W	CGR1	unknown	0.3595	1.3	0.0571443
YDL227C	HO	endonuclease	0.3598	1.3	0.0630797
YHR061C	GIC1	small GTPase regulator	0.3607	1.3	0.103102
YLR064W		unknown	0.3610	1.3	0.0182285
YDL230W	PTP1	protein tyrosine phosphatase	0.3610	1.3	0.144822

Table 1: continued.

ORF ID	Gene Name	Gene Function	Avg Log_2 Ratio	Fold Change	T-test
YML012W	ERV25	unknown	0.3610	1.3	0.160971
YFL053W	DAK2	glycerone kinase	0.3615	1.3	0.143986
YER032W	FIR1	unknown	0.3620	1.3	0.199377
YPL078C	ATP4	structural molecule *	0.3627	1.3	0.0119898
YDR375C	BCS1	ATPase	0.3633	1.3	0.137506
YJL051W	IRC8	unknown	0.3638	1.3	0.0194293
YDR513W	GRX2	thiol-disulfide exchange intermediate *	0.3642	1.3	0.10078
YLR197W	SIK1	unknown	0.3643	1.3	0.125653
YOR231W	MKK1	MAP kinase	0.3648	1.3	0.180798
YGL073W	HSF1	transcription factor	0.3648	1.3	0.0786332
YOL089C	HAL9	specific RNA polymerase II transcription factor	0.3650	1.3	0.00180215
YER086W	ILV1	threonine ammonia-lyase	0.3653	1.3	0.0356812
YDL122W	UBP1	ubiquitin-specific protease	0.3658	1.3	0.142034
YHR065C	RRP3	ATP-dependent RNA helicase	0.3667	1.3	0.0686174
YDR429C	TIF35	translation initiation factor	0.3668	1.3	0.107343
YJR010C-A	SPC1	unknown	0.3668	1.3	0.00503789
YFL040W		unknown	0.3670	1.3	0.10378
YLR264W	RPS28B	structural constituent of ribosome	0.3678	1.3	0.173261
YGR253C	PUP2	endopeptidase	0.3682	1.3	0.0531721
YDR392W	SPT3	transcription cofactor	0.3685	1.3	0.00165205
YJR152W	DAL5	allantoate transporter	0.3690	1.3	0.111736
YLR226W	BUR2	cyclin-dependent protein kinase	0.3697	1.3	0.0449872
YNL227C	JJJ1	unknown	0.3698	1.3	0.195103
YFR033C	QCR6	ubiquinol-cytochrome-c reductase	0.3702	1.3	0.0543097
YDR314C	RAD34	unknown	0.3707	1.3	0.0437755
YBR061C	TRM7	tRNA methyltransferase	0.3713	1.3	0.0909942
YDL123W	SNA4	unknown	0.3715	1.3	0.177047
YDL070W	BDF2	unknown	0.3717	1.3	0.0771189
YKL208W	CBT1	unknown	0.3720	1.3	0.271215
YGR037C	ACB1	long-chain fatty acid transporter	0.3722	1.3	0.148607
YDR001C	NTH1	alpha,alpha-trehalase	0.3725	1.3	0.0461789
YFL022C	FRS2	phenylalanine-tRNA ligase	0.3730	1.3	0.0541346
YBR194W	SOY1	unknown	0.3735	1.3	0.0361311
YDR201W	SPC19	structural constituent of cytoskeleton	0.3735	1.3	0.0611205
YPL104W	MSD1	aspartate-tRNA ligase	0.3742	1.3	0.0446667
YBR062C		unknown	0.3745	1.3	0.0511
YEL051W	VMA8	hydrogen-transporting ATPase , rotational mechanism	0.3747	1.3	0.0221746
YDR329C	PEX3	protein binding	0.3748	1.3	0.00340154
YFR034C	PHO4	transcription factor	0.3753	1.3	0.405673
YCR002C	CDC10	GTPase *	0.3763	1.3	0.0390753
YDR430C	CYM1	metalloendopeptidase	0.3763	1.3	0.244077
YPR085C		unknown	0.3775	1.3	0.0289033
YGL155W	CDC43	signal transducer *	0.3778	1.3	0.109475
YCR083W	TRX3	thiol-disulfide exchange intermediate	0.3778	1.3	0.117739
YLR268W	SEC22	v-SNARE	0.3785	1.3	0.0115942
YDR350C	TCM10	unknown	0.3787	1.3	0.103499
YLR265C	NEJ1	unknown	0.3797	1.3	0.0452802
YDR272W	GLO2	hydroxyacylglutathione hydrolase	0.3807	1.3	0.0121378
YNL284C	MRPL10	structural constituent of ribosome	0.3807	1.3	0.0146558
YJR019C	TES1	acyl-CoA thioesterase	0.3807	1.3	0.0481517
YHR110W	ERP5	unknown	0.3808	1.3	0.0633788
YNR034W	SOL1	unknown	0.3815	1.3	0.0465103
YKR080W	MTD1	methylenetetrahydrofolate dehydrogenase	0.3815	1.3	0.159451
YPL052W	OAZ1	enzyme inhibitor	0.3822	1.3	0.0488677
YEL072W	RMD6	unknown	0.3823	1.3	0.126648
YOR237W	HES1	oxysterol binding	0.3825	1.3	0.260569
YDR112W			0.3827	1.3	0.0775612
YKL081W	TEF4	translation elongation factor	0.3828	1.3	0.00256069
YDL020C	RPN4	transcriptional activator	0.3832	1.3	0.0735858
YBR087W	RFC5	DNA clamp loader	0.3832	1.3	0.00212711
YDR389W	SAC7	signal transducer *	0.3833	1.3	0.0822193
YAR033W	MST28	protein binding	0.3840	1.3	0.151429
YJR097W	JJJ3	unknown	0.3842	1.3	0.0780038
YER133W	GLC7	protein phosphatase type 1	0.3845	1.3	0.00582644
YJR022W	LSM8	RNA binding	0.3857	1.3	0.454422
YNR028W	CPR8	peptidyl-prolyl cis-trans isomerase	0.3860	1.3	0.0554568
YJR162C			0.3865	1.3	0.360675
YBR210W	ERV15	unknown	0.3870	1.3	0.0141565
YHR209W		S-adenosylmethionine-dependent methyltransferase	0.3877	1.3	0.0126853

Table 1: continued.

ORF ID	Gene Name	Gene Function	Avg Log_2 Ratio	Fold Change	T-test
YGR233C	PHO81	cyclin-dependent protein kinase	0.3878	1.3	0.241326
YPL168W		unknown	0.3892	1.3	0.0693092
YJR113C	RSM7	structural constituent of ribosome	0.3892	1.3	0.0766389
YDR527W	RBA50	DNA-directed RNA polymerase	0.3895	1.3	0.0481616
YMR022W	QRI8	ubiquitin conjugating enzyme	0.3897	1.3	0.00130401
YJL133W	MRS3	iron ion transporter	0.3898	1.3	0.0345282
YJR078W	BNA2	tryptophan 2,3-dioxygenase	0.3903	1.3	0.3433
YOL143C	RIB4	6,7-dimethyl-8-ribityllumazine synthase	0.3908	1.3	0.0219818
YFL061W	DDI2	unknown	0.3908	1.3	0.00674054
YHL024W	RIM4	RNA binding	0.3922	1.3	0.259553
YGL099W	LSG1	GTPase	0.3923	1.3	0.387602
YBR055C	PRP6	RNA splicing factor	0.3933	1.3	0.0939433
YAL003W	EFB1	translation elongation factor	0.3933	1.3	0.00260375
YDL136W	RPL35B	structural constituent of ribosome	0.3935	1.3	0.107267
YNL315C	ATP11	unfolded protein binding	0.3950	1.3	0.148398
YAL033W	POP5	ribonuclease P *	0.3952	1.3	0.108664
YDR145W	TAF12	general RNA polymerase II transcription factor	0.3953	1.3	0.0462536
YBR012C			0.3958	1.3	0.13285
YGL064C	MRH4	RNA helicase	0.3962	1.3	0.229261
YGL011C	SCL1	endopeptidase	0.3972	1.3	0.03885
YDL161W	ENT1	clathrin binding	0.3975	1.3	0.0950582
YFR008W	FAR7	unknown	0.3978	1.3	0.0522157
YLR328W	NMA1	nicotinamide-nucleotide adenylyltransferase	0.3980	1.3	0.000314098
YDL205C	HEM3	hydroxymethylbilane synthase	0.3985	1.3	0.18973
YAR068W		unknown	0.3987	1.3	0.0896942
YNL322C	KRE1	structural constituent of cell wall	0.3988	1.3	0.0454274
YOR085W	OST3	dolichyl-diphosphooligosaccharide-protein glycotransferase	0.3992	1.3	0.0604623
YPR057W	BRR1	RNA binding	0.3997	1.3	0.35368
YDR440W	DOT1	protein-lysine N-methyltransferase	0.3997	1.3	0.127816
YPL225W		unknown	0.3997	1.3	0.0290287
YBR291C	CTP1	tricarboxylate carrier	0.3998	1.3	0.0126561
YNL244C	SUI1	translation initiation factor	0.4002	1.3	0.0456726
YOL053W		unknown	0.4003	1.3	0.151764
YPL238C			0.4007	1.3	0.0613746
YPL252C	YAH1	electron carrier	0.4013	1.3	0.209866
YDR337W	MRPS28	structural constituent of ribosome*	0.4013	1.3	0.0752444
YMR257C	PET111	translation regulator	0.4015	1.3	0.202786
YDR280W	RRP45	3'-5'-exoribonuclease	0.4022	1.3	0.168241
YOR309C			0.4028	1.3	0.0527659
YDL209C	CWC2	unknown	0.4028	1.3	0.0628444
YDR139C	RUB1	protein tag	0.4033	1.3	0.021619
YDR351W	SBE2	unknown	0.4045	1.3	0.038492
YDL158C			0.4045	1.3	0.0276075
YKL114C	APN1	DNA-(apurinic or apyrimidinic site) lyase	0.4048	1.3	0.238965
YEL073C		unknown	0.4048	1.3	0.0302557
YHR143W-A	RPC10	DNA-directed RNA polymerase	0.4057	1.3	0.0682927
YJL189W	RPL39	structural constituent of ribosome	0.4060	1.3	0.0919081
YIL034C	CAP2	actin filament binding	0.4060	1.3	0.0395035
YDR261C-C			0.4065	1.3	0.128247
YOR147W	MDM32	unknown	0.4070	1.3	0.0430178
YDR253C	MET32	DNA binding	0.4075	1.3	0.0526674
YKR052C	MRS4	iron ion transporter	0.4082	1.3	0.0952343
YDR459C	PFA5	protein-cysteine S-palmitoleyltransferase	0.4090	1.3	0.210381
YPL129W	TAF14	general RNA polymerase II transcription factor	0.4093	1.3	0.262608
YHR187W	IKI1	RNA polymerase II transcription elongation factor	0.4097	1.3	0.0133826
YBR290W	BSD2	unknown	0.4115	1.3	0.0207699
YAL039C	CYC3	holocytochrome-c synthase	0.4118	1.3	0.000928542
YDR397C	NCB2	transcription corepressor	0.4133	1.3	0.0145439
YBR252W	DUT1	dUTP diphosphatase	0.4142	1.3	0.0325705
YDR441C	APT2	unknown	0.4143	1.3	0.12869
YOR192C-A			0.4147	1.3	0.0371685
YOL102C	TPT1	tRNA 2'-phosphotransferase	0.4150	1.3	0.318881
YBR033W	EDS1	unknown	0.4152	1.3	0.0171443
YDL079C	MRK1	glycogen synthase kinase	0.4157	1.3	0.0267702
YBR186W	PCH2	unknown	0.4158	1.3	0.125427
YJL011C	RPC17	DNA-directed RNA polymerase	0.4158	1.3	0.0575168
YGR182C			0.4162	1.3	0.220367
YBL093C	ROX3	RNA polymerase II transcription mediator	0.4167	1.3	0.311958
YNR026C	SEC12	guanyl-nucleotide exchange factor	0.4173	1.3	0.0733029

Table 1: continued.

ORF ID	Gene Name	Gene Function	Avg Log_2 Ratio	Fold Change	T-test
YDL018C	ERP3	unknown	0.4175	1.3	0.0775042
YNL175C	NOP13	RNA binding	0.4177	1.3	0.023322
YNL075W	IMP4	rRNA primary transcript binding	0.4180	1.3	0.0497298
YPL024W	RMI1	unknown	0.4183	1.3	0.151392
YNL161W	CBK1	protein kinase	0.4185	1.3	0.0107181
YAR075W			0.4190	1.3	0.148769
YDR524C	AGE1	ARF GTPase activator	0.4192	1.3	0.109806
YDR405W	MRP20	structural constituent of ribosome	0.4195	1.3	0.00542521
YKL063C		unknown	0.4197	1.3	0.10551
YDR470C	UGO1	transporter	0.4203	1.3	0.0573441
YOR262W		unknown	0.4217	1.3	0.0597271
YOL140W	ARG8	acetylornithine transaminase	0.4225	1.3	0.0259812
YKL190W	CNB1	calcium ion binding	0.4225	1.3	0.0636552
YGR235C		unknown	0.4242	1.3	0.0524528
YDR014W	RAD61	unknown	0.4247	1.3	0.0111871
YDL191W	RPL35A	structural constituent of ribosome	0.4253	1.3	0.0357698
YLR462W		unknown	0.4260	1.3	0.0943067
YBR059C	AKL1	protein kinase	0.4262	1.3	0.107159
YGR124W	ASN2	asparagine synthase (glutamine-hydrolyzing)	0.4268	1.3	0.134251
YLR049C		unknown	0.4270	1.3	0.0305927
YGR283C		unknown	0.4275	1.3	0.0132946
YOL071W	EMI5	unknown	0.4280	1.3	0.0477771
YLR225C		unknown	0.4285	1.3	0.132513
YCR036W	RBK1	ATP binding	0.4285	1.3	0.0424718
YKL143W	LTV1	unknown	0.4312	1.3	0.0801295
YMR149W	SWP1	dolichyl-diphosphooligosaccharide-protein glycotransferase	0.4323	1.3	0.026648
YML070W	DAK1	glycerone kinase	0.4327	1.3	0.224696
YDR344C			0.4328	1.3	0.174276
YML108W		unknown	0.4332	1.4	0.114318
YPL159C	PET20	unknown	0.4343	1.4	0.128292
YPL112C	PEX25	unknown	0.4355	1.4	0.119415
YKL107W		unknown	0.4367	1.4	0.0381975
YHR021C	RPS27B	structural constituent of ribosome	0.4367	1.4	0.0537606
YFL034C-B	MOB2	protein kinase	0.4368	1.4	0.0579427
YDL145C	COP1	unknown	0.4373	1.4	0.106422
YLR257W		unknown	0.4380	1.4	0.00559337
YDL156W		unknown	0.4385	1.4	0.0119992
YMR050C			0.4388	1.4	0.036899
YGL187C	COX4	cytochrome-c oxidase	0.4388	1.4	0.0877599
YMR021C	MAC1	specific RNA polymerase II transcription factor	0.4390	1.4	0.206785
YDR225W	HTA1	DNA binding	0.4393	1.4	0.161979
YGR246C	BRF1	RNA polymerase III transcription factor	0.4393	1.4	0.168143
YJL216C		alpha-galactosidase *	0.4400	1.4	0.0218329
YDR515W	SLF1	RNA binding	0.4403	1.4	0.0740588
YJL031C	BET4	Rab-protein geranylgeranyltransferase	0.4415	1.4	0.00258431
YOR023C	AHC1	histone acetyltransferase	0.4425	1.4	0.205194
YGR095C	RRP46	3'-5'-exoribonuclease	0.4432	1.4	0.086252
YEL050C	RML2	structural constituent of ribosome	0.4433	1.4	0.0341233
YLR204W	QRI5	unknown	0.4437	1.4	0.0623012
YKL139W	CTK1	protein kinase	0.4438	1.4	0.198831
YMR173W	DDR48	ATPase *	0.4440	1.4	0.0711408
YHR214W-A			0.4442	1.4	0.104409
YDR367W		unknown	0.4447	1.4	0.0351575
YNR061C		unknown	0.4450	1.4	0.0823606
YDL008W	APC11	protein binding	0.4460	1.4	0.00663904
YFL018W-A			0.4468	1.4	0.0780435
YDR210W-A			0.4472	1.4	0.000477681
YOR254C	SEC63	protein transporter	0.4473	1.4	0.17585
YDR027C	VPS54	unknown	0.4475	1.4	0.0846015
YHR100C		unknown	0.4477	1.4	0.0133828
YOL139C	CDC33	translation initiation factor	0.4477	1.4	0.0221916
YOR222W	ODC2	intracellular transporter	0.4477	1.4	0.311996
YML129C	COX14	unknown	0.4492	1.4	0.0677092
YMR012W	CLU1	unknown	0.4492	1.4	0.254401
YGR147C	NAT2	peptide alpha-N-acetyltransferase	0.4493	1.4	0.0441321
YBR172C	SMY2	unknown	0.4497	1.4	0.0108304
YMR177W	MMT1	unknown	0.4497	1.4	0.0136465
YIL076W	SEC28	unknown	0.4498	1.4	0.00542584
YLR250W	SSP120	unknown	0.4500	1.4	0.0343701

Table 1: continued.

ORF ID	Gene Name	Gene Function	Avg Log_2 Ratio	Fold Change	T-test
YOR248W			0.4500	1.4	0.129292
YKR100C	SKG1	unknown	0.4515	1.4	0.272004
YHR103W	SBE22	unknown	0.4517	1.4	0.13089
YGR093W		unknown	0.4518	1.4	0.0218532
YDR216W	ADR1	transcription factor	0.4523	1.4	0.0985205
YGL129C	RSM23	structural constituent of ribosome	0.4525	1.4	0.13619
YHL013C	OTU2	unknown	0.4528	1.4	0.0860462
YPL128C	TBF1	DNA binding	0.4533	1.4	0.204133
YJR055W	HIT1	unknown	0.4538	1.4	0.287507
YGR202C	PCT1	choline-phosphate cytidylyltransferase	0.4540	1.4	0.310226
YPL237W	SUI3	translation initiation factor	0.4550	1.4	0.0280956
YIL072W	HOP1	DNA binding	0.4562	1.4	0.073242
YPR120C	CLB5	cyclin-dependent protein kinase	0.4570	1.4	0.0899671
YGL219C	MDM34	unknown	0.4575	1.4	0.039917
YGR080W	TWF1	actin monomer binding	0.4575	1.4	0.0650006
YHL006C	SHU1	unknown	0.4578	1.4	0.101686
YDL054C	MCH1	transporter	0.4587	1.4	0.121718
YMR228W	MTF1	S-adenosylmethionine-dependent methyltransferase *	0.4592	1.4	0.146672
YDR486C	VPS60	unknown	0.4595	1.4	0.00029335
YMR051C			0.4597	1.4	0.250944
YDR085C	AFR1	receptor signaling protein	0.4610	1.4	0.158499
YGR257C	MTM1	transporter	0.4613	1.4	0.0341731
YHR186C	KOG1	unknown	0.4615	1.4	0.0298282
YBL064C	PRX1	thioredoxin peroxidase	0.4622	1.4	0.0455349
YJR032W	CPR7	unfolded protein binding	0.4622	1.4	0.0764775
YER182W	FMP10	unknown	0.4633	1.4	0.0834156
YJL166W	QCR8	ubiquinol-cytochrome-c reductase	0.4633	1.4	0.0199569
YOR182C	RPS30B	structural constituent of ribosome	0.4637	1.4	0.0422405
YDL147W	RPN5	unknown	0.4640	1.4	0.143632
YFR052W	RPN12	endopeptidase	0.4657	1.4	0.0550977
YLR354C	TAL1	transaldolase	0.4657	1.4	0.0421182
YKL151C		unknown	0.4660	1.4	0.0270596
YHR121W	LSM12	RNA binding	0.4660	1.4	0.0620676
YOR017W	PET127	unknown	0.4662	1.4	0.000291239
YBR010W	HHT1	DNA binding	0.4663	1.4	0.0427297
YBR021W	FUR4	uracil permease	0.4683	1.4	0.00678431
YLR252W			0.4697	1.4	0.0312779
YGL057C		unknown	0.4700	1.4	0.160958
YDR031W		unknown	0.4703	1.4	0.0218881
YJL151C	SNA3	unknown	0.4708	1.4	0.010204
YER134C		unknown	0.4712	1.4	0.0681911
YLR410W-A			0.4718	1.4	0.157633
YJR080C	FMP26	unknown	0.4718	1.4	0.0411835
YPR040W	TIP41	unknown	0.4722	1.4	0.00659972
YER028C	MIG3	DNA binding	0.4727	1.4	0.138613
YHR167W	THP2	nucleic acid binding	0.4727	1.4	0.135413
YDL101C	DUN1	protein kinase	0.4728	1.4	0.0072843
YIL056W	VHR1	DNA binding	0.4740	1.4	0.178737
YNL131W	TOM22	protein transporter	0.4740	1.4	0.0189604
YOR260W	GCD1	translation initiation factor	0.4748	1.4	0.0792931
YJR010W	MET3	sulfate adenylyltransferase (ATP)	0.4767	1.4	0.00783133
YGR001C		methyltransferase	0.4768	1.4	0.166606
YDR013W	PSF1	unknown	0.4775	1.4	0.149795
YCL031C	RRP7	unknown	0.4783	1.4	0.00567298
YGL169W	SUA5	unknown	0.4785	1.4	0.173407
YHL009C	YAP3	transcription factor	0.4788	1.4	0.198653
YOR174W	MED4	RNA polymerase II transcription mediator	0.4802	1.4	0.0712662
YNL137C	NAM9	structural constituent of ribosome	0.4807	1.4	0.0328999
YMR039C	SUB1	transcription coactivator	0.4823	1.4	0.0127394
YNR054C	ESF2	transcription regulator	0.4835	1.4	0.0436859
YOR087W	YVC1	calcium channel *	0.4835	1.4	0.0917948
YJL102W	MEF2	translation elongation factor	0.4837	1.4	0.00754178
YPL014W		unknown	0.4842	1.4	0.070502
YIL131C	FKH1	transcription factor	0.4857	1.4	0.274306
YLR294C			0.4858	1.4	0.023396
YBR037C	SCO1	thioredoxin peroxidase	0.4863	1.4	0.0361619
YFR025C	HIS2	histidinol-phosphatase	0.4873	1.4	0.247822
YHR051W	COX6	cytochrome-c oxidase	0.4878	1.4	0.0538899
YMR281W	GPI12	N-acetylglucosaminylphosphatidylinositol deacetylase	0.4880	1.4	0.213246

Table 1: continued.

ORF ID	Gene Name	Gene Function	Avg Log_2 Ratio	Fold Change	T-test
YDR281C	PHM6	unknown	0.4885	1.4	0.0241516
YFR017C		unknown	0.4893	1.4	0.216405
YEL066W	HPA3	histone acetyltransferase	0.4895	1.4	0.00210665
YOR158W	PET123	structural constituent of ribosome	0.4897	1.4	0.104932
YDR206W	EBS1	unknown	0.4898	1.4	0.100733
YOR045W	TOM6	protein transporter	0.4900	1.4	0.110627
YLR295C	ATP14	hydrogen-transporting ATP synthase , rotational mechanism	0.4915	1.4	0.0115678
YBR119W	MUD1	RNA binding	0.4925	1.4	0.0598601
YBR202W	CDC47	chromatin binding	0.4927	1.4	0.0580251
YDR299W	BFR2	unknown	0.4933	1.4	0.0469495
YMR073C		unknown	0.4942	1.4	0.0305443
YBL066C	SEF1	unknown	0.4962	1.4	0.0157141
YNR073C		mannitol dehydrogenase	0.4967	1.4	0.168241
YPL010W	RET3	protein binding	0.4972	1.4	0.0574156
YDR081C	PDC2	transcription regulator	0.4975	1.4	0.0223707
YCL007C			0.4975	1.4	0.174987
YDL114W		unknown	0.4982	1.4	0.164575
YLL014W		unknown	0.4993	1.4	0.063809
YDR049W		unknown	0.5002	1.4	0.395127
YFR003C	YPI1	protein phosphatase inhibitor	0.5007	1.4	0.0451772
YHR083W	SAM35	protein binding	0.5007	1.4	0.067767
YIL035C	CKA1	protein kinase	0.5010	1.4	0.0533489
YJL063C	MRPL8	structural constituent of ribosome	0.5013	1.4	0.0767068
YCR020C-A	MAK31	peptide alpha-N-acetyltransferase	0.5015	1.4	0.0163273
YER127W	LCP5	RNA binding	0.5017	1.4	0.00670135
YKL218C	SRY1	threo-3-hydroxyaspartate ammonia-lyase *	0.5020	1.4	0.0317813
YCL006C			0.5032	1.4	0.263108
YDR202C	RAV2	unknown	0.5048	1.4	0.0162182
YML127W	RSC9	chromatin binding	0.5050	1.4	0.183193
YDR532C		unknown	0.5053	1.4	0.0552863
YIR011C	STS1	unknown	0.5055	1.4	0.0311946
YOR372C	NDD1	transcriptional activator	0.5057	1.4	0.0649134
YDR529C	QCR7	ubiquinol-cytochrome-c reductase	0.5062	1.4	0.0913272
YKL161C		protein kinase	0.5063	1.4	0.0101032
YPL145C	KES1	oxysterol binding	0.5067	1.4	0.0949829
YKR007W	MEH1	unknown	0.5067	1.4	0.0412531
YGR015C		unknown	0.5073	1.4	0.0985756
YDR318W	MCM21	protein binding	0.5082	1.4	0.0181467
YGR013W	SNU71	RNA binding	0.5083	1.4	0.19209
YPL091W	GLR1	glutathione-disulfide reductase	0.5085	1.4	0.0188051
YDR332W	IRC3	helicase	0.5087	1.4	0.0594006
YIR021W	MRS1	RNA binding	0.5100	1.4	0.0860763
YFL043C			0.5102	1.4	0.0215182
YMR269W	TMA23	unknown	0.5103	1.4	0.149235
YDR140W	MTQ2	S-adenosylmethionine-dependent methyltransferase *	0.5143	1.4	0.00244867
YOR167C	RPS28A	structural constituent of ribosome	0.5147	1.4	0.0109307
YDR398W	UTP5	snoRNA binding	0.5157	1.4	0.273772
YDR096W	GIS1	transcription factor	0.5162	1.4	0.0165738
YBR039W	ATP3	hydrogen-transporting ATP synthase , rotational mechanism	0.5168	1.4	0.00768298
YDL235C	YPD1	transferase , transferring phosphorus-containing groups	0.5168	1.4	0.030936
YJL046W		unknown	0.5172	1.4	0.0786259
YOR187W	TUF1	GTPase *	0.5173	1.4	0.0045012
YBL113C		helicase	0.5183	1.4	0.0112937
YMR174C	PAI3	endopeptidase inhibitor	0.5185	1.4	0.0563961
YNL192W	CHS1	chitin synthase	0.5187	1.4	0.0346981
YBR120C	CBP6	unknown	0.5190	1.4	0.105301
YGL093W	SPC105	structural constituent of cytoskeleton	0.5193	1.4	0.040631
YAL047C	SPC72	structural constituent of cytoskeleton	0.5195	1.4	0.0531787
YDL048C	STP4	unknown	0.5198	1.4	0.000386249
YJL007C			0.5200	1.4	0.0460419
YGL242C		unknown	0.5203	1.4	0.0888156
YDR117C	TMA64	RNA binding	0.5215	1.4	0.348711
YCL043C	PDI1	protein disulfide isomerase	0.5220	1.4	0.00948149
YIL162W	SUC2	beta-fructofuranosidase	0.5223	1.4	0.00674801
YLR179C		unknown	0.5223	1.4	0.0161588
YNR012W	URK1	uridine kinase	0.5228	1.4	0.0799909
YPL092W	SSU1	sulfite transporter	0.5230	1.4	0.0372879
YNL310C	ZIM17	protein binding	0.5232	1.4	0.0147868
YKL183W	LOT5	unknown	0.5233	1.4	0.146996

Table 1: continued.

ORF ID	Gene Name	Gene Function	Avg Log_2 Ratio	Fold Change	T-test
YDL120W	YFH1	enzyme regulator	0.5235	1.4	0.0262338
YOR046C	DBP5	RNA helicase	0.5240	1.4	0.194869
YBR015C	MNN2	alpha-1,2-mannosyltransferase	0.5242	1.4	0.0328329
YLR050C		unknown	0.5253	1.4	0.0285192
YCR039C	MATALPHA2	transcription corepressor	0.5260	1.4	0.0609649
YOR062C		unknown	0.5262	1.4	0.0580951
YPR041W	TIF5	translation initiation factor	0.5263	1.4	0.0235665
YKL133C		unknown	0.5268	1.4	0.146588
YDR252W	BTT1	unfolded protein binding	0.5297	1.4	0.221855
YKR030W	GMH1	unknown	0.5297	1.4	0.155926
YOR236W	DFR1	dihydrofolate reductase	0.5302	1.4	0.0470777
YKL170W	MRPL38	structural constituent of ribosome	0.5310	1.4	0.0147879
YDR002W	YRB1	Ran GTPase binding	0.5318	1.4	0.00305125
YAL060W	BDH1	(R,R)-butanediol dehydrogenase	0.5327	1.4	0.0479707
YBR141C		unknown	0.5335	1.4	0.00282584
YNL281W	HCH1	chaperone activator	0.5338	1.4	0.057266
YOR297C	TIM18	protein transporter	0.5348	1.4	0.0431008
YOR208W	PTP2	protein tyrosine phosphatase	0.5352	1.4	0.0784979
YMR292W	GOT1	unknown	0.5355	1.4	0.0436418
TMR307W			0.5367	1.5	0.027773
YLR023C	IZH3	metal ion binding	0.5367	1.5	0.0859464
YLR053C		unknown	0.5372	1.5	0.042214
YDR530C	APA2	bis(5'-nucleosyl)-tetraphosphatase *	0.5373	1.5	0.0556706
YHR040W	BCD1	nucleic acid binding	0.5383	1.5	0.00665666
YBL002W	HTB2	DNA binding	0.5383	1.5	0.0273166
YDR412W	RRP17	unknown	0.5385	1.5	0.0622606
YOL137W	BSC6	unknown	0.5387	1.5	0.0190231
YNL132W	KRE33	unknown	0.5392	1.5	0.0706516
YGL263W	COS12	unknown	0.5393	1.5	0.046386
YDL157C		unknown	0.5410	1.5	0.0447279
YBL090W	MRP21	structural constituent of ribosome	0.5412	1.5	0.0317772
YJR077C	MIR1	inorganic phosphate transporter	0.5415	1.5	0.00792206
YHR137W	ARO9	aromatic-amino-acid transaminase	0.5423	1.5	0.0176031
YBR091C	MRS5	protein transporter	0.5425	1.5	0.0726096
YLR300W	EXG1	glucan 1,3-beta-glucosidase	0.5438	1.5	0.160733
YBR070C	ALG14	N-acetylglucosaminyldiphosphodolichol N-acetylglucosam	0.5440	1.5	0.00624406
YGL163C	RAD54	DNA-dependent ATPase *	0.5443	1.5	0.0598154
YCR080W			0.5445	1.5	0.136618
YDR331W	GPI8	GPI-anchor transamidase	0.5447	1.5	0.105054
YKL003C	MRP17	structural constituent of ribosome	0.5450	1.5	0.0536721
YLR016C	PML1	unknown	0.5475	1.5	0.0068785
YEL026W	SNU13	RNA binding	0.5477	1.5	0.0559199
YNL217W		phosphoric monoester hydrolase	0.5477	1.5	0.000190487
YPR100W	MRPL51	structural constituent of ribosome	0.5478	1.5	0.00524761
YNR017W	MAS6	protein transporter	0.5478	1.5	0.0219246
YDL241W		unknown	0.5480	1.5	0.0436493
YMR048W	CSM3	unknown	0.5490	1.5	0.00704276
YDL069C	CBS1	translation factor	0.5505	1.5	0.0490582
YFR011C		unknown	0.5508	1.5	0.0310636
YJR136C		unknown	0.5530	1.5	0.118162
YGR062C	COX18	protein transporter	0.5533	1.5	0.113301
YBR030W		unknown	0.5538	1.5	0.108062
YDL092W	SRP14	signal sequence binding	0.5543	1.5	0.0537937
YIL040W	APQ12	unknown	0.5550	1.5	0.129801
YGL107C	RMD9	unknown	0.5550	1.5	0.122977
YFL-TYA			0.5557	1.5	0.094898
YEL003W	GIM4	tubulin binding	0.5563	1.5	0.00555931
YNL031C	HHT2	DNA binding	0.5580	1.5	0.0133833
YDR462W	MRPL28	structural constituent of ribosome	0.5590	1.5	0.00962826
YDR273W	DON1	unknown	0.5603	1.5	0.00170895
YLR192C	HCR1	translation initiation factor	0.5603	1.5	0.00171666
YER150W	SPI1	unknown	0.5608	1.5	0.00880508
YCL026C			0.5612	1.5	0.0377089
YCL044C	MGR1	unknown	0.5612	1.5	0.00251144
YNL036W	NCE103	carbonate dehydratase	0.5613	1.5	0.000695624
YDR540C	IRC4	unknown	0.5622	1.5	0.170174
YFL010C	WWM1	unknown	0.5642	1.5	0.00405003
YOR305W		unknown	0.5653	1.5	0.0456689
YNR036C		structural constituent of ribosome	0.5657	1.5	0.0325287

Table 1: continued.

ORF ID	Gene Name	Gene Function	Avg Log_2 Ratio	Fold Change	T-test
YBR171W	SEC66	protein transporter	0.5658	1.5	0.0532421
YKR011C		unknown	0.5683	1.5	0.165897
YDR187C			0.5683	1.5	0.00615473
YDL089W		unknown	0.5683	1.5	0.0411234
YFL035C-A			0.5687	1.5	0.245016
YBR170C	NPL4	unknown	0.5697	1.5	0.0377509
YKL077W		unknown	0.5743	1.5	0.00426023
YIL063C	YRB2	unknown	0.5758	1.5	0.00334562
YER070W	RNR1	ribonucleoside-diphosphate reductase	0.5758	1.5	0.0390104
YDR378C	LSM6	RNA binding	0.5778	1.5	0.00871113
YJL097W	PHS1	unknown	0.5778	1.5	0.00374897
YFL041W	FET5	ferroxidase	0.5793	1.5	0.0528921
YJL221C	FSP2	alpha-glucosidase	0.5795	1.5	0.00854282
YPR094W	RDS3	unknown	0.5797	1.5	0.148855
YIL122W	POG1	specific RNA polymerase II transcription factor	0.5798	1.5	0.0537962
YLR251W	SYM1	unknown	0.5802	1.5	0.070233
YDR268W	MSW1	tryptophan-tRNA ligase	0.5805	1.5	0.0589518
YOL059W	GPD2	glycerol-3-phosphate dehydrogenase	0.5818	1.5	0.0497565
YPL204W	HRR25	casein kinase	0.5840	1.5	0.0151331
YJL062W	LAS21	transferase	0.5850	1.5	0.0290046
YIL008W	URM1	protein tag	0.5850	1.5	0.128733
YCR096C	HMRA2	unknown	0.5860	1.5	0.00763131
YHR081W	LRP1	unknown	0.5863	1.5	0.0419276
YAL069W			0.5863	1.5	0.0812503
YLR230W			0.5890	1.5	0.606237
YOL011W	PLB3	lysophospholipase	0.5898	1.5	0.0195474
YOR016C	ERP4	unknown	0.5913	1.5	0.0772978
YDR235W	PRP42	RNA binding	0.5913	1.5	0.0061686
YDL111C	RRP42	3'-5'-exoribonuclease	0.5913	1.5	0.0613521
YJR058C	APS2	unknown	0.5913	1.5	0.0135534
YBL107C		unknown	0.5920	1.5	0.0052672
Q0120	BI4	RNA binding	0.5930	1.5	0.108355
YGR078C	PAC10	tubulin binding	0.5932	1.5	0.0493755
YOR338W		unknown	0.5937	1.5	0.130278
YJL208C	NUC1	ribonuclease *	0.5945	1.5	0.0805223
Q0255		unknown	0.5947	1.5	0.0107965
YOR201C	MRM1	rRNA (guanine-N1-)-methyltransferase	0.5947	1.5	0.0781559
YDR517W	GRH1	unknown	0.5960	1.5	0.00537524
YMR173W-A			0.5963	1.5	0.0421073
YDR092W	UBC13	ubiquitin conjugating enzyme	0.5977	1.5	0.012112
YJL148W	RPA34	DNA-directed RNA polymerase	0.5980	1.5	0.0328234
YDL017W	CDC7	protein serine/threonine kinase	0.5980	1.5	0.10662
YFL016C	MDJ1	unfolded protein binding	0.5990	1.5	0.013336
YGR172C	YIP1	unknown	0.5997	1.5	0.0237079
YOL022C		unknown	0.6008	1.5	0.0614175
YDL055C	PSA1	mannose-1-phosphate guanylyltransferase	0.6012	1.5	0.013402
YKL082C	RRP14	unknown	0.6023	1.5	0.0951916
YPL106C	SSE1	ATP binding	0.6028	1.5	0.00288947
YKL150W	MCR1	cytochrome-b5 reductase	0.6030	1.5	0.00263223
YNL177C	MRPL22	structural constituent of ribosome	0.6030	1.5	0.0188789
YDR290W			0.6043	1.5	0.189285
YMR290C	HAS1	RNA binding	0.6045	1.5	0.0269443
YBR182C	SMP1	transcription factor	0.6052	1.5	0.0141909
YHR147C	MRPL6	structural constituent of ribosome	0.6060	1.5	0.0299516
YGL202W	ARO8	aromatic-amino-acid transaminase	0.6070	1.5	0.167251
YLL011W	SOF1	snoRNA binding	0.6078	1.5	0.0308592
YPL148C	PPT2	phosphopantetheinyltransferase	0.6082	1.5	0.0654919
YOR306C	MCH5	transporter	0.6083	1.5	0.104411
YCLX01W			0.6093	1.5	0.0203037
YLR186W	EMG1	unknown	0.6097	1.5	0.0908688
YML125C	PGA3	unknown	0.6128	1.5	0.0396362
YNL306W	MRPS18	structural constituent of ribosome	0.6142	1.5	0.0253688
YHR180W			0.6148	1.5	0.068993
YJL137C	GLG2	glycogenin glucosyltransferase	0.6148	1.5	0.025975
YDR028C	REG1	protein phosphatase type 1 regulator	0.6152	1.5	0.00565826
YKL011C	CCE1	endodeoxyribonuclease	0.6155	1.5	0.105211
YGR002C	SWC4	DNA binding	0.6160	1.5	0.103682
YEL001C		unknown	0.6160	1.5	0.0063596
YOL005C	RPB11	DNA-directed RNA polymerase	0.6168	1.5	0.0163654

Table 1: continued.

ORF ID	Gene Name	Gene Function	Avg Log_2 Ratio	Fold Change	T-test
YBR173C	UMP1	proteasome activator	0.6175	1.5	0.0240801
YLR275W	SMD2	RNA splicing factor	0.6180	1.5	0.0961118
YCR027C	RHB1	GTPase	0.6185	1.5	0.0921225
YKL089W	MIF2	centromeric DNA binding	0.6188	1.5	0.0108698
YGR156W	PTI1	RNA binding	0.6193	1.5	0.143618
YKL035W	UGP1	UTP:glucose-1-phosphate uridylyltransferase	0.6195	1.5	0.0231547
YDR044W	HEM13	coproporphyrinogen oxidase	0.6198	1.5	0.0148295
YDR079W	PET100	unfolded protein binding	0.6203	1.5	0.0273947
YGL070C	RPB9	DNA-directed RNA polymerase	0.6208	1.5	0.0836544
Q0250	COX2	cytochrome-c oxidase	0.6220	1.5	0.033301
YCL067C	HMLALPHA2	transcription corepressor	0.6222	1.5	0.0443276
YGR076C	MRPL25	structural constituent of ribosome	0.6225	1.5	0.070643
YGR020C	VMA7	hydrogen-transporting ATPase , rotational mechanism	0.6230	1.5	0.00698579
YOL023W	IFM1	RNA binding	0.6230	1.5	0.0737444
YML078W	CPR3	peptidyl-prolyl cis-trans isomerase	0.6233	1.5	0.0494883
YDR489W	SLD5	unknown	0.6238	1.5	0.00428904
YMR093W	UTP15	snoRNA binding	0.6242	1.5	0.109977
YAL007C	ERP2	unknown	0.6262	1.5	0.0525176
YDR373W	FRQ1	enzyme activator *	0.6278	1.5	0.00456051
YFL032W			0.6278	1.5	0.127398
YGL226W		unknown	0.6282	1.5	0.00366272
YGR152C	RSR1	GTPase *	0.6283	1.5	0.0115137
YGL143C	MRF1	translation release factor	0.6288	1.5	0.0788082
YNL153C	GIM3	tubulin binding	0.6293	1.5	0.109134
YKL225W			0.6298	1.5	0.0665314
YNL100W		unknown	0.6303	1.5	0.0180901
YPL271W	ATP15	hydrogen-transporting ATP synthase , rotational mechanism	0.6348	1.6	0.012649
YHR122W		unknown	0.6380	1.6	0.0317915
YDR173C	ARG82	inositol or phosphatidylinositol kinase	0.6392	1.6	0.0163209
YLR202C			0.6393	1.6	0.0496014
YCR034W	FEN1	fatty acid elongase	0.6393	1.6	0.0178405
YPL215W	CBP3	unknown	0.6397	1.6	0.0830257
YOR190W	SPR1	glucan 1,3-beta-glucosidase	0.6398	1.6	0.0863526
YJL196C	ELO1	fatty acid elongase	0.6432	1.6	0.100051
YBR267W	REI1	unknown	0.6462	1.6	0.0318328
YPR176C	BET2	Rab-protein geranylgeranyltransferase	0.6500	1.6	0.293145
YDR066C		unknown	0.6500	1.6	0.202496
YJL104W	PAM16	protein binding	0.6505	1.6	0.03308
YJL054W	TIM54	protein transporter	0.6515	1.6	0.0767007
YCL035C	GRX1	thiol-disulfide exchange intermediate *	0.6542	1.6	0.00238789
YHR116W	COX23	unknown	0.6558	1.6	0.0277786
YDL121C		unknown	0.6572	1.6	0.0951637
YGR063C	SPT4	RNA polymerase II transcription elongation factor	0.6647	1.6	0.13183
YOR354C	MSC6	unknown	0.6647	1.6	0.145648
YKL016C	ATP7	structural molecule *	0.6663	1.6	0.0258672
YKL085W	MDH1	L-malate dehydrogenase	0.6663	1.6	0.00284255
YNL108C		unknown	0.6665	1.6	0.107433
YJR156C	THI11	protein binding	0.6675	1.6	0.0200628
YLR221C	RSA3	unknown	0.6687	1.6	0.129387
YDR379W	RGA2	signal transducer *	0.6688	1.6	0.0701096
YOL136C	PFK27	6-phosphofructo-2-kinase	0.6692	1.6	0.0943872
YDL107W	MSS2	protein translocase	0.6700	1.6	0.0857198
YFL060C	SNO3	unknown	0.6703	1.6	0.00477158
YBL038W	MRPL16	structural constituent of ribosome*	0.6707	1.6	0.0164289
YPR166C	MRP2	structural constituent of ribosome	0.6720	1.6	0.0525754
YOR279C	RFM1	unfolded protein binding	0.6730	1.6	0.0121076
YGL043W	DST1	positive transcription elongation factor	0.6740	1.6	0.0338224
YDR377W	ATP17	hydrogen-transporting ATP synthase , rotational mechanism	0.6753	1.6	0.0351545
YBR251W	MRPS5	structural constituent of ribosome	0.6758	1.6	0.0865782
YGR159C	NSR1	RNA binding	0.6760	1.6	0.0291377
YKL023W		unknown	0.6767	1.6	0.0657252
YKR023W		unknown	0.6777	1.6	0.00906859
YJL114W			0.6787	1.6	0.00464335
YOR198C	BFR1	RNA binding	0.6788	1.6	0.00379246
YNL312W	RFA2	DNA binding	0.6792	1.6	0.0128626
YKR085C	MRPL20	structural constituent of ribosome	0.6812	1.6	0.0217817
YOR247W	SRL1	unknown	0.6815	1.6	0.0164093
YGL098W	USE1	SNAP receptor	0.6815	1.6	0.0690786
YFR007W		unknown	0.6832	1.6	0.159109

Table 1: continued.

ORF ID	Gene Name	Gene Function	Avg Log_2 Ratio	Fold Change	T-test
YER050C	RSM18	structural constituent of ribosome	0.6832	1.6	0.0146155
YNR037C	RSM19	structural constituent of ribosome	0.6837	1.6	0.0330487
YPL001W	HAT1	H3/H4 histone acetyltransferase	0.6838	1.6	0.250496
YGL136C	MRM2	rRNA (uridine-2'-O-)-methyltransferase	0.6842	1.6	0.0102949
YDR472W	TRS31	unknown	0.6843	1.6	0.0526128
YOR074C	CDC21	thymidylate synthase	0.6845	1.6	0.129474
YHR176W	FMO1	monooxygenase	0.6858	1.6	0.109132
YOR210W	RPB10	DNA-directed RNA polymerase	0.6888	1.6	0.00796331
YML039W			0.6890	1.6	0.19758
YIL098C	FMC1	unknown	0.6898	1.6	0.0174371
YGR260W	TNA1	nicotinamide mononucleotide permease	0.6918	1.6	0.0583647
YPR113W	PIS1	CDP-diacylglycerol-inositol 3-phosphatidyltransferase	0.6928	1.6	0.0794115
YKL109W	HAP4	transcriptional activator	0.6950	1.6	0.0191707
YOL002C	IZH2	metal ion binding	0.6982	1.6	0.214678
YML130C	ERO1	electron carrier	0.6985	1.6	0.030604
YBR268W	MRPL37	structural constituent of ribosome	0.7025	1.6	0.006982
YLR271W		unknown	0.7032	1.6	0.0312596
YGL232W	TAN1	RNA binding	0.7038	1.6	0.0598313
YJR059W	PTK2	protein kinase	0.7043	1.6	0.0177033
YDR320C	SWA2	protein binding	0.7060	1.6	0.0159393
YDR476C		unknown	0.7062	1.6	0.0129401
YBL043W	ECM13	unknown	0.7070	1.6	0.00649798
YLR217W			0.7072	1.6	0.0232707
YFR053C	HXK1	hexokinase	0.7078	1.6	0.140574
YKL024C	URA6	uridine kinase	0.7100	1.6	0.0826326
YPR073C	LTP1	protein tyrosine phosphatase	0.7115	1.6	0.0554634
YDR200C	VPS64	unknown	0.7142	1.6	0.00860777
YJL184W	GON7	unknown	0.7147	1.6	0.000183365
YOR271C		unknown	0.7163	1.6	0.00807593
YEL052W	AFG1	ATPase	0.7172	1.6	0.0761875
YBL018C	POP8	ribonuclease P *	0.7192	1.6	0.0364137
YJR063W	RPA12	DNA-directed RNA polymerase	0.7195	1.6	0.173241
YHR112C		cystathionine beta-lyase	0.7202	1.6	0.0867615
YFL012W		unknown	0.7215	1.6	0.0545161
YER177W	BMH1	protein binding	0.7215	1.6	0.00880142
YNL005C	MRP7	structural constituent of ribosome*	0.7218	1.6	0.00438703
YGL200C	EMP24	unknown	0.7252	1.7	0.0106196
YER083C	GET2	unknown	0.7253	1.7	0.0231585
YDR380W	ARO10	pyruvate decarboxylase	0.7260	1.7	0.0498865
YOR298W	MUM3	acyltransferase	0.7263	1.7	0.0366055
YDR510W	SMT3	protein tag	0.7270	1.7	0.0154042
YNL107W	YAF9	unknown	0.7288	1.7	0.181542
YJL174W	KRE9	unknown	0.7300	1.7	0.00546207
YJR117W	STE24	metalloendopeptidase *	0.7310	1.7	0.0617768
YDL100C	GET3	ATPase	0.7325	1.7	0.0100448
YDR241W			0.7332	1.7	0.00950221
YBR162W-A	YSY6	unknown	0.7375	1.7	0.0282321
YPR074C	TKL1	transketolase	0.7388	1.7	0.252939
YPR020W	ATP20	structural molecule	0.7392	1.7	0.0175005
YOR344C	TYE7	transcription factor	0.7395	1.7	0.0535386
YGR048W	UFD1	protein binding	0.7405	1.7	0.275455
YKL192C	ACP1	acyl carrier	0.7415	1.7	0.00593254
YDR494W	RSM28	structural constituent of ribosome	0.7422	1.7	0.0147008
YLR239C	LIP2	ligase	0.7438	1.7	0.0475392
YML009C	MRPL39	structural constituent of ribosome	0.7442	1.7	0.0140823
YFR050C	PRE4	endopeptidase	0.7443	1.7	0.011957
YNR040W		unknown	0.7477	1.7	0.225664
YGL089C	MF(ALPHA)2	mating pheromone	0.7498	1.7	0.163745
YHR041C	SRB2	RNA polymerase II transcription mediator	0.7515	1.7	0.0963786
YMR123W	PKR1	unknown	0.7540	1.7	0.0243693
YIL074C	SER33	phosphoglycerate dehydrogenase	0.7550	1.7	0.00306486
YDR260C	SWM1	unknown	0.7555	1.7	0.00232931
YLR051C	FCF2	unknown	0.7563	1.7	0.0350492
YDL022W	GPD1	glycerol-3-phosphate dehydrogenase	0.7568	1.7	0.00350797
YBR114W	RAD16	DNA-dependent ATPase	0.7573	1.7	0.0196294
YGR189C	CRH1	unknown	0.7573	1.7	0.00791711
YOR020C	HSP10	unfolded protein binding	0.7615	1.7	0.000738281
YJL192C	SOP4	unknown	0.7620	1.7	0.0103996
YOR357C	SNX3	protein binding	0.7623	1.7	0.0238469

Table 1: continued.

ORF ID	Gene Name	Gene Function	Avg Log_2 Ratio	Fold Change	T-test
YBR009C	HHF1	DNA binding	0.7630	1.7	0.00936158
YGL088W			0.7633	1.7	0.0501882
YLR183C	TOS4	transcription factor	0.7663	1.7	0.0176643
YBR262C	FMP51	unknown	0.7663	1.7	0.000555644
YBR146W	MRPS9	structural constituent of ribosome	0.7673	1.7	0.00505915
YMR260C	TIF11	translation initiation factor	0.7708	1.7	0.0117001
YMR157C	FMP39	unknown	0.7717	1.7	0.0514704
YGR183C	QCR9	ubiquinol-cytochrome-c reductase	0.7720	1.7	0.0335958
YBR201W	DER1	unknown	0.7728	1.7	0.0205069
YDL004W	ATP16	hydrogen-transporting ATP synthase , rotational mechanism	0.7730	1.7	0.00257301
YGR165W	MRPS35	structural constituent of ribosome	0.7733	1.7	0.0154686
YMR101C	SRT1	dehydrodolichyl diphosphate synthase	0.7735	1.7	0.000649768
YDR270W	CCC2	cation-transporting ATPase	0.7748	1.7	0.0443133
YMR188C	MRPS17	structural constituent of ribosome	0.7765	1.7	0.029002
YJR096W		aldo-keto reductase *	0.7793	1.7	0.00621474
YOR150W	MRPL23	structural constituent of ribosome	0.7797	1.7	0.0466981
YGR136W	LSB1	unknown	0.7875	1.7	0.0084724
YLR292C	SEC72	protein transporter	0.7902	1.7	0.0186406
YDR041W	RSM10	structural constituent of ribosome	0.7903	1.7	0.00054655
YHR128W	FUR1	uracil phosphoribosyltransferase	0.7942	1.7	0.0212612
YDR353W	TRR1	thioredoxin-disulfide reductase	0.7947	1.7	0.0193076
YOR224C	RPB8	DNA-directed RNA polymerase	0.7970	1.7	0.0757633
YML004C	GLO1	lactoylglutathione lyase	0.7982	1.7	5.85055E-05
YLR391W			0.7988	1.7	0.024883
YBR085W	AAC3	ATP:ADP antiporter	0.7993	1.7	0.0241274
YDR493W	FMP36	unknown	0.8005	1.7	0.0537485
YDR113C	PDS1	protein binding	0.8012	1.7	0.00346949
YDR220C			0.8030	1.7	0.0218942
YCL051W	LRE1	transcription regulator	0.8053	1.7	0.0044093
YLR203C	MSS51	unknown	0.8083	1.8	0.00957611
YBL021C	HAP3	transcriptional activator	0.8097	1.8	0.0113595
YDR151C	CTH1	transcription factor	0.8100	1.8	0.00504152
YDL021W	GPM2	unknown	0.8102	1.8	0.00337149
YHR034C	PIH1	unknown	0.8110	1.8	0.0174512
YCR071C	IMG2	structural constituent of ribosome	0.8113	1.8	9.61987E-05
YDL098C	SNU23	RNA splicing factor	0.8125	1.8	0.0190395
YHR214C-B			0.8142	1.8	0.0902069
YML045W			0.8157	1.8	0.0319898
YKL219W	COS9	unknown	0.8178	1.8	0.00531084
YGR166W	KRE11	unknown	0.8188	1.8	0.0768148
YDR410C	STE14	protein-S-isoprenylcysteine O-methyltransferase	0.8207	1.8	0.0164496
YKL154W	SRP102	GTPase *	0.8232	1.8	0.0903301
YFL045C	SEC53	phosphomannomutase	0.8275	1.8	0.00760547
YGR021W		unknown	0.8277	1.8	0.0030717
YNR077C			0.8285	1.8	0.000991682
YLR314C	CDC3	structural constituent of cytoskeleton*	0.8310	1.8	0.0150599
YKL195W	MIA40	unknown	0.8312	1.8	0.0534365
YER170W	ADK2	adenylate kinase	0.8363	1.8	0.0117105
YIL117C	PRM5	unknown	0.8365	1.8	0.0331854
YDR098C	GRX3	thiol-disulfide exchange intermediate	0.8378	1.8	0.358358
YJL171C		unknown	0.8415	1.8	0.0114316
YFL062W	COS4	unknown	0.8430	1.8	0.00660849
YHR148W	IMP3	snoRNA binding	0.8437	1.8	0.0823706
YMR067C	UBX4	unknown	0.8442	1.8	0.126909
YGR295C	COS6	unknown	0.8463	1.8	0.000228968
YDR244W	PEX5	peroxisome targeting sequence binding	0.8482	1.8	0.00416505
YKL110C	KTI12	enzyme regulator	0.8497	1.8	0.00756375
YLR146C	SPE4	spermine synthase	0.8508	1.8	0.00630244
YBR160W	CDC28	cyclin-dependent protein kinase	0.8523	1.8	0.0435165
YHR196W	UTP9	snoRNA binding	0.8540	1.8	0.156762
YBR183W	YPC1	ceramidase	0.8553	1.8	0.000860177
YGL127C	SOH1	unknown	0.8587	1.8	0.0410506
YKL167C	MRP49	structural constituent of ribosome	0.8588	1.8	0.0167323
YOL056W	GPM3	unknown	0.8605	1.8	0.111266
YDL248W	COS7	receptor	0.8615	1.8	0.000649638
YGL246C	RAI1	enzyme regulator	0.8630	1.8	0.0110987
YNL037C	IDH1	isocitrate dehydrogenase	0.8665	1.8	0.0010171
YCR003W	MRPL32	structural constituent of ribosome	0.8677	1.8	0.00542905
YLR113W	HOG1	MAP kinase	0.8693	1.8	0.0263236

Table 1: continued.

ORF ID	Gene Name	Gene Function	Avg Log_2 Ratio	Fold Change	T-test
YCR012W	PGK1	phosphoglycerate kinase	0.8720	1.8	0.0348544
YBR088C	POL30	DNA polymerase processivity factor	0.8733	1.8	0.0399572
YML132W	COS3	protein binding	0.8757	1.8	0.0164363
YBR299W	MAL32	alpha-glucosidase	0.8757	1.8	0.0382171
YJR057W	CDC8	thymidylate kinase	0.8765	1.8	0.0190524
YFL-TYB			0.8765	1.8	0.00677779
YOL041C	NOP12	RNA binding	0.8768	1.8	0.0817458
YDR181C	SAS4	acetyltransferase *	0.8770	1.8	0.027124
YER187W		unknown	0.8777	1.8	0.0724041
YNL193W		unknown	0.8780	1.8	0.0116237
YKL087C	CYT2	holocytochrome-c synthase	0.8780	1.8	0.00591817
YNL336W	COS1	unknown	0.8798	1.8	0.00122327
YBR008C	FLR1	multidrug transporter	0.8800	1.8	0.0270774
YFL063W			0.8838	1.8	0.157521
YKL060C	FBA1	fructose-bisphosphate aldolase	0.8840	1.8	0.0173647
YHL048W	COS8	unknown	0.8908	1.9	0.00720741
YPR060C	ARO7	chorismate mutase	0.8912	1.9	0.028491
YOR292C		unknown	0.8977	1.9	0.0338396
YGR207C		unknown	0.9017	1.9	0.00894998
YNL334C	SNO2	unknown	0.9048	1.9	0.192218
YDL202W	MRPL11	structural constituent of ribosome	0.9052	1.9	0.0193327
YER053C	PIC2	inorganic phosphate transporter	0.9072	1.9	0.0398808
YML025C	YML6	structural constituent of ribosome	0.9078	1.9	0.0275151
YDR166C	SEC5	protein binding	0.9085	1.9	0.0844186
YOR051C		unknown	0.9132	1.9	0.0737174
YMR286W	MRPL33	structural constituent of ribosome	0.9163	1.9	0.0848865
YMR304W	UBP15	ubiquitin-specific protease	0.9168	1.9	0.0045964
YCL047C		unknown	0.9222	1.9	0.038372
YOL122C	SMF1	di-, tri-valent inorganic cation transporter	0.9232	1.9	0.101084
YBR014C		unknown	0.9267	1.9	0.0113188
YPR138C	MEP3	ammonium transporter	0.9273	1.9	0.030441
YOR021C		unknown	0.9305	1.9	0.000372097
YKL001C	MET14	adenylylsulfate kinase	0.9312	1.9	0.0280655
YLR332W	MID2	transmembrane receptor	0.9347	1.9	0.00696463
YBR096W		unknown	0.9373	1.9	0.017836
YGR091W	PRP31	RNA splicing factor	0.9398	1.9	0.000015137
YKL067W	YNK1	nucleoside diphosphate kinase	0.9400	1.9	0.00192959
YOL007C		unknown	0.9442	1.9	0.137754
YIR043C		unknown	0.9458	1.9	0.00833612
YNL030W	HHF2	DNA binding	0.9513	1.9	0.00389126
YCL074W		protein binding	0.9518	1.9	0.012335
YDR050C	TPI1	triose-phosphate isomerase	0.9577	1.9	0.032662
YOL152W	FRE7	ferric-chelate reductase	0.9602	1.9	0.0174156
YDL168W	SFA1	alcohol dehydrogenase	0.9602	1.9	0.0166407
YBL028C		unknown	0.9605	1.9	0.00800421
YKL096W	CWP1	structural constituent of cell wall	0.9623	1.9	0.00734584
YKL066W			0.9635	2.0	0.00245309
YOR115C	TRS33	unknown	0.9653	2.0	0.0423615
YLR376C	PSY3	unknown	0.9697	2.0	0.152877
YDR322W	MRPL35	structural constituent of ribosome	0.9713	2.0	0.0111124
YBL010C		unknown	0.9793	2.0	0.100959
YLL009C	COX17	thioredoxin peroxidase	0.9812	2.0	0.0137056
YGL012W	ERG4	delta24(24-1) sterol reductase	0.9812	2.0	0.113517
YPL132W	COX11	copper ion binding	0.9823	2.0	0.00317913
YHR144C	DCD1	dCMP deaminase	0.9898	2.0	0.0896276
YPR158W		unknown	0.9975	2.0	0.0972752
YHR173C			0.9975	2.0	0.0185465
YML027W	YOX1	DNA binding	0.9987	2.0	0.00759221
YAL040C	CLN3	cyclin-dependent protein kinase	0.9995	2.0	0.00582507
YHR178W	STB5	transcription factor	1.0032	2.0	0.00467186
YHL004W	MRP4	structural constituent of ribosome*	1.0063	2.0	0.0104906
YML087C		unknown	1.0160	2.0	0.0442256
YBR282W	MRPL27	structural constituent of ribosome	1.0160	2.0	0.0598146
YDL127W	PCL2	cyclin-dependent protein kinase	1.0177	2.0	0.00680612
YOR131C		unknown	1.0182	2.0	0.0279522
YNL300W		unknown	1.0182	2.0	0.0024862
YKL200C			1.0238	2.0	0.02866
YMR225C	MRPL44	structural constituent of ribosome	1.0278	2.0	0.00105745
YKR093W	PTR2	peptide transporter	1.0362	2.1	0.00845347

Table 1: continued.

ORF ID	Gene Name	Gene Function	Avg Log_2 Ratio	Fold Change	T-test
YPL223C	GRE1	unknown	1.0418	2.1	0.00294154
YBL060W		unknown	1.0430	2.1	0.0213944
YMR226C	TMA29	oxidoreductase	1.0443	2.1	0.0261447
YDR511W	ACN9	unknown	1.0500	2.1	0.0208601
YGL256W	ADH4	alcohol dehydrogenase	1.0537	2.1	0.00619427
YNL231C	PDR16	phosphatidylinositol transporter	1.0583	2.1	0.014326
YKL138C	MRPL31	structural constituent of ribosome	1.0590	2.1	0.0522296
YGR215W	RSM27	structural constituent of ribosome	1.0600	2.1	0.0354891
YIL060W		unknown	1.0655	2.1	0.00435071
YHR059W	FYV4	unknown	1.0870	2.1	0.00671012
YBL030C	PET9	ATP:ADP antiporter	1.0905	2.1	0.0378908
YPR193C	HPA2	histone acetyltransferase	1.0942	2.1	0.00425003
YMR193W	MRPL24	structural constituent of ribosome	1.0952	2.1	0.00351365
YFR046C	CNN1	unknown	1.0982	2.1	0.0436128
YNL122C		unknown	1.1042	2.1	0.00916503
YDR333C		unknown	1.1045	2.2	0.00815121
YFR035C		unknown	1.1080	2.2	0.0198341
YKL113C	RAD27	5'-flap endonuclease	1.1113	2.2	0.0294076
YEL070W	DSF1	unknown	1.1157	2.2	0.0841826
YEL040W	UTR2	unknown	1.1167	2.2	0.0947613
YNL333W	SNZ2	protein binding	1.1173	2.2	0.0308249
YMR190C	SGS1	ATP-dependent DNA helicase	1.1185	2.2	0.0439944
YMR024W	MRPL3	structural constituent of ribosome	1.1188	2.2	0.0405321
YNL213C		unknown	1.1202	2.2	0.00510172
YDR115W		structural constituent of ribosome	1.1227	2.2	0.0181312
YKR077W		unknown	1.1255	2.2	0.00211103
YDL244W	THI13	unknown	1.1262	2.2	0.00209212
YDL080C	THI3	transcriptional activator *	1.1267	2.2	0.0229008
YHR145C			1.1277	2.2	0.0262777
YDL052C	SLC1	1-acylglycerol-3-phosphate O-acyltransferase	1.1408	2.2	0.010186
YER163C		unknown	1.1423	2.2	0.00683705
YBR122C	MRPL36	structural constituent of ribosome	1.1518	2.2	0.00105675
YGR084C	MRP13	structural constituent of ribosome	1.1530	2.2	0.0109299
YHR046C	INM1	inositol-1(or 4)-monophosphatase	1.1563	2.2	0.000892312
TDR261C-D			1.1580	2.2	0.0213298
YCL058C			1.1597	2.2	0.0136091
YMR316W	DIA1	unknown	1.1638	2.2	0.0186646
YJR026W			1.1652	2.2	0.0116285
YMR199W	CLN1	cyclin-dependent protein kinase	1.1667	2.2	0.00162298
YGR087C	PDC6	pyruvate decarboxylase	1.1667	2.2	0.00717395
YER003C	PMI40	mannose-6-phosphate isomerase	1.1673	2.2	0.0020648
YDR541C		dihydrokaempferol 4-reductase	1.1680	2.2	0.00599797
YDR534C	FIT1	unknown	1.1717	2.3	0.00545346
YML002W		unknown	1.1720	2.3	0.44113
YKR006C	MRPL13	structural constituent of ribosome	1.1727	2.3	0.00361926
YJR101W	RSM26	structural constituent of ribosome	1.1740	2.3	0.0029353
YCR061W(1)			1.1745	2.3	0.0373822
YLR410W-B			1.1752	2.3	0.00595837
YKR016W	FMP13	unknown	1.1753	2.3	0.00356851
YKL084W	HOT13	unknown	1.1792	2.3	0.0073707
YBL059W		unknown	1.1900	2.3	0.0182627
YKL137W		unknown	1.2010	2.3	0.0129598
YNL155W		unknown	1.2022	2.3	0.0421847
YBL101W-A			1.2045	2.3	0.000528526
YOR393W	ERR1	phosphopyruvate hydratase	1.2207	2.3	0.00967896
YBR185C	MBA1	unknown	1.2248	2.3	0.00575463
YOR286W	FMP31	unknown	1.2262	2.3	0.0170641
YOR136W	IDH2	isocitrate dehydrogenase	1.2342	2.4	0.0133421
YGL068W	MNP1	unknown	1.2360	2.4	0.0033026
YBR106W	PHO88	phosphate transporter	1.2443	2.4	0.0176661
YLR390W	ECM19	unknown	1.2453	2.4	0.0492809
YLR044C	PDC1	pyruvate decarboxylase	1.2467	2.4	0.00115598
YDR204W	COQ4	unknown	1.2493	2.4	0.00200241
YDR399W	HPT1	hypoxanthine phosphoribosyltransferase	1.2495	2.4	0.0162737
YMR184W	ADD37	unknown	1.2532	2.4	0.00862835
YOR347C	PYK2	pyruvate kinase	1.2593	2.4	0.00107906
YGR082W	TOM20	protein transporter	1.2612	2.4	0.00293878
YDR316W-B			1.2712	2.4	0.0025194
YDR503C	LPP1	phosphatidate phosphatase	1.2727	2.4	0.0131322

Table 1: continued.

ORF ID	Gene Name	Gene Function	Avg Log_2 Ratio	Fold Change	T-test
YAL038W	CDC19	pyruvate kinase	1.2733	2.4	0.00647856
YMR002W		unknown	1.2852	2.4	0.00527914
YFL059W	SNZ3	protein binding	1.2902	2.4	0.00473301
YGR208W	SER2	phosphoserine phosphatase	1.2927	2.4	0.0112336
YDR226W	ADK1	adenylate kinase	1.2943	2.5	0.00858258
YIL044C	AGE2	ARF GTPase activator	1.2950	2.5	0.0391057
YFL058W	THI5	unknown	1.3032	2.5	0.010547
YJR029W			1.3043	2.5	0.055112
YGR222W	PET54	RNA binding	1.3100	2.5	0.0148642
YHR174W	ENO2	phosphopyruvate hydratase	1.3123	2.5	0.00300659
YHR038W	RRF1	translation termination factor	1.3212	2.5	0.0475878
YHR087W		unknown	1.3237	2.5	0.00331972
YNL070W	TOM7	protein transporter	1.3268	2.5	0.00272651
YJR048W	CYC1	electron carrier	1.3350	2.5	0.00637233
YCL020W			1.3372	2.5	0.00301094
YAL012W	CYS3	cystathionine gamma-lyase	1.3387	2.5	0.00509558
YBR117C	TKL2	transketolase	1.3503	2.5	0.00690979
YGL225W	VRG4	nucleotide-sugar transporter	1.3572	2.6	0.0110224
YNL081C	SWS2	structural constituent of ribosome	1.3650	2.6	0.00855312
YPL171C	OYE3	NADPH dehydrogenase	1.3667	2.6	0.010552
YGR094W	VAS1	valine-tRNA ligase	1.3678	2.6	0.0163857
YPL281C	ERR2	phosphopyruvate hydratase	1.3727	2.6	0.00511442
YFL029C	CAK1	cyclin-dependent protein kinase	1.3787	2.6	0.00208134
YAR030C			1.3832	2.6	0.00504998
YDR213W	UPC2	RNA polymerase II transcription factor	1.3865	2.6	0.00495435
YCLX08C			1.3932	2.6	0.0251234
YNL185C	MRPL19	structural constituent of ribosome	1.4012	2.6	0.0124456
YJR149W		unknown	1.4022	2.6	0.00746424
YGL037C	PNC1	nicotinamidase	1.4173	2.7	0.000837184
YEL039C	CYC7	electron carrier	1.4238	2.7	0.00310728
YAR010C			1.4320	2.7	0.00511234
YHR181W	SVP26	protein binding	1.4367	2.7	0.0126539
YBR012W-A			1.4383	2.7	0.00946949
YJL096W	MRPL49	structural constituent of ribosome	1.4423	2.7	0.000174505
YER081W	SER3	phosphoglycerate dehydrogenase	1.4533	2.7	0.00242433
YGR254W	ENO1	phosphopyruvate hydratase	1.4620	2.8	0.0153733
YMR171C		unknown	1.4657	2.8	0.0804854
YIL070C	MAM33	unknown	1.4880	2.8	0.00561867
YLR227W-A			1.4977	2.8	0.016713
YFL051C		unknown	1.5142	2.9	0.0466355
YOR385W		unknown	1.5202	2.9	0.00158224
YHR104W	GRE3	aldo-keto reductase *	1.5240	2.9	0.00701331
YER067W		unknown	1.5273	2.9	0.00258942
YAL037C-B			1.5282	2.9	0.00161913
YCL075W		protein binding	1.5380	2.9	0.00508586
YGL253W	HXK2	hexokinase	1.5510	2.9	0.00594349
YHR179W	OYE2	NADPH dehydrogenase	1.5707	3.0	0.000618512
YER062C	HOR2	glycerol-1-phosphatase	1.5950	3.0	0.00123764
YGR142W	BTN2	unknown	1.5953	3.0	0.0357263
YGR088W	CTT1	catalase	1.6050	3.0	0.000809239
YIL053W	RHR2	glycerol-1-phosphatase	1.6108	3.1	0.00137762
YBR116C			1.6142	3.1	0.00182317
YDL219W	DTD1	hydrolase , acting on ester bonds	1.6208	3.1	0.0135482
YPL111W	CAR1	zinc ion binding	1.6462	3.1	0.0122879
YDR391C		unknown	1.6593	3.2	0.00768137
YGR151C			1.7575	3.4	0.00548375
YGL039W		oxidoreductase	1.7890	3.5	0.00140918
YGL157W		oxidoreductase	1.8280	3.6	0.00128667
YJR028W			1.8443	3.6	0.00951414
YFL021W	GAT1	specific RNA polymerase II transcription factor	1.8763	3.7	0.00226373
YBL005W-A			1.8923	3.7	0.00642121
YDR400W	URH1	ribosylpyrimidine nucleosidase	1.8978	3.7	0.0295183
YML040W			1.9135	3.8	0.000847626
YHR033W		unknown	1.9540	3.9	0.000486026
YJL107C		unknown	2.0235	4.1	0.0361086
YKL153W			2.0405	4.1	0.00705793
YFL013W-A			2.2030	4.6	0.00213463
YGR038C-A			2.2115	4.6	0.00210448
YFL014W	HSP12	unknown	2.2275	4.7	0.007048

Table 1: continued.

ORF ID	Gene Name	Gene Function	Avg Log_2 Ratio	Fold Change	T-test
YHR049W	FSH1	serine hydrolase	2.2737	4.8	0.00285462
YLR035C-A			2.2817	4.9	0.000973181
YNL054W-B		protein binding	2.3353	5.0	0.00859456
YPL163C	SVS1	unknown	2.3412	5.1	0.00346339
YDR210C-D			2.3965	5.3	0.00878016
YKL152C	GPM1	phosphoglycerate mutase	2.4405	5.4	0.000740055
YMR126C	DLT1	unknown	2.4488	5.5	0.00143872
YLR168C		unknown	2.5583	5.9	0.00126568
YOR382W	FIT2	unknown	2.6933	6.5	0.0105065
YHR044C	DOG1	2-deoxyglucose-6-phosphatase	2.8683	7.3	0.0112205
YMR169C	ALD3	3-chloroallyl aldehyde dehydrogenase	3.0673	8.4	0.00298248
YJL108C	PRM10	unknown	3.0900	8.5	0.000916524
YHR043C	DOG2	2-deoxyglucose-6-phosphatase	3.1953	9.2	0.00846285
YDR536W	STL1	transporter	3.5197	11.5	0.00666386

Table 2: Raw microarray data for fermentation day three.

ORF ID	Gene Name	Gene Function	Avg Log_2 Ratio	Fold Change	T-test
YGR254W	ENO1	phosphopyruvate hydratase	-3.6062	-12.2	0.0015155
YPL281C	ERR2	phosphopyruvate hydratase	-3.2245	-9.3	0.0036567
YHR181W	SVP26	protein binding	-3.1027	-8.6	0.0019187
YHR174W	ENO2	phosphopyruvate hydratase	-3.1002	-8.6	0.0036415
YOR393W	ERR1	phosphopyruvate hydratase	-2.9990	-8.0	0.0340413
YMR304C-A			-2.9637	-7.8	0.0047968
YCR012W	PGK1	phosphoglycerate kinase	-2.8532	-7.2	0.0138305
YGR192C	TDH3	glyceraldehyde-3-phosphate dehydrogenase	-2.7397	-6.7	0.0002674
YJL052W	TDH1	glyceraldehyde-3-phosphate dehydrogenase	-2.7353	-6.7	0.0021638
YJR009C	TDH2	glyceraldehyde-3-phosphate dehydrogenase	-2.5833	-6.0	0.0004105
YGR234W	YHB1	nitric oxide reductase	-2.5823	-6.0	0.0031394
YGR240C	PFK1	6-phosphofructokinase	-2.5133	-5.7	0.0125251
YAL037C-B			-2.3255	-5.0	0.0027095
Q0250	COX2	cytochrome-c oxidase	-2.2987	-4.9	0.0047764
YLR044C	PDC1	pyruvate decarboxylase	-2.2422	-4.7	0.0099584
YNL055C	POR1	voltage-gated ion-selective channel	-2.1995	-4.6	0.0098515
YGR094W	VAS1	valine-tRNA ligase	-2.1877	-4.6	0.0015225
YOL086C	ADH1	alcohol dehydrogenase	-2.1872	-4.6	0.013588
YGR087C	PDC6	pyruvate decarboxylase	-2.1603	-4.5	1.429E-05
YMR303C	ADH2	alcohol dehydrogenase	-2.1495	-4.4	0.0008692
YLR134W	PDC5	pyruvate decarboxylase	-2.1485	-4.4	0.0264216
YLR134W	PDC5	pyruvate decarboxylase	-2.1485	-4.4	0.0264216
YDR050C	TPI1	triose-phosphate isomerase	-2.1307	-4.4	0.002872
YJL005W	CYR1	adenylate cyclase	-2.1205	-4.3	0.0104521
YBR145W	ADH5	alcohol dehydrogenase	-2.0963	-4.3	0.0013869
YPL187W	MF(ALPHA)1	mating pheromone	-2.0948	-4.3	0.0110709
YHR173C			-2.0733	-4.2	0.0204469
YBR144C			-2.0662	-4.2	0.0025647
YNL015W	PBI2	endopeptidase inhibitor	-2.0497	-4.1	0.0064836
YNL072W	RNH201	ribonuclease H	-2.0482	-4.1	0.0054351
YKL152C	GPM1	phosphoglycerate mutase	-2.0472	-4.1	0.0012347
YGL089C	MF(ALPHA)2	mating pheromone	-2.0032	-4.0	0.0023197
YKL060C	FBA1	fructose-bisphosphate aldolase	-1.9920	-4.0	0.0020741
YKL174C	TPO5	polyamine transporter	-1.9703	-3.9	0.0053626
YFL030W	AGX1	alanine-glyoxylate transaminase	-1.9673	-3.9	0.0015463
YFL011W	HXT10	glucose transporter	-1.9588	-3.9	0.0058639
YLR153C	ACS2	acetate-CoA ligase	-1.8628	-3.6	0.0009635
YPR160W	GPH1	glycogen phosphorylase	-1.8208	-3.5	0.0123043
YPR160W	GPH1	glycogen phosphorylase	-1.8208	-3.5	0.0123043
YAL038W	CDC19	pyruvate kinase	-1.8033	-3.5	0.0001967
YDR246W	TRS23	unknown	-1.7960	-3.5	0.0019749
YBL030C	PET9	ATP:ADP antiporter	-1.7840	-3.4	0.0121792
YJR121W	ATP2	hydrogen-transporting ATP synthase , rotational mechanism	-1.7665	-3.4	0.0013171
YPL262W	FUM1	fumarate hydratase	-1.7648	-3.4	0.0080621
YFL018C	LPD1	glycine dehydrogenase	-1.7585	-3.4	0.0113803
YBL099W	ATP1	hydrogen-transporting ATP synthase , rotational mechanism	-1.7580	-3.4	0.0004718
YNL135C	FPR1	peptidyl-prolyl cis-trans isomerase	-1.7398	-3.3	0.0023218
YLR259C	HSP60	single-stranded DNA binding	-1.7267	-3.3	0.0154674
YJR048W	CYC1	electron carrier	-1.7030	-3.3	0.0050096
YKL153W			-1.6862	-3.2	0.0036681
YMR083W	ADH3	alcohol dehydrogenase	-1.6602	-3.2	0.017519
YDR247W	VHS1	protein kinase	-1.6598	-3.2	0.0099291
YDR249C		unknown	-1.6517	-3.1	0.0097933
YEL039C	CYC7	electron carrier	-1.6505	-3.1	0.0038712
YDR453C	TSA2	thioredoxin peroxidase	-1.5847	-3.0	0.017825
YJR016C	ILV3	dihydroxy-acid dehydratase	-1.5752	-3.0	0.0011641
YBR085W	AAC3	ATP:ADP antiporter	-1.5737	-3.0	0.0001426
YGL179C	TOS3	protein kinase	-1.5720	-3.0	0.004032
YHR092C	HXT4	glucose transporter	-1.5598	-2.9	0.0322082
YBR078W	ECM33	unknown	-1.5307	-2.9	0.0004679
YER133W	GLC7	protein phosphatase type 1	-1.5160	-2.9	0.0195183
YML028W	TSA1	thioredoxin peroxidase	-1.5123	-2.9	0.0050001
YNL053W	MSG5	prenylated protein tyrosine phosphatase	-1.5088	-2.8	6.246E-05
YDR380W	ARO10	pyruvate decarboxylase	-1.4992	-2.8	0.007323
YMR190C	SGS1	ATP-dependent DNA helicase	-1.4945	-2.8	0.047043
YGR244C	LSC2	succinate-CoA ligase	-1.4912	-2.8	0.0171706
YKL148C	SDH1	succinate dehydrogenase	-1.4842	-2.8	0.0233448
YBL001C	ECM15	unknown	-1.4735	-2.8	0.0042214
YNL052W	COX5A	cytochrome-c oxidase	-1.4733	-2.8	0.0017709

Table 2: continued.

ORF ID	Gene Name	Gene Function	Avg Log_2 Ratio	Fold Change	T-test
YCR074C			-1.4615	-2.8	0.0186611
YHR051W	COX6	cytochrome-c oxidase	-1.4555	-2.7	0.0053019
YJL153C	INO1	inositol-3-phosphate synthase	-1.4540	-2.7	0.0129276
YLR395C	COX8	cytochrome-c oxidase	-1.4505	-2.7	0.0040148
YER023W	PRO3	pyrroline-5-carboxylate reductase	-1.4472	-2.7	0.0083757
YCR013C			-1.4433	-2.7	0.178912
YHR008C	SOD2	manganese superoxide dismutase	-1.4285	-2.7	0.001679
YGL191W	COX13	enzyme regulator *	-1.4207	-2.7	0.0001805
YLL041C	SDH2	succinate dehydrogenase	-1.4120	-2.7	5.206E-05
YNL103W	MET4	transcription coactivator	-1.4093	-2.7	0.0002534
YGR279C	SCW4	glucosidase	-1.4013	-2.6	0.0438594
YJL152W			-1.3928	-2.6	0.0041552
YOR215C		unknown	-1.3892	-2.6	0.0227276
YHR001W-A	QCR10	ubiquinol-cytochrome-c reductase	-1.3537	-2.6	0.0086701
YDR322W	MRPL35	structural constituent of ribosome	-1.3517	-2.6	0.000573
YGR246C	BRF1	RNA polymerase III transcription factor	-1.3508	-2.6	0.0326688
YKL141W	SDH3	succinate dehydrogenase	-1.3158	-2.5	0.0037429
YBL100C			-1.3097	-2.5	0.0323298
YDR273W	DON1	unknown	-1.2945	-2.5	0.0016658
YIL155C	GUT2	glycerol-3-phosphate dehydrogenase	-1.2882	-2.4	0.0274819
YDL067C	COX9	cytochrome-c oxidase	-1.2878	-2.4	0.0461493
YKL160W	ELF1	RNA polymerase II transcription elongation factor	-1.2837	-2.4	0.0017938
YJR120W		unknown	-1.2828	-2.4	0.0003826
YDR119W		unknown	-1.2732	-2.4	0.0078908
YHR219W		unknown	-1.2722	-2.4	0.0171083
YBL098W	BNA4	kynurenine 3-monooxygenase	-1.2688	-2.4	0.0055453
YKL085W	MDH1	L-malate dehydrogenase	-1.2673	-2.4	0.0038412
YJL217W		unknown	-1.2667	-2.4	0.0479643
YJL217W		unknown	-1.2667	-2.4	0.0479643
YHR094C	HXT1	glucose transporter	-1.2655	-2.4	0.0098239
YJL214W	HXT8	glucose transporter	-1.2638	-2.4	0.0358475
YJL066C	MPM1	unknown	-1.2535	-2.4	0.015919
YJR148W	BAT2	branched-chain-amino-acid transaminase	-1.2505	-2.4	0.007391
YDR245W	MNN10	alpha-1,6-mannosyltransferase	-1.2335	-2.4	0.0113862
YDR202C	RAV2	unknown	-1.2270	-2.3	0.0135408
YOR133W	EFT1	translation elongation factor	-1.2250	-2.3	0.0679752
YMR145C	NDE1	NADH dehydrogenase	-1.2160	-2.3	0.0949257
YKL067W	YNK1	nucleoside diphosphate kinase	-1.2115	-2.3	0.0016627
YBL015W	ACH1	acetyl-CoA hydrolase	-1.2090	-2.3	0.0080694
YKL164C	PIR1	structural constituent of cell wall	-1.2010	-2.3	0.0299198
YJL045W		succinate dehydrogenase	-1.1980	-2.3	0.0009649
YKL145W	RPT1	ATPase *	-1.1978	-2.3	0.0374322
YKL145W	RPT1	ATPase *	-1.1978	-2.3	0.0374322
YKL026C	GPX1	glutathione peroxidase *	-1.1797	-2.3	0.0193568
YOR230W	WTM1	transcription corepressor	-1.1757	-2.3	0.0049473
YKL066W			-1.1743	-2.3	0.0367139
YER178W	PDA1	pyruvate dehydrogenase	-1.1707	-2.3	0.0048228
YMR256C	COX7	cytochrome-c oxidase	-1.1678	-2.2	0.002045
YIL170W	HXT12	unknown	-1.1670	-2.2	0.0020793
YIL170W	HXT12	unknown	-1.1670	-2.2	0.0020793
YGL253W	HXK2	hexokinase	-1.1618	-2.2	0.0208222
YEL030W	ECM10	unknown	-1.1598	-2.2	0.13813
YJR077C	MIR1	inorganic phosphate transporter	-1.1593	-2.2	0.0012406
YLL066W-A			-1.1532	-2.2	0.0420793
YPL134C	ODC1	intracellular transporter	-1.1513	-2.2	0.005421
YHR007C	ERG11	sterol 14-demethylase	-1.1313	-2.2	0.0215179
YNL220W	ADE12	adenylosuccinate synthase	-1.1282	-2.2	0.0175976
YFL038C	YPT1	GTPase	-1.1268	-2.2	0.008804
YBR039W	ATP3	hydrogen-transporting ATP synthase , rotational mechanism	-1.1240	-2.2	0.0552641
YIR037W	HYR1	thioredoxin peroxidase *	-1.1185	-2.2	0.0279486
YBR294W	SUL1	sulfate transporter	-1.1145	-2.2	0.0080761
YDR385W	EFT2	translation elongation factor	-1.1065	-2.2	0.0312713
YAR018C	KIN3	protein kinase	-1.1060	-2.2	0.0051538
YGL105W	ARC1	tRNA binding	-1.1048	-2.2	0.0153682
YLR303W	MET17	cysteine synthase *	-1.1033	-2.1	0.0546932
YBR244W	GPX2	glutathione peroxidase *	-1.1027	-2.1	0.0007172
YBR093C	PHO5	acid phosphatase *	-1.1022	-2.1	0.0198011
YCL058C			-1.1002	-2.1	0.0466576
YJR073C	OPI3	phosphatidyl-N-methylethanolamine N-methyltransferase	-1.0943	-2.1	0.0047786

Table 2: continued.

ORF ID	Gene Name	Gene Function	Avg Log_2 Ratio	Fold Change	T-test
YEL024W	RIP1	ubiquinol-cytochrome-c reductase	-1.0880	-2.1	0.0069601
YLR294C			-1.0695	-2.1	0.0021397
YEL066W	HPA3	histone acetyltransferase	-1.0658	-2.1	0.0229021
YEL066W	HPA3	histone acetyltransferase	-1.0658	-2.1	0.0229021
YFL039C	ACT1	structural constituent of cytoskeleton	-1.0655	-2.1	0.0120042
YKL016C	ATP7	structural molecule *	-1.0593	-2.1	0.0016204
YDR320C	SWA2	protein binding	-1.0588	-2.1	0.0431103
YHL050C		helicase	-1.0503	-2.1	0.0031794
YKL097W-A			-1.0437	-2.1	0.0006083
YML110C	COQ5	2-hexaprenyl-6-methoxy-1,4-benzoquinone methyltransferase	-1.0390	-2.1	0.0479456
YHR214W		unknown	-1.0318	-2.0	0.0180394
YPR020W	ATP20	structural molecule	-1.0255	-2.0	0.0010649
YEL077C		helicase	-1.0240	-2.0	0.002784
YEL065W	SIT1	siderophore-iron (ferrioxamine) uptake transporter	-1.0200	-2.0	0.0134719
YBL113W-A			-1.0152	-2.0	0.0042373
YHL034C	SBP1	RNA binding	-1.0132	-2.0	0.0048516
YPL078C	ATP4	structural molecule *	-1.0002	-2.0	0.0020795
YDL181W	INH1	enzyme inhibitor	-0.9997	-2.0	0.0071249
YCR004C	YCP4	electron carrier	-0.9735	-2.0	0.014026
YLR320W	MMS22	unknown	-0.9560	-1.9	0.0562386
YDR438W		unknown	-0.9538	-1.9	0.0397923
YHR126C		unknown	-0.9492	-1.9	0.0112156
YDL055C	PSA1	mannose-1-phosphate guanylyltransferase	-0.9452	-1.9	0.0086477
YBL002W	HTB2	DNA binding	-0.9392	-1.9	0.0188168
YJL143W	TIM17	protein transporter	-0.9383	-1.9	0.0650109
YLR150W	STM1	DNA binding*	-0.9362	-1.9	0.0100821
YBR067C	TIP1	structural constituent of cell wall*	-0.9323	-1.9	0.0027268
YDR268W	MSW1	tryptophan-tRNA ligase	-0.9292	-1.9	0.0036085
YDL078C	MDH3	L-malate dehydrogenase	-0.9092	-1.9	0.0225068
YNL037C	IDH1	isocitrate dehydrogenase	-0.9092	-1.9	0.0060415
YGR182C			-0.9003	-1.9	0.0346738
YAL008W	FUN14	unknown	-0.9000	-1.9	0.109014
YFR003C	YPI1	protein phosphatase inhibitor	-0.8968	-1.9	6.043E-05
YDL137W	ARF2	GTPase	-0.8950	-1.9	0.0160564
YER011W	TIR1	structural constituent of cell wall	-0.8910	-1.9	0.0206417
YDL215C	GDH2	glutamate dehydrogenase	-0.8852	-1.8	0.0142824
YNL064C	YDJ1	chaperone regulator *	-0.8830	-1.8	0.0830227
YKR013W	PRY2	unknown	-0.8778	-1.8	0.0225798
YBL078C	ATG8	microtubule binding	-0.8757	-1.8	0.0573605
YDL021W	GPM2	unknown	-0.8677	-1.8	0.0045561
YDL021W	GPM2	unknown	-0.8677	-1.8	0.0045561
YML132W	COS3	protein binding	-0.8665	-1.8	0.0077908
YDR529C	QCR7	ubiquinol-cytochrome-c reductase	-0.8472	-1.8	0.0060546
YBR025C		unknown	-0.8447	-1.8	0.0049425
YJR103W	URA8	CTP synthase	-0.8405	-1.8	0.0835693
YDR193W			-0.8392	-1.8	0.0085795
YDR033W	MRH1	unknown	-0.8385	-1.8	0.0005238
YLR377C	FBP1	fructose-bisphosphatase	-0.8233	-1.8	0.0738824
YNL142W	MEP2	ammonium transporter	-0.8227	-1.8	0.111587
YFR053C	HXK1	hexokinase	-0.8142	-1.8	0.0146429
YLL050C	COF1	protein binding	-0.8098	-1.8	0.101651
YIL111W	COX5B	cytochrome-c oxidase	-0.8067	-1.7	0.0204686
YKL117W	SBA1	chaperone binding	-0.7973	-1.7	0.0162102
YER053C	PIC2	inorganic phosphate transporter	-0.7935	-1.7	0.004651
YNR001C	CIT1	citrate (Si)-synthase	-0.7907	-1.7	0.0039411
YEL009C	GCN4	DNA binding*	-0.7893	-1.7	0.0013036
YLR258W	GSY2	glycogen (starch) synthase	-0.7845	-1.7	0.131435
YOR027W	STI1	unfolded protein binding*	-0.7800	-1.7	0.103367
YPL037C	EGD1	unfolded protein binding	-0.7800	-1.7	0.0296889
YBR094W		unknown	-0.7758	-1.7	0.0068261
YDL192W	ARF1	GTPase	-0.7753	-1.7	0.0196191
TMR307W			-0.7728	-1.7	0.0020019
YPL271W	ATP15	hydrogen-transporting ATP synthase , rotational mechanism	-0.7705	-1.7	0.0419803
YJL001W	PRE3	endopeptidase	-0.7700	-1.7	0.0661903
YIL123W	SIM1	unknown	-0.7668	-1.7	0.0555948
YKL192C	ACP1	acyl carrier	-0.7663	-1.7	0.0116203
YFR049W	YMR31	structural constituent of ribosome	-0.7653	-1.7	0.0024639
YFR049W	YMR31	structural constituent of ribosome	-0.7653	-1.7	0.0024639
YJR031C	GEA1	ARF guanyl-nucleotide exchange factor	-0.7608	-1.7	0.0114537

Table 2: continued.

ORF ID	Gene Name	Gene Function	Avg Log_2 Ratio	Fold Change	T-test
YLL026W	HSP104	chaperone binding*	-0.7602	-1.7	0.0250434
YHR040W	BCD1	nucleic acid binding	-0.7593	-1.7	0.0289917
YFL062W	COS4	unknown	-0.7565	-1.7	0.0238822
YBL075C	SSA3	ATPase *	-0.7562	-1.7	0.0299285
YBR054W	YRO2	unknown	-0.7555	-1.7	0.024774
YIL166C		transporter	-0.7520	-1.7	0.0242363
YJR045C	SSC1	ATPase *	-0.7508	-1.7	0.0233663
YBL045C	COR1	ubiquinol-cytochrome-c reductase	-0.7493	-1.7	0.0293268
YJL219W	HXT9	glucose transporter	-0.7388	-1.7	0.152974
YDR284C	DPP1	phosphatidate phosphatase *	-0.7358	-1.7	0.0849586
YDR032C	PST2	unknown	-0.7285	-1.7	0.0423654
YLR304C	ACO1	aconitate hydratase	-0.7272	-1.7	0.0083209
YOR136W	IDH2	isocitrate dehydrogenase	-0.7252	-1.7	0.0740756
YDL066W	IDP1	isocitrate dehydrogenase	-0.7230	-1.7	0.0028387
YJR001W	AVT1	neutral amino acid transporter	-0.7193	-1.6	0.0043982
YJL068C		S-formylglutathione hydrolase	-0.7135	-1.6	0.0044765
YDR133C			-0.7077	-1.6	0.0340978
YDR134C		unknown	-0.7057	-1.6	0.0016352
YGL062W	PYC1	pyruvate carboxylase	-0.7055	-1.6	0.031003
YIL136W	OM45	unknown	-0.7037	-1.6	0.0417209
YDL029W	ARP2	structural constituent of cytoskeleton*	-0.6987	-1.6	0.0857069
YMR203W	TOM40	protein transporter	-0.6987	-1.6	0.000612
YNL009W	IDP3	isocitrate dehydrogenase	-0.6985	-1.6	0.003158
YJL034W	KAR2	ATPase *	-0.6963	-1.6	0.0618993
YJR008W		unknown	-0.6962	-1.6	0.0435149
YJR008W		unknown	-0.6962	-1.6	0.0435149
YJL200C	ACO2	aconitate hydratase	-0.6947	-1.6	0.096495
YGL200C	EMP24	unknown	-0.6932	-1.6	0.04933
YEL034W	HYP2	protein binding*	-0.6910	-1.6	0.0130075
YDR327W			-0.6852	-1.6	0.0101475
YDR327W			-0.6852	-1.6	0.0101475
YBR139W		serine hydrolase *	-0.6830	-1.6	0.0061513
YMR295C		unknown	-0.6830	-1.6	0.0392713
YNL007C	SIS1	unfolded protein binding*	-0.6815	-1.6	0.0014455
YDL100C	GET3	ATPase	-0.6792	-1.6	0.0208688
YMR297W	PRC1	carboxypeptidase C	-0.6787	-1.6	0.0625163
YML078W	CPR3	peptidyl-prolyl cis-trans isomerase	-0.6785	-1.6	0.006109
YGL121C	GPG1	signal transducer	-0.6768	-1.6	0.0036963
YCL043C	PDI1	protein disulfide isomerase	-0.6720	-1.6	0.0105996
YIL138C	TPM2	actin lateral binding	-0.6720	-1.6	0.0003805
YBR080C	SEC18	ATPase	-0.6645	-1.6	0.0970178
YDL206W		unknown	-0.6642	-1.6	0.0344768
YOR020C	HSP10	unfolded protein binding	-0.6618	-1.6	0.032411
YER004W	FMP52	unknown	-0.6575	-1.6	0.0297763
YDR382W	RPP2B	structural constituent of ribosome	-0.6533	-1.6	0.0767667
YHL034W-A			-0.6515	-1.6	0.0723914
YIL033C	BCY1	cAMP-dependent protein kinase	-0.6437	-1.6	0.0054367
YDR377W	ATP17	hydrogen-transporting ATP synthase , rotational mechanism	-0.6413	-1.6	0.0019884
YDR148C	KGD2	dihydrolipoyllysine-residue succinyltransferase	-0.6405	-1.6	0.0036853
YBR221C	PDB1	pyruvate dehydrogenase	-0.6392	-1.6	0.0672441
YHR215W	PHO12	acid phosphatase	-0.6392	-1.6	0.0412283
YMR260C	TIF11	translation initiation factor	-0.6378	-1.6	0.0377335
YLR248W	RCK2	protein serine/threonine kinase	-0.6287	-1.5	0.0998243
YEL034C-A			-0.6280	-1.5	0.0763997
YJL158C	CIS3	structural constituent of cell wall	-0.6232	-1.5	0.0386436
YDL126C	CDC48	ATPase	-0.6207	-1.5	0.125145
YDR028C	REG1	protein phosphatase type 1 regulator	-0.6190	-1.5	0.160949
YOR007C	SGT2	unknown	-0.6023	-1.5	0.0440004
YIL018W	RPL2B	structural constituent of ribosome	-0.6010	-1.5	0.0942016
YAL013W	DEP1	transcription regulator	-0.6008	-1.5	0.0155276
YLR149C		unknown	-0.6003	-1.5	0.0570284
YLR043C	TRX1	thiol-disulfide exchange intermediate	-0.6002	-1.5	0.0166047
YBR243C	ALG7	UDP-N-acetylglucosamine-dolichyl-phosphate N-acetylglucosami	-0.6000	-1.5	0.0112551
YOL030W	GAS5	1,3-beta-glucanosyltransferase	-0.5978	-1.5	0.0491241
YJL026W	RNR2	ribonucleoside-diphosphate reductase	-0.5912	-1.5	0.133042
YCL035C	GRX1	thiol-disulfide exchange intermediate *	-0.5895	-1.5	0.0611118
YPR035W	GLN1	glutamate-ammonia ligase	-0.5880	-1.5	0.0211799
YER094C	PUP3	endopeptidase	-0.5863	-1.5	0.0298535
YML106W	URA5	orotate phosphoribosyltransferase	-0.5833	-1.5	0.0639159

Table 2: continued.

ORF ID	Gene Name	Gene Function	Avg Log_2 Ratio	Fold Change	T-test
YGR253C	PUP2	endopeptidase	-0.5820	-1.5	0.152895
YHR214W-A			-0.5805	-1.5	0.0033847
YHR057C	CPR2	peptidyl-prolyl cis-trans isomerase	-0.5798	-1.5	5.575E-05
YHR057C	CPR2	peptidyl-prolyl cis-trans isomerase	-0.5798	-1.5	5.575E-05
YCL009C	ILV6	enzyme regulator *	-0.5775	-1.5	0.147573
YIL011W	TIR3	unknown	-0.5722	-1.5	0.0526976
YPL033C		unknown	-0.5700	-1.5	0.0180346
YPL033C		unknown	-0.5700	-1.5	0.0180346
YKL216W	URA1	dihydroorotate dehydrogenase	-0.5687	-1.5	0.0004113
YER086W	ILV1	threonine ammonia-lyase	-0.5685	-1.5	0.214924
YHL048W	COS8	unknown	-0.5677	-1.5	0.0700487
YBR164C	ARL1	GTPase	-0.5667	-1.5	0.0294648
YNR036C		structural constituent of ribosome	-0.5595	-1.5	0.0608814
YDR086C	SSS1	protein transporter	-0.5593	-1.5	0.0117785
YBL003C	HTA2	DNA binding	-0.5588	-1.5	0.0139608
YJL159W	HSP150	structural constituent of cell wall	-0.5577	-1.5	0.0256999
YDL007W	RPT2	ATPase *	-0.5568	-1.5	0.0535129
YGR183C	QCR9	ubiquinol-cytochrome-c reductase	-0.5528	-1.5	0.0528061
YHR192W		unknown	-0.5472	-1.5	0.0007977
YIR041W	PAU15	unknown	-0.5462	-1.5	0.053258
YGR271W	SLH1	RNA helicase	-0.5458	-1.5	0.058332
YDR321W	ASP1	asparaginase	-0.5450	-1.5	0.0152668
YPL270W	MDL2	ATPase , coupled to transmembrane movement of substances	-0.5438	-1.5	0.0662755
YNL079C	TPM1	actin lateral binding	-0.5402	-1.5	0.185009
YJL207C	LAA1	unknown	-0.5393	-1.5	0.0113212
YBR111C	YSA1	phosphoribosyl-ATP diphosphatase	-0.5387	-1.5	0.283746
YMR056C	AAC1	ATP:ADP antiporter	-0.5370	-1.5	0.0662925
YDR163W	CWC15	unknown	-0.5333	-1.4	0.0393203
YGR282C	BGL2	glucan 1,3-beta-glucosidase	-0.5302	-1.4	0.0013714
YLR174W	IDP2	isocitrate dehydrogenase	-0.5297	-1.4	0.0493384
YDR388W	RVS167	cytoskeletal protein binding	-0.5288	-1.4	0.0285552
YNL208W		unknown	-0.5277	-1.4	0.109385
YAR020C	PAU7	unknown	-0.5165	-1.4	8.053E-05
YBR148W	YSW1	unknown	-0.5153	-1.4	0.001374
YMR205C	PFK2	6-phosphofructokinase	-0.5130	-1.4	0.142388
YBR184W		unknown	-0.5118	-1.4	0.308085
YGR180C	RNR4	ribonucleoside-diphosphate reductase	-0.5117	-1.4	0.0193124
YER177W	BMH1	protein binding*	-0.5098	-1.4	0.141298
YLR257W		unknown	-0.5087	-1.4	0.0086452
YEL032W	MCM3	chromatin binding*	-0.5028	-1.4	0.0398392
YGR209C	TRX2	thiol-disulfide exchange intermediate	-0.4998	-1.4	0.0114102
YJL167W	ERG20	dimethylallyltranstransferase *	-0.4997	-1.4	0.0353727
YDR198C	RKM2	unknown	-0.4978	-1.4	0.0080298
YDR198C	RKM2	unknown	-0.4978	-1.4	0.0080298
YAL023C	PMT2	dolichyl-phosphate-mannose-protein mannosyltransferase	-0.4962	-1.4	0.0299618
YIL176C	PAU14	unknown	-0.4953	-1.4	0.0086783
YBR023C	CHS3	chitin synthase	-0.4952	-1.4	0.0954594
YLL004W	ORC3	DNA replication origin binding	-0.4935	-1.4	0.0167494
YLL004W	ORC3	DNA replication origin binding	-0.4935	-1.4	0.0167494
YLR229C	CDC42	GTPase *	-0.4898	-1.4	0.0031201
YAL005C	SSA1	ATPase *	-0.4895	-1.4	0.0431829
YEL025C		unknown	-0.4887	-1.4	0.218472
YIL125W	KGD1	oxoglutarate dehydrogenase	-0.4863	-1.4	0.037867
YDR454C	GUK1	guanylate kinase	-0.4852	-1.4	0.0938369
YBR072W	HSP26	unfolded protein binding	-0.4848	-1.4	0.0065322
YDL130W	RPP1B	structural constituent of ribosome	-0.4847	-1.4	0.0816368
YJR047C	ANB1	translation initiation factor	-0.4833	-1.4	0.010185
YAL063C	FLO9	mannose binding	-0.4823	-1.4	0.0359755
YLR110C	CCW12	unknown	-0.4818	-1.4	0.0774241
YNL124W	NAF1	RNA binding	-0.4817	-1.4	0.218076
YOR362C	PRE10	endopeptidase	-0.4783	-1.4	0.258326
YKL163W	PIR3	structural constituent of cell wall	-0.4733	-1.4	0.0482333
YBR095C	RXT2	unknown	-0.4707	-1.4	0.0006189
YOR394W	PAU21	unknown	-0.4667	-1.4	0.0057981
YAL068C	PAU8	unknown	-0.4665	-1.4	0.0752435
YIL068C	SEC6	protein binding	-0.4653	-1.4	0.232778
YGL198W	YIP4	Rab GTPase binding	-0.4627	-1.4	0.0198333
YNR018W		unknown	-0.4625	-1.4	0.0884206
YBL113C		helicase	-0.4620	-1.4	0.0318955

Table 2: continued.

ORF ID	Gene Name	Gene Function	Avg Log_2 Ratio	Fold Change	T-test
YCR049C			-0.4605	-1.4	0.172441
YGL066W	SGF73	structural molecule *	-0.4557	-1.4	0.119983
YPL282C	PAU22	unknown	-0.4543	-1.4	0.0942943
YDR497C	ITR1	myo-inositol transporter	-0.4523	-1.4	0.0617382
YJL079C	PRY1	unknown	-0.4522	-1.4	0.0709253
YGL076C	RPL7A	structural constituent of ribosome	-0.4507	-1.4	0.0859879
YFL043C			-0.4473	-1.4	0.0095589
YPR165W	RHO1	GTPase *	-0.4420	-1.4	0.144566
YPR108W	RPN7	structural molecule	-0.4415	-1.4	0.0871089
YBR301W	DAN3	unknown	-0.4373	-1.4	0.0778786
YDR077W	SED1	structural constituent of cell wall	-0.4367	-1.4	0.0248061
YGR295C	COS6	unknown	-0.4360	-1.4	0.127048
YPR100W	MRPL51	structural constituent of ribosome	-0.4322	-1.3	0.153402
YJL166W	QCR8	ubiquinol-cytochrome-c reductase	-0.4295	-1.3	0.181686
YDR080W	VPS41	Rab guanyl-nucleotide exchange factor	-0.4268	-1.3	0.136035
YOR383C	FIT3	unknown	-0.4210	-1.3	0.306351
YBR088C	POL30	DNA polymerase processivity factor	-0.4165	-1.3	0.0010976
YBR088C	POL30	DNA polymerase processivity factor	-0.4165	-1.3	0.0010976
YPL048W	CAM1	translation elongation factor	-0.4132	-1.3	0.360113
YCL025C	AGP1	amino acid transporter	-0.4122	-1.3	0.0445531
YJR023C			-0.4122	-1.3	0.0651461
YJL151C	SNA3	unknown	-0.4105	-1.3	0.0842497
YER067W		unknown	-0.4103	-1.3	0.0751532
YER103W	SSA4	ATPase *	-0.4088	-1.3	0.21908
YDR253C	MET32	DNA binding*	-0.4057	-1.3	0.131526
YER057C	HMF1	unknown	-0.4050	-1.3	0.0253396
YCR087W			-0.4033	-1.3	0.163126
YOR332W	VMA4	hydrogen-transporting ATPase , rotational mechanism	-0.4032	-1.3	0.161853
YFL067W		unknown	-0.4018	-1.3	0.596477
YJL073W	JEM1	unfolded protein binding*	-0.3995	-1.3	0.0082648
YDR251W	PAM1	unknown	-0.3967	-1.3	0.0264071
YAL003W	EFB1	translation elongation factor	-0.3927	-1.3	0.0584031
YHR193C	EGD2	unfolded protein binding	-0.3907	-1.3	0.366134
YPR026W	ATH1	alpha,alpha-trehalase	-0.3903	-1.3	0.0047912
YIR014W		unknown	-0.3900	-1.3	0.164385
YMR008C	PLB1	lysophospholipase	-0.3897	-1.3	0.0161228
YEL011W	GLC3	1,4-alpha-glucan branching enzyme	-0.3878	-1.3	0.0152677
YGL112C	TAF6	general RNA polymerase II transcription factor	-0.3872	-1.3	0.117595
YDL171C	GLT1	glutamate synthase (NADH)	-0.3857	-1.3	0.263044
YDR329C	PEX3	protein binding	-0.3857	-1.3	0.0415069
YIR003W		unknown	-0.3855	-1.3	0.0160999
YKR096W		unknown	-0.3850	-1.3	0.069603
YJR085C		unknown	-0.3823	-1.3	0.0481058
YLL024C	SSA2	ATPase *	-0.3762	-1.3	0.0317893
YIL094C	LYS12	homoisocitrate dehydrogenase	-0.3730	-1.3	0.0869456
YDL248W	COS7	receptor	-0.3707	-1.3	0.0216969
YGR142W	BTN2	unknown	-0.3695	-1.3	0.485944
YLR190W	MMR1	unknown	-0.3695	-1.3	0.0571431
YHR200W	RPN10	endopeptidase	-0.3687	-1.3	0.138534
YPL224C	MMT2	unknown	-0.3682	-1.3	0.110035
YJL223C	PAU1	unknown	-0.3615	-1.3	0.0897186
YER052C	HOM3	aspartate kinase	-0.3575	-1.3	0.224273
YDR542W	PAU10	unknown	-0.3568	-1.3	0.193424
YJL216C		alpha-galactosidase *	-0.3530	-1.3	0.0213934
YJL216C		alpha-galactosidase *	-0.3530	-1.3	0.0213934
YKL058W	TOA2	general RNA polymerase II transcription factor	-0.3465	-1.3	0.0209133
YGR038W	ORM1	unknown	-0.3463	-1.3	0.0206693
YCR102C		unknown	-0.3437	-1.3	0.445094
YDL014W	NOP1	methyltransferase	-0.3407	-1.3	0.107289
YKL013C	ARC19	structural molecule	-0.3405	-1.3	0.357407
YIL097W	FYV10	unknown	-0.3335	-1.3	0.199443
YNL104C	LEU4	2-isopropylmalate synthase	-0.3332	-1.3	0.353002
YBR036C	CSG2	enzyme regulator	-0.3270	-1.3	0.0770719
YBR121C	GRS1	glycine-tRNA ligase	-0.3265	-1.3	0.183405
YDR167W	TAF10	general RNA polymerase II transcription factor	-0.3260	-1.3	0.174245
YAL061W		oxidoreductase , acting on the CH-OH group of donors, NAD or N	-0.3253	-1.3	0.0522863
YGR135W	PRE9	endopeptidase	-0.3250	-1.3	0.0800802
YAL062W	GDH3	glutamate dehydrogenase	-0.3237	-1.3	0.0251359
YPL118W	MRP51	structural constituent of ribosome	-0.3233	-1.3	0.0106163

Table 2: continued.

ORF ID	Gene Name	Gene Function	Avg Log_2 Ratio	Fold Change	T-test
YCR104W	PAU3	unknown	-0.3228	-1.3	0.0714356
YBR234C	ARC40	structural constituent of cytoskeleton	-0.3222	-1.3	0.151189
YJL202C			-0.3222	-1.3	0.46558
YBR047W	FMP23	unknown	-0.3205	-1.2	0.0364289
YIL085C	KTR7	mannosyltransferase	-0.3197	-1.2	0.875058
YFR017C		unknown	-0.3195	-1.2	0.0218165
YJL072C	PSF2	unknown	-0.3182	-1.2	0.0391689
YBL066C	SEF1	unknown	-0.3112	-1.2	0.253791
YOR374W	ALD4	aldehyde dehydrogenase	-0.3110	-1.2	0.0074353
YCR014C	POL4	beta DNA polymerase	-0.3105	-1.2	0.193762
YBR202W	CDC47	chromatin binding*	-0.3097	-1.2	0.0939306
YCL064C	CHA1	L-serine ammonia-lyase *	-0.3072	-1.2	0.0354441
YJL206C-A			-0.3067	-1.2	0.18422
YDR099W	BMH2	protein binding*	-0.3000	-1.2	0.403096
YDR266C		unknown	-0.2998	-1.2	0.0253857
YCL051W	LRE1	transcription regulator *	-0.2995	-1.2	0.342779
YDL213C	NOP6	unknown	-0.2987	-1.2	0.284312
YKL109W	HAP4	transcriptional activator	-0.2958	-1.2	0.184835
YBR102C	EXO84	protein binding	-0.2937	-1.2	0.261787
TDR261C-D			-0.2923	-1.2	0.195501
YKL093W	MBR1	unknown	-0.2897	-1.2	0.0637364
YBR247C	ENP1	snoRNA binding	-0.2890	-1.2	0.109716
YCL028W	RNQ1	unknown	-0.2883	-1.2	0.147312
YEL049W	PAU2	unknown	-0.2850	-1.2	0.145279
YBR052C	RFS1	unknown	-0.2835	-1.2	0.165765
YMR311C	GLC8	enzyme activator	-0.2825	-1.2	0.150182
YBR053C		unknown	-0.2793	-1.2	0.192995
YHL021C	FMP12	unknown	-0.2720	-1.2	0.421484
YBR218C	PYC2	pyruvate carboxylase	-0.2677	-1.2	0.198903
YCL001W	RER1	unknown	-0.2667	-1.2	0.126119
YMR325W	PAU19	unknown	-0.2662	-1.2	0.580808
YDR156W	RPA14	DNA-directed RNA polymerase	-0.2658	-1.2	0.246353
YBR287W	ZSP1	unknown	-0.2625	-1.2	0.817135
YDR496C	PUF6	specific transcriptional repressor	-0.2617	-1.2	0.261561
YHR026W	PPA1	hydrogen-transporting ATPase , rotational mechanism	-0.2593	-1.2	0.171852
YKL217W	JEN1	lactate transporter	-0.2590	-1.2	0.476441
YMR186W	HSC82	unfolded protein binding	-0.2563	-1.2	0.0485359
YBR263W	SHM1	glycine hydroxymethyltransferase	-0.2562	-1.2	0.0701914
YBR082C	UBC4	ubiquitin conjugating enzyme	-0.2553	-1.2	0.158767
YIL066C	RNR3	ribonucleoside-diphosphate reductase	-0.2550	-1.2	0.142169
YBR015C	MNN2	alpha-1,2-mannosyltransferase	-0.2532	-1.2	0.39925
YIL084C	SDS3	protein binding	-0.2532	-1.2	0.260757
YPR028W	YOP1	protein binding	-0.2532	-1.2	0.333069
YIL113W	SDP1	MAP kinase	-0.2518	-1.2	0.529468
YBR010W	HHT1	DNA binding	-0.2512	-1.2	0.14227
YML039W			-0.2512	-1.2	0.399605
YMR080C	NAM7	ATP-dependent RNA helicase *	-0.2507	-1.2	0.362955
YNL022C		unknown	-0.2500	-1.2	3.492E-05
YJL222W	VTH2	signal sequence binding	-0.2487	-1.2	0.113229
YBR170C	NPL4	unknown	-0.2483	-1.2	0.312997
YML012W	ERV25	unknown	-0.2480	-1.2	0.929802
YHR194W	MDM31	unknown	-0.2455	-1.2	0.254302
YGR008C	STF2	unknown	-0.2452	-1.2	0.143857
YLR437C		unknown	-0.2395	-1.2	0.0535503
YNL209W	SSB2	ATPase *	-0.2388	-1.2	0.194611
YCL037C	SRO9	RNA binding	-0.2387	-1.2	0.447294
YIL041W	GVP36	unknown	-0.2382	-1.2	0.0043406
YKR046C	PET10	unknown	-0.2365	-1.2	0.322573
YAL067C	SEO1	transporter	-0.2340	-1.2	0.0472514
YCL008C	STP22	protein binding	-0.2327	-1.2	0.149481
YDR232W	HEM1	5-aminolevulinate synthase	-0.2327	-1.2	0.502076
YHR211W	FLO5	mannose binding	-0.2325	-1.2	0.354771
YBR149W	ARA1	aldo-keto reductase *	-0.2317	-1.2	0.157737
YNL336W	COS1	unknown	-0.2307	-1.2	0.287355
YGR204W	ADE3	formate-tetrahydrofolate ligase	-0.2293	-1.2	0.363124
YHR183W	GND1	phosphogluconate dehydrogenase	-0.2247	-1.2	0.025193
YHR213W		unknown	-0.2192	-1.2	0.112611
YBR180W	DTR1	multidrug transporter	-0.2173	-1.2	0.793773
YOR141C	ARP8	unknown	-0.2163	-1.2	0.0915507

Table 2: continued.

ORF ID	Gene Name	Gene Function	Avg Log_2 Ratio	Fold Change	T-test
YGR037C	ACB1	long-chain fatty acid transporter	-0.2142	-1.2	0.199754
YPL190C	NAB3	poly(A) binding	-0.2138	-1.2	0.324583
YGR248W	SOL4	6-phosphogluconolactonase	-0.2112	-1.2	0.174259
YNL160W	YGP1	unknown	-0.2105	-1.2	0.313319
YDL086W		carboxymethylenebutenolidase	-0.2093	-1.2	0.253101
YKR094C	RPL40B	structural constituent of ribosome*	-0.2093	-1.2	0.393069
YDR201W	SPC19	structural constituent of cytoskeleton	-0.2073	-1.2	0.18729
YGR250C		RNA binding	-0.2070	-1.2	0.229686
YDL184C	RPL41A	structural constituent of ribosome	-0.2065	-1.2	0.17499
YLR055C	SPT8	transcription cofactor	-0.2043	-1.2	0.0635119
YBR280C		unknown	-0.2040	-1.2	0.0055926
YLR216C	CPR6	unfolded protein binding*	-0.2037	-1.2	0.0513457
YIL142W	CCT2	unfolded protein binding	-0.1995	-1.1	0.0212486
YER080W	FMP29	unknown	-0.1988	-1.1	0.106618
YHR157W	REC104	unknown	-0.1977	-1.1	0.254376
YMR196W		unknown	-0.1958	-1.1	0.469018
YIL156W	UBP7	ubiquitin-specific protease	-0.1892	-1.1	0.0608192
YBR269C	FMP21	unknown	-0.1882	-1.1	0.279132
YCL017C	NFS1	cystathionine gamma-lyase *	-0.1870	-1.1	0.269647
YBR100W			-0.1850	-1.1	0.0206199
YBR100W			-0.1850	-1.1	0.0206199
YDR310C	SUM1	transcriptional repressor	-0.1800	-1.1	0.959801
YJL160C		unknown	-0.1782	-1.1	0.0723843
YBR125C	PTC4	protein phosphatase type 2C	-0.1777	-1.1	0.63724
YDR427W	RPN9	structural molecule	-0.1762	-1.1	0.517973
YPL085W	SEC16	structural molecule	-0.1757	-1.1	0.553842
YPL105C		unknown	-0.1722	-1.1	0.438361
YKL171W		protein kinase	-0.1705	-1.1	0.47087
YFR031C-A	RPL2A	structural constituent of ribosome	-0.1687	-1.1	0.0372032
YOR375C	GDH1	glutamate dehydrogenase	-0.1675	-1.1	0.11877
YCL019W			-0.1650	-1.1	0.0460387
YIL050W	PCL7	cyclin-dependent protein kinase	-0.1650	-1.1	0.444316
YPR033C	HTS1	histidine-tRNA ligase	-0.1650	-1.1	0.0420972
YOR185C	GSP2	GTPase	-0.1632	-1.1	0.215822
YCR082W	AHC2	unknown	-0.1618	-1.1	0.103037
YOR372C	NDD1	transcriptional activator	-0.1615	-1.1	0.0196284
YJL210W	PEX2	protein binding	-0.1607	-1.1	0.378566
YPL240C	HSP82	ATPase , coupled	-0.1603	-1.1	0.0459967
YBR009C	HHF1	DNA binding	-0.1588	-1.1	0.341646
YBR069C	TAT1	amino acid transporter	-0.1557	-1.1	0.599037
YNL134C		alcohol dehydrogenase	-0.1557	-1.1	0.762409
YDR088C	SLU7	RNA splicing factor	-0.1552	-1.1	0.143022
YDR180W	SCC2	unknown	-0.1528	-1.1	0.0995337
YIL075C	RPN2	endopeptidase *	-0.1495	-1.1	0.249126
YJL101C	GSH1	glutamate-cysteine ligase	-0.1427	-1.1	0.0886188
YCL027W	FUS1	unknown	-0.1405	-1.1	0.155886
YIL162W	SUC2	beta-fructofuranosidase	-0.1400	-1.1	0.544858
YHR186C	KOG1	unknown	-0.1350	-1.1	0.764435
YJL123C		unknown	-0.1345	-1.1	0.965833
YBR150C	TBS1	unknown	-0.1332	-1.1	0.315707
YLR256W	HAP1	specific RNA polymerase II transcription factor	-0.1332	-1.1	0.544145
YAL030W	SNC1	v-SNARE	-0.1295	-1.1	0.718942
YAL011W	SWC3	unknown	-0.1288	-1.1	0.16215
YAL035W	FUN12	GTPase *	-0.1283	-1.1	0.0259497
YJL020C	BBC1	myosin I binding	-0.1268	-1.1	0.552426
YLR158C	ASP3-3	asparaginase	-0.1257	-1.1	0.245713
YOR123C	LEO1	RNA polymerase II transcription elongation factor	-0.1247	-1.1	0.857463
YJR015W		unknown	-0.1240	-1.1	0.742664
YKR048C	NAP1	protein binding	-0.1240	-1.1	0.146526
YCR021C	HSP30	unknown	-0.1225	-1.1	0.445803
YCRX21C			-0.1225	-1.1	0.196101
YJR105W	ADO1	adenosine kinase	-0.1222	-1.1	0.887085
YGL148W	ARO2	chorismate synthase *	-0.1215	-1.1	0.580228
YFR033C	QCR6	ubiquinol-cytochrome-c reductase	-0.1203	-1.1	0.352352
YBR289W	SNF5	general RNA polymerase II transcription factor	-0.1192	-1.1	0.71639
YFL066C		unknown	-0.1167	-1.1	0.983209
YJL021C			-0.1165	-1.1	0.19242
YAL042W	ERV46	unknown	-0.1153	-1.1	0.0072213
YNL030W	HHF2	DNA binding	-0.1147	-1.1	0.213936

Table 2: continued.

ORF ID	Gene Name	Gene Function	Avg Log_2 Ratio	Fold Change	T-test
YEL047C		fumarate reductase (NADH)	-0.1133	-1.1	0.038208
YHR217C			-0.1130	-1.1	0.245118
YIL154C	IMP2'	transcription coactivator	-0.1125	-1.1	0.623778
YBR255W		unknown	-0.1123	-1.1	0.673023
YKL150W	MCR1	cytochrome-b5 reductase	-0.1112	-1.1	0.191252
YBR159W	IFA38	ketoreductase	-0.1103	-1.1	0.432728
YCRX13W			-0.1093	-1.1	0.187926
YAL029C	MYO4	microfilament motor	-0.1092	-1.1	0.716549
YHR158C	KEL1	unknown	-0.1073	-1.1	0.638851
YCR046C	IMG1	structural constituent of ribosome	-0.1068	-1.1	0.872004
YPR002W	PDH1	unknown	-0.1068	-1.1	0.640189
YHR179W	OYE2	NADPH dehydrogenase	-0.1057	-1.1	0.521314
YLR204W	QRI5	unknown	-0.1052	-1.1	0.798823
YGR256W	GND2	phosphogluconate dehydrogenase	-0.1048	-1.1	0.700165
YLR247C		helicase	-0.1032	-1.1	0.156079
YBR008C	FLR1	multidrug transporter	-0.1005	-1.1	0.133196
YAL016W	TPD3	protein phosphatase type 2A	-0.0998	-1.1	0.779859
YOL039W	RPP2A	structural constituent of ribosome	-0.0957	-1.1	0.440778
YIL005W	EPS1	protein disulfide isomerase	-0.0917	-1.1	0.688447
YBR156C	SLI15	protein kinase	-0.0892	-1.1	0.639801
YBR143C	SUP45	translation release factor	-0.0885	-1.1	0.202823
YBR205W	KTR3	mannosyltransferase	-0.0882	-1.1	0.0554639
YJL130C	URA2	carbamoyl-phosphate synthase (glutamine-hydrolyzing) *	-0.0873	-1.1	0.830579
YBR245C	ISW1	ATPase	-0.0872	-1.1	0.621223
YDR059C	UBC5	ubiquitin conjugating enzyme	-0.0848	-1.1	0.837788
YER043C	SAH1	adenosylhomocysteinase	-0.0847	-1.1	0.0318519
YMR020W	FMS1	amine oxidase	-0.0835	-1.1	0.767023
YJL070C		unknown	-0.0822	-1.1	0.37809
YNL031C	HHT2	DNA binding	-0.0813	-1.1	0.807911
YDR154C			-0.0808	-1.1	0.346086
YKL056C	TMA19	unknown	-0.0778	-1.1	0.569459
YBR126C	TPS1	alpha,alpha-trehalose-phosphate synthase (UDP-forming)	-0.0747	-1.1	0.090745
YOR327C	SNC2	v-SNARE	-0.0732	-1.1	0.79496
YDL140C	RPO21	DNA-directed RNA polymerase	-0.0720	-1.1	0.620539
YBR239C		unknown	-0.0710	-1.1	0.222801
YMR226C	TMA29	oxidoreductase , acting on the aldehyde or oxo group of donors, N	-0.0660	-1.0	0.390916
YPL234C	TFP3	hydrogen-transporting ATPase , rotational mechanism	-0.0632	-1.0	0.998273
YKR002W	PAP1	polynucleotide adenylyltransferase	-0.0617	-1.0	0.78612
YAR042W	SWH1	phosphatidylinositol binding	-0.0597	-1.0	0.881636
YBR109C	CMD1	protein binding*	-0.0592	-1.0	0.422345
YGL221C	NIF3	unknown	-0.0588	-1.0	0.952809
YDL220C	CDC13	single-stranded DNA binding	-0.0587	-1.0	0.888505
YML100W	TSL1	enzyme regulator *	-0.0580	-1.0	0.994651
YLR299W	ECM38	protein-glutamine gamma-glutamyltransferase	-0.0572	-1.0	0.768608
YOR291W		unknown	-0.0560	-1.0	0.802987
YBR071W		unknown	-0.0558	-1.0	0.901496
YML010W	SPT5	RNA polymerase II transcription elongation factor	-0.0553	-1.0	0.671085
YLR436C	ECM30	unknown	-0.0535	-1.0	0.623946
YJL221C	FSP2	alpha-glucosidase	-0.0518	-1.0	0.656974
YEL053C	MAK10	peptide alpha-N-acetyltransferase	-0.0510	-1.0	0.867231
YOR120W	GCY1	aldo-keto reductase	-0.0508	-1.0	0.56991
YJL142C			-0.0502	-1.0	0.336986
YMR212C	EFR3	unknown	-0.0467	-1.0	0.976364
YBR137W		unknown	-0.0465	-1.0	0.824171
YJR007W	SUI2	translation initiation factor	-0.0430	-1.0	0.256203
YKR071C	DRE2	unknown	-0.0408	-1.0	0.555714
YBR079C	RPG1	translation initiation factor	-0.0375	-1.0	0.91121
YJL149W		unknown	-0.0372	-1.0	0.925782
YLR350W	ORM2	unknown	-0.0368	-1.0	0.758815
YER068W	MOT2	3'-5'-exoribonuclease *	-0.0365	-1.0	0.678687
YCL034W	LSB5	unknown	-0.0358	-1.0	0.439616
YKL142W	MRP8	structural constituent of ribosome	-0.0358	-1.0	0.342182
YBR132C	AGP2	amino acid transporter	-0.0352	-1.0	0.778329
YNL305C		unknown	-0.0343	-1.0	0.635317
YJL115W	ASF1	transcription regulator *	-0.0332	-1.0	0.467758
YDR513W	GRX2	thiol-disulfide exchange intermediate *	-0.0328	-1.0	0.74735
YLR249W	YEF3	translation elongation factor	-0.0323	-1.0	0.538453
YPR149W	NCE102	unknown	-0.0317	-1.0	0.409441
YDR091C	RLI1	ATPase *	-0.0305	-1.0	0.993499

Table 2: continued.

ORF ID	Gene Name	Gene Function	Avg Log_2 Ratio	Fold Change	T-test
YJL016W		unknown	-0.0302	-1.0	0.631493
YER026C	CHO1	CDP-diacylglycerol-serine O-phosphatidyltransferase	-0.0283	-1.0	0.966644
YLR270W	DCS1	hydrolase , acting on acid anhydrides, in phosphorus-containing a	-0.0278	-1.0	0.793073
YJR104C	SOD1	copper, zinc superoxide dismutase	-0.0265	-1.0	0.82633
YAR014C	BUD14	protein phosphatase type 1 regulator	-0.0257	-1.0	0.477668
YMR105C	PGM2	phosphoglucomutase	-0.0252	-1.0	0.870963
YDR250C			-0.0243	-1.0	0.092452
YER072W	VTC1	unknown	-0.0237	-1.0	0.626125
YBL041W	PRE7	endopeptidase	-0.0205	-1.0	0.566421
YHR131C		unknown	-0.0200	-1.0	0.536315
YPR080W	TEF1	translation elongation factor	-0.0187	-1.0	0.769361
YDL005C	MED2	RNA polymerase II transcription mediator	-0.0137	-1.0	0.595136
YFR016C		unknown	-0.0123	-1.0	0.695092
YOL129W	VPS68	unknown	-0.0110	-1.0	0.104815
YOR285W		unknown	-0.0088	-1.0	0.945477
YOR108W	LEU9	2-isopropylmalate synthase	-0.0082	-1.0	0.939298
YNL016W	PUB1	mRNA binding*	-0.0078	-1.0	0.924079
YBR177C	EHT1	serine hydrolase	-0.0075	-1.0	0.93439
YDR483W	KRE2	alpha-1,2-mannosyltransferase	-0.0073	-1.0	0.191345
YLR157C	ASP3-2	asparaginase	-0.0073	-1.0	0.869328
YHR096C	HXT5	glucose transporter	-0.0048	-1.0	0.671767
YCR042C	TAF2	general RNA polymerase II transcription factor	-0.0043	-1.0	0.774726
YJL140W	RPB4	DNA-directed RNA polymerase	-0.0043	-1.0	0.323239
YJL095W	BCK1	MAP kinase	-0.0042	-1.0	0.792483
YHR190W	ERG9	farnesyl-diphosphate farnesyltransferase	-0.0038	-1.0	0.71858
YBR090C		unknown	-0.0030	-1.0	0.547006
YBL097W	BRN1	unknown	-0.0027	-1.0	0.649356
YBR206W			-0.0020	-1.0	0.0744164
YDR520C		unknown	-0.0007	-1.0	0.826762
YGL243W	TAD1	tRNA specific adenosine deaminase	-0.0007	-1.0	0.31548
YJL156C	SSY5	amino acid binding	0.0030	1.0	0.773274
YBR115C	LYS2	L-aminoadipate-semialdehyde dehydrogenase	0.0032	1.0	0.469014
YDL099W	BUG1	unknown	0.0040	1.0	0.330018
YPR062W	FCY1	cytosine deaminase	0.0068	1.0	0.808286
YPL274W	SAM3	S-adenosylmethionine transporter	0.0070	1.0	0.866622
YDL095W	PMT1	dolichyl-phosphate-mannose-protein mannosyltransferase	0.0077	1.0	0.868196
YDL174C	DLD1	D-lactate dehydrogenase	0.0087	1.0	0.0028314
YPL222W	FMP40	unknown	0.0090	1.0	0.873304
YLR246W	ERF2	protein-cysteine S-palmitoleyltransferase	0.0093	1.0	0.0984154
YDR054C	CDC34	ubiquitin conjugating enzyme	0.0095	1.0	0.334444
YOR053W			0.0097	1.0	0.491963
YJL092W	HPR5	DNA helicase	0.0113	1.0	0.34034
YLR160C	ASP3-4	asparaginase	0.0127	1.0	0.947893
YML074C	FPR3	peptidyl-prolyl cis-trans isomerase	0.0148	1.0	0.405274
YDR316W-B			0.0150	1.0	0.862321
YAL039C	CYC3	holocytochrome-c synthase	0.0157	1.0	0.657798
YBR262C	FMP51	unknown	0.0173	1.0	0.881224
YDL131W	LYS21	homocitrate synthase	0.0180	1.0	0.902757
YBR118W	TEF2	translation elongation factor	0.0188	1.0	0.68477
YBR236C	ABD1	mRNA (guanine-N7-)-methyltransferase	0.0208	1.0	0.942208
YBL081W		unknown	0.0223	1.0	0.369428
YLR155C	ASP3-1	asparaginase	0.0232	1.0	0.0389851
YBR240C	THI2	transcriptional activator	0.0237	1.0	0.818587
YPL265W	DIP5	amino acid transporter	0.0243	1.0	0.354954
YHR009C		unknown	0.0268	1.0	0.383037
YCR044C	PER1	unknown	0.0277	1.0	0.745013
YLR381W	CTF3	protein binding	0.0305	1.0	0.392949
YMR302C	YME2	exonuclease	0.0323	1.0	0.0942745
YCRX17W			0.0360	1.0	0.883746
YBR251W	MRPS5	structural constituent of ribosome	0.0368	1.0	0.733327
YJL225C		helicase	0.0387	1.0	0.412489
YFL016C	MDJ1	unfolded protein binding*	0.0388	1.0	0.812296
YBR237W	PRP5	RNA splicing factor	0.0393	1.0	0.788099
YCR053W	THR4	threonine synthase	0.0413	1.0	0.841583
YDR473C	PRP3	RNA splicing factor	0.0430	1.0	0.985185
YBR070C	ALG14	N-acetylglucosaminyldiphosphodolichol N-acetylglucosaminyltra	0.0438	1.0	0.90828
YFL008W	SMC1	ATPase *	0.0465	1.0	0.586551
YCL041C			0.0488	1.0	0.797544
YDL124W		alpha-keto amide reductase *	0.0505	1.0	0.971075

Table 2: continued.

ORF ID	Gene Name	Gene Function	Avg Log_2 Ratio	Fold Change	T-test
YDL161W	ENT1	clathrin binding	0.0505	1.0	0.759655
YJR002W	MPP10	unknown	0.0507	1.0	0.353355
YOR304W	ISW2	ATPase	0.0507	1.0	0.806684
YBR250W		unknown	0.0523	1.0	0.453664
YBR119W	MUD1	RNA binding	0.0525	1.0	0.770962
YGL227W	VID30	unknown	0.0533	1.0	0.897366
YDR208W	MSS4	1-phosphatidylinositol-4-phosphate 5-kinase	0.0545	1.0	0.0877582
YKR042W	UTH1	unknown	0.0547	1.0	0.7362
YBR011C	IPP1	inorganic diphosphatase	0.0553	1.0	0.542188
YCR032W	BPH1	unknown	0.0567	1.0	0.978016
YBR208C	DUR1,2	allophanate hydrolase *	0.0568	1.0	0.786421
YCL003W			0.0573	1.0	0.675468
YLR178C	TFS1	lipid binding*	0.0573	1.0	0.924812
YEL027W	CUP5	hydrogen ion transporter	0.0600	1.0	0.935443
YFR008W	FAR7	unknown	0.0600	1.0	0.0528463
YJL174W	KRE9	unknown	0.0608	1.0	0.625319
YDL186W		unknown	0.0615	1.0	0.819761
YOR113W	AZF1	DNA binding*	0.0628	1.0	0.0594089
YGR155W	CYS4	cystathionine beta-synthase	0.0638	1.0	0.710362
YBR024W	SCO2	thioredoxin peroxidase	0.0640	1.0	0.4598
YNL102W	POL1	alpha DNA polymerase	0.0670	1.0	0.552319
YDR309C	GIC2	small GTPase regulator	0.0710	1.1	0.957103
YOR182C	RPS30B	structural constituent of ribosome	0.0718	1.1	0.957406
YJL138C	TIF2	translation initiation factor	0.0723	1.1	0.330517
YIL121W	QDR2	multidrug efflux pump	0.0738	1.1	0.904926
YDR433W			0.0745	1.1	0.627933
YDR145W	TAF12	general RNA polymerase II transcription factor	0.0760	1.1	0.094814
YKL107W		unknown	0.0762	1.1	0.882871
YER073W	ALD5	3-chloroallyl aldehyde dehydrogenase	0.0773	1.1	0.113367
YBR212W	NGR1	RNA binding*	0.0775	1.1	0.607473
YFL058W	THI5	unknown	0.0797	1.1	0.589852
YKL212W	SAC1	inositol or phosphatidylinositol phosphatase	0.0800	1.1	0.714299
YLR300W	EXG1	glucan 1,3-beta-glucosidase	0.0808	1.1	0.109759
YJL209W	CBP1	mRNA binding	0.0820	1.1	0.479526
YEL020C		unknown	0.0845	1.1	0.363063
YDL106C	PHO2	transcription factor	0.0858	1.1	0.687536
YPL206C		glycerophosphodiester phosphodiesterase	0.0870	1.1	0.490154
YIL036W	CST6	specific RNA polymerase II transcription factor	0.0873	1.1	0.704021
YDR330W	UBX5	unknown	0.0885	1.1	0.0172307
YKR090W	PXL1	protein binding	0.0932	1.1	0.283644
YER035W	EDC2	RNA binding	0.0955	1.1	0.247111
YKR059W	TIF1	translation initiation factor	0.0980	1.1	0.681532
YML058W	SML1	enzyme inhibitor	0.0997	1.1	0.108866
YDR127W	ARO1	3-dehydroquinate dehydratase *	0.0998	1.1	0.0940223
YGL237C	HAP2	transcriptional activator	0.1000	1.1	0.316126
YGR189C	CRH1	unknown	0.1027	1.1	0.302257
YBR224W			0.1055	1.1	0.594227
YJL129C	TRK1	potassium ion transporter	0.1063	1.1	0.645302
YLR264W	RPS28B	structural constituent of ribosome	0.1073	1.1	0.673035
YDR200C	VPS64	unknown	0.1077	1.1	0.749164
YIL026C	IRR1	protein binding	0.1102	1.1	0.57524
YPL260W		unknown	0.1113	1.1	0.347296
YNL023C	FAP1	transcription factor	0.1117	1.1	0.828141
YJL164C	TPK1	protein serine/threonine kinase	0.1120	1.1	0.0311745
YGR118W	RPS23A	structural constituent of ribosome	0.1140	1.1	0.731682
YER019C-A	SBH2	protein transporter	0.1143	1.1	0.28505
YLR325C	RPL38	structural constituent of ribosome	0.1153	1.1	0.562779
YBR261C		S-adenosylmethionine-dependent methyltransferase	0.1172	1.1	0.609125
YNL161W	CBK1	protein kinase	0.1173	1.1	0.0073165
YCR080W			0.1177	1.1	0.0556888
YFL059W	SNZ3	protein binding	0.1183	1.1	0.499157
YGR038C-A			0.1188	1.1	0.297821
YJR127C	RSF2	transcription factor	0.1207	1.1	0.341464
YAL019W	FUN30	unknown	0.1227	1.1	0.752596
YOL109W	ZEO1	unknown	0.1242	1.1	0.174605
YBR275C	RIF1	protein binding*	0.1250	1.1	0.67596
YDL081C	RPP1A	structural constituent of ribosome	0.1252	1.1	0.52939
YDR510W	SMT3	protein tag	0.1260	1.1	0.123016
YLR238W	FAR10	unknown	0.1260	1.1	0.166042

Table 2: continued.

ORF ID	Gene Name	Gene Function	Avg Log_2 Ratio	Fold Change	T-test
YEL044W	IES6	unknown	0.1262	1.1	0.277265
YER160C			0.1272	1.1	0.0450691
YML045W			0.1285	1.1	0.861791
YDR487C	RIB3	3,4-dihydroxy-2-butanone-4-phosphate synthase	0.1288	1.1	0.588451
YLR410W-B			0.1313	1.1	0.346615
YBR140C	IRA1	Ras GTPase activator	0.1333	1.1	0.633536
YBR260C	RGD1	Rho GTPase activator	0.1343	1.1	0.203981
YLR206W	ENT2	clathrin binding	0.1352	1.1	0.096404
YHR039BC			0.1375	1.1	0.433079
YJR066W	TOR1	protein binding*	0.1378	1.1	0.797059
YBR259W		unknown	0.1392	1.1	0.290645
YDR514C		unknown	0.1393	1.1	0.449497
YLR454W	FMP27	unknown	0.1403	1.1	0.428059
YBR081C	SPT7	structural molecule	0.1405	1.1	0.963621
YPL106C	SSE1	ATP binding*	0.1432	1.1	0.761594
YBR169C	SSE2	unknown	0.1447	1.1	0.18804
YJL111W	CCT7	unfolded protein binding	0.1478	1.1	0.294965
YFL021C-A			0.1488	1.1	0.60639
YOR321W	PMT3	dolichyl-phosphate-mannose-protein mannosyltransferase	0.1488	1.1	0.3494
YIL130W	ASG1	unknown	0.1490	1.1	0.341437
YPL111W	CAR1	zinc ion binding*	0.1503	1.1	0.0667393
YBR135W	CKS1	protein kinase	0.1523	1.1	0.347538
YBR204C		serine hydrolase	0.1523	1.1	0.435179
YPR023C	EAF3	histone acetyltransferase	0.1530	1.1	0.0414963
YAL017W	PSK1	protein serine/threonine kinase	0.1537	1.1	0.0515194
YIL047C	SYG1	unknown	0.1545	1.1	0.532192
YHR178W	STB5	transcription factor	0.1547	1.1	0.6834
YER109C	FLO8	specific RNA polymerase II transcription factor	0.1550	1.1	0.167306
YBR127C	VMA2	hydrogen-transporting ATPase , rotational mechanism	0.1568	1.1	0.0394191
YDL156W		unknown	0.1568	1.1	0.338632
YBR142W	MAK5	ATP-dependent RNA helicase	0.1572	1.1	0.129344
YDL097C	RPN6	structural molecule	0.1575	1.1	0.0220909
YIL105C	SLM1	phosphoinositide binding	0.1600	1.1	0.0047103
YMR168C	CEP3	DNA bending *	0.1618	1.1	0.127399
YLR301W		unknown	0.1620	1.1	0.895445
YMR241W	YHM2	DNA binding*	0.1632	1.1	0.124467
YNL126W	SPC98	structural constituent of cytoskeleton	0.1662	1.1	0.548123
YBR238C		unknown	0.1673	1.1	0.30045
YLR093C	NYV1	v-SNARE	0.1675	1.1	0.910825
YIL090W	ICE2	unknown	0.1680	1.1	0.181399
YIL104C	SHQ1	unknown	0.1692	1.1	0.770929
YOR128C	ADE2	phosphoribosylaminoimidazole carboxylase	0.1695	1.1	0.712344
YDR324C	UTP4	snoRNA binding	0.1712	1.1	0.116058
YMR046C			0.1725	1.1	0.642339
YOR315W	SFG1	specific RNA polymerase II transcription factor	0.1770	1.1	0.389039
YCR047C	BUD23	S-adenosylmethionine-dependent methyltransferase	0.1808	1.1	0.196023
YGL151W	NUT1	unknown	0.1818	1.1	0.894705
YNL099C	OCA1	protein tyrosine phosphatase	0.1842	1.1	0.315649
YCR025C			0.1855	1.1	0.517081
YAL054C	ACS1	acetate-CoA ligase	0.1862	1.1	0.262764
YBR157C	ICS2	unknown	0.1865	1.1	0.603056
YER117W	RPL23B	structural constituent of ribosome	0.1885	1.1	0.350012
YMR273C	ZDS1	protein binding	0.1887	1.1	0.423295
YBR227C	MCX1	unfolded protein binding*	0.1888	1.1	0.0966638
YHR135C	YCK1	casein kinase	0.1888	1.1	0.0757577
YMR016C	SOK2	transcription factor	0.1902	1.1	0.021014
YAL002W	VPS8	unknown	0.1927	1.1	0.0104272
YAL002W	VPS8	unknown	0.1927	1.1	0.0104272
YLR327C	TMA10	unknown	0.1930	1.1	0.0147312
YFR050C	PRE4	endopeptidase	0.1942	1.1	0.217265
YBL101W-A			0.1950	1.1	0.652759
YPR132W	RPS23B	structural constituent of ribosome	0.1950	1.1	0.230334
YKR066C	CCP1	cytochrome-c peroxidase	0.1967	1.1	0.432107
YJR113C	RSM7	structural constituent of ribosome	0.1968	1.1	0.0219174
YJR113C	RSM7	structural constituent of ribosome	0.1968	1.1	0.0219174
YMR002W		unknown	0.1982	1.1	0.180848
YBR286W	APE3	aminopeptidase	0.2000	1.1	0.0138792
YDR516C	EMI2	unknown	0.2002	1.1	0.215576
YGR014W	MSB2	osmosensor	0.2022	1.2	0.411294

Table 2: continued.

ORF ID	Gene Name	Gene Function	Avg Log_2 Ratio	Fold Change	T-test
YBR181C	RPS6B	structural constituent of ribosome	0.2027	1.2	0.330238
YOR167C	RPS28A	structural constituent of ribosome	0.2050	1.2	0.635452
YBR136W	MEC1	protein kinase	0.2052	1.2	0.601221
YJR059W	PTK2	protein kinase	0.2053	1.2	0.271615
YMR230W	RPS10B	structural constituent of ribosome	0.2070	1.2	0.273742
YML040W			0.2088	1.2	0.156966
YIL107C	PFK26	6-phosphofructo-2-kinase	0.2090	1.2	0.0389223
YLR227W-A			0.2092	1.2	0.691964
YDL084W	SUB2	protein binding*	0.2107	1.2	0.258949
YDR179W-A		unknown	0.2118	1.2	0.0062116
YDR179W-A		unknown	0.2118	1.2	0.0062116
YGL126W	SCS3	unknown	0.2155	1.2	0.563394
YJL064W			0.2158	1.2	0.0972282
YMR250W	GAD1	glutamate decarboxylase	0.2198	1.2	0.399388
YCLX06C			0.2237	1.2	0.153075
YBR134W			0.2242	1.2	0.81739
YCL002C		unknown	0.2247	1.2	0.0888468
YIL112W	HOS4	NAD-dependent histone deacetylase *	0.2270	1.2	0.722533
YOR317W	FAA1	long-chain-fatty-acid-CoA ligase	0.2278	1.2	0.0493882
YJL176C	SWI3	general RNA polymerase II transcription factor	0.2287	1.2	0.141799
YLR027C	AAT2	aspartate transaminase	0.2317	1.2	0.0294767
YBR207W	FTH1	iron ion transporter	0.2327	1.2	0.0993296
YBR120C	CBP6	unknown	0.2333	1.2	0.0739784
YDR244W	PEX5	peroxisome targeting sequence binding*	0.2360	1.2	0.149682
YAR003W	SWD1	histone lysine N-methyltransferase (H3-K4 specific)	0.2365	1.2	0.15794
YAR010C			0.2373	1.2	0.479165
YAR028W		unknown	0.2397	1.2	0.254112
YNR002C	ATO2	ammonium transporter	0.2435	1.2	0.316446
YCR036W	RBK1	ATP binding*	0.2453	1.2	0.174654
YLL010C	PSR1	phosphoprotein phosphatase	0.2460	1.2	0.149773
YJL204C	RCY1	protein binding	0.2462	1.2	0.414138
YEL012W	UBC8	ubiquitin conjugating enzyme	0.2495	1.2	0.202459
YBR230C	OM14	unknown	0.2497	1.2	0.111798
YMR096W	SNZ1	protein binding	0.2518	1.2	0.5897
YLR048W	RPS0B	structural constituent of ribosome	0.2535	1.2	0.109574
YOL011W	PLB3	lysophospholipase	0.2535	1.2	0.287428
YDL125C	HNT1	hydrolase *	0.2558	1.2	0.135089
YLR109W	AHP1	thioredoxin peroxidase	0.2577	1.2	0.253213
YMR110C	HFD1	3-chloroallyl aldehyde dehydrogenase	0.2580	1.2	0.444213
YGR027C	RPS25A	structural constituent of ribosome	0.2583	1.2	0.219048
YDR083W	RRP8	methyltransferase	0.2587	1.2	0.0396527
YDR083W	RRP8	methyltransferase	0.2587	1.2	0.0396527
YLR104W		unknown	0.2593	1.2	0.0771835
YIL045W	PIG2	protein phosphatase type 1 regulator	0.2612	1.2	0.377468
YOL106W			0.2628	1.2	0.168994
YIR016W		unknown	0.2632	1.2	0.450964
YAL014C	SYN8	SNAP receptor	0.2658	1.2	0.382028
YIL046W	MET30	protein binding	0.2665	1.2	0.0675293
YCL014W	BUD3	unknown	0.2708	1.2	0.376391
YDL190C	UFD2	ubiquitin conjugating enzyme	0.2722	1.2	0.215452
YLR293C	GSP1	GTPase	0.2725	1.2	0.245176
YHR154W	RTT107	unknown	0.2728	1.2	0.224814
YAL021C	CCR4	3'-5'-exoribonuclease	0.2735	1.2	0.133492
YER014W	HEM14	protoporphyrinogen oxidase	0.2743	1.2	0.0020775
YLR185W	RPL37A	structural constituent of ribosome	0.2750	1.2	0.0170647
YIL077C		unknown	0.2767	1.2	0.15259
YBR086C	IST2	unknown	0.2770	1.2	0.10021
YAL048C	GEM1	GTPase	0.2782	1.2	0.0444376
YPL090C	RPS6A	structural constituent of ribosome	0.2783	1.2	0.0693926
YCR062W			0.2785	1.2	0.051378
YMR070W	MOT3	DNA binding*	0.2793	1.2	0.341216
YDR210C-D			0.2807	1.2	0.0832661
YKL172W	EBP2	unknown	0.2808	1.2	0.220731
YBR012W-A			0.2832	1.2	0.0769723
YLR410W	VIP1	unknown	0.2852	1.2	0.27802
YIL118W	RHO3	GTPase *	0.2860	1.2	0.0241781
YIL043C	CBR1	cytochrome-b5 reductase	0.2865	1.2	0.105024
YLR340W	RPP0	structural constituent of ribosome	0.2867	1.2	0.0219009
YGL031C	RPL24A	structural constituent of ribosome*	0.2887	1.2	0.186987

Table 2: continued.

ORF ID	Gene Name	Gene Function	Avg Log_2 Ratio	Fold Change	T-test
YJR028W			0.2888	1.2	0.284732
Q0060	AI3	endonuclease	0.2902	1.2	0.0322297
YPR065W	ROX1	specific transcriptional repressor *	0.2902	1.2	0.240371
YGR148C	RPL24B	structural constituent of ribosome*	0.2907	1.2	0.0228892
YOL053C-A			0.2907	1.2	0.001846
YFL-TYB			0.2913	1.2	0.0545275
YIR023W	DAL81	specific RNA polymerase II transcription factor	0.2913	1.2	0.0761399
YNL042W	BOP3	unknown	0.2917	1.2	0.0396361
YOR043W	WHI2	phosphatase activator	0.2917	1.2	0.107319
YOL098C		metalloendopeptidase	0.2920	1.2	0.023922
YBL005W-A			0.2927	1.2	0.0987231
YBR214W	SDS24	unknown	0.2937	1.2	0.0616586
YBR200W	BEM1	protein binding	0.2948	1.2	0.128751
YBR112C	CYC8	transcription coactivator *	0.2985	1.2	0.164839
YBR256C	RIB5	riboflavin synthase	0.2993	1.2	0.134346
YER131W	RPS26B	structural constituent of ribosome	0.3003	1.2	0.0131872
YHR203C	RPS4B	structural constituent of ribosome	0.3007	1.2	0.0361563
YBR198C	TAF5	general RNA polymerase II transcription factor	0.3050	1.2	0.0776355
YHR089C	GAR1	RNA binding	0.3062	1.2	0.148651
YPL220W	RPL1A	structural constituent of ribosome	0.3073	1.2	0.112991
YGL150C	INO80	ATPase *	0.3080	1.2	0.0468705
YGL150C	INO80	ATPase *	0.3080	1.2	0.0468705
YDR533C	HSP31	unfolded protein binding*	0.3095	1.2	0.0030393
YCR107W	AAD3	aryl-alcohol dehydrogenase	0.3100	1.2	0.160967
YDR035W	ARO3	3-deoxy-7-phosphoheptulonate synthase	0.3110	1.2	0.0920598
YPL095C	EEB1	unknown	0.3110	1.2	0.491436
YLR177W		unknown	0.3137	1.2	0.611505
YGL197W	MDS3	unknown	0.3150	1.2	0.435973
YMR124W		unknown	0.3170	1.2	0.0685866
YBR213W	MET8	ferrochelatase *	0.3187	1.2	0.145926
YAL060W	BDH1	(R,R)-butanediol dehydrogenase	0.3200	1.2	0.157399
YOR293W	RPS10A	structural constituent of ribosome	0.3218	1.2	0.300713
YGL128C	CWC23	unknown	0.3223	1.3	0.0229767
YMR051C			0.3235	1.3	0.217876
YNL162W	RPL42A	structural constituent of ribosome	0.3235	1.3	0.505042
YBR129C	OPY1	unknown	0.3237	1.3	0.0533527
YBL072C	RPS8A	structural constituent of ribosome	0.3238	1.3	0.0011832
YBL072C	RPS8A	structural constituent of ribosome	0.3238	1.3	0.0011832
YBL101C	ECM21	unknown	0.3250	1.3	0.12519
YBR229C	ROT2	alpha-glucosidase	0.3270	1.3	0.450772
YBR108W		unknown	0.3278	1.3	0.0567532
YNL241C	ZWF1	glucose-6-phosphate 1-dehydrogenase	0.3280	1.3	0.0649378
YDR444W		unknown	0.3292	1.3	0.133095
YBR203W	COS111	unknown	0.3293	1.3	0.116873
YBR295W	PCA1	ATPase , coupled to transmembrane movement of ions, phosphory	0.3323	1.3	0.237237
YKL035W	UGP1	UTP:glucose-1-phosphate uridylyltransferase	0.3323	1.3	0.128612
YBR197C		unknown	0.3328	1.3	0.0120974
YOR359W	VTS1	RNA binding*	0.3328	1.3	0.031499
YCR038C	BUD5	signal transducer *	0.3338	1.3	0.333285
YNL027W	CRZ1	transcription factor	0.3347	1.3	0.0598415
YIL060W		unknown	0.3360	1.3	0.0623404
YMR125W	STO1	mRNA binding	0.3362	1.3	0.0148437
YCL020W			0.3372	1.3	0.273203
Q0140	VAR1	structural constituent of ribosome	0.3377	1.3	0.0330321
YKL180W	RPL17A	structural constituent of ribosome	0.3397	1.3	0.0045244
YKL094W	YJU3	serine hydrolase	0.3408	1.3	0.0042445
YKL094W	YJU3	serine hydrolase	0.3408	1.3	0.0042445
YBR113W			0.3417	1.3	0.0155249
YML113W	DAT1	AT DNA binding	0.3417	1.3	0.0977873
YBR302C	COS2	unknown	0.3418	1.3	0.105539
YGL122C	NAB2	poly(A) binding	0.3423	1.3	0.0495587
YBR089W			0.3485	1.3	0.167728
YOR234C	RPL33B	structural constituent of ribosome	0.3503	1.3	0.317068
YBR222C	PCS60	AMP binding	0.3507	1.3	0.0094451
YGL189C	RPS26A	structural constituent of ribosome	0.3522	1.3	0.0073061
YCR029C			0.3535	1.3	0.0147998
YIL108W		metalloendopeptidase	0.3567	1.3	0.0009852
YIL108W		metalloendopeptidase	0.3567	1.3	0.0009852
YBR128C	ATG14	unknown	0.3583	1.3	0.0955886

Table 2: continued.

ORF ID	Gene Name	Gene Function	Avg Log_2 Ratio	Fold Change	T-test
Q0255		unknown	0.3588	1.3	0.0691292
YEL060C	PRB1	serine-type endopeptidase	0.3597	1.3	0.13995
YAL056W	GPB2	signal transducer	0.3600	1.3	0.239646
YLR333C	RPS25B	structural constituent of ribosome	0.3607	1.3	0.0061303
YOR306C	MCH5	transporter	0.3627	1.3	0.0062809
YLR448W	RPL6B	structural constituent of ribosome*	0.3643	1.3	0.0996407
YOR312C	RPL20B	structural constituent of ribosome	0.3650	1.3	0.445677
YBR049C	REB1	RNA polymerase II transcription factor	0.3665	1.3	0.0020136
YNR052C	POP2	3'-5'-exoribonuclease	0.3668	1.3	0.0132947
YPL060W	LPE10	magnesium ion transporter	0.3678	1.3	0.0132464
YPL060W	LPE10	magnesium ion transporter	0.3678	1.3	0.0132464
YHR214C-B			0.3710	1.3	0.0597427
YDL227C	HO	endonuclease	0.3717	1.3	0.0209921
YOL143C	RIB4	6,7-dimethyl-8-ribityllumazine synthase	0.3738	1.3	0.0426318
YJL076W	NET1	rDNA binding	0.3743	1.3	0.201175
YMR264W	CUE1	protein binding	0.3745	1.3	0.0838317
YKR075C		unknown	0.3748	1.3	0.308079
YLR383W	SMC6	unknown	0.3752	1.3	0.0595504
YJL136C	RPS21B	structural constituent of ribosome	0.3757	1.3	0.0924836
YGR098C	ESP1	cysteine-type endopeptidase	0.3767	1.3	0.522543
YNL180C	RHO5	GTPase	0.3772	1.3	0.0093627
YNL180C	RHO5	GTPase	0.3772	1.3	0.0093627
YIL153W	RRD1	protein phosphatase type 2A regulator	0.3782	1.3	0.0362004
YIL153W	RRD1	protein phosphatase type 2A regulator	0.3782	1.3	0.0362004
YBR075W			0.3797	1.3	0.0320617
YDL046W	NPC2	unknown	0.3798	1.3	0.0016228
YAR019C	CDC15	protein kinase	0.3803	1.3	0.109336
YAR027W	UIP3	unknown	0.3817	1.3	0.0337224
YPL229W		unknown	0.3832	1.3	0.022244
YBR172C	SMY2	unknown	0.3845	1.3	0.0882636
YPL081W	RPS9A	structural constituent of ribosome	0.3850	1.3	0.0892798
YBR166C	TYR1	prephenate dehydrogenase	0.3855	1.3	0.0407031
YHR202W		unknown	0.3862	1.3	0.111643
YJL177W	RPL17B	structural constituent of ribosome	0.3878	1.3	0.0124636
YCR084C	TUP1	general transcriptional repressor	0.3892	1.3	0.0188019
YDR500C	RPL37B	structural constituent of ribosome	0.3898	1.3	0.107413
YML042W	CAT2	carnitine O-acetyltransferase	0.3918	1.3	0.0578596
YBR249C	ARO4	3-deoxy-7-phosphoheptulonate synthase	0.3933	1.3	0.0183409
YEL054C	RPL12A	structural constituent of ribosome	0.3938	1.3	0.403793
YPL238C			0.3992	1.3	0.0006738
YPL238C			0.3992	1.3	0.0006738
YBL027W	RPL19B	structural constituent of ribosome	0.3993	1.3	0.0243631
YCR052W	RSC6	unknown	0.4013	1.3	0.0364
YER088C	DOT6	unknown	0.4020	1.3	0.125387
YBR138C		unknown	0.4030	1.3	0.120619
YDR432W	NPL3	mRNA binding*	0.4045	1.3	0.0421114
YCR039C	MATALPHA2	transcription corepressor	0.4047	1.3	0.0600152
YJL015C			0.4057	1.3	0.0009602
YBR110W	ALG1	beta-1,4-mannosyltransferase	0.4103	1.3	0.0222501
YER074W	RPS24A	structural constituent of ribosome	0.4130	1.3	0.120579
YDL085W	NDE2	NADH dehydrogenase	0.4135	1.3	0.0352389
YHR142W	CHS7	unknown	0.4155	1.3	0.0808834
YJL141C	YAK1	protein kinase	0.4157	1.3	0.100752
YHR152W	SPO12	unknown	0.4168	1.3	0.326566
YNL069C	RPL16B	structural constituent of ribosome*	0.4210	1.3	0.0873251
YPR043W	RPL43A	structural constituent of ribosome	0.4213	1.3	0.0960937
YKL006W	RPL14A	structural constituent of ribosome*	0.4235	1.3	0.12409
YOR377W	ATF1	alcohol O-acetyltransferase	0.4262	1.3	0.133978
YJL165C	HAL5	protein kinase	0.4272	1.3	0.0223582
YER182W	FMP10	unknown	0.4277	1.3	0.0383488
YOL144W	NOP8	unknown	0.4278	1.3	0.0647453
YBL064C	PRX1	thioredoxin peroxidase	0.4280	1.3	0.0402983
YHR149C	SKG6	unknown	0.4280	1.3	0.0062213
YJR086W	STE18	GTPase	0.4285	1.3	0.115272
YCL011C	GBP2	RNA binding*	0.4298	1.3	0.0009988
YLR330W	CHS5	unknown	0.4302	1.3	0.101969
YIR017C	MET28	DNA binding*	0.4327	1.3	0.0513199
YER056C	FCY2	cytosine-purine permease	0.4358	1.4	0.0434912
YLR035C-A			0.4382	1.4	0.013454

Table 2: continued.

ORF ID	Gene Name	Gene Function	Avg Log_2 Ratio	Fold Change	T-test
YBR187W		unknown	0.4395	1.4	0.0110898
YDL222C	FMP45	unknown	0.4407	1.4	0.246699
YIL055C		unknown	0.4428	1.4	0.0382352
YCR096C	HMRA2	unknown	0.4430	1.4	0.0433916
YIR006C	PAN1	protein binding, bridging	0.4467	1.4	0.0071099
YOR173W	DCS2	unknown	0.4503	1.4	0.0080365
YJL139C	YUR1	mannosyltransferase	0.4505	1.4	0.0473155
YHR165C	PRP8	RNA splicing factor	0.4522	1.4	0.0734453
YPL237W	SUI3	translation initiation factor	0.4552	1.4	0.0786988
YHL033C	RPL8A	structural constituent of ribosome	0.4570	1.4	0.199437
YCL042W		unknown	0.4598	1.4	0.289034
YHR145C			0.4600	1.4	0.0079284
YML024W	RPS17A	structural constituent of ribosome	0.4615	1.4	0.0030291
YCL067C	HMLALPHA2	transcription corepressor	0.4633	1.4	0.0076669
YGR019W	UGA1	4-aminobutyrate transaminase	0.4637	1.4	0.0107372
YPL225W		unknown	0.4642	1.4	0.130315
YFL020C	PAU5	unknown	0.4672	1.4	0.0480115
YMR251W-A	HOR7	unknown	0.4703	1.4	0.0005489
YDR002W	YRB1	Ran GTPase binding	0.4705	1.4	0.31041
Q0070	AI5_ALPHA	endonuclease	0.4720	1.4	0.0212955
Q0070	AI5_ALPHA	endonuclease	0.4720	1.4	0.0212955
YPL004C	LSP1	protein kinase	0.4748	1.4	0.009949
YDR072C	IPT1	transferase , transferring phosphorus-containing groups	0.4757	1.4	0.176764
YJR026W			0.4777	1.4	0.165214
YHR134W	WSS1	unknown	0.4810	1.4	0.0067361
YPR102C	RPL11A	structural constituent of ribosome	0.4812	1.4	0.0245074
YDL075W	RPL31A	structural constituent of ribosome	0.4855	1.4	0.0346551
YDL142C	CRD1	cardiolipin synthase	0.4862	1.4	0.0005569
YDL142C	CRD1	cardiolipin synthase	0.4862	1.4	0.0005569
YDL232W	OST4	protein binding, bridging*	0.4865	1.4	0.0183406
YDL088C	ASM4	structural molecule	0.4878	1.4	0.167887
YMR194W	RPL36A	structural constituent of ribosome*	0.4903	1.4	0.0085836
YIR017W-A			0.4927	1.4	0.115578
YBR048W	RPS11B	structural constituent of ribosome	0.4943	1.4	0.0705719
YBR122C	MRPL36	structural constituent of ribosome	0.4948	1.4	0.163655
YBR062C		unknown	0.4957	1.4	0.0397618
YCR031			0.4963	1.4	0.0853844
YCL024W	KCC4	protein kinase	0.4987	1.4	0.0728841
YJL118W		unknown	0.4987	1.4	0.124295
YCR045C		serine-type peptidase	0.5000	1.4	0.169024
YDL191W	RPL35A	structural constituent of ribosome	0.5005	1.4	0.103185
YLR414C		unknown	0.5023	1.4	0.0111992
YNL284C-A			0.5025	1.4	0.0549954
YAR009C			0.5025	1.4	0.0040989
YML063W	RPS1B	structural constituent of ribosome	0.5028	1.4	0.004124
YJL065C	DLS1	unknown	0.5045	1.4	0.0538968
YIR012W	SQT1	unknown	0.5067	1.4	0.100443
YOL127W	RPL25	structural constituent of ribosome*	0.5103	1.4	0.12283
YIL074C	SER33	phosphoglycerate dehydrogenase	0.5158	1.4	0.010749
YOL040C	RPS15	structural constituent of ribosome	0.5160	1.4	0.273104
YDL188C	PPH22	protein phosphatase type 2A	0.5198	1.4	0.0550047
YLR237W	THI7	thiamin transporter	0.5210	1.4	0.0427702
YGL078C	DBP3	ATP-dependent RNA helicase	0.5217	1.4	0.15154
YIL173W	VTH1	signal sequence binding	0.5225	1.4	0.244468
YLR344W	RPL26A	structural constituent of ribosome*	0.5235	1.4	0.0825584
YDL053C	PBP4	unknown	0.5237	1.4	0.0990367
YER102W	RPS8B	structural constituent of ribosome	0.5258	1.4	0.005912
YBR084C-A	RPL19A	structural constituent of ribosome	0.5270	1.4	0.0244341
YML073C	RPL6A	structural constituent of ribosome*	0.5292	1.4	0.0214537
YDR041W	RSM10	structural constituent of ribosome	0.5327	1.4	0.0096728
YDL243C	AAD4	aryl-alcohol dehydrogenase	0.5348	1.4	0.0060642
YDL082W	RPL13A	structural constituent of ribosome	0.5392	1.5	0.256101
YOR052C		unknown	0.5397	1.5	0.137075
YDL136W	RPL35B	structural constituent of ribosome	0.5422	1.5	0.125916
YGR137W			0.5445	1.5	8.151E-05
YNL244C	SUI1	translation initiation factor	0.5460	1.5	0.0053681
YGL135W	RPL1B	structural constituent of ribosome	0.5503	1.5	0.0087886
YER159C	BUR6	transcription corepressor	0.5523	1.5	0.0147145
YDL020C	RPN4	transcriptional activator	0.5535	1.5	0.0598933

Table 2: continued.

ORF ID	Gene Name	Gene Function	Avg Log_2 Ratio	Fold Change	T-test
YCR024C-A	PMP1	enzyme regulator	0.5552	1.5	0.0023886
YDR261C-C			0.5552	1.5	0.0020688
YCR008W	SAT4	protein kinase	0.5563	1.5	0.0170853
YDR210W-A			0.5570	1.5	0.186916
YLR384C	IKI3	RNA polymerase II transcription elongation factor	0.5592	1.5	0.0575922
YDR261W-A			0.5607	1.5	0.0048746
YHR010W	RPL27A	structural constituent of ribosome	0.5617	1.5	0.0254427
YDR447C	RPS17B	structural constituent of ribosome	0.5633	1.5	0.295822
YLR441C	RPS1A	structural constituent of ribosome	0.5658	1.5	0.076886
YHR155W	YSP1	unknown	0.5687	1.5	0.0970743
YBR068C	BAP2	amino acid transporter	0.5702	1.5	0.0664958
YAR031W	PRM9	unknown	0.5723	1.5	0.219092
YLR250W	SSP120	unknown	0.5730	1.5	0.0039065
YJL117W	PHO86	unknown	0.5767	1.5	0.0304931
YOR122C	PFY1	actin monomer binding	0.5872	1.5	0.109343
YPL143W	RPL33A	structural constituent of ribosome	0.5910	1.5	0.0781045
YPL131W	RPL5	structural constituent of ribosome*	0.5928	1.5	0.0278664
YHR141C	RPL42B	structural constituent of ribosome	0.5947	1.5	0.0040292
YHL015W	RPS20	structural constituent of ribosome	0.6025	1.5	0.0375388
YEL046C	GLY1	threonine aldolase	0.6060	1.5	0.0162237
YER064C		unknown	0.6093	1.5	0.114616
YIL069C	RPS24B	structural constituent of ribosome	0.6097	1.5	0.0138118
YDR074W	TPS2	trehalose-phosphatase	0.6127	1.5	0.10452
YHR097C		unknown	0.6127	1.5	0.0033287
YDR365W-A			0.6128	1.5	0.0082528
YBR154C	RPB5	DNA-directed RNA polymerase	0.6132	1.5	0.283729
YJL122W	ALB1	unknown	0.6147	1.5	0.136374
YGL095C	VPS45	unfolded protein binding	0.6153	1.5	0.0130891
YLR382C	NAM2	mRNA binding*	0.6177	1.5	0.0317762
YBR183W	YPC1	ceramidase	0.6182	1.5	0.0486957
YMR143W	RPS16A	structural constituent of ribosome	0.6187	1.5	0.0354319
YDL048C	STP4	unknown	0.6193	1.5	0.0489642
YMR107W	SPG4	unknown	0.6218	1.5	0.15285
YDR418W	RPL12B	structural constituent of ribosome	0.6225	1.5	0.0178555
YMR142C	RPL13B	structural constituent of ribosome	0.6235	1.5	0.0087378
YKL096W	CWP1	structural constituent of cell wall	0.6240	1.5	0.0539334
YDR366C		unknown	0.6243	1.5	0.0298718
YNL067W	RPL9B	structural constituent of ribosome	0.6250	1.5	0.0875433
YOR192C-A			0.6257	1.5	0.0534534
YJL191W	RPS14B	structural constituent of ribosome*	0.6272	1.5	0.0040079
YJL189W	RPL39	structural constituent of ribosome	0.6295	1.5	0.0222771
YNL268W	LYP1	basic amino acid transporter	0.6315	1.5	0.0568801
YGL077C	HNM1	choline transporter	0.6335	1.6	0.355304
YLR107W	REX3	3'-5' exonuclease	0.6347	1.6	0.134479
YLR388W	RPS29A	structural constituent of ribosome	0.6367	1.6	0.0117181
YPL061W	ALD6	3-chloroallyl aldehyde dehydrogenase	0.6368	1.6	0.0187111
YDR269C			0.6383	1.6	0.0001662
YBL035C	POL12	alpha DNA polymerase	0.6437	1.6	0.0223498
YBR190W			0.6440	1.6	0.0243461
YER049W	TPA1	unknown	0.6458	1.6	0.0726418
YBR114W	RAD16	DNA-dependent ATPase	0.6507	1.6	0.0018041
YDL061C	RPS29B	structural constituent of ribosome	0.6518	1.6	0.0702054
YIL152W		unknown	0.6540	1.6	0.0139991
YOR309C			0.6545	1.6	0.0631489
YCR050C			0.6575	1.6	0.0312211
YJL192C	SOP4	unknown	0.6612	1.6	0.0380758
YJL192C	SOP4	unknown	0.6612	1.6	0.0380758
YCL040W	GLK1	glucokinase	0.6623	1.6	0.0435096
YDR034C-C			0.6717	1.6	0.010173
YOR080W	DIA2	DNA replication origin binding	0.6753	1.6	0.0061567
YHL002W	HSE1	protein binding	0.6760	1.6	0.0183859
YHR166C	CDC23	protein binding*	0.6782	1.6	0.0133522
YHR187W	IKI1	RNA polymerase II transcription elongation factor	0.6812	1.6	0.0506781
YGR085C	RPL11B	structural constituent of ribosome	0.6815	1.6	0.0106195
YJL144W		unknown	0.6815	1.6	0.146826
YBR191W	RPL21A	structural constituent of ribosome	0.6820	1.6	0.0224524
YKL065C	YET1	unknown	0.6908	1.6	0.0149104
YHL001W	RPL14B	structural constituent of ribosome*	0.6952	1.6	0.0124379
YCRX16C			0.6958	1.6	0.0465628

Table 2: continued.

ORF ID	Gene Name	Gene Function	Avg Log_2 Ratio	Fold Change	T-test
YDR025W	RPS11A	structural constituent of ribosome	0.6967	1.6	0.0171773
YIL144W	TID3	structural constituent of cytoskeleton	0.7028	1.6	0.0248803
YMR170C	ALD2	3-chloroallyl aldehyde dehydrogenase	0.7032	1.6	0.116715
YKR097W	PCK1	phosphoenolpyruvate carboxykinase	0.7040	1.6	0.0130773
YGL123W	RPS2	structural constituent of ribosome	0.7088	1.6	0.0029485
YDL077C	VAM6	Rab guanyl-nucleotide exchange factor	0.7118	1.6	0.0281424
YKL006C-A	SFT1	v-SNARE	0.7140	1.6	0.0118243
YDL083C	RPS16B	structural constituent of ribosome	0.7155	1.6	0.0033495
YJL089W	SIP4	specific RNA polymerase II transcription factor	0.7180	1.6	0.0646857
YER056C-A	RPL34A	structural constituent of ribosome	0.7208	1.6	0.0106918
YIR031C	DAL7	malate synthase	0.7313	1.7	0.0109947
YNL054W-A			0.7348	1.7	0.0386707
YIL052C	RPL34B	structural constituent of ribosome	0.7393	1.7	0.0467228
YHR138C		endopeptidase inhibitor	0.7437	1.7	0.0011383
YLR410W-A			0.7458	1.7	0.0009951
YBR188C	NTC20	RNA splicing factor	0.7475	1.7	0.0117737
YJR123W	RPS5	structural constituent of ribosome	0.7492	1.7	0.0536007
YJL171C		unknown	0.7520	1.7	0.0277478
YKL156W	RPS27A	structural constituent of ribosome	0.7547	1.7	0.0727957
YGR136W	LSB1	unknown	0.7552	1.7	0.0254165
YKL024C	URA6	uridine kinase	0.7587	1.7	0.0737835
YBL092W	RPL32	structural constituent of ribosome	0.7623	1.7	0.0333798
YLL045C	RPL8B	structural constituent of ribosome	0.7663	1.7	0.0074899
YFL031W	HAC1	transcription factor	0.7707	1.7	0.0417002
YHR021C	RPS27B	structural constituent of ribosome	0.7717	1.7	0.0141383
YAR037W			0.7727	1.7	0.0830785
YNL113W	RPC19	DNA-directed RNA polymerase	0.7785	1.7	0.0580063
YDL051W	LHP1	RNA binding	0.7820	1.7	0.0227754
YLL039C	UBI4	protein tag*	0.7848	1.7	0.0007606
YDR203W			0.7855	1.7	0.0129925
YPL079W	RPL21B	structural constituent of ribosome	0.7868	1.7	0.0651095
YJR095W	SFC1	succinate:fumarate antiporter	0.7895	1.7	0.0225915
YMR316W	DIA1	unknown	0.7928	1.7	0.0027432
YDL134C	PPH21	protein phosphatase type 2A	0.7975	1.7	0.013999
YJL190C	RPS22A	structural constituent of ribosome	0.7998	1.7	0.0013096
YJR096W		aldo-keto reductase *	0.8017	1.7	0.121383
YHR095W			0.8072	1.7	0.0694593
YMR242C	RPL20A	structural constituent of ribosome	0.8078	1.8	0.0002689
YMR243C	ZRC1	di-, tri-valent inorganic cation transporter	0.8082	1.8	0.117849
YLR076C			0.8155	1.8	0.016312
YMR191W	SPG5	unknown	0.8167	1.8	0.0200889
YLR267W	BOP2	unknown	0.8172	1.8	0.015504
YLR267W	BOP2	unknown	0.8172	1.8	0.015504
YDL170W	UGA3	transcription factor	0.8173	1.8	0.0202773
YCR035C	RRP43	3'-5'-exoribonuclease	0.8242	1.8	0.0046852
YML026C	RPS18B	structural constituent of ribosome	0.8287	1.8	0.131321
YDR471W	RPL27B	structural constituent of ribosome	0.8310	1.8	0.0159222
YDL134C-A			0.8322	1.8	0.0421843
YDR450W	RPS18A	structural constituent of ribosome	0.8353	1.8	0.0071381
YDR055W	PST1	unknown	0.8372	1.8	0.0160348
YEL026W	SNU13	RNA binding*	0.8375	1.8	0.0614777
YKL151C		unknown	0.8380	1.8	0.0009637
YER013W	PRP22	RNA splicing factor	0.8392	1.8	0.0037659
YIR033W	MGA2	transcriptional activator	0.8393	1.8	0.0177476
YDL110C	TMA17	unknown	0.8412	1.8	0.0084966
YHR137W	ARO9	aromatic-amino-acid transaminase	0.8435	1.8	0.01094
YCR041W			0.8443	1.8	0.0286948
YMR176W	ECM5	unknown	0.8462	1.8	0.0143677
YMR116C	ASC1	unknown	0.8542	1.8	0.0607158
YCR033W	SNT1	NAD-dependent histone deacetylase *	0.8575	1.8	0.0187163
YHR199C	FMP34	unknown	0.8585	1.8	0.01634
YOR096W	RPS7A	structural constituent of ribosome	0.8640	1.8	0.0035532
YDL047W	SIT4	protein serine/threonine phosphatase	0.8682	1.8	0.0194416
YBR004C	GPI18	mannosyltransferase	0.8723	1.8	0.0351371
YBR117C	TKL2	transketolase	0.8727	1.8	0.0238077
YBR116C			0.8772	1.8	0.0255202
YPL057C	SUR1	mannosyltransferase *	0.8797	1.8	0.0398194
YNL192W	CHS1	chitin synthase	0.8813	1.8	0.0507604
YGR086C	PIL1	protein kinase	0.8832	1.8	0.0068342

Table 2: continued.

ORF ID	Gene Name	Gene Function	Avg Log_2 Ratio	Fold Change	T-test
YKR040C			0.8837	1.8	0.0099214
YML128C	MSC1	unknown	0.8883	1.9	0.0095036
YDL204W	RTN2	unknown	0.8890	1.9	0.0026248
YOR316C	COT1	di-, tri-valent inorganic cation transporter	0.8907	1.9	0.0109291
YIL133C	RPL16A	structural constituent of ribosome*	0.8953	1.9	0.0154846
YEL074W			0.8975	1.9	0.0178998
YNL096C	RPS7B	structural constituent of ribosome	0.8980	1.9	0.0790623
YCR028C	FEN2	pantothenate transporter	0.9075	1.9	0.0068358
YGL103W	RPL28	structural constituent of ribosome*	0.9087	1.9	0.0103456
YOR095C	RKI1	ribose-5-phosphate isomerase	0.9110	1.9	0.0153279
YNL117W	MLS1	malate synthase	0.9125	1.9	0.0173036
YLR075W	RPL10	structural constituent of ribosome	0.9155	1.9	0.042146
YDL212W	SHR3	unfolded protein binding	0.9160	1.9	0.0024472
YFL050C	ALR2	di-, tri-valent inorganic cation transporter	0.9200	1.9	0.0048175
YNL157W	IGO1	unknown	0.9290	1.9	0.0123405
YBR031W	RPL4A	structural constituent of ribosome	0.9317	1.9	0.0108182
YBR050C	REG2	protein phosphatase type 1 regulator	0.9388	1.9	0.008376
YBR297W	MAL33	transcription factor	0.9447	1.9	0.0159806
YIL148W	RPL40A	structural constituent of ribosome*	0.9465	1.9	0.0067275
YOL126C	MDH2	L-malate dehydrogenase	0.9487	1.9	0.0028429
YMR262W		unknown	0.9533	1.9	0.0271089
YLR375W	STP3	unknown	0.9573	1.9	0.0050155
YDL182W	LYS20	homocitrate synthase	0.9578	1.9	0.0231322
YCL039W	GID7	unknown	0.9585	1.9	0.0417765
YGR034W	RPL26B	structural constituent of ribosome*	0.9658	2.0	0.0021637
YLR029C	RPL15A	structural constituent of ribosome*	0.9703	2.0	0.032712
YDR001C	NTH1	alpha,alpha-trehalase	0.9763	2.0	0.0546775
YDL123W	SNA4	unknown	0.9892	2.0	0.022495
YNL195C		unknown	0.9907	2.0	0.0125122
YGR088W	CTT1	catalase	0.9985	2.0	0.0019508
YBR033W	EDS1	unknown	1.0075	2.0	0.111556
YDR368W	YPR1	oxidoreductase *	1.0172	2.0	0.0406334
YMR272C	SCS7	oxidoreductase	1.0177	2.0	0.0009907
YER081W	SER3	phosphoglycerate dehydrogenase	1.0217	2.0	0.0029483
YLR355C	ILV5	ketol-acid reductoisomerase	1.0233	2.0	0.0031752
YER025W	GCD11	translation initiation factor	1.0372	2.1	0.0159438
YDR012W	RPL4B	structural constituent of ribosome	1.0437	2.1	0.0033139
YBR161W	CSH1	mannosyltransferase *	1.0477	2.1	0.0041389
YNL143C			1.0530	2.1	0.0145176
YML004C	GLO1	lactoylglutathione lyase	1.0553	2.1	0.000554
YBR034C	HMT1	protein-arginine N-methyltransferase	1.0607	2.1	0.0004575
YMR174C	PAI3	endopeptidase inhibitor	1.0615	2.1	0.0139104
YNL178W	RPS3	structural constituent of ribosome	1.0698	2.1	0.0004945
YER150W	SPI1	unknown	1.0750	2.1	0.0338064
YHR049W	FSH1	serine hydrolase	1.0812	2.1	0.0863549
YHR071W	PCL5	cyclin-dependent protein kinase	1.0830	2.1	0.0369871
YDR508C	GNP1	amino acid transporter	1.0887	2.1	0.0089435
YDL023C			1.0908	2.1	0.0343537
YCR005C	CIT2	citrate (Si)-synthase	1.0922	2.1	0.0174329
YOR063W	RPL3	structural constituent of ribosome	1.0960	2.1	0.0107875
YMR175W	SIP18	phospholipid binding	1.0990	2.1	0.000566
YDR070C	FMP16	unknown	1.1073	2.2	0.0165054
YBL043W	ECM13	unknown	1.1287	2.2	0.0023883
YDR064W	RPS13	structural constituent of ribosome	1.1408	2.2	0.0580586
YGR043C		transaldolase	1.1483	2.2	0.0072384
YBR189W	RPS9B	structural constituent of ribosome	1.1552	2.2	0.0069421
YHR161C	YAP1801	clathrin binding	1.1663	2.2	0.0023362
YML070W	DAK1	glycerone kinase	1.1700	2.3	0.0455597
YGR057C	LST7	protein transporter	1.1775	2.3	0.0033761
YGR057C	LST7	protein transporter	1.1775	2.3	0.0033761
YML131W		unknown	1.1815	2.3	0.0427881
YML131W		unknown	1.1815	2.3	0.0427881
YER065C	ICL1	isocitrate lyase	1.1993	2.3	0.0087595
YBL093C	ROX3	RNA polymerase II transcription mediator	1.2070	2.3	0.0064967
YBL093C	ROX3	RNA polymerase II transcription mediator	1.2070	2.3	0.0064967
YGR138C	TPO2	spermine transporter	1.2137	2.3	0.0014605
YGR051C			1.2417	2.4	0.0067508
YMR173W	DDR48	ATPase *	1.2450	2.4	0.0176233
YDR037W	KRS1	lysine-tRNA ligase	1.2452	2.4	0.006399

Table 2: continued.

ORF ID	Gene Name	Gene Function	Avg Log_2 Ratio	Fold Change	T-test
YGL037C	PNC1	nicotinamidase	1.2557	2.4	0.0090876
YHR171W	ATG7	APG12 activating enzyme *	1.2777	2.4	0.0007471
YHR104W	GRE3	aldo-keto reductase *	1.3027	2.5	0.002315
YMR173W-A			1.3243	2.5	0.0064815
YDR492W	IZH1	metal ion binding	1.3452	2.5	0.0159989
YLR194C		structural constituent of cell wall	1.3477	2.5	0.0121587
YLR194C		structural constituent of cell wall	1.3477	2.5	0.0121587
YOL125W		unknown	1.3705	2.6	0.0233996
YOL125W		unknown	1.3705	2.6	0.0233996
YMR090W		unknown	1.3865	2.6	0.0319874
YNL112W	DBP2	RNA helicase	1.3868	2.6	0.0633853
YFL021W	GAT1	specific RNA polymerase II transcription factor	1.3957	2.6	0.0314206
YPL223C	GRE1	unknown	1.4073	2.7	0.0008462
YBL033C	RIB1	cyclohydrolase	1.4123	2.7	0.0519619
YFL029C	CAK1	cyclin-dependent protein kinase	1.4128	2.7	0.0009785
YER024W	YAT2	carnitine O-acetyltransferase	1.4378	2.7	0.0105631
YBR105C	VID24	unknown	1.5025	2.8	0.0160432
YNL036W	NCE103	carbonate dehydratase	1.5077	2.8	0.0046861
YIL117C	PRM5	unknown	1.5107	2.8	0.0013873
YIL117C	PRM5	unknown	1.5107	2.8	0.0013873
YOR348C	PUT4	L-proline permease	1.5480	2.9	0.0034499
YDR038C	ENA5	ATPase , coupled to transmembrane movement of ions, phosphory	1.5610	3.0	0.0144567
YDR038C	ENA5	ATPase , coupled to transmembrane movement of ions, phosphory	1.5610	3.0	0.0144567
YDR502C	SAM2	methionine adenosyltransferase	1.5610	3.0	0.0020633
YMR195W	ICY1	unknown	1.6000	3.0	0.0062503
YDL168W	SFA1	alcohol dehydrogenase	1.6098	3.1	0.0072298
YHR054C		unknown	1.6337	3.1	0.042637
YER032W	FIR1	unknown	1.6533	3.1	0.0069945
YIL099W	SGA1	glucan 1,4-alpha-glucosidase	1.6637	3.2	0.0273178
YCR010C	ADY2	ammonium transporter	1.6937	3.2	0.0198648
YPL135W	ISU1	protein binding	1.7005	3.3	0.0026833
YHR139C	SPS100	unknown	1.7403	3.3	0.015393
YJL088W	ARG3	ornithine carbamoyltransferase	1.7542	3.4	0.0138
YDR040C	ENA1	ATPase , coupled to transmembrane movement of ions, phosphory	1.7885	3.5	0.0563136
YOR031W	CRS5	copper ion binding	1.9118	3.8	0.0165351
YFL013W-A			1.9137	3.8	0.0008942
YEL071W	DLD3	D-lactate dehydrogenase	1.9187	3.8	0.0016436
YFL014W	HSP12	unknown	1.9348	3.8	0.0012294
YHR103W	SBE22	unknown	1.9427	3.8	0.0115856
YDR039C	ENA2	ATPase , coupled to transmembrane movement of ions, phosphory	1.9688	3.9	0.005857
YLR061W	RPL22A	structural constituent of ribosome	2.0047	4.0	0.0090796
YHR162W		unknown	2.0162	4.0	0.0030272
YOR303W	CPA1	carbamoyl-phosphate synthase (glutamine-hydrolyzing)	2.0510	4.1	0.0016321
YDL022W	GPD1	glycerol-3-phosphate dehydrogenase	2.0962	4.3	0.0007573
YDR043C	NRG1	DNA binding*	2.1978	4.6	0.0213979
YHR070W	TRM5	tRNA (guanine) methyltransferase	2.2173	4.7	0.0342632
YER145C	FTR1	iron ion transporter	2.2430	4.7	0.0084955
YCL065W			2.2572	4.8	0.0163941
YDL214C	PRR2	receptor signaling protein serine/threonine kinase	2.2830	4.9	0.0124674
YHR033W		unknown	2.4160	5.3	0.0027482
YHR056C	RSC30	DNA binding	2.4358	5.4	0.0027017
YFL035C-B			2.5072	5.7	0.0324437
YHR087W		unknown	2.5665	5.9	0.0054202
YGL039W		oxidoreductase *	2.6283	6.2	0.031805
YOR100C	CRC1	carnitine:acyl carnitine antiporter	2.7913	6.9	0.0004714
YOL150C			2.8075	7.0	0.0182197
YJL106W	IME2	protein kinase	3.1218	8.7	0.0085618
YIL053W	RHR2	glycerol-1-phosphatase	3.1282	8.7	0.0009198
YGL157W		oxidoreductase *	3.2108	9.3	0.0064748
YER062C	HOR2	glycerol-1-phosphatase	3.2197	9.3	0.0005317
YOR107W	RGS2	GTPase activator	3.2452	9.5	0.0051711
YMR169C	ALD3	3-chloroallyl aldehyde dehydrogenase	3.2817	9.7	0.0119141
YBR281C		unknown	3.4813	11.2	0.0001763
YDR536W	STL1	transporter	3.5778	11.9	0.0024304
YHR055C	CUP1-2	copper ion binding	3.7490	13.4	0.0004694
YOL151W	GRE2	oxidoreductase *	3.7803	13.7	0.0034423
YHR053C	CUP1-1	copper ion binding	3.8430	14.4	0.0003756
YGR159C	NSR1	RNA binding*	3.8437	14.4	0.0007395
YGR066C		unknown	4.3562	20.5	0.0112158

Table 3: Raw microarray data for fermentation day four.

ORF ID	Gene Name	Gene Function	Avg Log_2 Ratio	Fold Change	T-test
YGR254W	ENO1	phosphopyruvate hydratase	-3.5377	-11.6	0.0005211
YPL281C	ERR2	phosphopyruvate hydratase	-3.5108	-11.4	5.267E-05
YDR246W	TRS23	unknown	-3.3958	-10.5	0.0013327
YFL011W	HXT10	glucose transporter	-3.2197	-9.3	0.0088991
YDR247W	VHS1	protein kinase	-3.1373	-8.8	0.0029673
YDR249C		unknown	-2.8802	-7.4	0.0049436
YNL142W	MEP2	ammonium transporter	-2.8245	-7.1	0.0029756
YHR174W	ENO2	phosphopyruvate hydratase	-2.8163	-7.0	0.016026
YFL030W	AGX1	alanine-glyoxylate transaminase	-2.7903	-6.9	0.0019559
YGR087C	PDC6	pyruvate decarboxylase	-2.7440	-6.7	0.0040176
YHR173C			-2.7333	-6.6	0.0685791
YHR181W	SVP26	protein binding	-2.7217	-6.6	0.0053433
YLR153C	ACS2	acetate-CoA ligase	-2.6993	-6.5	0.0523336
YOL086C	ADH1	alcohol dehydrogenase	-2.6982	-6.5	7.147E-05
YMR303C	ADH2	alcohol dehydrogenase	-2.6880	-6.4	0.0007619
YMR323W	ERR3	phosphopyruvate hydratase	-2.6003	-6.1	0.0160369
YCR012W	PGK1	phosphoglycerate kinase	-2.5973	-6.1	0.0027821
YLR259C	HSP60	single-stranded DNA binding	-2.5663	-5.9	0.0284376
YLR134W	PDC5	pyruvate decarboxylase	-2.5590	-5.9	0.0105047
YOL058W	ARG1	argininosuccinate synthase	-2.5527	-5.9	0.270517
YGR240C	PFK1	6-phosphofructokinase	-2.5485	-5.9	0.0025216
YGR094W	VAS1	valine-tRNA ligase	-2.5400	-5.8	0.0021247
YHR092C	HXT4	glucose transporter	-2.5200	-5.7	0.0501148
YGL055W	OLE1	stearoyl-CoA 9-desaturase	-2.5098	-5.7	0.0029415
YGL008C	PMA1	hydrogen-exporting ATPase , phosphorylative mechanism	-2.4883	-5.6	0.141586
YBR144C			-2.4625	-5.5	0.0134941
YGR192C	TDH3	glyceraldehyde-3-phosphate dehydrogenase	-2.4508	-5.5	0.0056974
YLR044C	PDC1	pyruvate decarboxylase	-2.4458	-5.4	0.0013079
YHL032C	GUT1	glycerol kinase	-2.4197	-5.4	0.0316138
YAL037C-B			-2.3870	-5.2	0.0004363
YCR013C			-2.3687	-5.2	0.0360705
YBR145W	ADH5	alcohol dehydrogenase	-2.2932	-4.9	0.0057532
YHR094C	HXT1	glucose transporter	-2.2655	-4.8	0.0067767
YJL052W	TDH1	glyceraldehyde-3-phosphate dehydrogenase	-2.2213	-4.7	0.0057361
YGR234W	YHB1	nitric oxide reductase	-2.2198	-4.7	0.010346
YJL005W	CYR1	adenylate cyclase	-2.2127	-4.6	0.0115928
YDR245W	MNN10	alpha-1,6-mannosyltransferase	-2.1832	-4.5	0.0208124
YLR056W	ERG3	C-5 sterol desaturase	-2.1518	-4.4	0.288339
YBL100C			-2.1470	-4.4	0.0145585
YIL171W		unknown	-2.1300	-4.4	0.0214632
YPL028W	ERG10	acetyl-CoA C-acetyltransferase	-2.1157	-4.3	0.0386839
YDR357C		unknown	-2.1038	-4.3	0.0132799
YLL066W-A			-2.0112	-4.0	0.0062855
YJL045W		succinate dehydrogenase (ubiquinone)	-2.0098	-4.0	0.0050414
Q0250	COX2	cytochrome-c oxidase	-2.0087	-4.0	0.0002256
YEL077C		helicase	-1.9065	-3.7	0.004981
YBL030C	PET9	ATP:ADP antiporter	-1.8978	-3.7	0.0021073
YKL148C	SDH1	succinate dehydrogenase (ubiquinone)	-1.8787	-3.7	0.0072915
YPL187W	MF(ALPHA)1	mating pheromone	-1.8728	-3.7	0.003322
YGL089C	MF(ALPHA)2	mating pheromone	-1.8093	-3.5	0.0003334
YIR036C		unknown	-1.7878	-3.5	0.0096615
YNL055C	POR1	voltage-gated ion-selective channel	-1.7758	-3.4	0.0041243
YBL099W	ATP1	hydrogen-transporting ATP synthase , rotational mechanism	-1.7740	-3.4	0.0013101
YAL038W	CDC19	pyruvate kinase	-1.7672	-3.4	0.0026264
YKL060C	FBA1	fructose-bisphosphate aldolase	-1.7640	-3.4	0.0057646
YJR048W	CYC1	electron carrier	-1.7638	-3.4	0.0043225
YFL018C	LPD1	glycine dehydrogenase (decarboxylating) *	-1.7500	-3.4	0.0069931
YOR187W	TUF1	GTPase *	-1.7400	-3.3	0.0161058
YBL113W-A			-1.7173	-3.3	0.0059674
YDR050C	TPI1	triose-phosphate isomerase	-1.7088	-3.3	0.001759
YNL135C	FPR1	peptidyl-prolyl cis-trans isomerase	-1.7083	-3.3	0.0016081
YML110C	COQ5	2-hexaprenyl-6-methoxy-1,4-benzoquinone methyltransferase	-1.7035	-3.3	0.0241298
YGR244C	LSC2	succinate-CoA ligase (ADP-forming)	-1.6993	-3.2	0.0146377
YMR304C-A			-1.6962	-3.2	0.0422933
YJR009C	TDH2	glyceraldehyde-3-phosphate dehydrogenase	-1.6778	-3.2	0.0663943
YJR016C	ILV3	dihydroxy-acid dehydratase	-1.6523	-3.1	0.0021943
YBR085W	AAC3	ATP:ADP antiporter	-1.6435	-3.1	0.0005171
YGR287C		hydrolase , hydrolyzing O-glycosyl compounds	-1.6390	-3.1	0.116654
YPL127C	HHO1	DNA binding	-1.6355	-3.1	0.0336075

Table 3: continued.

ORF ID	Gene Name	Gene Function	Avg Log_2 Ratio	Fold Change	T-test
YDL055C	PSA1	mannose-1-phosphate guanylyltransferase	-1.6302	-3.1	0.012652
YPL262W	FUM1	fumarate hydratase	-1.6232	-3.1	0.0035527
YPR204W		DNA helicase	-1.6188	-3.1	0.0694302
YJR120W		unknown	-1.6173	-3.1	0.0027704
YKL152C	GPM1	phosphoglycerate mutase	-1.6137	-3.1	0.045952
YNL339C	YRF1-6	DNA helicase	-1.5880	-3.0	0.0031108
YNL052W	COX5A	cytochrome-c oxidase	-1.5753	-3.0	0.0040669
YCR074C			-1.5665	-3.0	0.005856
TMR307W			-1.5593	-2.9	0.0138625
YKL085W	MDH1	L-malate dehydrogenase	-1.5432	-2.9	0.0049448
YJL214W	HXT8	glucose transporter	-1.5372	-2.9	0.0406361
YOR133W	EFT1	translation elongation factor	-1.5342	-2.9	0.0057968
YMR145C	NDE1	NADH dehydrogenase	-1.5298	-2.9	0.0080462
YGR279C	SCW4	glucosidase	-1.5277	-2.9	0.0421182
YBL015W	ACH1	acetyl-CoA hydrolase	-1.5243	-2.9	0.001791
YOR230W	WTM1	transcription corepressor	-1.5232	-2.9	0.003855
YHR218W		unknown	-1.5163	-2.9	0.021105
YGL156W	AMS1	alpha-mannosidase	-1.5097	-2.8	0.0833606
YIR021W	MRS1	RNA binding	-1.5072	-2.8	0.146316
YGL179C	TOS3	protein kinase	-1.5000	-2.8	0.0294567
YJR077C	MIR1	inorganic phosphate transporter	-1.4997	-2.8	0.0078868
YGL202W	ARO8	aromatic-amino-acid transaminase	-1.4847	-2.8	0.0277173
YNL009W	IDP3	isocitrate dehydrogenase (NADP+)	-1.4800	-2.8	0.0153217
YBL112C		unknown	-1.4675	-2.8	0.0238395
YEL030W	ECM10	unknown	-1.4557	-2.7	0.0147754
YLR420W	URA4	dihydroorotase	-1.4477	-2.7	0.117124
YNL072W	RNH201	ribonuclease H	-1.4187	-2.7	0.0114425
YLL026W	HSP104	chaperone binding	-1.4185	-2.7	0.0789263
YGL253W	HXK2	hexokinase	-1.4103	-2.7	0.0165731
YNL053W	MSG5	prenylated protein tyrosine phosphatase	-1.4002	-2.6	0.0045382
YMR056C	AAC1	ATP:ADP antiporter	-1.3943	-2.6	0.0132202
YGR143W	SKN1	glucosidase	-1.3917	-2.6	0.0102354
YHR051W	COX6	cytochrome-c oxidase	-1.3872	-2.6	0.002703
YML028W	TSA1	thioredoxin peroxidase	-1.3855	-2.6	0.0066019
YDL021W	GPM2	unknown	-1.3822	-2.6	0.0126967
YJR103W	URA8	CTP synthase	-1.3815	-2.6	0.0375282
YEL066W	HPA3	histone acetyltransferase	-1.3765	-2.6	0.0015326
YLR174W	IDP2	isocitrate dehydrogenase (NADP+)	-1.3750	-2.6	0.0037159
YJL217W		unknown	-1.3702	-2.6	0.0006493
YHL034C	SBP1	RNA binding	-1.3697	-2.6	0.0234807
YEL024W	RIP1	ubiquinol-cytochrome-c reductase	-1.3682	-2.6	0.0128749
YNR036C		structural constituent of ribosome	-1.3630	-2.6	0.0271336
YMR199W	CLN1	cyclin-dependent protein kinase regulator	-1.3627	-2.6	0.0350652
YJR148W	BAT2	branched-chain-amino-acid transaminase	-1.3610	-2.6	0.0177124
YGL191W	COX13	enzyme regulator *	-1.3572	-2.6	0.0054378
YHL050C		helicase	-1.3523	-2.6	0.0358242
YOR393W	ERR1	phosphopyruvate hydratase	-1.3355	-2.5	0.220241
YOR142W	LSC1	succinate-CoA ligase (ADP-forming)	-1.3352	-2.5	0.0005867
YMR015C	ERG5	C-22 sterol desaturase	-1.3238	-2.5	0.0469431
YBR026C	ETR1	enoyl-[acyl-carrier protein] reductase	-1.3205	-2.5	7.395E-06
YGR191W	HIP1	L-histidine transporter	-1.3102	-2.5	0.0027607
YDR385W	EFT2	translation elongation factor	-1.3068	-2.5	0.0039284
YJR031C	GEA1	ARF guanyl-nucleotide exchange factor	-1.2995	-2.5	0.0164891
YFR053C	HXK1	hexokinase	-1.2933	-2.5	0.0070769
YHR219W		unknown	-1.2927	-2.4	0.0065523
YGL062W	PYC1	pyruvate carboxylase	-1.2910	-2.4	0.019084
YLR395C	COX8	cytochrome-c oxidase	-1.2893	-2.4	0.0146455
YDR202C	RAV2	unknown	-1.2888	-2.4	0.0007558
YDR119W		unknown	-1.2875	-2.4	0.0012483
YLL041C	SDH2	succinate dehydrogenase (ubiquinone)	-1.2683	-2.4	0.0082625
YDL185W	TFP1	hydrogen-transporting ATPase , rotational mechanism*	-1.2658	-2.4	0.0237687
YER023W	PRO3	pyrroline-5-carboxylate reductase	-1.2652	-2.4	0.0012985
YNL220W	ADE12	adenylosuccinate synthase	-1.2637	-2.4	0.0001225
YGL105W	ARC1	tRNA binding	-1.2623	-2.4	0.0085279
YKL097W-A			-1.2552	-2.4	0.0162569
YKL067W	YNK1	nucleoside diphosphate kinase	-1.2533	-2.4	0.0032047
YKL153W			-1.2488	-2.4	0.0168587
YER178W	PDA1	pyruvate dehydrogenase (acetyl-transferring)	-1.2483	-2.4	0.0091187
YPL134C	ODC1	intracellular transporter	-1.2475	-2.4	0.0061971

Table 3: continued.

ORF ID	Gene Name	Gene Function	Avg Log_2 Ratio	Fold Change	T-test
YKL217W	JEN1	lactate transporter	-1.2455	-2.4	0.0558608
YEL039C	CYC7	electron carrier	-1.2420	-2.4	0.0019586
YHR212C			-1.2417	-2.4	0.145285
YCL025C	AGP1	amino acid transporter	-1.2355	-2.4	0.0037559
YGL188C			-1.2317	-2.3	0.0336314
YFL039C	ACT1	structural constituent of cytoskeleton	-1.2285	-2.3	0.0084709
YDR453C	TSA2	thioredoxin peroxidase	-1.2272	-2.3	0.0077252
YPL078C	ATP4	structural molecule *	-1.2218	-2.3	0.0033471
YBL098W	BNA4	kynurenine 3-monooxygenase	-1.2158	-2.3	0.0178262
YNR001C	CIT1	citrate (Si)-synthase	-1.2085	-2.3	0.0021957
YBR078W	ECM33	unknown	-1.2015	-2.3	0.0015443
YMR190C	SGS1	ATP-dependent DNA helicase	-1.1968	-2.3	0.0018184
YMR208W	ERG12	mevalonate kinase	-1.1950	-2.3	0.0526759
YDR273W	DON1	unknown	-1.1930	-2.3	0.0052203
YER053C	PIC2	inorganic phosphate transporter	-1.1862	-2.3	0.002229
YDL100C	GET3	ATPase	-1.1862	-2.3	0.0198745
YIR037W	HYR1	thioredoxin peroxidase *	-1.1848	-2.3	0.0324715
YNL103W	MET4	transcription coactivator	-1.1798	-2.3	0.0017762
YIR035C		unknown	-1.1687	-2.2	0.013592
YMR297W	PRC1	carboxypeptidase C	-1.1672	-2.2	0.0058152
YER133W	GLC7	protein phosphatase type 1	-1.1610	-2.2	0.0084142
YGR292W	MAL12	alpha-glucosidase	-1.1568	-2.2	0.0960076
YJR139C	HOM6	homoserine dehydrogenase	-1.1497	-2.2	0.0071506
YHR007C	ERG11	sterol 14-demethylase	-1.1395	-2.2	0.0049116
YOR084W		lipase	-1.1385	-2.2	0.0039637
YDL126C	CDC48	ATPase	-1.1323	-2.2	0.0240621
YDR148C	KGD2	dihydrolipoyllysine-residue succinyltransferase	-1.1323	-2.2	0.0018843
YDR284C	DPP1	phosphatidate phosphatase *	-1.1293	-2.2	0.0041214
YKL176C	LST4	protein transporter	-1.1257	-2.2	0.339576
YBR244W	GPX2	glutathione peroxidase *	-1.1227	-2.2	0.0040126
YKL141W	SDH3	succinate dehydrogenase (ubiquinone)	-1.1197	-2.2	0.0064126
YLR460C		unknown	-1.1190	-2.2	0.0404649
YDL215C	GDH2	glutamate dehydrogenase	-1.1168	-2.2	0.0244043
YBL001C	ECM15	unknown	-1.1123	-2.2	0.0186059
YMR215W	GAS3	1,3-beta-glucanosyltransferase	-1.1123	-2.2	0.0490475
YKL066W			-1.1013	-2.1	0.0051052
YML132W	COS3	protein binding	-1.0953	-2.1	0.0048383
YKL192C	ACP1	acyl carrier	-1.0917	-2.1	0.014706
YLL018C	DPS1	RNA binding	-1.0917	-2.1	0.0193234
YKR046C	PET10	unknown	-1.0903	-2.1	0.0395881
YDL210W	UGA4	putrescine transporter	-1.0775	-2.1	0.083624
YBR185C	MBA1	unknown	-1.0762	-2.1	0.0167391
YBL075C	SSA3	ATPase *	-1.0710	-2.1	0.0055408
YER152C		unknown	-1.0665	-2.1	0.115109
YKL157W	APE2	leucyl aminopeptidase	-1.0643	-2.1	0.000473
YHR008C	SOD2	manganese superoxide dismutase	-1.0640	-2.1	0.0058543
YGL200C	EMP24	unknown	-1.0520	-2.1	0.0414524
YKL174C	TPO5	polyamine transporter	-1.0508	-2.1	0.128647
YML078W	CPR3	peptidyl-prolyl cis-trans isomerase	-1.0508	-2.1	0.0186655
YKL069W		unknown	-1.0442	-2.1	0.112305
YEL009C	GCN4	DNA binding	-1.0337	-2.0	0.0097289
YDR438W		unknown	-1.0330	-2.0	0.002288
YDL067C	COX9	cytochrome-c oxidase	-1.0290	-2.0	0.0015579
YDR200C	VPS64	unknown	-1.0273	-2.0	0.242927
YBR067C	TIP1	structural constituent of cell wall*	-1.0262	-2.0	0.0311461
YHL034W-A			-1.0245	-2.0	0.0514341
YHR126C		unknown	-1.0212	-2.0	0.0043803
YPL082C	MOT1	ATPase	-1.0182	-2.0	0.0625089
YCRX18C			-1.0172	-2.0	0.0930517
YFL062W	COS4	unknown	-1.0137	-2.0	0.0043981
YHR214W		unknown	-1.0113	-2.0	0.0006442
YER011W	TIR1	structural constituent of cell wall	-1.0028	-2.0	0.0148515
YHR028C	DAP2	dipeptidyl-peptidase and tripeptidyl-peptidase	-1.0017	-2.0	0.0039903
YKL160W	ELF1	RNA polymerase II transcription elongation factor	-0.9982	-2.0	0.0409732
YGR167W	CLC1	structural molecule	-0.9933	-2.0	0.0137311
YLR304C	ACO1	aconitate hydratase	-0.9883	-2.0	0.0341339
YPL080C			-0.9882	-2.0	0.0301871
YBL045C	COR1	ubiquinol-cytochrome-c reductase	-0.9868	-2.0	0.0011312
YHR001W-A	QCR10	ubiquinol-cytochrome-c reductase	-0.9818	-2.0	0.0243084

Table 3: continued.

ORF ID	Gene Name	Gene Function	Avg Log_2 Ratio	Fold Change	T-test
YBL102W	SFT2	unknown	-0.9788	-2.0	0.0469287
YJL068C		S-formylglutathione hydrolase	-0.9782	-2.0	0.0029145
YBL078C	ATG8	microtubule binding	-0.9772	-2.0	0.0238878
YIL166C		transporter	-0.9752	-2.0	0.0027811
YGR175C	ERG1	squalene monooxygenase *	-0.9740	-2.0	0.0041998
YAR018C	KIN3	protein kinase	-0.9685	-2.0	0.0155214
YLR150W	STM1	DNA binding	-0.9665	-2.0	0.0482563
YIL125W	KGD1	oxoglutarate dehydrogenase (succinyl-transferring)	-0.9652	-2.0	0.0669744
YFL049W	SWP82	transcriptional activator	-0.9628	-1.9	0.0244383
YDL066W	IDP1	isocitrate dehydrogenase (NADP+)	-0.9600	-1.9	0.0016617
YIL057C		unknown	-0.9572	-1.9	0.023131
YKR013W	PRY2	unknown	-0.9455	-1.9	0.247454
YGR121C	MEP1	ammonium transporter	-0.9423	-1.9	0.368745
YMR205C	PFK2	6-phosphofructokinase	-0.9413	-1.9	0.0038085
YLR303W	MET17	cysteine synthase *	-0.9403	-1.9	0.0102335
YDR327W			-0.9383	-1.9	0.0063162
YPR020W	ATP20	structural molecule	-0.9380	-1.9	0.0218309
YNL071W	LAT1	dihydrolipoyllysine-residue acetyltransferase	-0.9350	-1.9	0.01109
YJL066C	MPM1	unknown	-0.9325	-1.9	0.0049339
YMR206W		unknown	-0.9315	-1.9	0.0173931
YNL336W	COS1	unknown	-0.9305	-1.9	0.0080794
YDR047W	HEM12	uroporphyrinogen decarboxylase	-0.9270	-1.9	0.0240862
YER003C	PMI40	mannose-6-phosphate isomerase	-0.9263	-1.9	0.0071212
YFL038C	YPT1	GTPase	-0.9255	-1.9	0.0057113
YIL157C	FMP35	unknown	-0.9255	-1.9	0.0011721
YBR025C		unknown	-0.9253	-1.9	0.0007142
YBR243C	ALG7	UDP-N-acetylglucosamine-dolichyl-phosphate N-acetylglucosa	-0.9253	-1.9	0.0358139
YLL052C	AQY2	water channel	-0.9215	-1.9	0.037856
YBR148W	YSW1	unknown	-0.9202	-1.9	0.0274711
YCL057W	PRD1	metalloendopeptidase *	-0.9110	-1.9	0.0505244
YGR246C	BRF1	RNA polymerase III transcription factor	-0.9107	-1.9	0.0120764
YDR193W			-0.9100	-1.9	0.0027404
YDL120W	YFH1	enzyme regulator	-0.9063	-1.9	0.0008325
YDL078C	MDH3	L-malate dehydrogenase	-0.9043	-1.9	0.0007158
YAL062W	GDH3	glutamate dehydrogenase	-0.9028	-1.9	0.0829544
YGR295C	COS6	unknown	-0.8932	-1.9	0.0233409
YGR142W	BTN2	unknown	-0.8875	-1.8	0.127621
YJL213W		unknown	-0.8865	-1.8	0.0070708
YDR032C	PST2	unknown	-0.8860	-1.8	0.0097202
YEL065W	SIT1	siderophore-iron (ferrioxamine) uptake transporter	-0.8780	-1.8	0.0025091
YJR080C	FMP26	unknown	-0.8747	-1.8	0.0051612
YDR007W	TRP1	phosphoribosylanthranilate isomerase	-0.8745	-1.8	0.0511363
YJL048C	UBX6	unknown	-0.8720	-1.8	0.0006909
YLR231C	BNA5	kynureninase	-0.8720	-1.8	0.135077
YIL123W	SIM1	unknown	-0.8695	-1.8	0.0469092
YOR007C	SGT2	unknown	-0.8687	-1.8	0.0062891
YHR057C	CPR2	peptidyl-prolyl cis-trans isomerase	-0.8682	-1.8	0.178201
YKL216W	URA1	dihydroorotate dehydrogenase	-0.8667	-1.8	0.0028603
YHR018C	ARG4	argininosuccinate lyase	-0.8643	-1.8	0.0131009
YAL008W	FUN14	unknown	-0.8628	-1.8	0.0025063
YKR020W	VPS51	protein binding	-0.8627	-1.8	0.175689
YGR132C	PHB1	unknown	-0.8623	-1.8	0.0238722
YIR044C		unknown	-0.8613	-1.8	0.0067745
YML039W			-0.8602	-1.8	0.113936
YLR294C			-0.8593	-1.8	0.0185024
YFL005W	SEC4	GTPase	-0.8590	-1.8	0.0094263
YGL026C	TRP5	tryptophan synthase	-0.8500	-1.8	0.11978
YFR044C		unknown	-0.8477	-1.8	0.0633565
YBR294W	SUL1	sulfate transporter	-0.8468	-1.8	0.0223382
YGR021W		unknown	-0.8463	-1.8	0.0452241
YML120C	NDI1	NADH dehydrogenase (ubiquinone)	-0.8417	-1.8	0.0094716
YDR268W	MSW1	tryptophan-tRNA ligase	-0.8390	-1.8	0.008626
YGL164C	YRB30	protein binding	-0.8355	-1.8	0.106843
YMR074C		unknown	-0.8355	-1.8	0.0106242
YDL181W	INH1	enzyme inhibitor	-0.8330	-1.8	0.0336067
YGL068W	MNP1	unknown	-0.8325	-1.8	0.0212398
YNL037C	IDH1	isocitrate dehydrogenase (NAD+)	-0.8230	-1.8	0.0188632
YJR073C	OPI3	phosphatidyl-N-methylethanolamine N-methyltransferase	-0.8185	-1.8	0.0331786
YGR253C	PUP2	endopeptidase	-0.8150	-1.8	0.000143

Table 3: continued.

ORF ID	Gene Name	Gene Function	Avg Log_2 Ratio	Fold Change	T-test
YBR039W	ATP3	hydrogen-transporting ATP synthase , rotational mechanism	-0.8148	-1.8	0.0102082
YJR109C	CPA2	carbamoyl-phosphate synthase (glutamine-hydrolyzing)	-0.8132	-1.8	0.0905807
YER010C		unknown	-0.8112	-1.8	0.444645
YPR033C	HTS1	histidine-tRNA ligase	-0.8100	-1.8	0.0051138
YNL144C		unknown	-0.8055	-1.7	0.183034
YEL052W	AFG1	ATPase	-0.8032	-1.7	0.0369059
YDL237W		unknown	-0.8028	-1.7	0.0107521
YJL079C	PRY1	unknown	-0.7997	-1.7	0.0032116
YKR076W	ECM4	unknown	-0.7987	-1.7	0.0189093
YGL148W	ARO2	chorismate synthase *	-0.7973	-1.7	0.062767
YCR021C	HSP30	unknown	-0.7970	-1.7	0.0112727
YFR003C	YPI1	protein phosphatase inhibitor	-0.7953	-1.7	0.0347147
YGR183C	QCR9	ubiquinol-cytochrome-c reductase	-0.7947	-1.7	0.029432
YGL004C	RPN14	unknown	-0.7943	-1.7	0.0302875
YDL248W	COS7	receptor	-0.7927	-1.7	0.0090428
YMR108W	ILV2	acetolactate synthase *	-0.7923	-1.7	0.0066842
YNL057W			-0.7885	-1.7	0.139776
YDR163W	CWC15	unknown	-0.7867	-1.7	0.0265685
YBR299W	MAL32	alpha-glucosidase	-0.7815	-1.7	0.025647
YGR182C			-0.7792	-1.7	0.0436314
YDL195W	SEC31	structural molecule	-0.7775	-1.7	0.0054941
YPR088C	SRP54	signal sequence binding	-0.7770	-1.7	0.0858451
YHR074W	QNS1	hydrolase , acting on carbon-nitrogen (but not peptide) bonds, i	-0.7753	-1.7	0.378315
YHL048W	COS8	unknown	-0.7737	-1.7	0.0130009
YMR276W	DSK2	protein binding	-0.7735	-1.7	0.0480635
YAL055W	PEX22	unknown	-0.7727	-1.7	0.0669845
YIL136W	OM45	unknown	-0.7725	-1.7	0.0169707
YHL019W-A			-0.7703	-1.7	0.18253
YJL001W	PRE3	endopeptidase	-0.7703	-1.7	0.0377976
YDR031W		unknown	-0.7692	-1.7	0.0012387
YPL265W	DIP5	amino acid transporter	-0.7660	-1.7	0.0286061
YJL207C	LAA1	unknown	-0.7643	-1.7	0.0315624
YIL124W	AYR1	acylglycerone-phosphate reductase	-0.7625	-1.7	0.0880242
YDL174C	DLD1	D-lactate dehydrogenase (cytochrome)	-0.7615	-1.7	0.0139759
YKR048C	NAP1	protein binding	-0.7610	-1.7	0.0386136
YIR043C		unknown	-0.7595	-1.7	0.0033023
YBR221C	PDB1	pyruvate dehydrogenase (acetyl-transferring)	-0.7580	-1.7	0.0147966
YER056C	FCY2	cytosine-purine permease *	-0.7563	-1.7	0.108878
YCL058C			-0.7530	-1.7	0.0382909
YIR038C	GTT1	glutathione transferase	-0.7527	-1.7	0.0203948
YBR219C		unknown	-0.7518	-1.7	0.0233464
YKL164C	PIR1	structural constituent of cell wall	-0.7518	-1.7	0.0092288
YCL009C	ILV6	enzyme regulator *	-0.7505	-1.7	0.0087365
YDL171C	GLT1	glutamate synthase (NADH)	-0.7493	-1.7	0.0157805
YPL048W	CAM1	translation elongation factor	-0.7467	-1.7	0.0047668
YNR018W		unknown	-0.7445	-1.7	0.0393113
YPR156C	TPO3	spermine transporter	-0.7422	-1.7	0.058331
YDR157W			-0.7415	-1.7	0.0330321
YOL071W	EMI5	unknown	-0.7372	-1.7	0.0220893
YDR388W	RVS167	cytoskeletal protein binding	-0.7368	-1.7	0.0366519
YNL064C	YDJ1	chaperone regulator *	-0.7345	-1.7	0.0410423
YBR094W		unknown	-0.7335	-1.7	0.001266
YCL030C	HIS4	phosphoribosyl-ATP diphosphatase	-0.7307	-1.7	0.0471703
YGL048C	RPT6	ATPase *	-0.7280	-1.7	0.0341018
YLR028C	ADE16	IMP cyclohydrolase	-0.7262	-1.7	0.0107976
YIL137C	TMA108	metalloendopeptidase	-0.7255	-1.7	0.125156
YCR079W		phosphoprotein phosphatase	-0.7242	-1.7	0.0464033
YDL192W	ARF1	GTPase	-0.7237	-1.7	0.0199873
YOR243C	PUS7	pseudouridine synthase	-0.7217	-1.6	0.0269627
YOR215C		unknown	-0.7203	-1.6	0.0006178
YDR129C	SAC6	protein binding	-0.7160	-1.6	0.0715468
YCR058C			-0.7150	-1.6	0.266776
YER004W	FMP52	unknown	-0.7143	-1.6	0.0035528
YFR031C-A	RPL2A	structural constituent of ribosome	-0.7118	-1.6	0.0094638
YHR037W	PUT2	1-pyrroline-5-carboxylate dehydrogenase	-0.7110	-1.6	0.0044512
YKL103C	LAP4	aminopeptidase I	-0.7053	-1.6	0.0286373
YER103W	SSA4	ATPase *	-0.7045	-1.6	0.0973909
YCR004C	YCP4	electron carrier	-0.7020	-1.6	0.0363207
YCR014C	POL4	beta DNA polymerase	-0.7017	-1.6	0.140327

Table 3: continued.

ORF ID	Gene Name	Gene Function	Avg Log_2 Ratio	Fold Change	T-test
YBR046C	ZTA1	unknown	-0.6998	-1.6	7.841E-06
YLR248W	RCK2	protein serine/threonine kinase	-0.6997	-1.6	0.0040415
YHR214W-A			-0.6997	-1.6	0.080264
YGR231C	PHB2	unknown	-0.6987	-1.6	0.0250179
YPL270W	MDL2	ATPase , coupled to transmembrane movement of substances	-0.6985	-1.6	0.0241096
YDR310C	SUM1	transcriptional repressor	-0.6975	-1.6	0.0007879
YDL137W	ARF2	GTPase	-0.6948	-1.6	0.0250585
YFR024C			-0.6937	-1.6	0.0249951
YOR289W		unknown	-0.6935	-1.6	0.051487
YGL115W	SNF4	protein kinase activator	-0.6917	-1.6	0.0393142
YLR257W		unknown	-0.6860	-1.6	0.0098596
YEL025C		unknown	-0.6858	-1.6	0.347913
YJR001W	AVT1	neutral amino acid transporter	-0.6825	-1.6	0.0168642
YPL031C	PHO85	cyclin-dependent protein kinase	-0.6825	-1.6	0.0059765
YJL081C	ARP4	chromatin binding	-0.6797	-1.6	0.0894538
YDR325W	YCG1	unknown	-0.6795	-1.6	0.0257903
YPL274W	SAM3	S-adenosylmethionine transporter	-0.6787	-1.6	0.0428522
YBR298C	MAL31	alpha-glucoside:hydrogen symporter	-0.6783	-1.6	0.0030428
YGL121C	GPG1	signal transducer	-0.6750	-1.6	0.0086372
YLL024C	SSA2	ATPase *	-0.6732	-1.6	0.023702
YIL065C	FIS1	unknown	-0.6730	-1.6	0.0232047
YEL032W	MCM3	chromatin binding	-0.6725	-1.6	0.0296826
YGR038W	ORM1	unknown	-0.6725	-1.6	0.0568904
YJL034W	KAR2	ATPase *	-0.6698	-1.6	0.0194184
YER012W	PRE1	endopeptidase	-0.6693	-1.6	0.0629897
YPL034W		unknown	-0.6687	-1.6	0.373552
YFL045C	SEC53	phosphomannomutase	-0.6667	-1.6	0.0270839
YGR250C		RNA binding	-0.6667	-1.6	0.000825
YBR139W		serine hydrolase *	-0.6622	-1.6	0.0049168
YJR023C			-0.6613	-1.6	0.0192836
YCL018W	LEU2	3-isopropylmalate dehydrogenase	-0.6597	-1.6	0.0063544
YIL078W	THS1	threonine-tRNA ligase	-0.6595	-1.6	0.0125413
YAL023C	PMT2	dolichyl-phosphate-mannose-protein mannosyltransferase	-0.6578	-1.6	0.0073141
YKL200C			-0.6575	-1.6	0.0263667
YPR024W	YME1	ATP-dependent peptidase	-0.6548	-1.6	0.191781
YLR354C	TAL1	transaldolase	-0.6543	-1.6	0.0634906
YML106W	URA5	orotate phosphoribosyltransferase	-0.6480	-1.6	0.0026807
YPR083W	MDM36	unknown	-0.6452	-1.6	0.129119
YJR079W		unknown	-0.6433	-1.6	0.13572
YLR095C	IOC2	protein binding	-0.6368	-1.6	0.0097903
YDL029W	ARP2	structural constituent of cytoskeleton*	-0.6367	-1.6	0.0048151
YHR117W	TOM71	protein transporter	-0.6330	-1.6	0.0315424
YPL059W	GRX5	thiol-disulfide exchange intermediate	-0.6285	-1.5	0.203837
YDR023W	SES1	serine-tRNA ligase	-0.6282	-1.5	0.007585
YER031C	YPT31	GTPase	-0.6250	-1.5	0.0240893
YBL003C	HTA2	DNA binding	-0.6233	-1.5	0.0513053
YBR088C	POL30	DNA polymerase processivity factor	-0.6232	-1.5	0.0115579
YDR177W	UBC1	ubiquitin conjugating enzyme	-0.6227	-1.5	0.001769
YML054C	CYB2	L-lactate dehydrogenase (cytochrome)	-0.6225	-1.5	0.0152554
YER136W	GDI1	Rab GDP-dissociation inhibitor	-0.6218	-1.5	0.0543204
YIL051C	MMF1	unknown	-0.6212	-1.5	0.0220292
YFL066C		unknown	-0.6177	-1.5	0.0117956
YPL282C	PAU22	unknown	-0.6138	-1.5	0.0428703
YIR022W	SEC11	signal peptidase	-0.6132	-1.5	0.001555
YGR214W	RPS0A	structural constituent of ribosome	-0.6070	-1.5	0.0203501
YNL100W		unknown	-0.6058	-1.5	0.0295146
YOL111C	MDY2	unknown	-0.6058	-1.5	0.0614107
YBR074W		metalloendopeptidase	-0.6047	-1.5	0.0153701
YMR099C		unknown	-0.5987	-1.5	0.0688834
YCR011C	ADP1	ATPase	-0.5898	-1.5	0.0220968
YER091C	MET6	5-methyltetrahydropteroyltriglutamate-homocysteine S-methylt	-0.5895	-1.5	0.104279
YER095W	RAD51	recombinase	-0.5878	-1.5	0.158913
YEL034C-A			-0.5863	-1.5	0.0616625
YJL014W	CCT3	unfolded protein binding	-0.5853	-1.5	0.0123731
YJL012C	VTC4	unknown	-0.5852	-1.5	0.113078
YBR280C		unknown	-0.5807	-1.5	0.0332498
YPR035W	GLN1	glutamate-ammonia ligase	-0.5800	-1.5	0.0130086
YDR529C	QCR7	ubiquinol-cytochrome-c reductase	-0.5793	-1.5	0.0832114
YOR335C	ALA1	alanine-tRNA ligase	-0.5790	-1.5	0.145233

Table 3: continued.

ORF ID	Gene Name	Gene Function	Avg Log$_2$ Ratio	Fold Change	T-test
YDR429C	TIF35	translation initiation factor	-0.5782	-1.5	0.0236947
YGL066W	SGF73	structural molecule *	-0.5778	-1.5	0.0289986
YCL061C	MRC1	unknown	-0.5730	-1.5	0.0227256
YMR203W	TOM40	protein transporter	-0.5712	-1.5	0.0408657
YJL143W	TIM17	protein transporter	-0.5705	-1.5	0.000366
YDR198C	RKM2	unknown	-0.5702	-1.5	0.0394924
YLR326W		unknown	-0.5697	-1.5	0.0382259
YPR028W	YOP1	protein binding	-0.5677	-1.5	0.116211
YDR496C	PUF6	specific transcriptional repressor	-0.5652	-1.5	0.0444239
YBR206W			-0.5643	-1.5	0.0509919
YDL093W	PMT5	dolichyl-phosphate-mannose-protein mannosyltransferase	-0.5630	-1.5	0.148798
YOR168W	GLN4	glutamine-tRNA ligase	-0.5627	-1.5	0.0028085
YOR259C	RPT4	ATPase *	-0.5623	-1.5	0.0217712
YEL042W	GDA1	guanosine-diphosphatase	-0.5613	-1.5	0.0444184
YJR014W	TMA22	RNA binding	-0.5605	-1.5	0.0890437
YPR080W	TEF1	translation elongation factor	-0.5558	-1.5	0.0850207
YKR070W		unknown	-0.5547	-1.5	0.0165033
YBR121C	GRS1	glycine-tRNA ligase	-0.5535	-1.5	0.0040589
YEL011W	GLC3	1,4-alpha-glucan branching enzyme	-0.5535	-1.5	0.0515006
YCL064C	CHA1	L-serine ammonia-lyase *	-0.5522	-1.5	0.0077958
YGR271W	SLH1	RNA helicase	-0.5475	-1.5	0.0124169
YER009W	NTF2	Ran GTPase binding	-0.5455	-1.5	0.0210792
YOR020C	HSP10	unfolded protein binding	-0.5433	-1.5	0.03817
YDL007W	RPT2	ATPase *	-0.5405	-1.5	0.010477
YDR253C	MET32	DNA binding	-0.5402	-1.5	0.146406
YML012W	ERV25	unknown	-0.5395	-1.5	0.012581
YEL049W	PAU2	unknown	-0.5368	-1.5	0.0479029
YJL062W	LAS21	transferase	-0.5358	-1.4	0.0018635
YLR378C	SEC61	protein transporter	-0.5355	-1.4	0.052101
YML010W	SPT5	RNA polymerase II transcription elongation factor	-0.5353	-1.4	0.0234722
YPL181W	CTI6	transcription factor binding	-0.5332	-1.4	0.0626876
YBR054W	YRO2	unknown	-0.5330	-1.4	0.0420432
YNL134C		alcohol dehydrogenase (NADP+)	-0.5302	-1.4	0.0194446
YEL034W	HYP2	protein binding	-0.5297	-1.4	0.0165189
YFL022C	FRS2	phenylalanine-tRNA ligase	-0.5258	-1.4	0.0023064
YIL075C	RPN2	endopeptidase *	-0.5253	-1.4	0.0473779
YFL037W	TUB2	structural constituent of cytoskeleton	-0.5240	-1.4	0.0165442
YKL109W	HAP4	transcriptional activator	-0.5240	-1.4	0.0089356
YBR208C	DUR1,2	allophanate hydrolase *	-0.5230	-1.4	0.0170561
YIL039W		unknown	-0.5230	-1.4	0.0190342
YDR086C	SSS1	protein transporter	-0.5228	-1.4	0.0070185
YPR026W	ATH1	alpha,alpha-trehalase	-0.5203	-1.4	0.0173272
YBR301W	DAN3	unknown	-0.5182	-1.4	0.0297179
YKL163W	PIR3	structural constituent of cell wall	-0.5173	-1.4	0.0252202
YJL080C	SCP160	RNA binding	-0.5172	-1.4	0.0491651
YKR094C	RPL40B	structural constituent of ribosome*	-0.5167	-1.4	0.0231704
YLR249W	YEF3	translation elongation factor	-0.5167	-1.4	0.078223
YOR394W	PAU21	unknown	-0.5167	-1.4	0.0543114
YMR104C	YPK2	protein kinase	-0.5165	-1.4	0.127505
YOR136W	IDH2	isocitrate dehydrogenase (NAD+)	-0.5142	-1.4	0.0216685
YPL224C	MMT2	unknown	-0.5138	-1.4	0.0440024
YDL206W		unknown	-0.5130	-1.4	0.0046788
YOR135C			-0.5120	-1.4	0.0647748
YPL179W	PPQ1	protein serine/threonine phosphatase	-0.5103	-1.4	0.0072955
YKL212W	SAC1	inositol or phosphatidylinositol phosphatase	-0.5092	-1.4	0.0424713
YNL173C	MDG1	unknown	-0.5087	-1.4	0.0809204
YDR377W	ATP17	hydrogen-transporting ATP synthase , rotational mechanism	-0.5085	-1.4	0.0171782
YHL040C	ARN1	siderophore-iron transporter	-0.5083	-1.4	0.0553052
YJR047C	ANB1	translation initiation factor	-0.5077	-1.4	0.0265618
YOR270C	VPH1	hydrogen-transporting ATPase , rotational mechanism	-0.5073	-1.4	0.328298
YIL018W	RPL2B	structural constituent of ribosome	-0.5068	-1.4	0.045769
YOL038W	PRE6	endopeptidase	-0.5058	-1.4	0.0178029
YGR037C	ACB1	long-chain fatty acid transporter	-0.5038	-1.4	0.121755
YBL113C		helicase	-0.5020	-1.4	0.0549479
YDR134C		unknown	-0.5003	-1.4	0.0989924
YHR027C	RPN1	endopeptidase	-0.4963	-1.4	0.0531673
YDR300C	PRO1	glutamate 5-kinase	-0.4957	-1.4	0.0155524
YER072W	VTC1	unknown	-0.4933	-1.4	0.100826
YKR074W		unknown	-0.4923	-1.4	0.169534

Table 3: continued.

ORF ID	Gene Name	Gene Function	Avg Log_2 Ratio	Fold Change	T-test
YKL107W		unknown	-0.4913	-1.4	0.471983
YBR095C	RXT2	unknown	-0.4863	-1.4	0.0195059
YNL209W	SSB2	ATPase *	-0.4847	-1.4	0.042555
YNL151C	RPC31	DNA-directed RNA polymerase	-0.4830	-1.4	0.0393664
YGR235C		unknown	-0.4823	-1.4	0.0581392
YDR542W	PAU10	unknown	-0.4807	-1.4	0.0064604
YLR314C	CDC3	structural constituent of cytoskeleton*	-0.4807	-1.4	0.27661
YBR080C	SEC18	ATPase	-0.4805	-1.4	0.0162414
YOR027W	STI1	unfolded protein binding	-0.4797	-1.4	0.0921955
YJL161W	FMP33	unknown	-0.4790	-1.4	0.1197
YLL050C	COF1	protein binding	-0.4773	-1.4	0.0410656
YIL047C	SYG1	unknown	-0.4772	-1.4	0.219427
YJL159W	HSP150	structural constituent of cell wall	-0.4762	-1.4	0.0321015
YNL015W	PBI2	endopeptidase inhibitor	-0.4752	-1.4	0.648855
YJL121C	RPE1	ribulose-phosphate 3-epimerase	-0.4735	-1.4	0.0205524
YOR198C	BFR1	RNA binding	-0.4702	-1.4	0.0099157
YMR271C	URA10	orotate phosphoribosyltransferase	-0.4698	-1.4	0.052667
YJL210W	PEX2	protein binding	-0.4695	-1.4	0.0126098
YDR063W		unknown	-0.4670	-1.4	0.13161
YIL147C	SLN1	osmosensor *	-0.4657	-1.4	0.0022519
YPL091W	GLR1	glutathione-disulfide reductase	-0.4633	-1.4	0.0355704
YDR028C	REG1	protein phosphatase type 1 regulator	-0.4623	-1.4	0.025451
YHR001W	OSH7	oxysterol binding	-0.4612	-1.4	0.0819638
YDR512C	EMI1	unknown	-0.4607	-1.4	0.106574
YIR032C	DAL3	ureidoglycolate hydrolase	-0.4607	-1.4	0.0464308
YKR096W		unknown	-0.4577	-1.4	0.0077315
YFR039C		unknown	-0.4562	-1.4	0.180178
YER177W	BMH1	protein binding	-0.4548	-1.4	0.0616217
YLR258W	GSY2	glycogen (starch) synthase	-0.4548	-1.4	0.253974
YAL067C	SEO1	transporter	-0.4523	-1.4	0.0732858
YBR180W	DTR1	multidrug transporter	-0.4467	-1.4	0.0440688
YDR321W	ASP1	asparaginase	-0.4465	-1.4	0.0151755
YFR004W	RPN11	endopeptidase	-0.4443	-1.4	0.0214781
YIL176C	PAU14	unknown	-0.4425	-1.4	0.0757757
YEL047C		fumarate reductase (NADH)	-0.4418	-1.4	0.0369753
YBR224W			-0.4417	-1.4	0.122312
YOR196C	LIP5	lipoic acid synthase	-0.4412	-1.4	0.132005
YJL216C		alpha-galactosidase *	-0.4408	-1.4	0.0190883
YFR033C	QCR6	ubiquinol-cytochrome-c reductase	-0.4407	-1.4	0.0155085
YPL015C	HST2	NAD-dependent histone deacetylase	-0.4407	-1.4	0.0033929
YPR100W	MRPL51	structural constituent of ribosome	-0.4397	-1.4	0.0499669
YAL063C	FLO9	mannose binding	-0.4392	-1.4	0.0452028
YDR454C	GUK1	guanylate kinase	-0.4388	-1.4	0.0526079
YNL131W	TOM22	protein transporter	-0.4382	-1.4	0.0659353
YLR193C		unknown	-0.4380	-1.4	0.0005422
YBR234C	ARC40	structural constituent of cytoskeleton	-0.4370	-1.4	0.0397934
YOR141C	ARP8	unknown	-0.4368	-1.4	0.025171
YPL234C	TFP3	hydrogen-transporting ATPase , rotational mechanism	-0.4347	-1.4	0.182705
YCRX17W			-0.4318	-1.3	0.146365
YBR036C	CSG2	enzyme regulator	-0.4315	-1.3	0.108648
YNL121C	TOM70	protein transporter	-0.4307	-1.3	0.0039095
YEL044W	IES6	unknown	-0.4287	-1.3	0.0572575
YPL037C	EGD1	unfolded protein binding	-0.4283	-1.3	0.0148963
YGL210W	YPT32	GTPase	-0.4253	-1.3	0.112283
YLR429W	CRN1	protein binding	-0.4247	-1.3	0.0868638
YJL223C	PAU1	unknown	-0.4245	-1.3	0.0038577
YJR017C	ESS1	peptidyl-prolyl cis-trans isomerase	-0.4233	-1.3	0.0522744
YJL158C	CIS3	structural constituent of cell wall	-0.4225	-1.3	0.32418
YBR218C	PYC2	pyruvate carboxylase	-0.4223	-1.3	0.155177
YML008C	ERG6	sterol 24-C-methyltransferase	-0.4180	-1.3	0.0140024
YDR272W	GLO2	hydroxyacylglutathione hydrolase	-0.4172	-1.3	0.0705474
YOL030W	GAS5	1,3-beta-glucanosyltransferase	-0.4165	-1.3	0.0530601
YML055W	SPC2	protein binding	-0.4152	-1.3	0.0367222
YJL112W	MDV1	unknown	-0.4145	-1.3	0.0023037
YGR255C	COQ6	ubiquinone biosynthesis monooxygenase	-0.4122	-1.3	0.0146451
YLR149C		unknown	-0.4117	-1.3	0.0187874
YDL220C	CDC13	single-stranded DNA binding	-0.4092	-1.3	0.204353
YOR332W	VMA4	hydrogen-transporting ATPase , rotational mechanism	-0.4080	-1.3	0.0298209
YDR494W	RSM28	structural constituent of ribosome	-0.4078	-1.3	0.231802

Table 3: continued.

ORF ID	Gene Name	Gene Function	Avg Log_2 Ratio	Fold Change	T-test
YJL073W	JEM1	unfolded protein binding	-0.4065	-1.3	0.0172061
YMR008C	PLB1	lysophospholipase	-0.4058	-1.3	0.0436741
YPR188C	MLC2	myosin II binding	-0.4055	-1.3	0.15973
YAL049C		unknown	-0.4048	-1.3	0.0154981
YCL043C	PDI1	protein disulfide isomerase	-0.4033	-1.3	0.0204957
YCL017C	NFS1	cystathionine gamma-lyase *	-0.4025	-1.3	0.0820098
YNL079C	TPM1	actin lateral binding	-0.4023	-1.3	0.0002213
YER174C	GRX4	thiol-disulfide exchange intermediate	-0.4018	-1.3	0.0834665
YMR027W		unknown	-0.4007	-1.3	0.0303282
YOR008C	SLG1	transmembrane receptor	-0.4007	-1.3	0.12183
YBR047W	FMP23	unknown	-0.4002	-1.3	0.0768826
YCR077C	PAT1	unknown	-0.3997	-1.3	0.152069
YJL206C-A			-0.3988	-1.3	0.27333
YDR161W		unknown	-0.3982	-1.3	0.0124273
YDR027C	VPS54	unknown	-0.3968	-1.3	0.413022
YFR015C	GSY1	glycogen (starch) synthase	-0.3958	-1.3	0.295452
YPL087W	YDC1	ceramidase	-0.3950	-1.3	0.0612491
YAL068C	PAU8	unknown	-0.3932	-1.3	0.0152362
YGL003C	CDH1	enzyme activator	-0.3932	-1.3	0.0087865
YBR197C		unknown	-0.3928	-1.3	0.0273176
YIL150C	MCM10	chromatin binding	-0.3928	-1.3	0.193376
YNL022C		unknown	-0.3922	-1.3	0.0431623
YCL028W	RNQ1	unknown	-0.3903	-1.3	0.0402925
YGR044C	RME1	specific transcriptional repressor	-0.3897	-1.3	0.0137378
YJR133W	XPT1	xanthine phosphoribosyltransferase	-0.3897	-1.3	0.0138571
YOL120C	RPL18A	structural constituent of ribosome	-0.3892	-1.3	0.101527
YJL105W	SET4	unknown	-0.3853	-1.3	0.0464239
YIL094C	LYS12	homoisocitrate dehydrogenase	-0.3838	-1.3	0.068896
YBR158W	AMN1	protein binding	-0.3830	-1.3	0.136506
YHR121W	LSM12	RNA binding	-0.3812	-1.3	0.0055828
YCR102C		unknown	-0.3795	-1.3	0.0525116
YDR201W	SPC19	structural constituent of cytoskeleton	-0.3787	-1.3	0.0574842
YPR023C	EAF3	histone acetyltransferase	-0.3763	-1.3	0.0535381
YMR260C	TIF11	translation initiation factor	-0.3757	-1.3	0.051849
YBR082C	UBC4	ubiquitin conjugating enzyme	-0.3750	-1.3	0.101735
YLR055C	SPT8	transcription cofactor	-0.3750	-1.3	0.0440691
YIL156W	UBP7	ubiquitin-specific protease	-0.3705	-1.3	0.057431
YIL087C		unknown	-0.3703	-1.3	0.073208
YHR208W	BAT1	branched-chain-amino-acid transaminase	-0.3693	-1.3	0.0252525
YBR006W	UGA2	succinate-semialdehyde dehydrogenase [NAD(P)+]	-0.3687	-1.3	0.102173
YJR008W		unknown	-0.3680	-1.3	0.0023637
YDR150W	NUM1	tubulin binding	-0.3672	-1.3	0.123314
YBR269C	FMP21	unknown	-0.3663	-1.3	0.025059
YHL028W	WSC4	transmembrane receptor	-0.3620	-1.3	0.373484
YOR108W	LEU9	2-isopropylmalate synthase	-0.3613	-1.3	0.278176
YLR242C	ARV1	unknown	-0.3607	-1.3	0.0431188
YIL109C	SEC24	protein binding	-0.3532	-1.3	0.0583009
YCR049C			-0.3527	-1.3	0.129834
YMR325W	PAU19	unknown	-0.3527	-1.3	0.191408
YER052C	HOM3	aspartate kinase	-0.3517	-1.3	0.0395801
YDR109C		kinase	-0.3502	-1.3	0.0862926
YER094C	PUP3	endopeptidase	-0.3502	-1.3	0.199199
YJR064W	CCT5	unfolded protein binding	-0.3500	-1.3	0.189069
YBL002W	HTB2	DNA binding	-0.3490	-1.3	0.0963136
YGL112C	TAF6	general RNA polymerase II transcription factor	-0.3475	-1.3	0.0965273
YGR181W	TIM13	protein transporter	-0.3452	-1.3	0.291063
YEL002C	WBP1	dolichyl-diphosphooligosaccharide-protein glycotransferase	-0.3450	-1.3	0.020492
YIL086C			-0.3447	-1.3	0.0208902
YJL025W	RRN7	RNA polymerase I transcription factor	-0.3435	-1.3	0.524392
YLL013C	PUF3	mRNA binding	-0.3425	-1.3	0.0467786
YOR362C	PRE10	endopeptidase	-0.3385	-1.3	0.183092
YPL033C		unknown	-0.3342	-1.3	0.127051
YJL055W		unknown	-0.3335	-1.3	0.116933
YJL202C			-0.3333	-1.3	0.275421
YER022W	SRB4	RNA polymerase II transcription mediator	-0.3328	-1.3	0.296652
YHR009C		unknown	-0.3313	-1.3	0.013602
YER066C-A			-0.3308	-1.3	0.280224
YDL135C	RDI1	signal transducer	-0.3278	-1.3	0.0184586
YJL153C	INO1	inositol-3-phosphate synthase	-0.3277	-1.3	0.0728575

Table 3: continued.

ORF ID	Gene Name	Gene Function	Avg Log_2 Ratio	Fold Change	T-test
YHR026W	PPA1	hydrogen-transporting ATPase , rotational mechanism	-0.3270	-1.3	0.01885
YDR079W	PET100	unfolded protein binding	-0.3248	-1.3	0.12494
YPR004C		electron carrier	-0.3232	-1.3	0.0088409
YDR033W	MRH1	unknown	-0.3228	-1.3	0.129756
YJL070C		unknown	-0.3210	-1.2	0.0965442
YPR019W	CDC54	chromatin binding	-0.3208	-1.2	0.0691866
YDR394W	RPT3	ATPase *	-0.3200	-1.2	0.0142985
YIL005W	EPS1	protein disulfide isomerase	-0.3187	-1.2	0.0147456
YBR132C	AGP2	amino acid transporter	-0.3160	-1.2	0.0530281
YEL046C	GLY1	threonine aldolase	-0.3110	-1.2	0.0473239
YDR133C			-0.3107	-1.2	0.245479
YCR087W			-0.3103	-1.2	0.328557
YCR104W	PAU3	unknown	-0.3093	-1.2	0.463135
YDL086W		carboxymethylenebutenolidase	-0.3058	-1.2	0.108362
YDR320C	SWA2	protein binding	-0.3053	-1.2	0.129512
YBR090C		unknown	-0.3045	-1.2	0.0116947
YHR217C			-0.3043	-1.2	0.0116195
YGL073W	HSF1	transcription factor	-0.3038	-1.2	0.14289
YMR311C	GLC8	enzyme activator	-0.3027	-1.2	0.0116322
YGL147C	RPL9A	structural constituent of ribosome	-0.3020	-1.2	0.121024
YDR059C	UBC5	ubiquitin conjugating enzyme	-0.3007	-1.2	0.128747
YLR048W	RPS0B	structural constituent of ribosome	-0.2995	-1.2	0.018032
YIL098C	FMC1	unknown	-0.2973	-1.2	0.236249
YLR102C	APC9	protein binding	-0.2965	-1.2	0.213915
YBR227C	MCX1	unfolded protein binding	-0.2962	-1.2	0.204366
YDR255C	RMD5	unknown	-0.2952	-1.2	0.0875604
YNL138W	SRV2	cytoskeletal protein binding	-0.2920	-1.2	0.100936
YOR383C	FIT3	unknown	-0.2915	-1.2	0.411951
YDL178W	DLD2	actin binding	-0.2910	-1.2	0.454079
YPR090W			-0.2907	-1.2	0.0998667
YAL005C	SSA1	ATPase *	-0.2905	-1.2	0.286351
YBR222C	PCS60	AMP binding	-0.2898	-1.2	0.0200898
YGR008C	STF2	unknown	-0.2895	-1.2	0.0064264
YPL094C	SEC62	protein binding	-0.2893	-1.2	0.095558
YIL162W	SUC2	beta-fructofuranosidase	-0.2890	-1.2	0.113941
YFR017C		unknown	-0.2887	-1.2	0.189414
YGR135W	PRE9	endopeptidase	-0.2868	-1.2	0.201021
YOR374W	ALD4	aldehyde dehydrogenase (NAD)	-0.2868	-1.2	0.0791755
YGR232W	NAS6	unknown	-0.2867	-1.2	0.0187189
YLR299W	ECM38	protein-glutamine gamma-glutamyltransferase	-0.2863	-1.2	0.187261
YMR100W	MUB1	unknown	-0.2858	-1.2	0.0711819
YMR196W		unknown	-0.2837	-1.2	0.277547
YNL268W	LYP1	basic amino acid transporter	-0.2835	-1.2	0.426689
YGR209C	TRX2	thiol-disulfide exchange intermediate	-0.2827	-1.2	0.189644
YNL104C	LEU4	2-isopropylmalate synthase	-0.2812	-1.2	0.0032684
YER057C	HMF1	unknown	-0.2803	-1.2	0.281469
YOL078W	AVO1	unknown	-0.2793	-1.2	0.0549599
YKR051W		unknown	-0.2775	-1.2	0.0474545
YPL106C	SSE1	ATP binding	-0.2773	-1.2	0.126718
YFL004W	VTC2	unknown	-0.2747	-1.2	0.195109
YBR245C	ISW1	ATPase	-0.2737	-1.2	0.05567
YDL130W	RPP1B	structural constituent of ribosome	-0.2732	-1.2	0.106492
YGL056C	SDS23	unknown	-0.2723	-1.2	0.0126981
YBR262C	FMP51	unknown	-0.2708	-1.2	0.0120791
YJL166W	QCR8	ubiquinol-cytochrome-c reductase	-0.2697	-1.2	0.0387817
YLR204W	QRI5	unknown	-0.2695	-1.2	0.199011
YPL190C	NAB3	poly(A) binding	-0.2685	-1.2	0.131304
YDL184C	RPL41A	structural constituent of ribosome	-0.2672	-1.2	0.191252
YBR164C	ARL1	GTPase	-0.2667	-1.2	0.160548
YJL167W	ERG20	dimethylallyltranstransferase *	-0.2667	-1.2	0.0354019
YBR102C	EXO84	protein binding	-0.2665	-1.2	0.139396
YCL051W	LRE1	transcription regulator *	-0.2625	-1.2	0.54067
YJL115W	ASF1	transcription regulator *	-0.2602	-1.2	0.370579
YPL177C	CUP9	specific RNA polymerase II transcription factor	-0.2598	-1.2	0.0465961
YGR193C	PDX1	protein binding	-0.2577	-1.2	0.12853
YML100W	TSL1	enzyme regulator *	-0.2568	-1.2	0.370253
YGR189C	CRH1	unknown	-0.2565	-1.2	0.137615
YGL108C		unknown	-0.2552	-1.2	0.132556
YDR329C	PEX3	protein binding	-0.2523	-1.2	0.125236

Table 3: continued.

ORF ID	Gene Name	Gene Function	Avg Log_2 Ratio	Fold Change	T-test
YMR043W	MCM1	DNA binding	-0.2513	-1.2	0.0104057
YPR002W	PDH1	unknown	-0.2512	-1.2	0.0285461
YLR340W	RPP0	structural constituent of ribosome	-0.2507	-1.2	0.12604
YIL138C	TPM2	actin lateral binding	-0.2503	-1.2	0.136127
YML103C	NUP188	structural molecule	-0.2503	-1.2	0.47276
YCL037C	SRO9	RNA binding	-0.2495	-1.2	0.670089
YDR091C	RLI1	ATPase *	-0.2487	-1.2	0.0577111
YIL160C	POT1	acetyl-CoA C-acyltransferase	-0.2480	-1.2	0.290992
YBL027W	RPL19B	structural constituent of ribosome	-0.2478	-1.2	0.288063
YPL040C	ISM1	isoleucine-tRNA ligase	-0.2468	-1.2	0.404087
YBR202W	CDC47	chromatin binding	-0.2465	-1.2	0.0574305
YIL084C	SDS3	protein binding	-0.2452	-1.2	0.196977
YGL019W	CKB1	protein kinase	-0.2447	-1.2	0.184944
YNL160W	YGP1	unknown	-0.2443	-1.2	0.296927
YEL027W	CUP5	hydrogen ion transporter	-0.2412	-1.2	0.0395769
YLR043C	TRX1	thiol-disulfide exchange intermediate	-0.2412	-1.2	0.368864
YIL088C	AVT7	transporter	-0.2407	-1.2	0.151876
YKL058W	TOA2	general RNA polymerase II transcription factor	-0.2397	-1.2	0.181891
YPL085W	SEC16	structural molecule	-0.2387	-1.2	0.711948
YBR184W		unknown	-0.2375	-1.2	0.540746
YDR080W	VPS41	Rab guanyl-nucleotide exchange factor	-0.2368	-1.2	0.0940768
YBR147W		unknown	-0.2363	-1.2	0.313067
YCL027W	FUS1	unknown	-0.2353	-1.2	0.0037438
YCL056C		unknown	-0.2347	-1.2	0.204913
YBR216C	YBP1	unknown	-0.2323	-1.2	0.185157
YGL219C	MDM34	unknown	-0.2323	-1.2	0.0003069
YHR129C	ARP1	structural constituent of cytoskeleton	-0.2320	-1.2	0.687546
YPR108W	RPN7	structural molecule	-0.2313	-1.2	0.0626768
YER002W	NOP16	unknown	-0.2297	-1.2	0.0468075
YDR115W		structural constituent of ribosome	-0.2267	-1.2	0.118588
YLR247C		helicase	-0.2267	-1.2	0.120682
YER035W	EDC2	RNA binding	-0.2262	-1.2	0.0925406
YDR427W	RPN9	structural molecule	-0.2262	-1.2	0.0070353
YJL123C		unknown	-0.2245	-1.2	0.179128
YAL013W	DEP1	transcription regulator	-0.2237	-1.2	0.265207
YHR131C		unknown	-0.2233	-1.2	0.203873
YER119C	AVT6	amino acid transporter	-0.2232	-1.2	0.0782718
YOR239W	ABP140	S-adenosylmethionine-dependent methyltransferase *	-0.2205	-1.2	0.0022359
YGL104C	VPS73	unknown	-0.2202	-1.2	0.480298
YBR237W	PRP5	RNA splicing factor , transesterification mechanism*	-0.2197	-1.2	0.0681174
YNL125C	ESBP6	transporter	-0.2195	-1.2	0.324223
YBR017C	KAP104	nuclear localization sequence binding	-0.2192	-1.2	0.23811
YHR215W	PHO12	acid phosphatase	-0.2125	-1.2	0.02025
YJL209W	CBP1	mRNA binding	-0.2113	-1.2	0.451795
YCL033C		protein-methionine-R-oxide reductase	-0.2110	-1.2	0.0413544
YLR355C	ILV5	ketol-acid reductoisomerase	-0.2095	-1.2	0.176056
YGR284C	ERV29	unknown	-0.2050	-1.2	0.0496765
YMR295C		unknown	-0.2050	-1.2	0.182676
YER158C		unknown	-0.2048	-1.2	0.256225
YEL051W	VMA8	hydrogen-transporting ATPase , rotational mechanism	-0.2042	-1.2	0.0897327
YMR135C	GID8	unknown	-0.2032	-1.2	0.419044
YDR169C	STB3	unknown	-0.2025	-1.2	0.389068
YMR233W		unknown	-0.2003	-1.1	0.123669
YBR261C		S-adenosylmethionine-dependent methyltransferase	-0.1990	-1.1	0.323767
YLR216C	CPR6	unfolded protein binding	-0.1990	-1.1	0.121774
YER063W	THO1	unknown	-0.1972	-1.1	0.115254
YDR116C	MRPL1	structural constituent of ribosome	-0.1962	-1.1	0.217686
YAL003W	EFB1	translation elongation factor	-0.1957	-1.1	0.18672
YDR481C	PHO8	alkaline phosphatase	-0.1948	-1.1	0.17067
YGL031C	RPL24A	structural constituent of ribosome*	-0.1920	-1.1	0.150615
YHR025W	THR1	homoserine kinase	-0.1917	-1.1	0.112021
YMR264W	CUE1	protein binding	-0.1915	-1.1	0.357225
YDR232W	HEM1	5-aminolevulinate synthase	-0.1912	-1.1	0.0846545
YKL204W	EAP1	eukaryotic initiation factor 4E binding	-0.1885	-1.1	0.372457
YOR197W	MCA1	caspase	-0.1880	-1.1	0.0302436
YEL053C	MAK10	peptide alpha-N-acetyltransferase	-0.1852	-1.1	0.297628
YPL093W	NOG1	GTP binding	-0.1830	-1.1	0.494304
YCR026C	NPP1	nucleoside-triphosphatase *	-0.1822	-1.1	0.329519
YDR517W	GRH1	unknown	-0.1822	-1.1	0.240009

Table 3: continued.

ORF ID	Gene Name	Gene Function	Avg Log_2 Ratio	Fold Change	T-test
YGL059W		protein kinase	-0.1818	-1.1	0.0240171
YHR200W	RPN10	endopeptidase	-0.1792	-1.1	0.328357
YPL105C		unknown	-0.1782	-1.1	0.13231
YGR180C	RNR4	ribonucleoside-diphosphate reductase	-0.1768	-1.1	0.23795
YBR137W		unknown	-0.1752	-1.1	0.0905536
YCL001W	RER1	unknown	-0.1748	-1.1	0.396328
YJL124C	LSM1	RNA binding	-0.1743	-1.1	0.492226
YPL271W	ATP15	hydrogen-transporting ATP synthase , rotational mechanism	-0.1737	-1.1	0.666933
YLR436C	ECM30	unknown	-0.1733	-1.1	0.663404
YJR005W	APL1	unknown	-0.1725	-1.1	0.617463
YNL067W	RPL9B	structural constituent of ribosome	-0.1718	-1.1	0.259672
YPL259C	APM1	clathrin binding	-0.1708	-1.1	0.0661125
YJL095W	BCK1	MAP kinase	-0.1700	-1.1	0.0708709
YBR151W	APD1	unknown	-0.1675	-1.1	0.300384
YJL026W	RNR2	ribonucleoside-diphosphate reductase	-0.1673	-1.1	0.210331
YNL102W	POL1	alpha DNA polymerase	-0.1663	-1.1	0.285585
YBR250W		unknown	-0.1653	-1.1	0.286503
YFL010C	WWM1	unknown	-0.1650	-1.1	0.0138209
YMR241W	YHM2	DNA binding	-0.1632	-1.1	0.019435
YIR014W		unknown	-0.1625	-1.1	0.308478
YJL129C	TRK1	potassium ion transporter	-0.1607	-1.1	0.44731
YLR350W	ORM2	unknown	-0.1598	-1.1	0.301149
YNL241C	ZWF1	glucose-6-phosphate 1-dehydrogenase	-0.1588	-1.1	0.0377215
YLR064W		unknown	-0.1582	-1.1	0.482771
YER060W-A	FCY22	cytosine-purine permease	-0.1567	-1.1	0.43332
YKR049C	FMP46	oxidoreductase	-0.1552	-1.1	0.493468
YIR007W		unknown	-0.1530	-1.1	0.235529
YNL245C	CWC25	unknown	-0.1515	-1.1	0.111736
YBR118W	TEF2	translation elongation factor	-0.1512	-1.1	0.512129
YBR149W	ARA1	aldo-keto reductase *	-0.1512	-1.1	0.693718
YDL173W		unknown	-0.1507	-1.1	0.169142
YPL203W	TPK2	protein serine/threonine kinase	-0.1505	-1.1	0.136663
YBR101C	FES1	adenyl-nucleotide exchange factor	-0.1502	-1.1	0.286266
YDL014W	NOP1	methyltransferase	-0.1498	-1.1	0.165326
YHR089C	GAR1	RNA binding	-0.1497	-1.1	0.570321
YGL150C	INO80	ATPase *	-0.1493	-1.1	0.215053
YCL052C	PBN1	mannosyltransferase	-0.1482	-1.1	0.402806
YER142C	MAG1	alkylbase DNA N-glycosylase	-0.1482	-1.1	0.523804
YOR261C	RPN8	unknown	-0.1478	-1.1	0.413071
YPL240C	HSP82	ATPase , coupled	-0.1437	-1.1	0.140038
YHR194W	MDM31	unknown	-0.1422	-1.1	0.26376
YIL154C	IMP2'	transcription coactivator	-0.1415	-1.1	0.0942467
YIL062C	ARC15	structural molecule *	-0.1410	-1.1	0.200793
YJL156C	SSY5	amino acid binding	-0.1393	-1.1	0.484104
YJR127C	RSF2	transcription factor	-0.1392	-1.1	0.130358
YEL012W	UBC8	ubiquitin conjugating enzyme	-0.1370	-1.1	0.192647
YLR190W	MMR1	unknown	-0.1348	-1.1	0.107811
YLR437C		unknown	-0.1348	-1.1	0.444345
YGR155W	CYS4	cystathionine beta-synthase	-0.1345	-1.1	0.184863
YJL137C	GLG2	glycogenin glucosyltransferase	-0.1342	-1.1	0.292176
YKR062W	TFA2	general RNA polymerase II transcription factor	-0.1337	-1.1	0.121212
YJR104C	SOD1	copper, zinc superoxide dismutase	-0.1328	-1.1	0.229208
YOR327C	SNC2	v-SNARE	-0.1327	-1.1	0.240595
YDR156W	RPA14	DNA-directed RNA polymerase	-0.1325	-1.1	0.283442
YKL064W	MNR2	magnesium ion transporter	-0.1312	-1.1	0.334449
YKR059W	TIF1	translation initiation factor	-0.1308	-1.1	0.399465
YJL151C	SNA3	unknown	-0.1260	-1.1	0.349272
YAL039C	CYC3	holocytochrome-c synthase	-0.1255	-1.1	0.226222
YBR240C	THI2	transcriptional activator	-0.1247	-1.1	0.184372
YJR105W	ADO1	adenosine kinase	-0.1243	-1.1	0.258849
YAL061W		oxidoreductase	-0.1230	-1.1	0.396
YLR005W	SSL1	general RNA polymerase II transcription factor	-0.1218	-1.1	0.716853
YGL084C	GUP1	O-acyltransferase	-0.1203	-1.1	0.117724
YGR236C	SPG1	unknown	-0.1203	-1.1	0.0253991
YBR053C		unknown	-0.1200	-1.1	0.0275542
YFL018W-A			-0.1197	-1.1	0.295279
YAL011W	SWC3	unknown	-0.1187	-1.1	0.589352
YBR156C	SLI15	protein kinase	-0.1182	-1.1	0.238679
YML048W	GSF2	unknown	-0.1178	-1.1	0.41546

Table 3: continued.

ORF ID	Gene Name	Gene Function	Avg Log_2 Ratio	Fold Change	T-test
YDR128W		unknown	-0.1167	-1.1	0.19689
YBL050W	SEC17	soluble NSF attachment protein	-0.1165	-1.1	0.572066
YDR378C	LSM6	RNA binding	-0.1165	-1.1	0.192762
YLR192C	HCR1	translation initiation factor *	-0.1165	-1.1	0.713732
YHR096C	HXT5	glucose transporter	-0.1163	-1.1	0.674733
YIL046W	MET30	protein binding	-0.1155	-1.1	0.652273
YBR204C		serine hydrolase	-0.1143	-1.1	0.615932
YGR285C	ZUO1	unfolded protein binding	-0.1133	-1.1	0.136678
YBR059C	AKL1	protein kinase	-0.1132	-1.1	0.465755
YHR158C	KEL1	unknown	-0.1123	-1.1	0.896318
YDR382W	RPP2B	structural constituent of ribosome	-0.1120	-1.1	0.190768
YGL011C	SCL1	endopeptidase	-0.1110	-1.1	0.507073
YHR179W	OYE2	NADPH dehydrogenase	-0.1105	-1.1	0.317048
YIL050W	PCL7	cyclin-dependent protein kinase	-0.1103	-1.1	0.363737
YPR062W	FCY1	cytosine deaminase	-0.1088	-1.1	0.0745763
YAL035W	FUN12	GTPase *	-0.1080	-1.1	0.326953
YDL156W		unknown	-0.1058	-1.1	0.216533
YIL142W	CCT2	unfolded protein binding	-0.1055	-1.1	0.202652
YDR179W-A		unknown	-0.1052	-1.1	0.131808
YJL138C	TIF2	translation initiation factor *	-0.1033	-1.1	0.319223
YNL208W		unknown	-0.1025	-1.1	0.523182
YOR185C	GSP2	GTPase	-0.1018	-1.1	0.0915285
YKL013C	ARC19	structural molecule	-0.1008	-1.1	0.271515
YBR238C		unknown	-0.0993	-1.1	0.267861
YGL197W	MDS3	unknown	-0.0983	-1.1	0.849497
YBR159W	IFA38	ketoreductase	-0.0977	-1.1	0.844389
YOR286W	FMP31	unknown	-0.0977	-1.1	0.476641
YPL090C	RPS6A	structural constituent of ribosome	-0.0935	-1.1	0.235743
YOR015W			-0.0920	-1.1	0.656495
YJL101C	GSH1	glutamate-cysteine ligase	-0.0905	-1.1	0.164251
YBR255W		unknown	-0.0897	-1.1	0.576046
YJR085C		unknown	-0.0890	-1.1	0.556205
YHR192W		unknown	-0.0882	-1.1	0.570074
YBR247C	ENP1	snoRNA binding	-0.0872	-1.1	0.773009
YNL056W	OCA2	unknown	-0.0872	-1.1	0.136971
YBR200W	BEM1	protein binding	-0.0868	-1.1	0.371361
YMR302C	YME2	exonuclease	-0.0868	-1.1	0.684504
YCL008C	STP22	protein binding	-0.0863	-1.1	0.32417
YOL016C	CMK2	calcium- and calmodulin-dependent protein kinase	-0.0858	-1.1	0.692862
YPL111W	CAR1	zinc ion binding	-0.0852	-1.1	0.406608
YDR497C	ITR1	myo-inositol transporter	-0.0847	-1.1	0.415047
YIL085C	KTR7	mannosyltransferase	-0.0842	-1.1	0.47342
YJR024C		unknown	-0.0820	-1.1	0.195425
YBR069C	TAT1	amino acid transporter	-0.0765	-1.1	0.686578
YBR070C	ALG14	N-acetylglucosaminyldiphosphodolichol N-acetylglucosaminyl	-0.0758	-1.1	0.459492
YOR123C	LEO1	RNA polymerase II transcription elongation factor	-0.0752	-1.1	0.13178
YDL095W	PMT1	dolichyl-phosphate-mannose-protein mannosyltransferase	-0.0738	-1.1	0.483306
YBR272C	HSM3	unknown	-0.0737	-1.1	0.69541
YDR208W	MSS4	1-phosphatidylinositol-4-phosphate 5-kinase	-0.0698	-1.0	0.123837
YKR097W	PCK1	phosphoenolpyruvate carboxykinase	-0.0695	-1.0	0.394403
YDR358W	GGA1	ubiquitin binding	-0.0693	-1.0	0.610278
YCR018C	SRD1	unknown	-0.0665	-1.0	0.642644
YJL113W			-0.0652	-1.0	0.7457
YJL221C	FSP2	alpha-glucosidase	-0.0638	-1.0	0.821865
YCRX13W			-0.0627	-1.0	0.153112
YJL016W		unknown	-0.0618	-1.0	0.748095
YBR223C	TDP1	tyrosyl-DNA phosphodiesterase	-0.0590	-1.0	0.829929
YER067W		unknown	-0.0588	-1.0	0.656957
YBR111C	YSA1	phosphoribosyl-ATP diphosphatase	-0.0567	-1.0	0.326224
YHR193C	EGD2	unfolded protein binding	-0.0562	-1.0	0.813478
YMR186W	HSC82	unfolded protein binding	-0.0558	-1.0	0.571664
YKL100C		unknown	-0.0547	-1.0	0.83955
YBR259W		unknown	-0.0543	-1.0	0.451349
YDR056C		unknown	-0.0533	-1.0	0.367201
YIL068C	SEC6	protein binding	-0.0523	-1.0	0.510106
YBR252W	DUT1	dUTP diphosphatase	-0.0513	-1.0	0.757945
YNL147W	LSM7	RNA binding	-0.0510	-1.0	0.402097
YMR230W	RPS10B	structural constituent of ribosome	-0.0503	-1.0	0.631628
YOL032W	OPI10	unknown	-0.0500	-1.0	0.223904

Table 3: continued.

ORF ID	Gene Name	Gene Function	Avg Log_2 Ratio	Fold Change	T-test
YBR057C	MUM2	unknown	-0.0497	-1.0	0.692495
YNL126W	SPC98	structural constituent of cytoskeleton	-0.0475	-1.0	0.726938
YAL029C	MYO4	microfilament motor	-0.0472	-1.0	0.916709
YIL158W		unknown	-0.0470	-1.0	0.702289
YGR118W	RPS23A	structural constituent of ribosome	-0.0463	-1.0	0.400155
YBR198C	TAF5	general RNA polymerase II transcription factor	-0.0458	-1.0	0.302126
YIL130W	ASG1	unknown	-0.0458	-1.0	0.664978
YKR075C		unknown	-0.0440	-1.0	0.7065
YML063W	RPS1B	structural constituent of ribosome	-0.0437	-1.0	0.814976
YLR345W		6-phosphofructo-2-kinase	-0.0427	-1.0	0.612659
YMR020W	FMS1	amine oxidase	-0.0423	-1.0	0.61925
YML073C	RPL6A	structural constituent of ribosome*	-0.0420	-1.0	0.544518
YBR170C	NPL4	unknown	-0.0407	-1.0	0.77877
YNR021W		unknown	-0.0372	-1.0	0.601968
YIL076W	SEC28	unknown	-0.0362	-1.0	0.851407
YMR061W	RNA14	RNA binding	-0.0357	-1.0	0.747233
YFL008W	SMC1	ATPase *	-0.0355	-1.0	0.807287
YER054C	GIP2	protein phosphatase regulator	-0.0343	-1.0	0.738647
YBR126C	TPS1	alpha,alpha-trehalose-phosphate synthase (UDP-forming)	-0.0327	-1.0	0.29786
YBR302C	COS2	unknown	-0.0327	-1.0	0.870826
YCRX02C			-0.0307	-1.0	0.764771
YAL002W	VPS8	unknown	-0.0302	-1.0	0.618338
YIL041W	GVP36	unknown	-0.0282	-1.0	0.623516
YBL095W		unknown	-0.0275	-1.0	0.823013
YKL198C	PTK1	protein kinase	-0.0273	-1.0	0.8231
YEL016C	NPP2	nucleoside-triphosphatase *	-0.0267	-1.0	0.727216
YER117W	RPL23B	structural constituent of ribosome	-0.0263	-1.0	0.730651
YCL035C	GRX1	thiol-disulfide exchange intermediate *	-0.0245	-1.0	0.901073
YGR138C	TPO2	spermine transporter	-0.0225	-1.0	0.888756
YMR273C	ZDS1	protein binding	-0.0192	-1.0	0.886538
YKL086W	SRX1	oxidoreductase	-0.0190	-1.0	0.971947
YDL147W	RPN5	unknown	-0.0173	-1.0	0.846439
YOR080W	DIA2	DNA replication origin binding	-0.0165	-1.0	0.702658
YDL213C	NOP6	unknown	-0.0145	-1.0	0.881505
YMR188C	MRPS17	structural constituent of ribosome	-0.0140	-1.0	0.930087
YBR236C	ABD1	mRNA (guanine-N7-)-methyltransferase	-0.0133	-1.0	0.887663
YER073W	ALD5	3-chloroallyl aldehyde dehydrogenase	-0.0123	-1.0	0.899672
YDR444W		unknown	-0.0120	-1.0	0.977128
YBR207W	FTH1	iron ion transporter	-0.0117	-1.0	0.54532
YKL116C	PRR1	receptor signaling protein serine/threonine kinase	-0.0097	-1.0	0.925469
YKL211C	TRP3	anthranilate synthase *	-0.0093	-1.0	0.971409
YLR381W	CTF3	protein binding	-0.0093	-1.0	0.948143
YCR023C		unknown	-0.0050	-1.0	0.973556
YER131W	RPS26B	structural constituent of ribosome	-0.0038	-1.0	0.973754
YLR160C	ASP3-4	asparaginase	-0.0025	-1.0	0.975087
YBR210W	ERV15	unknown	-0.0023	-1.0	0.990589
YHR120W	MSH1	ATP binding	-0.0022	-1.0	0.99433
YGR196C	FYV8	unknown	0.0002	1.0	0.996927
YLR447C	VMA6	hydrogen-transporting ATPase , rotational mechanism	0.0003	1.0	0.973757
YBL066C	SEF1	unknown	0.0013	1.0	0.998359
YOR375C	GDH1	glutamate dehydrogenase (NADP+)	0.0013	1.0	0.992311
YBR188C	NTC20	RNA splicing factor , transesterification mechanism	0.0015	1.0	0.983857
YDR514C		unknown	0.0022	1.0	0.992061
YBR035C	PDX3	pyridoxamine-phosphate oxidase	0.0030	1.0	0.978258
YAL030W	SNC1	v-SNARE	0.0035	1.0	0.817056
YCL019W			0.0037	1.0	0.983595
YJL059W	YHC3	basic amino acid transporter	0.0038	1.0	0.94726
YBR072W	HSP26	unfolded protein binding	0.0040	1.0	0.963297
YOR063W	RPL3	structural constituent of ribosome	0.0040	1.0	0.915429
YDR127W	ARO1	3-dehydroquinate dehydratase *	0.0042	1.0	0.931692
YJL111W	CCT7	unfolded protein binding	0.0045	1.0	0.941228
YMR148W		unknown	0.0050	1.0	0.987813
YOR089C	VPS21	GTPase	0.0067	1.0	0.968212
YIR031C	DAL7	malate synthase	0.0068	1.0	0.952106
YBR009C	HHF1	DNA binding	0.0078	1.0	0.952965
YBR286W	APE3	aminopeptidase	0.0093	1.0	0.361603
YLR155C	ASP3-1	asparaginase	0.0093	1.0	0.883431
YCR009C	RVS161	cytoskeletal protein binding	0.0113	1.0	0.913926
YDL232W	OST4	protein binding	0.0115	1.0	0.932106

Table 3: continued.

ORF ID	Gene Name	Gene Function	Avg Log_2 Ratio	Fold Change	T-test
YJL225C		helicase	0.0148	1.0	0.896168
YKL056C	TMA19	unknown	0.0150	1.0	0.825276
YFL006W			0.0165	1.0	0.936657
YBR120C	CBP6	unknown	0.0167	1.0	0.909303
YLR448W	RPL6B	structural constituent of ribosome*	0.0182	1.0	0.929721
YJL071W	ARG2	amino-acid N-acetyltransferase	0.0197	1.0	0.901738
YJL021C			0.0200	1.0	0.764018
YIL059C			0.0215	1.0	0.752012
YBR232C			0.0217	1.0	0.907517
YHR195W	NVJ1	protein binding	0.0220	1.0	0.849372
YIR026C	YVH1	protein tyrosine phosphatase *	0.0225	1.0	0.953713
YIL097W	FYV10	unknown	0.0227	1.0	0.797355
YOL039W	RPP2A	structural constituent of ribosome	0.0240	1.0	0.798216
YBR125C	PTC4	protein phosphatase type 2C	0.0257	1.0	0.867112
YDL097C	RPN6	structural molecule	0.0258	1.0	0.851374
YHL021C	FMP12	unknown	0.0267	1.0	0.741442
YIR008C	PRI1	alpha DNA polymerase	0.0277	1.0	0.874719
YBR073W	RDH54	DNA-dependent ATPase *	0.0283	1.0	0.69516
YNL031C	HHT2	DNA binding	0.0305	1.0	0.814157
YIL143C	SSL2	general RNA polymerase II transcription factor *	0.0308	1.0	0.779992
YLR375W	STP3	unknown	0.0333	1.0	0.571388
YNL149C	PGA2	unknown	0.0335	1.0	0.782749
YDL075W	RPL31A	structural constituent of ribosome	0.0347	1.0	0.555455
YGR098C	ESP1	cysteine-type endopeptidase	0.0348	1.0	0.925403
YBR010W	HHT1	DNA binding	0.0360	1.0	0.863754
YEL020C		unknown	0.0385	1.0	0.790251
YBR100W			0.0405	1.0	0.865627
YER043C	SAH1	adenosylhomocysteinase	0.0430	1.0	0.676812
YHR178W	STB5	transcription factor	0.0432	1.0	0.597239
YHR198C	FMP22	unknown	0.0438	1.0	0.698314
YDL081C	RPP1A	structural constituent of ribosome	0.0443	1.0	0.894563
YFR016C		unknown	0.0443	1.0	0.783366
YAL054C	ACS1	acetate-CoA ligase	0.0445	1.0	0.853367
YOL027C	MDM38	unknown	0.0470	1.0	0.580167
YMR044W	IOC4	protein binding	0.0487	1.0	0.699442
YNL197C	WHI3	RNA binding	0.0493	1.0	0.752765
YLR157C	ASP3-2	asparaginase	0.0513	1.0	0.559126
YGL221C	NIF3	unknown	0.0517	1.0	0.884325
YIL177C		helicase	0.0523	1.0	0.712893
YPR043W	RPL43A	structural constituent of ribosome	0.0528	1.0	0.5684
YOR053W			0.0530	1.0	0.519903
YIL146C	ECM37	unknown	0.0538	1.0	0.70498
YBL058W	SHP1	protein phosphatase type 1 regulator	0.0540	1.0	0.652117
YIL036W	CST6	specific RNA polymerase II transcription factor	0.0558	1.0	0.625373
YDL234C	GYP7	Rab GTPase activator	0.0567	1.0	0.620932
YJL176C	SWI3	general RNA polymerase II transcription factor	0.0570	1.0	0.149109
YIL026C	IRR1	protein binding	0.0572	1.0	0.790645
YJL149W		unknown	0.0572	1.0	0.784475
YIL090W	ICE2	unknown	0.0573	1.0	0.815598
YBR134W			0.0583	1.0	0.717538
YKL180W	RPL17A	structural constituent of ribosome	0.0588	1.0	0.713634
YCR107W	AAD3	aryl-alcohol dehydrogenase	0.0595	1.0	0.723654
YOR315W	SFG1	specific RNA polymerase II transcription factor	0.0608	1.0	0.882602
YBR079C	RPG1	translation initiation factor	0.0623	1.0	0.849129
YPL235W	RVB2	ATPase *	0.0623	1.0	0.636872
YLL019C	KNS1	protein serine/threonine kinase	0.0632	1.0	0.731721
YNL115C		unknown	0.0638	1.0	0.400503
YNL305C		unknown	0.0643	1.0	0.625113
YBR203W	COS111	unknown	0.0650	1.0	0.830386
YGR148C	RPL24B	structural constituent of ribosome*	0.0650	1.0	0.592386
YPR042C	PUF2	mRNA binding	0.0662	1.0	0.709883
YPR148C		unknown	0.0662	1.0	0.197285
YFL007W	BLM10	proteasome activator	0.0673	1.0	0.788506
YOR285W		unknown	0.0678	1.0	0.564548
YKL171W		protein kinase	0.0680	1.0	0.85326
YCL050C	APA1	bis(5'-nucleosyl)-tetraphosphatase	0.0682	1.0	0.698987
YAL053W	FLC2	unknown	0.0683	1.0	0.867804
YJL110C	GZF3	transcription factor *	0.0688	1.0	0.559607
YGL227W	VID30	unknown	0.0708	1.1	0.0128979

Table 3: continued.

ORF ID	Gene Name	Gene Function	Avg Log_2 Ratio	Fold Change	T-test
YBR176W	ECM31	3-methyl-2-oxobutanoate hydroxymethyltransferase	0.0718	1.1	0.239951
YAR014C	BUD14	protein phosphatase type 1 regulator	0.0735	1.1	0.31085
YFL021C-A			0.0735	1.1	0.291533
YKR002W	PAP1	polynucleotide adenylyltransferase	0.0742	1.1	0.83087
YOR194C	TOA1	general RNA polymerase II transcription factor	0.0742	1.1	0.366512
YCR051W		unknown	0.0767	1.1	0.691641
YGL189C	RPS26A	structural constituent of ribosome	0.0767	1.1	0.392322
YNL016W	PUB1	mRNA binding	0.0792	1.1	0.523818
YDR330W	UBX5	unknown	0.0808	1.1	0.481804
YOL026C	MIM1	unknown	0.0813	1.1	0.241457
YCL016C	DCC1	unknown	0.0815	1.1	0.429242
YOR372C	NDD1	transcriptional activator	0.0820	1.1	0.510075
YEL001C		unknown	0.0827	1.1	0.439822
YJR074W	MOG1	Ran GTPase binding	0.0833	1.1	0.376654
YPL260W		unknown	0.0850	1.1	0.533537
YBR177C	EHT1	serine hydrolase	0.0873	1.1	0.206581
YIL112W	HOS4	NAD-dependent histone deacetylase *	0.0878	1.1	0.336896
YBL101C	ECM21	unknown	0.0880	1.1	0.130741
YAL056W	GPB2	signal transducer	0.0887	1.1	0.581451
YAL016W	TPD3	protein phosphatase type 2A	0.0898	1.1	0.558172
YBR181C	RPS6B	structural constituent of ribosome	0.0905	1.1	0.0788305
YCL042W		unknown	0.0910	1.1	0.652731
YPL219W	PCL8	cyclin-dependent protein kinase	0.0918	1.1	0.143769
YGR117C		unknown	0.0930	1.1	0.482923
YOR043W	WHI2	phosphatase activator	0.0932	1.1	0.563934
YKR042W	UTH1	unknown	0.0937	1.1	0.695054
YDR418W	RPL12B	structural constituent of ribosome	0.0938	1.1	0.520595
YBR175W	SWD3	histone lysine N-methyltransferase (H3-K4 specific)	0.0948	1.1	0.704378
YGL058W	RAD6	ubiquitin conjugating enzyme	0.0953	1.1	0.729575
YCR053W	THR4	threonine synthase	0.0988	1.1	0.370164
YDL099W	BUG1	unknown	0.0992	1.1	0.263134
YKL093W	MBR1	unknown	0.1000	1.1	0.43462
YJL020C	BBC1	myosin I binding	0.1002	1.1	0.430835
YMR152W	YIM1	unknown	0.1007	1.1	0.260185
YIL107C	PFK26	6-phosphofructo-2-kinase	0.1013	1.1	0.185519
YER021W	RPN3	unknown	0.1018	1.1	0.180763
YPL081W	RPS9A	structural constituent of ribosome	0.1022	1.1	0.367343
YMR282C	AEP2	unknown	0.1050	1.1	0.46097
YCL003W			0.1057	1.1	0.526202
YNL042W	BOP3	unknown	0.1057	1.1	0.721034
YPL222W	FMP40	unknown	0.1070	1.1	0.649179
YLR237W	THI7	thiamin transporter	0.1075	1.1	0.737274
YHR203C	RPS4B	structural constituent of ribosome	0.1080	1.1	0.206443
YEL060C	PRB1	serine-type endopeptidase	0.1083	1.1	0.081507
YBR109C	CMD1	protein binding	0.1085	1.1	0.498652
YJL191W	RPS14B	structural constituent of ribosome*	0.1095	1.1	0.384347
YDR233C	RTN1	unknown	0.1103	1.1	0.2583
YJL140W	RPB4	DNA-directed RNA polymerase	0.1115	1.1	0.150697
YDR263C	DIN7	nuclease	0.1117	1.1	0.142271
YKL006W	RPL14A	structural constituent of ribosome*	0.1145	1.1	0.165822
YBR127C	VMA2	hydrogen-transporting ATPase , rotational mechanism	0.1152	1.1	0.609987
YFL043C			0.1157	1.1	0.45262
YHR132C	ECM14	metalloendopeptidase	0.1158	1.1	0.364983
YDL218W		unknown	0.1182	1.1	0.705368
YLR178C	TFS1	lipid binding	0.1185	1.1	0.294337
YBR131W	CCZ1	guanyl-nucleotide exchange factor	0.1193	1.1	0.252601
YNL030W	HHF2	DNA binding	0.1203	1.1	0.325061
YLR454W	FMP27	unknown	0.1212	1.1	0.307638
YBL081W		unknown	0.1222	1.1	0.225264
YNR047W		protein kinase	0.1223	1.1	0.643167
YMR002W		unknown	0.1235	1.1	0.447
YFR008W	FAR7	unknown	0.1240	1.1	0.272748
YER160C			0.1245	1.1	0.585023
YER159C	BUR6	transcription corepressor	0.1247	1.1	0.0176098
YBR260C	RGD1	Rho GTPase activator	0.1248	1.1	0.18176
YDL140C	RPO21	DNA-directed RNA polymerase	0.1250	1.1	0.41749
YPR016C	TIF6	unknown	0.1258	1.1	0.269512
YOR251C		thiosulfate sulfurtransferase	0.1267	1.1	0.398732
YCR042C	TAF2	general RNA polymerase II transcription factor	0.1268	1.1	0.318437

Table 3: continued.

ORF ID	Gene Name	Gene Function	Avg Log_2 Ratio	Fold Change	T-test
YER080W	FMP29	unknown	0.1282	1.1	0.436598
YCL049C		unknown	0.1292	1.1	0.290869
YJR002W	MPP10	unknown	0.1295	1.1	0.348597
YDR062W	LCB2	serine C-palmitoyltransferase	0.1300	1.1	0.478307
YER100W	UBC6	ubiquitin conjugating enzyme	0.1328	1.1	0.138897
YJL072C	PSF2	unknown	0.1348	1.1	0.398719
YDR500C	RPL37B	structural constituent of ribosome	0.1353	1.1	0.362215
YMR168C	CEP3	DNA bending *	0.1358	1.1	0.183822
YOR099W	KTR1	alpha-1,2-mannosyltransferase	0.1363	1.1	0.0384063
YMR105C	PGM2	phosphoglucomutase	0.1378	1.1	0.589437
YCR059C	YIH1	unknown	0.1385	1.1	0.288575
YDR217C	RAD9	protein binding	0.1387	1.1	0.0942463
YDR309C	GIC2	small GTPase regulator	0.1408	1.1	0.189636
YKR071C	DRE2	unknown	0.1410	1.1	0.61076
YDR473C	PRP3	RNA splicing factor , transesterification mechanism	0.1412	1.1	0.295316
YBR136W	MEC1	protein kinase	0.1452	1.1	0.549302
YMR236W	TAF9	general RNA polymerase II transcription factor	0.1475	1.1	0.170939
YER074W	RPS24A	structural constituent of ribosome	0.1482	1.1	0.301609
YJL015C			0.1482	1.1	0.271545
YMR143W	RPS16A	structural constituent of ribosome	0.1513	1.1	0.405787
YDR035W	ARO3	3-deoxy-7-phosphoheptulonate synthase	0.1528	1.1	0.544787
YNL118C	DCP2	mRNA binding	0.1532	1.1	0.46221
YOR120W	GCY1	aldo-keto reductase	0.1545	1.1	0.29807
YJL165C	HAL5	protein kinase	0.1572	1.1	0.223009
YBR081C	SPT7	structural molecule	0.1573	1.1	0.210179
YGL243W	TAD1	tRNA specific adenosine deaminase	0.1573	1.1	0.743083
YHR039BC			0.1575	1.1	0.270592
YBR263W	SHM1	glycine hydroxymethyltransferase	0.1590	1.1	0.110675
YAL019W	FUN30	unknown	0.1595	1.1	0.119214
YDL045C	FAD1	FMN adenylyltransferase	0.1602	1.1	0.28881
YOR182C	RPS30B	structural constituent of ribosome	0.1607	1.1	0.397334
YBR249C	ARO4	3-deoxy-7-phosphoheptulonate synthase	0.1613	1.1	0.300001
YHR190W	ERG9	farnesyl-diphosphate farnesyltransferase	0.1613	1.1	0.0929202
YBR215W	HPC2	transcription regulator	0.1620	1.1	0.159109
YOR312C	RPL20B	structural constituent of ribosome	0.1628	1.1	0.382632
YBR290W	BSD2	unknown	0.1632	1.1	0.0225144
YAL058W	CNE1	unfolded protein binding	0.1640	1.1	0.469466
YKL063C		unknown	0.1657	1.1	0.178941
YML045W			0.1665	1.1	0.0178715
YDR099W	BMH2	protein binding	0.1668	1.1	0.26254
YBR212W	NGR1	RNA binding	0.1672	1.1	0.0951895
YEL054C	RPL12A	structural constituent of ribosome	0.1682	1.1	0.378921
YDR516C	EMI2	unknown	0.1692	1.1	0.316558
YOR377W	ATF1	alcohol O-acetyltransferase	0.1702	1.1	0.451847
YDR130C	FIN1	unknown	0.1708	1.1	0.382842
YCL002C		unknown	0.1713	1.1	0.165626
YLR256W	HAP1	specific RNA polymerase II transcription factor	0.1713	1.1	0.397353
YPR132W	RPS23B	structural constituent of ribosome	0.1733	1.1	0.0253757
YCR032W	BPH1	unknown	0.1745	1.1	0.291174
YNL117W	MLS1	malate synthase	0.1755	1.1	0.148843
YBR160W	CDC28	cyclin-dependent protein kinase	0.1757	1.1	0.108491
YDL165W	CDC36	3'-5'-exoribonuclease	0.1762	1.1	0.25734
YER182W	FMP10	unknown	0.1762	1.1	0.476109
YOL139C	CDC33	translation initiation factor	0.1768	1.1	0.269887
YER049W	TPA1	unknown	0.1770	1.1	0.166726
YAR042W	SWH1	phosphatidylinositol binding	0.1777	1.1	0.82101
YOL011W	PLB3	lysophospholipase	0.1777	1.1	0.0345318
YDL083C	RPS16B	structural constituent of ribosome	0.1780	1.1	0.137987
YKR066C	CCP1	cytochrome-c peroxidase	0.1790	1.1	0.200555
YHR191C	CTF8	unknown	0.1793	1.1	0.0080886
YIL121W	QDR2	multidrug efflux pump	0.1793	1.1	0.0350443
YIL043C	CBR1	cytochrome-b5 reductase	0.1803	1.1	0.442247
YAL021C	CCR4	3'-5'-exoribonuclease	0.1822	1.1	0.380068
YBL049W	MOH1	unknown	0.1840	1.1	0.199181
YPL156C	PRM4	unknown	0.1840	1.1	0.38523
YBR289W	SNF5	general RNA polymerase II transcription factor	0.1845	1.1	0.15961
YKL122C	SRP21	signal sequence binding	0.1845	1.1	0.201753
YML024W	RPS17A	structural constituent of ribosome	0.1848	1.1	0.345004
YER079W		unknown	0.1855	1.1	0.51985

Table 3: continued.

ORF ID	Gene Name	Gene Function	Avg Log_2 Ratio	Fold Change	T-test
YDL131W	LYS21	homocitrate synthase	0.1857	1.1	0.132558
YML026C	RPS18B	structural constituent of ribosome	0.1867	1.1	0.124204
YMR016C	SOK2	transcription factor	0.1867	1.1	0.157004
YKL006C-A	SFT1	v-SNARE	0.1887	1.1	0.287021
Q0060	AI3	endonuclease	0.1905	1.1	0.0746155
YDL084W	SUB2	protein binding	0.1907	1.1	0.0291847
YBR295W	PCA1	ATPase , coupled to transmembrane movement of ions, phosph	0.1922	1.1	0.0819892
YAR015W	ADE1	phosphoribosylaminoimidazolesuccinocarboxamide synthase	0.1925	1.1	0.008313
YJL177W	RPL17B	structural constituent of ribosome	0.1933	1.1	0.0645773
YMR125W	STO1	mRNA binding	0.1945	1.1	0.187596
YCR082W	AHC2	unknown	0.1947	1.1	0.327742
YLR158C	ASP3-3	asparaginase	0.1962	1.1	0.224188
YBL085W	BOI1	phospholipid binding	0.1968	1.1	0.179566
YHL011C	PRS3	ribose phosphate diphosphokinase	0.1978	1.1	0.268141
YDL016C			0.2007	1.1	0.299784
YOR293W	RPS10A	structural constituent of ribosome	0.2055	1.2	0.13611
YBL037W	APL3	unknown	0.2075	1.2	0.130578
YAL017W	PSK1	protein serine/threonine kinase	0.2080	1.2	0.0869401
YGR046W		unknown	0.2082	1.2	0.123359
YBR119W	MUD1	RNA binding	0.2092	1.2	0.130848
YML042W	CAT2	carnitine O-acetyltransferase	0.2097	1.2	0.0453306
YLR168C		unknown	0.2102	1.2	0.0088148
YCR036W	RBK1	ATP binding	0.2103	1.2	0.112399
YDL085W	NDE2	NADH dehydrogenase	0.2115	1.2	0.0451916
YLR438W	CAR2	ornithine-oxo-acid transaminase	0.2117	1.2	0.213545
YLR441C	RPS1A	structural constituent of ribosome	0.2117	1.2	0.175398
YNL078W	NIS1	unknown	0.2125	1.2	0.213784
YMR116C	ASC1	unknown	0.2133	1.2	0.167254
YCR002C	CDC10	GTPase *	0.2155	1.2	0.0145124
YER019C-A	SBH2	protein transporter	0.2155	1.2	0.394379
YJR007W	SUI2	translation initiation factor	0.2155	1.2	0.47037
YOR321W	PMT3	dolichyl-phosphate-mannose-protein mannosyltransferase	0.2162	1.2	0.227859
YBR048W	RPS11B	structural constituent of ribosome	0.2163	1.2	0.0904646
YOR317W	FAA1	long-chain-fatty-acid-CoA ligase	0.2165	1.2	0.0842238
YOR064C	YNG1	histone acetyltransferase	0.2182	1.2	0.0350022
YPL131W	RPL5	structural constituent of ribosome*	0.2188	1.2	0.174037
YBR066C	NRG2	transcriptional repressor	0.2190	1.2	0.161822
YPL220W	RPL1A	structural constituent of ribosome	0.2193	1.2	0.227748
YER020W	GPA2	GTPase	0.2198	1.2	0.0893473
YER019W	ISC1	phospholipase C	0.2207	1.2	0.325469
YBR287W	ZSP1	unknown	0.2227	1.2	0.0494068
YER081W	SER3	phosphoglycerate dehydrogenase	0.2242	1.2	0.0045936
YBR051W			0.2257	1.2	0.0517947
YJR100C		unknown	0.2273	1.2	0.414574
YMR064W	AEP1	unknown	0.2275	1.2	0.0462257
YJL127C	SPT10	histone acetyltransferase	0.2283	1.2	0.498844
YBR253W	SRB6	RNA polymerase II transcription mediator	0.2293	1.2	0.278533
YHL033C	RPL8A	structural constituent of ribosome	0.2300	1.2	0.137696
YCR057C	PWP2	snoRNA binding	0.2303	1.2	0.0348982
YDL010W		unknown	0.2318	1.2	0.272822
YKR098C	UBP11	ubiquitin-specific protease	0.2318	1.2	0.0463327
YLR327C	TMA10	unknown	0.2330	1.2	0.1726
YGL237C	HAP2	transcriptional activator	0.2335	1.2	0.0793536
YKL032C	IXR1	DNA binding	0.2340	1.2	0.315165
YBR169C	SSE2	unknown	0.2353	1.2	0.0641767
YAL009W	SPO7	unknown	0.2362	1.2	0.565516
YLR238W	FAR10	unknown	0.2372	1.2	0.106673
YDR511W	ACN9	unknown	0.2378	1.2	0.252092
YMR212C	EFR3	unknown	0.2383	1.2	0.652341
YIL077C		unknown	0.2407	1.2	0.226894
YCR031			0.2413	1.2	0.046791
YMR051C			0.2425	1.2	0.099358
YHR006W	STP2	specific RNA polymerase II transcription factor	0.2432	1.2	0.133915
YDR266C		unknown	0.2435	1.2	0.128454
YFL-TYB			0.2442	1.2	0.103945
YLR264W	RPS28B	structural constituent of ribosome	0.2450	1.2	0.202117
YCR045C		serine-type peptidase	0.2452	1.2	0.577389
YGL122C	NAB2	poly(A) binding	0.2478	1.2	0.170935
YDR077W	SED1	structural constituent of cell wall	0.2483	1.2	0.294513

Table 3: continued.

ORF ID	Gene Name	Gene Function	Avg Log_2 Ratio	Fold Change	T-test
YDL226C	GCS1	actin binding	0.2485	1.2	0.0310436
YDR068W	DOS2	unknown	0.2495	1.2	0.0837498
YDR071C	PAA1	aralkylamine N-acetyltransferase *	0.2505	1.2	0.0933319
YPR086W	SUA7	general RNA polymerase II transcription factor	0.2505	1.2	0.113247
YBR049C	REB1	RNA polymerase II transcription factor *	0.2507	1.2	0.092407
YDL223C	HBT1	unknown	0.2525	1.2	0.0393533
YIL021W	RPB3	DNA-directed RNA polymerase	0.2527	1.2	0.0074357
YLR206W	ENT2	clathrin binding	0.2537	1.2	0.0017845
YDR092W	UBC13	ubiquitin conjugating enzyme	0.2542	1.2	0.309298
YPL079W	RPL21B	structural constituent of ribosome	0.2547	1.2	0.195736
YMR110C	HFD1	3-chloroallyl aldehyde dehydrogenase	0.2548	1.2	0.0151451
YDR090C		unknown	0.2555	1.2	0.0702783
YFL016C	MDJ1	unfolded protein binding	0.2562	1.2	0.0070729
YBR071W		unknown	0.2563	1.2	0.270707
YMR046C			0.2570	1.2	0.13098
YDL186W		unknown	0.2580	1.2	0.0272931
YDR324C	UTP4	snoRNA binding	0.2580	1.2	0.124495
YNL023C	FAP1	transcription factor	0.2583	1.2	0.716553
YAL033W	POP5	ribonuclease P *	0.2590	1.2	0.0767786
YDR167W	TAF10	general RNA polymerase II transcription factor	0.2598	1.2	0.0630406
YCR008W	SAT4	protein kinase	0.2605	1.2	0.0558661
YCR024C-A	PMP1	enzyme regulator	0.2607	1.2	0.0841958
YIR010W	DSN1	unknown	0.2610	1.2	0.085467
YDL005C	MED2	RNA polymerase II transcription mediator	0.2617	1.2	0.177827
YCR044C	PER1	unknown	0.2620	1.2	0.521016
YIL135C	VHS2	unknown	0.2637	1.2	0.2734
YBR157C	ICS2	unknown	0.2648	1.2	0.0172777
YJR076C	CDC11	structural constituent of cytoskeleton*	0.2657	1.2	0.197752
YDL092W	SRP14	signal sequence binding	0.2658	1.2	0.0113611
YBR115C	LYS2	L-aminoadipate-semialdehyde dehydrogenase	0.2660	1.2	0.502537
YER014W	HEM14	protoporphyrinogen oxidase	0.2673	1.2	0.0026705
YHR213W		unknown	0.2693	1.2	0.0410299
YDR088C	SLU7	RNA splicing factor , transesterification mechanism*	0.2710	1.2	0.144377
YNL154C	YCK2	casein kinase I	0.2715	1.2	0.0243373
YDR533C	HSP31	unfolded protein binding	0.2738	1.2	0.0956208
YLR325C	RPL38	structural constituent of ribosome	0.2748	1.2	0.304616
YKL150W	MCR1	cytochrome-b5 reductase	0.2753	1.2	0.0699198
YLR094C	GIS3	unknown	0.2768	1.2	0.253976
YBR031W	RPL4A	structural constituent of ribosome	0.2827	1.2	0.119102
YLR040C		unknown	0.2835	1.2	0.0655853
YLR250W	SSP120	unknown	0.2835	1.2	0.150086
YCR062W			0.2858	1.2	0.0008532
YDR356W	SPC110	structural constituent of cytoskeleton	0.2862	1.2	0.370205
YFR029W	PTR3	amino acid binding	0.2868	1.2	0.0125929
YLR246W	ERF2	protein-cysteine S-palmitoleyltransferase	0.2898	1.2	0.0354252
YDL091C	UBX3	unknown	0.2912	1.2	0.18028
YDL190C	UFD2	ubiquitin conjugating enzyme	0.2912	1.2	0.0933201
YGR146C		unknown	0.2915	1.2	0.0253532
YLR093C	NYV1	v-SNARE	0.2920	1.2	0.120326
YBR123C	TFC1	RNA polymerase III transcription factor	0.2928	1.2	0.168292
YJR058C	APS2	unknown	0.2942	1.2	0.0314166
YBR256C	RIB5	riboflavin synthase	0.2980	1.2	0.912071
YJR123W	RPS5	structural constituent of ribosome	0.2980	1.2	0.199123
YOL106W			0.2987	1.2	0.0515506
YDR012W	RPL4B	structural constituent of ribosome	0.2990	1.2	0.0087733
YCR025C			0.3017	1.2	0.601868
YDL106C	PHO2	transcription factor	0.3022	1.2	0.274582
YKL172W	EBP2	unknown	0.3027	1.2	0.0001707
YOR113W	AZF1	DNA binding	0.3033	1.2	0.0429644
YOR184W	SER1	phosphoserine transaminase	0.3038	1.2	0.252962
YPL206C		glycerophosphodiester phosphodiesterase	0.3067	1.2	0.0830177
YGL123W	RPS2	structural constituent of ribosome	0.3077	1.2	0.0147807
YLL045C	RPL8B	structural constituent of ribosome	0.3085	1.2	0.0219904
YMR194W	RPL36A	structural constituent of ribosome*	0.3085	1.2	0.0337608
YBR166C	TYR1	prephenate dehydrogenase	0.3087	1.2	0.384681
YBR190W			0.3098	1.2	0.0853908
YJL069C	UTP18	unknown	0.3103	1.2	0.28073
YGR007W	MUQ1	ethanolamine-phosphate cytidylyltransferase	0.3117	1.2	0.0214033
YJL164C	TPK1	protein serine/threonine kinase	0.3117	1.2	0.0565868

Table 3: continued.

ORF ID	Gene Name	Gene Function	Avg Log_2 Ratio	Fold Change	T-test
YMR250W	GAD1	glutamate decarboxylase	0.3117	1.2	0.320592
YCL066W	HMLALPHA1	transcription coactivator	0.3118	1.2	0.0915848
YDR269C			0.3132	1.2	0.0544512
YBR113W			0.3140	1.2	0.0322234
YGL095C	VPS45	unfolded protein binding	0.3142	1.2	0.107025
YDL188C	PPH22	protein phosphatase type 2A	0.3148	1.2	0.0332659
YDL020C	RPN4	transcriptional activator	0.3157	1.2	0.0720395
YDL048C	STP4	unknown	0.3163	1.2	0.0312737
YBR112C	CYC8	transcription coactivator *	0.3167	1.2	0.0276492
YDR350C	TCM10	unknown	0.3178	1.2	0.0509807
YNL162W	RPL42A	structural constituent of ribosome	0.3182	1.2	0.0600358
YHR149C	SKG6	unknown	0.3195	1.2	0.0068105
YBR168W	PEX32	unknown	0.3200	1.2	0.279415
YGL126W	SCS3	unknown	0.3210	1.2	0.369375
YDR180W	SCC2	unknown	0.3217	1.2	0.222937
YCL041C			0.3228	1.3	0.0152257
YNL166C	BNI5	unknown	0.3257	1.3	0.0390715
YDL161W	ENT1	clathrin binding	0.3258	1.3	0.0197532
YOR095C	RKI1	ribose-5-phosphate isomerase	0.3270	1.3	0.0710363
YMR235C	RNA1	Ran GTPase activator	0.3272	1.3	0.0349585
YMR022W	QRI8	ubiquitin conjugating enzyme	0.3298	1.3	0.0583425
YBR012W-A			0.3308	1.3	0.116522
YBR084C-A	RPL19A	structural constituent of ribosome	0.3312	1.3	0.0315089
YDR055W	PST1	unknown	0.3312	1.3	0.0099697
YIR006C	PAN1	protein binding	0.3312	1.3	0.1055
YJR003C		unknown	0.3320	1.3	0.110934
YGR229C	SMI1	unknown	0.3332	1.3	0.392184
YBR172C	SMY2	unknown	0.3352	1.3	0.0035667
Q0140	VAR1	structural constituent of ribosome	0.3353	1.3	0.0080991
YOR122C	PFY1	actin monomer binding	0.3353	1.3	0.0569877
YNL161W	CBK1	protein kinase	0.3357	1.3	0.220263
YHR141C	RPL42B	structural constituent of ribosome	0.3362	1.3	0.104475
YBL041W	PRE7	endopeptidase	0.3365	1.3	0.142208
YOR389W		unknown	0.3390	1.3	0.286057
YAL060W	BDH1	(R,R)-butanediol dehydrogenase	0.3405	1.3	0.0019043
YLR197W	SIK1	unknown	0.3407	1.3	0.104173
YBR089W			0.3420	1.3	0.0224113
YJL076W	NET1	rDNA binding	0.3433	1.3	0.107821
YNR002C	ATO2	ammonium transporter	0.3453	1.3	0.0120224
YML040W			0.3457	1.3	0.0432481
YIL074C	SER33	phosphoglycerate dehydrogenase	0.3465	1.3	0.0189035
YDR153C	ENT5	clathrin binding	0.3468	1.3	0.0712946
YGR256W	GND2	phosphogluconate dehydrogenase (decarboxylating)	0.3468	1.3	0.255532
YBR229C	ROT2	alpha-glucosidase	0.3470	1.3	0.292602
YHR010W	RPL27A	structural constituent of ribosome	0.3478	1.3	0.138529
YGR019W	UGA1	4-aminobutyrate transaminase	0.3487	1.3	0.138266
YLR309C	IMH1	unknown	0.3500	1.3	0.031425
YOR304W	ISW2	ATPase	0.3502	1.3	0.473588
YMR097C	MTG1	GTPase	0.3505	1.3	0.0806746
YLR301W		unknown	0.3507	1.3	0.0976603
YNR057C	BIO4	dethiobiotin synthase	0.3512	1.3	0.0454883
YIL149C	MLP2	ribonucleoprotein binding	0.3520	1.3	0.0097889
YDR476C		unknown	0.3537	1.3	0.0146229
YDR067C	OCA6	unknown	0.3550	1.3	0.0281261
YOR311C	HSD1	unknown	0.3553	1.3	0.234589
YOR128C	ADE2	phosphoribosylaminoimidazole carboxylase	0.3563	1.3	0.0312847
YER102W	RPS8B	structural constituent of ribosome	0.3567	1.3	0.0143663
YJL147C		unknown	0.3570	1.3	0.218333
YGR251W		unknown	0.3577	1.3	0.0348247
YDR060W	MAK21	unknown	0.3580	1.3	0.0141598
YER109C	FLO8	specific RNA polymerase II transcription factor	0.3585	1.3	0.0026077
YGR147C	NAT2	peptide alpha-N-acetyltransferase	0.3587	1.3	0.0049887
YPL239W	YAR1	unknown	0.3588	1.3	0.0012312
YOR096W	RPS7A	structural constituent of ribosome	0.3603	1.3	0.045111
YCL034W	LSB5	unknown	0.3610	1.3	0.172697
YBR189W	RPS9B	structural constituent of ribosome	0.3612	1.3	0.0013001
YML074C	FPR3	peptidyl-prolyl cis-trans isomerase	0.3613	1.3	0.0369408
YOL082W	ATG19	protein binding	0.3625	1.3	0.140094
YJR066W	TOR1	protein binding	0.3627	1.3	0.0301496

Table 3: continued.

ORF ID	Gene Name	Gene Function	Avg Log_2 Ratio	Fold Change	T-test
YDR298C	ATP5	structural molecule *	0.3642	1.3	0.0285107
YCR061W(1)			0.3643	1.3	0.181657
YDL243C	AAD4	aryl-alcohol dehydrogenase	0.3650	1.3	0.167374
YPL061W	ALD6	3-chloroallyl aldehyde dehydrogenase	0.3653	1.3	0.0460235
YER068W	MOT2	3'-5'-exoribonuclease *	0.3665	1.3	0.0115801
YIL048W	NEO1	phospholipid-translocating ATPase *	0.3673	1.3	0.105522
YDR250C			0.3683	1.3	0.0733077
YGL103W	RPL28	structural constituent of ribosome*	0.3708	1.3	0.114567
YHR146W	CRP1	DNA binding	0.3727	1.3	0.0301264
YNR052C	POP2	3'-5'-exoribonuclease	0.3727	1.3	0.0213755
YOR359W	VTS1	RNA binding	0.3737	1.3	0.075993
YMR315W		unknown	0.3740	1.3	0.138719
YGR014W	MSB2	osmosensor	0.3742	1.3	0.568245
YBR297W	MAL33	transcription factor	0.3743	1.3	0.040974
YBR264C	YPT10	GTPase *	0.3757	1.3	0.0980819
Q0255		unknown	0.3760	1.3	0.0575876
YDR452W	PPN1	endopolyphosphatase	0.3777	1.3	0.0742538
YBR230C	OM14	unknown	0.3818	1.3	0.139045
YCR052W	RSC6	unknown	0.3820	1.3	0.111431
YCR047C	BUD23	S-adenosylmethionine-dependent methyltransferase	0.3822	1.3	0.166106
YLL010C	PSR1	phosphoprotein phosphatase	0.3825	1.3	0.0219582
YDL124W		alpha-keto amide reductase *	0.3832	1.3	0.0152227
YMR272C	SCS7	oxidoreductase	0.3838	1.3	0.079297
YMR163C		unknown	0.3840	1.3	0.191744
YDL166C	FAP7	nucleoside-triphosphatase	0.3845	1.3	0.16134
YPR036W	VMA13	hydrogen-transporting ATPase , rotational mechanism	0.3852	1.3	0.0018528
YHR202W		unknown	0.3853	1.3	0.0792575
YOR298W	MUM3	acyltransferase	0.3858	1.3	0.364013
YDL072C	YET3	unknown	0.3872	1.3	0.0332545
YLR177W		unknown	0.3898	1.3	0.015294
YCL011C	GBP2	RNA binding	0.3902	1.3	0.085295
YGR027C	RPS25A	structural constituent of ribosome	0.3923	1.3	0.0417248
YOR276W	CAF20	translation regulator	0.3940	1.3	0.0374735
YML051W	GAL80	transcription corepressor	0.3943	1.3	0.0583907
YJR095W	SFC1	succinate:fumarate antiporter	0.3953	1.3	0.113921
YDL121C		unknown	0.3958	1.3	0.209981
YLR104W		unknown	0.3968	1.3	0.0283164
YPL199C		unknown	0.3980	1.3	0.0073836
YIL113W	SDP1	MAP kinase	0.3990	1.3	0.0187789
YHL001W	RPL14B	structural constituent of ribosome*	0.3993	1.3	0.0243855
YCL024W	KCC4	protein kinase	0.4015	1.3	0.164817
YLR384C	IKI3	RNA polymerase II transcription elongation factor *	0.4022	1.3	0.235114
YMR070W	MOT3	DNA binding	0.4023	1.3	0.0828388
YDL061C	RPS29B	structural constituent of ribosome	0.4025	1.3	0.226787
YDL125C	HNT1	hydrolase *	0.4062	1.3	0.110569
YPL052W	OAZ1	enzyme inhibitor	0.4068	1.3	0.0534972
YJL017W			0.4070	1.3	0.118868
YPL273W	SAM4	homocysteine S-methyltransferase	0.4070	1.3	0.489671
YER056C-A	RPL34A	structural constituent of ribosome	0.4083	1.3	0.0114097
YCR029C			0.4095	1.3	0.197745
YLR333C	RPS25B	structural constituent of ribosome	0.4108	1.3	0.164936
YOR167C	RPS28A	structural constituent of ribosome	0.4112	1.3	0.0826127
YDL142C	CRD1	cardiolipin synthase	0.4140	1.3	0.0718081
YOL040C	RPS15	structural constituent of ribosome	0.4155	1.3	0.117769
YDL217C	TIM22	protein transporter	0.4157	1.3	0.0730385
YMR242C	RPL20A	structural constituent of ribosome	0.4162	1.3	0.0949676
YDL225W	SHS1	structural constituent of cytoskeleton	0.4175	1.3	0.0136115
YER027C	GAL83	AMP-activated protein kinase	0.4177	1.3	0.0304636
YML113W	DAT1	AT DNA binding	0.4195	1.3	0.0660129
YBR129C	OPY1	unknown	0.4197	1.3	0.0607726
YKL186C	MTR2	protein binding	0.4205	1.3	0.0382333
YDR072C	IPT1	transferase , transferring phosphorus-containing groups	0.4208	1.3	0.0306595
YIL104C	SHQ1	unknown	0.4217	1.3	0.053
YDR351W	SBE2	unknown	0.4218	1.3	0.0174488
YGL080W	FMP37	unknown	0.4225	1.3	0.0517235
YLR335W	NUP2	structural molecule	0.4232	1.3	0.0215867
YBR062C		unknown	0.4258	1.3	0.0737451
YFL-TYA			0.4278	1.3	0.139567
YMR142C	RPL13B	structural constituent of ribosome	0.4288	1.3	0.026996

Table 3: continued.

ORF ID	Gene Name	Gene Function	Avg Log_2 Ratio	Fold Change	T-test
YDL046W	NPC2	unknown	0.4290	1.3	0.0765605
YPL143W	RPL33A	structural constituent of ribosome	0.4312	1.3	0.0870198
YER088C	DOT6	unknown	0.4340	1.4	0.0029541
YBR214W	SDS24	unknown	0.4342	1.4	0.0276292
YGR009C	SEC9	t-SNARE	0.4355	1.4	0.12963
YBR114W	RAD16	DNA-dependent ATPase	0.4360	1.4	0.0626064
YLR383W	SMC6	unknown	0.4365	1.4	0.135411
YOR173W	DCS2	unknown	0.4365	1.4	0.0686687
YIL027C	KRE27	unknown	0.4372	1.4	0.107721
YBR106W	PHO88	phosphate transporter	0.4373	1.4	0.0943904
YHR134W	WSS1	unknown	0.4375	1.4	0.0212561
YHR209W		S-adenosylmethionine-dependent methyltransferase	0.4387	1.4	0.0411227
YBR086C	IST2	unknown	0.4388	1.4	0.076393
YLR052W	IES3	unknown	0.4407	1.4	0.0376626
YCLX10C			0.4412	1.4	0.0877594
YNL021W	HDA1	histone deacetylase	0.4420	1.4	0.185184
YFL058W	THI5	unknown	0.4427	1.4	0.0851235
YJL030W	MAD2	unknown	0.4427	1.4	0.0465429
YKR091W	SRL3	unknown	0.4467	1.4	0.0030785
YOL126C	MDH2	L-malate dehydrogenase	0.4482	1.4	0.0095309
YOR283W		unknown	0.4502	1.4	0.10103
YHR163W	SOL3	6-phosphogluconolactonase	0.4517	1.4	0.0070757
YJR012C		unknown	0.4520	1.4	0.0161885
YBR130C	SHE3	mRNA binding	0.4523	1.4	0.0319372
YOR245C	DGA1	diacylglycerol O-acyltransferase	0.4527	1.4	0.0843416
YJL117W	PHO86	unknown	0.4548	1.4	0.0008273
YBL092W	RPL32	structural constituent of ribosome	0.4552	1.4	0.258129
YDR447C	RPS17B	structural constituent of ribosome	0.4555	1.4	0.0391831
YJL064W			0.4560	1.4	0.121646
YLR053C		unknown	0.4563	1.4	0.0201412
YHR030C	SLT2	MAP kinase	0.4572	1.4	0.102423
YBR167C	POP7	ribonuclease P *	0.4577	1.4	0.0125835
YLR253W		unknown	0.4580	1.4	0.0403765
YDR145W	TAF12	general RNA polymerase II transcription factor	0.4590	1.4	0.0394653
YDR022C	CIS1	unknown	0.4603	1.4	0.496707
YDR513W	GRX2	thiol-disulfide exchange intermediate *	0.4603	1.4	0.0796488
TDR261C-D			0.4617	1.4	0.131645
YMR073C		unknown	0.4617	1.4	0.198626
YJL141C	YAK1	protein kinase	0.4620	1.4	0.0264559
YBR128C	ATG14	unknown	0.4643	1.4	0.0699366
YHR152W	SPO12	unknown	0.4655	1.4	0.0200978
YBR075W			0.4662	1.4	0.0065598
YLR410W-B			0.4668	1.4	0.0081619
YOR046C	DBP5	RNA helicase	0.4673	1.4	0.11785
YBR191W	RPL21A	structural constituent of ribosome	0.4682	1.4	0.0187838
YGL077C	HNM1	choline transporter	0.4682	1.4	0.0295363
YBR138C		unknown	0.4685	1.4	0.223255
YDL088C	ASM4	structural molecule	0.4685	1.4	0.0179667
YAR037W			0.4697	1.4	0.246423
YBR213W	MET8	ferrochelatase	0.4697	1.4	0.012594
YLR382C	NAM2	mRNA binding	0.4697	1.4	0.0349826
YDR510W	SMT3	protein tag	0.4700	1.4	0.0711014
YIR023W	DAL81	specific RNA polymerase II transcription factor	0.4707	1.4	0.0145459
YDL082W	RPL13A	structural constituent of ribosome	0.4708	1.4	0.0195166
YKL028W	TFA1	general RNA polymerase II transcription factor	0.4708	1.4	0.0946728
YIL116W	HIS5	histidinol-phosphate transaminase	0.4710	1.4	0.0323842
YDR034C	LYS14	transcriptional activator	0.4713	1.4	0.088733
YIL045W	PIG2	protein phosphatase type 1 regulator	0.4730	1.4	0.0305551
YML053C		unknown	0.4745	1.4	0.0084153
YIL133C	RPL16A	structural constituent of ribosome*	0.4758	1.4	0.0315509
YDL177C		unknown	0.4765	1.4	0.0381995
YIL111W	COX5B	cytochrome-c oxidase	0.4767	1.4	0.262548
YHR135C	YCK1	casein kinase	0.4797	1.4	0.0532657
YDL053C	PBP4	unknown	0.4837	1.4	0.0087411
YPL095C	EEB1	unknown	0.4838	1.4	0.0188507
YDR471W	RPL27B	structural constituent of ribosome	0.4853	1.4	0.0868826
YOL133W	HRT1	protein binding	0.4855	1.4	0.130335
YOR145C	PNO1	unfolded protein binding	0.4863	1.4	0.139019
YLR388W	RPS29A	structural constituent of ribosome	0.4890	1.4	0.07198

Table 3: continued.

ORF ID	Gene Name	Gene Function	Avg Log_2 Ratio	Fold Change	T-test
YOR054C	VHS3	phosphopantothenoylcysteine decarboxylase *	0.4910	1.4	0.027021
YOL068C	HST1	NAD-dependent histone deacetylase *	0.4915	1.4	0.0738916
YMR243C	ZRC1	di-, tri-valent inorganic cation transporter	0.4918	1.4	0.0656337
YFL067W		unknown	0.4932	1.4	0.64905
YBL101W-A			0.4947	1.4	0.004212
YLR330W	CHS5	unknown	0.4953	1.4	0.0196172
YDR450W	RPS18A	structural constituent of ribosome	0.4958	1.4	0.0149866
YER036C	ARB1	ATPase	0.4958	1.4	0.0280296
YBL040C	ERD2	HDEL sequence binding	0.4973	1.4	0.028403
YGL135W	RPL1B	structural constituent of ribosome	0.4973	1.4	0.0214487
YDL079C	MRK1	glycogen synthase kinase	0.4982	1.4	0.0958719
YPR041W	TIF5	translation initiation factor *	0.4995	1.4	0.101006
YER065C	ICL1	isocitrate lyase	0.4997	1.4	0.0095397
YCR041W			0.4998	1.4	0.2451
YIL105C	SLM1	phosphoinositide binding	0.5017	1.4	0.0071928
YJL118W		unknown	0.5033	1.4	0.0547805
YNL178W	RPS3	structural constituent of ribosome	0.5055	1.4	0.0043822
YDR025W	RPS11A	structural constituent of ribosome	0.5063	1.4	0.0552956
YML058W	SML1	enzyme inhibitor	0.5070	1.4	0.12005
YBL097W	BRN1	unknown	0.5075	1.4	0.281202
YIL069C	RPS24B	structural constituent of ribosome	0.5078	1.4	0.007055
YKL156W	RPS27A	structural constituent of ribosome	0.5095	1.4	0.0562405
YBR140C	IRA1	Ras GTPase activator	0.5097	1.4	0.0292406
YIL007C	NAS2	unknown	0.5100	1.4	0.0793274
YAR010C			0.5145	1.4	0.0581187
YBL072C	RPS8A	structural constituent of ribosome	0.5162	1.4	0.189202
YDL025C		protein kinase	0.5205	1.4	0.146723
YIR012W	SQT1	unknown	0.5222	1.4	0.0949048
YBL064C	PRX1	thioredoxin peroxidase	0.5225	1.4	0.0425174
YOL098C		metalloendopeptidase	0.5232	1.4	0.33902
YJR028W			0.5252	1.4	0.0315859
YGL128C	CWC23	unknown	0.5255	1.4	0.0029366
YDL191W	RPL35A	structural constituent of ribosome	0.5270	1.4	0.0553661
YCR084C	TUP1	general transcriptional repressor	0.5277	1.4	0.017961
YDR408C	ADE8	phosphoribosylglycinamide formyltransferase	0.5307	1.4	0.0435428
YJL065C	DLS1	unknown	0.5308	1.4	0.018932
YNL027W	CRZ1	transcription factor	0.5322	1.4	0.0157153
YLL023C		unknown	0.5328	1.4	0.037853
YHR097C		unknown	0.5340	1.4	0.036475
YBR135W	CKS1	protein kinase	0.5357	1.4	0.0125355
YAR002W	NUP60	structural constituent of nuclear pore	0.5368	1.5	0.0145382
YFL031W	HAC1	transcription factor *	0.5368	1.5	0.181046
YDR508C	GNP1	amino acid transporter	0.5378	1.5	0.0344047
YBL005W-A			0.5390	1.5	0.0549268
YMR124W		unknown	0.5398	1.5	0.0144626
YDR354W	TRP4	anthranilate phosphoribosyltransferase	0.5402	1.5	0.0161396
YNL244C	SUI1	translation initiation factor	0.5410	1.5	0.0709532
YNL099C	OCA1	protein tyrosine phosphatase	0.5412	1.5	0.0227138
YER148W	SPT15	DNA binding	0.5420	1.5	0.0299641
YMR197C	VTI1	v-SNARE	0.5445	1.5	0.0362647
YNL059C	ARP5	unknown	0.5455	1.5	0.061866
YLR290C		unknown	0.5472	1.5	0.0954273
YPL049C	DIG1	DNA binding	0.5475	1.5	0.237246
YCR038C	BUD5	signal transducer *	0.5492	1.5	0.0310974
YHR122W		unknown	0.5495	1.5	0.0016139
YDL224C	WHI4	RNA binding	0.5498	1.5	0.0645596
YHL002W	HSE1	protein binding	0.5508	1.5	0.0751863
YHR154W	RTT107	unknown	0.5520	1.5	0.050038
YLR198C			0.5523	1.5	0.0246025
YKL065C	YET1	unknown	0.5527	1.5	0.0526849
YNL133C	FYV6	unknown	0.5528	1.5	0.0089595
YOR052C		unknown	0.5535	1.5	0.0426082
YBR050C	REG2	protein phosphatase type 1 regulator	0.5555	1.5	0.0287962
YBR030W		unknown	0.5583	1.5	0.112549
YDL047W	SIT4	protein serine/threonine phosphatase	0.5598	1.5	0.0045282
YAR027W	UIP3	unknown	0.5613	1.5	0.0202892
YDL134C	PPH21	protein phosphatase type 2A	0.5613	1.5	0.025438
YLR029C	RPL15A	structural constituent of ribosome*	0.5618	1.5	0.0170283
YFL059W	SNZ3	protein binding	0.5623	1.5	0.0841028

Table 3: continued.

ORF ID	Gene Name	Gene Function	Avg Log_2 Ratio	Fold Change	T-test
YDR154C			0.5638	1.5	0.0412276
YBR024W	SCO2	thioredoxin peroxidase	0.5688	1.5	0.0025094
YDR492W	IZH1	metal ion binding	0.5695	1.5	0.0337674
YPR040W	TIP41	unknown	0.5732	1.5	0.0498624
YDR412W	RRP17	unknown	0.5737	1.5	0.0097174
YJL189W	RPL39	structural constituent of ribosome	0.5743	1.5	0.0179627
YIL004C	BET1	v-SNARE	0.5752	1.5	0.0578862
YDR244W	PEX5	peroxisome targeting sequence binding	0.5757	1.5	0.013908
YBR279W	PAF1	RNA polymerase II transcription elongation factor	0.5770	1.5	0.0056696
YKL012W	PRP40	RNA binding	0.5770	1.5	0.0371327
YDL134C-A			0.5793	1.5	0.0077575
YDL169C	UGX2	unknown	0.5795	1.5	0.011808
YLL039C	UBI4	protein tag*	0.5797	1.5	0.0067012
YJL190C	RPS22A	structural constituent of ribosome	0.5798	1.5	0.0301632
YDR121W	DPB4	epsilon DNA polymerase	0.5802	1.5	0.00634
YBR211C	AME1	unknown	0.5813	1.5	0.141025
YJR096W		aldo-keto reductase *	0.5823	1.5	0.0362997
YLR391W			0.5835	1.5	0.0889035
YCL005W	LDB16	unknown	0.5843	1.5	0.124221
YER026C	CHO1	CDP-diacylglycerol-serine O-phosphatidyltransferase	0.5845	1.5	0.002478
YDR064W	RPS13	structural constituent of ribosome	0.5860	1.5	0.0312294
YHR142W	CHS7	unknown	0.5893	1.5	0.0109231
YAR009C			0.5893	1.5	0.0463007
YOR103C	OST2	dolichyl-diphosphooligosaccharide-protein glycotransferase	0.5898	1.5	0.0175108
YKL214C	YRA2	RNA binding	0.5900	1.5	0.642384
YCR020C-A	MAK31	peptide alpha-N-acetyltransferase	0.5912	1.5	0.0017026
YGL078C	DBP3	ATP-dependent RNA helicase	0.5917	1.5	0.0085144
YDL136W	RPL35B	structural constituent of ribosome	0.5922	1.5	0.0330865
YMR255W	GFD1	unknown	0.6005	1.5	0.01597
YPL054W	LEE1	unknown	0.6010	1.5	0.0335987
YLR075W	RPL10	structural constituent of ribosome	0.6032	1.5	0.0106968
YDL070W	BDF2	unknown	0.6053	1.5	0.0078577
YPR102C	RPL11A	structural constituent of ribosome	0.6055	1.5	0.0026455
YOR234C	RPL33B	structural constituent of ribosome	0.6063	1.5	0.0912172
YNL096C	RPS7B	structural constituent of ribosome	0.6070	1.5	0.0665578
YDR432W	NPL3	mRNA binding	0.6080	1.5	0.0993888
YPL237W	SUI3	translation initiation factor	0.6088	1.5	0.0963182
YBR162W-A	YSY6	unknown	0.6102	1.5	0.015102
YBR077C	SLM4	phosphatidylinositol-3,4-bisphosphate binding	0.6107	1.5	0.0166044
YOL149W	DCP1	mRNA binding	0.6113	1.5	0.0041306
YDR498C	SEC20	v-SNARE	0.6113	1.5	0.0097686
YAL014C	SYN8	SNAP receptor	0.6118	1.5	0.0402033
YHR214C-B			0.6175	1.5	0.0107341
YDL077C	VAM6	Rab guanyl-nucleotide exchange factor	0.6188	1.5	0.0043489
YMR005W	TAF4	RNA polymerase II transcription factor	0.6192	1.5	0.002214
YNL062C	GCD10	tRNA binding	0.6198	1.5	0.0047471
YJL136C	RPS21B	structural constituent of ribosome	0.6203	1.5	0.0064227
YJL018W			0.6252	1.5	0.0458914
YLR332W	MID2	transmembrane receptor	0.6278	1.5	0.0162083
YAL031C	GIP4	unknown	0.6280	1.5	0.0331935
YBL036C		alanine racemase	0.6283	1.5	0.0350416
YPL229W		unknown	0.6293	1.5	0.0434246
YDR343C	HXT6	glucose transporter	0.6313	1.5	0.0460598
YAL015C	NTG1	DNA-(apurinic or apyrimidinic site) lyase	0.6333	1.6	0.0641866
YPL238C			0.6363	1.6	0.0291676
YLL027W	ISA1	unknown	0.6368	1.6	0.0044931
YDR433W			0.6375	1.6	0.0037363
YNL116W	DMA2	unknown	0.6427	1.6	0.0118315
YOL073C		unknown	0.6428	1.6	0.0332842
YIL040W	APQ12	unknown	0.6450	1.6	0.0455902
YCR069W(1)			0.6453	1.6	0.0242917
YBL032W	HEK2	mRNA binding	0.6462	1.6	0.110691
YGR137W			0.6492	1.6	0.0098867
YBL033C	RIB1	cyclohydrolase	0.6495	1.6	0.0430691
YDL228C			0.6510	1.6	0.0614825
YCL039W	GID7	unknown	0.6512	1.6	0.0227334
YDR069C	DOA4	endopeptidase	0.6525	1.6	0.0039496
YOR152C		unknown	0.6605	1.6	0.101074
YAR028W		unknown	0.6613	1.6	0.0181914

Table 3: continued.

ORF ID	Gene Name	Gene Function	Avg Log$_2$ Ratio	Fold Change	T-test
YJL142C			0.6645	1.6	0.0343115
YDR373W	FRQ1	enzyme activator	0.6650	1.6	0.0351373
YGR085C	RPL11B	structural constituent of ribosome	0.6678	1.6	0.0083789
YLR243W		signal sequence binding	0.6678	1.6	0.033278
YOR244W	ESA1	histone acetyltransferase	0.6718	1.6	0.0142352
YNL180C	RHO5	GTPase	0.6752	1.6	0.0137025
YDR251W	PAM1	unknown	0.6755	1.6	0.360361
YOR357C	SNX3	protein binding	0.6782	1.6	0.0322226
YML097C	VPS9	guanyl-nucleotide exchange factor	0.6788	1.6	0.022509
YCR070W			0.6837	1.6	0.0191098
YHR021C	RPS27B	structural constituent of ribosome	0.6843	1.6	0.0513548
YDL170W	UGA3	transcription factor	0.6923	1.6	0.0040976
YCL044C	MGR1	unknown	0.6935	1.6	0.002867
YHR150W	PEX28	unknown	0.6945	1.6	0.0076472
YMR298W	LIP1	sphingosine N-acyltransferase	0.7003	1.6	0.10402
YCRX16C			0.7005	1.6	0.000299
YMR191W	SPG5	unknown	0.7018	1.6	0.0222206
YCR020C	PET18	unknown	0.7027	1.6	0.0132927
YPR149W	NCE102	unknown	0.7047	1.6	0.0335362
YMR096W	SNZ1	protein binding	0.7097	1.6	0.0041331
YJR086W	STE18	GTPase	0.7127	1.6	0.0380325
YLR254C	NDL1	unknown	0.7133	1.6	0.0487382
YDL233W		unknown	0.7197	1.6	0.0115499
YBR183W	YPC1	ceramidase	0.7220	1.6	0.0264319
YGL166W	CUP2	ligand-regulated transcription factor	0.7227	1.7	0.0006974
YNL001W	DOM34	unknown	0.7243	1.7	0.0397806
YJL133W	MRS3	iron ion transporter	0.7258	1.7	0.03809
YPR065W	ROX1	specific transcriptional repressor	0.7258	1.7	0.0016087
YER013W	PRP22	RNA splicing factor , transesterification mechanism	0.7295	1.7	0.044427
YIL148W	RPL40A	structural constituent of ribosome*	0.7297	1.7	0.0006812
YOL144W	NOP8	unknown	0.7337	1.7	0.0195138
YDR073W	SNF11	general RNA polymerase II transcription factor	0.7363	1.7	0.0505516
YPL004C	LSP1	protein kinase	0.7373	1.7	0.0104057
YMR121C	RPL15B	structural constituent of ribosome	0.7375	1.7	0.0032652
YDL212W	SHR3	unfolded protein binding	0.7397	1.7	0.0051169
YDL110C	TMA17	unknown	0.7413	1.7	0.0109625
YLR076C			0.7455	1.7	0.0111283
YIL152W		unknown	0.7462	1.7	0.0106222
YCR096C	HMRA2	unknown	0.7497	1.7	0.0059965
YCR039C	MATALPHA2	transcription corepressor	0.7568	1.7	0.0099801
YBR201W	DER1	unknown	0.7575	1.7	0.0230302
YLR270W	DCS1	hydrolase , acting on acid anhydrides, in phosphorus-containing	0.7578	1.7	0.0234946
YBR083W	TEC1	specific RNA polymerase II transcription factor	0.7617	1.7	0.0287579
YOR385W		unknown	0.7630	1.7	0.0432233
YHR170W	NMD3	protein binding	0.7645	1.7	0.0076408
YGR248W	SOL4	6-phosphogluconolactonase	0.7660	1.7	0.0018052
YOR367W	SCP1	protein binding	0.7678	1.7	0.0269859
YDR397C	NCB2	transcription corepressor	0.7748	1.7	0.0073126
YCL067C	HMLALPHA2	transcription corepressor	0.7758	1.7	0.0176063
YNL195C		unknown	0.7763	1.7	0.0208827
YCL040W	GLK1	glucokinase	0.7798	1.7	0.0129569
YIR017C	MET28	DNA binding	0.7800	1.7	0.0758299
YIL052C	RPL34B	structural constituent of ribosome	0.7853	1.7	0.0072553
YEL074W			0.7868	1.7	0.0377551
YDR002W	YRB1	Ran GTPase binding	0.7923	1.7	0.0774179
YNL156C	NSG2	unknown	0.7937	1.7	0.0455285
YCR080W			0.7945	1.7	0.0009706
YDL182W	LYS20	homocitrate synthase	0.8002	1.7	0.0029764
YHL015W	RPS20	structural constituent of ribosome	0.8023	1.7	0.0371291
YBR182C	SMP1	transcription factor	0.8027	1.7	0.0142551
YDL208W	NHP2	RNA binding	0.8077	1.8	0.0117274
YPL057C	SUR1	mannosyltransferase	0.8095	1.8	0.0126662
YIL060W		unknown	0.8175	1.8	0.0265058
YHR145C			0.8182	1.8	0.0196212
YNL192W	CHS1	chitin synthase	0.8285	1.8	0.0439633
YDR366C		unknown	0.8287	1.8	0.0163353
YMR153W	NUP53	structural molecule	0.8300	1.8	0.0820494
YGL070C	RPB9	DNA-directed RNA polymerase	0.8307	1.8	0.0511236
YDL230W	PTP1	protein tyrosine phosphatase	0.8313	1.8	0.0067083

Table 3: continued.

ORF ID	Gene Name	Gene Function	Avg Log_2 Ratio	Fold Change	T-test
YER087C-A			0.8340	1.8	0.0864664
YMR251W-A	HOR7	unknown	0.8340	1.8	0.0571777
YCL031C	RRP7	unknown	0.8360	1.8	0.0141313
YAR031W	PRM9	unknown	0.8370	1.8	0.0107993
YIR016W		unknown	0.8392	1.8	0.0091005
YCR005C	CIT2	citrate (Si)-synthase	0.8480	1.8	0.0523574
YFR013W	IOC3	protein binding	0.8507	1.8	0.0511829
YHR140W		unknown	0.8512	1.8	0.0062437
YMR195W	ICY1	unknown	0.8540	1.8	0.0242994
YNL119W	NCS2	unknown	0.8573	1.8	0.0219324
YGR051C			0.8588	1.8	0.132115
YMR149W	SWP1	dolichyl-diphosphooligosaccharide-protein glycotransferase	0.8595	1.8	0.0499717
YDL128W	VCX1	calcium ion transporter	0.8645	1.8	0.0129911
YOR309C			0.8673	1.8	0.0597032
YDL227C	HO	endonuclease	0.8693	1.8	0.0036788
YOR091W	TMA46	unknown	0.8700	1.8	0.0095877
YHR199C	FMP34	unknown	0.8758	1.8	0.0050944
YDL129W		unknown	0.8773	1.8	0.0567164
YOR348C	PUT4	L-proline permease	0.8805	1.8	0.0015679
YDR306C		protein binding	0.8842	1.8	0.0438353
YDL051W	LHP1	RNA binding	0.8850	1.8	0.0192443
YPR113W	PIS1	CDP-diacylglycerol-inositol 3-phosphatidyltransferase	0.8887	1.9	0.0167012
YOR104W	PIN2	unknown	0.8907	1.9	0.0079078
YBR014C		unknown	0.8920	1.9	0.0201327
YDR178W	SDH4	succinate dehydrogenase (ubiquinone)	0.8943	1.9	0.0296624
YNL157W	IGO1	unknown	0.8953	1.9	0.0047717
YHR049W	FSH1	serine hydrolase	0.8962	1.9	0.0206594
YDR120C	TRM1	tRNA (guanine-N2-)-methyltransferase	0.8963	1.9	0.0147429
YKL024C	URA6	uridine kinase	0.8965	1.9	0.0146188
YDR203W			0.9038	1.9	0.0259082
YBR065C	ECM2	unknown	0.9042	1.9	0.0022371
YJL192C	SOP4	unknown	0.9068	1.9	0.0025798
YPL060W	LPE10	magnesium ion transporter	0.9075	1.9	0.0154464
YHR155W	YSP1	unknown	0.9083	1.9	0.0443863
YOR057W	SGT1	chaperone binding	0.9155	1.9	0.0253564
YGR241C	YAP1802	clathrin binding	0.9222	1.9	0.0173609
YGL172W	NUP49	structural molecule	0.9258	1.9	0.0074146
YDR083W	RRP8	methyltransferase	0.9353	1.9	0.0271996
YCR050C			0.9420	1.9	0.0577847
YOR316C	COT1	di-, tri-valent inorganic cation transporter	0.9422	1.9	0.0329205
YJL089W	SIP4	specific RNA polymerase II transcription factor	0.9442	1.9	0.0099058
YOR021C		unknown	0.9527	1.9	0.0186045
YNR046W	TRM112	zinc ion binding	0.9548	1.9	0.0388793
YLR107W	REX3	3'-5' exonuclease	0.9560	1.9	0.0159249
YOL109W	ZEO1	unknown	0.9563	1.9	0.0379235
YIL144W	TID3	structural constituent of cytoskeleton	0.9583	1.9	0.0064321
YNL191W		unknown	0.9645	2.0	0.0176501
YGR136W	LSB1	unknown	0.9688	2.0	0.0222979
YML128C	MSC1	unknown	0.9702	2.0	0.0105665
YLR109W	AHP1	thioredoxin peroxidase	0.9712	2.0	0.0038796
YDR074W	TPS2	trehalose-phosphatase	0.9730	2.0	0.0289385
YGR034W	RPL26B	structural constituent of ribosome	0.9808	2.0	0.0885126
YLR022C	SDO1	unknown	0.9823	2.0	0.0091679
YGL117W		unknown	0.9872	2.0	0.0133172
YLR328W	NMA1	nicotinamide-nucleotide adenylyltransferase	0.9883	2.0	0.0133009
YHR187W	IKI1	RNA polymerase II transcription elongation factor	0.9890	2.0	0.007731
YLR292C	SEC72	protein transporter	0.9930	2.0	0.0019322
YBR034C	HMT1	protein-arginine N-methyltransferase	0.9942	2.0	0.0053895
YKR025W	RPC37	DNA-directed RNA polymerase	0.9970	2.0	0.0389254
YJL125C	GCD14	tRNA (adenine-N1-)-methyltransferase	1.0000	2.0	0.003202
YHR043C	DOG2	2-deoxyglucose-6-phosphatase	1.0052	2.0	0.0246612
YGR230W	BNS1	unknown	1.0062	2.0	0.0216224
YGR069W			1.0148	2.0	0.0008504
YJL060W	BNA3	arylformamidase	1.0352	2.0	0.0506385
YKR040C			1.0392	2.1	0.0097195
YER025W	GCD11	translation initiation factor	1.0402	2.1	0.0365487
YCR028C	FEN2	pantothenate transporter	1.0405	2.1	0.0236263
YIL106W	MOB1	kinase	1.0433	2.1	0.0001591
YLR252W			1.0562	2.1	0.0404698

Table 3: continued.

ORF ID	Gene Name	Gene Function	Avg Log_2 Ratio	Fold Change	T-test
YHR133C	NSG1	protein binding	1.0582	2.1	0.0038236
YIL063C	YRB2	unknown	1.0637	2.1	0.0160592
YDR256C	CTA1	catalase	1.0642	2.1	0.0422466
YBR155W	CNS1	unfolded protein binding	1.0655	2.1	0.0022346
YDL031W	DBP10	ATP-dependent RNA helicase	1.0657	2.1	0.0409663
YCL065W			1.0702	2.1	0.0234966
YLR267W	BOP2	unknown	1.0703	2.1	0.0027182
YCR033W	SNT1	NAD-dependent histone deacetylase	1.0733	2.1	0.0120961
YDL222C	FMP45	unknown	1.0790	2.1	0.0101303
YDL076C	RXT3	unknown	1.0815	2.1	0.0062744
YDR527W	RBA50	DNA-directed RNA polymerase	1.0913	2.1	0.0138646
YDL074C	BRE1	ubiquitin-protein ligase	1.0925	2.1	0.0071606
YBR021W	FUR4	uracil permease	1.0927	2.1	0.0223852
YDL123W	SNA4	unknown	1.0927	2.1	0.000194
YAL059W	ECM1	unknown	1.1005	2.1	0.0392358
YMR170C	ALD2	3-chloroallyl aldehyde dehydrogenase	1.1058	2.2	0.0154439
YHR171W	ATG7	APG12 activating enzyme	1.1080	2.2	0.0170534
YPR025C	CCL1	general RNA polymerase II transcription factor	1.1100	2.2	0.109907
YKL050C		unknown	1.1175	2.2	0.120823
YNL194C		unknown	1.1220	2.2	0.0005191
YMR262W		unknown	1.1272	2.2	0.0229439
YKL151C		unknown	1.1275	2.2	0.0571066
YBR165W	UBS1	unknown	1.1475	2.2	0.0023997
YDR181C	SAS4	acetyltransferase *	1.1503	2.2	0.015197
YOR023C	AHC1	histone acetyltransferase	1.1563	2.2	0.0270164
YJL122W	ALB1	unknown	1.1597	2.2	0.0716043
YHR138C		endopeptidase inhibitor	1.1625	2.2	0.0018937
YNL112W	DBP2	RNA helicase	1.1717	2.3	0.0030629
YJL144W		unknown	1.1767	2.3	0.0026914
YCR035C	RRP43	3'-5'-exoribonuclease	1.1787	2.3	0.0128518
YCLX01W			1.1955	2.3	0.011882
YDR399W	HPT1	hypoxanthine phosphoribosyltransferase	1.1975	2.3	0.0464471
YER024W	YAT2	carnitine O-acetyltransferase	1.2010	2.3	0.0089968
YBL043W	ECM13	unknown	1.2050	2.3	0.0036862
YIR018W	YAP5	RNA polymerase II transcription factor	1.2080	2.3	0.0159803
YBL093C	ROX3	RNA polymerase II transcription mediator	1.2083	2.3	0.0245215
YDR361C	BCP1	unknown	1.2132	2.3	0.0208792
YNL143C			1.2200	2.3	0.0046535
YOR262W		unknown	1.2250	2.3	0.0104374
YHR054C		unknown	1.2358	2.4	0.0104088
YDR252W	BTT1	unfolded protein binding	1.2360	2.4	0.0011034
YHR071W	PCL5	cyclin-dependent protein kinase	1.2392	2.4	0.0036633
YLR251W	SYM1	unknown	1.2575	2.4	0.0037094
YDL133W		unknown	1.2590	2.4	0.0009272
YBR063C		unknown	1.2793	2.4	0.0501857
YCR027C	RHB1	GTPase	1.2892	2.4	0.0481794
YOR220W	WSP1	unknown	1.2978	2.5	0.102601
YOL077C	BRX1	rRNA primary transcript binding	1.3110	2.5	0.0045937
YGR057C	LST7	protein transporter	1.3122	2.5	0.0108821
YDR037W	KRS1	lysine-tRNA ligase	1.3157	2.5	4.485E-05
YCR016W		unknown	1.3220	2.5	0.0040942
YLR414C		unknown	1.3288	2.5	0.0057038
YEL026W	SNU13	RNA binding	1.3315	2.5	0.0466166
YAL012W	CYS3	cystathionine gamma-lyase	1.3347	2.5	0.0485253
YNL046W		unknown	1.3482	2.5	0.166658
YHR161C	YAP1801	clathrin binding	1.3502	2.5	0.0003253
YHR095W			1.3560	2.6	0.0596932
YLR061W	RPL22A	structural constituent of ribosome	1.3692	2.6	0.0045889
YNL002C	RLP7	rRNA binding	1.3708	2.6	0.007672
YOL053C-A			1.3720	2.6	0.014656
YDR368W	YPR1	oxidoreductase	1.3863	2.6	0.0029524
YBR105C	VID24	unknown	1.4198	2.7	0.0019282
YPL135W	ISU1	protein binding	1.4242	2.7	0.0011447
YHR104W	GRE3	aldo-keto reductase *	1.4313	2.7	0.0036065
YML070W	DAK1	glycerone kinase	1.4385	2.7	0.0010459
YDL204W	RTN2	unknown	1.4515	2.7	0.0033247
YGR043C		transaldolase	1.4565	2.7	0.005118
YGR086C	PIL1	protein kinase	1.4580	2.7	0.0033372
YER150W	SPI1	unknown	1.4653	2.8	0.0089646

Table 3: continued.

ORF ID	Gene Name	Gene Function	Avg Log_2 Ratio	Fold Change	T-test
YNL113W	RPC19	DNA-directed RNA polymerase	1.4870	2.8	0.0030432
YMR316W	DIA1	unknown	1.5038	2.8	0.0101384
YNL110C	NOP15	unknown	1.5062	2.8	0.0020962
YNL107W	YAF9	unknown	1.5532	2.9	0.0088094
YGR242W			1.5540	2.9	0.0499112
YMR090W		unknown	1.5587	2.9	0.0062352
YBR004C	GPI18	mannosyltransferase	1.5660	3.0	0.0095197
YBR005W	RCR1	unknown	1.5703	3.0	0.0053983
YJL088W	ARG3	ornithine carbamoyltransferase	1.5882	3.0	0.0012621
YIL003W	CFD1	ATPase	1.5893	3.0	0.0063768
YFL050C	ALR2	di-, tri-valent inorganic cation transporter	1.5905	3.0	0.0061501
YOL142W	RRP40	3'-5'-exoribonuclease	1.6503	3.1	0.0068724
YOR303W	CPA1	carbamoyl-phosphate synthase (glutamine-hydrolyzing)	1.6518	3.1	0.0501503
YML004C	GLO1	lactoylglutathione lyase	1.6558	3.2	0.0002869
YDR502C	SAM2	methionine adenosyltransferase	1.6602	3.2	0.0007113
YHR137W	ARO9	aromatic-amino-acid transaminase	1.6668	3.2	0.0001437
YDR070C	FMP16	unknown	1.6943	3.2	0.0051151
YMR107W	SPG4	unknown	1.6987	3.2	0.0025338
YER032W	FIR1	unknown	1.7165	3.3	0.003199
YEL071W	DLD3	D-lactate dehydrogenase (cytochrome)	1.7180	3.3	0.0003916
YBR117C	TKL2	transketolase	1.7185	3.3	0.0006054
YDL168W	SFA1	alcohol dehydrogenase	1.7803	3.4	0.0011891
YLR164W		unknown	1.8252	3.5	0.0058369
YGR088W	CTT1	catalase	1.8363	3.6	3.037E-05
YNL193W		unknown	1.8413	3.6	0.003302
YMR176W	ECM5	unknown	1.8672	3.6	0.0032719
YGR243W	FMP43	unknown	1.8707	3.7	0.0098761
YML005W	TRM12	S-adenosylmethionine-dependent methyltransferase	1.8733	3.7	0.0023663
YMR174C	PAI3	endopeptidase inhibitor	1.8782	3.7	0.00829
YNL075W	IMP4	rRNA primary transcript binding	1.8830	3.7	0.0138137
YOR031W	CRS5	copper ion binding	1.9465	3.9	0.0019572
YGL037C	PNC1	nicotinamidase	1.9810	3.9	0.000148
YHR070W	TRM5	tRNA (guanine) methyltransferase	1.9837	4.0	0.0174053
YJL171C		unknown	2.0557	4.2	0.122607
YLR194C		structural constituent of cell wall	2.0742	4.2	0.0058299
YML131W		unknown	2.0768	4.2	0.0002212
YHR034C	PIH1	unknown	2.0827	4.2	0.0055576
YOR100C	CRC1	carnitine:acyl carnitine antiporter	2.0887	4.3	0.0012696
YMR173W-A			2.1310	4.4	0.0017235
YHR162W		unknown	2.2008	4.6	0.0005867
YDR039C	ENA2	ATPase , coupled to transmembrane movement of ions, phosph	2.2312	4.7	0.0032162
YMR175W	SIP18	phospholipid binding	2.2352	4.7	0.0039071
YHR056C	RSC30	DNA binding	2.2843	4.9	0.0044164
YDR040C	ENA1	ATPase , coupled to transmembrane movement of ions, phosph	2.3302	5.0	0.008578
YDL023C			2.3502	5.1	0.0038876
YBR116C			2.3518	5.1	0.0050972
YNL036W	NCE103	carbonate dehydratase	2.3613	5.1	0.0071273
YIL117C	PRM5	unknown	2.4263	5.4	0.0007718
YHR103W	SBE22	unknown	2.4640	5.5	0.0006885
YOR107W	RGS2	GTPase activator	2.4728	5.6	0.0009944
YCR010C	ADY2	ammonium transporter	2.4952	5.6	0.0004029
YFL021W	GAT1	specific RNA polymerase II transcription factor	2.5605	5.9	0.0012964
YNR014W		unknown	2.5733	6.0	0.0038867
YFL029C	CAK1	cyclin-dependent protein kinase	2.6262	6.2	0.0004148
YDL022W	GPD1	glycerol-3-phosphate dehydrogenase (NAD+)	2.7333	6.6	3.523E-05
YPL223C	GRE1	unknown	2.7528	6.7	0.0010662
YJL106W	IME2	protein kinase	2.7968	6.9	0.0002579
YGL039W		oxidoreductase	2.8945	7.4	0.0048832
YGR159C	NSR1	RNA binding	2.9822	7.9	0.0061362
YDR043C	NRG1	DNA binding	3.0162	8.1	2.901E-05
YFL013W-A			3.0492	8.3	0.0023316
YDL214C	PRR2	receptor signaling protein serine/threonine kinase	3.0513	8.3	0.0042473
YFL014W	HSP12	unknown	3.0805	8.5	0.0051355
YHR139C	SPS100	unknown	3.1183	8.7	0.0352836
YHR033W		unknown	3.2067	9.2	0.0006293
YGL157W		oxidoreductase	3.4043	10.6	0.0032501
YOL150C			3.4392	10.8	0.0075217
YBR281C		unknown	3.5735	11.9	0.0061927
YER062C	HOR2	glycerol-1-phosphatase	3.6217	12.3	0.0010461

Table 3: continued.

ORF ID	Gene Name	Gene Function	Avg Log_2 Ratio	Fold Change	T-test
YHR087W		unknown	3.6385	12.5	0.0004163
YIL053W	RHR2	glycerol-1-phosphatase	3.8072	14.0	0.0022372
YMR169C	ALD3	3-chloroallyl aldehyde dehydrogenase	3.8642	14.6	0.0011308
YHR055C	CUP1-2	copper ion binding	3.9318	15.3	0.0027359
YHR053C	CUP1-1	copper ion binding	3.9465	15.4	0.0026594
YDR536W	STL1	transporter	4.3728	20.7	0.0003767
YOL151W	GRE2	oxidoreductase	4.6408	24.9	0.0013843

Table 4: Raw microarray data for fermentation day five.

ORF ID	Gene Name	Gene Function	Avg Log_2 Ratio	Fold Change	T-test
YDR444W		unknown	-5.3392	-40.5	0.051763
YAL048C	GEM1	GTPase	-4.5062	-22.7	0.0344011
YCR045C		serine-type peptidase	-4.2547	-19.1	0.0440621
YLR382C	NAM2	mRNA binding	-4.2263	-18.7	0.0289843
YGR204W	ADE3	formate-tetrahydrofolate ligase	-4.1873	-18.2	0.0548038
YMR212C	EFR3	unknown	-3.9447	-15.4	0.0062186
YBR229C	ROT2	alpha-glucosidase	-3.9010	-14.9	0.026299
YGR098C	ESP1	cysteine-type endopeptidase	-3.7858	-13.8	0.0679902
YGR254W	ENO1	phosphopyruvate hydratase	-3.7653	-13.6	0.0074388
YKR002W	PAP1	polynucleotide adenylyltransferase	-3.7153	-13.1	0.0256818
YBL101C	ECM21	unknown	-3.6018	-12.1	0.0211561
YLR410W	VIP1	unknown	-3.5778	-11.9	0.0305307
YGR087C	PDC6	pyruvate decarboxylase	-3.3335	-10.1	0.0353946
YGL253W	HXK2	hexokinase	-3.2457	-9.5	0.0435592
YBL066C	SEF1	unknown	-3.1123	-8.6	0.207726
YGL243W	TAD1	tRNA specific adenosine deaminase	-3.0443	-8.2	0.0676653
YHR092C	HXT4	glucose transporter	-2.9675	-7.8	0.0073077
Q0255		unknown	-2.9470	-7.7	0.0239738
YCR041W			-2.9003	-7.5	0.0201269
YLR304C	ACO1	aconitate hydratase	-2.8653	-7.3	0.0766614
YDR385W	EFT2	translation elongation factor	-2.7742	-6.8	0.076096
YGR192C	TDH3	glyceraldehyde-3-phosphate dehydrogenase	-2.7288	-6.6	0.0159984
YFR053C	HXK1	hexokinase	-2.7267	-6.6	0.0465588
YMR302C	YME2	exonuclease	-2.7135	-6.6	0.0355041
YBR115C	LYS2	L-aminoadipate-semialdehyde dehydrogenase	-2.6073	-6.1	0.0422329
YOR306C	MCH5	transporter	-2.5742	-6.0	0.0580967
YCR025C			-2.5660	-5.9	0.0501329
YKL171W		protein kinase	-2.5295	-5.8	0.023167
YCR044C	PER1	unknown	-2.5255	-5.8	0.0482678
YDR249C		unknown	-2.4080	-5.3	0.0256315
YOR375C	GDH1	glutamate dehydrogenase (NADP+)	-2.3998	-5.3	0.0137396
YBR084W	MIS1	formate-tetrahydrofolate ligase	-2.3965	-5.3	0.0266945
YMR303C	ADH2	alcohol dehydrogenase	-2.2927	-4.9	0.0428944
YHR094C	HXT1	glucose transporter	-2.2070	-4.6	0.20141
YPR035W	GLN1	glutamate-ammonia ligase	-2.0923	-4.3	0.0213266
YHR096C	HXT5	glucose transporter	-2.0707	-4.2	0.0139458
YIL026C	IRR1	protein binding	-2.0672	-4.2	0.0960565
YBR127C	VMA2	hydrogen-transporting ATPase	-2.0652	-4.2	0.0232156
YDR516C	EMI2	unknown	-2.0278	-4.1	0.0430584
YHR174W	ENO2	phosphopyruvate hydratase	-2.0000	-4.0	0.0394261
YLR044C	PDC1	pyruvate decarboxylase	-1.9802	-3.9	0.0226271
YBL075C	SSA3	ATPase	-1.9228	-3.8	0.022582
YBR166C	TYR1	prephenate dehydrogenase	-1.9082	-3.8	0.0565102
YLR454W	FMP27	unknown	-1.8977	-3.7	0.018047
YHR181W	SVP26	protein binding	-1.8647	-3.6	0.082482
YNL072W	RNH201	ribonuclease H	-1.8630	-3.6	0.0426152
YMR083W	ADH3	alcohol dehydrogenase	-1.8503	-3.6	0.0911022
YDR247W	VHS1	protein kinase	-1.8400	-3.6	0.0152159
YMR163C		unknown	-1.8355	-3.6	0.0534559
YEL060C	PRB1	serine-type endopeptidase	-1.8322	-3.6	0.0182008
YMR297W	PRC1	carboxypeptidase C	-1.8112	-3.5	0.0035305
YHL048W	COS8	unknown	-1.8012	-3.5	0.0344361
YDR246W	TRS23	unknown	-1.7747	-3.4	0.0161081
YJL034W	KAR2	ATPase	-1.7743	-3.4	0.0532092
YFL062W	COS4	unknown	-1.7330	-3.3	0.047555
YNL209W	SSB2	ATPase	-1.6767	-3.2	0.0339435
YOL086C	ADH1	alcohol dehydrogenase	-1.6753	-3.2	0.0227968
YML132W	COS3	protein binding	-1.6287	-3.1	0.0225979
YCL024W	KCC4	protein kinase	-1.6078	-3.0	0.11384
YJR016C	ILV3	dihydroxy-acid dehydratase	-1.6025	-3.0	0.0231506
YMR125W	STO1	mRNA binding	-1.5743	-3.0	0.0507185
YBL099W	ATP1	hydrogen-transporting ATP synthase	-1.5735	-3.0	0.0448278
YKL103C	LAP4	aminopeptidase I	-1.5043	-2.8	0.0028877
YJR121W	ATP2	hydrogen-transporting ATP synthase	-1.5003	-2.8	0.0009516
YGR295C	COS6	unknown	-1.4972	-2.8	0.0492923
YDR129C	SAC6	protein binding	-1.4763	-2.8	0.0492033
YOR007C	SGT2	unknown	-1.4702	-2.8	0.0545219
YGR282C	BGL2	glucan 1,3-beta-glucosidase	-1.4538	-2.7	0.0393614
YAL037C-B			-1.4488	-2.7	0.0424666

Table 4: continued.

ORF ID	Gene Name	Gene Function	Avg Log_2 Ratio	Fold Change	T-test
YNL336W	COS1	unknown	-1.4452	-2.7	0.0542555
YGR248W	SOL4	6-phosphogluconolactonase	-1.4103	-2.7	0.0447699
YNL007C	SIS1	unfolded protein binding	-1.4067	-2.7	0.035954
YNL055C	POR1	voltage-gated ion-selective channel	-1.4002	-2.6	0.0474275
YBR128C	ATG14	unknown	-1.3803	-2.6	0.0351967
YJL052W	TDH1	glyceraldehyde-3-phosphate dehydrogenase	-1.3770	-2.6	0.010066
YDR432W	NPL3	mRNA binding	-1.3710	-2.6	0.0297018
YFL039C	ACT1	structural constituent of cytoskeleton	-1.3562	-2.6	0.0388893
YCR029C			-1.3558	-2.6	0.014576
YJR009C	TDH2	glyceraldehyde-3-phosphate dehydrogenase	-1.3525	-2.6	0.0546887
YAL062W	GDH3	glutamate dehydrogenase	-1.3248	-2.5	0.103498
YHR126C		unknown	-1.3195	-2.5	0.0325986
YJL160C		unknown	-1.2820	-2.4	0.0105725
YPL240C	HSP82	ATPase	-1.2735	-2.4	0.0281381
YML028W	TSA1	thioredoxin peroxidase	-1.2655	-2.4	0.0325153
YHR214W		unknown	-1.2520	-2.4	0.0587032
YBL045C	COR1	ubiquinol-cytochrome-c reductase	-1.2448	-2.4	0.035604
YCR004C	YCP4	electron carrier	-1.2435	-2.4	0.0344376
YDR032C	PST2	unknown	-1.2425	-2.4	0.037142
YKL117W	SBA1	chaperone binding	-1.2380	-2.4	0.0399051
YLR257W		unknown	-1.2313	-2.3	0.0924239
YDL029W	ARP2	structural constituent of cytoskeleton*	-1.2243	-2.3	0.178642
YMR186W	HSC82	unfolded protein binding	-1.2205	-2.3	0.0007939
YOR027W	STI1	unfolded protein binding	-1.1647	-2.2	0.0468117
YBR144C			-1.1547	-2.2	0.0182665
YPR033C	HTS1	histidine-tRNA ligase	-1.1540	-2.2	0.0207082
YCL042W		unknown	-1.1455	-2.2	0.0527729
YML100W	TSL1	enzyme regulator	-1.1102	-2.2	0.0200636
YLR258W	GSY2	glycogen (starch) synthase	-1.1092	-2.2	0.0075418
YPR080W	TEF1	translation elongation factor	-1.0617	-2.1	0.0257002
YPR113W	PIS1	CDP-diacylglycerol-inositol 3-phosphatidyltransferase	-1.0612	-2.1	0.0497974
YJL079C	PRY1	unknown	-1.0538	-2.1	0.050628
YGL076C	RPL7A	structural constituent of ribosome	-1.0323	-2.0	0.0160039
YBL001C	ECM15	unknown	-1.0195	-2.0	0.0485627
YLR149C		unknown	-1.0177	-2.0	0.0998473
YDR453C	TSA2	thioredoxin peroxidase	-1.0160	-2.0	0.0330834
YHR051W	COX6	cytochrome-c oxidase	-1.0148	-2.0	0.0169114
YDR322W	MRPL35	structural constituent of ribosome	-0.9937	-2.0	0.0511027
YAL002W	VPS8	unknown	-0.9903	-2.0	0.401723
YNL037C	IDH1	isocitrate dehydrogenase (NAD+)	-0.9893	-2.0	0.0766296
YKL163W	PIR3	structural constituent of cell wall	-0.9827	-2.0	0.0361575
YPL037C	EGD1	unfolded protein binding	-0.9800	-2.0	0.0541988
YLR109W	AHP1	thioredoxin peroxidase	-0.9773	-2.0	0.04681
YER053C	PIC2	inorganic phosphate transporter	-0.9753	-2.0	0.012701
YBR218C	PYC2	pyruvate carboxylase	-0.9668	-2.0	0.067544
YBR286W	APE3	aminopeptidase	-0.9597	-1.9	0.094082
YKL067W	YNK1	nucleoside diphosphate kinase	-0.9515	-1.9	0.0193619
YDR163W	CWC15	unknown	-0.9508	-1.9	0.0245781
YIL018W	RPL2B	structural constituent of ribosome	-0.9340	-1.9	0.0347385
YGR180C	RNR4	ribonucleoside-diphosphate reductase	-0.9320	-1.9	0.027898
YDR157W			-0.9258	-1.9	0.0415326
YNL208W		unknown	-0.9232	-1.9	0.121175
YAL005C	SSA1	ATPase	-0.9035	-1.9	0.00993
YBL030C	PET9	ATP:ADP antiporter	-0.9015	-1.9	0.24093
YIL094C	LYS12	homoisocitrate dehydrogenase	-0.8955	-1.9	0.0934259
YJL129C	TRK1	potassium ion transporter	-0.8778	-1.8	0.0894357
YCL009C	ILV6	enzyme regulator	-0.8747	-1.8	0.0663351
YCL064C	CHA1	L-serine ammonia-lyase	-0.8688	-1.8	0.206763
YHR219W		unknown	-0.8632	-1.8	0.0186118
YNL064C	YDJ1	chaperone regulator	-0.8600	-1.8	0.21054
YKL013C	ARC19	structural molecule	-0.8495	-1.8	0.178514
YMR233W		unknown	-0.8493	-1.8	0.0104045
YIL138C	TPM2	actin lateral binding	-0.8487	-1.8	0.0239481
YJL223C	PAU1	unknown	-0.8458	-1.8	0.01429
YBR079C	RPG1	translation initiation factor	-0.8167	-1.8	0.0203147
YJR103W	URA8	CTP synthase	-0.7887	-1.7	0.0035963
YEL027W	CUP5	hydrogen ion transporter	-0.7868	-1.7	0.0142962
YMR260C	TIF11	translation initiation factor	-0.7867	-1.7	0.0541752
YBR203W	COS111	unknown	-0.7847	-1.7	0.0256541

Table 4: continued.

ORF ID	Gene Name	Gene Function	Avg Log_2 Ratio	Fold Change	T-test
YJL159W	HSP150	structural constituent of cell wall	-0.7770	-1.7	0.0324755
YEL077C		helicase	-0.7742	-1.7	0.0517198
YAR020C	PAU7	unknown	-0.7555	-1.7	0.0127277
YLR441C	RPS1A	structural constituent of ribosome	-0.7533	-1.7	0.0517316
YLR388W	RPS29A	structural constituent of ribosome	-0.7532	-1.7	0.502622
YHL033C	RPL8A	structural constituent of ribosome	-0.7343	-1.7	0.0251955
YPR108W	RPN7	structural molecule	-0.7202	-1.6	0.186524
YOR185C	GSP2	GTPase	-0.7197	-1.6	0.0402039
YIR043C		unknown	-0.7132	-1.6	0.0508439
YKL152C	GPM1	phosphoglycerate mutase	-0.7105	-1.6	0.0322486
YKL058W	TOA2	general RNA polymerase II transcription factor	-0.6935	-1.6	0.0162936
YHL050C		helicase	-0.6908	-1.6	0.042141
YDL137W	ARF2	GTPase	-0.6883	-1.6	0.0986587
YOR332W	VMA4	hydrogen-transporting ATPase	-0.6848	-1.6	0.0515079
YDR086C	SSS1	protein transporter	-0.6682	-1.6	0.152408
YKL056C	TMA19	unknown	-0.6680	-1.6	0.130941
YLR264W	RPS28B	structural constituent of ribosome	-0.6642	-1.6	0.0213802
YOR167C	RPS28A	structural constituent of ribosome	-0.6625	-1.6	0.0292391
YAL056W	GPB2	signal transducer	-0.6580	-1.6	0.0421383
YAL013W	DEP1	transcription regulator	-0.6548	-1.6	0.0955915
YBR237W	PRP5	RNA splicing factor	-0.6533	-1.6	0.0745361
YGR118W	RPS23A	structural constituent of ribosome	-0.6513	-1.6	0.0279966
YKL160W	ELF1	RNA polymerase II transcription elongation factor	-0.6422	-1.6	0.0492036
YIR037W	HYR1	thioredoxin peroxidase	-0.6337	-1.6	0.0036256
YIL011W	TIR3	unknown	-0.6213	-1.5	0.0372393
YCL018W	LEU2	3-isopropylmalate dehydrogenase	-0.6213	-1.5	0.01219
YNL079C	TPM1	actin lateral binding	-0.6210	-1.5	0.0307504
YBR170C	NPL4	unknown	-0.6182	-1.5	0.0744633
YBL002W	HTB2	DNA binding	-0.6155	-1.5	0.294039
YKL006W	RPL14A	structural constituent of ribosome	-0.6150	-1.5	0.0006214
YCR032W	BPH1	unknown	-0.6087	-1.5	0.259111
YKR042W	UTH1	unknown	-0.6080	-1.5	0.173422
YBR301W	DAN3	unknown	-0.6070	-1.5	0.0276601
YBR263W	SHM1	glycine hydroxymethyltransferase	-0.6060	-1.5	0.0027566
YBR121C	GRS1	glycine-tRNA ligase	-0.6042	-1.5	0.0469617
YHR008C	SOD2	manganese superoxide dismutase	-0.5990	-1.5	0.0392052
YOR215C		unknown	-0.5953	-1.5	0.0125881
YLR238W	FAR10	unknown	-0.5887	-1.5	0.0507794
YLR325C	RPL38	structural constituent of ribosome	-0.5853	-1.5	0.0236712
YIL155C	GUT2	glycerol-3-phosphate dehydrogenase	-0.5823	-1.5	0.210418
YIR041W	PAU15	unknown	-0.5755	-1.5	0.0400524
YBR164C	ARL1	GTPase	-0.5698	-1.5	0.0646627
YEL054C	RPL12A	structural constituent of ribosome	-0.5673	-1.5	0.139228
YBR010W	HHT1	DNA binding	-0.5668	-1.5	0.053004
YJL177W	RPL17B	structural constituent of ribosome	-0.5557	-1.5	0.0615107
YBR082C	UBC4	ubiquitin conjugating enzyme	-0.5533	-1.5	0.277941
YDR033W	MRH1	unknown	-0.5392	-1.5	0.043695
YLR227W-A			-0.5375	-1.5	0.0497666
YIL142W	CCT2	unfolded protein binding	-0.5350	-1.4	0.0500548
YBR221C	PDB1	pyruvate dehydrogenase (acetyl-transferring)	-0.5342	-1.4	0.0522371
YCR047C	BUD23	S-adenosylmethionine-dependent methyltransferase	-0.5338	-1.4	0.157489
YER057C	HMF1	unknown	-0.5293	-1.4	0.0478953
YKR094C	RPL40B	structural constituent of ribosome	-0.5022	-1.4	0.148783
YJL158C	CIS3	structural constituent of cell wall	-0.5017	-1.4	0.0727102
YBR081C	SPT7	structural molecule	-0.4840	-1.4	0.365906
YBR067C	TIP1	structural constituent of cell wall*	-0.4827	-1.4	0.251577
YKL060C	FBA1	fructose-bisphosphate aldolase	-0.4808	-1.4	0.278732
YBR126C	TPS1	alpha,alpha-trehalose-phosphate synthase (UDP-forming)	-0.4728	-1.4	0.0825319
YPL090C	RPS6A	structural constituent of ribosome	-0.4703	-1.4	0.0035684
YKL085W	MDH1	L-malate dehydrogenase	-0.4592	-1.4	0.0489727
YHR135C	YCK1	casein kinase I	-0.4468	-1.4	0.413325
YER102W	RPS8B	structural constituent of ribosome	-0.4345	-1.4	0.0049872
YLR043C	TRX1	thiol-disulfide exchange intermediate	-0.4305	-1.3	0.0060027
YML045W			-0.4202	-1.3	0.0193989
YEL049W	PAU2	unknown	-0.4198	-1.3	0.0016843
YCR104W	PAU3	unknown	-0.4102	-1.3	0.0137731
YLR216C	CPR6	unfolded protein binding	-0.4013	-1.3	0.0084931
YGR037C	ACB1	long-chain fatty acid transporter	-0.3985	-1.3	0.0046039
YJR073C	OPI3	phosphatidyl-N-methylethanolamine N-methyltransferase	-0.3958	-1.3	0.0340325

Table 4: continued.

ORF ID	Gene Name	Gene Function	Avg Log_2 Ratio	Fold Change	T-test
YIL176C	PAU14	unknown	-0.3848	-1.3	0.16288
YDR201W	SPC19	structural constituent of cytoskeleton	-0.3767	-1.3	0.475063
YBR234C	ARC40	structural constituent of cytoskeleton	-0.3733	-1.3	0.0467256
YBR255W		unknown	-0.3728	-1.3	0.0621633
YMR190C	SGS1	ATP-dependent DNA helicase	-0.3702	-1.3	0.215257
YDR500C	RPL37B	structural constituent of ribosome	-0.3658	-1.3	0.0677628
YBR208C	DUR1,2	allophanate hydrolase	-0.3618	-1.3	0.14266
YBR094W		unknown	-0.3533	-1.3	0.0108237
YDR119W		unknown	-0.3513	-1.3	0.0295702
YHR192W		unknown	-0.3432	-1.3	0.195677
YBR080C	SEC18	ATPase	-0.3407	-1.3	0.226605
YBL027W	RPL19B	structural constituent of ribosome	-0.3385	-1.3	0.525091
YBR224W			-0.3185	-1.2	0.0180677
YBL113C		helicase	-0.2948	-1.2	0.191124
YBR191W	RPL21A	structural constituent of ribosome	-0.2843	-1.2	0.0247335
YIL051C	MMF1	unknown	-0.2795	-1.2	0.473004
YDR382W	RPP2B	structural constituent of ribosome	-0.2795	-1.2	0.0472885
YNL160W	YGP1	unknown	-0.2737	-1.2	0.200024
YAL068C	PAU8	unknown	-0.2683	-1.2	0.0073871
YHR183W	GND1	phosphogluconate dehydrogenase (decarboxylating)	-0.2590	-1.2	0.742296
YNL161W	CBK1	protein kinase	-0.2577	-1.2	0.656745
YLR340W	RPP0	structural constituent of ribosome	-0.2555	-1.2	0.220982
YCR053W	THR4	threonine synthase	-0.2548	-1.2	0.0314283
YLL066W-A			-0.2465	-1.2	0.68185
YBR012W-A			-0.2445	-1.2	0.209382
YBR031W	RPL4A	structural constituent of ribosome	-0.2412	-1.2	0.787372
YGR148C	RPL24B	structural constituent of ribosome	-0.2347	-1.2	0.257877
YJR028W			-0.2337	-1.2	0.0340705
YOR096W	RPS7A	structural constituent of ribosome	-0.2308	-1.2	0.0456217
YBR125C	PTC4	protein phosphatase type 2C	-0.2285	-1.2	0.179713
YMR264W	CUE1	protein binding	-0.2262	-1.2	0.0467298
YER068W	MOT2	3'-5'-exoribonuclease	-0.2248	-1.2	0.0062249
YGL095C	VPS45	unfolded protein binding	-0.2145	-1.2	0.0225472
YBR212W	NGR1	RNA binding	-0.2125	-1.2	0.71913
YBR072W	HSP26	unfolded protein binding	-0.2118	-1.2	0.290927
YDL082W	RPL13A	structural constituent of ribosome	-0.2072	-1.2	0.291089
YBR086C	IST2	unknown	-0.2028	-1.2	0.374258
YLR333C	RPS25B	structural constituent of ribosome	-0.2002	-1.1	0.0631351
YDR202C	RAV2	unknown	-0.1908	-1.1	0.695319
YAL035W	FUN12	GTPase	-0.1877	-1.1	0.261907
YJL020C	BBC1	myosin I binding	-0.1867	-1.1	0.0357772
YBR069C	TAT1	amino acid transporter	-0.1833	-1.1	0.825265
YJL210W	PEX2	protein binding	-0.1742	-1.1	0.0424187
YBR095C	RXT2	unknown	-0.1717	-1.1	0.432364
YBR009C	HHF1	DNA binding	-0.1688	-1.1	0.0446996
YLR185W	RPL37A	structural constituent of ribosome	-0.1630	-1.1	0.0507136
YCR028C	FEN2	pantothenate transporter	-0.1535	-1.1	0.835791
YBR148W	YSW1	unknown	-0.1465	-1.1	0.445584
YJL111W	CCT7	unfolded protein binding	-0.1455	-1.1	0.485339
YJL174W	KRE9	unknown	-0.1437	-1.1	0.515636
YDR321W	ASP1	asparaginase	-0.1402	-1.1	0.0219457
YDR329C	PEX3	protein binding	-0.1383	-1.1	0.0065111
YBR111C	YSA1	phosphoribosyl-ATP diphosphatase	-0.1202	-1.1	0.46628
YDR080W	VPS41	Rab guanyl-nucleotide exchange factor	-0.1170	-1.1	0.470536
YCL025C	AGP1	amino acid transporter	-0.1077	-1.1	0.451172
YBR280C		unknown	-0.1060	-1.1	0.458173
YBR053C		unknown	-0.0850	-1.1	0.567644
YLR294C			-0.0837	-1.1	0.554822
YGL135W	RPL1B	structural constituent of ribosome	-0.0812	-1.1	0.605322
YDR542W	PAU10	unknown	-0.0712	-1.1	0.20482
YBR302C	COS2	unknown	-0.0512	-1.0	0.788207
YBR008C	FLR1	multidrug transporter	-0.0457	-1.0	0.776315
YJL070C		unknown	-0.0335	-1.0	0.862868
YBR205W	KTR3	mannosyltransferase	0.0028	1.0	0.987206
YAL021C	CCR4	3'-5'-exoribonuclease	0.0102	1.0	0.954663
YMR143W	RPS16A	structural constituent of ribosome	0.0120	1.0	0.965284
YCRX13W			0.0140	1.0	0.949018
YER177W	BMH1	protein binding	0.0255	1.0	0.626577
YMR242C	RPL20A	structural constituent of ribosome	0.0318	1.0	0.565757

Table 4: continued.

ORF ID	Gene Name	Gene Function	Avg Log_2 Ratio	Fold Change	T-test
YOR182C	RPS30B	structural constituent of ribosome	0.0530	1.0	0.925237
YGL189C	RPS26A	structural constituent of ribosome	0.0543	1.0	0.713676
YER067W		unknown	0.0617	1.0	0.450352
YBR259W		unknown	0.0647	1.0	0.738226
YDR025W	RPS11A	structural constituent of ribosome	0.0705	1.1	0.41071
YER011W	TIR1	structural constituent of cell wall	0.0707	1.1	0.67071
YDL136W	RPL35B	structural constituent of ribosome	0.0735	1.1	0.607779
YBR262C	FMP51	unknown	0.0795	1.1	0.599434
YCL020W			0.1157	1.1	0.587526
YIL043C	CBR1	cytochrome-b5 reductase	0.1212	1.1	0.568691
YDR377W	ATP17	hydrogen-transporting ATP synthase	0.1287	1.1	0.0463994
YIL074C	SER33	phosphoglycerate dehydrogenase	0.1287	1.1	0.0528452
YHR190W	ERG9	farnesyl-diphosphate farnesyltransferase	0.1307	1.1	0.758866
YOR285W		unknown	0.1383	1.1	0.548149
YDR273W	DON1	unknown	0.1590	1.1	0.297698
YDR473C	PRP3	RNA splicing factor	0.1812	1.1	0.0011975
YLR395C	COX8	cytochrome-c oxidase	0.1837	1.1	0.0267468
YBL092W	RPL32	structural constituent of ribosome	0.1968	1.1	0.283901
YNL149C	PGA2	unknown	0.1978	1.1	0.447352
YJL225C		helicase	0.2048	1.2	0.0025009
YDL075W	RPL31A	structural constituent of ribosome	0.2070	1.2	0.477447
YJL021C			0.2092	1.2	0.0208446
YMR022W	QRI8	ubiquitin conjugating enzyme	0.2112	1.2	0.0129973
YLR193C		unknown	0.2177	1.2	0.0363107
YPR020W	ATP20	structural molecule	0.2223	1.2	0.0425931
YER019C-A	SBH2	protein transporter	0.2225	1.2	0.566916
YIL105C	SLM1	phosphoinositide binding	0.2287	1.2	0.015514
YDR154C			0.2290	1.2	0.020685
YHR104W	GRE3	aldo-keto reductase	0.2337	1.2	0.0392109
YNL099C	OCA1	protein tyrosine phosphatase	0.2358	1.2	0.502156
YCL002C		unknown	0.2395	1.2	0.031586
YBR135W	CKS1	protein kinase activator	0.2397	1.2	0.0667429
YOR113W	AZF1	DNA binding	0.2483	1.2	0.051918
YJR048W	CYC1	electron carrier	0.2588	1.2	0.0315101
YOR394W	PAU21	unknown	0.2638	1.2	0.758736
YGL227W	VID30	unknown	0.2778	1.2	0.0204272
YOR310C	NOP58	unknown	0.2788	1.2	0.0046976
YLR158C	ASP3-3	asparaginase	0.2813	1.2	0.261902
YDR145W	TAF12	general RNA polymerase II transcription factor	0.2833	1.2	0.0472565
YAL016W	TPD3	protein phosphatase type 2A	0.2882	1.2	0.216513
YOR359W	VTS1	RNA binding	0.2905	1.2	0.0517269
YJR104C	SOD1	copper, zinc superoxide dismutase	0.2927	1.2	0.261885
YBR238C		unknown	0.2982	1.2	0.0092437
YER056C-A	RPL34A	structural constituent of ribosome	0.2995	1.2	0.0129893
YHR146W	CRP1	DNA binding	0.3000	1.2	0.035565
YDR002W	YRB1	Ran GTPase binding	0.3002	1.2	0.433006
YOR042W	CUE5	unknown	0.3065	1.2	0.0020051
YBR172C	SMY2	unknown	0.3128	1.2	0.0021384
YJL136C	RPS21B	structural constituent of ribosome	0.3163	1.2	0.0276983
YCR024C-A	PMP1	enzyme regulator	0.3173	1.2	0.152376
YCRX16C			0.3207	1.2	0.0640786
YBR102C	EXO84	protein binding	0.3283	1.3	0.329939
YCR084C	TUP1	general transcriptional repressor	0.3310	1.3	0.0360097
YBR261C		S-adenosylmethionine-dependent methyltransferase	0.3343	1.3	0.0067372
YHR152W	SPO12	unknown	0.3378	1.3	0.107735
YER080W	FMP29	unknown	0.3388	1.3	0.0069813
YDL124W		alpha-keto amide reductase	0.3392	1.3	0.26327
YNL284C-A			0.3402	1.3	0.0209582
YDR034C	LYS14	transcriptional activator	0.3420	1.3	0.0443624
YDL134C	PPH21	protein phosphatase type 2A	0.3435	1.3	0.27363
YER109C	FLO8	specific RNA polymerase II transcription factor	0.3557	1.3	0.0110862
YIL068C	SEC6	protein binding	0.3567	1.3	0.452916
YBR268W	MRPL37	structural constituent of ribosome	0.3572	1.3	0.0070668
YJL141C	YAK1	protein kinase	0.3653	1.3	0.112743
YDR134C		unknown	0.3703	1.3	0.177762
YDR510W	SMT3	protein tag	0.3722	1.3	0.0119308
YDR309C	GIC2	small GTPase regulator	0.3752	1.3	0.350099
YAL030W	SNC1	v-SNARE	0.3765	1.3	0.0967859
YLR204W	QRI5	unknown	0.3785	1.3	0.0028322

Table 4: continued.

ORF ID	Gene Name	Gene Function	Avg Log_2 Ratio	Fold Change	T-test
YHR200W	RPN10	endopeptidase	0.3908	1.3	0.0867604
YIL045W	PIG2	protein phosphatase type 1 regulator	0.3923	1.3	0.0317944
YIL052C	RPL34B	structural constituent of ribosome	0.3963	1.3	0.0234255
YNL027W	CRZ1	transcription factor	0.3967	1.3	0.010022
YLR093C	NYV1	v-SNARE	0.3972	1.3	0.0210133
YCR042C	TAF2	general RNA polymerase II transcription factor	0.3993	1.3	0.0430635
YBR117C	TKL2	transketolase	0.4085	1.3	0.0265663
YBR071W		unknown	0.4103	1.3	0.0156187
YOR327C	SNC2	v-SNARE	0.4108	1.3	0.0424408
YOR065W	CYT1	electron transporter	0.4218	1.3	0.017113
YNR052C	POP2	3'-5'-exoribonuclease	0.4298	1.3	0.0398091
YBR090C		unknown	0.4330	1.4	0.117835
YDR261C-C			0.4348	1.4	0.0394559
YDL147W	RPN5	unknown	0.4350	1.4	0.0127133
YBR162W-A	YSY6	unknown	0.4353	1.4	0.0094113
YDR208W	MSS4	1-phosphatidylinositol-4-phosphate 5-kinase	0.4397	1.4	0.286168
YCR082W	AHC2	unknown	0.4468	1.4	0.0212216
YMR002W		unknown	0.4538	1.4	0.0464385
YPL271W	ATP15	hydrogen-transporting ATP synthase	0.4665	1.4	0.0300279
YBR267W	REI1	unknown	0.4710	1.4	0.0084363
YDL097C	RPN6	structural molecule	0.4710	1.4	0.218294
YBR297W	MAL33	transcription factor	0.4782	1.4	0.40255
YJL144W		unknown	0.4787	1.4	0.0291092
YFL021C-A			0.4793	1.4	0.222885
YAL063C	FLO9	mannose binding	0.4820	1.4	0.0511794
YLR330W	CHS5	unknown	0.4863	1.4	0.0320483
YBR134W			0.4897	1.4	0.0093899
YIR016W		unknown	0.4918	1.4	0.134715
YBR256C	RIB5	riboflavin synthase	0.4933	1.4	0.0786972
YJL118W		unknown	0.5017	1.4	0.0488577
YBR105C	VID24	unknown	0.5028	1.4	0.0489352
YDL083C	RPS16B	structural constituent of ribosome	0.5122	1.4	0.0499676
YBL101W-A			0.5127	1.4	0.0761509
YDL005C	MED2	RNA polymerase II transcription mediator	0.5163	1.4	0.005962
YDL212W	SHR3	unfolded protein binding	0.5238	1.4	0.0448283
YFR008W	FAR7	unknown	0.5318	1.4	0.0289027
YIL152W		unknown	0.5338	1.4	0.0120596
YNL118C	DCP2	mRNA binding	0.5342	1.4	0.0170435
YMR124W		unknown	0.5412	1.5	0.0749135
YMR070W	MOT3	DNA binding	0.5435	1.5	0.0172109
YDR476C		unknown	0.5437	1.5	0.033795
YKL065C	YET1	unknown	0.5555	1.5	0.0510764
YBR024W	SCO2	thioredoxin peroxidase	0.5707	1.5	0.046428
YAL061W		oxidoreductase	0.5815	1.5	0.181938
YHR198C	FMP22	unknown	0.5830	1.5	0.0365646
YJL117W	PHO86	unknown	0.5858	1.5	0.0242786
YDR365W-A			0.5933	1.5	0.0270192
YPR065W	ROX1	specific transcriptional repressor	0.5937	1.5	0.240102
YIL063C	YRB2	unknown	0.5987	1.5	0.0532592
YNL113W	RPC19	DNA-directed RNA polymerase	0.6105	1.5	0.0450949
YHR154W	RTT107	unknown	0.6182	1.5	0.0122228
YJR008W		unknown	0.6260	1.5	0.0528628
YDR034C-C			0.6343	1.6	0.0446272
YCL011C	GBP2	RNA binding	0.6418	1.6	0.0001894
YNL054W-A			0.6478	1.6	0.0547295
YKL172W	EBP2	unknown	0.6508	1.6	0.0394215
YDR261W-A			0.6510	1.6	0.0256109
YLR410W-A			0.6545	1.6	0.0468589
YGL037C	PNC1	nicotinamidase	0.6548	1.6	0.0403934
YGL237C	HAP2	transcriptional activator	0.6697	1.6	0.0248453
YGR086C	PIL1	protein kinase inhibitor	0.6742	1.6	0.0354637
YHR095W			0.6878	1.6	0.0106695
YDL020C	RPN4	transcriptional activator	0.7053	1.6	0.046169
YJL142C			0.7128	1.6	0.0471679
YAR015W	ADE1	phosphoribosylaminoimidazolesuccinocarboxamide synthas	0.7187	1.6	0.0198603
YBR034C	HMT1	protein-arginine N-methyltransferase	0.7282	1.7	0.0218337
YDL134C-A			0.7485	1.7	0.104724
YGR069W			0.7593	1.7	0.0024741
YIL006W	YIA6	transporter	0.7617	1.7	0.204415

Table 4: continued.

ORF ID	Gene Name	Gene Function	Avg Log_2 Ratio	Fold Change	T-test
YHR138C		endopeptidase inhibitor	0.7718	1.7	0.0429167
YCR080W			0.7753	1.7	0.0319661
YNL112W	DBP2	RNA helicase	0.7760	1.7	0.0158107
YBR068C	BAP2	amino acid transporter	0.7792	1.7	0.0936009
YOR298W	MUM3	acyltransferase	0.7823	1.7	0.0088567
YHR166C	CDC23	protein binding	0.8003	1.7	0.0753333
YCL067C	HMLALPHA	transcription corepressor	0.8032	1.7	0.020451
YNL143C			0.8048	1.7	0.0127135
YER079W		unknown	0.8088	1.8	0.032764
YNL133C	FYV6	unknown	0.8183	1.8	0.0064089
YKR071C	DRE2	unknown	0.8277	1.8	0.0887988
YAL039C	CYC3	holocytochrome-c synthase	0.8285	1.8	0.0075338
YMR121C	RPL15B	structural constituent of ribosome	0.8292	1.8	0.0128724
YEL071W	DLD3	D-lactate dehydrogenase (cytochrome)	0.8443	1.8	0.045225
YOL143C	RIB4	6,7-dimethyl-8-ribityllumazine synthase	0.8468	1.8	0.0470601
YMR090W		unknown	0.8622	1.8	0.0460975
YKR040C			0.8778	1.8	0.0263266
YDR203W			0.8782	1.8	0.102064
YBR122C	MRPL36	structural constituent of ribosome	0.8928	1.9	0.0345816
YJR047C	ANB1	translation initiation factor	0.9015	1.9	0.406705
YBR249C	ARO4	3-deoxy-7-phosphoheptulonate synthase	0.9033	1.9	0.0395766
YGR034W	RPL26B	structural constituent of ribosome	0.9062	1.9	0.0161455
YAL060W	BDH1	(R,R)-butanediol dehydrogenase	0.9090	1.9	0.0296579
YHR187W	IKI1	RNA polymerase II transcription elongation factor	0.9115	1.9	0.0309065
YDL048C	STP4	unknown	0.9160	1.9	0.0454473
YDR529C	QCR7	ubiquinol-cytochrome-c reductase	0.9263	1.9	0.0298725
YFR017C		unknown	0.9315	1.9	0.0450418
YHL015W	RPS20	structural constituent of ribosome	0.9440	1.9	0.0257441
YKL141W	SDH3	succinate dehydrogenase (ubiquinone)	0.9558	1.9	0.233962
YIL144W	TID3	structural constituent of cytoskeleton	0.9593	1.9	0.054765
YFL-TYB			0.9787	2.0	0.0448005
YCL065W			0.9825	2.0	0.0175075
YNL157W	IGO1	unknown	0.9865	2.0	0.0441041
YKR066C	CCP1	cytochrome-c peroxidase	0.9895	2.0	0.0091674
YNL178W	RPS3	structural constituent of ribosome	1.0010	2.0	0.0379982
YOR020C	HSP10	unfolded protein binding	1.0115	2.0	0.030164
YCR096C	HMRA2	unknown	1.0132	2.0	0.0324899
YDL051W	LHP1	RNA binding	1.0195	2.0	0.0536717
YPL058C	PDR12	xenobiotic-transporting ATPase	1.0252	2.0	0.20091
YHR097C		unknown	1.0355	2.0	0.0346253
YOR052C		unknown	1.0378	2.1	0.144021
YGR183C	QCR9	ubiquinol-cytochrome-c reductase	1.0418	2.1	0.0751807
YER032W	FIR1	unknown	1.0543	2.1	0.0523615
YHR137W	ARO9	aromatic-amino-acid transaminase	1.0658	2.1	0.0942575
YDL169C	UGX2	unknown	1.0682	2.1	0.0261166
YKR049C	FMP46	oxidoreductase	1.0758	2.1	0.174838
YMR251W-A	HOR7	unknown	1.0838	2.1	0.0922112
YOL106W			1.0888	2.1	0.0328209
YNL180C	RHO5	GTPase	1.1487	2.2	0.028897
YBR101C	FES1	adenyl-nucleotide exchange factor	1.1603	2.2	0.0205651
YLR309C	IMH1	unknown	1.1613	2.2	0.0186924
YDR368W	YPR1	oxidoreductase	1.1630	2.2	0.0361984
YKL093W	MBR1	unknown	1.2308	2.3	0.0486059
YGL062W	PYC1	pyruvate carboxylase	1.2363	2.4	0.0459513
YBL015W	ACH1	acetyl-CoA hydrolase	1.2407	2.4	0.0388953
YHR214C-B			1.2627	2.4	0.0532289
YCL040W	GLK1	glucokinase	1.2673	2.4	0.0381918
YMR173W-A			1.2678	2.4	0.0466505
YHR155W	YSP1	unknown	1.2897	2.4	0.128931
YFR016C		unknown	1.3243	2.5	0.0459536
YHR054C		unknown	1.3395	2.5	0.0265463
YEL009C	GCN4	DNA binding	1.3403	2.5	0.0382242
YAR009C			1.3413	2.5	0.0114855
YEL012W	UBC8	ubiquitin conjugating enzyme	1.3488	2.5	0.0521475
YDR210C-D			1.3710	2.6	0.0296608
YOR031W	CRS5	copper ion binding	1.3805	2.6	0.0265957
YHR145C			1.3915	2.6	0.0788772
YLR256W	HAP1	specific RNA polymerase II transcription factor	1.3978	2.6	0.113426
YHR149C	SKG6	unknown	1.4077	2.7	0.0385228

Table 4: continued.

ORF ID	Gene Name	Gene Function	Avg Log_2 Ratio	Fold Change	T-test
YHR070W	TRM5	tRNA (guanine) methyltransferase	1.4293	2.7	0.0320838
TDR261C-D			1.4402	2.7	0.04881
YHR087W		unknown	1.4628	2.8	0.0438919
YDR244W	PEX5	peroxisome targeting sequence binding	1.4683	2.8	0.0511298
YER062C	HOR2	glycerol-1-phosphatase	1.4755	2.8	0.0441064
YLR035C-A			1.4912	2.8	0.0209809
YGR088W	CTT1	catalase	1.5060	2.8	0.135822
Q0060	AI3	endonuclease	1.5138	2.9	0.0431973
YJL116C	NCA3	unknown	1.5418	2.9	0.0909263
YMR096W	SNZ1	protein binding	1.5512	2.9	0.0658355
YOL053C-A			1.5812	3.0	0.0462657
YIL060W		unknown	1.5883	3.0	0.0331232
YBR230C	OM14	unknown	1.6172	3.1	0.0502337
YHR165C	PRP8	RNA splicing factor	1.6178	3.1	0.0352883
YER024W	YAT2	carnitine O-acetyltransferase	1.6467	3.1	0.0457763
YHR171W	ATG7	APG12 activating enzyme	1.6627	3.2	0.0530414
YBR116C			1.6698	3.2	0.0604677
YHR103W	SBE22	unknown	1.6850	3.2	0.0194832
YHR161C	YAP1801	clathrin binding	1.6862	3.2	0.037702
YHR144C	DCD1	dCMP deaminase	1.7098	3.3	0.0438885
YDR041W	RSM10	structural constituent of ribosome	1.7302	3.3	0.0532902
YFL029C	CAK1	cyclin-dependent protein kinase activating kinase	1.7960	3.5	0.0370991
YLR410W-B			1.8005	3.5	0.0058466
YDL182W	LYS20	homocitrate synthase	1.8177	3.5	0.0255799
YNL110C	NOP15	unknown	1.8192	3.5	0.0420959
YIL099W	SGA1	glucan 1,4-alpha-glucosidase	1.8200	3.5	0.0408364
YIL053W	RHR2	glycerol-1-phosphatase	1.8332	3.6	0.0308083
YFL021W	GAT1	specific RNA polymerase II transcription factor	1.9022	3.7	0.048557
YOL150C			1.9847	4.0	0.0398114
YGR243W	FMP43	unknown	1.9980	4.0	0.0476662
YMR174C	PAI3	endopeptidase inhibitor	2.0182	4.1	0.0382856
YDR070C	FMP16	unknown	2.0265	4.1	0.0371171
YGR182C			2.0555	4.2	0.0106683
YOL151W	GRE2	oxidoreductase	2.1938	4.6	0.0417326
YHR139C	SPS100	unknown	2.1995	4.6	0.042501
YCR005C	CIT2	citrate (Si)-synthase	2.2268	4.7	0.0099217
YJL106W	IME2	protein kinase	2.3285	5.0	0.0508438
YBR050C	REG2	protein phosphatase type 1 regulator	2.3793	5.2	0.0456598
YLR346C		unknown	2.4018	5.3	0.0338526
YPL135W	ISU1	protein binding	2.4313	5.4	0.0459425
YMR195W	ICY1	unknown	2.4578	5.5	0.0283315
YHR033W		unknown	2.4952	5.6	0.0476181
YPL223C	GRE1	unknown	2.5318	5.8	0.0477036
YHR162W		unknown	2.5717	5.9	0.0417935
YBR281C		unknown	2.5802	6.0	0.0436952
YHR056C	RSC30	DNA binding	2.5825	6.0	0.0005777
YFL013W-A			2.5992	6.1	0.0431277
YHR055C	CUP1-2	copper ion binding	2.6320	6.2	0.0505493
YFL014W	HSP12	unknown	2.6625	6.3	0.0461229
YHR053C	CUP1-1	copper ion binding	2.7475	6.7	0.0360849
YKL096W	CWP1	structural constituent of cell wall	3.1493	8.9	0.0515745
YER065C	ICL1	isocitrate lyase	3.2103	9.3	0.0446256
YMR107W	SPG4	unknown	3.2662	9.6	0.0388049
YJR095W	SFC1	succinate:fumarate antiporter	3.5115	11.4	0.0203382
YNL036W	NCE103	carbonate dehydratase	3.7867	13.8	0.0378788
YCR010C	ADY2	ammonium transporter	3.8223	14.1	0.0387718
YDR536W	STL1	transporter	3.9488	15.4	0.0341034
YMR175W	SIP18	phospholipid binding	4.6685	25.4	0.0458001

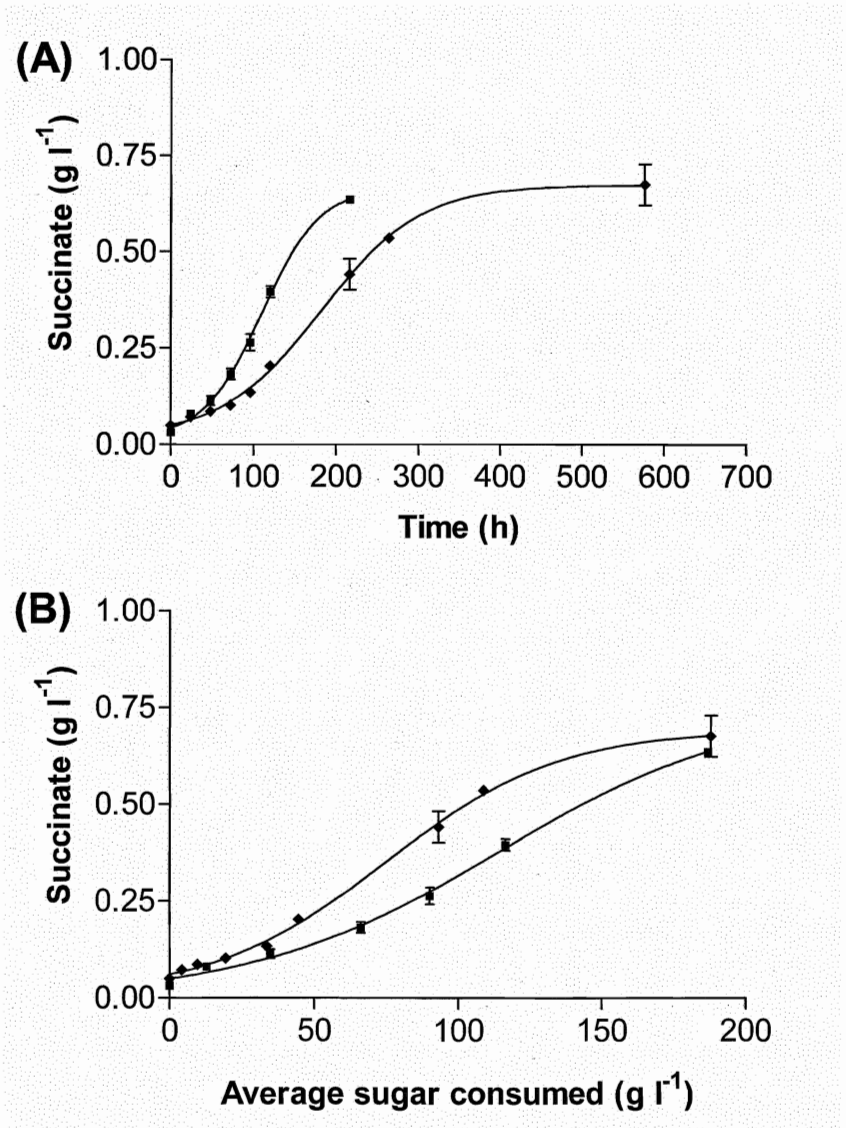

Figure 1: Yeast succinate production. The concentration of extracellular succinate (A) was measured in duplicate throughout the course of the fermentations of Icewine juice (♦) and diluted Icewine juice (■) and was plotted as a function of sugar consumed (B). The values represent the average ± standard deviation of the mean of triplicate fermentations.